Annulation and Directing Group Strategies as Tools for the Construction of Heterocycles

A dissertation submitted in partial fulfillment for the degree of

Doctor of Philosophy

Submitted By

Bubul Das

Roll No. 196122010

Under the supervision of

Prof. Bhisma K. Patel

Department of Chemistry

Indian Institute of Technology Guwahati

Guwahati-781039, Assam, India

August, 2024

DEDICATED WITH LOVE

TO

My Maa, Deuta & Baideu

INDIAN INSTITUTE OF TECHNOLOGY GUWAHATI

Department of Chemistry

STATEMENT

I do hereby declare that the matter embodied in this thesis is the result of investigations carried out by me in the Department of Chemistry, Indian Institute of Technology Guwahati, India, under the guidance of Prof. Bhisma K. Patel. I have submitted this thesis to the Department of Chemistry, Indian Institute of Technology Guwahati for the award of the degree of Doctor of Philosophy.

In keeping with the general practice of reporting scientific observations, due acknowledgments have been made wherever the work described is based on the findings of other investigators. I further declare that this work has not been submitted anywhere else for any degree, diploma, associateship or membership, etc. of any Institute or University to the best of my knowledge.

August, 2024

IIT Guwahati **Bubul Das**

INDIAN INSTITUTE OF TECHNOLOGY GUWAHATI

Department of Chemistry

CERTIFICATE

This is to certify that Bubul Das has been working under my supervision since July 2019 as a registered Ph.D. student. His thesis entitled "**Annulation and Directing Group Strategies as Tools for the Construction of Heterocycles**" is an authentic record of the results obtained from the research work in the Department of Chemistry, Indian Institute of Technology Guwahati, Assam, India. I am forwarding his thesis to submit for the Ph.D. (Science) degree from this institute. I certify that he has fulfilled all the requirements according to the rules of this institute regarding the investigations embodied in his thesis, and this work has not been submitted elsewhere for a degree.

August, 2024

Prof. Bhisma K. Patel
(Thesis Supervisor)
Department of Chemistry
IIT Guwahati

ACKNOWLEDGEMENT

Reaching the stage very close to accomplishing the highest academic qualification, a Ph.D. degree, if I look back I can see a lot of people to whom I am forever indebted for their encouragement, support, guidance, belief in me, love, and every little push they offer me towards achieving it.

First and foremost, I want to express my deepest respect and profound gratitude to my supervisor, Prof. Bhisma K. Patel, for providing me the opportunity to work under his guidance in his research group. His creative and unique scientific ideas, continuous support, guidance, and motivation throughout the journey shaped my path and helped me to explore the domain of my work assembled in this thesis. I am fortunate enough to have him as my mentor, who offered full freedom to explore my ideas, supported me when things were not working as planned, and motivated me towards achieving excellence in this journey.

I would also like to extend my heartiest gratitude to the doctoral committee (DC) members, Prof. A. S. Achalkumar, Prof. Chandan Das, and Dr. Dipankar Srimani, for the timely evaluation of my Ph.D. work and all the precious suggestions, which helped me a lot in the betterment of my thesis. I also sincerely thank Prof. Bhubaneswar Mandal and Dr. Kalyan Raidongia for their evaluation of my work during the absence of any DC members.

My honest gratitude to all the faculty and staff members of the Department of Chemistry, IIT Guwahati, for their cooperative nature. I would like to thank Imdadul da for NMR, Babulal da for single-crystal XRD, Basab da, Diganta da, Anirudha da, Tapu da, and Michel for various official work and support in the Department of Chemistry.

I wish to express sincere gratitude to MHRD or the Ministry of Education for the financial support and to IIT Guwahati for all the facilities that were made available to me for learning several analytical instruments required during my research work. I am grateful to the Central Instruments Facility (CIF) for the 600 MHz NMR and single-crystal XRD facilities, MHRD for the 400 MHz NMR facility under the COE-FAST program, DST for the 500 MHz NMR facility under the DST-FIST program, NECBH, IIT Guwahati, and DBT, Govt. of India for the 400 MHz NMR and single-crystal XRD facilities.

Thanks to all the operators inside and outside IIT Guwahati for successfully carrying out all the instrumental experiments required during my research. Further, I am extremely thankful to all the co-authors, editors, associate editors, and reviewers for their valuable comments and suggestions.

The entire CHEL-106, past and present members deserve tremendous credit for completing the most memorable journey of academia among them. I would like to express my deepest gratitude to my Ph.D. senior, Anjali Di, for her guidance throughout the journey. She left no stone unturned to teach me every lab technique that was necessary to complete this journey. I am also thankful to senior-cum-my close neighbour from the lab Nikita Baa for making the tough Ph.d journey smooth with her guidance, support, and encouragement. Starting from her initial days of guidance, she always up for scientic and non-scientific discussions and tea. I would also like to thank my other lab seniors Ashish bhaiya, Tipu bhaiya, Amitava bhaiya, Subhendu bhaiya, Bilal bhaiya, Suresh bhaiya. I am fortunate enough that I could share the lab space with these wonderful seniors and able to enrich my knowledge through discussions with them. In the form of batch mates, I found Hiru and Tamanna who also deserve full credit for maintaining a friendly environment in the lab. I am also thankful to postdoctoral lab seniors Dr. Binoyargha Dam, Dr. Kamal Krishna Rajbongshi, Dr. Pakiza Begum, Dr. Bhaskar Deka, Dr. Gongutri Borah for their help, and support. Specially Binoy bhaiya and Kamal Sir are always there to provide valuable suggestions in every tough time.

I want to heartily appreciate all my talented and hard-working juniors Pritishree, Raju, Dinabandhu, Shalini, Deepjyoti, Supriyo, and Manjunath for their extreme enthusiasm for research and for creating a friendly environment in the lab. I shall forever cherish all the lab trips, outings, and parties, those were some of the most memorable days of my life. I also had the opportunity to work with some dedicated summer and M.Sc. trainees like Priyabrta, Prashant, Pankaj, Akshar, Abhishek, Angshuman, Sourasish, Uday, Pratip, Kaustav, Debasis, Debolina, Gaurav, Amisha and Shalini.

I would like to express millions of gratitude to my closest friend Biman for his help and support, and for staying by my side since we first met in the campus. From discussing lab worries to watching movies in the hostel or movie theatre, making fun of each other it was always great to have you throughout the journey. Thank you for

your strong belive in me and keeping me motivated towards achieving more goals. I would also like to thank my friends Surjya, Hirak, Sukesh, Rabu, Pallav, and Raktim for all their help and joyful moments here at IITG.

I would also like to thank some of my Ph.D. fellowmates, seniors, and juniors here at IITG; Subhamoy da, Bipin bhaiya, Sudip da, Pallab bhaiya, Sandip da, Partha da, Samir bhaiya, Arup bhaiya, Altaf bhaiya, Monuranjan da, Bikoshita baa, Priyanka baa, Himangshu da, Bittu baa, Rahul da, Kishan da, Debjyoti bhaiya, Rahul da, Abhy, Jagnyesh, Rajdikshit, Kirti, Himani, Niharika, Upasana, Monalisha, Santanu, Subhankar, Rupkumar, Dipankar, Archana, Suravi, Satyajit, Subham, Deepak, Hrisikesh for making the journey a lot better, easier, and entertaining.

I would like to express my heartiest gratitude to Biren Khura and Anjan Khura along with his family for making life more comfortable inside the campus.

Back in home, I have a few good friends who always trust and push me to do something bigger than my capacity. Ranjan, Hemen, and Manash-they deserve full credit for their efforts to make my journey a whole lot easier. They are like the three wheels of the car I drive during the journey to reach my goals. I am highly thankful to the people of my locality for their motivation, encouragement, and honest blessing on me throughout the journey.

No words would suffice to express my feelings towards my teachers to whom I owe my obligations for their great teachings and philosophy to be a good human. Dimbeswar Das, Dr. Rupam Sarma, Dr. Purabi Sharma, and all the teachers from Dr. B. R. Ambedkar M.E. School have been always supportive throughout this journey. Further, I owe a lot to the entire fraternity from my school, Nalbari College (Gauhati University), and University of Delhi.

Lastly, and most importantly, my Ph.D. endeavour could not have been completed without the endless love, unending support, tolerance, freedom, and blessings from my family. I would like to express my deepest gratitude to my Maa, Deuta, and Baideu, whose unconditional love in every stage of my life motivated me to overcome all the challenges, and I owe my entire life to them. Dedicating this thesis to them is a minor recognition of their love, support, and encouragement. I am forever indebted to the sufferings they faced, and the patience and calmness they showed to make their son get the highest academic degree. I wish Deuta were here to see his son

finishing the line and holding this prestigious degree, but I know he is always watching and blessing me from the Above. Special mention to my Baideu, Kangkan vindeu and their family for being caring and supportive over the years. Two extended members of my family Mahi and brother Kulojit deserve credit for the love and care they showed towards me in this journey. Equal credit to my mama Pramod Baishya for his guidance and concerns to get the work done as soon as possible.

I would also like to thank the new family of Bagadhar Brahma Kishan College (BBKC) for the support and encouragement to smoothly complete this journey. I am thankful to Principal Sir Dr. Keshab Basumatary, and Chemistry Department HOD Dr. Hiya Talukdar for approving my leave to finish the pending formalities in the later part of this journey.

Lastly, I am thankful to Almighty for continuous blessing throughout my life, especially during my research career, and for providing me the willpower and strength to accomplish this remarkable journey.

Bubul Das

SYNOPSIS

The contents of the thesis have been divided into four chapters with initial one as introductory and the rest of the chapters are based on experimental results obtained during the research period. The introductory chapter of the thesis is a summary of alkyl isocyanoacetate's reactivity and its usefulness in diverse (3 + n) annulation/cycloaddition reactions. Along with this, a brief description of the directing group (DG) strategy for the functionalization of C–H bond has also been added. A brief account of the formation of important heterocyclic scaffolds following annulation/cycloaddition and DG-assisted C–H activation has been included.

Chapter II demonstrates a step-economical *in situ* cycloaddition lactonization strategy for the synthesis of chromenopyrrole. The developed protocol exploits all the reactive centres of alkyl isocyanoacetate while reacting with 2-hydroxy chalcone.

Chapter III demonstrates a tandem cycloaddition and C–O coupling strategy for the efficient construction of chromenopyrrole. This step economical Ag salt-catalyzed reaction proceeded in mild reaction conditions with excellent functional group tolerance.

Chapter IV illustrates the utilization of phenyl isocyanate as a transient directing group for *o*-olefination. Synthesized *o*-alkenylated anilines have been further transformed into substituted aza-coumarins.

Each of these chapters comprises seven subsections which include an introduction, previous work, present work, experimental section, references, spectral data, and a few representative spectra.

CHAPTER I. A Brief Outline of Annulation/Cycloaddition Using Alkyl Isocyanoacetate and General Description of Directing Group Strategy

The introductory chapter presents a brief description of annulation/cycloaddition and directing group strategy. Initially, the chemistry of ethyl isocyanoacetate and its utilization in (3 + n) annulation reactions has been described. The latter half elaborates on the directing group strategy for the efficient construction of heterocycles *via* C–H activation.

Carbocycles with at least one heteroatom are known as heterocycles. *N*, *O*, and *S* are some of the most common heteroatoms used to design these rings. Moreover, boron, phosphorous, iron, magnesium, and selenium are a few other additional heteroatoms frequently used in the construction of heterocycles. Heterocycles are widespread in natural products and many medicinally active compounds. Most of the FDA-approved drugs contain at least one heterocyclic ring. The presence of such a ring increases the bioactive nature of the compounds. Hemoglobin, chlorophyll, vitamins, enzymes, DNA, and RNA are prime examples of bioactive compounds having at least one heterocycle. Many heterocycles are also the building blocks of protein and other important biomolecules that constitute our body. Apart from their usefulness in drug design, heterocycles are gaining attention in agriculture, veterinary items, cosmetics design, etc. The high chemical adaptability of heterocycles makes them suitable to respond to diverse demands of biological activity. A wide section of pharmaceutical modifications has been covered by heterocycles on the basis of their significant medicinal value. A range of heterocyclic moieties with a condensed ring system are found to have a variety of physiological activities. Owing to such biological relevance, over the years, scientists have kept themselves engaged in the design and construction of heterocyclic scaffolds.

A widely popular tool for the construction of carbocyclic and heterocyclic scaffolds is annulation. This interesting cyclization concept allows the formation of two bonds and one ring in a single step. In the modern era of drug design and discovery, annulation proves to be an efficient step economical pathway for the construction of prominent structural motifs. Alkyl isocyanoacetate or α-isocyano ester has been serving as an annulating partner in diverse annulation for the synthesis of functionalized pyrrole. Isocyanoacetates and their derivatives are versatile and powerful building blocks in organic synthesis. They have found applications in diverse fields of organic, inorganic, medicinal, and coorditional chemistry. The versatility that lies in this molecule is due to the presence of three reactive centres *viz*., an isocyano unit,

the acidic CH, and an electrophilic ester functionality (Scheme I.1.a). The combination of these three potential reactive centers in the molecule results in exceptional reactivity and broad synthetic potential. Additionally, the chiral version of this reagent can also be obtained from protected natural amino acids. In an ideal world, isocyanoacetates feature in many (3 + n) cycloaddition reactions through the nucleophilicity of the active methylene and electrophilicity of the isocyanide for the construction of the heterocycles (Scheme I.1.b).

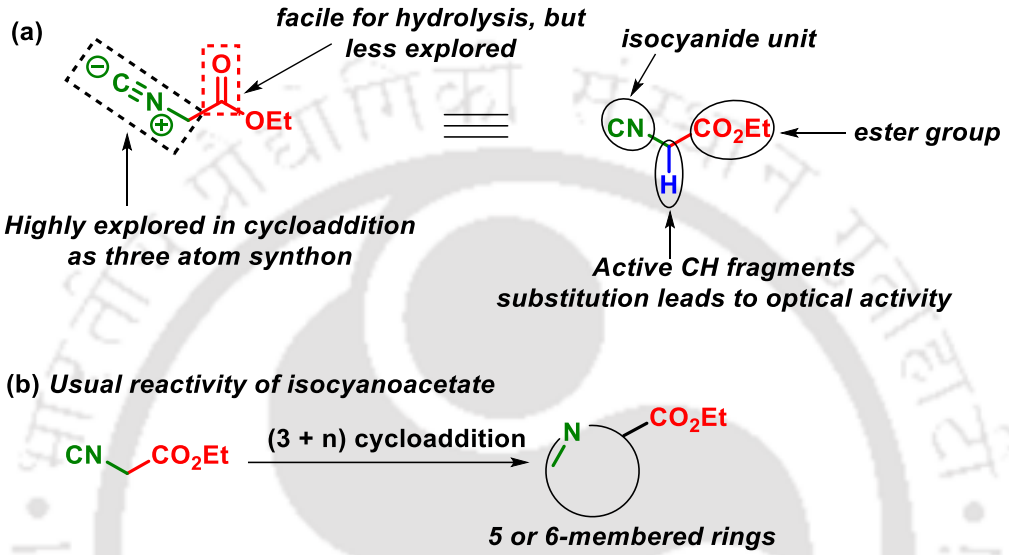

Scheme I.1. *Reactive centers of ethyl isocyanoacetate.*

Nenajdenko *et al.* described an efficient strategy for the synthesis of fluorinated pyrrole utilizing the reactivity of ethyl isocyanoacetate. The protocol proceeded following Barton-Zard pathway where *β*-nitrostyrene was functionalized to 4-fluoropyrrole *via* annulation with ethyl isocyanoacetate (Scheme I.2).

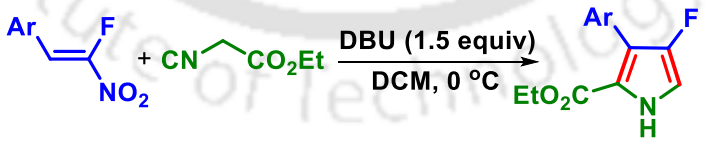

Scheme I.2. *Barton-Zard reaction of β-nitrostyrene with isocyanoacetate.*

Yang *et al*. disclosed a convenient silver-catalyzed cascade cyclization approach for the synthesis of chromenopyrrolones. A nucleophilic conjugate addition of the ethyl isocyanoacetate anion on the double bond of 3-iodochromanone and subsequent ring opening of chromanone leads to the formation of pyrrole. The tethered pyrrole ring eventually leads to chromenopyrrole *via* C–O bond formation (Scheme I.3).

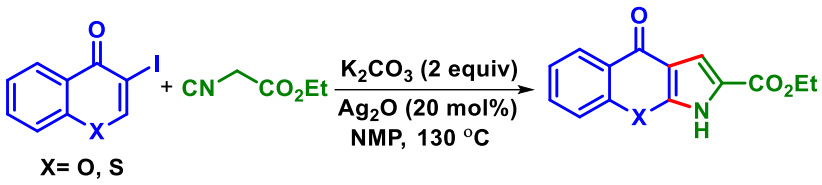

Scheme I.3. *Ag-catalyzed cascade reaction of ethyl isocyanoacetate.*

The exploitation of the nucleophilicity of the α-carbon atom and the electrophilicity of the divalent carbon atom of the isocyanide for the effective construction of C–C and C–N bonds characterizes the reactivity of α-isocyano ester. However, in most of these cycloaddition reactions, the ester group acts only as an activator and remains an unreactive spectator without undergoing any participation in the bond-forming process. To explore the reactivity of this inert ester group, Zhu group in 2007 synthesized strategically designed isocyanoacetate where α-position is substituted by electron-rich nitrobenzene. This makes α-hydrogen more acidic and subsequent anion is highly stabilized due to the strong electron-withdrawing nitro group in the ring. Consequently, the anion becomes less acidic and rather more nucleophilic divalent carbon of isocyanide initiated the reaction with a polar double bond such as imine. Such type of reactivity tuning gives different heterocycles by trapping nitrilium intermediates through the *O*-nucleophile of ester (Scheme I.4).

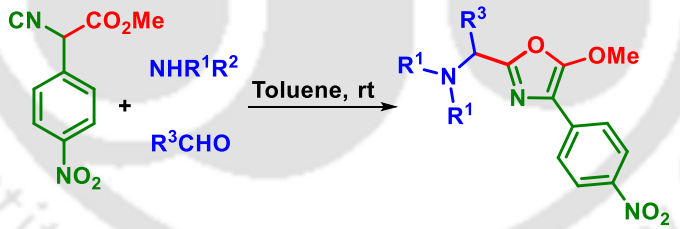

Scheme I.4. *Rare reactivity of isocyanoacetate: ester group as O-nucleophile.*

Apart from annulation, C–H activation is another emerging methodology for the smooth construction of heterocycles through C–H bond functionalization. The C–H bonds are ubiquitously available in organic compounds. There are three types of C–H bonds in organic molecules: alkynes C(sp)–H, alkene C(sp^2)–H, and alkane C(sp^3)–H bonds. The three types of C–H bonds have different acidity and *p*Ka values. These C–H bonds offer very limited reactivity and are thus difficult to functionalize. The acidity or reactivity of these C–H bonds is highly dependent on the surrounding environment of the molecule. The less acidic alkane

C(sp^3)–H and alkene C(sp^2)–H bonds are difficult to functionalize as compared to alkyne C(sp)–H bonds. However, various techniques have been developed for the activation or functionalization of these inert C–H bonds. The two best methodologies for the transformation of these ubiquitous C–H bonds into C–C or C–heteroatoms are C–H activation and cross-dehydrogenative coupling (CDC). These two methodologies have been gaining attention for the synthesis of complex molecular scaffolds, natural products, pharmaceuticals and are being used for the late-stage functionalization of diverse bioactive molecules.

The diverse coupling reactions such as Negishi, Stille, Suzuki–Miyaura, etc. present multiple ways for constructing C–C bonds through the coupling of organic halides with an organometallic intermediate or with a functional alkene as in the Heck reaction. However, with the assistance of transition metal (TM) catalysts a direct C–H bond activation becomes possible without any pre-activation of the substrate. Such regioselective functionalization of inert C–H bonds can be achieved with the help of directing groups (DG) and transition metal catalysts like Pd, Rh, Ru, etc. The catalysts interact with the directing group through some heteroatoms and assist the C–H bond-breaking process. This type of C–H bond can be considered as a semi-activated C–H bond *i.e.*, although they are not inherently activated the reactivity can be enhanced with aid from the neighbouring directing group. The directing groups are well-known for their role in activating the selective C–H bonds from a bucket of C–H bonds. Through the coordination with the metal *via* heteroatom of the directing group, it forms a metallacycle in proximity to the targeted C–H bond. Various functional groups, such as amide, carboxylic acid, amine, anilide, imine, ketone, hydroxyl, *etc*. have been employed as directing groups for C–H functionalization. The traditional directing groups preferentially activate the proximal or *ortho*-C–H bonds without any change in the chemistry of the directing groups. However, a directing group can transform into another functionality within the reaction condition or after completion of the desired transformations (Scheme I.5). Further, progress has been achieved in the direction of distal C–H bond activation. However, distal C–H functionalization requires more strenuous conditions and advanced techniques. In the distal C–H bond activation, the directing group coordinates to the furthest located C–H bond and functionalizes it.

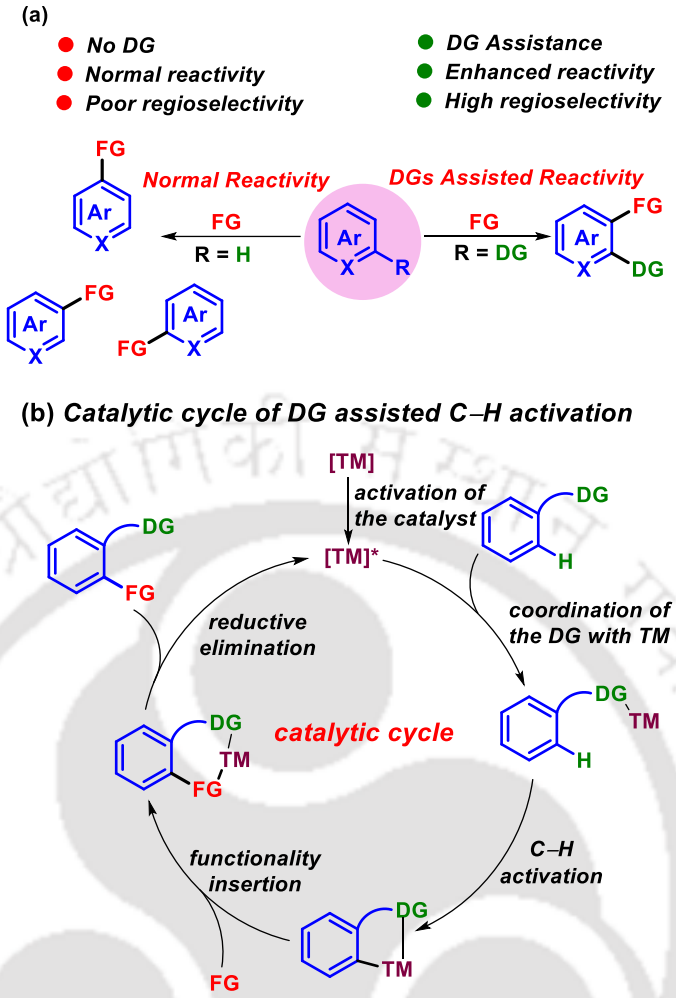

Scheme I.5. *Directing group (DG)-assisted C–H activation.*

CHAPTER II. Synthesis of Chromeno-pyrroles (Azacoumestans) from Functionalized Enones and Alkyl Isocyanoacetates

This chapter demonstrates an elegant synthetic strategy for chromeno-pyrroles (azacoumestans) *via* cycloaddition of 2-hydroxychalcone/cyclic enones and alkyl isocyanoacetate, followed by lactonization. Herein, ethyl isocyanoacetate acts as a C–NH–C–C=O synthon contrary to its hitherto applications as a C–NH–C synthon. Subsequently, pentacyclic fused pyrroles were also constructed from the *o*-iodo benzoyl chromeno-pyrroles using Pd(II) catalyst.

Azacoumestans, specifically chromenopyrroles, are found in marine natural products and synthetic compounds. Among them, lamellarins and ningalin B, are a class of marine

alkaloids, having a pyrrole polyaromatic core differing in the substitution pattern and the arrangement of rings (Figure II.1). A few of them have shown various biological activities, including multidrug-resistant cancer cell lines and anti-HIV-1 activity at non-cytotoxic concentrations and have served as organic redox switches. Pharmacologists are engaged in the chemical modifications of these natural products to get synthetic analogues which may result in new innovative drugs conferred with potential antitumor, and anti-angiogenesis activities.

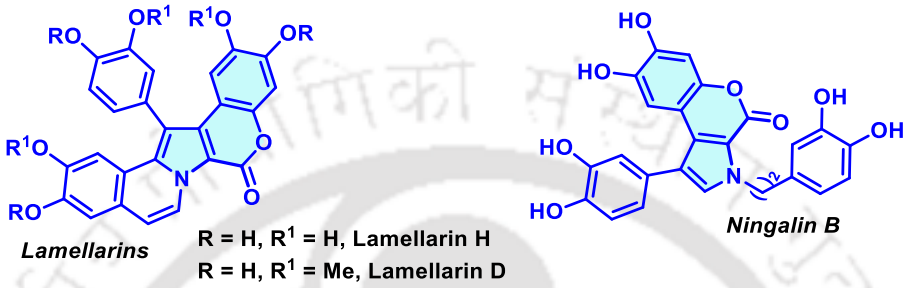

Figure II.1. *Bioactive pyrrolo-coumarins.*

Due to their potential biological activities and functional properties, synthetic routes involving multi-step condensation, cyclization, and subsequent lactonization have been developed. Some of the protocols adopt transition metal-catalyzed dehydrogenative coupling or cyclization of pre-functionalized coumarins. A one-pot multi-component strategy uses 4-chloro-3-nitrocoumarin (Scheme II.1.a), while others adopted a metal-catalyzed cyclization of functionalized coumarins with alkynes (Scheme II.1.b). While numerous methods to construct pyrrolo-fused coumarins have been developed, but direct access to this heterocyclic skeleton in a single step remains elusive.

Alkyl isocyanoacetates are efficient 1,3-dipolar coupling partners towards a range of annulation/cycloaddition reactions. In the presence of a base and Ag salt, they undergo cycloaddition (non-concerted) with dipolarophiles providing diverse heterocycles (Scheme II.1.c). The Barton-Zard reaction is one such strategy for synthesizing substituted pyrrole from alkyl isocyanoester and conjugated nitroalkene (Scheme II.1.d). The requirement of nitro group is essential in the starting alkenes, which is eventually eliminated. Herein, we report a methodology, where the ethyl isocyanoacetate undergoes (3 + 2) cycloaddition with the alkene part of the 2-hydroxychalcone, followed by an intramolecular lactonization to furnish pyrrolocoumarin in a single step (Scheme II.1.e).

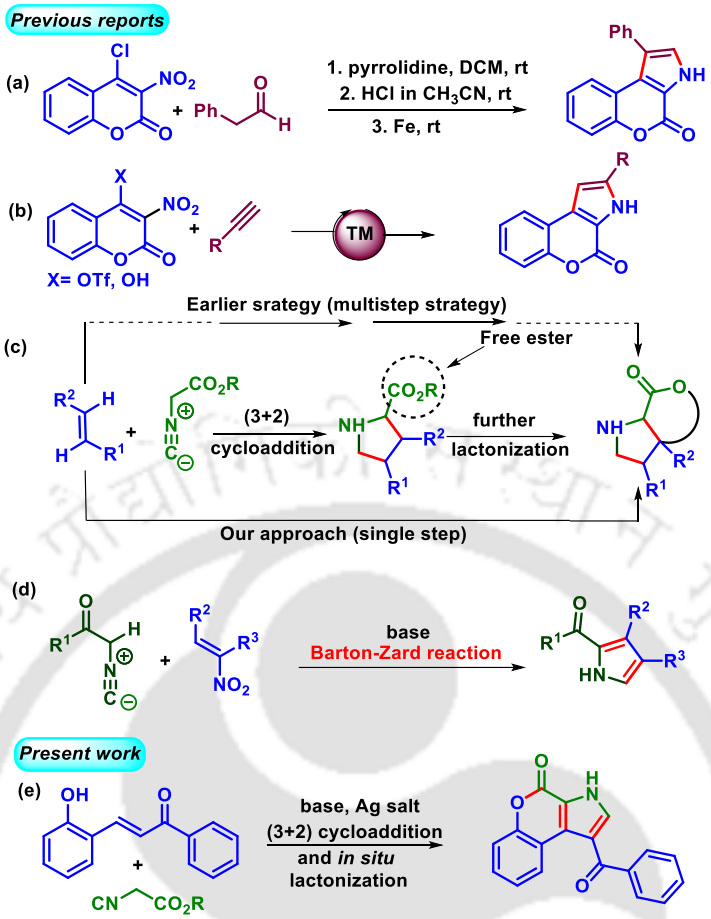

Scheme II.1. *Different approaches for the synthesis of pyrrolo-coumarin.*

Initially, we commenced our exploration by taking 2-hydroxychalcone (**1**) and ethyl isocyanoacetate (**a**) in the presence of Cs_2CO_3 (2 equiv), Ag_2CO_3 (3 equiv) in 1,4-dioxane (3 mL). To our delight, the reaction was completed within 12 h with the formation of chromeno-pyrrole moiety (**1a**) in 71% yield. The product (**1a**) formation without the ethoxy group suggests a (3 + 2) cycloaddition followed by lactonization. The use of methyl isocyanoacetate (**b**) in lieu of ethyl isocyanoacetate (**a**) under an identical condition yielded the same product (**1a**), thereby supporting the lactonization path. The XRD analysis of the product unambiguously confirmed the structure to be 1-benzoylchromeno[3,4-*b*]pyrrol-4(3*H*)-one (**1a**) (CCDC 2245374). Here, ethyl isocyanoacetate serves as a four-atom (C–NH–C–C=O) synthon, unlike its well-established three-atom (C–NH–C–) synthon. An extensive optimization study revealed the optimization condition to be the use of 2-hydroxychalcone (**1**) (1 equiv), ethyl isocyanoacetate (**a**) (1.2 equiv), Ag_2CO_3 (3 equiv), Cs_2CO_3 (2 equiv) in 1,4 dioxane (3 mL) at 80 °C.

After having a set optimized condition, the generality of this cycloaddition-lactonization strategy was tested with diverse 2-hydroxychalcones prepared from substituted acetophenone and salicylaldehyde. The reactions proceeded well with all kinds of 2-hydroxychalcones having no significant effect from the electronic environment. The methodology shows scalability when performed in a gram scale with a 57% yield of the desired chromenopyrrole. A base free-reaction gives unlactonized intermediate **D** which indicates rapid (3 + 2) cycloaddition as the initial step and subsequent lactonization in the presence of a base. A similar kind of cycloaddition was tested with lactonized enones such as coumarin and alkyl isocyanoacetate. The methodology yielded pyrrolocoumarin with concomitant cycloaddition and elimination of ester or ketone counterpart from enone *via* a path similar to the Barton-Zard reaction.

Based on literature precedents, a plausible reaction mechanism is proposed as shown in Scheme II.2. Initially, treatment of AgOAc with ethyl isocyanoacetate (**a**) generates an active 1,3-dipolar intermediate (**a'**) *via* elimination of AcOH. Next, the active 1,3-dipolar intermediate (**a'**) undergoes a (3 + 2) cycloaddition at the C=C bond of chalcone (**1**) to give a cycloadduct intermediate (**B**). The intermediate **B** provides the pyrrole moiety (**D**) through tautomerization followed by aromatization. The intermediate **D** undergoes intramolecular lactonization in the presence of Cs_2CO_3 to provide the resultant pyrrolocoumarin (**1a**) (Scheme II.2.a). A similar mechanism is proposed for the Barton-Zard equivalent reaction of coumarin-3-carboxylate/acetyl and ethyl isocyanoacetate (**a**). A rapid (3 + 2) cycloaddition between both the coupling partners followed by tautomerization and double bond rearrangement/oxidation leads to the chromenopyrrole (**1a'**).

(a) Cascade (3 + 2) cycloaddition-lactonization

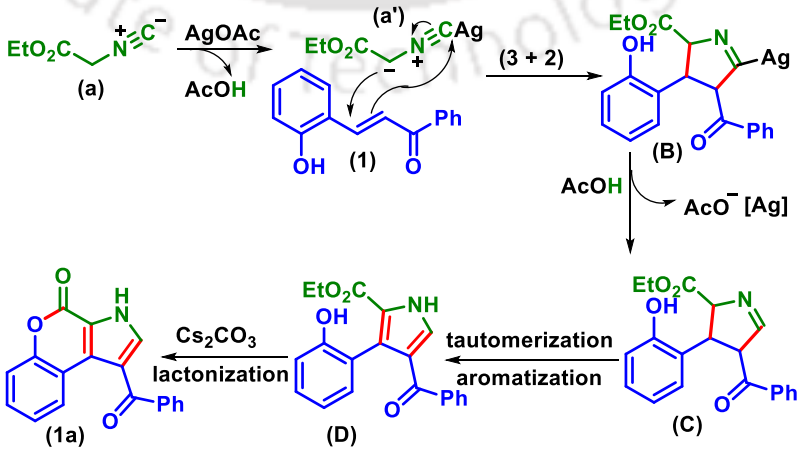

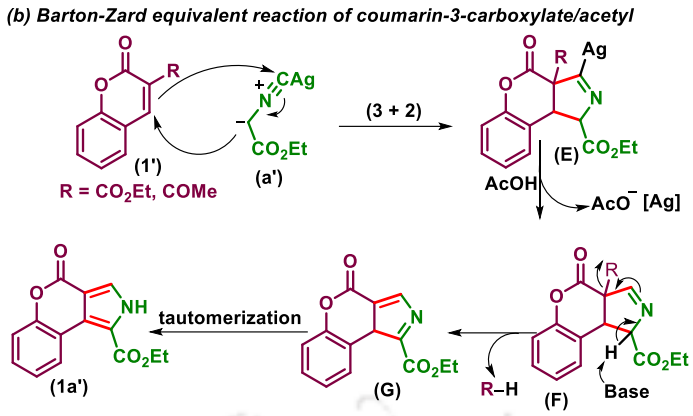

Scheme II.2. *A plausible mechanism for (3 + 2) cycloaddition-lactonization.*

In summary, we have developed an efficient cycloaddition and *in situ* lactonization strategy for the synthesis of diverse chromenopyrrole in a step-economical way. This tandem cycloaddition-lactonization strategy is the best example of employing ethyl isocyanoacetate as a new type of four-atom synthon (C–NH–C–C=O) contrary to its application as a three-atom synthon (C–NH–C). This methodology can be further extended to the synthesis of chromeno-pyrrole-carboxylate from the cyclic enones *via* an equivalent Barton-Zard reaction. A few post-synthetic modifications have also been carried out for the synthesis of pentacyclic fused pyrrolo-coumarin.

CHAPTER III: Access to Chromenopyrrole *via* Tandem (3 + 2) Cycloaddition and Intramolecular C–O Coupling

This chapter illustrates a mild and concise method for the synthesis of chromenopyrrole from 2′-hydroxychalcone and alkyl isocyanoacetate. The reaction proceeds *via* an initial [3 + 2] cycloaddition on the C=C bond of 2′-hydroxychalcone and 1,3-dipole, generated *in situ* by the reaction of ethyl isocyanoacetate and AgOAc. This is then followed by an intramolecular C–O bond formation with the –OH group and C5-H of the *in situ* generated pyrrole leading to chromenopyrroles.

Pyrrole is a well-known structural motif, often found in natural products and pharmacologically active molecules. Chromene, too, is a privileged core that occurs in many natural and synthetic biological molecules. Individually, these rings bring different kinds of bioactivity. However, the fused form of these two rings, pyrrolocoumarin/chromenopyrrole interests chemists and pharmacists as an exciting and versatile building block because of their excellent biological profile. For example, pyralomicins, a group of antibiotics isolated from the

soil bacterium *Nonomuraea spiralis* IMC A-0156, contain a chromenopyrrole core. This core is linked to a C7-cyclitol (pyralomicins I–IV) or glycosylated by glucose (pyralomicins V–VII) (Figure III.1). The pyralomicins are active against Gram-positive bacteria and their antibacterial activity depends on the position and number of chlorine atoms attached within the molecule and nature and methylation of glycone. The aglycon region of the molecule resembles pyoluteorin, the marinopyrroles, TAN-876A, and TAN-876B. Considering the wide utility of chromenopyrroles, it is essential to plan newer sustainable methodologies for their synthesis.

Pyrrole synthesis has achieved a greater height with classical methods such as Paal–Knorr pyrrole synthesis and Hantzsch pyrrole synthesis along with other transition metal-catalyzed reactions. However, at present, the synthesis of chromenopyrrole has limited reports. Most of them require synthesis of both pyrrole and chromenone *via* different approaches and then their fusion at some stage through transition metal-catalyzed reactions. Thus, the development of new synthetic strategies from readily accessible raw materials in step economical way under mild reaction conditions finds attention.

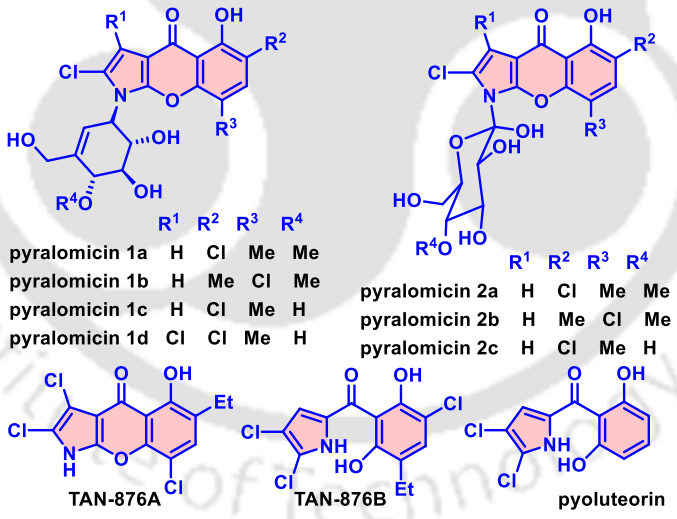

Figure III.1. *Bioactive pyrrole and chromenopyrrole core.*

Most of the existing methods for the synthesis of chromenopyrrole involve the construction of pyrrole moiety from a functionalized chromenone *via* transition metal-catalyzed coupling reactions. Such coupling often demands the presence of halide groups in the starting precursors for the efficient construction of pyrrolocoumarin. Recently, Yan *et al.* demonstrated a Cu-catalyzed decarboxylative annulation of *N*-substituted glycines with 3-

formylchromones. Requirement of pre-synthesized 3-formylchromones demands an additional step for its synthesis (Scheme III.1.a). Earlier, Hu *et al*. demonstrated a Cu-catalyzed synthesis of imidazochromones by reacting 3-iodochromone and acetamidine hydrochloride in the presence of a base. 3-Iodochromone when treated with acetamidine hydrochloride in the presence of a catalytic amount of copper and base resulted in the formation of imidazochromone through a tandem C–H activation/C–O formation process (Scheme III.1.b). Recently, our group reported a one-pot tandem (3 + 2) cycloaddition-lactonization strategy utilizing 2-hydroxychalcone and ethyl isocyanoacetate for the synthesis of fused 2-chromenopyrroles. The rapid (3 + 2) cycloaddition and *in situ* lactonization of 2-hydroxy chalcone with ethyl isocyanoacetate afforded a library of aza-coumestans (Scheme III.1.c). The presence of hydroxy functional group at the strategic position helps in the step-economical construction of chromenopyrrole in a straightforward condition.

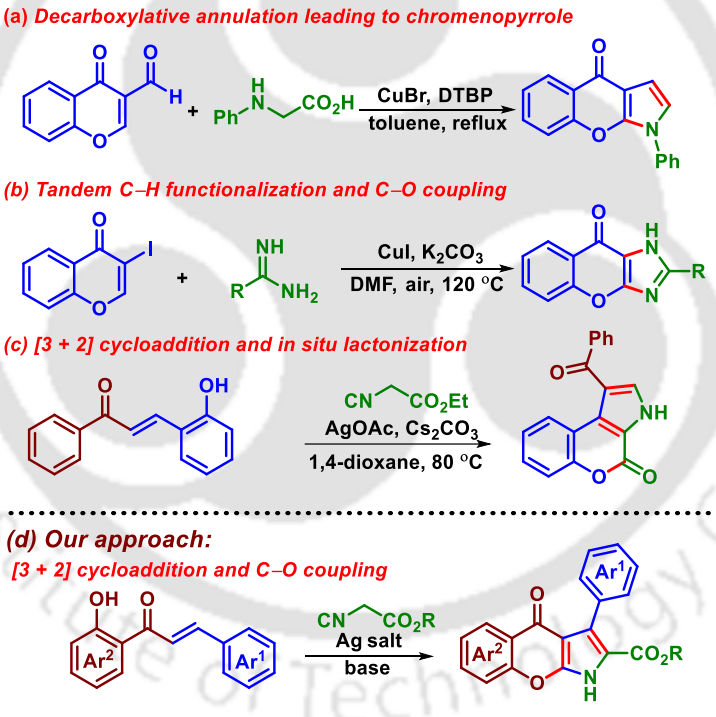

Scheme III.1. *Different approaches for the synthesis of pyrrolo-coumarin.*

Inspired by this approach, we envisioned applying this strategy to an appropriately designed substituted chalcone, where the hydroxy group is kept at a distal phenyl ring, thereby avoiding the chances of lactonization. Hence, 2′-hydroxychalcone (**1**) derived from 2′-hydroxyacetophenone and benzaldehyde was treated with ethyl isocyanoacetate (**a**) in the presence of AgOAc and K_2CO_3 in CH_3CN at 60 °C. Delightfully, after 12 h of reaction, two

new products were obtained which were isolated and characterized by spectroscopic techniques (^{1}H, ^{13}C{^{1}H}, and IR). The one having higher R_f was obtained in 37% yield and was found to be a formal (3 + 2) cycloadduct pyrrole. The other compound having lower R_f was isolated in 45% yield, was characterized to be ethyl 4-oxo-3-phenyl-1,4-dihydrochromeno[2,3-*b*]pyrrole-2-carboxylate (**1a**). Here, unlike the previous approach, the furthest located hydroxy group prefers C–O coupling with 2-*H* of the *in situ* generated pyrrole over lactonization. The exact structure of the molecule was confirmed through diverse spectroscopic techniques. Then, we screened various reaction parameters such as solvents, bases, and silver salts for optimum yield of the protocol. The use of 2′-hydroxychalcone (**1**) (1 equiv), ethyl isocyanoacetate (**a**) (1.2 equiv), AgOAc (3 equiv), K_2CO_3 (2 equiv) in ethanolic solvent (3 mL) at 80 ^{o}C was turning out to be the optimum condition for this tandem cycloaddition and C–O coupling protocol.

With the optimized condition in our hand, we examine the competence of this protocol with different 2′-hydroxychalcone. A library of chromenopyrroles were obtained with no significant impact from the substituted functionality in the chalcone. A few control experiments were performed to gain some insight into the mechanism. Guided by those observations and from the literature reports, a possible Ag-promoted mechanism for this transformation has been proposed as shown in Scheme III.2. Initially, ethyl isocyanoacetate (**a**) generates a 1,3-dipolar intermediate (**a'**) in the presence of AgOAc with the elimination of AcOH. Next, this 1,3-dipole (**a'**) undergoes a (3 + 2) cycloaddition at the C=C double bond of chalcone (**1**) which results in the generation of pyrrole intermediate **1a'**. Following this, a six-membered cyclic transition state (**A**) arises because of the interaction between AgOAc and C5–*H* of pyrrole ring of **1a'** which also involves the participation of deprotonated phenolic group. Elimination of AcOH followed by activation of the pyrrole ring *via* insertion of Ag at C5 resulted in the formation of another intermediate **B**. Finally, C–O coupling at the electrophilic C5 site with the release of Ag(0) gives the desired chromenopyrrole (**1a**) (Scheme III.2). The formation of Ag mirror at the surface of the reaction flask confirms the reduction of Ag(I) salt supporting the proposed mechanism.

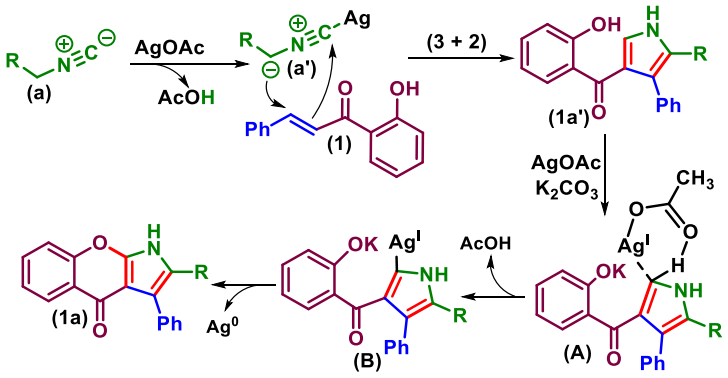

Scheme III.2. *Plausible mechanism.*

In summary, a synthetically new tandem cycloaddition cum C–O coupling strategy was developed for the synthesis of pyrrolocoumarin. This elegant approach leads to the construction of C=C and C–O bonds in a step-economical manner under operationally simple conditions. Mechanistic studies revealed that Ag salts are essential for the initial cycloaddition and subsequent C–O coupling.

CHAPTER IV: Transformable Transient Directing Group Assisted C(sp^2)–H Activation: Synthesis and Late-Stage Functionalizations of *o*-Alkenylanilines

This chapter describes the utilization of phenyl isocyanate as a transformable transient directing group in a Ru(II)-catalyzed *o*-olefination for the formation of alkenylanilines. Alcoholic solvents, particularly, ^{t}AmOH serve the dual role of solvent-cum transient directing mediator. The *o*-alkenylanilines are converted to azacoumarins and subsequently into C-4 aryl-substituted azacoumarins using aryl iodides as coupling partners *via* Pd(II) catalyzed C–H functionalizations.

The formation of C–C, and C–X bonds *via* C–H bond activation continues to be an important and stimulating thrust into academic and industrial research. In recent years, outstanding progress has been achieved in *o*-C−H alkenylation using activated alkenes. Alkenes are essential feedstock in industrial processes, and their utilization for the synthesis of a variety of important biological and materially relevant molecules has become immensely important in organic synthesis. However, the direct introduction of olefinic C(sp^2)–H bonds into aryl rings is challenging and thus becomes a potential area of research for organic chemists.

Directing groups (DGs)-assisted C–H activation has overcome many such limitations and has significantly improved the arsenal of synthetic chemistry for synthesizing exotic molecules.

DGs are usually *σ*-coordinating functional groups that in combination with a transition metal control the site selectivity and activate the relatively strong C–H bonds by coordinating through the heteroatoms of DGs to the reactive metal catalysts. Transition metals like Pd, Rh, Ru, Co, Mn, etc. are being used for the activation of inert C–H bonds found in different organic moieties. The field of directed C–H bond activations has grown tremendously and many chelating groups have been explored that can serve as auxiliaries. Though the directing group-assisted C–H olefinations are well-established but the detachment of these groups after completion of the desired C–H bond activation is a cumbersome process. Thus, the step economical issue is an added disadvantage of DGs-assisted C–H activation.

Compared to traditional DG-assisted C–H bond activation, transient DG (TDG) assisted C–H bond activation has become a new strategy for the challenges of prior installation and removal of auxiliaries. TDGs are modified *in situ* with an external transient directing mediator (TDM), used either in catalytic or stoichiometric amounts. TDMs are functional moieties inherent to the compounds that transform a weakly coordinating functional group into a better *σ*-donor motif by tethering to the TDGs. Moreover, this TDM must be cleaved *in situ* after the functionalization. For instance, derivatives of phenols, aldehydes, and ketones, *viz*. imines, oximes, hydrazones, etc. are some examples of transient DGs that have been utilized in the C–H bond functionalizations. However, new transient directing groups for the selective C–H functionalizations are still highly desirable as well as appreciable. *o*-Alkenylanilines are important building blocks in many organic transformations and are prevalent in many bioactive compounds. *o*-Alkenylanilines can be synthesized using DG-assisted *o*-C–H alkenylations. Activated olefins are widely introduced in the *ortho* position of anilines with the assistance of some directing groups like –NHCOMe, urea (Scheme IV.1.a). In 2017, Satoh, and Miura group reported a carbamate (Boc) directed olefination protocol using the Rh catalyst (Scheme IV.1.b). The weakly coordinating carbonyl oxygen of carbamate coordinates to the Rh metal in an environmentally benign alcoholic solvent (^{t}BuOH). However, an additional step is required for the cleavage of the Boc directing group. Recently, Li and co-workers developed a method that enables the Rh(III)-catalyzed C−H alkenylation of aryldiazenecarboxylates using acrylate esters as the alkenylating partner with concomitant hydrogenation of the N=N bond in the

resulting product (Scheme IV.1.c). Yi *et al*. in 2017, disclosed a regioselective monoalkenylation of arenes with polar acrylates using urea moiety as a transformable directing group (Scheme IV.1.d). Searching for new and innovative TDG, we came across a relatively unexplored phenyl isocyanate. To the best of our knowledge, in DG-assisted C–H activation reactions, alkyl and phenyl isocyanates have been widely employed only as a reacting partner due to their electrophilic nature. However, the use of phenyl isocyanate as a transient directing group in the proximal C–H bond activation is unexplored. Thus, herein we report an efficient synthesis of *o*-alkenylanilines *via* a regioselective *o*-C–H olefination using phenyl isocyanate as the transient directing group under Ru catalysis (Scheme IV.1.e).

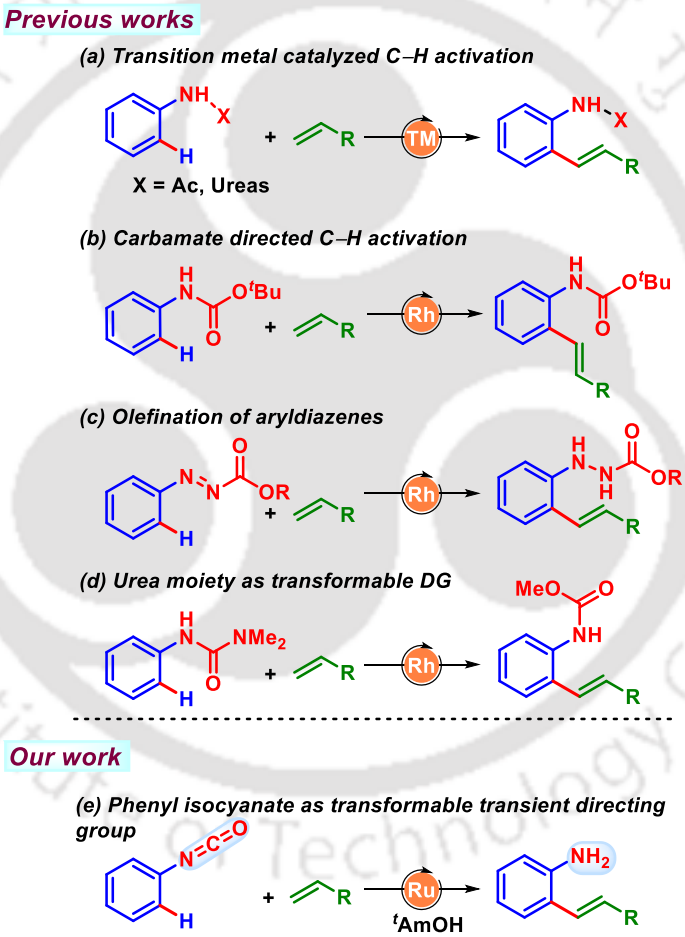

Scheme IV.1. *Metal-catalyzed DG-assisted C–H activation.*

We commenced our investigation using *p*-tolyl isocyanate (**2**) and methyl acrylate (**a**) as the coupling partner in the presence of $[Ru(p\text{-cymene})Cl_2]_2$ (5 mol %), $AgSbF_6$ (15 mol %), $Cu(OAc)_2{\cdot}H_2O$ (0.5 equiv), and *tert*-amyl alcohol (^{t}AmOH) (2 mL) in a sealed tube at 120 °C. To our delight, a yellow fluorescent spot was observed which was isolated and identified by

spectroscopic analysis (^{1}H NMR, ^{13}C{^{1}H} NMR, and IR) as an *ortho*-olefinated product of *p*-tolylaniline (**2a**). The new product was obtained in a satisfactory yield of 78%. XRD analysis of one of the substrates reconfirmed its structure to be *p*-tolyl (*E*)-3-(2-amino-5-methylphenyl)acrylate (**1l**).

An extensive screening of different solvents, bases, catalysts and oxidants sets the optimized condition to be use of phenyl isocyanate (**1**) (1 equiv), methyl acrylate (**a**) (2 equiv), [Ru(*p*-cymene)Cl_2]$_2$ (5 mol %), $AgSbF_6$ (15 mol %), $Cu(OAc)_2{\cdot}H_2O$ (0.5 equiv), and ^{t}AmOH (2 mL) in a 21 mL sealed tube at 120 ^{o}C for 24 h. After gaining the optimum yield from the protocol, a series of acrylates and phenyl isocyanates were treated in the standard conditions for efficient formation of diverse *o*-alkenyl aniline. A series of control experiments were performed including intermolecular competition experiment, kinetic isotope effect, etc. Based on the performed control experiments and literature precedent, a plausible mechanism for the *ortho* alkenylation (**1** with **a**) is illustrated in Scheme IV.2. Initially, the nucleophilic attack of the solvent ^{t}AmOH on the phenyl isocyanate forms a carbamate intermediate (**P**). The *in situ*-generated carbamate coordinates to the ruthenium centre *via* the carbonyl oxygen. This coordination triggers the activation of the proximal C(sp^2)–H bond forming a six-membered ruthenocycle intermediate (**A**). Intermediate **A** undergoes an olefin insertion to give intermediate **B** with subsequent elimination of acetic acid. Later, a *β*-hydride elimination gives the *ortho*-alkenylated carbamate (**C**). Finally, the acetic acid cleaves the *ortho*-alkenylated carbamate (**C**) to afford the final product (**1a**) with the release of 2-methylbut-2-ene (**E**) and carbon dioxide. The removal of carbamate depends on the stability of the carbocation formed after its cleavage to produce a substituted alkene. In the case of a primary alcohol such as methanol and ethanol, the reaction stops prior to the removal of carbamate, which is due to the lower stability of the primary carbocation (Scheme IV.2).

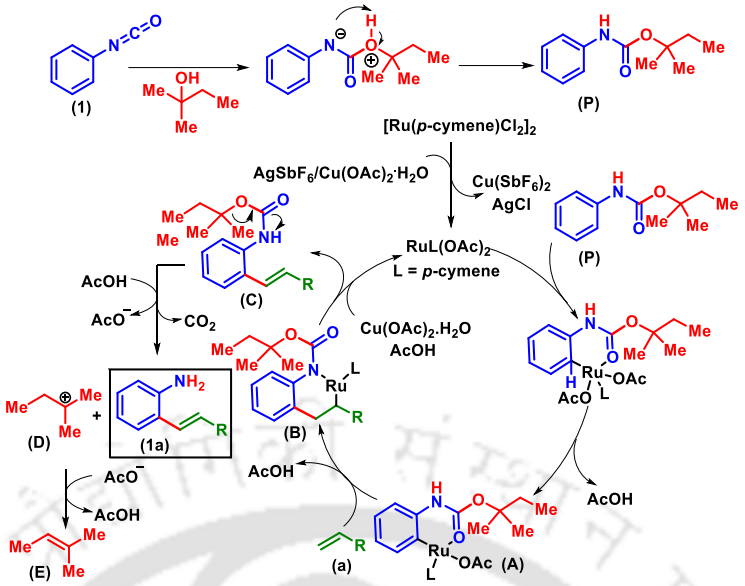

Scheme IV.2. *Proposed mechanism for o-olefination.*

In conclusion, we have developed a Ru-catalyzed *o*-olefination strategy taking phenyl isocyanate as the transformable transient directing group. Solvent *t*-amyl alcohol, not only acts as the solvent but is also used as a transient directing mediator (TDM) by forming carbamate. The *in situ* transformation of the transient directing group (NCO to NH_2) is a key feature of this methodology.

LIST OF ABBREVIATIONS

CCDC	*Cambridge Crystallographic Data Centre*
ORTEP	*oak ridge thermal ellipsoid plot*
NMR	*Nuclear Magnetic Resonance*
MHz	*Megahertz*
HRMS	*High-Resolution Mass Spectrometry*
ESI-MS	*Electrospray Ionization Mass Spectrometry*
IR	*Infrared*
TLC	*Thin layer chromatography*
XRD	*X-ray diffraction*
LED	*Light-emitting diode*
M.p.	*Melting point*
DMSO	*Dimethyl sulfoxide*
DMF	*Dimethylformamide*
DCM	*Dichloromethane*
DCE	*1,2-Dichloroethane*
THF	*Tetrahydrofuran*
^{t}*AmOH*	*tert-Amyl accohol*
TFE	*Trifluoroethanol*
NIS	*N-Iodosuccinimide*
NCS	*N-Chlorosuccinimide*
PIDA	*Phenyliodonium Diacetate*
FDA	*(US) Food and Drug Administration*
DNA	*Deoxyribonucleic Acid*
RNA	*Ribonucleic acid*
CDC	*Cross-Dehydrogenative Coupling*

TM	*Transition Metal*
DG	*Directing Group*
TDG	*Transient Directing Group*
TDM	*Transient Directing Mediator*
FG	*Functional Group*
TosMIC	*Tosylmethyl phenyl isocyanide*
KIE	*Kinetic Isotope Effect*
o-QM	*o-Quinone methides*
NBE	*Norbornene*
TMS	*Trimethylsilane*
MDR	*Multidrug-resistant*
UV	*Ultraviolet*
OBO	*oxabicyclo[2.2.2]octyl orthoester*

CONTENTS

CHAPTER I

An Overview of Annulation/Cycloaddition and Directing Group Strategies for Synthesis of Heterocycles

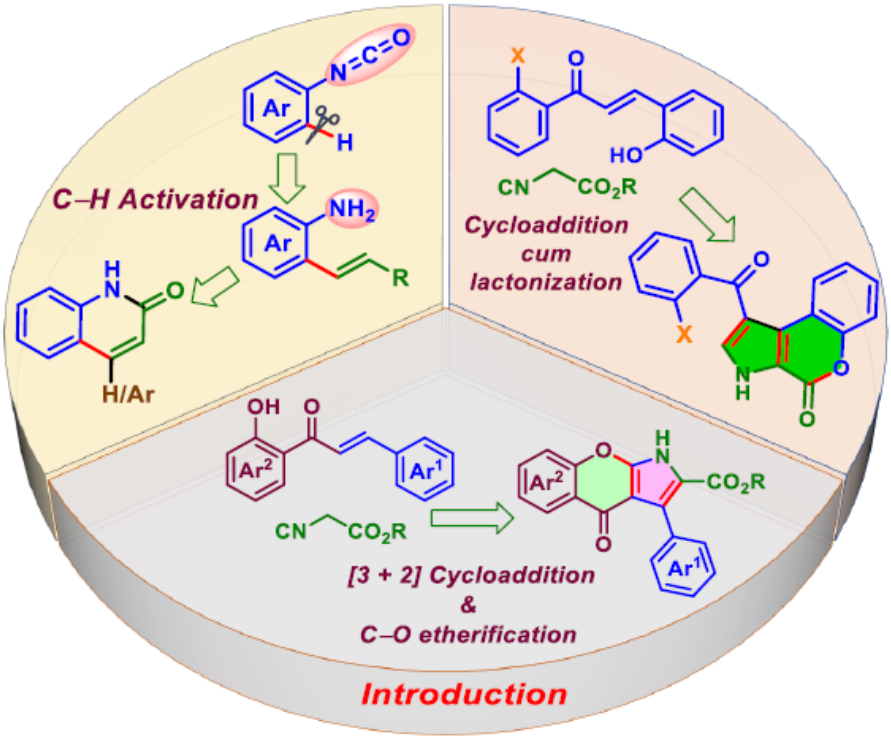

CHAPTER I

An Overview of Annulation/Cycloaddition and Directing Group Strategies for Synthesis of Heterocycles

I.1. Introduction

Carbocycles with at least one heteroatom are known as heterocycles. *N* and O are the most common heteroatoms found in these rings (Figure I.1.1). Moreover, sulfur, boron, phosphorous, iron, magnesium, selenium are other heteroatoms frequently used in the construction of heterocycles. Out of over 50 million registered organic compounds, it is estimated that more than half are heterocycles, and this number is still growing.[1a] Heterocycles are widespread in natural products and many medicinally active compounds (Figure I.1.2). Most of the FDA-approved drugs contain at least one heterocyclic ring.[1b,c] The nature of hetero atoms and strain in the ring influence the properties of such rings. The presence of such a ring increases the bioactive nature of the compounds. Haemoglobin, chlorophyll, vitamins, enzymes, DNA, RNA, etc. are a few examples of bioactive heterocycles. Many heterocycles are also the building blocks of protein and other important biomolecules that constitute our body. Thus, heterocyclic structures are all-pervading and are an integral part of almost every biologically and physiologically active organic molecule.[1d,e] Apart from their usefulness in drug design, heterocycles are drawing attention in agriculture, veterinary items, cosmetics design, etc. The high chemical adaptability of heterocycles makes them suitable to respond diverse demands in the biological field. A wide section of pharmaceutical modifications has been covered by heterocycles owing to their significant medicinal value. A range of heterocyclic moieties with a condensed ring system is found to have a variety of physiological activities. *N*-heterocycles *i.e.*, a carbocycle with at least one *N* atom, have found considerable attention for their remarkable biological properties and their role as pharmacophores. Pyrrole, one of the five-membered *N*-heterocycles constructs the core of the porphyrin rings which act as a key moiety in haemoglobin, chlorophyll, and vitamin B_{12}. Six-membered *N*-heterocyclic scaffolds are ubiquitous in anti-malarial drugs, dyes, and high-performing materials.[1f] Pyridine, quinolines are core heterocycles found in antimalarial drugs such as chloroquine, quinine,

mefloquine, etc.[1g] Pyrimidine, purines are another class of six-membered *N*-heterocycles having their presence in the nucleoside and nucleotides.[1d]

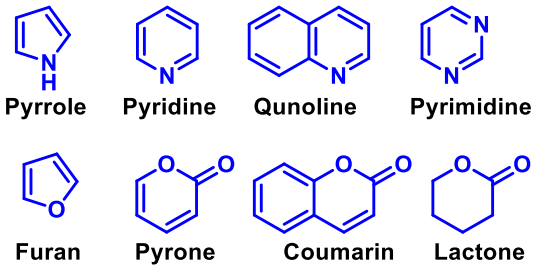

Figure I.1.1. *Common five or six-membered N, O-containing rings.*

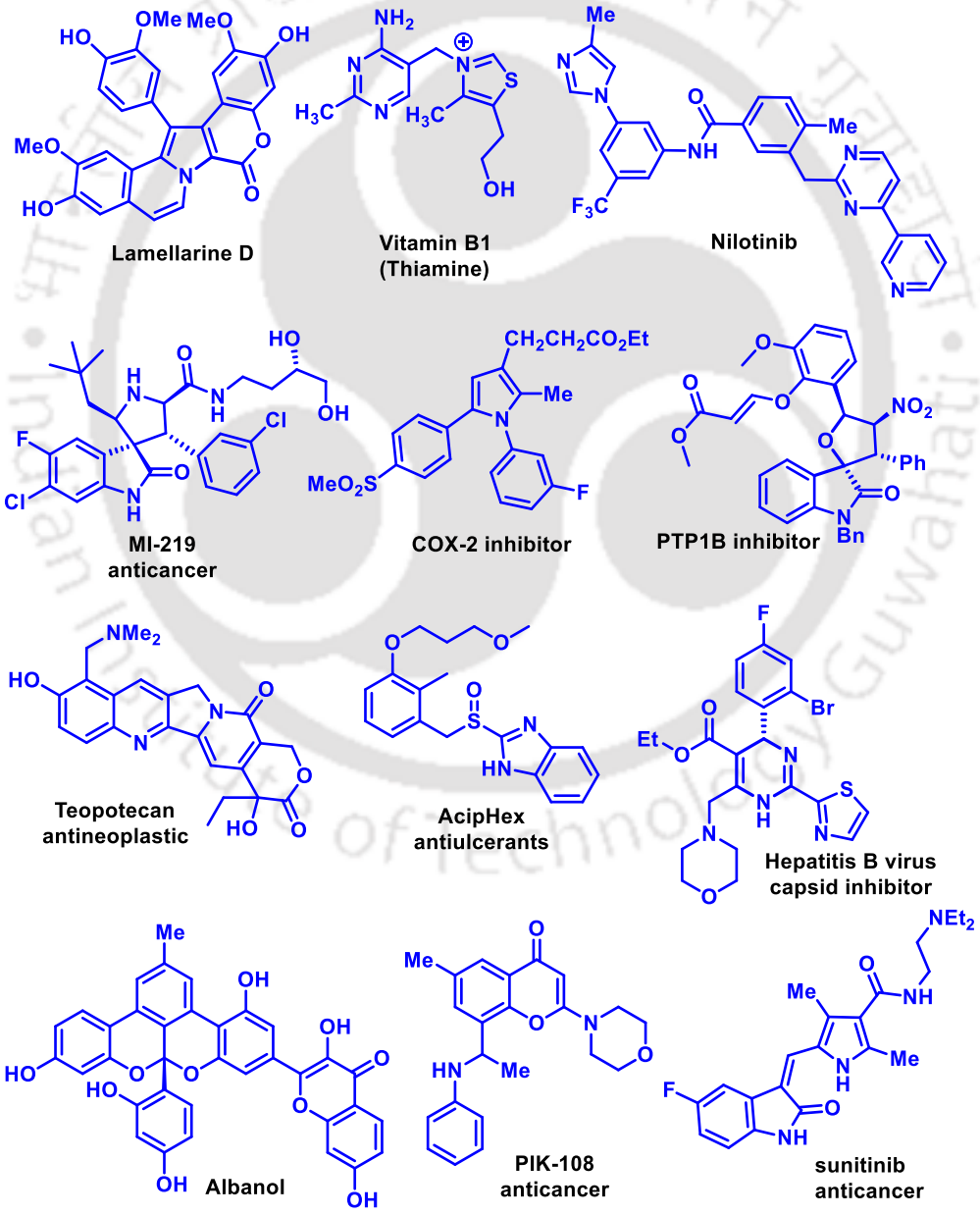

Figure I.1.2. *Bioactive N, O-containing heterocycles.*

Coumarins with *O* atoms in the ring are also known for their role in anti-HIV drug calanolide A, anticoagulant drug warfarin, etc.[1h,i] Pyrones are another class of six-membered *O*-containing heterocycles, found to exhibit a wide range of pharmacological properties such as antibiotic, antifungal, cytotoxic, neurotoxic activities.[1j] Other *O*-containing rings such as lactone are also found in many natural products or drugs including anticancer, neurotransmitters, antibiotics, etc (Figure I.1.2).[1k]

Due to their role in pharmaceuticals, agrochemicals, cosmetics, material chemistry, and synthesis of natural products, their synthesis has garnered considerable attention and this area is rapidly evolving. Over the last few decades, several pioneering strategies have emerged for the synthesis of *N*, *O*-containing heterocycles such as pyrrole, pyridine, pyrimidines, indole, imidazole, quinoline, azacoumarin, coumarin, flavone, etc. A popular tool for the construction of carbocyclic and heterocyclic moieties is annulation. This interesting cyclization concept allows the generation of a ring through two new bonds in a single step. In the modern era of drug design and discovery, annulation proves to be an efficient step-economical pathway for the construction of prominent structural motifs. Alkyl isocyanoacetate or α-isocyano ester has been serving as a coupling partner in diverse annulation and cycloaddition reactions leading to the synthesis of functionalized pyrrole.[2a,b] Isocyanoacetate and its derivatives are versatile and powerful building blocks in organic synthesis. They have found applications in the diverse fields of organic, inorganic, medicinal, and coorditional chemistry.[2c-e] The versatility this molecule possesses is due to the presence of three reactive centers *viz.*, an isocyano unit, the acidic C–H, and an electrophilic ester functionality (Scheme I.1.a). The combination of these three potential reactive centers brings exceptional reactivity and broad synthetic potential to the molecule. Additionally, the chiral version of this reagent can also be obtained from protected natural amino acids. In organic synthesis, the isocyanoacetates feature in many (3 + n) cycloaddition reactions through the nucleophilicity of the acidic C–H and electrophilicity of the isocyanide for the synthesis of the five or six-membered heterocycles (Scheme I.1.c).[2f-h]

Another α-methylene isocyanide is *p*-toluenesulfonylmethyl isocyanide (TosMIC), known for its odourless, solid-state stability and impressive structural features. Like alkyl isocyanoacetate, it also has three functionalities except arylsulfonyl functionality. Sulfonyl being α-to the active methylene and a good leaving group enhances the acidity of the α-carbon (pK$_a$=14). The reagent was first introduced into organic synthesis in 1972 by a Dutch

researchers van Leusen and so known as van-Leusen reagent. All these crucial factors in a single molecule collectively enrich its chemistry (Scheme 1.1.b).[1i]

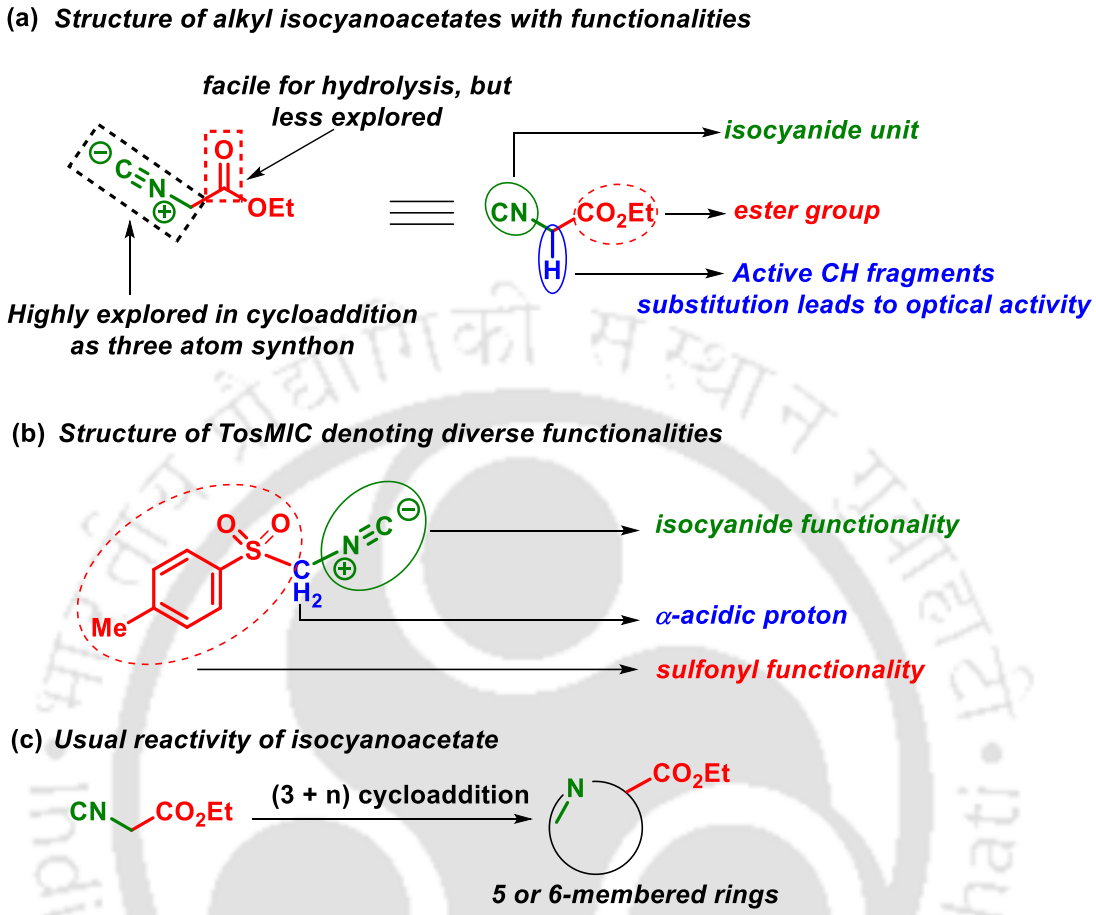

Scheme 1.1. *Reactive centers of isocyanoacetate.*

I.2. Strategies for Construction of Heterocycles *via* (3 + 2) Cycloaddition of Isocyanoacetates:

I.2.1. Synthesis of five-membered heterocycles from alkyl isocyanoacetate

The (3 + 2) cycloaddition between a 1,3-dipole and a dienophile is considered as one of the established and frequently used methodologies for the construction of heterocyclic scaffolds. The excellent regio-selectivity and the ease of handling of reagents make this strategy suitable for the construction of five-membered heterocycles. These (3 + 2) cycloaddition reactions deliver diverse *N*- or *O*-containing heterocycles *viz.*, pyrrole, oxazole, imidazole, pyrrolocoumarin, etc. Alkyl isocyanoacetate is an effective 1,3-dipole for (3 + 2) cycloaddition with the simultaneous presence of an activated methylene and isocyanide moiety. The classical heterocycle synthesis strategies such as Barton-Zard and van-Leusen pyrrole

syntheses follow such (3 + 2) cycloaddition of isocyanoacetates with an alkene.[1e,f,3a] The formal (3 + 2) cycloaddition of isocyanoacetate usually involves nucleophilic addition of the α-enolate to an electron-deficient dienophile which is associated with an intramolecular cycloaddition of the resulting anion to the empty orbital of the isocyanide. Additionally, alkyl isocyanoacetates have been extensively used in diverse asymmetric syntheses through a chiral Lewis acid-, organometallic-, or organo/metalo cooperatively catalyzed formal (3 + 2) cycloaddition with various electrophiles *viz*. carbonyls, imine or with a carbon-carbon multiple bonds.[3b-i]

In 2012, Nenajdenko *et al*. described a synthetic strategy for the construction of fluorinated pyrroles. The protocol proceeded following the Barton-Zard pathway where β-nitrostyrene was functionalized to a 4-fluoropyrrole *via* annulation with ethyl isocyanoacetate (Scheme I.2.1).[4a]

Scheme I.2.1. *Barton-Zard strategy of β-nitrostyrene and isocyanoacetate.*

Bi and Wang group developed a catalyst-selective synthesis of 1,3-and 1,5-disubstituted 1,2,4-triazoles *via* a (3 + 2) cycloaddition between aryl diazonium salt and isocyanoacetates under two different catalytic conditions. The two catalysts *viz.* Ag_2CO_3 and $Cu(OAc)_2$ used in this strategy follow two different mechanisms at the same reaction temperature (0 °C) to deliver both disubstituted triazoles regio-selectively (Scheme I.2.2).[4b]

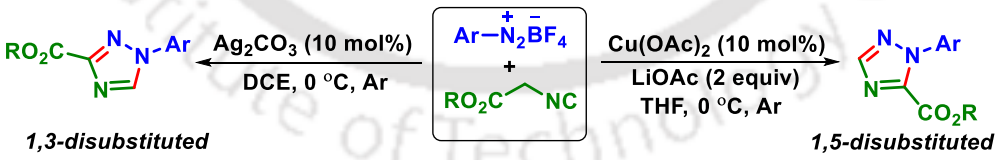

Scheme I.2.2. *Synthesis of 1,2,4-triazole via (3 + 2) cycloaddition of isocyanoacetate and diazonium salt.*

Liu *et al*. utilized the reactivity of the van-Leusen reagent (TosMIC) for a metal-free synthesis of imidazoles through (3 + 2) cyclization with ketenimines. The mild conditions of the reaction help to keep sulfonyl moiety intact in the final 1,4,5-trisubstituted imidazoles.

Thus, the reaction proceeded in high atom economy under this ^{t}BuONa catalytic condition compared to classical van-Leusen imidazole synthesis (Scheme I.2.3).[4c]

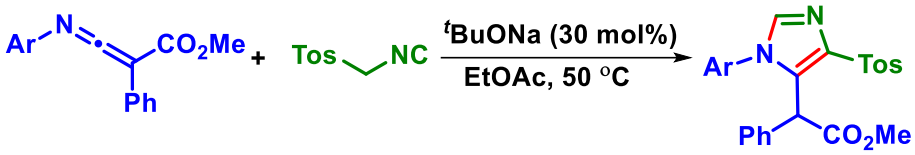

Scheme I.2.3. *Synthesis of imidazoles via cyclization of TosMIC.*

Isocyanoacetates have also been used in the asymmetric synthesis of heterocyclic building blocks. He and Shao group developed a chiral Ag-complex-catalyzed enantioselective formal (3 + 2) cycloaddition of aurone and α-benzyl isocyanoacetate to synthesize optically enriched spiro-1-pyrrolidines (Scheme I.2.4).[4d]

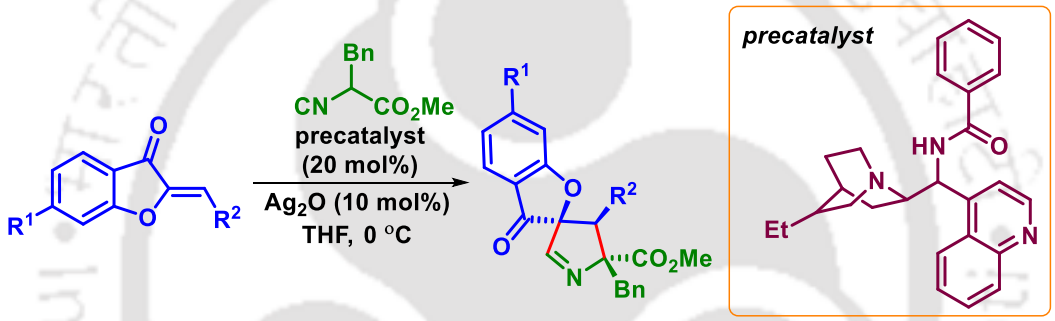

Scheme I.2.4. *(3 + 2) Cycloaddition of alkyl isocyanoacetates and aurones.*

Blay and Pedro group synthesized a quaternary carbon center containing chiral oxazolines *via* (3 + 2) cycloaddition of *tert*-butyl isocyanoacetate and unactivated ketone. This high diastereo-and enantoselective *cis*-oxazoline synthesis was carried out utilizing a dual catalytic system of bi-functional Brønsted base squaramide and Lewis acid Ag_2O. The H-bonding interaction of the squaramide catalyst activates the ketone and at the same time, Ag-catalyst enhances the reactivity of the isocyanoacetate towards nucleophilic addition (Scheme I.2.5).[4e]

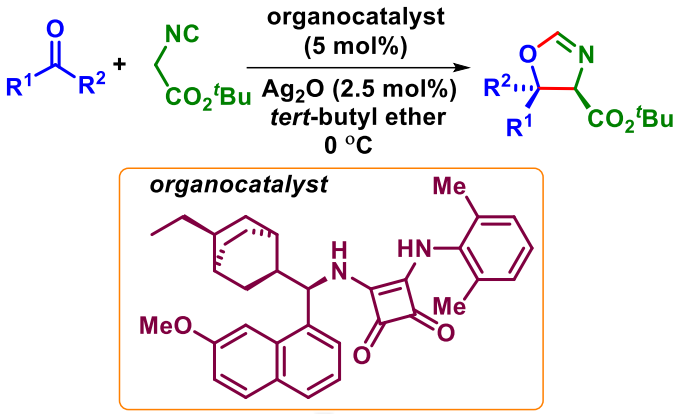

Scheme I.2.5. *Enantioselective synthesis of chiral oxazolines.*

I.2.2. Synthesis of fused heterocycles from alkyl isocyanoacetate

In 2022, Pedro *et al.* carried out a dearomative (3 + 2) cycloaddition of α-aryl isocyanoacetates and 2-nitrobenzofurans to synthesize chiral polycyclic compounds with full diastereoselectivity and excellent enantioselectivity. This metal-free approach utilizes electron deficient 2-nitobenzofuran as dipolorophile and α-aryl-α-isocyanoacetate as the corresponding 1,3-dipole for interrupted Barton-Zard reaction. The curepine-derived oraganocatalyst having free phenolic OH group and basic amine acts synergistically and controls the stereochemistry of this chiral heterocycle that has three consecutive stereogenic centers (Scheme I.2.6).[5a]

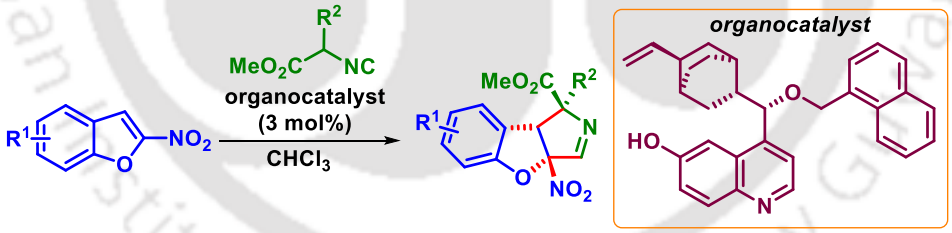

Scheme I.2.6. *(3 + 2) Cycloaddition of 2-nitrobenzofuran and isocyanoacetate ester.*

Samet group described an appealing strategy for the synthesis of pyrrolocoumarin core utilizing 1,2-diaryl-1-nitroethenes and alkyl isocyanoacetates. The reaction proceeded *via* initial Barton-Zard reaction of the nitrostilbene to deliver substituted pyrrole-2-carboxylate which follows selective *O*-demethylation and final lactonization. The selective *O*-demethylation of the *ortho*-methoxy group is chemo-selectively completed using 1 equiv. of BBr_3 and lactonization is achieved on treatment with ethanolic NaOH to deliver pyrrolocoumarin. Further, the Barton-Zard component of the reaction is extended for the construction of natural product lamellarin Q (Scheme I.2.7).[5b]

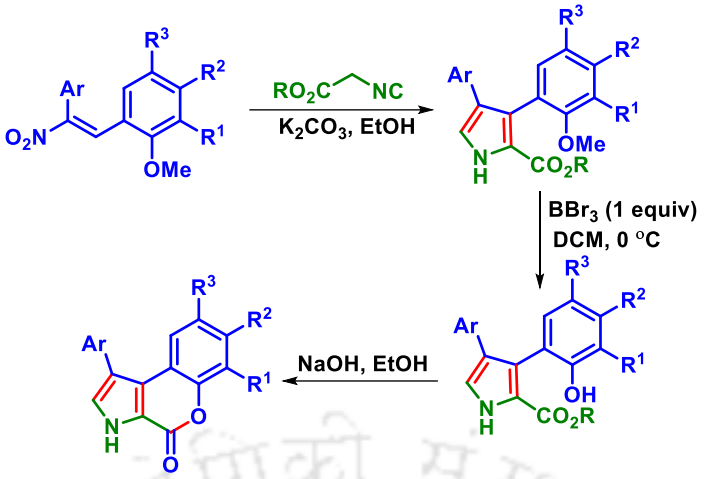

Scheme I.2.7. *Synthesis of pyrrolo-coumarin core via Barton-Zard reaction.*

Yang *et al*. disclosed a convenient silver-catalyzed cascade cyclization approach for the synthesis of chromenopyrrolones. Initially, activated ethyl isocyanoacetate undergoes conjugate nucleophilic addition to the double bond of 3-iodochromanone and subsequent ring opening of chromanone leads to the formation of pyrrole. The tethered pyrrole ring eventually forms chromenopyrrole *via* C–O etherification (Scheme I.2.8).[5c]

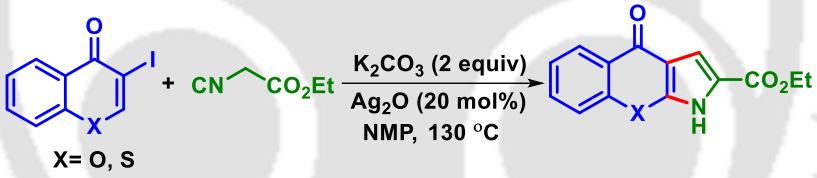

Scheme I.2.8. *Ag-catalyzed cascade reaction of ethyl isocyanoacetate.*

Kim and Oh group accomplished asymmetric desymmetrization of cyclohexadienones following van-Leusen pyrrole synthesis methodology utilizing a complex of Ag(I) salt and chiral phosphino-carboamide ligand. The optimum condition for this chiral pyrrole synthesis was found to be the use of 4-alkoxy cyclohexadienones and naphthylsulfonic methyl isocyanide (NasMIC) in the presence of quinine-derived phosphino carboamide ligand. Initially, deprotonated NasMIC undergoes (3 + 2) cycloaddition with alkene of cyclohexadienone to form 3,4-dihydropyrrole which on subsequent isomerization and sulfinic acid elimination delivers chiral pyrrole. The rigid naphthyl moiety of arylsulfonyl isocyanides and 4-alkoxy substituent of cyclohexadienone is expected to influence the enantioselectivity of the resulting pyrrole (Scheme I.2.9).[5d]

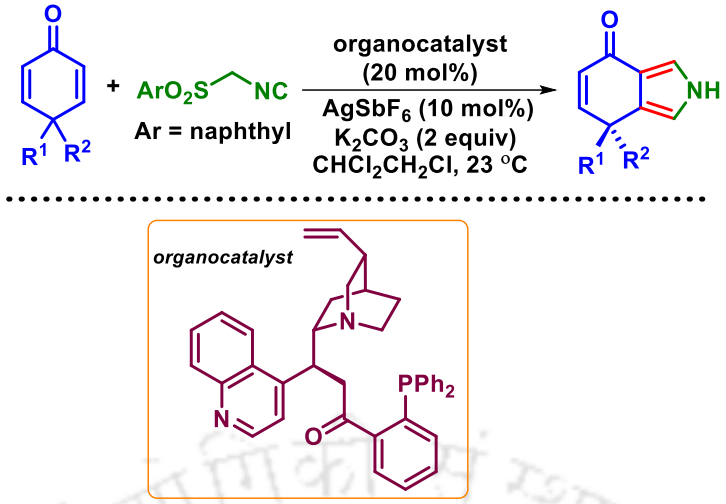

Scheme I.2.9. *Ag-catalyzed asymmetric van-Leusen pyrrole synthesis.*

Shaabani *et al*. disclosed a cyclization strategy for the synthesis of chromenopyrrole from 3-acetyl coumarin. Under an alcoholic medium, the acetyl group of the starting precursors gets eliminated and TosMIC-derived anion preferentially undergoes addition to the double bond of cyclic enone to deliver the desired polyheterocycle. The reaction proceeds following a van-Leusen type (3 + 2) cycloaddition between C=C of 3-acetyl coumarin and 1,3-dipole derived from TosMIC (Scheme I.2.10).[5e]

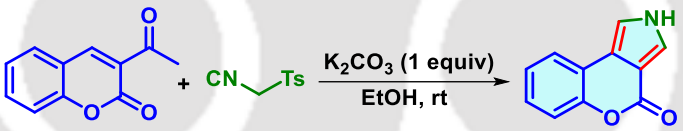

Scheme I.2.10. *Synthesis of chromenopyrrole from 3-acetyl coumarin.*

I.2.3. Reactivity of ester group of alkyl isocyanoacetate

The reactivity of alkyl isocyanoacetate is best known due to the nucleophilic character of the acidic α-carbon and electrophilicity of the divalent carbon atom of isocyanide. Such reactivity of α-isocyano ester has been exploited in various cycloaddition reactions for the effective construction of C–C and C–N bonds. However, in most of these cycloadditions, the ester group acts only as an activator and remains an unreactive spectator without undergoing any participation in the bond-forming processes. To exploit this inertness of ester functionality, Zhu group in 2007 synthesized strategically designed isocyanoacetate where α-position is substituted with electron-rich nitrobenzene. This makes α-hydrogen more acidic and the resultant anion is stabilized due to the strong electron-accepting nitro group in the phenyl ring.

Consequently, the anion becomes less acidic and more nucleophilic divalent carbon of isocyanide initiates the reaction with an electron-deficient double bond such as imine. Such type of reactivity tuning gives different heterocycles by trapping the nitrilium intermediates through *O*-nucleophile of ester (Scheme I.2.11).[6a]

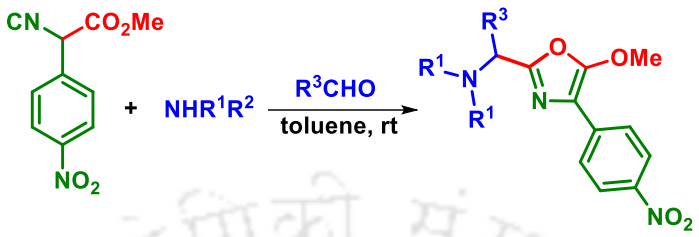

Scheme I.2.11. *Rare reactivity of isocyanoacetate: ester group as O-nucleophile.*

Dong and Xu group also explored all reactivity centers of an alkyl isocyanoacetate for the diastereodivergent synthesis of chromeno[2,3-*b*]chromenes. They exploited the less reactive ester functionality of alkyl isocyanoacetate and accomplished the synthesis of complicated architectures with four adjacent stereocentres. All the three functionalities of isocyanoacetate sequentially reacted with two *o*-quinone methides (*o*-QMs) in this diastereoselectively switchable domino process (Scheme I.2.12).[6b]

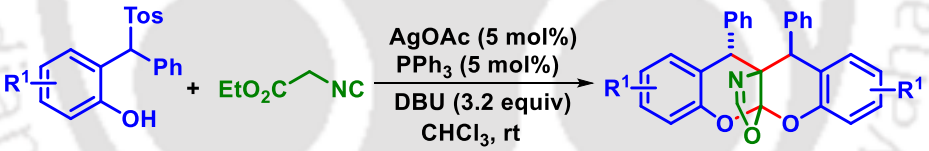

Scheme I.2.12. *Synthesis of chromeno[2,3-b]chromeno by exploring all reactivity of isocyanoacetate.*

I.3. Directing Group-Assisted C–H Activation

1.3.1. What is C–H activation:

The carbon-hydrogen (C–H) bonds are ubiquitous in all kinds of organic molecules. The three types of C–H bonds present in organic molecules *viz*., C(sp)–H bonds in alkynes, C(sp^2)–H bonds in alkene, and C(sp^3)–H bonds in alkane have different acidity and pK_a values. The C–H bonds offer very limited reactivity due to high bond dissociation energies and thus difficult to functionalize. The acidity or reactivity of these C–H bonds is strongly dependent on the surrounding environment of the molecule. The less acidic C(sp^3)–H, C(sp^2)–H bonds

are more difficult to functionalize compared to alkyne C(sp)–H bonds. However, various techniques have emerged for the activation of these inert C–H bonds. The two best methodologies for the conversion of these ubiquitous C–H bonds into C–C or C–heteroatom bonds are C–H activation and cross-dehydrogenative coupling (CDC). These two methodologies have been gaining attention for the synthesis of complex molecular scaffolds, natural products, pharmaceuticals and are being used for the late-stage modifications of diverse bioactive molecules.[7a-f]

The C–H functionalization of organic molecules can be accomplished *via* a number of pathways-

(i) α-C–H functionalization of carbonyl, amine, or ester through acid-base promoted or radical pathways.

(ii) The undirected C–H functionalization of heterocycles with lack of selectivity.

(iii) Directed C–H functionalization through functional groups selectively at α (*ortho*), β, γ, δ or even at more distal positions.

With the advent of innovations and technology, the synthesis of complex molecules is no longer an intractable venture. However, these new approaches should carry the burden of synthetic ideality and economy.[8a-b] The advance of C–H functionalization-the net conversion of C–H bonds to different functionalities has widened the toolbox for organic chemists. A C–H bond can be considered as dormant synthetic equivalents of different functional groups. This novel innovation helps in the construction of diverse functionalized C–C/C–heteroatom bonds in a step-economical way. In a simple word, the skeletal construction and modification *via* C–C bond formation through C–H activation can offer the expeditious generation of complex molecular entities by providing an alternative route to the traditional coupling reactions. For example, coupling reactions such Negishi, Stille, Suzuki–Miyaura, etc. present multiple ways for the formation of C–C bonds through the coupling of organic halides with an organometallic intermediate or with an activated alkene as in Heck reaction. But these transition-metal-catalyzed coupling reactions need a suitable coupling handle to be installed in the substrate before C–C transformation.[8c-e] Thus, C–H activation has emerged to overcome such difficulties as substrates having inert C–H bonds can be coupled with a range of electrophiles or nucleophiles. The activation of inert C–H bonds maximizes operational simplicity and reduces the amount of chemical waste generated in traditional coupling reactions. In a nutshell, such

strengths considerably broaden the range of potential coupling partners for given transformations and provide larger flexibility to accomplish a desired synthetic target. Thus, C–H activation has the potential to impact and redefine how synthesis can be conceptualized.

Usually, with the assistance from a transition metal catalyst, a direct C–H bond activation becomes possible without any pre-activation of the substrate. A transition metal can cleave the strong C–H bonds to generate carbon-metal bonds, which can be intercepted by various coupling partners to convert an inert C–H bond omnipresent in organic molecules to a diversely functionalized C–C or C–X bonds (Figure I.3.1).

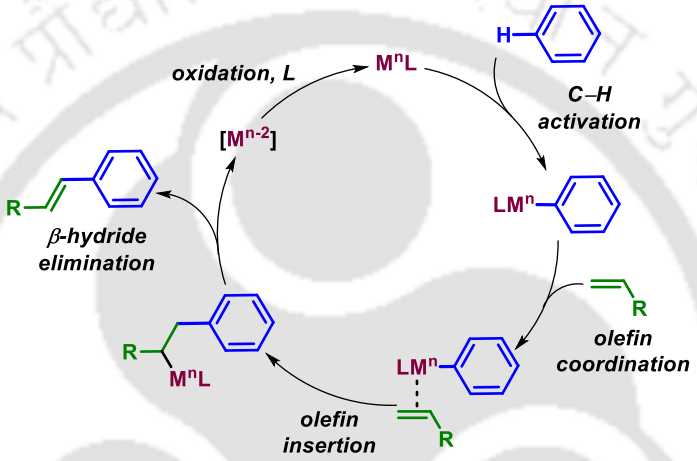

Figure I.3.1. *General mechanism for direct C–H olefination.*

Initially, progress was achieved utilizing rare and noble second- or third-row transition metals such as Pd, Rh, Ru, Ir.[7a,8a-e] Apart from this, various metal complexes of earth-abundant metals such as Ni, Co, Mn, Cu in their different oxidation states are found to have high catalytic activity in various C–C bond forming reactions that proceeded through C–H activation strategy.[9e-h] Such a larger pool of catalysts helps in the development of this methodology and encourages a larger variety of possible transformations.

1.3.2. Directing groups (DGs)

However, to make C–H activation as an inclusive strategy selectivity is the key issue to resolve. The ubiquity of C–H bonds in organic molecules raises challenges in the selective modification of a desired C–H bond to a C–C or C–X bond. Thus, selective activation of a target C–H bond in an organic compound must be achieved over all the other C–H bonds available in the molecule. The selectivity issue, however, can be resolved to some extent by

employing molecules having differently reactive C–H bonds. Such a strategy has already been employed in the functionalization of C–H bonds of heterocycles, as the presence of heteroatom in the ring brings disparity among C–H bonds. However, due to its symmetrical nature, such discrepancy is generally less pronounced in the case of benzene derivatives, thus demanding regioselectivity controlling elements to achieve selective C–H transformations in arenes (Figure I.3.2).[7a]

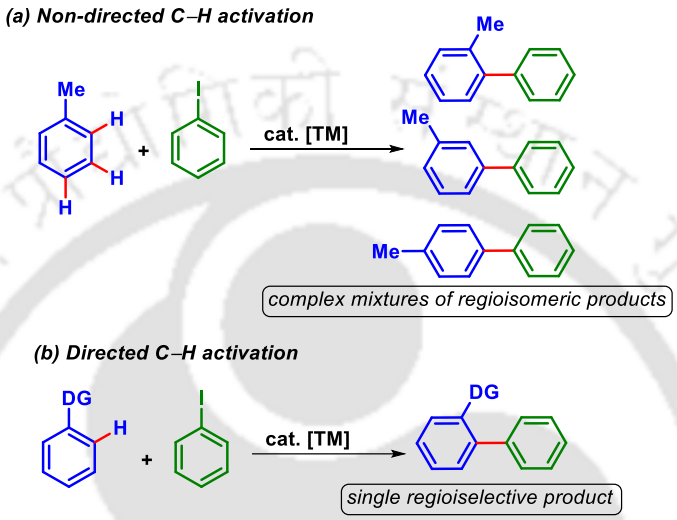

Figure I.3.2. *Non-directed vs directed C–H functionalization.*

Transition metal complexes that activate a C–H bond are necessarily of high energy which makes it difficult to control chemo-, regio-, and stereoselectivity of the C–H cleavage event. To tackle the challenges such as the inertness of C–H bonds and to control site selectivity, a variety of creative innovations especially directing group and ligand design has been made in this promising methodology (Figure I.3.3).

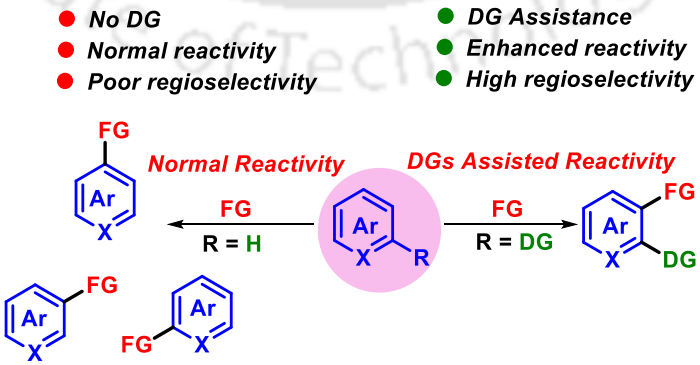

Figure I.3.3. *Advantages of directing groups.*

Directing groups (DGs) are Lewis basic functionality that is inherent to the substrates and possess some σ-donating heteroatoms. These functionalities contain non-bonding lone pairs of electrons that facilitate the pre-coordination between metal and the substrate. The role of the directing groups in these reactions is usually twofold. The DGs enhance the reactivity of a transition metal-catalyzed C–H activation and also control the site selectivity of such reactions. The coordination ability of a directing group brings the transition metal into close proximity to the targeted C–H bonds.[10a] The higher concentration of the metal in the proximity of the functional group accelerates regioselectivity and reactivity and thus preferentially leads to the functionalization of the *ortho* C–H bonds. Such type of C–H bonds can be considered as semi-activated C–H bonds *i.e.*, although they are not inherently activated but the reactivity can be enhanced with aid from the neighbouring directing group. Directing groups coordinate with the active metal catalyst through its heteroatom and form a metallacycle in the vicinity of the targeted C–H bonds (Figure I.3.4).[10b] Metallacycles are efficiently generated by the activation of arenes with the aid of strongly coordinating *N*-atom or weakly coordinating *O*-atoms of the directing group. This coordination enhances the pre-requisite substrate catalyst interactions to activate a C–H bond. This chelation-driven C–H bond activation has become a more powerful and popular strategy for *o*-C–H functionalization.

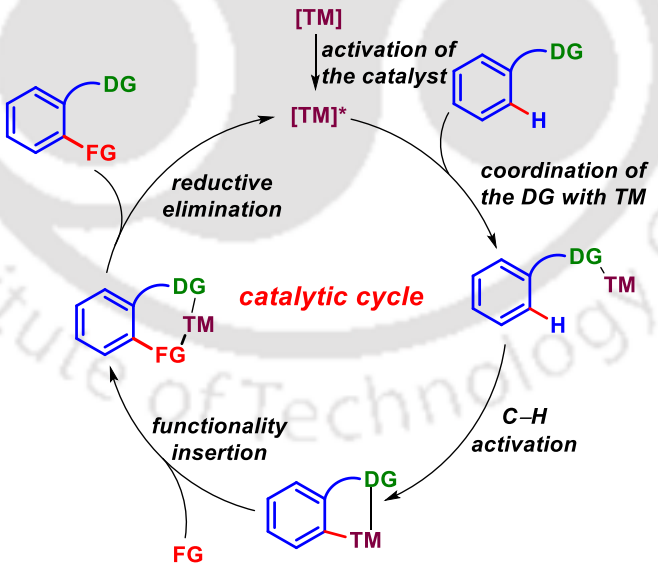

Figure I.3.4. *General mechanism of DG-assisted C–H activation.*

There is a wide scope of coupling partners for C–C bond construction through C–H activation which includes alkenylation, alkylation, alkynylation, arylation, allylation, carbonylation, and other valuable organic transformations.[10c] Furthermore, these coupling

partners may act as an electrophile, nucleophile or a free radical species in such C–H functionalization and thus offer diverse and attractive synthetic routes.

1.3.2.1. Classification of directing group

The revolutionary work on directing groups was first realized in 1986 by Lewis and co-workers. They regioselectivity achieved mono and di-*ortho*-alkylation of phenol with ethene under *ortho*-metallated ruthenium phosphite complex.[11a] The knowledge about directing groups greatly enhances the discovery of new methodology in the C–H bonds functionalization by chelation-assisted C–H activation strategy. Diverse functional groups including pyridine, amide, carboxylic acid, amine, anilide, imine, ketone, hydroxyl, etc. have been employed as directing groups for catalytic C–H functionalization.[9a] Additionally, C–H activation directed by sulfur, phosphorous, silicon-containing functionality and π-chelation have also been achieved. Over the years, the directing group-assisted C–H functionalization has been intensively investigated and several intriguing C–C and C–X bond-forming processes have been realized enriching the perception of *o*-C(sp^2)–H bond activation. The large pool of DGs can be categorized either by their structure (eg., denticity, types of coordinating atoms and moieties), or by their utilization strategy.

1.3.2.1.1. Directing groups based on the number of coordinating atoms

Based on the denticity *i.e.*, the number of coordinating atoms, DGs can be divided into monodentate and bidentate directing groups. These DGs are mostly heterocyclic and coordinate through a basic *N*-atom and associate with the metal center (Figure I.3.5). 2-Phenylpyridine and its close structural relatives are one of the most widely utilized classes of monodentate directing group. However, the inherent disadvantage associated with them is their inertness towards cleavage and unless such DGs are a part of the targeted framework, they have limited applications. Due to such inertness of these directing groups, they are often termed permanent DGs.[12a]

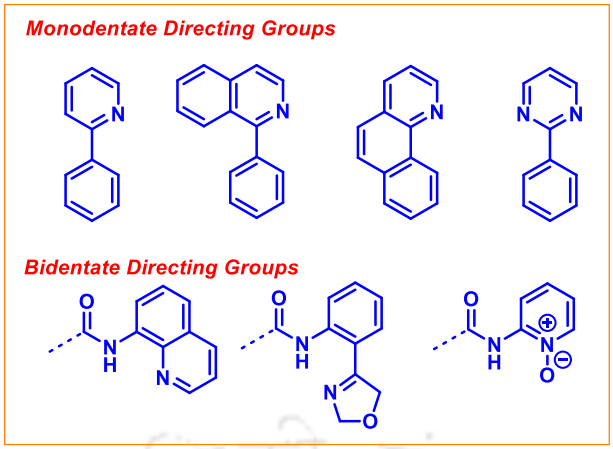

Figure I.3.5. *Classification of DGs based on the number of coordinating atoms.*

Sames *et al*. reported a C(sp^3)–H arylation strategy of pyrrolidines with a catalytic amount of low valent transition metal catalyst with the assistance of a permanent directing group. They took 2-(pyrrolidin-1-yl)pyridine derivative and treated with phenylboronic ester as the arylating source in the presence of 10 mol% of trinuclear $Ru_3(CO)_{12}$ catalyst and a ketone. The arylated product was isolated in moderate to good yield, although the catalyst loading and reaction time was longer than that of corresponding pyrrolidine derived amidine (Scheme I.3.1.).[11b]

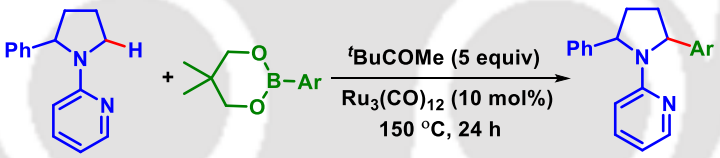

Scheme I.3.1. *C(sp^3)–H Arylation utilizing monodentate DG.*

Although pyridine as a directing group is quite difficult to remove when connected to the substrate through a C–C bond, the prevalence of pyridine ring in a vast number of bioactive molecules partially compensates for this disadvantage, as the ring may be part of the targeted molecule. Loh *et al*. achieved alkenylation of the C7 position of indolines with the assistance of Rh(II) catalyst and $Cu(OAc)_2$. The *N*-atom of the indoline is attached to a pyridine ring and this acts as a non-removable directing group for this regioselective olefination (Scheme I.3.2).[11c]

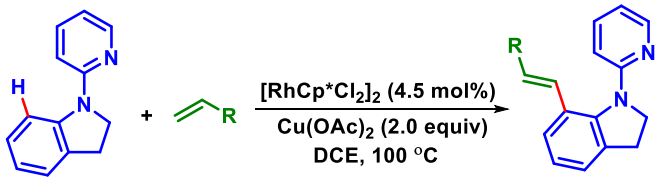

Scheme I.3.2. *Pyridine directed C–H olefination.*

Niu and Song group extended this monodentate direction strategy for oxidative C2 arylation of indole under a readily available Co(II) catalyst utilizing *N*-pyrimidine as monodentate DG. This Grignard reagent-free arylation utilized aryl boronic acid as an arylating source and $Mn(OAc)_2{\cdot}4H_2O$ as the oxidant in the highly C2 regioselective C–H functionalization pathways. After the desired arylation, the pyrimidine auxiliary can be easily cleaved under basic hydrolysis (Scheme I.3.3).[11d]

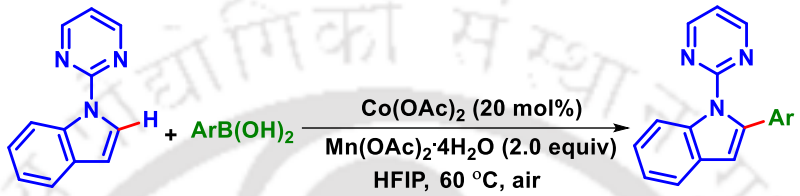

Scheme I.3.3. *Regioselective C–H arylation of indole.*

The seminal work on the bidentate group-promoted C–H functionalization was accomplished by Daugulis *et al.*[11e] The amide derived from 2-aminoquinoline acts as a bidentate directing auxiliary for such transformation. Since then, the scientific community left no stone unturned to design and use a large family of bidentate directing groups and thus widen the C–H functionalization toolbox.[11e,f] Striking examples of the application of such bidentate directing groups are also found in total syntheses of various target molecules. Baran and co-workers designed their approach to synthesize pipercyclobutanamide-A through a direct C(sp^3)–H bond arylation using 8-aminoquinoline derived bidentate DG (Scheme I.3.4.).[11g]

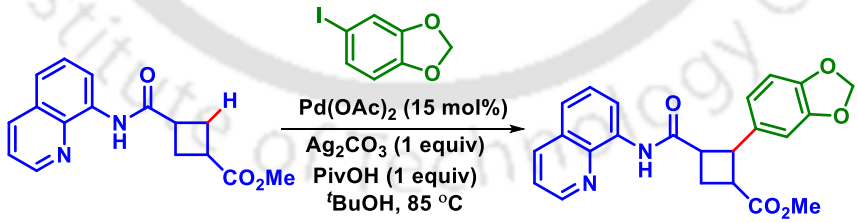

Scheme I.3.4. *C(sp^3)–H arylation using bidentate DG.*

In 2015, Li and Ge group developed amide-tethered oxazoline as a *N*, *N*-bidentate directing group for direct *o*-acetoxylation. This DG activates the *ortho*-C–H bond by forming a six-membered metallacycle with Pd(II) through both *N*-atoms and simultaneously coordinates with the aryl C–H bonds. Eventually, *ortho* acetoxylation with PIDA delivered the desired product (Scheme 1.3.5).[11h]

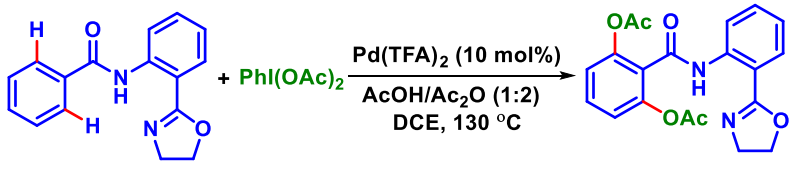

Scheme I.3.5. *Pd(II)-catalyzed ortho-acetoxylation via amide-oxazoline bidentate DG.*

Another amide bidentate directing group derived from 2-aminopyridine-*N*-oxide has been found to have remarkable features in C–H transformation reactions.[11i,j] Eco-friendly transition metal catalysts such as Co and Ni efficiently catalyzed C–H bond of aromatic molecules with the help of such *N*, *O*- bidentate DGs. Besides the efficient functionalization of *ortho* C–H bonds, another key advantage of 2-aminopyridine-*N*-oxide bidentate DGs is their easy removal after the desired transformations. Niu and Song group reported an inexpensive $Co(H_2O)_2{\cdot}4H_2O$ catalyzed C–H activation-annulation strategy directed by *N*,*O*-bidentate DG. The alkynyl carboxylic acid undergoes decarboxylative addition to the C–H bond of the arene to deliver isoquinolones with diverse amides (Scheme I.3.6).[11k]

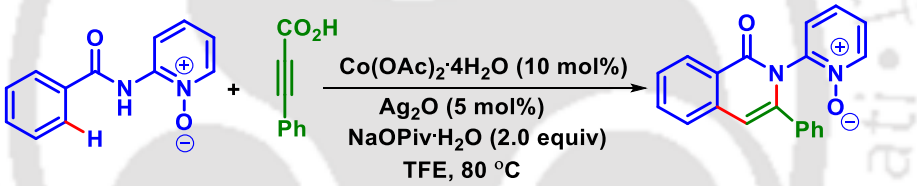

Scheme I.3.6. *Co(II)-catalyzed C–H activation/annulation utilizing bidentate DG.*

1.3.2.1.2. Directing groups based on their approaching action:

Directing groups further can be classified based on the approaching action or by their utilization strategy. Based on this the DGs can be categorized as follows-

- ❖ Non-removable/permanent directing group
- ❖ Removable/modifiable directing group
- ❖ Transient directing Group
- ❖ Traceless directing Groups

Non-removable/permanent directing groups

Removal of the directing group is an alarming issue of C–H functionalization strategy, as the DG might not be still useful after the desired transformation and its removable thus becomes necessary. Several directing groups cannot be removed after the desired C–H

functionalization. However, this is not an issue if the directing group is part of the targeted molecule. So, the directing group that could not be easily removed is considered as non-removable or permanent directing group.[12a] *N*-heterocycles (azine) such as pyridine and pyrimidine are often regarded as non-removable directing groups. Although the removal of these DGs is tricky, especially with mono-heterocycles (*i.e.*, pyridine), a number of strategies have emerged over the years. Again, the omnipresence of pyridine in many bioactive molecules partly compensates for this challenge, as cleavage of the DG might not be required at all. This difficulty arises if heterocycles are linked to the precursors through a C–C bond, in which case they are considered as permanent DG.[12a-c] However, the electron-deficient nature of *N*-heterocycles and the strong coordinating ability of the ring's *N*-atom reduce the ring's reactivity towards further transformations. This limits the scope of this C–H functionalization strategy.

Yu group in 2011 developed C3-selective C–H alkenylation of pyridine with the assistance of Pd catalyst and ligand 1,10-phenanthroline. The C3 selectivity with pyridine was observed due to bidentate ligand 1,10-phenanthroline enabled *trans* effect which weakens the coordination of the catalyst with ring *N*-atom. This bis-dentate ligand enhances the ligand exchange and could form an intermediate **II** albeit in small amounts where Pd is potentially coordinated to the electron-deficient pyridine ring. It is anticipated that solvent, additive, or ligands could significantly enhance the equilibrium resulting in the efficient construction of pyridine C3–C bond with olefin (Scheme I.3.7).[12d]

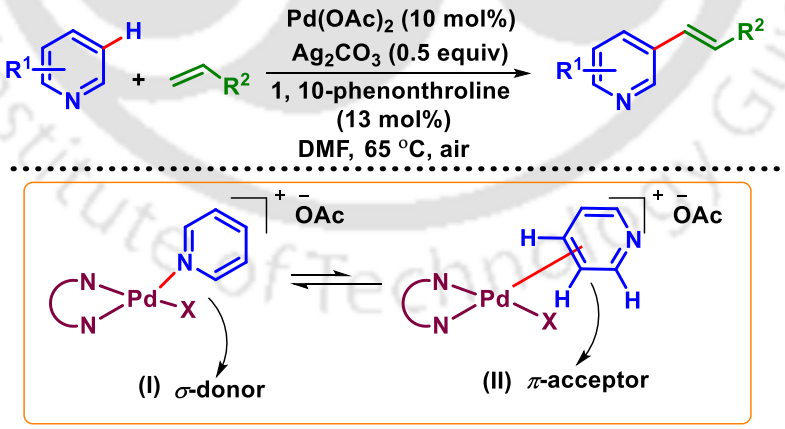

Scheme I.3.7. *C–H olefination of pyridine.*

Tobisu and Chatani group achieved a Ni-catalyzed C2–H arylation of pyridine using diphenyl zinc as an aryl source. This methodology delivers straightforward access to a range of arylated *N*-heteroarenes, which otherwise are poor substrates for direct catalytic arylation.

This nucleophilic oxidative arylation under the catalytic system of $[Ni(cod)_2]/PCy_3$ provides an alternative C–H functionalization strategy over well-established direct arylations by S_EAr pathway (Scheme I.3.8).[12e]

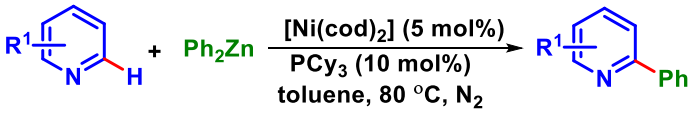

Scheme I.3.8. *Pyridine directed C–H arylation.*

Removable/modifiable directing groups

The directing groups can be termed as removable or modifiable if, after the desired C–H functionalization of the substrate, it can be removed or modified by some easy additional steps on the functionalized product. The DG removal must be achieved relatively easily (Figure I.3.6).[13a] However, removal of the directing group can be completed *in situ* after the desired C–H functionalization, which in such cases is called a traceless directing group. The traceless directing group is separately discussed in the following section. Different functional groups have been utilized as removable/modifiable DG for C–H functionalization. For example, imine has evolved as a modifiable directing group for carbonyl-containing compounds, as hydrolysis allows the generation original carbonyl group. Similarly, modification of carboxylic acid or sulfonic acid into corresponding amide or ester group can serve as modifiable DG. Subsequent removal of these directing groups then delivers the original compound.[13b]

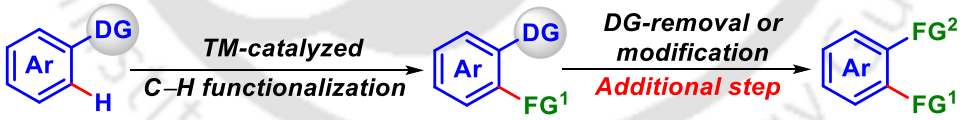

Figure I.3.6. *C–H activation using removable/modifiable DG.*

Aryl carbamates are frequently used for *o*-C–H functionalization due to their easy derivatization from phenols, high stability, and readily removal after the desired functionalization. Thus, functionalization of phenols can be achieved by transforming them into carbamates. Li and Wang group achieved Ru-catalyzed *ortho*-C–H alkenylation *via* a carbamate-directing group. The carbamate DG can be readily removed by hydrolysis with a base, and thus recovers the phenol functionality (Scheme I.3.9).[13c]

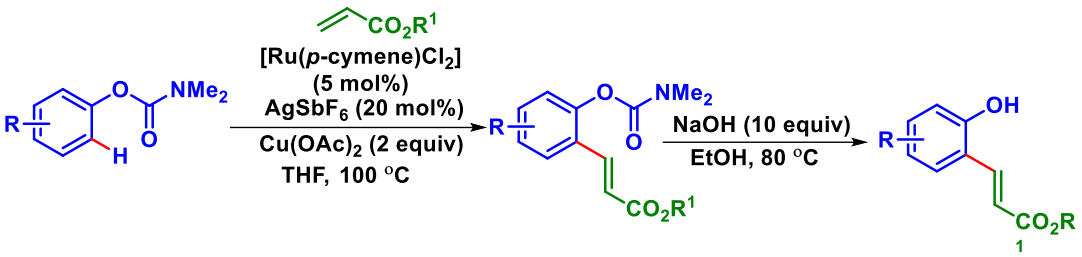

Scheme I.3.9. *o-C–H olefination via carbamate as a removable DG.*

Shi group utilized the removable directing group nature of 2-picolinamide to functionalize C(sp^3)–H bonds of an imide *via* Pd catalysis. They synthesized imide as a substrate for these primary and secondary C–H arylations by reacting 2-picolinamide with a proper acyl chloride in the presence of a base. The *N*-atom of the imide linker serves as the coordinating atom for promoting arylations with different aryl iodides. The removal ability of the DG has been verified by easy hydrolysis of the product under mild reaction conditions and in short reaction time (Scheme I.3.10).[13d]

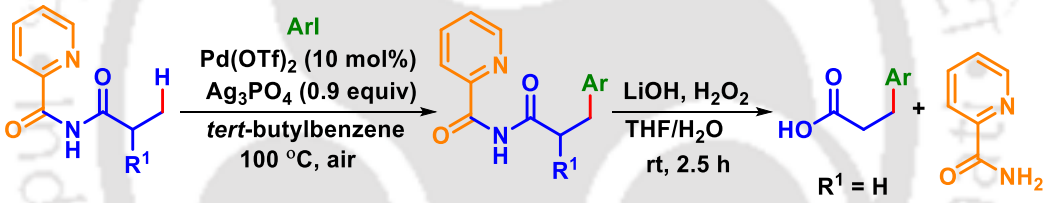

Scheme I.3.10. *Removable DG-assisted C–H arylation.*

A modifiable directing group is highly desirable in C–H functionalization. Such a directing group could be converted into various transformations after the desired C–H functionalization. Huang and co-workers selected 1,2,3-thiadiazoles to serve as a modifiable DG. The less acidic C–H bonds of 5-*H*-1,2,3-thiadiazoles enable easy deprotonation of such heterocycles and subsequently release nitrogen to generate thioketenes or alkynyl thiolate anion intermediate. Such intermediates are further trapped by electrophiles or nucleophiles to deliver different synthetically valuable compounds. To execute a modifiable DG *o*-C–H alkynylation approach, they treated 1,2,3-thiadiazoles with bromoalkyne in the presence of Ir-complex. Mild base K_2CO_3 triggers the ring-opening of thiadiazoles which show the modifiability of the directing group. Thus, in the presence of base K_2CO_3 in DMF the alkynylated product delivers thioamide. Similarly, under a combination of Ag(I) salt and acetylacetone, the functionalized product undergoes annulation to give polysubstituted furan (Scheme I.3.11).[13e]

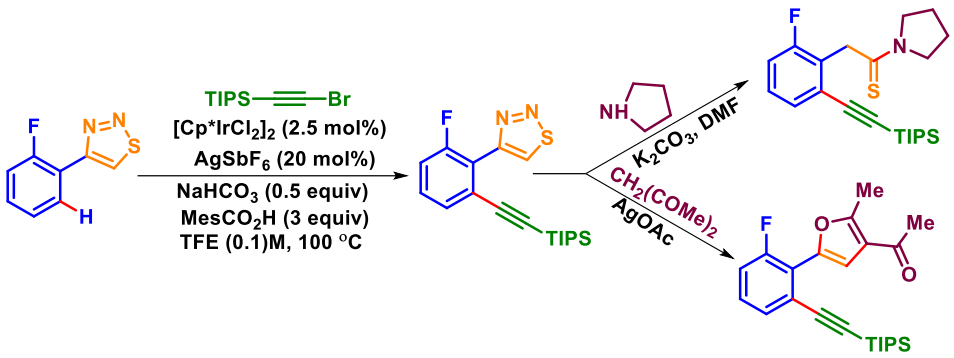

Scheme I.3.11. *1,2,3-Thiadiazoles as modifiable DG.*

Gao and Yoshikai developed a Co(II)-phenanthroline-catalyzed *ortho*-alkylation of imines. Imine derived from acetophenone and *p*-methoxyaniline when treated with vinyltrimethylsilane under an inexpensive catalytic system of cobalt and phenanthroline delivers *o*-alkylated acetophenone after acidic hydrolysis (Scheme I.3.12).[13f]

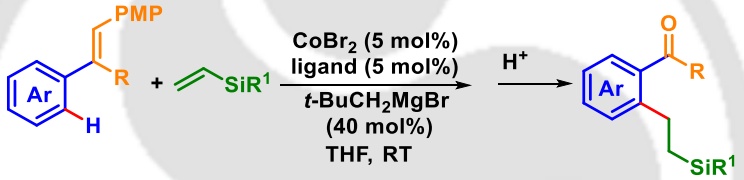

Scheme I.3.12. *Co(II)-catalyzed modifiable DG-assisted C–H functionalization.*

Transient directing groups

Despite having significant usefulness of removable DGs, this approach demands additional steps for installation and cleavage of DGs, thus again a step-economical and chemical waste issue. Instead, a reversible *in situ* preparation and removal of the DGs in a transient way has the ability to reduce synthetic steps through the use of catalytic additives. Thus, transient DGs have surfaced as a new progressive approach for C–H functionalization with a high level of selectivity.[14a] A directing group that could not effectively coordinate with metal catalyst alone, however, can activate a C–H bond with the aid of a co-catalytic modifier known as a transient directing modifier (TDM). The important criteria for the design of a transient DG include:[14b]

i. The transient directing modifier should chemo-selectively form transient DG
ii. The TDM should not interfere with the desired modification.
iii. The TDM must be stable throughout the process.
iv. The formation of transient DG must be reversible.

Mechanistically, the reaction between the substrate functional group and the suitable catalyst (TDM) temporarily and reversibly installed a transient directing group on the substrate. This transient DG coordinates selectively with the transition metal catalyst and thus behaves as a monodentate or bidentate ligand. Such coordination generates corresponding five or six-membered metallacycles, which react with the incoming coupling partner leading to species **III** which eventually regenerates the metal catalyst and forms intermediate **IV**. Finally, cleavage of the transient directing group delivers the anticipated C–H functionalized product with the regeneration of the TDM (Figure I.3.7).[14c]

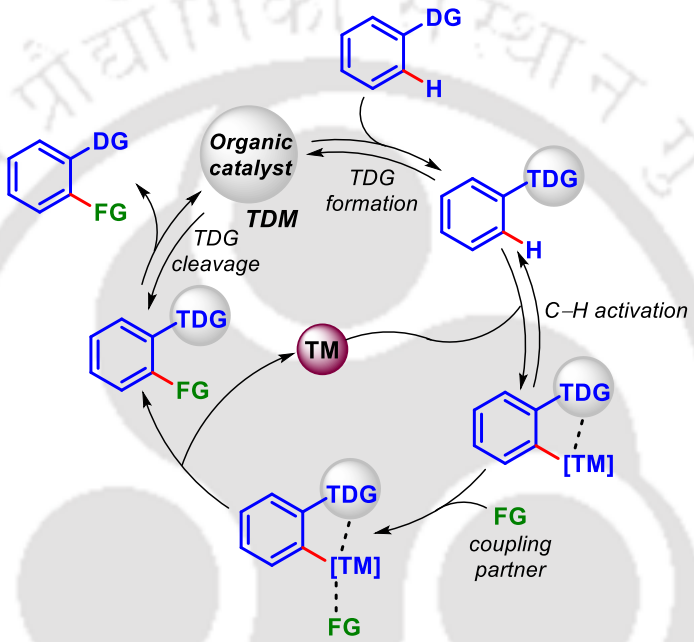

Figure I.3.7. *General mechanism for transient DG-assisted C–H functionalization.*

The pioneering work on transient directing groups in a catalytic way was achieved by Lewis and Smith in 1985.[11a] Lewis independently analyzed the *ortho* deuteration of phenols catalyzed by Ru complex (TDM-1) through transesterification of the phenoxy group to phosphites under deuterium atmosphere.[14d] The catalytic KOPh was found to be very crucial for rapid transesterification. The *ortho* selectivity of the protocol was believed to be due to the formation *o*-metallated complex as the key intermediate (Scheme I.3.13).

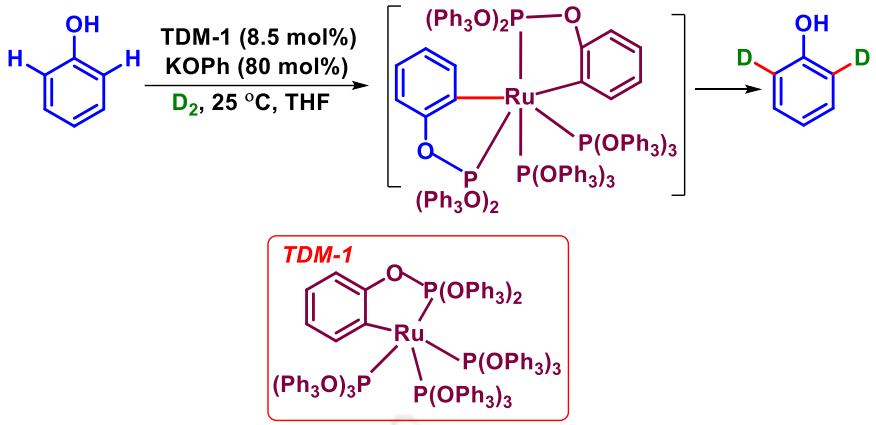

Scheme I.3.13. *Pioneering o-C–H deuteration by Lewis using transient DG.*

In 2016, Yu group outlined an arylation approach of a library of carbonyl compounds at inert β or γ-C–H bond under catalytic conditions of palladium. Amino acids form imine while reacting with aldehydes or ketones, thus acting as transient directing mediators. The imine generated by such condensation serves as a bidentate transient DG and activates the inert C(sp^3)–H bond. Activated C–H bonds eventually coupled with aryl or heteroaryl iodides to deliver arylated aldehydes or ketones through *in situ* modifications (Scheme I.3.14).[14e]

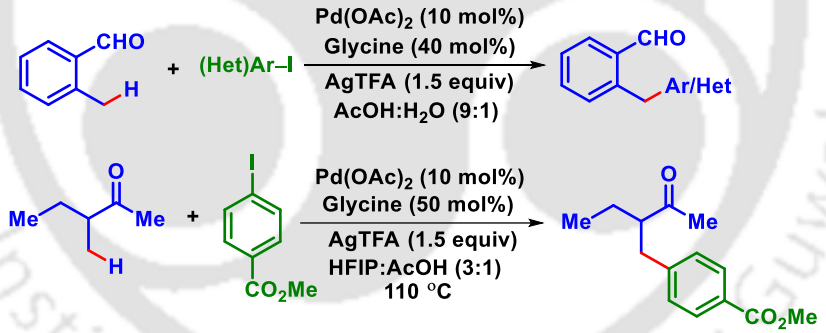

Scheme I.3.14. *C(sp^3)–H arylation through imine transient DG.*

Sorensen *et al*. carried out a Pd-catalyzed *ortho*-C–H hydroxylation of benzaldehyde using 4-chloroanthranilic acid as a transient directing mediator. The functionalization starts with the initial formation of imine between the substrate benzaldehyde and 4-chloro anthranilic acid which is the resultant transient directing group and undergoes metal coordination. Subsequent cyclopalladation of the imine generates a six-membered palladacycle which on oxidative addition with by standing F^+ oxidant eventually delivers *o*-C–H hydroxylated product. It is assumed that *p*-toluenesulfonic acid acts an external hydroxyl nucleophile for the Pd(IV) reductive elimination (Scheme I.3.15).[14f]

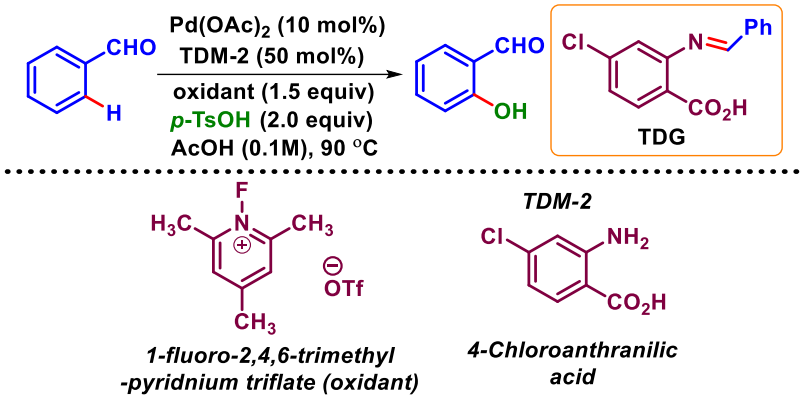

Scheme I.3.15. *Transient DG-assisted o-C–H hydroxylation of benzaldehyde.*

Norbornene (NBE) as transient directing mediator

The concept of TDGs largely depends on the coordination of the active metal through the heteroatom. However, recent progress has surfaced where strained alkenes especially norbornene have been employed as transient directing mediators in Pd-catalyzed *ortho*-C–H functionalization.[14g,h] The procedure, also termed as "Catellani reaction" allows selective functionalization of *ipso or o*-C–H bond of aryl halides.

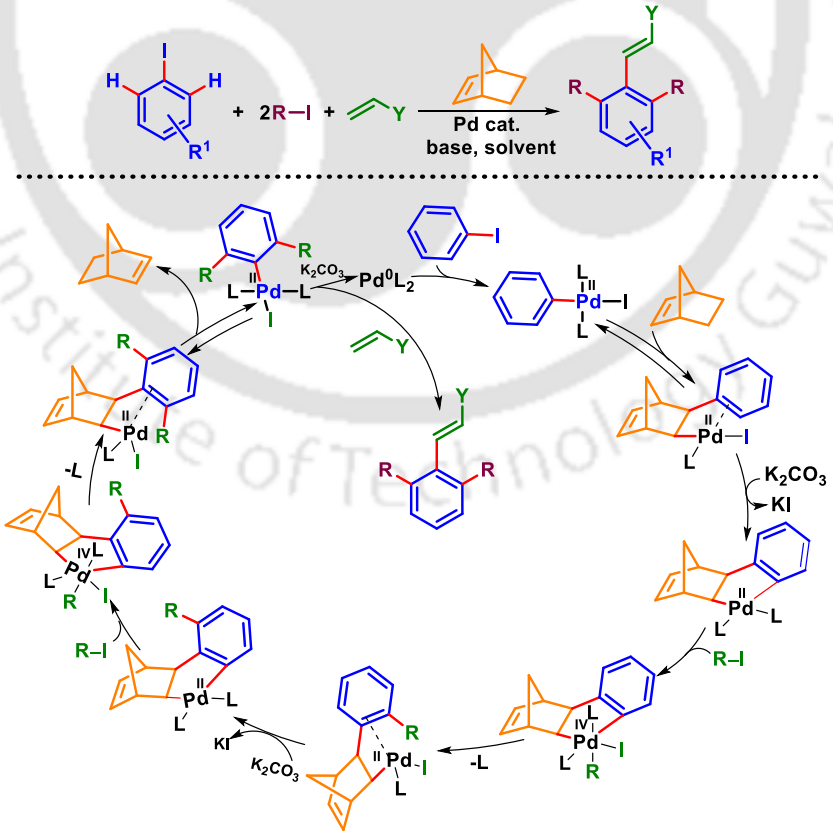

Scheme I.3.16. *ortho-C–H functionalization by Catellini reaction.*

The combined action of aryl halide, norbornene, and Pd catalyst construct the palladacycle through the *o*-C–H activation of the aryl halide. The resulting complex serves as a transient directing mediator and directs the alkyl halide or in some cases amine towards the C(sp^2)–Pd bond. In the end, due to large steric hindrance, the palladacycle gets dismantled with the extrusion of norbornene along with C–C/C–X bond formation (Scheme I.3.16).[14g]

Li *et al*. reported a Pd/norbornene (NBE)-catalyzed regioselective silylation of *NH*-free indoles. A diverse silylated indole were synthesized using hexamethyldisilane as a silylating source following a Catellani-type regioselective C2–H silylation (Scheme I.3.17).[14i]

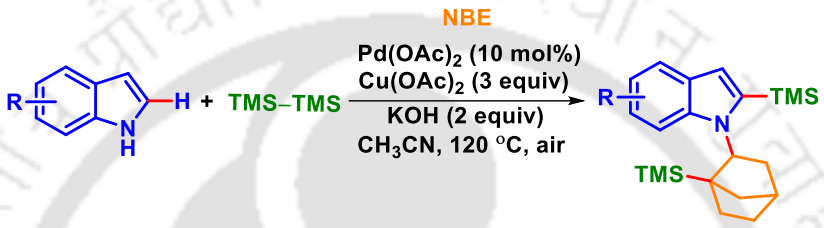

Scheme I.3.17. *Pd/NBE-catalyzed regioselective C–H silylation.*

Traceless directing groups

Traceless directing groups enabled functionalization of the C–H bond and simultaneous cleavage of the DGs in a cascade fashion. Such directing groups are considered as ideal directing groups as they do not persist in the target molecule but rather are removed during the catalytic cycle (Figure I.3.8). However, the line of differentiation between transient and traceless directing groups is very thin. The former demands additional steps for installation with some mediator while the later are inherent to the substrate to be functionalized. Moreover, transient directing groups require specific functionality on the molecule for reversible formation of functionality such as phosphinite, imine, or enamine to tether to the transition metal. These groups act as a transient handle to which the mediators could tether themselves.[15a-c] Since the introduction by Satoh and Miura in 2008, traceless directing group-assisted C–H activation has evolved as an elegant approach over traditional methodology largely due to their step-economy.[15d] Functional groups like carboxylic acids, imines, nitroso, *N*-oxides, sulfoxonium, etc. are attractive functionality for directing C–H functionality in a traceless way.[15c,e]

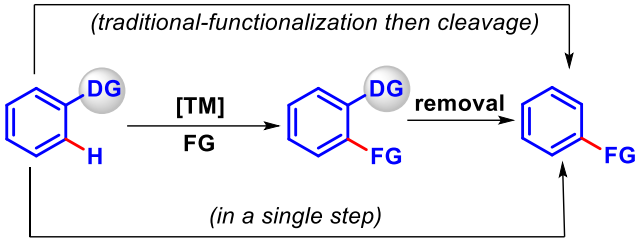

Figure I.3.8. *Traceless directing group strategies.*

Thus, a directing group should possess the following desirable features to achieve effective traceless behaviour-

(i) Directing group should be stable enough during the reaction and reversibly associated with the metal center.

(ii) Post functionalization, the directing group must be eliminated in a single step.

(iii) The desired compound should be free from the directing group.

Due to its abundance in organic molecules and versatility, while considering its further modifications, aromatic carboxylic acid functionality is an effective candidate for C–H functionalization. Moreover, the easy removal of carboxylate by extrusion of CO_2 makes it an ideal functionality for traceless directing groups.[15c,f] In 2019, Cai *et al.* developed a decarboxylative *ortho*-halogenation strategy using traceless character of carboxylic acid for the synthesis of *m*-nitrohalobenzenes. To execute this Pd-catalyzed *o*-C–H halogenation, they treated readily available *o*-nitrobenzoic acid and sodium halide with multiple additives at high temperatures. Mechanism investigation suggested a possible intermediacy of 2-halo-6-nitrobenzoic acid derivative in this *o*-C–H halogenation (Scheme I.3.18).[15g]

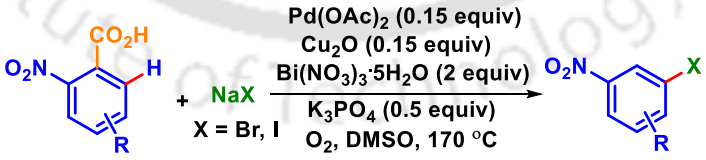

Scheme I.3.18. *Carboxylic acid as traceless DG for o-halogenation.*

Dey and Volla reported a Co(II)-catalyzed traceless bidentate directing group-directed C–H functionalization/annulation strategy for the construction of 2-alkynylated isoquinolines derivatives. 2-Aminopyridine acts a bidentate traceless directing group in this inexpensive and earth-abundant Co-catalyzed C(sp^2)–H activation of aryl/hetroaryl hydrazone and their simultaneous annulation with 1,3-diynes. 2-Aminopyridine also serves as the internal oxidant

and obviates the requirement of any external oxidant to carry out this oxidative annulation. This [4 + 2] annulation strategy is further extended for the synthesis of biologically active 3,3′-bisisoquinolines in one-pot or sequential manner (Scheme I.3.19).[15h]

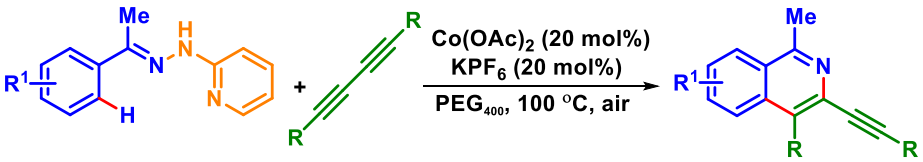

Scheme I.3.19. *Traceless bidentate DG assisted C(sp2)–H activation.*

In 2021, Lin *et al*. accomplished a Pd-catalyzed alkyl C–H borylation utilizing bromide as an effective traceless directing group. The reaction proceeded with the initial oxidative addition of aryl bromide to Pd(0) catalyst which forms an aryl Pd(II) species. This intermediate undergoes intramolecular C(sp^3)–H activation and generates a five-membered metallacycle. Subsequent proton transfers and transmetalation with B_2pin_2 delivers alkyl boronates with excellent site-selectivity (Scheme I.3.20).[15i]

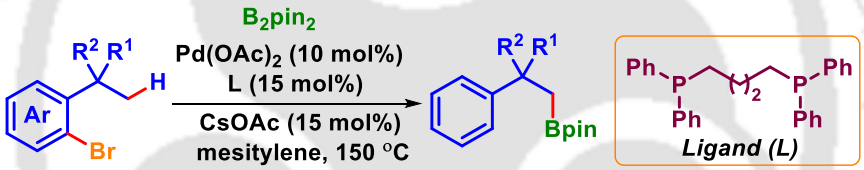

Scheme I.3.20. *Alkyl C–H borylation using bromide as traceless DG.*

Niu and co-workers developed a Co(III)-catalyzed C–H activation/annulation strategy for the construction of isoquinolines by α-imino-oxy traceless directing group. Both terminal, as well as internal alkyne, effectively serve as annulating partners for this inexpensive and readily available Co salt-catalyzed one-step process. The substrate α-imino-oxy acid serves as a traceless oxidizing *N*, *O*-bidentate directing group, coordinating through both strong *N*- and weak carboxyl *O*-atoms (Scheme I.3.21).[15j]

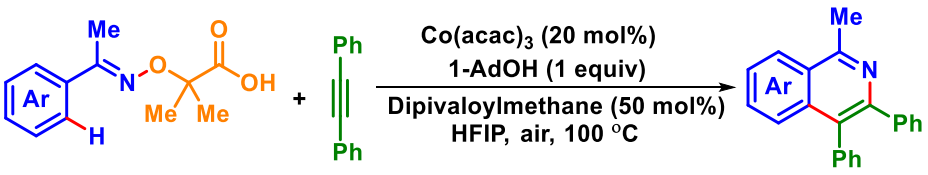

Scheme I.3.21. *C–H activation/annulation using traceless N, O-bidentate DG.*

1.3.2.2. Challenges and potential of C–H activation

Despite all those advantages of directing groups, it has a few limitations as well. The functionalization of benzene derivatives largely occurs only at proximal C–H bonds of the DG, so restricts the range of the accessible products. Moreover, extra steps are necessary for the installation of the DG in the substrate and for their manipulation after the desired C–H bond transformations. A DG might not be always required after the desired C–H functionalization, and its removal therefore is necessary. Several DGs are not easily removable and some of them constitute part of the targeted molecule. Thus, a more appealing strategy for C–H functionalization would be the one that avoids the use of DGs or DGs that are easily removed either during the reaction or after completion of the desired functionalization. Therefore, scientists have put their attention towards achieving reactivity as well as selectivity without the control of the DGs. Such strategy involves "undirected" C–H activation *i.e,* activation of C–H bonds of substrates that are devoid of any functionality capable of pre-coordinating the metal catalyst and deciding the position of C–H activation. Such undirected C–H activation could not get the benefit of the electronic and steric bias associated with all substituted arenes.[16a] Thus, for synthetic acceptance of the C–H activation strategy, a growing interest has been observed where the use of the DG can be completely avoided. This allows direct C–H functionalization of the simple arenes. Such strategy is called "Cross-Dehydrogenative Coupling" (CDC) involving the activation of two rather inert C–H bonds. [7d,e,16b]

Unlike C(sp^2)–H bond functionalization, there are fewer reports available for C(sp^3)–H bond activation because of the lower reactivity of these bonds. The activation of chemically unreactive alkyl C(sp^3)–H bonds is very challenging as such bonds have no pre-coordination site. The low acidity of the C(sp^3)–H bonds, and lack of empty low-energy or filled high-energy orbitals that interact with the *d*-orbital electrons of the transition metal makes functionalization of C(sp^3)–H bonds difficult. However, lately, scientists have turned their attention towards the functionalization of such sp^3 alkyl C–H bonds.[16c,d] The Majority of such processes involve the utilization of proximal DG that enhances chemical reactivity and brings site-selectivity. The activation of such bonds proceeded through the generation of a five- or six-membered metallacycle intermediate. The resulting C–H functionalization may take place either at γ- or δ– positions to the coordinating heteroatoms.[16e,f]

Although the transition metal-catalyzed *o*-C–H bond activation is thermodynamically favourable *via* formation of a five, six, or seven-membered metallacycle intermediate, the selective functionalization of the C–H bond that is distal to the directing group is an arduous task.[17a] Such metallacycles are not possible for distal C–H functionalization as it requires generation of 11-12-membered rings which are not feasible due to angle strain. For distal C–H bond activation, the DG coordinates to the furthest located C–H bond and functionalizes it. Further, the activation of the distal alkyl C–H bonds is more strenuous due to unfavourable thermodynamic conditions. However, in recent years enormous progress has been achieved towards the regioselective functionalization of remote *meta* and *para* position of arenes[17b,c] or distal sp^3-alkyl C–H bonds.[17d]

I.4. Cascade Reactions

Cascade reactions are also termed as 'domino', 'tandem', 'sequential,' or 'one-pot'/'one-flask' reactions in which multiple transformations are carried out one after another in a single reaction vessel. The key feature in the cascade synthesis is that at least two transformations must happen and each conversion step should be dependent on functionality generated in the earlier step of the cascade event. The cascade approach avoids the requirement of isolation of the reactive intermediates, thus reducing cost, waste, and time for organic synthesis. Also, being a one-pot process, all the elementary reactions of the cascade event proceed under a single reaction condition, avoiding interim work-up and purification steps. Thus, traditional step-by-step synthesis can be replaced with upgraded or integrated synthesis to speed up the synthetic process. Overall, an economical and easier way has evolved through a cascade strategy to create complex molecular entities.[18a-d]

The reaction integration in cascade methodology can be achieved in the following ways[18b]

(i) By mixing all the components at once to perform the sequence of reactions.

(ii) By time integration *i.e.*, adding the reaction components in a single reactor at intervals of time to complete the required transformations.

(iii) Or by space integration *i.e.*, performing the reactions in a continuous flow method where elementary reactions are carried out in different reactors situated at different locations in space of the continuous flow system.

The undeniable benefits of the cascade processes have made it as an intellectual tool for constructing step-economical synthesis of the targeted molecules.[18e,f] Over the years, a large variety of cascade approaches have emerged for the synthesis of considerable structurally and stereo-chemically complex molecules including total synthesis of natural products.[18a] Here, we have discussed a few of them that lead to the construction of heterocycles or carbocycles through cascade cycloaddition or C–H activation strategy.

In 2021, Dash *et al.* established a cascade strategy involving initial (3 + 2) cycloaddition, 1,2-acyl migration, and subsequent hydrolysis in a single step all within 2 hours of reaction time. They executed this strategy utilizing ethyl azidoformate and alkyne as two coupling partners. Under the presence of catalytic CuI and ligand prolinamide in aqueous media, both coupling partners reacted regio-selectively to furnish N^2-carboxyalkylated triazoles rather than N^1-carboxyalkylated triazoles. The substituted triazoles can be further hydrolyzed in the presence of Cu salt and prolinamide catalyst in a cascade fashion if kept for a longer duration. This leads to free 2*H*-1,2,3-triazoles through the removal of N^2-carboxyalkyl functional groups (Scheme I.4.1).[18h]

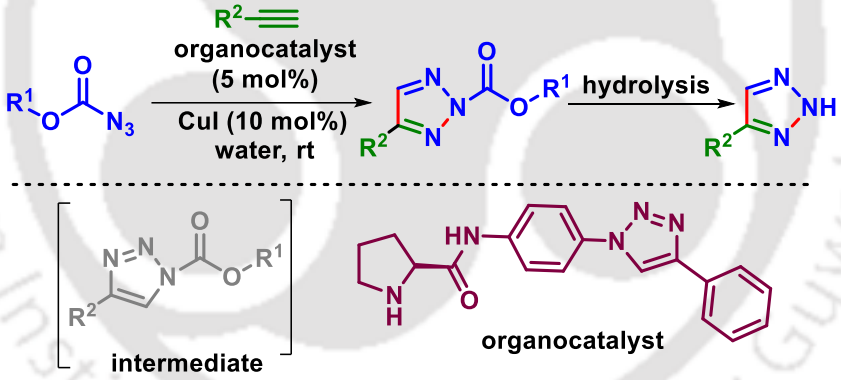

Scheme I.4.1. *Cascade regioselective synthesis of 1,2,3-triazoles in water.*

In 2015 Xu and Yi group developed a one-pot Rh(III)-catalyzed cascade strategy for construction of *N*-methoxyisoquinolinediones. The cascade methodology involves regio-selectively carbenoid insertion C–H activation into *N*-methoxybenzamide with cyclic α-diazotized Meldrum's acid and subsequent cyclization to deliver *N*-methoxyisoquinolinediones (Scheme I.4.2).[18i]

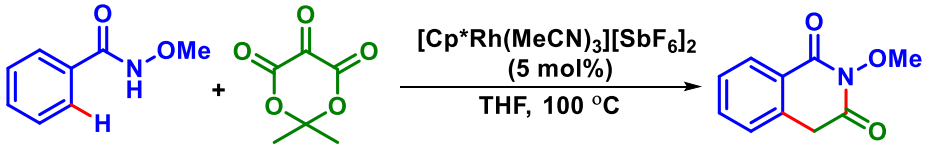

Scheme I.4.2. *One-pot synthesis of N-methoxyisoquinolinedione.*

Extending the cascade strategy, Huang and Yang group in 2021 reported the synthesis of 3-substituted phthalides from carboxylic acids and cyclopropanols through a cascade event of C–H activation/ring opening and C–C cleavage/cyclization. The reaction proceeds with initial C–H activation of aryl carboxylic acid by Rh(III) catalyst and subsequent ring opening and cyclization of cyclopropanols in a cascade way to deliver substituted phthalides (Scheme I.4.3).[18j]

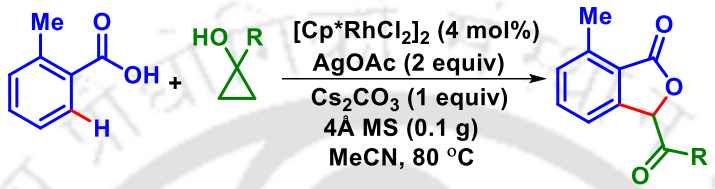

Scheme I.4.3. *Cascade C–H activation and C–C cleavage.*

In 2023, Parasram group developed a photoinduced cascade arylation/cyclization strategy for phenanthrene synthesis. This simple and mild photochemical setup involves initial photo-induced homolysis of aryl iodide bond to form aryl radical. Then, radical recombination to diphenylethylene gives stilbene intermediate which follows a Mallory-type cyclization in the presence of *in situ* formed iodine and delivers phenanthrene. Thus, this cascade strategy provides an efficient route to unsymmetrical phenanthrenes without using any transition metal or Lewis acid catalyst (Scheme I.4.4).[18k]

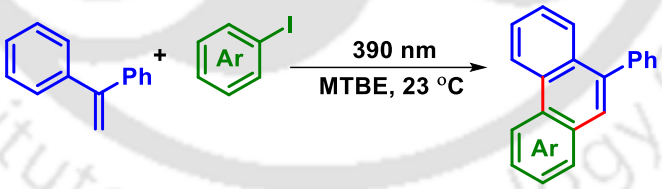

Scheme I.4.4. *Photo-induced cascade synthesis of phenanthrene.*

I.5. Conclusion

In conclusion, cycloaddition/annulation and C–H activation are presented as two remarkable strategies for synthesizing diverse heterocycles. The construction of heterocycles through these two approaches can be extended to deliver important bioactive molecules or effective natural products. The cascade version of these two methodologies offers step and atom-economical ways to deliver *N* or *O*-heterocycles. The appropriate pick of the coupling

partners and effective design of the starting materials can lead to the construction of efficient heterocycles by saving time as well as money through a cascade way. Thus, throughout this thesis, we report newer cascade (3 + 2) cycloaddition and C–H functionalization of some previously unexplored starting precursors.

I.6. References

[1] (a) Lipkus, A. H.; Yuan, Q.; Lucas, K. A.; Funk, S. A.; Bartelt, W. F.; Schenck, R. J.; Trippe, A. J. *J. Org. Chem.* **2008**, *73*, 4443–4451. (b) Brown, D. G.; Wobst, H. J. *J. Med. Chem.* **2021**, *64*, 2312–2338. (c) Benedetto Tiz, D.; Bagnoli, L.; Rosati, O.; Marini, F.; Sancineto, L.; Santi, C. *Molecules* **2022**, *27*, 1643. (d) De Coen, L. M.; Heugebaert, T. S. A.; García, D.; Stevens, C. V. *Chem. Rev.* **2016**, *116*, 80–139. (e) Bhardwaj, V.; Gumber, D.; Abbot, V.; Dhiman, S.; Sharma, P. *RSC Adv.* **2015**, *5*, 15233–15266. (f) Kalaria, P. N.; Karad, S. C.; Raval, D. K. *Eur. J. Med. Chem.* **2018**, *158*, 917–936. (g) Egan, T. J.; Ncokazi, K. K. *J. Inorg. Biochem.* **2005**, *99*, 1532–1539. (h) Ma, T.; Liu, L.; Xue, H.; Li, L.; Han, C.; Wang, L.; Chen, Z.; Liu, G. *J. Med. Chem.* **2008**, *51*, 1432–1446. (i) Tiwari, G.; Khanna, A.; Mishra, V. K.; Sagar, R. *RSC Adv.* **2023**, *13*, 32858–32892. (j) Singh, P. K.; Silakari, O. *ChemMedChem* **2018**, *13*, 1071–1087. (k) Heravi, M. M.; Ghanbarian, M.; Zadsirjan, V.; Alimadadi Jani, B. *Monatsh Chem* **2019**, *150*, 1365–1407.

[2] (a) Luo, J.; Chen, G.; Chen, S.; Li, Z.; Liu, Y. *Chem. Eur. J.* **2021**, *27*, 6598–6619. (b) Gulevich, A. V.; Zhdanko, A. G.; Orru, R. V. A.; Nenajdenko, V. G. *Chem. Rev.* **2010**, *110*, 5235–5331. (c) Lygin, A. V.; de Meijere, A. *Angew. Chem. Int. Ed.* **2010**, *49*, 9094–9124. (d) Ito, Y.; Sawamura, M.; Hayashi, T. *Tetrahedron Lett.* **1987**, *28*, 6215–6218. (e) Efimov, I. V.; Kulikova, L. N.; Zhilyaev, D. I.; Voskressensky, L. G. *Eur. J. Org. Chem.* **2020**, *2020*, 7284–7303. (f) Wang, Y.; Zhang, C.; Li, S.; Liu, L.; Feng, X.; Liu, G. *Eur. J. Org. Chem.* **2023**, *26*, e202300323. (g) Arróniz, C.; Gil-González, A.; Semak, V.; Escolano, C.; Bosch, J.; Amat, M. *Eur. J. Org. Chem.* **2011**, *2011*, 3755–3760. (h) Giustiniano, M.; Basso, A.; Mercalli, V.; Massarotti, A.; Novellino, E.; Tron, G. C.; Zhu, J. *Chem. Soc. Rev.* **2017**, *46*, 1295–1357.

[3] (a) Kaur, T.; Wadhwa, P.; Sharma, A. *RSC Adv.* **2015**, *5*, 52769–52787. (b) De La Campa, R.; Ortín, I.; Dixon, D. J. *Angew. Chem. Int. Ed.* **2015**, *54*, 4895–4898. (c) Franchino, A.; Jakubec, P.; Dixon, D. J. *Org. Biomol. Chem.* **2016**, *14*, 93–96. (d) Zhang, Z.-W.; Lu, G.; Chen, M.-M.; Lin, N.; Li, Y.-B.; Hayashi, T.; Chan, A. S. C. *Tetrahedron: Asymmetry*

2010, *21*, 1715–1721. (e) Nakamura, S.; Maeno, Y.; Ohara, M.; Yamamura, A.; Funahashi, Y.; Shibata, N. *Org. Lett.* **2012**, *14*, 2960–2963. (f) De La Campa, R.; Gammack Yamagata, A. D.; Ortín, I.; Franchino, A.; Thompson, A. L.; Odell, B.; Dixon, D. J. *Chem. Commun.* **2016**, *52*, 10632–10635. (g) Padilla, S.; Adrio, J.; Carretero, J. C. *J. Org. Chem.* **2012**, *77*, 4161–4166. (h) Liao, J.-Y.; Shao, P.-L.; Zhao, Y. *J. Am. Chem. Soc.* **2015**, *137*, 628–631. (i) Monge, D.; Jensen, K. L.; Marín, I.; Jørgensen, K. A. *Org. Lett.* **2011**, *13*, 328–331.

[4] (a) Serdyuk, O.; Muzalevskiy, V.; Nenajdenko, V. *Synthesis* **2012**, *44*, 2115–2137. (b) Liu, J.-Q.; Shen, X.; Wang, Y.; Wang, X.-S.; Bi, X. *Org. Lett.* **2018**, *20*, 6930–6933. (c) Zhao, C.; Gu, M.-Z.; Chen, Y.-Y.; Hu, X.-W.; Xu, Y.-B.; Lin, X.-M.; Liu, X.-N.; Chen, L.; Chen, G.-S.; Liu, Y.-L. *Org. Biomol. Chem.* **2022**, *20*, 8623–8627. (d) Wang, Z.-P.; Xiang, S.; Shao, P.-L.; He, Y. *J. Org. Chem.* **2018**, *83*, 10995–11007. (e) Martínez-Pardo, P.; Blay, G.; Muñoz, M. C.; Pedro, J. R.; Sanz-Marco, A.; Vila, C. *Chem. Commun.* **2018**, *54*, 2862–2865.

[5] (a) Laviós, A.; Sanz-Marco, A.; Vila, C.; Muñoz, M. C.; Pedro, J. R.; Blay, G. *Org. Lett.* **2022**, *24*, 2149–2154. (b) Silyanova, E. A.; Samet, A. V.; Salamandra, L. K.; Khrustalev, V. N.; Semenov, V. V. *Eur. J. Org. Chem.* **2020**, *2020*, 2093–2100. (c) Qi, X.; Xiang, H.; Yang, C. *Org. Lett.* **2015**, *17*, 5590–5593. (d) Abozeid, M. A.; Kim, H. Y.; Oh, K. *Org. Lett.* **2022**, *24*, 1812–1816. (e) Shaabani, A.; Sepahvand, H.; Bazgir, A.; Khavasi, H. R. *Tetrahedron* **2018**, *74*, 7058–7067.

[6] (a) Bonne, D.; Dekhane, M.; Zhu, J. *Angew. Chem. Int. Ed.* **2007**, *46*, 2485–2488. (b) Wang, L.; Huang, Z.; Guo, X.; Liu, J.; Dong, J.; Xu, X. *Chem. Commun.* **2022**, *58*, 6433–6436.

[7] (a) Dyker, G. *Angew. Chem. Int. Ed.* **1999**, *38*, 1698–1712. (b) Crabtree, R. H.; Lei, A. *Chem. Rev.* **2017**, *117*, 8481–8482. (c) Dalton, T.; Faber, T.; Glorius, F. *ACS Cent. Sci.* **2021**, *7*, 245–261. (d) Li, C.-J. *Acc. Chem. Res.* **2009**, *42*, 335–344. (e) Tian, T.; Li, Z.; Li, C.-J. *Green Chem.* **2021**, *23*, 6789–6862. (f) Girard, S. A.; Knauber, T.; Li, C. *Angew. Chem. Int. Ed.* **2014**, *53*, 74–100.

[8] (a) Newhouse, T.; Baran, P. S.; Hoffmann, R. W. *Chem. Soc. Rev.* **2009**, *38*, 3010. (b) Gaich, T.; Baran, P. S. *J. Org. Chem.* **2010**, *75*, 4657–4673. (c) Campeau, L.-C.; Hazari, N. *Organometallics* **2019**, *38*, 3–35. (d) Littke, A. F.; Fu, G. C. *Angew. Chem. Int. Ed.*

2002, *41*, 4176–4211. (e) Gildner, P. G.; Colacot, T. J. *Organometallics* **2015**, *34*, 5497–5508.

[9] (a) Chen, Z.; Wang, B.; Zhang, J.; Yu, W.; Liu, Z.; Zhang, Y. *Org. Chem. Front.* **2015**, *2*, 1107–1295. (b) Arockiam, P. B.; Bruneau, C.; Dixneuf, P. H. *Chem. Rev.* **2012**, *112*, 5879–5918. (c) Li, X.; Ouyang, W.; Nie, J.; Ji, S.; Chen, Q.; Huo, Y. *ChemCatChem* **2020**, *12*, 2358–2384. (d) Colby, D. A.; Bergman, R. G.; Ellman, J. A. *Chem. Rev.* **2010**, *110*, 624–655. (e) Ujwaldev, S. M.; Harry, N. A.; Divakar, M. A.; Anilkumar, G. *Catal. Sci. Technol.* **2018**, *8*, 5983–6018. (f) Mei, R.; Dhawa, U.; Samanta, R. C.; Ma, W.; Wencel-Delord, J.; Ackermann, L. *ChemSusChem* **2020**, *13*, 3306–3356. (g) Chatani, N. *Acc. Chem. Res.* **2023**, *56*, 3053–3064. (h) Guo, X.-X.; Gu, D.-W.; Wu, Z.; Zhang, W. *Chem. Rev.* **2015**, *115*, 1622–1651.

[10] (a) Meng, G.; Lam, N. Y. S.; Lucas, E. L.; Saint-Denis, T. G.; Verma, P.; Chekshin, N.; Yu, J.-Q. *J. Am. Chem. Soc.* **2020**, *142*, 10571–10591. (b) Murali, K.; Machado, L. A.; Carvalho, R. L.; Pedrosa, L. F.; Mukherjee, R.; Da Silva Júnior, E. N.; Maiti, D. *Chem. Eur. J.* **2021**, *27*, 12453–12508. (c) Zhao, B.; Prabagar, B.; Shi, Z. *Chem* **2021**, *7*, 2585–2634.

[11] (a) Lewis, L. N.; Smith, J. F. *J. Am. Chem. Soc.* **1986**, *108*, 2728–2735. (b) Pastine, S. J.; Gribkov, D. V.; Sames, D. *J. Am. Chem. Soc.* **2006**, *128*, 14220–14221. (c) Yang, X.-F.; Hu, X.-H.; Feng, C.; Loh, T.-P. *Chem. Commun.* **2015**, *51*, 2532–2535. (d) Zhu, X.; Su, J.-H.; Du, C.; Wang, Z.-L.; Ren, C.-J.; Niu, J.-L.; Song, M.-P. *Org. Lett.* **2017**, *19*, 596–599. (e) Zaitsev, V. G.; Shabashov, D.; Daugulis, O. *J. Am. Chem. Soc.* **2005**, *127*, 13154–13155. (f) Corbet, M.; De Campo, F. *Angew. Chem. Int. Ed.* **2013**, *52*, 9896–9898. (g) Gutekunst, W. R.; Gianatassio, R.; Baran, P. S. *Angew. Chem. Int. Ed.* **2012**, *51*, 7507–7510. (h) Liu, B.; Huang, X.; Wang, X.; Ge, Z.; Li, R. *Org. Chem. Front.* **2015**, *2*, 797–800. (i) Mei, R.; Wang, H.; Warratz, S.; Macgregor, S. A.; Ackermann, L. *Chem. Eur. J.* **2016**, *22*, 6759–6763. (j) Zhang, S.-K.; Yang, X.-Y.; Zhao, X.-M.; Li, P.-X.; Niu, J.-L.; Song, M.-P. *Organometallics* **2015**, *34*, 4331–4339. (k) Hao, X.-Q.; Du, C.; Zhu, X.; Li, P.-X.; Zhang, J.-H.; Niu, J.-L.; Song, M.-P. *Org. Lett.* **2016**, *18*, 3610–3613.

[12] (a) Sambiagio, C.; Schönbauer, D.; Blieck, R.; Dao-Huy, T.; Pototschnig, G.; Schaaf, P.; Wiesinger, T.; Zia, M. F.; Wencel-Delord, J.; Besset, T.; Maes, B. U. W.; Schnürch, M. *Chem. Soc. Rev.* **2018**, *47*, 6603–6743. (b) Schröter, S.; Stock, C.; Bach, T. *Tetrahedron*

2005, *61*, 2245–2267. (c) Murakami, K.; Yamada, S.; Kaneda, T.; Itami, K. *Chem. Rev.* **2017**, *117*, 9302–9332. (d) Ye, M.; Gao, G.-L.; Yu, J.-Q. *J. Am. Chem. Soc.* **2011**, *133*, 6964–6967. (e) Hyodo, I.; Tobisu, M.; Chatani, N. *Chem. Asian J.* **2012**, *7*, 1357–1365.

[13] (a) Rej, S.; Chatani, N. *Angew. Chem. Int. Ed.* **2019**, *58*, 8304–8329. (b) Zhang, F.; Spring, D. R. *Chem. Soc. Rev.* **2014**, *43*, 6906–6919. (c) Li, B.; Ma, J.; Liang, Y.; Wang, N.; Xu, S.; Song, H.; Wang, B. *Eur. J. Org. Chem.* **2013**, *2013*, 1950–1962. (d) Zhang, Y.; Zhao, H.; Wang, H.; Wei, J.; Shi, Z. *Angew. Chem. Int. Ed.* **2015**, *54*, 13686–13690. (e) Jia, X.; Xing, D.; Shen, J.; Li, B.; Zeng, Y.; Jiang, H.; Huang, L. *Org. Lett.* **2024**, *26*, 1544–1549. (f) Gao, K.; Yoshikai, N. *Angew. Chem. Int. Ed.* **2011**, *50*, 6888–6892.

[14] (a) Liao, G.; Zhang, T.; Lin, Z.-K.; Shi, B.-F. *Angew. Chem. Int. Ed.* **2020**, *59*, 19773–19786. (b) Gandeepan, P.; Ackermann, L. *Chem* **2018**, *4*, 199–222. (c) Zhao, Q.; Poisson, T.; Pannecoucke, X.; Besset, T. *Synthesis* **2017**, *49*, 4808–4826. (d) Lewis, L. N. *Inorg. Chem.* **1985**, *24*, 4433–4435. (e) Zhang, F.-L.; Hong, K.; Li, T.-J.; Park, H.; Yu, J.-Q. *Science* **2016**, *351*, 252–256. (f) Chen, X.-Y.; Ozturk, S.; Sorensen, E. J. *Org. Lett.* **2017**, *19*, 6280–6283. (g) Catellani, M.; Frignani, F.; Rangoni, A. *Angew. Chem. Int. Ed.* **1997**, *36*, 119–122. (h) Della Ca', N.; Fontana, M.; Motti, E.; Catellani, M. *Acc. Chem. Res.* **2016**, *49*, 1389–1400. (i) Li, W.; Cao, M.; Zhang, C.; Shi, S.; Liu, J.; Li, W.; Zhang, X.; Yu, Y.; Li, T. *Org. Lett.* **2024**, *26*, 1143–1147.

[15] (a) Preshlock, S. M.; Plattner, D. L.; Maligres, P. E.; Krska, S. W.; Maleczka, R. E.; Smith, M. R. *Angew. Chem. Int. Ed.* **2013**, *52*, 12915–12919. (b) Rani, G.; Luxami, V.; Paul, K. *Chem. Commun.* **2020**, *56*, 12479–12521. (c) Font, M.; Quibell, J. M.; Perry, G. J. P.; Larrosa, I. *Chem. Commun.* **2017**, *53*, 5584–5597. (d) Maehara, A.; Tsurugi, H.; Satoh, T.; Miura, M. *Org. Lett.* **2008**, *10*, 1159–1162. (e) Zarkadoulas, A.; Zgouleta, I.; Tzouras, N. V.; Vougioukalakis, G. C. *Catalysts* **2021**, *11*, 554. (f) Dutta, S.; Bhattacharya, T.; Geffers, F. J.; Bürger, M.; Maiti, D.; Werz, D. B. *Chem. Sci.* **2022**, *13*, 2551–2573. (g) Fu, Z.; Jiang, Y.; Wang, S.; Song, Y.; Guo, S.; Cai, H. *Org. Lett.* **2019**, *21*, 3003–3007. (h) Dey, A.; Volla, C. M. R. *Org. Lett.* **2020**, *22*, 7480–7485. (i) Zhang, G.; Li, M.-Y.; Ye, W.-B.; He, Z.-T.; Feng, C.-G.; Lin, G.-Q. *Org. Lett.* **2021**, *23*, 2948–2953. (j) Li, X.-C.; Du, C.; Zhang, H.; Niu, J.-L.; Song, M.-P. *Org. Lett.* **2019**, *21*, 2863–2866.

[16] (a) Kuhl, N.; Hopkinson, M. N.; Wencel-Delord, J.; Glorius, F. *Angew. Chem. Int. Ed.* **2012**, *51*, 10236–10254. (b) Ackerman, L. J.; Sadighi, J. P.; Kurtz, D. M.; Labinger, J.

A.; Bercaw, J. E. *Organometallics* **2003**, *22*, 3884–3890. (c) He, J.; Wasa, M.; Chan, K. S. L.; Shao, Q.; Yu, J.-Q. *Chem. Rev.* **2017**, *117*, 8754–8786. (d) Xu, Y.; Dong, G. *Chem. Sci.* **2018**, *9*, 1424–1432. (e) Chen, Z.; Rong, M.-Y.; Nie, J.; Zhu, X.-F.; Shi, B.-F.; Ma, J.-A. *Chem. Soc. Rev.* **2019**, *48*, 4921–4942. (f) Das, S.; Incarvito, C. D.; Crabtree, R. H.; Brudvig, G. W. *Science* **2006**, *312*, 1941–1943.

[17] (a) Dey, A.; Sinha, S. K.; Achar, T. K.; Maiti, D. *Angew. Chem. Int. Ed.* **2019**, *58*, 10820–10843. (b) Dutta, U.; Maiti, S.; Bhattacharya, T.; Maiti, D. *Science* **2021**, *372*, eabd5992. (c) Sinha, S. K.; Guin, S.; Maiti, S.; Biswas, J. P.; Porey, S.; Maiti, D. *Chem. Rev.* **2022**, *122*, 5682–5841. (d) Das, J.; Guin, S.; Maiti, D. *Chem. Sci.* **2020**, *11*, 10887–10909.

[18] (a) Nicolaou, K. C.; Edmonds, D. J.; Bulger, P. G. *Angew. Chem. Int. Ed.* **2006**, *45*, 7134–7186. (b) Yadav, M. K.; Chowdhury, S. *Green Chem.* **2023**, *25*, 10144–10181. (c) Huang, H.-M.; Garduño-Castro, M. H.; Morrill, C.; Procter, D. J. *Chem. Soc. Rev.* **2019**, *48*, 4626–4638. (d) Shivam; Tiwari, G.; Kumar, M.; Chauhan, A. N. S.; Erande, R. D. *Org. Biomol. Chem.* **2022**, *20*, 3653–3674. (e) Tietze, L. F. *Chem. Rev.* **1996**, *96*, 115–136. (f) Pellissier, H. *Tetrahedron* **2006**, *62*, 2143–2173. (g) Pellissier, H. *Adv. Synth. Catal.* **2020**, *362*, 2289–2325. (h) Chakraborti, G.; Mandal, T.; Roy, C. P.; Dash, J. *Chem. Commun.* **2021**, *57*, 7970–7973. (i) Shi, J.; Zhou, J.; Yan, Y.; Jia, J.; Liu, X.; Song, H.; Xu, H. E.; Yi, W. *Chem. Commun.* **2015**, *51*, 668–671. (j) Wang, S.; Miao, E.; Wang, H.; Song, B.; Huang, W.; Yang, W. *Chem. Commun.* **2021**, *57*, 5929–5932. (k) Li, Y.; Wise, D. E.; Mitchell, J. K.; Parasram, M. *J. Org. Chem.* **2023**, *88*, 717–721.

CHAPTER II

Synthesis of Chromeno-pyrroles (Azacoumestans) from Functionalized Enones and Alkyl Isocyanoacetates

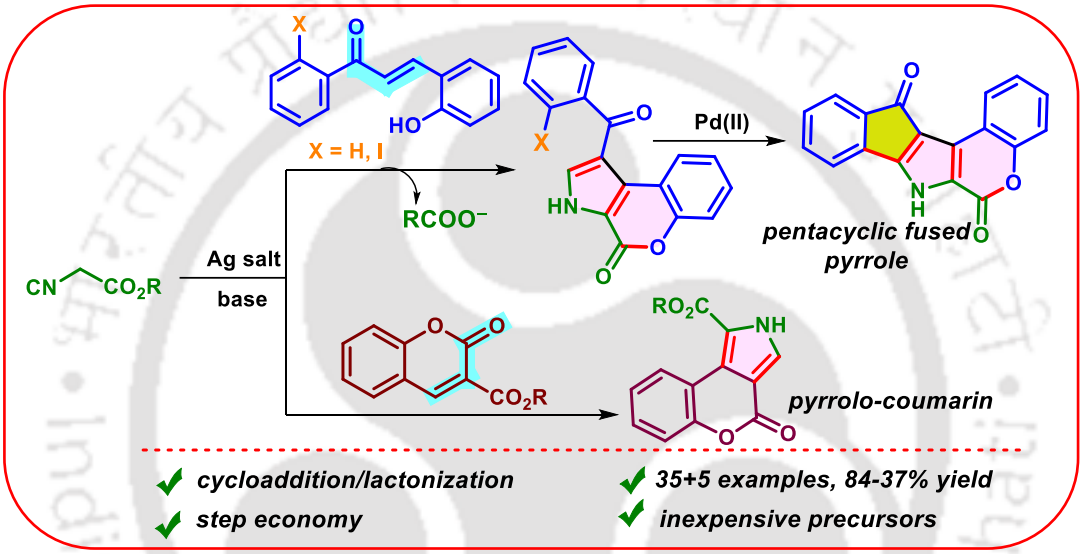

OL Organic Letters

Org. Lett. **2023**, *25*, 5209−5213.

pubs.acs.org/OrgLett Letter

ABSTRACT: ***Elegant synthetic strategies for chromeno-pyrroles (azacoumestans) have been devised via cycloaddition of 2-hydroxychalcone/cyclic enones and alkyl isocyanoacetate, followed by lactonization. Herein, ethyl isocyanoacetate acts as a C–NH–C–C=O synthon contrary to its hitherto applications as a C–NH–C synthon. Subsequently, pentacyclic fused pyrroles were also constructed from the o-iodo benzoyl chromeno-pyrroles using Pd(II) catalyst.***

CHAPTER II

Synthesis of Chromeno-pyrroles (Azacoumestans) from Functionalized Enones and Alkyl Isocyanoacetates

II.1. Introduction

Azacoumestans, specifically chromenopyrroles, are found in marine natural products and synthetic compounds.[1] Among them, lamellarins and ningalin B, are a class of marine alkaloids, having a pyrrole polyaromatic core differing in the substitution pattern and the arrangement of rings (Figure II.1.1).[2] Since the first discovery of lamellarin A–D by Faulkner in 1985, more than 50 lamellarins have been isolated from diverse marine organisms such as mollusks, sponges, and tunicates.[2f] Most of those isolated lamellarins possess a fused pentacyclic ring system as a common structural moiety and are called type I lamellarin. The aromatic rings of the type I lamellarins are heavily substituted by hydroxy or methoxy groups. A few lamellarins contain much simpler non-fused 3,4-diarylpyrrole-2-carboxylate scaffold and are called type II lamellarins. These pentacyclic lamellarins core are composed of pyrrolocoumarin and isoquinoline segments which suggest that these lamellarins could be synthesized from these heterocycles.

The ability of the nitrogen atoms of pyrrolocoumarin ring to form extra hydrogen bonds helps in binding to the active site of biological targets. A few of them have shown various potent biological activities, including anti-tumor, anti-HIV-1 activity at non-cytotoxic concentrations, immunomodulatory activity, multidrug-resistant (MDR) reversal, analgesic activity, and are important precursors for the antibiotic martinelline.[3a] Many lamellarins displayed biological effects both on mammalian cells and viruses, including antiproliferative, cytotoxicity, etc. This type of core structure is also present in novel drug candidates, such as a series of LAM-D derivatives, which show promising activity such as topoisomerase I inhibitor.[2g-h,3] Some pyrrolocoumarin rings are known for their susceptibility to oxidation upon UV irradiation which makes them potential candidates for organic redox switches.[3]

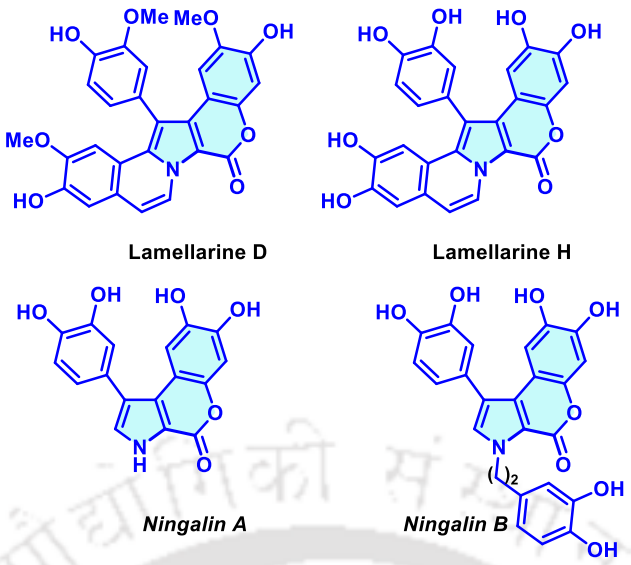

Figure II.1.1. *Bioactive pyrrolo-coumarins.*

II.2. Strategies for the Construction of Azacoumestans

Due to their potential biological activities and functional properties, several synthetic routes involving multi-step condensation, cyclization, and subsequent lactonization have been developed.[4] The synthesis of pyrrolocoumarin can be divided into following two categories-

(i) Multi-step synthesis of functionalized pyrrole and subsequent lactonization.

(ii) Transition metal-catalyzed coupling of functionalized coumarin.

Syntheses through the first category involve introduction of aryl moiety at position 3 of the pyrrole ring and a carboxy group at position 2. Carboxy group eventually brings lactonization with the help of a properly substituted hydroxy group of aryl ring at position 3.[2b,4f-g] The second approach involves the well-known pyrrole synthetic methodology such as Paal-Knorr, Hantch, Barton-Zard reactions, and interaction of α-aminoester with α,β-unsaturated carbonyl compounds, cyclization of properly substituted 3-aminocoumarin, etc.[4d,f,h]

II.2.1. Synthesis of pyrrolocoumarin *via* multi-step synthesis of functionalized pyrrole and subsequent lactonization.

Okano *et al.* described a methodology for the total synthesis of lamellarins *via* a one-pot halogen dance/Neigshi coupling of lithiated dibromopyrrole derivative.[5a] The easily available dibromo pyrrole having an ester moiety quickly underwent halogen dance at –78 °C. Subsequent modification with transition metal smoothly delivers lamellarin derivatives (Scheme II.2.1).

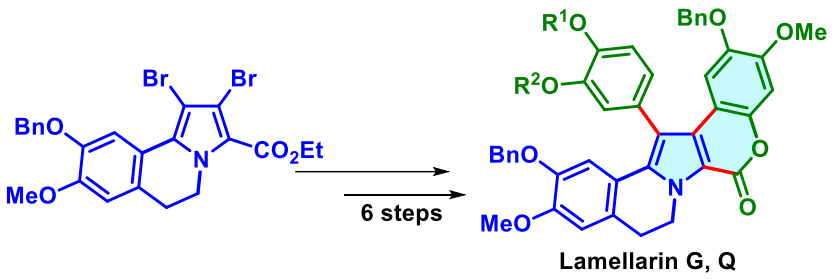

Scheme II.2.1. *A bottom-up synthesis of lamellarin derivatives.*

Ackermann *et al*. reported a sustainable Ru(II) catalyzed oxidative alkyne annulation for the step-economical synthesis of lamellarin alkaloids.[5b] This transition metal catalyzed strategy proceeded with a couple of C–H/N–H activation of enamides which leads to the generation of key pyrrole intermediate. Subsequent Suzuki-Miyaura-based coupling delivers tetrasubstituted chromenopyrrole which on further modification leads to lamellarin H and D (Scheme II.2.2).

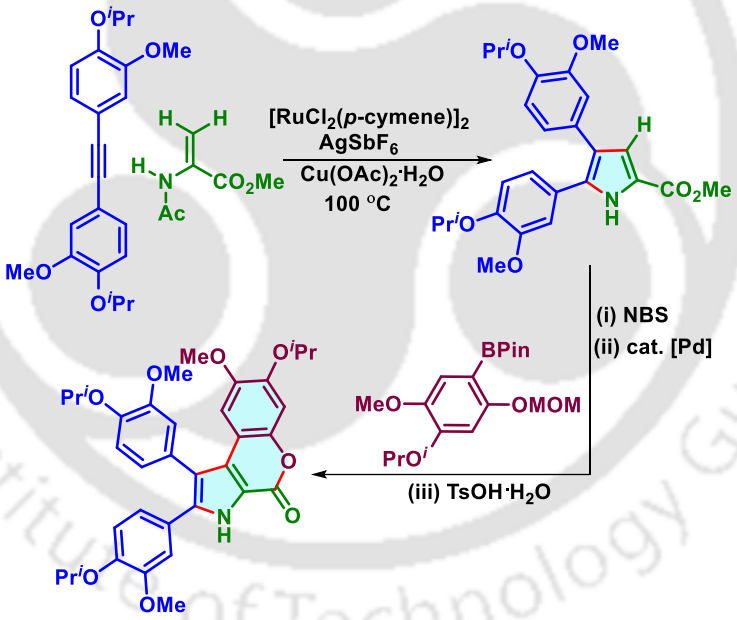

Scheme II.2.2. *Ru-catalyzed oxidative annulation for the synthesis of lamellarins.*

Donohoe *et al.* explored the synthetic utility of OBO ester (oxabicyclo[2.2.2]octyl orthoester) masked α-keto acid as a key intermediate in the synthesis of lamellatrin alkaloids.[4b] The one-pot strategy leads to the construction of a 1,4-dicarbonyl fragment from masked α-keto ester which eventually undergoes condensation to pyrrole core. Subsequent deprotection of phenol assists in the lactonization to give pyrrolocoumarin in good yield (Scheme II.2.3).

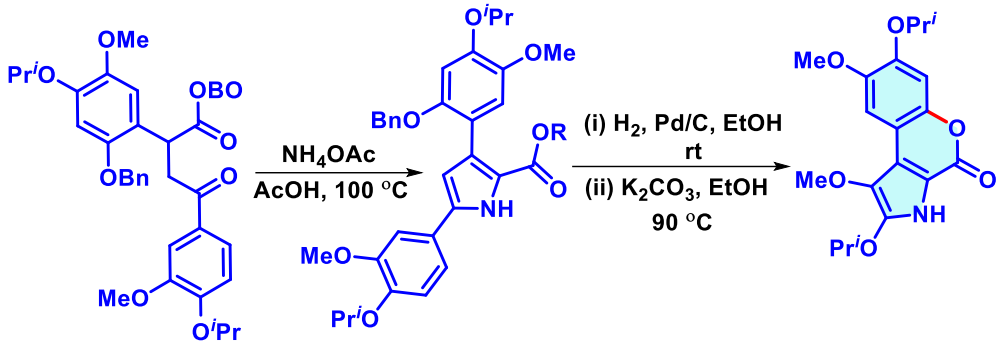

Scheme II.2.3. *Synthesis of lamellarin derivatives from masked α-keto ester.*

Samet group disclosed a methodology for the synthesis of pyrrolocoumarin utilizing methylated pyrrole.[5c] Selective demethylation with 1 equiv. BBr_3 and subsequent base-promoted cyclization deliver hexacyclic methylated lamellarin core. On the other hand, in the presence of excess BBr_3 complete demethylated product could be achieved (Scheme II.2.4).

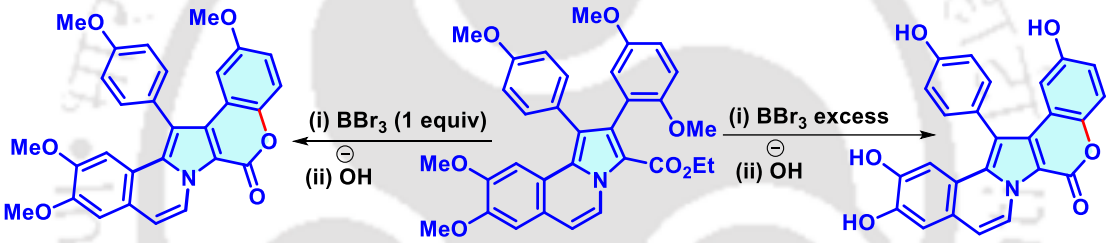

Scheme II.2.4*. BBr_3-catalyzed and base-induced cyclization.*

II.2.2. Synthesis of pyrrolocoumarin *via* transition metal-catalyzed coupling of functionalized coumarin.

Some of the protocols adopt transition metal-catalyzed dehydrogenative coupling or cyclization of pre-functionalized coumarins.[6] Chen and Xu group disclosed a base-free atom-economic Pd-catalyzed cross-dehydrogenative coupling (CDC) for the synthesis of indole-fused polyheterocycle.[7a] The strategy delivers a diverse array of targeted polyheteroycles from differently substituted 4-aniline coumarin (Scheme II.2.5).

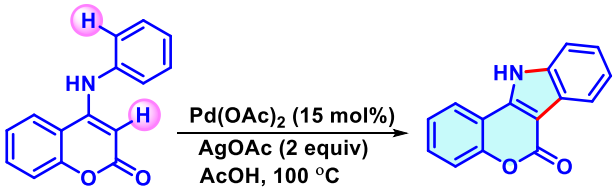

Scheme II.2.5. *CDC strategy for synthesis of indole-fused polyheterocycle.*

Samanta *et al*. developed a weakly coordinated *tert-amide-directed* protocol for the synthesis of azacoumestans. This Ru(II)-catalyzed cyclization utilized corresponding azaheterocycle derivatives and diazonaphthoquinones as coupling partners and delivers diverse azacoumestans including bioactive natural compound isolamellarin A and B. The methodology proceeded through the migratory insertion of quinoid carbene followed by Brønsted-acid mediated cyclization (Scheme II.2.6).[4e]

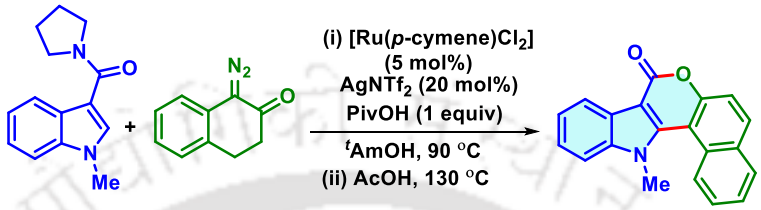

Scheme II.2.6. *Ru(II)-catalyzed cyclization for synthesis of azacoumestans.*

An efficient one-pot strategy for the construction of pyrrolocoumarin scaffolds was reported by Weng and Yang group in 2019.[6b] The protocol proceeded through coupling of 4-chloro-3-nitrocoumarin and 1-styrylpyrrolidine in the key step and reduction and cyclization *via* nitro functionality in the subsequent step. The protocol was then successfully extended for the synthesis of ningalin B in five linear steps with an overall yield of 41.5% (Scheme II.2.7).

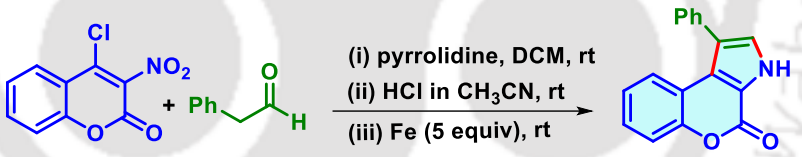

Scheme II.2.7. *One-pot strategy for synthesis of chromenopyrrole.*

A similar kind of approach was designed by Xu and Chen for the synthesis of these polycyclic hetero skeletons.[6d] The key strategy involves construction of a pyrrole ring through Pd-catalyzed intramolecular hydroamination of corresponding acetylenic aminocoumarins. Through this expeditious protocol polyheterocyclic lamellarin scaffold was synthesized in four steps with 73% yield (Scheme II.2.8).

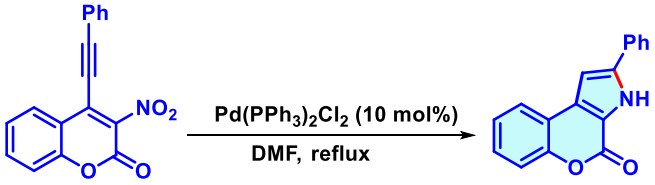

Scheme II.2.8. *Pd-catalyzed intramolecular coupling for synthesis of pyrrolocoumarin.*

Saito and Mutoh *et al*. developed a Ru(II)-catalyzed cycloisomerization of 3-amino-4-alkynylcoumarin for the synthesis of chromenopyrrole.[6e] The said protocol was extended for formal total synthesis of marine natural products ningalin B, lamellarin H (Scheme II.2.9).

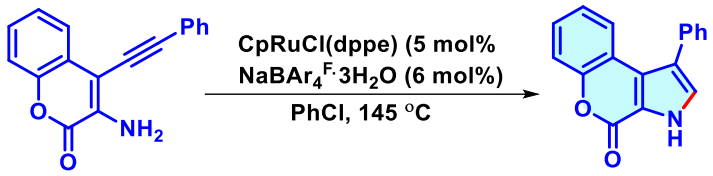

Scheme II.2.9. *Synthesis of pyrrolocoumarin via Ru-catalyzed cycloisomerization.*

Another methodology designed by Langer *et al*. demonstrated the step-economical synthesis of pyrrolocoumarin subunit.[7b] In this protocol, the key step is the formation of a pyrrole ring *via* Pd-catalyzed one-pot sequential C–N coupling/intramolecular hydroamination of 3-bromo-4-ethynylcoumarin (Scheme II.2.10).

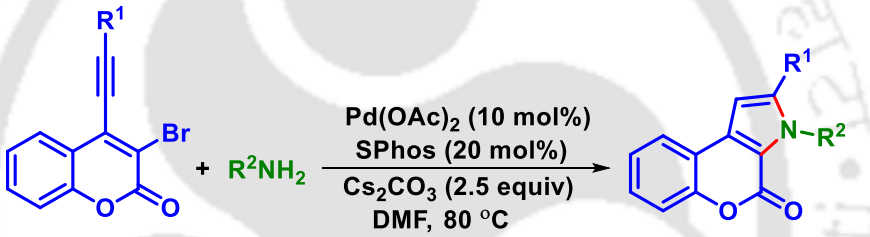

Scheme II.2.10. *Synthesis of pyrrolocoumarin via Pd-catalyzed coupling.*

Saahbani *et al*. disclosed a cyclization strategy for the synthesis of chromenopyrrole from 3-acetyl coumarin.[7c] Under alcoholic conditions, the acetyl group of the starting precursors gets eliminated and TosMIC (*p*-tosyl methyl isocyanide) preferentially adds to the double bond of cyclic enone to deliver the desired polyheterocycle (Scheme II.2.11).

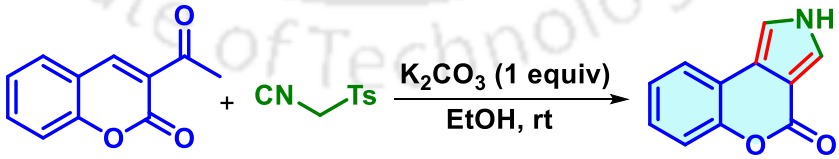

Scheme II.2.11. *Synthesis of chromenopyrrole from 3-acetyl coumarin.*

Alkyl isocyanoacetates are efficient 1,3-dipolar coupling partners towards a range of annulation/cycloaddition reactions.[8] The presence of three reactive centres *viz*., acidic CH unit, isocyanide unit, and a neighbouring ester makes this molecule a versatile reagent for construction of *N*-heterocycles. In the presence of a base and Ag salt, they undergo

cycloaddition (non-concerted) with dipolarophiles providing diverse heterocycles (Scheme II.2.12).[8e] In most of these reactions, alkyl isocyanoacetate delivers three atoms *i.e.*, it serves as a three-atom synthon towards cycloaddition reactions. Ester group remains inert throughout such cycloaddition reactions or is used in the subsequent lactonization or hydrolyzed to another functionality.

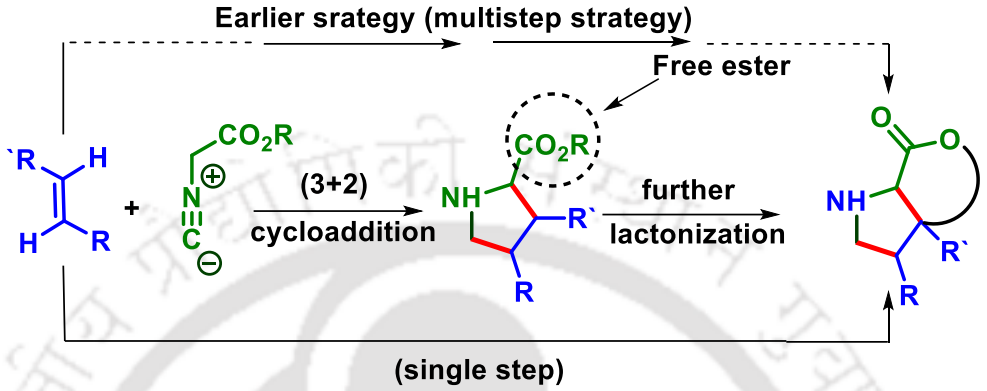

Scheme II.2.12. *Reactivity of alkyl isocyanoacetate.*

The Barton-Zard reaction is one such strategy for synthesizing substituted pyrrole from alkyl isocyanoester and conjugated nitroalkene (Scheme II.2.13).[9] The requirement of nitro group is essential in the starting alkenes, which is eventually eliminated.

Scheme II.2.13. *Barton-Zard reaction of alkyl isocyanoacetate.*

II.3. Present Work

II.3.1. Our approach:

Herein, we report a methodology, where the alkyl isocyanoacetate undergoes (3 + 2) cycloaddition with the alkene part of the 2-hydroxychalcone, followed by an intramolecular lactonization to furnish pyrrolocoumarin in a single step (Scheme II.3.1).

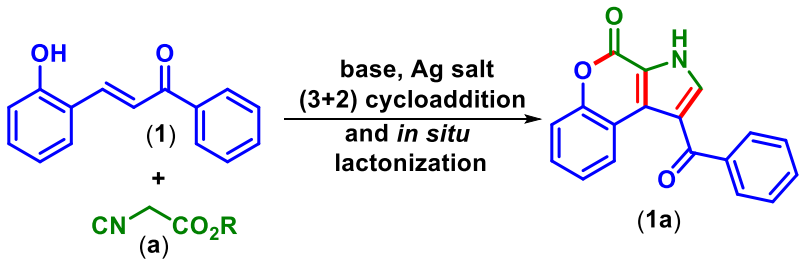

Scheme II.3.1. *Tandem cycloadditon and lactonization for pyrrolocoumarin synthesis.*

Initially, we commenced our exploration by taking 2-hydroxychalcone (**1**) and ethyl isocyanoacetate (**a**) in the presence of Cs_2CO_3 (2 equiv), Ag_2CO_3 (3 equiv) in 1,4-dioxane (3 mL). To our delight, the reaction was completed within 12 h with the formation of pyrrolocoumarin moiety (**1a**) in 71% yield. The product (**1a**) formation without the ethoxy group suggests a (3 + 2) cycloaddition followed by lactonization. The use of methyl isocyanoacetate (**b**) in lieu of ethyl isocyanoacetate (**a**) under an identical condition yielded the same product (**1a**), thereby supporting the lactonization path. The XRD analysis of the product unambiguously confirmed the structure to be 1-benzoylchromeno[3,4-*b*]pyrrol-4(3*H*)-one (**1a**) (CCDC 2245374) (Figure II.3.1). Here, ethyl isocyanoacetate serves as a four-atom (C–NH–C–C=O) synthon, unlike its well-established three-atom (C–NH–C–) synthon.

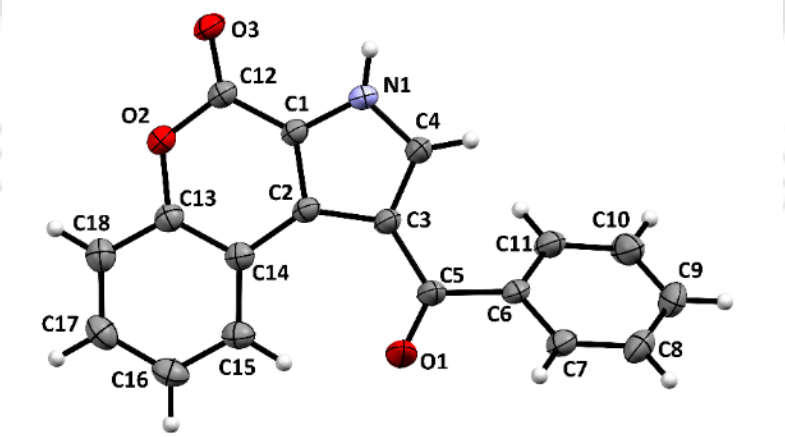

Figure II.3.1. *ORTEP view of 1-benzoylchromeno[3,4-b]pyrrol-4(3H)-one (**1a**) with 30% ellipsoid probability (CCDC 2245374).*

II.3.2. Optimization of the reaction conditions:

Table II.1. *Optimizations of the reaction conditions*[a,b]

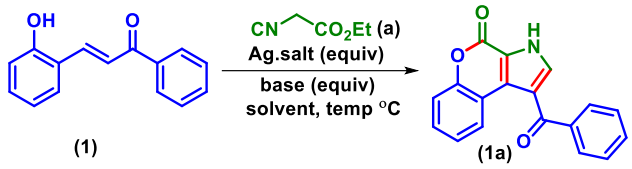

Sl No.	Ag (or Cu) salt. (equiv)	Base (equiv)	Solvent	Temp (°C)	Yield [c]
1	Ag_2CO_3 (3)	Cs_2CO_3 (2)	1,4-dioxane	80	71
2	**AgOAc (3)**	**Cs_2CO_3 (2)**	**1,4-dioxane**	**80**	**75**
3	AgOTf (3)	Cs_2CO_3 (2)	1,4-dioxane	80	60
4	$AgBF_4$ (3)	Cs_2CO_3 (2)	1,4-dioxane	80	43
5	$AgSO_4$ (3)	Cs_2CO_3 (2)	1,4-dioxane	80	41
6	$AgOCOCF_3$ (3)	Cs_2CO_3 (2)	1,4-dioxane	80	Trace
7	Ag_2O (3)	Cs_2CO_3 (2)	1,4-dioxane	80	68
8	AgCl (3)	Cs_2CO_3 (2)	1,4-dioxane	80	30
9	$AgNO_3$ (3)	Cs_2CO_3 (2)	1,4-dioxane	80	Trace
10	AgOAc (3)	K_2CO_3 (2)	1,4-dioxane	80	48
11	AgOAc (3)	^tBuOK (2)	1,4-dioxane	80	35
12	AgOAc (3)	K_3PO_4 (2)	1,4-dioxane	80	32
13	AgOAc (3)	DBU (2)	1,4-dioxane	80	57
14	AgOAc (3)	Cs_2CO_3 (2)	ethanol	80	65
15	AgOAc (3)	Cs_2CO_3 (2)	1,2-DCE	80	30
16	AgOAc (3)	Cs_2CO_3 (2)	CH_3CN	80	35
17	AgOAc (3)	Cs_2CO_3 (2)	TFE	80	Trace
18	AgOAc (3)	Cs_2CO_3 (2)	DMSO	80	50
19	CuI (3)	Cs_2CO_3 (2)	1,4-dioxane	80	42
20	$Cu(OAc)_2 \cdot H_2O$ (3)	Cs_2CO_3 (2)	1,4-dioxane	80	48
21	AgOAc (2)	Cs_2CO_3 (2)	1,4-dioxane	80	45
22	AgOAc (2)	Cs_2CO_3 (1)	1,4-dioxane	80	65
23	AgOAc(3)	Cs_2CO_3 (2)	1,4-dioxane	60	47

[a]Reaction conditions: **2** (0.15 mmol), **a** (0.18 mmol, 1.2 equiv), Ag/Cu Salt. (3 equiv), base (2 equiv), solvent (3 mL), 80 °C, 12 h. [b]Isolated yield of the product.

After, having the confirmed structure, we moved towards the selecting optimum condition for the proposed cascade cycloaddition lactonization approach. The optimization studies were started by taking 2-hydroxychalcone (**1**) and ethyl isocyanoacetate (**a**) as the model substrate for this one-pot reaction. Initially, we screened different silver salts for effective cycloaddition. As the reaction was completely unproductive in the absence of Ag_2CO_3, other Ag salts were also screened. Silver salts such as AgOAc, AgOTf, $AgBF_4$, $AgSO_4$, $AgOCOCF_3$, Ag_2O, AgCl, and $AgNO_3$ were screened for optimum yield. Among these Ag salts, the use of AgOAc was the most efficient in delivering the product (**1a**) in 75% yield (Table II.1, entries 1–9). Other bases screened such as K_2CO_3, ^tBuOK, K_3PO_4, and DBU were found to be inferior to Cs_2CO_3 (Table II.1, entries 10–13). Further, the solvent 1,4-dioxane was ideal compared to other solvents scrutinized, *viz*. ethanol, 1,2-DCE, CH_3CN, TFE (2,2,2-trifluoro ethanol), and DMSO (Table II.1, entries 14–18). Further, the use of CuI (42%) and $Cu(OAc)_2{\cdot}H_2O$ (48%) turned out to be ineffective compared to AgOAc (Table II.1, entries 19 and 20). Lowering the amount of AgOAc (2 equiv) and base Cs_2CO_3 (1 equiv) decreases the yield (Table II.1, entries 21 and 22). Reducing the reaction temperature to 60 ^oC was found detrimental to the product yield (Table II.1, entry 23). After extensive optimization, the best condition for this cycloaddition-lactonization strategy was found to be use of **1** (1 equiv), **a** (1.2 equiv), AgOAc (3 equiv), Cs_2CO_3 (2 equiv) in 1,4-dioxane (3 mL) at 80 ^oC (Table II.1, entry 2).

II.3.3. Substrate scopes of acetophenone and salicylaldehyde.[a,b,c]

With the set optimized conditions, the generality of this cycloaddition-lactonization protocol was tested with various 2-hydroxychalcones (**1**–**35**). Initially, 2-hydroxychalcones with substituents (R^1) at the ketone part were varied (Scheme II.3.2). 2-Hydroxychalcones bearing electron-neutral (–H) (**1**) and electron-releasing substituents (*p*-Me (**2**), *m*-Me (**3**), *p*-OMe (**4**), *p*-OEt (**5**), *p*-O^{i}Pr (**6**) at the phenyl ring of ketone reacted well with ethyl isocyanoacetate (**a**) resulting in their pyrrolocoumarins (**1a**–**6a**) in 63–75% yields. The scalability of the reaction has been tested in gram scale by reacting **1** with **a** which yielded the product **1a** in a slightly lower yield (57%). Halo-substituted 2-hydroxychalcones {*p*-F (**7**), *p*-Cl (**8**), *p*-Br (**9**), *p*-I (**10**), *o*-Br (**11**), *o*-I (**12**)} delivered the anticipated products (**7a**–**12a**) in higher yields (63%–82%). Strongly electron-withdrawing $–NO_2$ substituted chalcones (**13** and **14**) successfully yielded the products (**13a**, 84%) and (**14a**, 80%).

Scheme II.3.2. *Synthesis of pyrrolocoumarin via varying acetophenones.*

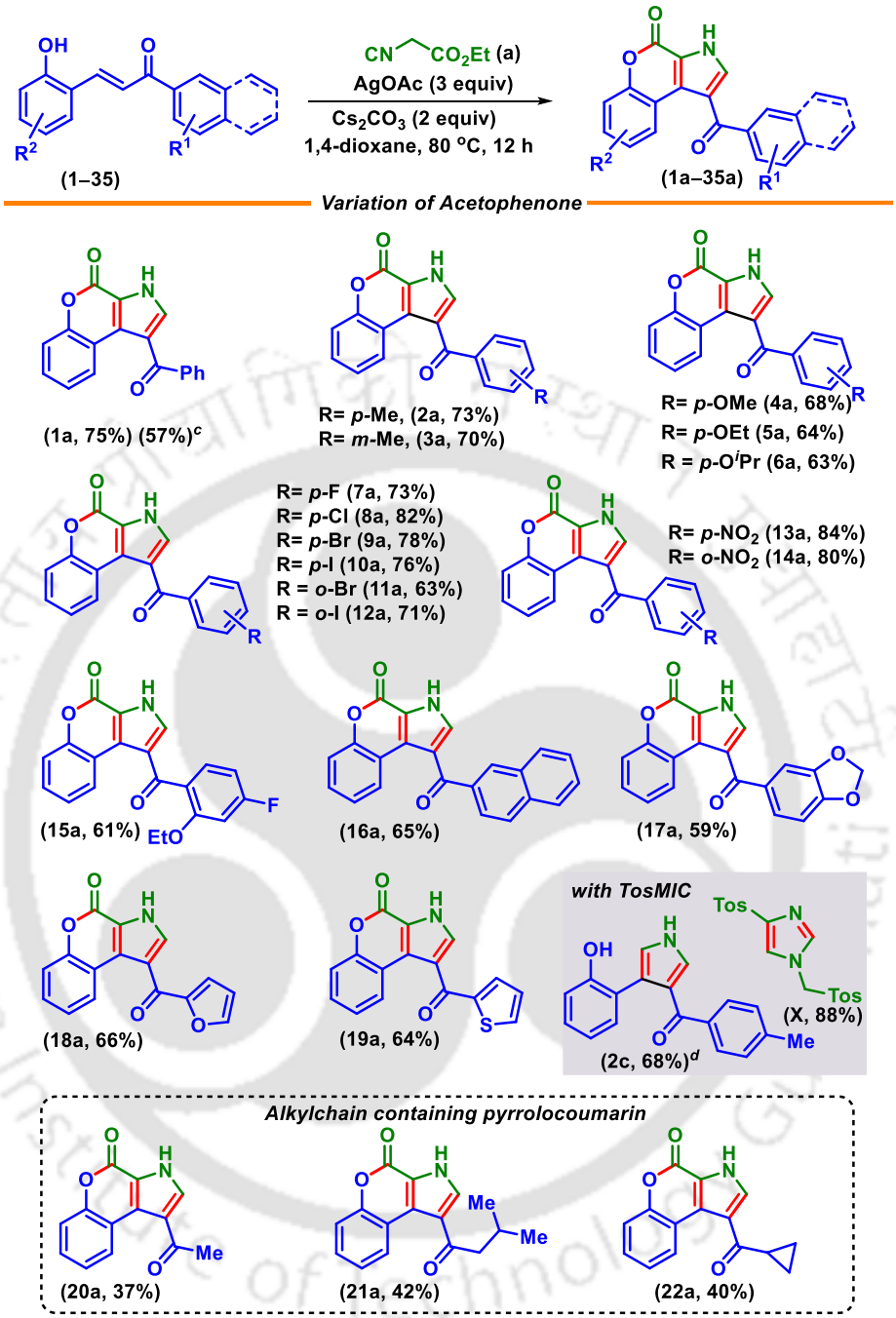

[a]Reaction conditions: **1**–**22** (0.25 mmol), **a** (1.2 equiv, 0.3 mmol), AgOAc (3 equiv, 0.75 mmol), Cs_2CO_3 (2 equiv, 0.5 mmol), 1,4-dioxane (3 mL), 80 °C, 12 h. [b]Isolated yield of the product. [c]5 mmol scale. [d]without AgOAc.

A di-substituted 2-hydroxychalcone (**15**) also provided the lactonized product (**15a**) in 61% yield. Naphthyl (**16**), and heteroaryl (**17**–**19**) derived 2-hydroxychalcone were well compatible and gave the pyrrolocoumarins **16a**–**19a** in moderate yields (59–65%). However, aliphatic 2-hydroxychalcones (**20**–**22**) delivered the requisite products (**20a**–**22a**) in lower

yields (37–42%) (Scheme II.3.2.). Further, the flexibility of the 1,3-dipolar coupling partner was tested by varying ethyl part of the alkyl isocyanoacetate by tosyl group. This tosylmethyl isocyanide (TosMIC) popularly known as Van Leusen reagent has gained considerable attention among synthetic researchers owing to its stability and reactivity as well as its odorless nature.[10] However, employment of TosMIC (**c**) in our protocol resulted in the intermolecular dimerization of itself (**X**). In contrast, an AgOAc-free reaction of TosMIC stops at pyrrole with the elimination of the tosyl group (**2c**). Such reactivity of TosMIC *viz.*, dimerization and elimination might be due to the high reactivity of TosMIC in the presence of AgOAc and better-leaving tendency of tosyl group respectively (Scheme II.3.2).

Then, the substituents in the salicylaldehyde part (R^2) of the 2-hydroxychalcone were varied (Scheme II.3.3).

Scheme II.3.3. *Synthesis of pyrrolocoumarin via varying salicylaldehyde.*

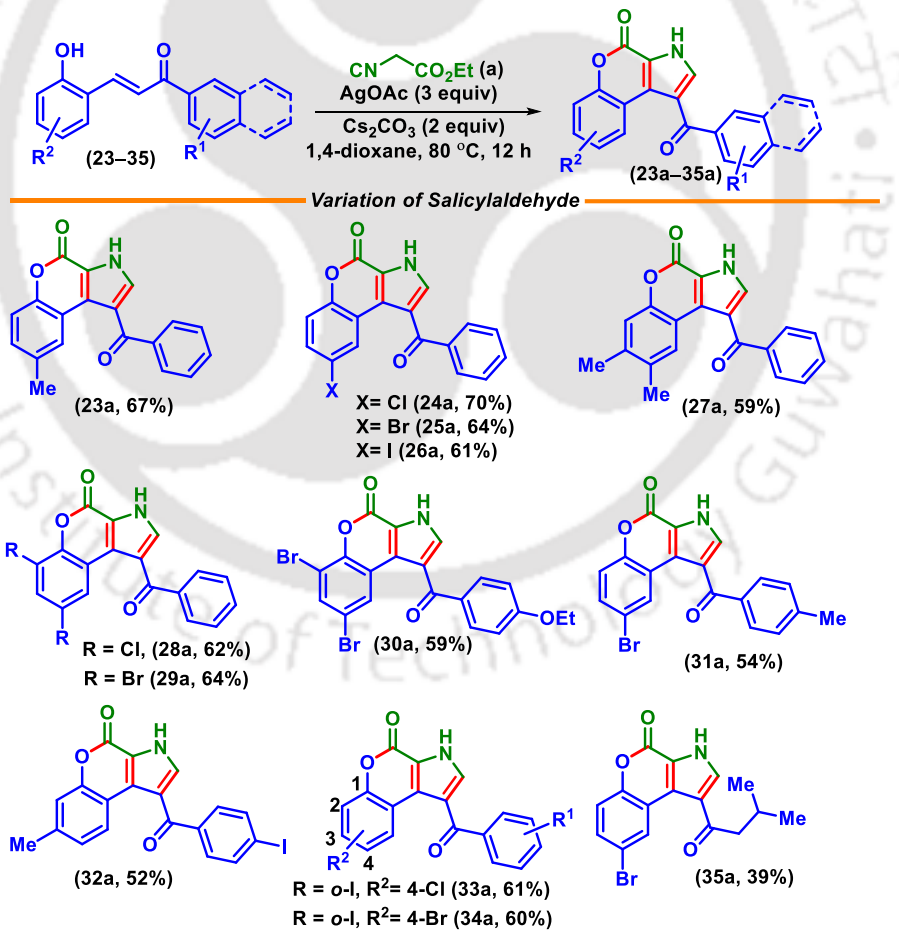

[a]Reaction conditions: **23**–**35** (0.25 mmol), **a** (1.2 equiv, 0.3 mmol), AgOAc (3 equiv, 0.75 mmol), Cs_2CO_3 (2 equiv, 0.5 mmol), 1,4-dioxane (3 mL), 80 °C, 12 h. [b]Isolated yield of the product.

Substrates possessing electron-releasing as well as electron-withdrawing groups in the *para* position as in –Me (**23**), –Cl (**24**), –Br (**25**), –I (**26**) successfully resulted in the products **23a**–**26a** in 61–70% yields. Various disubstituted 2-hydroxychalcones (**27**–**29**) were treated under standard conditions and corresponding pyrrolocoumarins (**27a**–**29a**) were obtained in modest yield (59–64%). Next, the substitution at both rings of 2-hydroxychalcone (**30**–**34**) was varied and the products (**32a**–**34a**) were isolated in 52–61% yield. However, chalcone derived from an aliphatic ketone (**35**) yielded pyrolocoumarin (**35**) albeit in a lower yield (39%) (Scheme II.3.3).

In an attempt to further exemplify the cycloaddition strategy, a reaction was conducted between lactonized enone such as coumarin (**1'**) and ethyl isocyanoacetate (**a**). This strategy resulted in the pyrrolocoumarin (**1a'**, 87%) with concomitant cycloaddition and elimination of ester or ketone counterpart from enone *via* a path similar to Barton-Zard reaction (Scheme II.3.4).

Scheme II.3.4. *Synthesis of fused pyrrolocoumarins from coumarin-3-carboxylate/acetyl*[a,b]

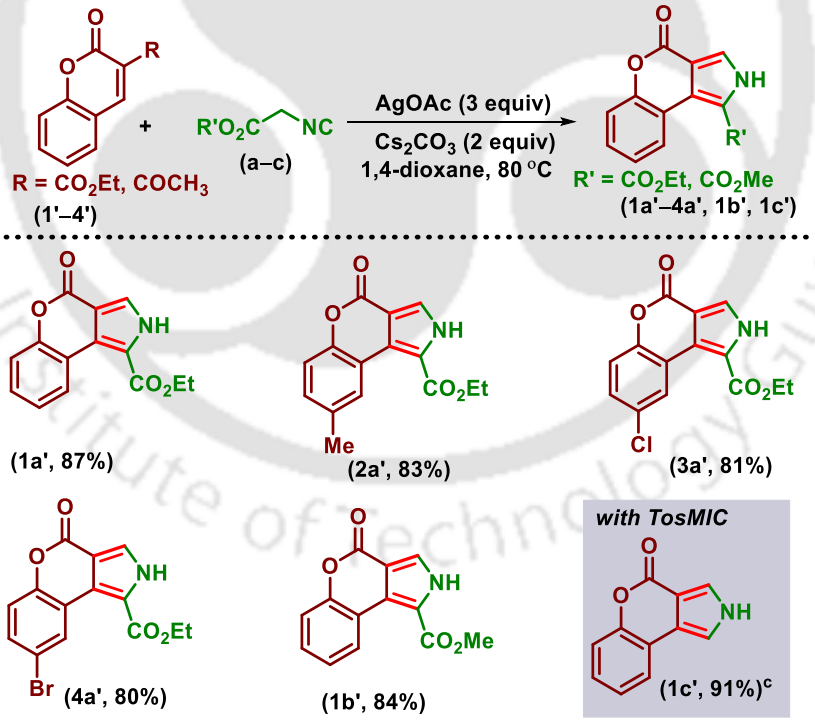

[a]Reaction conditions: **1'**–**4'** (0.5 mmol), **a**–**c** (1.2 equiv, 0.6 mmol), AgOAc (3 equiv, 1.5 mmol), Cs_2CO_3 (2 equiv, 1 mmol), 1,4-dioxane (3 mL), 80 °C, 12 h. [b]Isolated yield of the product. [c]Without AgOAc

The single crystal XRD-analysis confirmed the structure of this cycloadduct (CCDC 2251681) (Figure II.3.2). Here, instead of the nitro group, the ester or ketone moiety is

eliminated. After having the confirmed structure, a few other lactonized enones (**1'**–**4'**) having different electronic and steric effects were subjected to the same reaction conditions, all of which led to the formation of pyrrolocoumarins (**1a'**–**4a'**) in good yields (80–87%). Interestingly, the same product was isolated in good yield when the reaction was performed with 3-acetylcoumarin instead of carboxylate. Similarly, when a reaction was conducted between **1** and methyl isocyanoacetate (**b**), the pyrrolocoumarin (**1b'**) was obtained in 84% yield. Further, treatment of **1'** with TosMIC (**c**) in the absence of AgOAc leads to the formation of carboxylate-free pyrrolocoumarin (**1c'**) in exclusive yield (91%) (Scheme II.3.4).

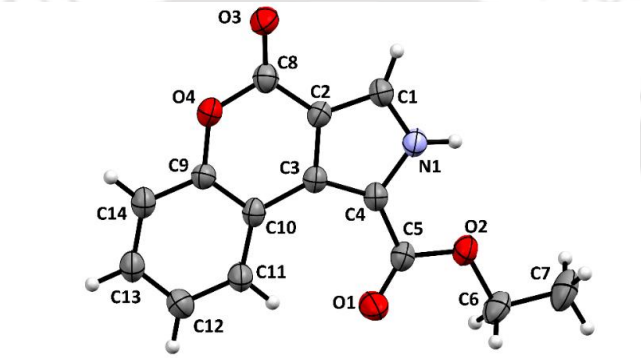

Figure II.3.2. *ORTEP view of ethyl 4-oxo-2,4-dihydrochromeno[3,4-c]pyrrole-1-carboxylate (CCDC 2251681) (**1a'**) with 30% ellipsoid probability.*

II.3.4. Plausible reaction mechanism:

Based on literature precedents, a plausible reaction mechanism is proposed in Scheme II.3.5.[11-12] Initially, treatment of AgOAc with ethyl isocyanoacetate (**a**) generates an active 1,3-dipolar intermediate (**a'**) *via* the elimination of AcOH.[12d] Next, the active 1,3-dipolar intermediate (**a'**) undergoes a (3 + 2) cycloaddition at the C=C bond of chalcone (**1**) to give a cycloadduct intermediate (**B**).[12d] The intermediate **B** provides the pyrrole moiety (**D**) through tautomerization followed by aromatization. The intermediate **D** undergoes intramolecular lactonization in the presence of Cs_2CO_3 to provide the resultant pyrrolocoumarin (**1a**) (Scheme II.3.5.a). A similar mechanism is proposed for the Barton-Zard equivalent reaction of coumarin-3-carboxylate/acetyl (**1'**) and ethyl isocyanoacetate (**a**).[12g] A rapid (3 + 2) cycloaddition between both the coupling partners followed by tautomerization and double bond rearrangement/oxidation leads to the pyrrolocoumarin (**1a'**) (Scheme II.3.5.b).

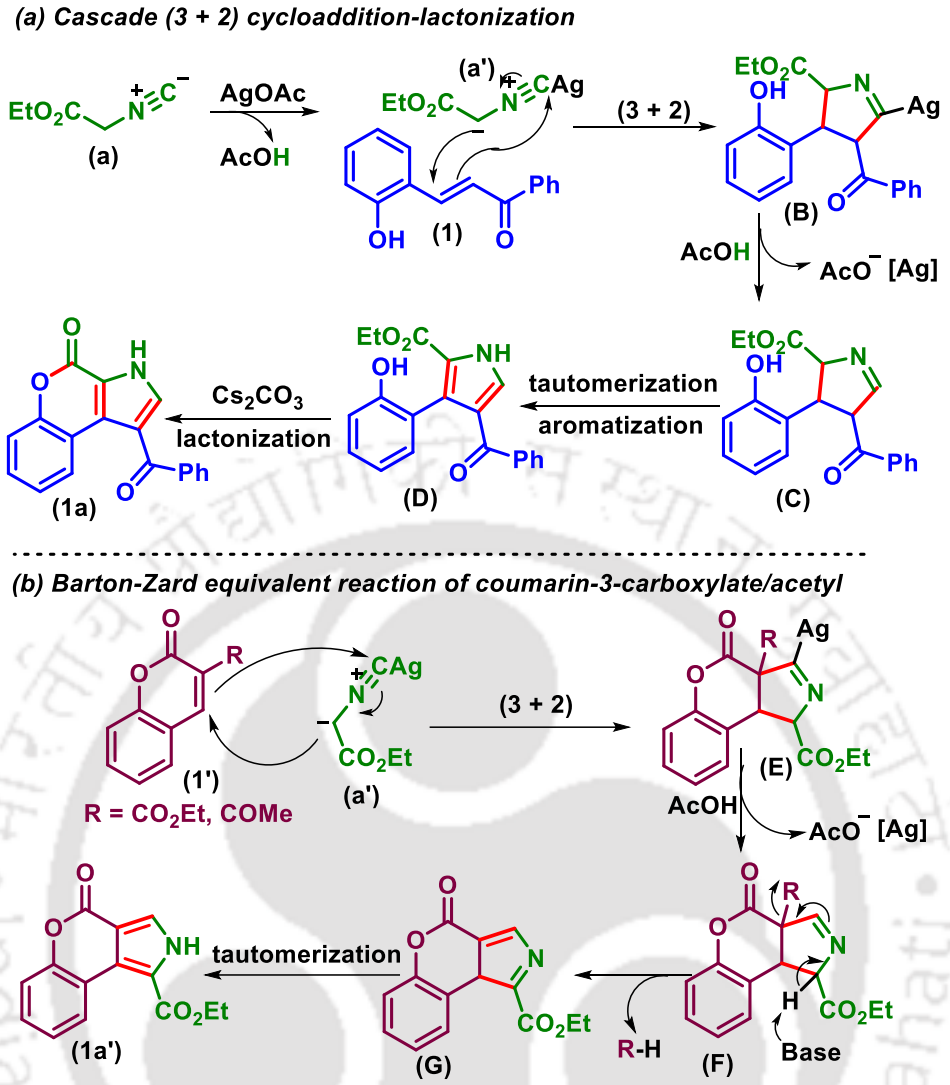

Scheme II.3.5. *A plausible mechanism for (3 + 2) cycloaddition-lactonization.*

II.3.5. Post-synthetic modifications:

To portray the robust synthetic utility of the present cycloaddition-lactonization strategy, the isolated fused 2-iodo pyrrolocoumarins (**12a** and **34a**) were subjected to Pd(II)-catalyzed cross-coupling reactions (Scheme II.3.6.a). The reaction provided pentacyclic pyrroles in good yields **12aa** (87%) and **34aa** (83%). On the other hand, a Sonogashira coupling of di halo substituted pyrrolocoumarin **34a** with phenylacetylene (**c**) produces dialkynyled product (**34ac**) (Scheme II.3.6.b).

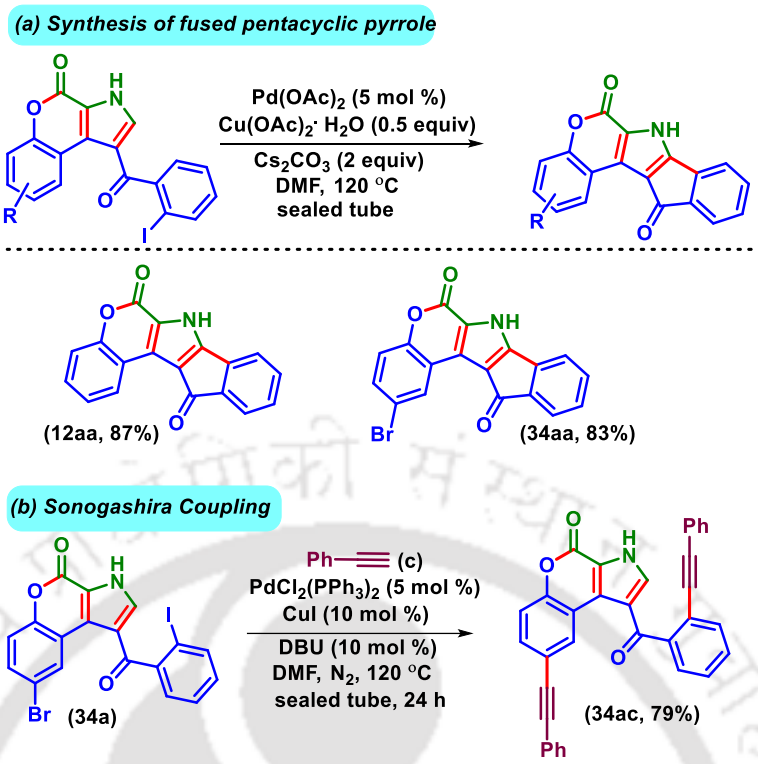

Scheme II.3.6. *Late-stage functionalizations.*

II.3.6. Conclusions:

In conclusion, we have developed a step economical way for the synthesis of pyrrolocoumarins from easily accessible precursors. This tandem cycloaddition-lactonization strategy is the best example of employing ethyl isocyanoacetate as a new type of four-atom synthon (C–NH–C–C=O) contrary to its earlier application as a three-atom synthon (C–NH–C). This methodology can be further extended to the synthesis of pyrrolocoumarin-carboxylate from the cyclic enones *via* an equivalent Barton-Zard reaction. Moreover, Pd(II) mediated cross-coupling reactions of the 2-halo substituted pyrrolocoumarins provide easy access to fused pentacyclic pyrrole. Thus, this hitherto unexploited AgOAc-mediated cascade cycloadditon-lactonization strategy is expected to find wide synthetic applications in pharmaceutical industry.

II.4 Experimental Section

II.4.1. General information

All the reagents were commercial grade and used without further purification unless otherwise stated. 2-Hydroxychalcones are prepared following the literature procedure from

salicylaldehyde and acetophenone. All the reactions were carried out in a 10 mL oven-dried round-bottom flask under aerobic conditions. Reactions were monitored by thin layer chromatography (TLC) on a 0.25 mm silica gel plates ($60F_{254}$) and visualized under UV illumination at 254 nm. Organic extracts were dried over anhydrous sodium sulfate (Na_2SO_4). Column chromatography was performed to purify the crude product on silica gel 60–120 mesh using a mixture of hexane and ethyl acetate as eluent. The isolated compounds were characterized by spectroscopic [^1H, $^{13}C\{^1H\}$ NMR, and IR] techniques and HRMS analysis. NMR spectra were recorded in deuterochloroform ($CDCl_3$) and in some cases deuterated dimethyl sulphoxide (CD_3SOCD_3). ^1H, $^{13}C\{^1H\}$ were recorded in 500 (125) or 400 (100) MHz spectrometer and were calibrated using tetramethylsilane or residual undeuterated solvent for ^1H NMR, deuterochloroform for $^{13}C\{^1H\}$ NMR as an internal reference {$Si(CH_3)_4$: 0.00 ppm or $CHCl_3$: 7.260 ppm for ^1H NMR, 77.230 ppm for $^{13}C\{^1H\}$ NMR}. ^{19}F NMR was calibrated without any internal standard in $CDCl_3$. The chemical shifts are quoted in δ units, parts per million (ppm). ^1H NMR data is represented as follows: chemical shift, multiplicity (s = singlet, d = doublet, t = triplet, q = quartet, m = multiplet, dd = doublet of doublet, dt = doublet of triplet), integration and coupling constant(s) *J* in hertz (Hz). High-resolution mass spectra (HRMS) were recorded on a mass spectrometer using electrospray ionization-time of flight (ESI-TOF) reflection experiments. FT-IR spectra were recorded in neat and reported in the frequency of absorption (cm^{-1}).

II.4.2. Crystallographic information:

Sample preparation: The single crystals of compounds **1a** and **1a'** were prepared by the slow evaporation method for which 10 mg of the compound (**1a** and **1a'**) was dissolved in 1 mL of DCM in a clean and dry 10 mL glass vial. MeOH (0.5 mL) was added to this solution slowly with a dropper. The mouth of the glass vial was covered with a cap having a small hole and kept for slow evaporation at room temperature. Crystals of **1a** and **1a'** were obtained after approximately 3–4 days as a transparent block-shaped crystal.

Data collection: Diffraction data were collected at 292 K with MoKα radiation (λ = 0.71073 Å) using a Bruker Nonius SMART APEX CCD diffractometer equipped with graphite monochromator and Apex CD camera. The SMART software was used for data collection and indexing the reflections and determining the unit cell parameters. Data reduction and cell refinement were performed using SAINT[13a-b] software and the space groups of these crystals were determined from systematic absences by XPREP and further justified by the refinement

results. The structures were solved by direct methods and refined by full-matrix least-squares calculations using SHELXTL-973 software. All the non-H atoms were refined in the anisotropic approximation against F2 of all reflections.[13c]

Crystallographic description of 1-benzoylchromeno[3,4-*b*]pyrrol-4(3*H*)-one (1a):

$C_{18}H_{11}NO_3$, colourless block shaped crystal; crystal dimensions 0.25 x 0.23 x 0.17 mm, M_r = 289.28, Triclinic, space group P(-1), a = 6.0521(8), b = 11.2758(16), c = 11.6157(15) Å, α = 66.982(3)°, β = 82.613(3)°, γ = 76.191(3)°, V = 707.93(17) Å^3, Z = 2, ρ = 1.357 g/cm^3, μ = 0.094 mm^{-1} , F(000)= 300, reflection collected / unique = 2490 / 2192, refinement method = full-matrix least-squares on F^2, final *R* indices [I > 2\s(I)]: R_1 = 0.0462, wR_2 = 0.1495, *R* indices (all data): R_1 = 0.0533, wR_2 = 0.1663, goodness of fit = 1.127; CCDC = 2245374 for ***1-benzoylchromeno[3,4-b]pyrrol-4(3H)-one*** **(1a)** contains the supplementary crystallographic data for this paper. These data can be obtained free of charge from The Cambridge Crystallographic Data Centre via www.ccdc.cam.ac.uk/data_request/cif.

Crystallographic description of ethyl 4-oxo-2,4-dihydrochromeno[3,4-*c*]pyrrole-1-carboxylate (1a'):

$C_{14}H_{11}NO_4$, colourless block shaped crystal; crystal dimensions 0.29 x 0.25 x 0.14 mm, M_r = 257.24, orthorhombic, space group P 21 21 21, a = 4.4163(2), b = 12.9777(6), c = 20.7587(9) Å, α = 90°, β = 90°, γ = 90°, V = 1189.75(9) Å^3, Z = 4, ρ = 1.436 g/cm^3, μ = 0.107 mm^{-1} , F(000)= 536, reflection collected / unique = 2095 / 1309, refinement method = full-matrix least-squares on F^2, final *R* indices [I > 2\s(I)]: R_1 = 0.0589, wR_2 = 0.1439, *R* indices (all data): R_1 = 0.1280, wR_2 = 0.2114, goodness of fit = 1.072; CCDC = 2251681 for **ethyl 4-oxo-2,4-dihydrochromeno[3,4-*c*]pyrrole-1-carboxylate (1a')** contains the supplementary crystallographic data for this paper. These data can be obtained free of charge from The Cambridge Crystallographic Data Centre via www.ccdc.cam.ac.uk/data_request/cif.

II.4.3. General procedures

II.4.3.1. General procedures for the synthesis of 2-hydroxychalcones (1):

2-Hydroxychalones were synthesized according to the available literature procedure.[14a-d]

II.4.3.2. General procedure for the synthesis of 1-benzoylchromeno[3,4-*b*]pyrrol-4(3*H*)-one (1a):

To a 10 mL oven-dried round bottom flask equipped with a magnetic bar was added (*E*)-3-(2-hydroxyphenyl)-1-phenylprop-2-en-1-one (**1**) (0.5 mmol, 112 mg), ethyl isocyanoacetate (**a**) (1.2 equiv, 68 mg), AgOAc (3 equiv, 250 mg), Cs_2CO_3 (2 equiv, 325 mg) and 1,4-dioxane (3 mL). The reaction mixture was allowed to stir at 80 ^oC for 12 h. After completion of the reaction as confirmed by TLC monitoring, the mixture was filtered through a thin bed of celite. The crude mixture was diluted by adding 20 mL ethyl acetate and washed with water (1 x 10 mL) followed by brine solution (1 x 5 mL). The organic layer was dried over anhydrous Na_2SO_4 and concentrated under reduced pressure. The crude product thus obtained was purified over a column of silica gel using hexane and ethyl acetate (3:1) to give pure product **1a** in 75% yield (108 mg).

II.4.3.3. General procedure for the synthesis of ethyl 2-oxo-2*H*-chromene-3-carboxylate/acetyl (1'):

Alkyl 2-oxo-2*H*-chromene-3-carboxylate/acetyl was synthesized according to modified literature reports.[14e,f]

II.4.3.4. General procedure for the synthesis of ethyl 4-oxo-2,4-dihydrochromeno[3,4-*c*]pyrrole-1-carboxylate (1a'):

An oven-dried 10 mL round bottom flask equipped with magnetic bar was added ethyl 2-oxo-2*H*-chromene-3-carboxylate (**1'**) (0.5 mmol, 109 mg), ethyl isocyanoacetate (**a**) (1.2 equiv, 0.6 mmol, 68 mg), AgOAc (3 equiv, 250 mg), Cs_2CO_3 (2 equiv, 325 mg) and 1,4-dioxane (3 mL). The reaction mixture was stirred in a pre-heated oil bath at 80 ^oC for 12 h. After completion of the reaction (monitored by TLC analysis), the crude mixture was filtered through a thin bed of celite and then diluted with EtOAc (20 mL). The organic layer was washed with water (2 x 10 mL), and brine solution (1 x 5 mL). The organic layer was dried over anhydrous Na_2SO_4 and the solvent was concentrated under reduced pressure. The crude product so obtained was purified over a column of silica gel using ethyl acetate in hexane (4:1) to give pure ethyl 4-oxo-2,4-dihydrochromeno[3,4-*c*]pyrrole-1-carboxylate (**1a'**) 78% yield (100 mg). The identity and purity of the product were confirmed by spectroscopic analysis.

II.4.3.5. General procedure for gram-scale synthesis:

To a 25 mL oven-dried round bottom flask equipped with a magnetic bar was added (*E*)-3-(2-hydroxyphenyl)-1-phenylprop-2-en-1-one (**1a**) (5 mmol, 1.12 g), ethyl isocyanoacetate (**a**) (1.2 equiv, 6 mmol, 678 mg), AgOAc (3 equiv, 15 mmol, 2.50 g), Cs_2CO_3

(2 equiv, 10 mmol, 3.25 g) and 1,4-dioxane (20 mL). The reaction mixture was allowed to stir at 80 ^{o}C for 12 h. After completion of the reaction as confirmed by TLC monitoring, the mixture was filtered through a thin bed of celite. The crude mixture was diluted by adding 50 mL ethyl acetate and washed with water (1 x 30 mL) followed by brine solution (1 x 10 mL). The organic layer was dried over anhydrous Na_2SO_4 and concentrated under reduced pressure. The crude product thus obtained was purified over a column of silica gel using hexane and ethyl acetate (3:1) to give pure product **1a** in 57% yield (824 mg).

II.4.4. Post-synthetic transformations:

II.4.4.1. General procedure for the synthesis of 6H-chromeno[3,4-*b*]indeno[2,1-*d*]pyrrole-6,12(7*H*)-dione (12aa) from 1-(2-iodobenzoyl)chromeno[3,4-*b*]pyrrol-4(3*H*)-one (12a):

An oven-dried 15 mL sealed tube equipped with a magnetic bar was charged with 1-(2-iodobenzoyl)chromeno[3,4-*b*]pyrrol-4(3*H*)-one (**12a**) (0.15 mmol, 62 mg), $Pd(OAc)_2$ (5 mol %, 0.0075 mmol, 1.7 mg), $Cu(OAc)_2 \cdot H_2O$ (0.5 equiv, 0.075 mmol, 15 mg), PPh_3 (10 mol %, 0.015 mmol, 4 mg), Cs_2CO_3 (2 equiv, 0.3 mmol, 98 mg), DMF (2 mL). The reaction mixture was allowed to stir for 24 h at 120 ^{o}C. After completion of the reaction as confirmed by TLC analysis, the mixture was filtered through a thin bed of celite. The filtrate was evaporated and diluted with EtOAc (10 mL). The organic layer was washed with water (1 x 10 mL) followed by brine solution (1 x 5 mL). The organic layer was dried over anhydrous Na_2SO_4 and solvent was concentrated under reduced pressure. The crude product so obtained was purified over a column of silica gel using ethyl acetate in hexane (1:3) to give the product (**12aa**) in 87% yield (37 mg).

II.4.4.2. General procedure for Sonogashira coupling of 34a:

To a 10 mL oven-dried round bottom flask equipped with a magnetic bar was added 8-bromo-1-(2-iodobenzoyl)chromeno[3,4-*b*]pyrrol-4(3*H*)-one (**34a**) (0.15 mmol, 74 mg), phenylacetylene (**c**) (2.4 equiv, 0.36 mmol, 37 mg), $PdCl_2(PPh_3)_2$ (5 mol %, 0.075 mmol, 5.3 mg,), CuI (10 mol %, 0.015 mmol, 2.9 mg,), DBU (2 equiv, 0.3 mmol, 46 mg) and dry DMF (2 mL) under nitrogen atmosphere. The reaction mixture was stirred in a pre-heated oil bath at 120 ^{o}C for 24 h. After completion of the reaction (monitored by TLC analysis), the crude mixture was diluted with EtOAc (15 mL). The organic layer was washed with water (1 x 10 mL), and brine solution (1 x 5 mL). The organic layer was dried over anhydrous Na_2SO_4 and

solvent and concentrated under reduced pressure. The crude product so obtained was purified over a column of silica gel using ethyl acetate in hexane (3:7) to give pure dialkynylated 8-(phenylethynyl)-1-(2-(phenylethynyl)benzoyl)chromeno[3,4-*b*]pyrrol-4(3*H*)-one (**34ac**) in 79% yield (58 mg). The identity and purity of the product were confirmed by spectroscopic analysis.

II.5. Spectral Data

Spectral data of all compounds:

1-Benzoylchromeno[3,4-b]pyrrol-4(3H)-one (1a):

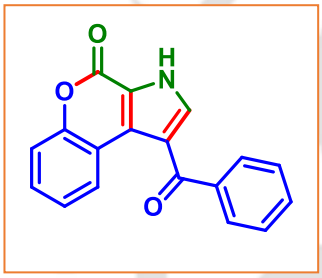

As off-white solid (108 mg, 75% yield); m.p. 226–228 °C; purified over a column of silica gel (20% EtOAc in hexane); ^{1}H NMR ($CDCl_3$, 500 MHz): δ 11.50 (s. 1H), 8.89 (d, 1H, J = 3.0 Hz), 7.88 (d, 2H, J = 7.5 Hz), 7.74 (s, 1H), 7.62 (t, 1H, J = 7.5 Hz), 7.52 (t, 2H, J = 7.5 Hz), 7.46 (d, 2H, J = 8 Hz), 7.36 (dt, 1H, J_1 = 6.0 Hz, J_2 = 2.5 Hz); ^{13}C{^{1}H} NMR ($CDCl_3$, 125 MHz): δ 191.2, 156.6, 151.8, 139.8, 136.2, 132.7, 129.9, 129.7, 129.5, 128.7, 127.6, 125.0, 121.4, 119.5, 117.6, 117.4; IR (neat, cm^{-1}): 3194, 2957, 2919, 1724, 1645, 1468, 1401, 1320, 1275; HRMS (ESI/Q-TOF) (m/z): calcd. for $C_{18}H_{12}NO_3$, $[M + H]^+$: 290.0812, found: 290.0810.

1-(4-Methylbenzoyl)chromeno[3,4-b]pyrrol-4(3H)-one (2a):

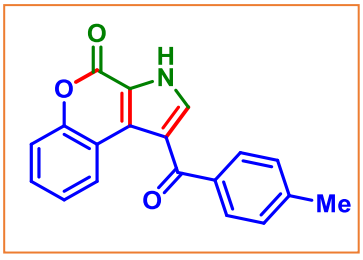

As white solid (110 mg, 73% yield); m.p. 230–232 °C; purified over a column of silica gel (20% EtOAc in hexane); ^{1}H NMR ($CDCl_3$, 400 MHz): δ 11.35 (s, 1H), 8.82 (d, 1H, J = 8.0 Hz), 7.81 (d, 2H, J = 8.4 Hz), 7.73 (s, 1H), 7.46 (d, 2H, J = 4.8 Hz), 7.36–7.31 (m, 3H), 2.46 (s, 3H); ^{13}C{^{1}H} NMR ($CDCl_3$ + DMSO-d_6, 100 MHz): δ 191.0, 155.6, 151.7, 143.1, 137.0, 135.8, 129.6, 129.1, 128.7, 128.6, 127.1, 124.3, 120.6, 119.5, 117.6, 117.0, 21.6; IR (neat, cm^{-1}): 3195, 2963, 2921, 1721, 1651, 1463, 1398, 1271; HRMS (ESI/Q-TOF) (m/z): calcd. for $C_{19}H_{14}NO_3$, $[M + H]^+$: 304.0968, found: 304.0977.

1-(3-Methylbenzoyl)chromeno[3,4-b]pyrrol-4(3H)-one (3a):

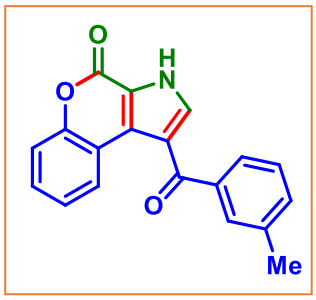

As white solid (106 mg, 70% yield); m.p. 231–235 °C; purified over a column of silica gel (20% EtOAc in hexane); ^{1}H NMR (DMSO-d$_6$, 500 MHz): δ 13.45 (s, 1H), 8.72 (dd, 1H, J_1 = 8.0 Hz, J_2 = 1.5 Hz), 7.81 (s, 1H), 7.65 (s, 1H), 7.63 (d, 1H, J = 7.5 Hz), 7.50–7.42 (m, 4H), 7.36–7.32 (m, 1H), 2.40 (s, 3H); ^{13}C{^{1}H} NMR (DMSO-d$_6$, 125 MHz): δ 190.7, 154.2, 151.2, 139.3, 138.0, 136.7, 133.1, 129.6, 128.9, 128.4, 127.6, 126.6, 126.3, 124.1, 119.8, 118.9, 117.1, 116.9, 20.9; IR (neat, cm^{-1}): 3189, 2960, 2918, 1699, 1646, 1467, 1261; HRMS (ESI/Q-TOF) (m/z): calcd. for $C_{19}H_{13}NO_3Na$, $[M + Na]^+$: 326.0788, found: 326.0790.

1-(4-Methoxybenzoyl)chromeno[3,4-b]pyrrol-4(3H)-one (4a):

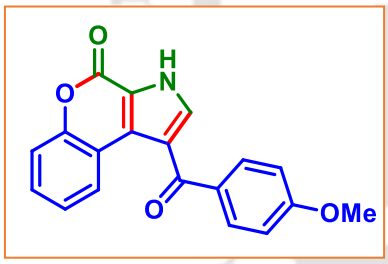

As off-white solid (108 mg, 68% yield); m.p. 234–236 °C; purified over a column of silica gel (20% EtOAc in hexane); ^{1}H NMR ($CDCl_3$, 500 MHz): δ 11.07 (s, 1H), 8.89 (d, 1H, J = 8.0 Hz), 7.92 (d, 2H, J = 9.0 Hz), 7.33 (d, 1H, J = 3.0 Hz), 7.46 (dd, 2H, J_1 = 4.5 Hz, J_2 = 1.0 Hz), 7.35–7.32 (m, 1H), 7.01 (d, 2H, J = 9.0 Hz) 3.92 (s, 3H); ^{13}C{^{1}H} NMR ($CDCl_3$, 125 MHz): δ 189.9, 163.7, 156.4, 151.8, 137.7, 132.2, 132.1, 129.5, 129.3, 127.2, 124.9, 121.4, 119.3, 117.6, 117.4, 114.1, 55.8; IR (neat, cm^{-1}): 3233, 2968, 2923, 1715, 1653, 1480, 1399, 1271; HRMS (ESI/Q-TOF) (m/z): calcd. for $C_{19}H_{14}NO_4$, $[M + H]^+$: 320.0917, found: 320.0928.

1-(4-Ethoxybenzoyl)chromeno[3,4-b]pyrrol-4(3H)-one (5a):

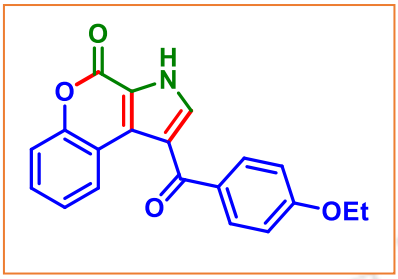

As white solid (106 mg, 64% yield); m.p. 250–252 °C; purified over a column of silica gel (20% EtOAc in hexane); ^{1}H NMR($CDCl_3$, 400 MHz): δ 10.87 (s, 1H), 8.67 (d, 1H, J = 8.0 Hz), 7.91 (d, 2H, J = 8.4 Hz), 7.71 (d, 1H, J = 3.2 Hz), 7.46 (d, 2H, J = 4.0 Hz), 7.34–7.30 (m, 1H), 6.98 (d, 2H, J = 8.4 Hz), 4.14 (q, 2H, J = 7.2 Hz), 1.48 (t, 3H, J = 6.8 Hz); ^{13}C{^{1}H} NMR (DMSO-d_6, 100 MHz): δ 189.2, 162.2, 154.1, 151.1, 135.5, 131.8, 131.3, 128.7, 127.4, 126.1, 124.1, 119.6, 118.6, 117.2, 116.9, 114.2, 63.5, 14.5; IR (neat, cm^{-1}): 3351, 2981, 2923, 1715, 1653, 1463, 1398, 1267; HRMS (ESI/Q-TOF) (m/z): calcd. for $C_{20}H_{16}NO_4$, $[M + H]^+$: 334.1074, found: 334.1079.

1-(4-Isopropoxybenzoyl)chromeno[3,4-b]pyrrol-4(3H)-one (6a):

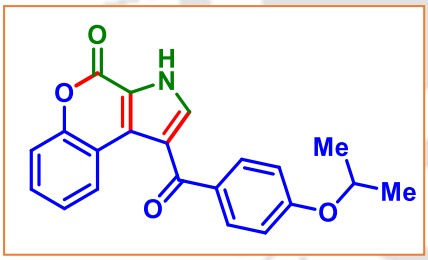

As off-white solid (109 mg, 63% yield); m.p. 235–237 °C; purified over a column of silica gel (20% EtOAc in hexane); ^{1}H NMR (DMSO-d_6, 500 MHz): δ 13.40 (s, 1H), 8.54 (d, 1H, J = 8.0 Hz), 7.85 (d, 3H, J = 9.5 Hz), 7.48–7.46 (m, 2H), 7.33–7.30 (m, 1H), 7.06 (d, 2H, J = 8.5 Hz), 4.79–4.74 (m, 1H), 1.31 (d, 6H, J = 6.0 Hz); ^{13}C{^{1}H} NMR (DMSO-d_6, 100 MHz): δ 189.1, 161.2, 154.1, 151.1, 135.5, 131.9, 131.1, 128.7, 127.4, 126.0, 124.1, 119.6, 118.6, 117.2, 116.9, 115.1, 69.6, 21.7; IR (neat, cm^{-1}): 3321, 2971, 2928, 1719, 1649, 1470, 1397, 1260; HRMS (ESI/Q-TOF) (m/z): calcd. for $C_{21}H_{18}NO_4$, $[M + H]^+$: 348.1230, found: 348.1230.

1-(4-Fluorobenzoyl)chromeno[3,4-b]pyrrol-4(3H)-one (7a)

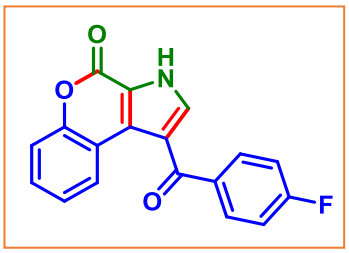

As yellow solid (112 mg, 73% yield); m.p. 239–241 °C; purified over a column of silica gel (20% EtOAc in hexane); ^{1}H NMR (DMSO-d$_6$, 500 MHz): δ 13.47 (s. 1H), 8.68 (d, 1H, J = 8.0 Hz), 7.94–7.92 (m, 2H), 7.86 (s, 1H), 7.51–7.46 (m, 2H), 7.39–7.32 (m, 3H); ^{13}C{^{1}H} NMR (DMSO-d$_6$, 125 MHz): δ 198.7, 165.9, 163.9, 154.6, 151.4, 137.1, 136.1 (d, J = 2.2 Hz), 132.5 (d, J = 7.5 Hz), 129.4, 128.0, 126.6, 124.6, 119.8, 119.2, 117.3 (d, J = 5.9 Hz), 115.9 (d, J = 17.4 Hz); ^{19}F NMR (DMSO-d$_6$, 471 MHz): δ –107.1; IR (neat, cm^{-1}): 3169, 2970, 2925, 1720, 1649, 1468, 1401, 1269; HRMS (ESI/Q-TOF) (m/z): calcd. for $C_{18}H_{11}FNO_3$, $[M + H]^+$: 308.0717, found: 308.0715.

1-(4-Chlorobenzoyl)chromeno[3,4-b]pyrrol-4(3H)-one (8a)

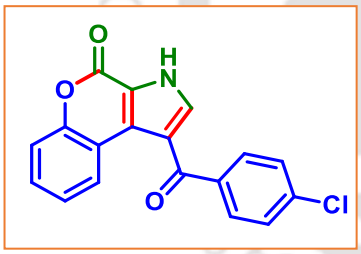

As white solid (132 mg, 82% yield); m.p. 257–259 °C; purified over a column of silica gel (20% EtOAc in hexane); ^{1}H NMR (DMSO-d$_6$, 500 MHz): δ 13.50 (s, 1H), 8.73 (d, 1H, J = 8.0 Hz), 7.86 (t, 3H, J = 8.0 Hz), 7.62 (d, 2H, J = 7.5 Hz), 7.52–7.46 (m, 2H), 7.35 (t, 1H, J = 7.5 Hz); ^{13}C{^{1}H} NMR (DMSO-d$_6$, 125 MHz): δ 189.5, 154.3, 151.3, 138.1, 137.4, 137.2, 131.2, 129.2, 128.8, 127.8, 126.5, 124.3, 119.5, 119.2, 117.2, 117.1; IR (neat, cm^{-1}): 3213, 2998, 2932, 1709, 1655, 1585, 1468, 1398, 1268; HRMS (ESI/Q-TOF) (m/z): calcd. for $C_{18}H_{11}ClNO_3$, $[M + H]^+$: 324.0422, found: 324.0421.

1-(4-Bromobenzoyl)chromeno[3,4-b]pyrrol-4(3H)-one (9a)

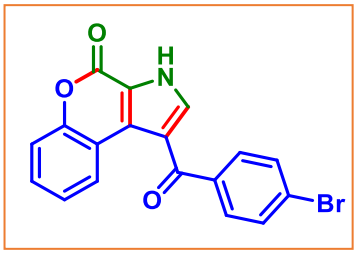

As white solid (143 mg, 78% yield); m.p. 263–265 °C; purified over a column of silica gel (20% EtOAc in hexane); ^{1}H NMR (DMSO-d_6, 500 MHz): δ 13.51 (s, 1H), 8.74 (d, 1H, J = 8.0 Hz), 7.89 (s, 1H), 7.79–7.75 (m, 4H), 7.52–7.46 (m, 2H), 7.37–7.33 (m, 1H); ^{13}C{^{1}H} NMR (DMSO-d_6, 125 MHz): δ 189.7, 154.2, 151.3, 138.4, 137.2, 131.7, 131.3, 129.1, 127.8, 126.5, 126.4, 124.3, 119.5, 119.1, 117.1, 117.0; IR (neat, cm^{-1}): 3198, 2973, 2921, 1719, 1658, 1465, 1397, 1265; HRMS (ESI/Q-TOF) (m/z): calcd. for $C_{18}H_{11}BrNO_3$, $[M + H]^+$: 367.9917, found: 367.9916.

1-(4-Iodobenzoyl)chromeno[3,4-b]pyrrol-4(3H)-one (10a)

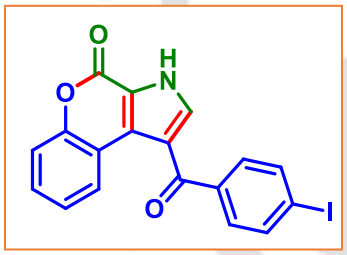

As white solid (158 mg, 76% yield); m.p. 273–275 °C; purified over a column of silica gel (20% EtOAc in hexane); ^{1}H NMR (DMSO-d_6, 500 MHz): δ 13.51 (s, 1H), 8.74 (d, 1H, J = 8.0 Hz), 7.95 (d, 2H, J = 8.0 Hz), 7.89 (s, 1H), 7.61 (d, 2H, J = 8.0 Hz), 7.51–7.47 (m, 2H), 7.36 (t, 1H, J = 7.5 Hz); ^{13}C{^{1}H} NMR (DMSO-d_6, 125 MHz): δ 190.0, 154.2, 151.2, 138.7, 137.5, 137.1, 131.1, 129.1, 127.7, 126.4, 124.4, 119.4, 119.1, 117.1, 117.0, 100.6; IR (neat, cm^{-1}): 3223, 2974, 2923, 1714, 1651, 1473, 1396, 1271; HRMS (ESI/Q-TOF) (m/z): calcd. for $C_{18}H_{11}INO_3$, $[M + H]^+$: 415.9778, found: 415.9786.

1-(2-Bromobenzoyl)chromeno[3,4-b]pyrrol-4(3H)-one (11a):

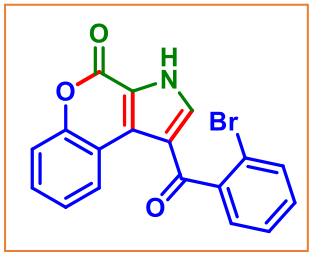

As brown solid (115 mg, 63% yield); m.p. 259–261 °C; purified over a column of silica gel (20% EtOAc in hexane); ^{1}H NMR ($CDCl_3$, 400 MHz): δ 13.63 (s, 1H), 9.26 (dd, 1H, J_1 = 8.0 Hz, J_2 = 1.6 Hz), 7.75 (d, 1H, J = 8.0 Hz), 7.57–7.45 (m, 6H); ^{13}C{^{1}H} NMR (DMSO-d_6, 100 MHz): δ 188.7, 153.1, 150.3, 140.9, 137.9, 131.9, 130.4, 128.3, 127.7, 126.7, 126.6, 126.2, 123.3, 119.4, 118.7, 117.4, 116.0, 115.9; IR (neat, cm^{-}

^{1}): 3198, 2981, 2931, 1719, 1657, 1458, 1401, 1257; HRMS (ESI/Q-TOF) (m/z): calcd. for $C_{18}H_{11}BrNO_3$, $[M + H]^+$: 367.9917, found: 367.9899.

1-(2-Iodobenzoyl)chromeno[3,4-b]pyrrol-4(3H)-one (12a):

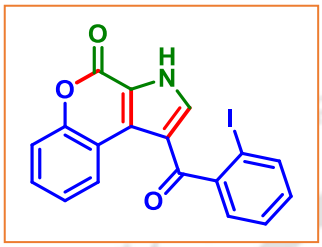

As white solid (147 mg, 71% yield); m.p. 271–273 °C; purified over a column of silica gel (20% EtOAc in hexane); ^{1}H NMR $CDCl_3$, 400 MHz): δ 11.49 (s, 1H), 9.41–9.38 (m, 1H), 7.95 (dd, 1H, J_1 = 8.0 Hz, J_2 = 1.2 Hz), 7.53 (dd, 1H, J_1 = 6.8 Hz, J_2 = 1.6 Hz), 7.49–7.48 (m, 3H), 7.47–7.46 (m, 1H), 7.42 (dd, 1H, J_1 = 5.6 Hz, J_2 = 2.0 Hz), 7.24–7.20 (m, 1H); ^{13}C{^{1}H} NMR (DMSO-d_6, 100 MHz): δ 191.6, 154.2, 151.3, 145.8, 139.1, 139.0, 131.2, 129.3, 128.1, 127.9, 127.7, 127.2, 124.4, 120.1, 119.8, 117.1, 116.9, 93.1; IR (neat, cm^{-1}): 3200, 2973, 2921, 1701, 1650, 1580, 1464, 1399; HRMS (ESI/Q-TOF) (m/z): calcd. for $C_{18}H_{11}INO_3$, $[M + H]^+$: 415.9778, found: 415.9754.

1-(4-Nitrobenzoyl)chromeno[3,4-b]pyrrol-4(3H)-one (13a):

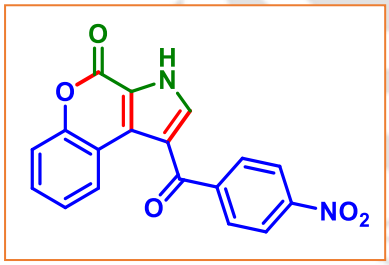

As brown solid (140 mg, 84% yield); m.p. 272–274 °C; purified over a column of silica gel (25% EtOAc in hexane); ^{1}H NMR (DMSO-d_6, 400 MHz): δ 13.63 (s, 1H), 8.91 (dd, 1H, J_1 = 8.0 Hz, J_2 = 1.6 Hz), 8.37 (d, 2H, J = 8.8 Hz), 8.04 (d, 2H, J = 8.8 Hz), 7.91 (s, 1H), 7.55–7.48 (m, 2H), 7.41–7.37 (m, 1H); ^{13}C{^{1}H} NMR (DMSO-d_6, 100 MHz): δ 189.1, 154.1, 151.2, 149.2, 144.9, 138.3, 130.3, 129.2, 127.8, 126.6, 124.2, 123.6, 119.5, 119.4, 117.0, 116.9; IR (neat, cm^{-1}): 3191, 2955, 2923, 1693, 1650, 1599, 1520, 1463, 1346; HRMS (ESI/Q-TOF) (m/z): calcd. for $C_{18}H_{11}N_2O_5$, $[M + H]^+$: 335.0662, found: 335.0668.

1-(2-Nitrobenzoyl)chromeno[3,4-b]pyrrol-4(3H)-one (14a):

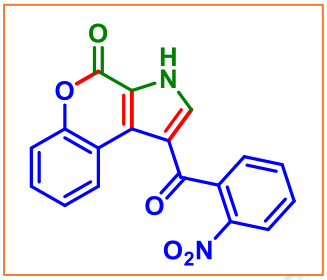

As brown solid (136 mg, 80% yield); m.p. 268–270 °C; purified over a column of silica gel (25% EtOAc in hexane); ^{1}H NMR (DMSO-d$_6$, 500 MHz): δ 13.59 (s, 1H), 9.18 (dd, 1H, J_1= 8.5 Hz, J_2 = 2.0 Hz), 8.25 (d, 1H, J = 8.0 Hz), 7.91 (dt, 1H, J_1 = 7.5 Hz, J_2 = 1.0 Hz), 7.82 (dt, 1H, J_1 = 7.5 Hz, J_2 = 1.5 Hz), 7.74–7.72 (m, 2H), 7.58– 7.54 (m, 1H), 7.51 (dd, 1H, J_1 = 7.0 Hz, J_2 = 1.5 Hz), 7.46–7.42 (m, 1H); ^{13}C{^{1}H} NMR (DMSO-d$_6$, 125 MHz): δ 187.8, 154.1, 151.3, 146.3, 138.3, 136.6, 134.5, 131.1, 129.3, 129.1, 127.6, 127.1, 124.8, 124.4, 120.4, 119.6, 117.0, 116.9; IR (neat, cm^{-1}): 3180, 2960, 2921, 1699, 1647, 1591, 1515, 1461; HRMS (ESI/Q-TOF) (m/z): calcd. for $C_{18}H_{11}N_2O_5$, $[M + H]^+$: 335.0662, found: 335.0663.

1-(2-Ethoxy-4-fluorobenzoyl)chromeno[3,4-b]pyrrol-4(3H)-one (15a):

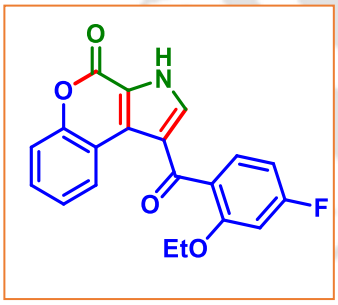

As off white solid (107 mg, 61% yield); m.p. 269–271 °C; purified over a column of silica gel (25% EtOAc in hexane); ^{1}H NMR (DMSO-d$_6$, 400 MHz): δ 13.49 (s, 1H), 9.20 (dd, 1H, J_1 = 8.0 Hz, J_2 = 1.6 Hz), 7.65 (s, 1H), 7.57–7.53 (m, 1H), 7.49 (dd, 1H, J_1 = 8.4 Hz, J_2 = 1.6 Hz), 7.45–7.41 (m, 1H), 7.33 (dt, 1H, J_1 = 8.4 Hz, J_2 = 3.2 Hz), 7.27 (dd, 1H, J_1 = 8.4 Hz, J_2 = 3.2 Hz), 7.18 (dd, 1H, J_1 = 9.2 Hz, J_2 = 4.4 Hz), 4.01 (q, 2H, J = 6.8 Hz), 1.06 (t, 3H, J = 6.8 Hz); ^{13}C{^{1}H} NMR (DMSO-d$_6$, 100 MHz): δ 188.5, 157.0, 154.4 (d, J = 48.4 Hz), 151.8 (d, J = 1.9 Hz), 151.2, 138.7, 131.8 (d, J = 6.3 Hz), 129.2, 127.3 (d, J = 7.7 Hz), 124.2, 121.2, 119.2, 117.6, 117.4, 117.1, 116.9, 115.3, 115.0 (d, J = 7.8 Hz), 64.4, 14.3; ^{19}F NMR (DMSO-d$_6$, 376 MHz): δ –123.3; IR (neat, cm^{-1}): 3221, 2998, 2931, 1721, 1642, 1465, 1395, 1261; HRMS (ESI/Q-TOF) (m/z): calcd. for $C_{20}H_{15}FNO_4$, $[M + H]^+$: 352.0980, found: 352.0997.

1-(2-Naphthoyl)chromeno[3,4-b]pyrrol-4(3H)-one (16a):

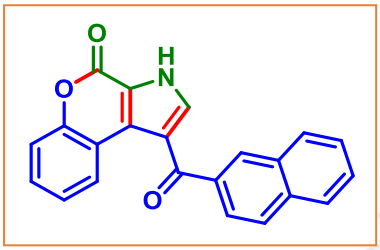

As brown solid (110 mg, 65% yield); m.p. 283–285 ^{o}C; purified over a column of silica gel (20% EtOAc in hexane); ^{1}H NMR (DMSO-d$_6$, 500 MHz): δ 13.49 (s, 1H), 8.74 (d, 1H, J = 8.5 Hz), 8.47 (s, 1H), 8.11 (dd, 2H, J_1 = 16 Hz, J_2 = 8.5 Hz), 8.03 (d, 1H, J = 8.5 Hz), 7.95 (d, 2H, J = 9.0 Hz), 7.68 (t, 1H, J = 8.0 Hz), 7.62 (t, 1H, J = 7.5 Hz), 7.52–7.47 (m, 2H), 7.37–7.33 (m, 1H); ^{13}C{^{1}H} NMR (DMSO-d$_6$, 125 MHz): δ 190.6. 154.2, 151.2, 137.0, 136.5, 134.7, 132.0, 131.1, 129.5, 128.9, 128.4, 128.3, 127.7, 127.6, 126.9, 126.3, 125.1, 124.2, 119.8, 118.9, 117.2, 116.9; IR (neat, cm^{-1}): 3400, 2923, 2850, 1725, 1643, 1467, 1400, 1264; HRMS (ESI/Q-TOF) (m/z): calcd. for $C_{22}H_{14}NO_3$, $[M + H]^+$: 340.0968, found: 340.0981.

1-(Benzo[d][1,3]dioxole-5-carbonyl)chromeno[3,4-b]pyrrol-4(3H)-one (17a):

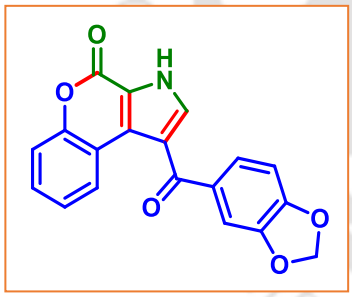

As brown solid (98 mg, 59% yield); m.p. 267–269 ^{o}C; purified over a column of silica gel (20% EtOAc in hexane); ^{1}H NMR (DMSO-d$_6$, 500 MHz): δ 13.39 (s, 1H), 8.53 (d, 1H, J = 8.5 Hz), 7.85 (s, 1H), 7.48–7.43 (m, 3H), 7.38 (d, 1H, J = 1.5 Hz), 7.33–7.30 (m, 1H), 7.04 (d, 1H, J = 8.0 Hz), 6.16 (s, 2H); ^{13}C{^{1}H} NMR (DMSO-d$_6$, 125 MHz): δ 188.9, 154.2, 151.2, 151.1, 147.7, 135.8, 133.4, 128.8, 127.4, 126.0, 124.1, 119.5, 118.7, 117.1, 116.9, 108.8, 107.9, 102.1; IR (neat, cm^{-1}): 3412, 2960, 2921, 1723, 1646, 1478, 1439, 1399, 1260; HRMS (ESI/Q-TOF) (m/z): calcd. for $C_{19}H_{12}NO_5$, $[M + H]^+$: 334.0710, found: 334.0715.

1-(Furan-2-carbonyl)chromeno[3,4-b]pyrrol-4(3H)-one (18a):

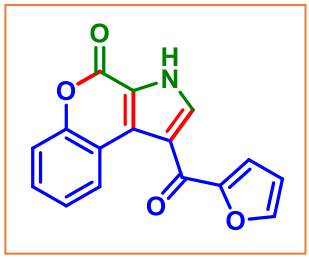

As brown solid (92 mg, 66% yield); m.p. 237–239 °C; purified over a column of silica gel (20% EtOAc in hexane); ^{1}H NMR (DMSO-d_6, 500 MHz): δ 13.51 (s, 1H), 8.70 (d, 1H, J = 7.5 Hz), 8.29 (s, 1H), 8.09 (s, 1H), 7.49–7.45 (m, 3H), 7.36–7.33 (m, 1H), 6.79–6.78 (m, 1H); ^{13}C{^{1}H} NMR (DMSO-d_6, 125 MHz): δ 176.4, 154.1, 152.5, 151.1, 148.0, 136.6, 128.9, 127.5, 126.3, 124.2, 120.1, 118.7, 117.1, 116.9, 112.7; IR (neat, cm^{-1}): 3405, 2957, 2921, 1724, 1634, 1466, 1400, 1278; HRMS (ESI/Q-TOF) (m/z): calcd. for $C_{16}H_{10}NO_4$, $[M + H]^+$: 280.0604, found: 280.0603.

1-(Thiophene-2-carbonyl)chromeno[3,4-b]pyrrol-4(3H)-one (19a):

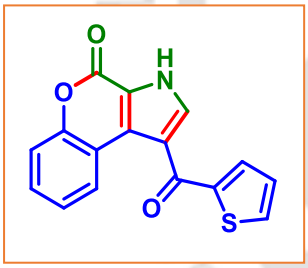

As yellow solid (94 mg, 64% yield); m.p. 247–249 °C; purified over a column of silica gel (20% EtOAc in hexane); ^{1}H NMR (DMSO-d_6, 500 MHz): δ 13.49 (s, 1H), 8.53 (d, 1H, J = 8.5 Hz), 8.17 (s, 1H), 8.09 (d, 1H, J = 5.0 Hz), 7.87 (d, 1H, J = 3.5 Hz), 7.51–7.45 (m, 2H), 7.35–7.32 (m, 1H), 7.29 (t, 1H, J = 4.5 Hz); ^{13}C{^{1}H} NMR (DMSO-d_6, 125 MHz): δ 182.0, 154.1, 151.1, 144.7, 135.2, 135.1, 134.8, 128.9, 128.8, 127.1, 125.9, 124.2, 119.1, 118.8, 117.0, 116.9; IR (neat, cm^{-1}): 3204, 2960, 2918, 1701, 1624, 1465, 1413, 1275; HRMS (ESI/Q-TOF) (m/z): calcd. for $C_{16}H_{10}NO_3S$, $[M + H]^+$: 296.0376, found: 296.0381.

1-Acetylchromeno[3,4-b]pyrrol-4(3H)-one (20a):

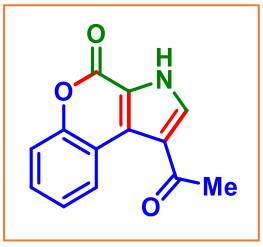

As yellow solid (42 mg, 37% yield); m.p. 222–224 °C; purified over a column of silica gel (15% EtOAc in hexane); ^{1}H NMR ($CDCl_3$, 400MHz): δ 10.84 (s, 1H), 9.32 (d, 1H, J = 8.0 Hz), 8.02 (d, 1H, J = 3.2 Hz), 7.51–7.46 (m, 2H), 7.44–7.38 (m, 1H), 2.64 (s, 3H); ^{13}C{^{1}H} NMR ($CDCl_3$ + DMSO-d_6, 100 MHz): δ 192.7, 155.3, 151.4, 135.1, 128.5,

127.9, 127.6, 124.1, 121.8, 119.6, 117.5, 116.6, 28.6; IR (neat, cm^{-1}): 3429, 3064, 3008, 1742, 1634, 1441, 1272; HRMS (ESI/Q-TOF) (m/z): calcd. for $C_{17}H_{10}NO_3$, $[M + H]^+$: 228.0655, found: 228.0652.

1-(3-Methylbutanoyl)chromeno[3,4-b]pyrrol-4(3H)-one (21a):

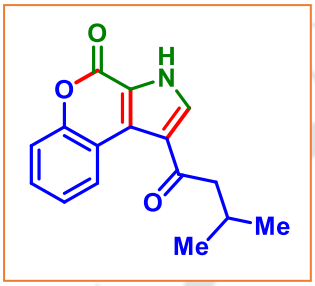

As brown solid (56 mg, 42% yield); m.p. 233–235 °C; purified over a column of silica gel (15% EtOAc in hexane); ^1H NMR ($CDCl_3$, 400 MHz): δ 11.00 (s, 1H), 9.33 (dd, 1H, J_1= 8.0 Hz, J_2 = 1.6 Hz), 8.02 (d, 1H, J = 3.2 Hz), 7.51–7.45 (m, 2H), 7.43–7.38 (m, 1H), 2.80 (d, 2H, J = 6.8 Hz), 2.41–2.31 (m, 1H), 1.04 (d, 6H, J = 6.8 Hz); $^{13}C\{^1H\}$ NMR ($CDCl_3$, 125 MHz): δ 195.6, 156.4, 151.8, 134.1, 129.5, 129.0, 128.5, 125.1, 123.3, 119.7, 117.7, 117.3, 50.2, 25.9, 23.0; IR (neat, cm^{-1}): 3251, 3011, 2925, 1725, 1667, 1461, 1398, 1273; HRMS (ESI/Q-TOF) (m/z): calcd. for $C_{16}H_{16}NO_3$, $[M + H]^+$: 270.1125, found: 270.1129.

1-(Cyclopropanecarbonyl)chromeno[3,4-b]pyrrol-4(3H)-one (22a):

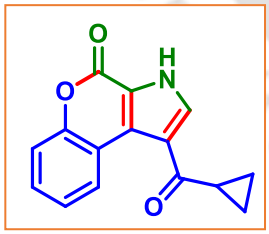

As white solid (50 mg, 40% yield); m.p. 241–243 °C; purified over a column of silica gel (15% EtOAc in hexane); ^1H NMR ($CDCl_3$, 400 MHz): δ 13.47 (s, 1H), 9.22 (dd, 1H, J_1 = 8.0 Hz, J_2 = 1.6 Hz), 8.68 (d, 1H, J = 3.2 Hz), 7.49–7.42 (m, 2H), 7.36–7.31 (m, 1H), 2.89–2.85 (m, 1H), 1.29–1.19 (m, 1H), 1.06–1.03 (m, 1H), 0.99–0.94 (m, 2H); $^{13}C\{^1H\}$ NMR ($CDCl_3$, 125 MHz): δ 194.9, 154.3, 151.2, 136.5, 128.9, 127.6, 126.5, 124.1, 122.0, 119.1, 117.3, 116.7, 18.5, 10.6; IR (neat, cm^{-1}): 3202, 2956, 2920, 1701, 1658, 1466, 1401, 1262; HRMS (ESI/Q-TOF) (m/z): calcd. for $C_{15}H_{12}NO_3$, $[M + H]^+$: 254.0812, found: 254.0812.

(4-(2-Hydroxyphenyl)-1H-pyrrol-3-yl)(p-tolyl)methanone (2c):

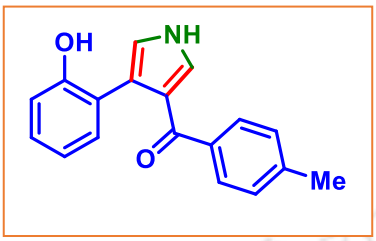

As a white solid (87 mg, 63% yield); m.p. 181–183 °C; purified over a column of silica gel (15% EtOAc in hexane);^{1}H NMR ($CDCl_3$, 500 MHz): δ 9.36 (s, 1H), 9.24 (s, 1H), 7.73 (dd, 2H, J_1 = 8.0 Hz, J_2 = 1.5 Hz), 7.24–7.22 (m, 3H), 7.15 (dd, 1H, J_1 = 7.5 Hz, J_2 = 1.5 Hz), 7.09 (d, 2H, J = 7.5 Hz), 6.91 (dt, 1H, J_1 = 7.0 Hz, J_2 = 1.5 Hz), 6.72 (s, 1H), 2.41 (s, 3H); ^{13}C{^{1}H} NMR ($CDCl_3$, 125 MHz): δ 194.4, 155.5, 143.5, 136.5, 132.1, 130.5, 129.3, 129.1, 128.4, 124.9, 122.9, 122.8, 121.2, 121.0, 119.5, 21.8; IR (neat, cm^{-1}): 3278, 2957, 2924, 1678, 1600, 1545, 1452, 1381, 1282; HRMS (ESI/Q-TOF) (m/z): calcd. for $C_{18}H_{16}NO_2$, [M + H]$^{+}$: 278.1176, found: 278.1171.

4-Tosyl-1-(tosylmethyl)-1H-imidazole (2c'):

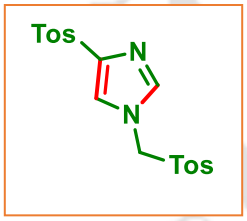

As yellow solid (68 mg, 77% yield); m.p. 177–179 °C; purified over a column of silica gel (80% EtOAc in hexane); ^{1}H NMR ($CDCl_3$, 500 MHz): δ 7.86 (d, 2H, J = 8.0 Hz), 7.45 (d, 2H, J = 8.0 Hz), 7.39 (s, 1H), 7.33 (d, 2H, J = 8.0 Hz), 7.29 (s, 1H), 7.23 (d, 2H, J = 8.0 Hz), 5.11 (s, 2H), 2.44 (s, 3H), 2.43 (s, 3H); ^{13}C{^{1}H} NMR (125 MHz): δ 147.0, 144.7, 143.3, 139.7, 137.6, 131.5, 130.7, 129.9, 128.8, 128.1, 124.0, 65.5, 21.9, 21.8; IR (neat, cm^{-1}): 3377, 2924, 1705, 1622, 1438, 1264, 1172; HRMS (ESI/Q-TOF) (m/z): calcd. for $C_{18}H_{18}N_2O_4S_2Na$, [M + H]$^{+}$: 413.0600, found: 413.0601.

1-Benzoyl-8-methylchromeno[3,4-b]pyrrol-4(3H)-one (23a):

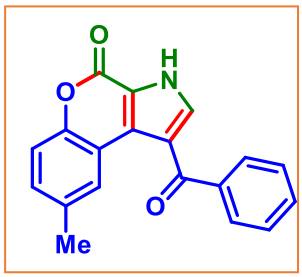

As brown solid (101 mg, 67% yield); m.p. 237–239 °C; purified over a column of silica gel (15% EtOAc in hexane); ^{1}H NMR (DMSO-d$_6$, 400 MHz): δ 13.46 (s, 1H), 8.51 (s, 1H), 7.85 (d, 2H, J = 8.4 Hz), 7.82 (s, 1H), 7.69 (t, 1H, J = 7.2 Hz), 7.57 (t, 2H, J = 7.6 Hz), 7.37 (d, 1H, J = 8.4 Hz), 7.31 (d, 1H, J = 8.8 Hz), 2.36 (s, 3H); ^{13}C{^{1}H} NMR (DMSO-d$_6$, 100 MHz): δ 190.6, 154.3, 149.3, 139.3, 136.8, 133.1, 132.5, 129.6, 129.3, 128.6, 127.6, 126.2, 119.7, 119.1, 116.8, 116.6, 20.7; IR (neat, cm^{-1}): 3193, 3973, 3937, 1710, 1660, 1458, 1398, 1271; HRMS (ESI/Q-TOF) (m/z): calcd. for $C_{19}H_{14}NO_3$, $[M + H]^+$: 304.0968, found: 304.0953.

1-Benzoyl-8-chlorochromeno[3,4-b]pyrrol-4(3H)-one (24a):

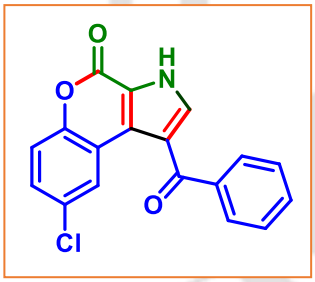

As brown solid (113 mg, 70% yield); m.p. 244–246 °C; purified over a column of silica gel (20% EtOAc in hexane); ^{1}H NMR (DMSO-d$_6$, 500 MHz): δ 13.63 (s, 1H), 8.88 (d, 1H, J = 2.5 Hz), 7.87 (d, 1H, J = 3.0 Hz), 7.85 (dd, 2H, J_1 = 8.5 Hz, J_2 = 1.5 Hz), 7.68–7.67 (m, 1H), 7.59–7.56 (m, 2H), 7.54–7.51 (m, 2H); ^{13}C{^{1}H} NMR (DMSO-d$_6$, 125 MHz): δ 190.7, 153.8, 149.9, 139.2, 137.4, 132.5, 129.4, 128.7, 128.6, 128.1, 126.6, 125.7, 119.8, 119.4, 118.9, 118.7; IR (neat, cm^{-1}): 3325, 2973, 2927, 1722, 1661, 1471, 1399, 1269; HRMS (ESI/Q-TOF) (m/z): calcd. for $C_{18}H_{11}ClNO_3$, $[M + H]^+$: 324.0422, found: 324.0426.

1-Benzoyl-8-bromochromeno[3,4-b]pyrrol-4(3H)-one (25a):

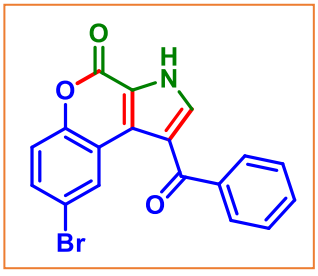

As yellow solid (117 mg, 64% yield); m.p. 251–253 °C; purified over a column of silica gel (20% EtOAc in hexane); ^{1}H NMR (DMSO-d$_6$,, 500 MHz): δ 13.75 (s, 1H), 8.85 (d, 1H, J = 2.5 Hz), 7.92 (s, 1H), 7.85–7.83 (m, 4H), 7.69 (t, 1H, J = 7.0 Hz), 7.58 (t, 2H, J = 7.5 Hz); ^{13}C{^{1}H} NMR (DMSO-d$_6$, 125 MHz): δ 190.6, 152.8, 145.6, 139.1, 137.7, 137.1, 132.6,

130.6, 129.4, 128.6, 128.3, 127.9, 126.2, 124.7, 121.6, 119.9; IR (neat, cm^{-1}): 3220, 2983, 2951, 1702, 1653, 1458, 1397, 1259; HRMS (ESI/Q-TOF) (m/z): calcd. for $C_{18}H_{11}BrNO_3$, [M + H] : 367.9917, found: 367.9914.

1-Benzoyl-8-iodochromeno[3,4-b]pyrrol-4(3H)-one (26a):

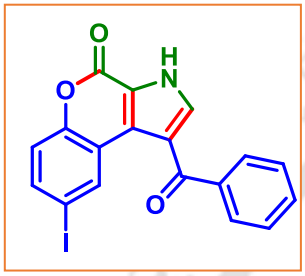

As brown solid (126 mg, 61% yield); m.p. 258–260 °C; purified over a column of silica gel (20% EtOAc in hexane); ^{1}H NMR (DMSO-d_6, 400 MHz): δ 13.60 (s, 1H), 9.16 (d, 1H, J = 2.0 Hz), 7.85–7.83 (m, 3H), 7.78 (dd, 1H, J_1 = 8.4 Hz, J_2 = 2.0 Hz), 7.01–7.66 (m, 1H), 7.57 (t, 2H, J = 7.6 Hz), 7.29 (d, 1H, J = 8.4 Hz); ^{13}C{^{1}H} NMR (DMSO-d_6, 100 MHz): δ 190.7, 153.7, 150.8, 139.2, 137.2, 137.1, 134.7, 132.5, 129.3, 128.6, 127.9, 126.3, 119.7, 119.5, 119.2, 88.3; IR (neat, cm^{-1}): 3295, 2981, 2923, 1717, 1659, 1468, 1396, 1271; HRMS (ESI/Q-TOF) (m/z): calcd. for $C_{18}H_{10}INO_3Na$, $[M + Na]^+$: 437.9598, found: 437.9638.

1-Benzoyl-7,8-dimethylchromeno[3,4-b]pyrrol-4(3H)-one (27a):

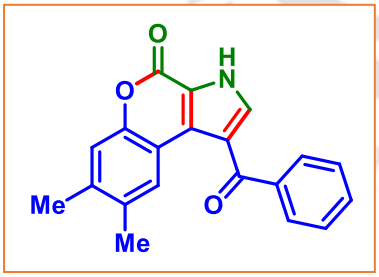

As brown solid (93 mg, 59% yield); m.p. 239–241 °C; purified over a column of silica gel (20% EtOAc in hexane); ^{1}H NMR (DMSO-d_6, 400 MHz): δ 8.46 (s, 1H), 7.85–7.83 (m, 2H), 7.79 (s, 1H), 7.70–7.65 (m, 1H), 7.57 (t, 2H, J = 6.8 Hz), 7.28 (s, 1H), 2.31 (s, 3H), 2.26 (s, 3H); ^{13}C{^{1}H} NMR (DMSO-d_6, 100 MHz): δ 190.5, 154.4, 149.6, 139.4, 137.9, 136.7, 132.4, 132.2, 129.3, 128.6, 127.9, 125.5, 119.4, 118.6, 117.3, 114.5, 19.4, 19.2; IR (neat, cm^{-1}): 3211, 2977, 2921, 1702, 1651, 1460, 1399, 1268; HRMS (ESI/Q-TOF) (m/z): calcd. for $C_{20}H_{16}NO_3$, $[M + H]^+$: 318.1125, found: 318.1131.

1-Benzoyl-6,8-dichlorochromeno[3,4-b]pyrrol-4(3H)-one (28a):

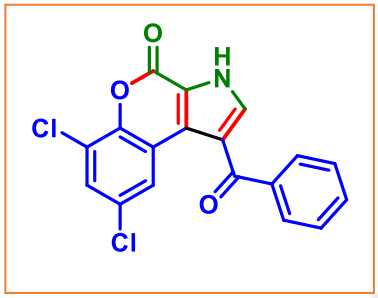

As white solid (111 mg, 62% yield); m.p. 281–283 °C; purified over a column of silica gel (20% EtOAc in hexane); ^{1}H NMR (DMSO-d$_6$, 400 MHz): δ 13.61 (s, 1H), 9.01 (d, 1H, J = 2.4 Hz), 7.86–7.83 (m, 3H), 7.66–7.63 (m, 1H), 7.59–7.55 (m, 2H), 7.44–7.42 (d, 1H, J = 8.8 Hz); ^{13}C{^{1}H} NMR (DMSO-d$_6$, 100 MHz): δ 190.6, 153.7, 150.2, 139.2, 137.3, 132.5, 131.3, 129.3, 128.7, 128.6, 126.4, 119.7, 119.4, 119.14, 119.12, 116.1; IR (neat, cm^{-1}): 3401, 2978, 2927, 1719, 1657, 1458, 1391, 1259.

1-Benzoyl-6,8-dibromochromeno[3,4-b]pyrrol-4(3H)-one (29a):

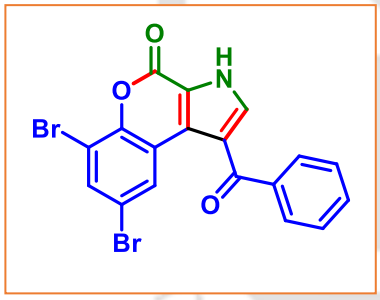

As off-white solid (143 mg, 64% yield); m.p. 289–291 °C; purified over a column of silica gel (20% EtOAc in hexane); ^{1}H NMR (DMSO-d$_6$, 500 MHz): δ 13.72 (s, 1H), 9.01 (d, 1H, J = 2.5 Hz), 8.00 (d, 1H, J = 2.5 Hz), 7.90 (s, 1H), 7.84 (d, 2H, J = 7.5 Hz), 7.70–7.66 (m, 1H), 7.57 (t, 2H, J = 7.5 Hz); ^{13}C{^{1}H} NMR (DMSO-d$_6$, 125 MHz): δ 190.6, 152.8, 146.9, 139.1, 137.7, 133.7, 132.5, 129.3, 128.5, 128.2, 126.1, 120.2, 119.8, 119.5, 115.9, 110.9; IR (neat, cm^{-1}): 3201, 2960, 2920, 1739, 1647, 1592, 1464, 1261; HRMS (ESI/Q-TOF) (m/z): calcd. for $C_{18}H_{10}Br_2NO_3$, $[M + H]^+$: 445.9022, found: 445.9013.

6,8-Dibromo-1-(4-ethoxybenzoyl)chromeno[3,4-b]pyrrol-4(3H)-one (30a):

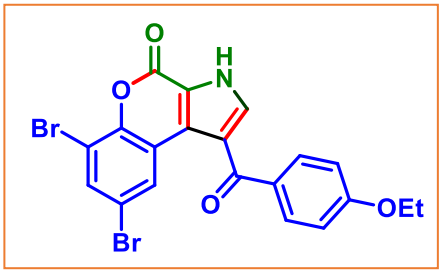

As white solid (145 mg, 59% yield); m.p. 279–281 °C; purified over a column of silica gel (20% EtOAc in hexane); ^{1}H NMR (DMSO-d$_6$, 400 MHz): δ 13.66 (s, 1H), 8.83 (d, 1H, J = 2.4 Hz), 8.01 (d, 1H, J = 2.4 Hz), 7.94 (s, 1H), 7.84 (d, 2H, J = 8.8 Hz), 7.07 (d, 2H, J = 8.8 Hz), 4.14 (q, 2H, J = 6.8 Hz), 1.37 (t, 3H, J = 6.8 Hz); ^{13}C{^{1}H} NMR (DMSO-d$_6$, 100 MHz): δ 189.2, 162.3, 152.9,

146.9, 136.6, 133.5, 131.9, 131.2, 129.9, 125.9, 120.3, 119.9, 119.2, 115.9, 114.3, 110.0, 63.6, 14.5; IR (neat, cm^{-1}): 3185, 2971, 2930, 1700, 1653, 1458, 1401, 1261; HRMS (ESI/Q-TOF) (m/z): calcd. for $C_{20}H_{14}Br_2NO_4$, $[M + H]^+$: 489.9284, found: 489.9251.

8-Bromo-1-(4-methylbenzoyl)chromeno[3,4-b]pyrrol-4(3H)-one (31a):

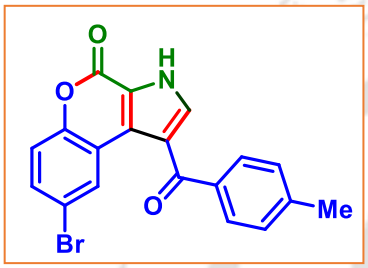

As white solid (103 mg, 54% yield); m.p. 281–283 °C; purified over a column of silica gel (20% EtOAc in hexane); ^1H NMR (DMSO-d_6, 400 MHz): δ 13.60 (s, 1H), 8.95 (d, 1H, J = 2.4 Hz), 8.87 (d, 1H, J = 2.8 Hz), 7.76 (d, 2H, J = 8.4 Hz), 7.65 (dd, 1H, J_1 = 8.8 Hz, J_2 = 2.4 Hz), 7.45 (d, 1H, J = 8.8 Hz), 7.38 (d, 2H, J = 7.6 Hz), 2.42 (s, 3H); $^{13}C\{^1H\}$ NMR (DMSO-d_6, 100 MHz): δ 190.3, 153.7, 150.2, 142.9, 136.8, 136.4, 131.3, 129.6, 129.2, 128.6, 126.4, 119.8, 119.23, 119.19, 119.15, 116.1, 21.1; IR (neat, cm^{-1}): 3205, 2973, 2941, 1721, 1658, 1461, 1393, 1271; HRMS (ESI/Q-TOF) (m/z): calcd. for $C_{19}H_{13}BrNO_3$, $[M + H]^+$: 382.0073, found: 382.0069.

1-(2-Iodobenzoyl)-7-methylchromeno[3,4-b]pyrrol-4(3H)-one (32a):

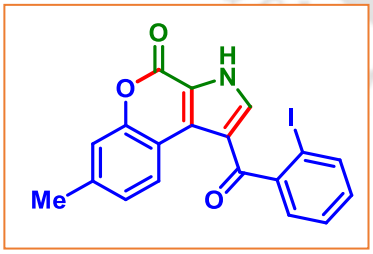

As yellow solid (111 mg, 52% yield); m.p. 291–293 °C; purified over a column of silica gel (20% EtOAc in hexane); ^1H NMR ($CDCl_3$ + DMSO-d_6, 500 MHz): δ 13.28 (s, 1H), 9.24 (d, 1H, J = 8.0 Hz), 7.98 (d, 1H, J = 8.0 Hz), 7.55–7.52 (m, 1H), 7.46–7.44 (m, 1H), 7.36 (s, 1H), 7.29–7.27 (m, 3H), 2.54 (s, 3H); $^{13}C\{^1H\}$ NMR ($CDCl_3$ + DMSO-d_6, 125 MHz): δ 190.7, 154.4, 151.1, 145.3, 138.9, 138.8, 137.6, 130.7, 128.2, 127.2, 127.1, 126.9, 124.7, 119.5, 119.0, 116.3, 114.1, 91.6, 20.6; IR (neat, cm^{-1}): 3250, 2981, 2950, 1710, 1649, 1458, 1397, 1263; HRMS (ESI/Q-TOF) (m/z): calcd. for $C_{19}H_{13}INO_3$, $[M + H]^+$: 429.9935, found: 429.9940.

8-Chloro-1-(2-iodobenzoyl)chromeno[3,4-b]pyrrol-4(3H)-one (33a):

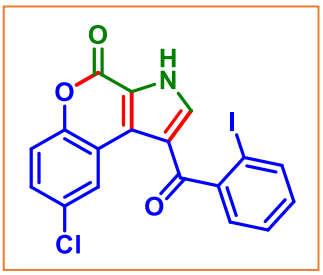

As brown solid (137 mg, 61% yield); m.p. 295–297 °C; purified over a column of silica gel (20% EtOAc in hexane); ^{1}H NMR (DMSO-d_6, 400 MHz): δ 13.74 (s, 1H), 9.33 (d, 1H, J = 2.4 Hz), 7.98 (d, 1H, J = 7.6 Hz), 7.60 (dd, 1H, J_1 = 6.4 Hz, J_2 = 2.4 Hz), 7.57–7.52 (m, 2H), 7.49 (dd, 1H, J_1 = 6.0 Hz, J_2 = 1.6 Hz), 7.32–7.28 (m, 2H); ^{13}C{^{1}H} NMR (DMSO-d_6, 125 MHz): δ 190.9, 153.7, 149.9, 145.5, 139.2, 139.1, 131.3, 128.9, 128.7, 128.1, 128.0, 126.6, 126.3, 120.1, 120.0, 118.9, 118.5, 92.9; IR (neat, cm^{-1}): 3301, 2971, 2928, 1720, 1653, 1460, 1401, 1273; HRMS (ESI/Q-TOF) (m/z): calcd. for $C_{18}H_{10}ClINO_3$, $[M + H]^+$: 449.9388, found: 449.9394.

8-Bromo-1-(2-iodobenzoyl)chromeno[3,4-b]pyrrol-4(3H)-one (34a):

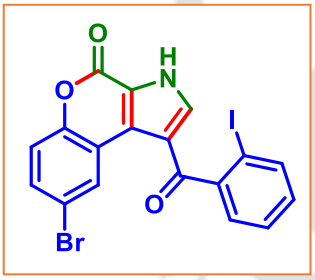

As brown solid (148 mg, 60% yield); m.p. 296–298 °C; purified over a column of silica gel (20% EtOAc in hexane); ^{1}H NMR (DMSO-d_6, 500 MHz): δ 13.72 (s, 1H), 9.45 (d, 1H, J = 2.5 Hz), 7.97 (d, 1H, J = 7.5 Hz), 7.69 (dd, 1H, J_1 = 9.0 Hz, J_2 = 2.5 Hz), 7.55–7.45 (m, 4H), 7.29 (t, 1H, J = 7.5 Hz); ^{13}C{^{1}H} NMR (DMSO-d_6, 125 MHz): δ 192.3, 154.1, 150.8, 146.0, 139.7, 139.6, 132.2, 131.8, 129.7, 129.1, 128.6, 128.5, 127.0, 120.5, 119.6, 119.5, 116.7, 93.5; IR (neat, cm^{-1}): 3295, 2983, 2927, 1699, 1647, 1468, 1395, 1261; HRMS (ESI/Q-TOF) (m/z): calcd. for $C_{18}H_{10}BrINO_3$, $[M + H]^+$: 493.8883, found: 493.8874.

8-Bromo-1-(3-methylbutanoyl)chromeno[3,4-b]pyrrol-4(3H)-one (35a):

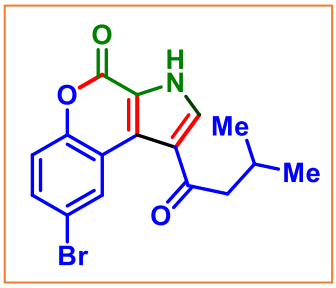

As brown solid (68 mg, 39% yield); m.p. 239–241 °C; purified over a column of silica gel (20% EtOAc in hexane); ^{1}H NMR ($CDCl_3$, 400 MHz): δ 10.97 (s, 1H), 9.58 (d, 1H, J = 2.4 Hz), 8.03 (s, 1H), 7.58 (dd, 1H, J_1 = 8.8 Hz, J_2 = 2.8 Hz), 7.32 (d, 1H, J = 8.8 Hz), 2.79 (d, 2H, J = 7.2 Hz), 2.42–2.34 (m, 1H), 1.04 (d, 6H, J = 6.0 Hz); ^{13}C{^{1}H} NMR ($CDCl_3$, 100 MHz): δ 195.4, 155.6, 150.7, 133.7, 132.4, 131.1, 127.8, 123.5, 119.9, 119.4, 118.9, 117.9, 50.1, 25.9, 23.0; IR (neat, cm^{-1}): 3253, 3012, 2922, 1727, 1679, 1465, 1397, 1274; HRMS (ESI/Q-TOF) (m/z): calcd. for $C_{16}H_{15}BrNO_3$, $[M + H]^+$: 348.0230, found: 348.0228.

Ethyl 4-oxo-2,4-dihydrochromeno[3,4-c]pyrrole-1-carboxylate (1a'):

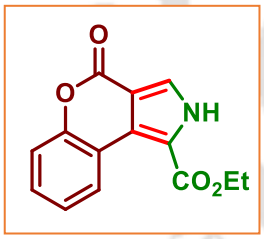

As white solid (112 mg, 87% yield); m.p. 249–251 °C; purified over a column of silica gel (15% EtOAc in hexane); ^{1}H NMR ($CDCl_3$, 400 MHz): δ 9.98 (s, 1H), 9.14 (dd, 1H, J_1 = 8.0 Hz, J_2 = 1.6 Hz), 7.86 (d, 1H, J = 3.6 Hz), 7.46–7.42 (m, 1H), 7.36 (d, 1H, J = 8.0 Hz), 7.32 (t, 1H, J = 7.6 Hz), 2.49 (q, 2H, J = 7.2 Hz), 1.48 (t, 3H, J = 7.2 Hz); ^{13}C{^{1}H} NMR ($CDCl_3$, 100 MHz): δ 163.7, 156.1, 151.8, 134.5, 129.3, 128.1, 126.5, 125.0, 119.1, 117.5, 117.4, 113.8, 60.9, 14.6; IR (neat, cm^{-1}): 3222, 2931, 2897, 1703, 1651, 1613, 1261; HRMS (ESI/Q-TOF) (m/z): calcd. for $C_{14}H_{12}NO_4$, $[M + H]^+$: 258.0761, found: 258.0765.

Ethyl 7-methyl-4-oxo-2,4-dihydrochromeno[3,4-c]pyrrole-1-carboxylate (2a'):

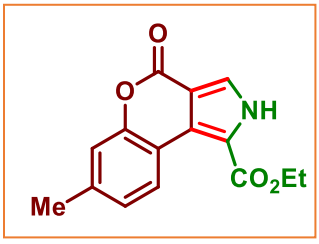

As yellow solid (112 mg, 83% yield); m.p. 254–256 °C; purified over a column of silica gel (15% EtOAc in hexane); ^{1}H NMR (DMSO-d_6, 400 MHz): δ 13.35 (s, 1H), 8.99 (d, 1H, J = 8.4 Hz), 8.07 (d, 1H, J = 3.2 Hz), 7.26 (s, 1H), 7.19 (dd, 1H, J_1 = 8.4 Hz, J_2 = 1.6 Hz), 4.30 (q, 2H, J = 7.2 Hz), 2.40 (s, 3H), 1.33 (t, 3H, J = 7.2 Hz); ^{13}C{^{1}H} NMR (DMSO-d_6, 125

MHz): δ 163.4, 154.1, 151.2, 139.0, 135.0, 127.5, 126.6, 125.2, 118.2, 116.9, 114.4, 111.1, 60.1, 20.8, 14.2; IR (neat, cm^{-1}): 3377, 2924, 1705, 1622, 1438, 1264, 1172; HRMS (ESI/Q-TOF) (m/z): calcd. for $C_{15}H_{14}NO_4$, $[M + H]^+$: 272.0917, found: 272.0937.

Ethyl 8-chloro-4-oxo-2,4-dihydrochromeno[3,4-c]pyrrole-1-carboxylate (3a')

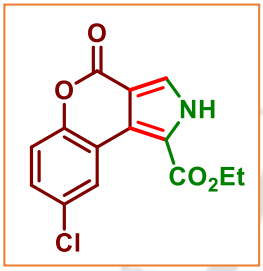

As yellow solid (118 mg, 81% yield); m.p. 262–264 °C; purified over a column of silica gel (15% EtOAc in hexane); ^1H NMR (DMSO-d_6, 400 MHz): δ 13.52 (s, 1H), 9.18 (d, 1H, J = 2.4 Hz), 8.09 (s, 1H), 7.50 (dd, 1H, J_1 = 8.8 Hz, J_2 = 2.4 Hz), 7.45 (d, 1H, J = 8.8 Hz), 4.31 (q, 2H, J = 7.2 Hz), 1.35 (t, 3H, J = 7.2 Hz); $^{13}C\{^1H\}$ NMR (DMSO-d_6, 125 MHz): δ 163.3, 153.5, 149.7, 135.3, 128.4, 128.1, 125.99, 125.96, 118.9, 118.7, 118.4, 111.7, 60.3, 14.2; IR (neat, cm^{-1}): 3220, 3127, 2987, 2923, 1733, 1679, 1528, 1468, 1400, 1263; HRMS (ESI/Q-TOF) (m/z): calcd. for $C_{14}H_{11}ClNO_4$, $[M + H]^+$: 292.0371, found: 292.0374.

Ethyl 8-bromo-4-oxo-2,4-dihydrochromeno[3,4-c]pyrrole-1-carboxylate (4a'):

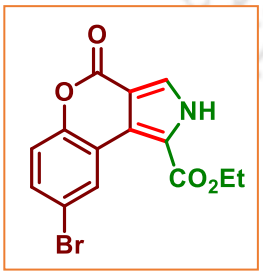

As white solid (134 mg, 80% yield); m.p. 276–278 °C; purified over a column of silica gel (15% EtOAc in hexane); ^1H NMR (DMSO-d_6, 400 MHz): δ 13.50 (s, 1H), 9.28 (d, 1H, J = 2.8 Hz), 8.06 (s, 1H), 7.59 (dd, 1H, J_1 = 8.8 Hz, J_2= 2.4 Hz), 7.36 (d, 1H, J = 8.8 Hz), 4.30 (q, 2H, J = 7.2 Hz), 1.35 (t, 3H, J = 7.2 Hz); $^{13}C\{^1H\}$ NMR (DMSO-d_6,125 MHz): δ 163.2, 153.4, 150.1, 135.3, 131.1, 128.9, 125.8, 119.0, 118.9, 118.8, 116.1, 111.7, 60.3, 14.2; IR (neat, cm^{-1}): 3107, 2987, 2931, 1721, 1658, 1460, 1409, 1268; HRMS (ESI/Q-TOF) (m/z): calcd. for $C_{14}H_{11}BrNO_4$, $[M + H]^+$: 335.9866, found:335.9865.

Methyl 4-oxo-2,4-dihydrochromeno[3,4-c]pyrrole-1-carboxylate (1b'):

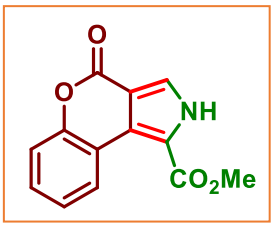

As white solid (102 mg, 84% yield); m.p. 239–241 °C; purified over a column of silica gel (15% EtOAc in hexane); ^{1}H NMR ($CDCl_3$ + DMSO-d_6, 400 MHz): δ 12.79 (s, 1H), 9.17 (dd, 1H, J_1= 8.0 Hz, J_2 = 6.4 Hz), 7.87 (d, 1H, J = 6.8 Hz), 7.37–7.25 (m, 3H), 3.83 (s, 3H); ^{13}C{^{1}H} NMR ($CDCl_3$ + DMSO-d_6, 125 MHz): δ 164.3, 155.3, 151.5, 134.6, 128.5, 128.3, 127.4, 124.3, 119.1, 117.5, 116.9, 112.0, 51.5; IR (neat, cm^{-1}): 3310, 2981, 2927, 1721, 1659, 1530, 1458, 1398, 1271; HRMS (ESI/Q-TOF) (m/z): calcd. for $C_{13}H_{10}NO_4$, [M + H]$^+$: 244.0604, found: 244.0610.

Chromeno[3,4-c]pyrrol-4(2H)-one (1c'):

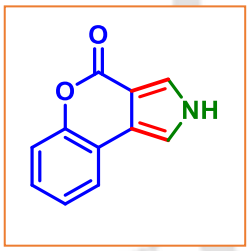

As reddish solid (84 mg, 91% yield); m.p. 200–202 °C; purified over a column of silica gel (20% EtOAc in hexane);; ^{1}H NMR ($CDCl_3$, 500 MHz): δ 9.70 (s, 1H), 7.73 (s, 1H), 7.68 (d, 1H, J = 7.5 Hz), 7.33–7.29 (m, 3H), 7.23–7.20 (m, 1H); ^{13}C{^{1}H} NMR ($CDCl_3$, 125 MHz): δ 160.1, 151.4, 127.9, 124.3, 123.1, 122.4, 121.7, 117.7, 117.2, 111.5, 109.8; IR (neat, cm^{-1}): 3218, 2927, 2899, 1700, 1617, 1457, 1262; HRMS (ESI/Q-TOF) (m/z): calcd. for $C_{11}H_8NO$, [M + H]$^+$: 186.0550, found: 186.0550.

6H-Chromeno[3,4-b]indeno[2,1-d]pyrrole-6,12(7H)-dione (12aa):

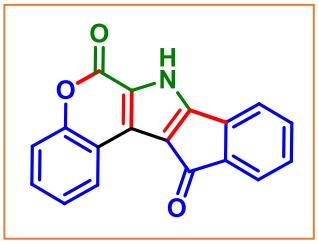

As yellow solid (37 mg, 87% yield); m.p. 288–291 °C; purified over a column of silica gel (15% EtOAc in hexane); ^{1}H NMR (DMSO-d_6, 400 MHz): δ 13.72 (s, 1H), 8.14 (dd, 1H, J_1 = 7.6 Hz, J_2 = 1.6 Hz), 7.49–7.43 (m, 3H), 7.40–7.37 (m, 3H), 7.32 (t, 1H, J = 7.2 Hz); ^{13}C{^{1}H} NMR (DMSO-d_6, 125 MHz): δ 184.7, 157.2, 154.1, 151.5, 139.5, 133.8, 133.7, 130.3, 129.8, 126.5, 126.1, 124.7, 123.6, 121.5, 120.3, 117.4, 116.8, 116.3; IR (neat, cm^{-1}): 3391, 2967, 2931, 1721, 1650,

1463, 1400, 1259; HRMS (ESI/Q-TOF) (m/z): calcd. for $C_{18}H_{10}NO_3$, $[M + H]^+$: 288.0655, found: 288.0661.

2-Bromo-6H-chromeno[3,4-b]indeno[2,1-d]pyrrole-6,12(7H)-dione (34aa):

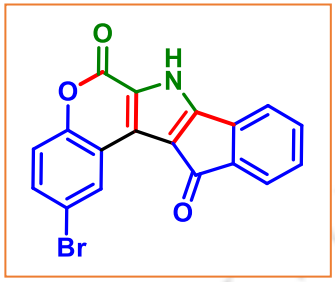

As red solid (45 mg, 83% yield); m.p. 297–299 °C; purified over a column of silica gel (15% EtOAc in hexane); ^{1}H NMR (DMSO-d_6, 400 MHz): δ 13.72 (s, 1H), 8.15 (dd, 1H, J_1 = 7.2 Hz, J_2 = 1.2 Hz), 7.49–7.44 (m, 2H), 7.40–7.37 (m, 3H), 7.33 (t, 1H, J = 7.2 Hz); ^{13}C{^{1}H} NMR (DMSO-d_6, 125 MHz): δ 184.6, 157.1, 153.9, 151.4, 139.4, 133.8, 133.7, 130.2, 129.7, 126.4, 126.1, 124.6, 123.5, 121.4, 120.2, 117.3, 116.7, 116.3; IR (neat, cm^{-1}): 3397, 2922, 2850, 1728, 1649, 1491, 1404, 1273; HRMS (ESI/Q-TOF) (m/z): calcd. for $C_{18}H_9BrNO_3$, $[M + H]^+$: 365.9760, found: 365.9766.

8-(Phenylethynyl)-1-(2-(phenylethynyl)benzoyl)chromeno[3,4-b]pyrrol-4(3H)-one (34ac):

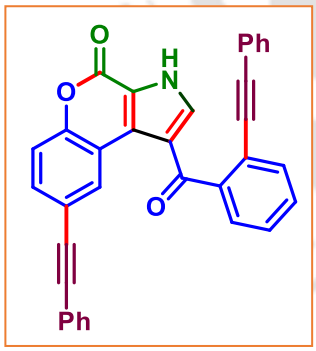

As yellow solid (58 mg, 79% yield); m.p. 269–271 °C; purified over a column of silica gel (35% EtOAc in hexane); ^{1}H NMR (DMSO-d_6, 500 MHz): δ 13.66 (s, 1H), 9.31 (d, 1H, J = 2.0 Hz), 7.73–7.69 (m, 3H), 7.67 (d, 1H, J = 7.5 Hz), 7.65–7.61 (m, 1H), 7.59–7.54 (m, 4H), 7.42 (t, 3H, J = 3.0 Hz), 7.28 (t, 1H, J = 7.0 Hz), 7.21 (t, 2H, J = 7.5 Hz), 7.09 (d, 2H, J = 8.0 Hz); ^{13}C{^{1}H} NMR (DMSO-d_6, 125 MHz): δ 190.9, 153.7, 151.1, 143.1, 138.7, 132.5, 132.1, 131.4, 130.9, 130.5, 129.7, 128.9, 128.8, 128.7, 128.6, 128.5, 128.0, 126.6, 122.1, 121.7, 121.2, 120.2, 119.5, 118.3, 117.7, 117.5, 93.9, 89.1, 88.8, 87.5; IR (neat, cm^{-1}): 3395, 2957, 2922, 2258, 2128, 1725, 1672, 1460, HRMS (ESI/Q-TOF) (m/z): calcd. for $C_{34}H_{20}NO_3$, $[M + H]^+$: 490.1438, found: 490.1427.

(E)-1-(4-Ethoxyphenyl)-3-(2-hydroxyphenyl)prop-2-en-1-one (5)[14a]:

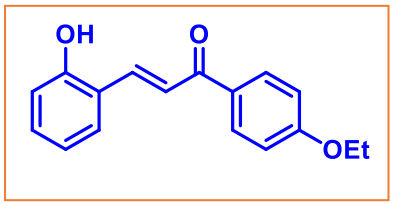

^{1}H NMR ($CDCl_3$, 400 MHz): δ 8.24 (d, 1H, J = 15.6 Hz), 8.05 (d, 2H, J = 8.8 Hz), 7.72 (d, 1H, J = 15.6 Hz), 7.58 (dd, 1H, J_1 = 8.0 Hz, J_2 = 1.6 Hz), 7.27–7.23 (m, 1H), 6.99–6.90 (m, 4H), 4.11 (q, 2H, J = 7.2 Hz), 1.92 (s, 1H), 1.45 (t, 3H, J = 7.2 Hz). The obtained ^{1}H NMR spectra matched with the reported procedure in ref. 14a.

(E)-3-(2-Hydroxyphenyl)-1-(4-isopropoxyphenyl)prop-2-en-1-one (6):

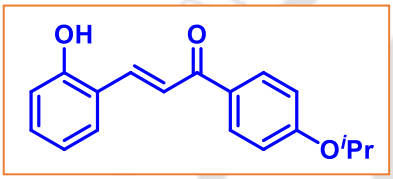

As yellowish solid (440 mg, 78% yield), m.p. 118–120 °C; purified over a column of silica gel (10% EtOAc in hexane); ^{1}H NMR ($CDCl_3$, 400 MHz): δ 8.19 (dd, 1H, J_1 = 16.0 Hz, J_2 = 3.6 Hz), 8.04 (d, 2H, J = 8.8 Hz), 7.70 (d, 1H, J = 15.6 Hz), 7.60 (dd, 1H, J_1 = 7.6 Hz, J_2 = 1.6 Hz), 7.28–7.24 (m, 1H), 6.96–6.92 (m, 4H), 4.72–4.61 (m, 1H), 1.38 (d, 6H, J = 6.0 Hz); ^{13}C{^{1}H} NMR (125 MHz) 190.5, 162.3, 156.2, 140.5, 131.8, 131.3, 130.9, 129.3, 122.7, 122.6, 120.9, 116.9, 115.4, 70.4, 22.2; IR (neat, cm^{-1}): 3265, 2982, 2928, 1720, 1672, 1635, 1600, 1559, 1490, 1256.

(E)-1-(2-Ethoxy-4-fluorophenyl)-3-(2-hydroxyphenyl)prop-2-en-1-one (15):

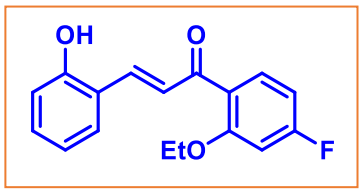

As yellowish solid (429 mg, 75% yield); m.p. 127–129 °C; purified over a column of silica gel (10% EtOAc in hexane); ^{1}H NMR ($CDCl_3$, 400 MHz): δ 8.04 (d, 1H, J = 16.0 Hz), 7.63 (d, 1H, J = 16.0 Hz), 7.52 (dd, 1H, J_1 = 8.0 Hz, J_2 = 1.6 Hz), 7.37 (dd, 1H, J_1 = 8.4 Hz, J_2 = 3.2 Hz), 7.27–7.23 (m, 1H), 7.17–7.12 (m, 2H), 6.94–6.90 (m, 3H), 4.09 (q, 2H, J = 6.4 Hz), 1.41 (t, 3H, J = 6.8 Hz); ^{13}C{^{1}H} NMR ($CDCl_3$, 125 MHz): δ 193.1, 158.0, 156.1 (d, J_{C-F} = 12.38 Hz), 154.1 (d, J_{C-F} = 2.13 Hz), 140.2, 132.0, 130.5 (d, J_{C-F} = 11.25 Hz), 129.3, 127.1, 122.4, 120.9, 119.4 (d, J_{C-F} = 23.13 Hz), 117.0 (d, J_{C-F} = 23.88 Hz), 116.9, 114.5 (d, J_{C-F} = 75 Hz), 65.4, 15.0;

^{19}F NMR ($CDCl_3$, 470 MHz): δ –123.1; IR (neat, cm^{-1}): 3261, 2980, 2928, 1723, 1670, 1636, 1601, 1556, 1491, 1256.

(E)-4-(2-Hydroxyphenyl)but-3-en-2-one (20)[14c]:

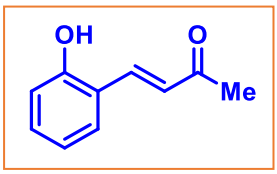

^{1}H NMR ($CDCl_3$, 400 MHz): δ 7.85 (d, 1H, J = 16.4 Hz), 7.48 (dd, 1H, J_1 = 7.6 Hz, J_2 = 1.6 Hz), 7.29–7.24 (m, 1H), 7.07 (s, 1H), 7.02 (d, 1H, J = 16.4 Hz), 6.95–6.89 (m, 2H), 2.43 (s, 3H); ^{13}C{^{1}H} NMR ($CDCl_3$, 100 MHz): δ 201.0, 156.0, 140.6, 132.1, 129.8, 128.0, 121.8, 121.0, 116.7, 27.1. The obtained ^{1}H NMR spectra matched with the reported procedure in ref. 14c.

(***E)-1-Cyclopropyl-3-(2-hydroxyphenyl)prop-2-en-1-one (22):***

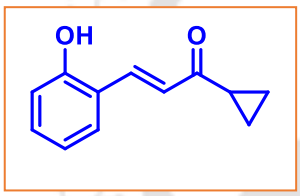

As yellowish solid (267 mg, 71% yield) ^{1}H NMR ($CDCl_3$, 400 MHz): δ 8.05 (d, 1H, J = 16.4 Hz), 7.63 (s, 1H), 7.53 (dd, 1H, J_1 = 7.6 Hz, J_2 = 1.6 Hz), 7.29 (d, 1H, J = 7.2 Hz), 7.16 (d, 1H, J = 16.4 Hz), 6.94 (d, 2H, J = 8.0 Hz), 2.39–2.35 (m, 1H), 1.26–1.22 (m, 2H), 1.06–1.01 (m, 2H); ^{13}C{^{1}H} NMR ($CDCl_3$, 100 MHz): δ 202.7, 156.4, 139.2, 131.9, 129.5, 127.1, 122.1, 120.8, 116.9, 19.4, 11.8.

(E)-3-(3,5-Dibromo-2-hydroxyphenyl)-1-(4-ethoxyphenyl)prop-2-en-1-one (30):

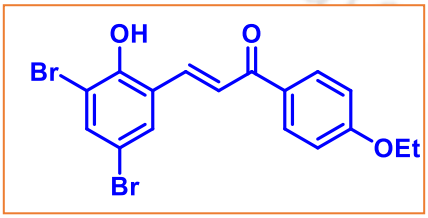

As yellowish solid (622 mg, 73% yield); m.p. 154–156 ^{o}C; purified over a column of silica gel (10% EtOAc in hexane); ^{1}H NMR ($CDCl_3$, 400 MHz): δ 8.03 (d, 2H, J = 8.8 Hz), 7.93 (d, 1H, J = 15.6 Hz), 7.65–7.63 (m, 2H), 7.62 (d, 1H, J = 2.4 Hz), 6.97 (d, 2H, J = 8.8 Hz), 6.14 (s, 1H), 4.12 (q, 2H, J = 6.8 Hz), 1.46 (t, 3H, J = 6.8 Hz); ^{13}C{^{1}H} NMR ($CDCl_3$, 125 MHz): δ 188.7, 163.3, 150.8, 137.1, 136.4, 135.2, 131.5, 131.2, 130.9, 125.3, 114.6, 113.0, 112.4, 64.0, 14.9; IR (neat, cm^{-1}): 3340, 2979, 2931, 1647, 1602, 1560, 1450, 1308, 1261.

(E)-3-(2-Hydroxy-4-methylphenyl)-1-(2-iodophenyl)prop-2-en-1-one (32):

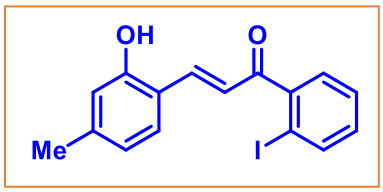

As yellowish solid (502 mg, 69% yield); m.p. 148–150 °C; purified over a column of silica gel (10% EtOAc in hexane); ^{1}H NMR ($CDCl_3$, 400 MHz): δ 7.93 (dd, 1H, J_1 = 8.0 Hz, J_2 = 1.0 Hz), 7.64 (d, 1H, J = 16.0 Hz), 7.44–7.39 (m, 3H), 7.35–7.32 (m, 1H), 7.17–7.13 (m, 1H), 6.75–6.73 (m, 2H), 2.30 (s, 3H); ^{13}C{^{1}H} NMR ($CDCl_3$, 125 MHz): δ 124.8, 144.9, 143.8, 140.8, 140.2, 131.3, 130.5, 128.7, 128.1, 128.0, 125.6, 122.1, 119.2, 117.5, 92.6, 21.8; IR (neat, cm^{-1}): 3282, 3057, 2920, 1693, 1595, 1454, 1419, 1304, 1245.

II.6. References

[1] (a) Lončarić, M.; Gašo-Sokač, D.; Jokić, S.; Molnar, M. *Biomolecules* **2020**, *10*, 151. (b) Samanta, K.; Patra, P.; Kar, G. K.; Dinda, S. K.; Mahanty, D. S. *New J. Chem*. **2021**, *45*, 7450–7485. (c) Fan, H.; Peng, J.; Hamann, M. T.; Hu, J.-F. *Chem. Rev*. **2008**, *108*, 264–287. (d) Bailly, C. *Curr. Med. Chem.: Anti-Cancer Agents* **2004**, *4*, 363–378. (e) Cironi, P.; Albericio, F.; A´lvarez, M. Prog. *Heterocycl. Chem*. **2005**, *16*, 1–26.

[2] (a) Ishibashi, F.; Tanabe, S.; Oda, T.; Iwao, M. *J. Nat. Prod*. **2002**, *65*, 500–504. (b) Fukuda, T.; Ishibashi, F.; Iwao, M. *The Alkaloids: Chemistry and Biology*, Elsevier, **2020**, *83*, 1–112. (c) Zhang, H.; Conte, M. M.; Huang, X.-C.; Khalil, Z.; Capon, R. J. *Org. Biomol. Chem*. **2012**, *10*, 2656–2663. (d) Krishnaiah, P.; Reddy, V. L. N.; Venkataramana, G.; Ravinder, K.; Srinivasulu, M.; Raju, T. V.; Ravikumar, K.; Chandrasekar, D.; Ramakrishna, S.; Venkateswarlu, Y. *J. Nat. Prod*. **2004**, *67*, 1168–1171. (e) Pla, D.; Albericio, F.; Alvarez, M. *Med. Chem. Commun*. **2011**, *2*, 689–697. (f) Andersen, R. J.; Faulkner, D. J.; Cun-heng, H.; Van Duyne, G. D.; Clardy, J. *J. Am. Chem. Soc*. **1985**, *107*, 5492–5495. (g) Kamiyama, H.; Kubo, Y.; Sato, H.; Yamamoto, N.; Fukuda, T.; Ishibashi, F.; Iwao, M. *Bioorg. Med. Chem.* **2011**, *19*, 7541–7550. (h) Pla, D; Albericio, F.; Alvarez, M. *Anti-Cancer Agents Med. Chem*. **2008**, *8*, 746–760.

[3] (a) Zheng, L.; Gao, T.; Ge, Z.; Ma, Z.; Xu, J.; Ding W.; Shen, L. *Eur. J. Med. Chem.* **2021**, *214*, 113226. (b) Bailly, C. *Mar. Drugs* **2015**, *13*, 1105–1123. (c) Lin, C.-H.; Yang, D.-Y. *Org. Lett*. **2013**, *15*, 2802–2805. (d) Reddy, M. V. R.; Rao, M. R.; Rhodes, D.;

Hansen, M. S. T.; Rubins, K.; Bushman, F. D.; Venkateswarlu, Y.; Faulkner, D. J. *J. Med. Chem*. **1999**, *42*, 1901–1907. (e) Marco, E.; Laine, W.; Tardy, C.; Lansiaux, A.; Iwao M.; Ishibashi, F.; Bailly, C.; Gago, F. *J. Med. Chem*. **2005**, *48*, 3796–3807.

[4] (a) Silyanova, E. A.; Samet, A. V.; Salamandra, L. K.; Khrustalev, V. N.; Semenov, V. V. *Eur. J. Org. Chem*. **2020**, *2020*, 2093–2100. (b) Shirley, H. J.; Koyioni, M.; Muncan, F.; Donohoe, T. J. *Chem. Sci*. **2019**, *10*, 4334–4338. (c) Balanna, K.; Barik, S.; Shee, S.; Gonnade, R. G.; Biju, A. T. *Chem. Sci*. **2022**, *13*, 11513–11518. (d) Ueda, K.; Amaike, K.; Maceiczyk, R. M.; Itami, K.; Yamaguchi, J. *J. Am. Chem. Soc*. **2014**, *136*, 13226–13232. (e) Sarkar, S.; Samanta, R. *Org. Lett*. **2022**, *24*, 4536–4541. (f) Imbri, D.; Tauber, J.; Opatz, T. *Mar. Drugs* **2014**, *12*, 6142–6177. (g) Shen, L.; Xie, N.; Yang, B.; Hu, Y.; Zhang, Y. *Eur. J. Med. Chem*. **2014**, *85*, 807–817. (h) Li, Q.; Jiang, J.; Fan, A.; Cui, Y.; Jia, Y. *Org. Lett*. **2011**, *13*, 312–315.

[5] (a) Morii, K.; Yasuda, Y.; Morikawa, D.; Mori, A.; Okano, K. *J. Org. Chem*. **2021**, *86*, 13388–13401. (b) Mei, R.; Zhang, S.-K.; Ackermann, L. *Synlett* **2017**, *28*, 1715–1718. (c) Silyanova, E. A.; Samet, A. V.; Semenov, V. V. *J. Org. Chem*. **2022**, *87*, 6444–6453.

[6] (a) Patra, P. *New J. Chem*. **2021**, *45*, 14269–14327. (b) Wu, C.-K.; Weng, Z.; Yang, D.-Y. *Org. Lett*. **2019**, *21*, 5225–5228. (c) Wang, Z.; Xing, X.; Xue, L.; Gao, F.; Fang, L. *Org. Biomol. Chem.* **2013**, *11*, 7334–7341. (d) Chen, L.; Xu, M.-H. *Adv. Synth. Catal.* **2009**, *351*, 2005–2012. (e) Watanabe, T.; Mutoh, Y.; Saito, S. *Org. Biomol. Chem*. **2020**, *18*, 81–85. (f) Verma, S.; Kumar, M.; Verma, A. K. *Chem. Commun*. **2023**, *59*, 3723–3726. (g) Qi, X.; Xiang, H.; Yang, C. *Org. Lett*. **2015**, *17*, 5590–5593.

[7] (a) Cheng, C.; Chen, W.-W.; Xu, B.; Xu, M.-H. *J. Org. Chem*. **2016**, *81*, 11501–11507. (b) Ngo, T. N.; Akrawi, O. A.; Dang, T. T.; Villinger, A.; Langer, P. *Tetrahedron Lett.* **2015**, *56*, 86–88. (c) Shaabani, A.; Sepahvand, H.; Bazgir, A.; Khavasi, H. R. *Tetrahedron* **2018**, *74*, 7058–7067.

[8] (a) Giustiniano, M.; Basso, A.; Mercalli, V.; Massarotti, A.; Novellino, E.; Tron, G. C.; Zhu, *J. Chem. Soc. Rev*. **2017**, *46*, 1295–1357. (b) Mathiyazhagan, A. D.; Anilkumar, G. *Org. Biomol. Chem*. **2019**, *17*, 6735–6747. (c) Gulevich, A. V.; Zhdanko, A. G.; Orru, R. V. A.; Nenajdenko, V. G. *Chem. Rev*. **2010**, *110*, 5235–5331. (d) Li, Y.; Xu, X.; Tan, J.; Xia, C.; Zhang, D.; Liu, Q. *J. Am. Chem. Soc*. **2011**, *133*, 1775–1777. (e) Liu, J.; Fang,

Z.; Zhang, Q.; Liu, Q.; Bi, X. *Angew. Chem. Int. Ed*. **2013**, *52*, 6953–6957. (f) Shao, R.; Zhao, H.; Ding, S.; Li, L.; Chen, C.; Wang, J.; Shang, Y. *Chem. Commun*. **2022**, *58*, 4771–4774. (g) Dong, P.; Majeed, K.; Wang, L.; Guo, Z.; Zhou, F.; Zhang, Q. *Chem. Commun*. **2021**, *57*, 4855–4858.

[9] (a) He, X.-L.; Zhao, H.-R.; Song, X.; Jiang, B.; Du, W.; Chen, Y.-C. *ACS Catal*. **2019**, *9*, 4374–4381. (b) Zheng, S.; Wang, Q.; Zhu, J. *Angew. Chem. Int. Ed*. **2019**, *58*, 9215–9219.

[10] (a) Leusen, D. V.; Leusen, A. M. V. John Wiley & Sons, Inc., Ed.; John Wiley & Sons, Inc.: Hoboken, NJ, USA, **2001**; pp 417–666. (b) Salehi, P.; Tanbakouchian, Z.; Farajinia-Lehi, N.; Shiri, M. *RSC Adv*. **2021**, *11*, 13292–13296. (c) Abozeid, M. A.; Kim, H. Y.; Oh, K. *Org. Lett.* **2022**, *24*, 1812–1816.

[11] Zheng, X.; Liu, W.; Zhang, D. *Molecules* **2020**, *25*, 1594.

[12] (a) Gao, M.; He, C.; Chen, H.; Bai, R.; Cheng, B.; Lei, A. *Angew. Chem. Int. Ed*. **2013**, *52*, 6958–6961. (b) Chakrabarty, S.; Choudhary, S.; Doshi, A.; Liu, F.-Q.; Mohan, R.; Ravindra, M. P.; Shah, D.; Yang, X.; Fleming, F. F. *Adv. Synth. Catal*. **2014**, *356*, 2135–2196. (c) Liu, Q.; Chen, J.-H.; Yao, M.; Zhao, Z.-Y.; Liu, X.-Y.; Zhao, X.-L.; Shi, M.; Zhao, M.-X. *Tetrahedron* **2021**, *88*, 132122. (d) Wang, Z.-P.; He, Y.; Shao, P.-L. *Org. Biomol. Chem*. **2018**, *16*, 5422–5426. (e) Tang, B.-Z.; Hao, W.-J.; Li, J.-Z.; Zhu, S.-S.; Tu, S.-J.; Jiang, B. *Chem. Commun*. **2020**, *56*, 7749–7752. (f) Duan, W.-D.; Zhang, Y.-F.; Hu, Y. *ACS Omega* **2020**, *5*, 13454–13461. (g) Yuan, W.-C.; Chen, X.-M.; Zhao, J.-Q.; Zhang, Y.-P.; Wang, Z.-H.; You, Y. *Org. Lett*. **2022**, *24*, 826–831. (h) Wang, Z.-P.; Xiang, S.; Shao, P.-L.; He, Y. *J. Org. Chem*. **2018**, *83*, 10995–11007.

[13] (a) Sheldrick, G. M. SHELXL-2014, Program for the Refinement of Crystal Structures; University of Göttingen: Göttingen (Germany), **1997**. (b) Dolomanov, O.V.; Bourhis, L.J.; Gildea, R.J.; Howard, J. A. K.; Puschmann, H. *J. Appl. Crystallogr.* **2009**, *42*, *339–341*.. (c) Sheldrick, G.M. *Acta. Crystallogr. A Found. Adv.* **2015**, *71*, *3–8*...

[14] (a) Rouh, H.; Liu, Y.; Katakam, N.; Pham, L.; Zhu, Y.-L.; Li, G. *J. Org. Chem*. **2018**, *83*, 15372–15379. (b) Gao, Y.-Q.; Hou, Y.; Zhu, L.; Chen, G.; Xu, D.; Zhang, S.-Y.; He, Y.; Xie, W. *RSC Adv*. **2019**, *9*, 29005–29009. (c) Yin, G.; Fan, L.; Ren, T.; Zheng, C.; Tao, Q.; Wu, A.; She, N. *Org. Biomol. Chem.* **2012**, *10*, 8877–8883. (d) Zheng, Y.-

Q.; Luan, C.-F.; Wang, Z.-J.; Yao, Y.-Q.; Shi, Z.-C.; Li, X.-F.; Zhao, Z.-G.; Chen, F. *Chin. Chem. Lett*. **2016**, *27*, 25–30. (e) Wang, D.; Sun, J.; Han, Y.; Sun, Q.; Yan, C.-G. *Org. Lett*. **2022**, *24*, 7790–7795. (f) Sepay, N.; Guha, C.; Maity, S.; Mallik, A. K. *Eur. J. Org. Chem*. **2017**, *2017*, 6013–6022.

II.7. Representative Spectra

1-Benzoylchromeno[3,4-b]pyrrol-4(3H)-one (1a): **^{1}H NMR ($CDCl_3$, 500 MHz)**

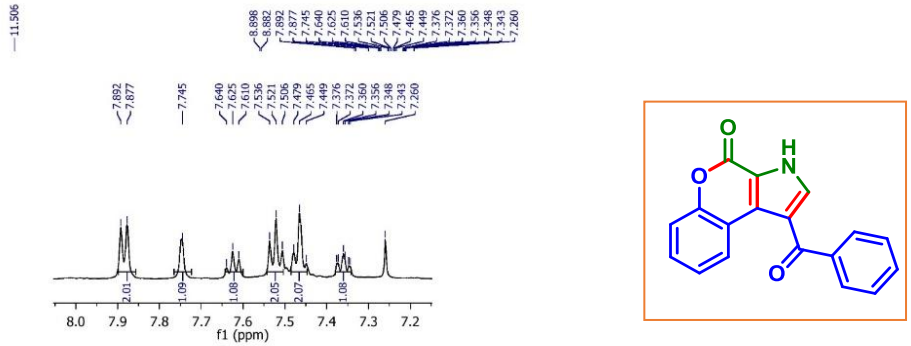

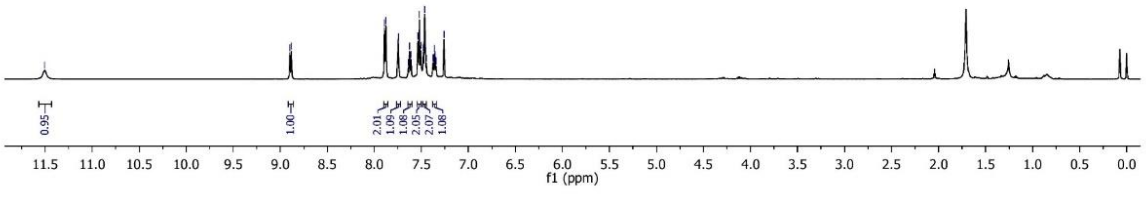

1-Benzoylchromeno[3,4-b]pyrrol-4(3H)-one (1a): **^{13}C {^{1}H} NMR (CDCl$_3$, 125 MHz)**

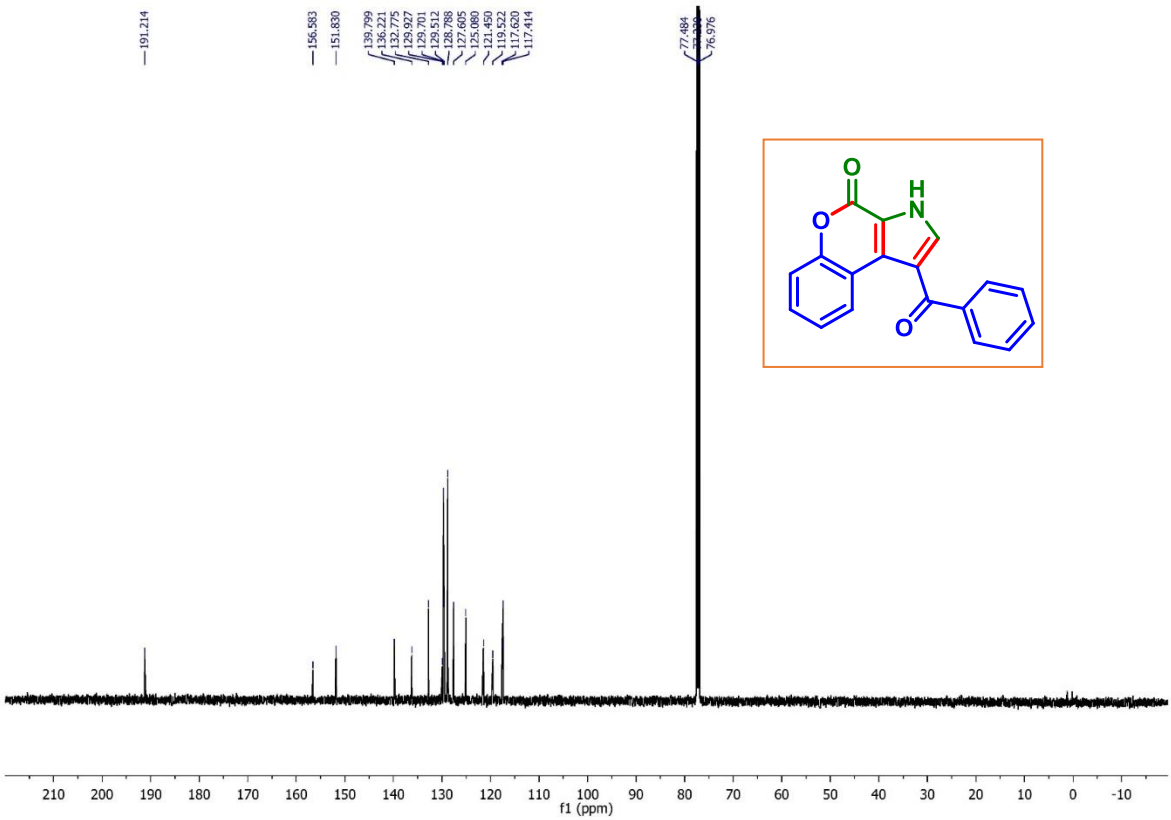

1-(4-Methylbenzoyl)chromeno[3,4-b]pyrrol-4(3H)-one (2a): **^{1}H NMR (CDCl$_3$, 500 MHz)**

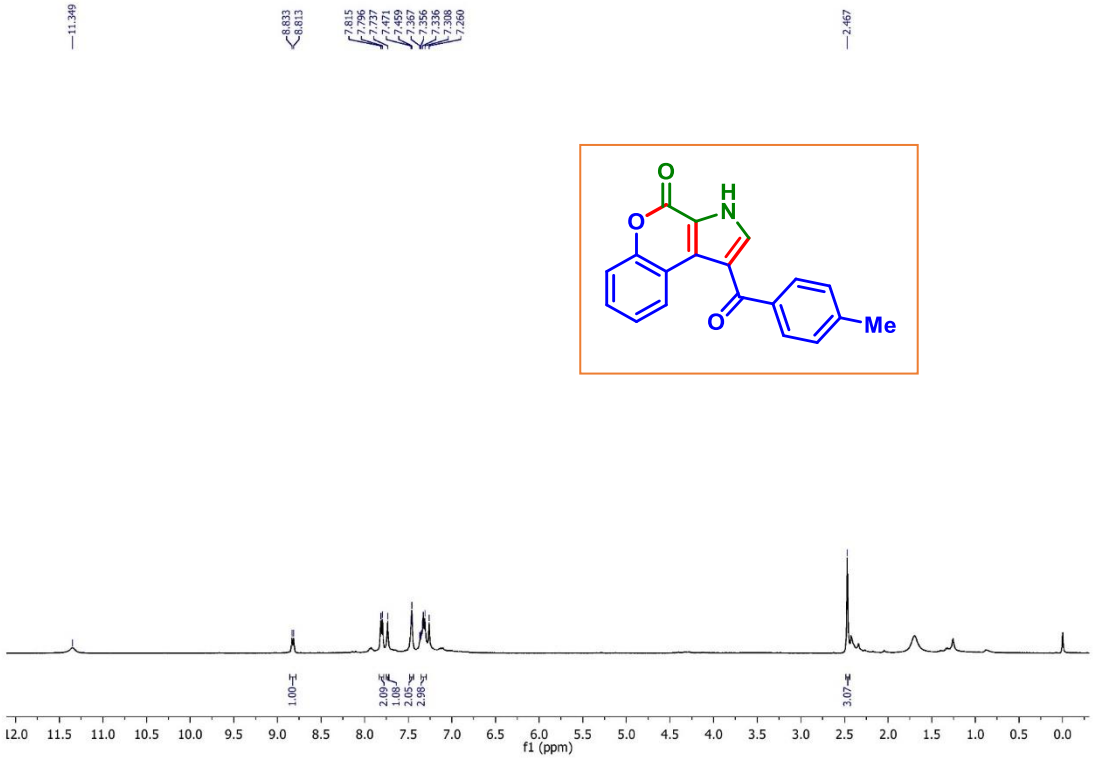

1-(4-Methylbenzoyl)chromeno[3,4-b]pyrrol-4(3H)-one (2a)): **^{13}C {^{1}H} NMR (CDCl$_3$ + DMSO-d$_6$, 100 MHz)**

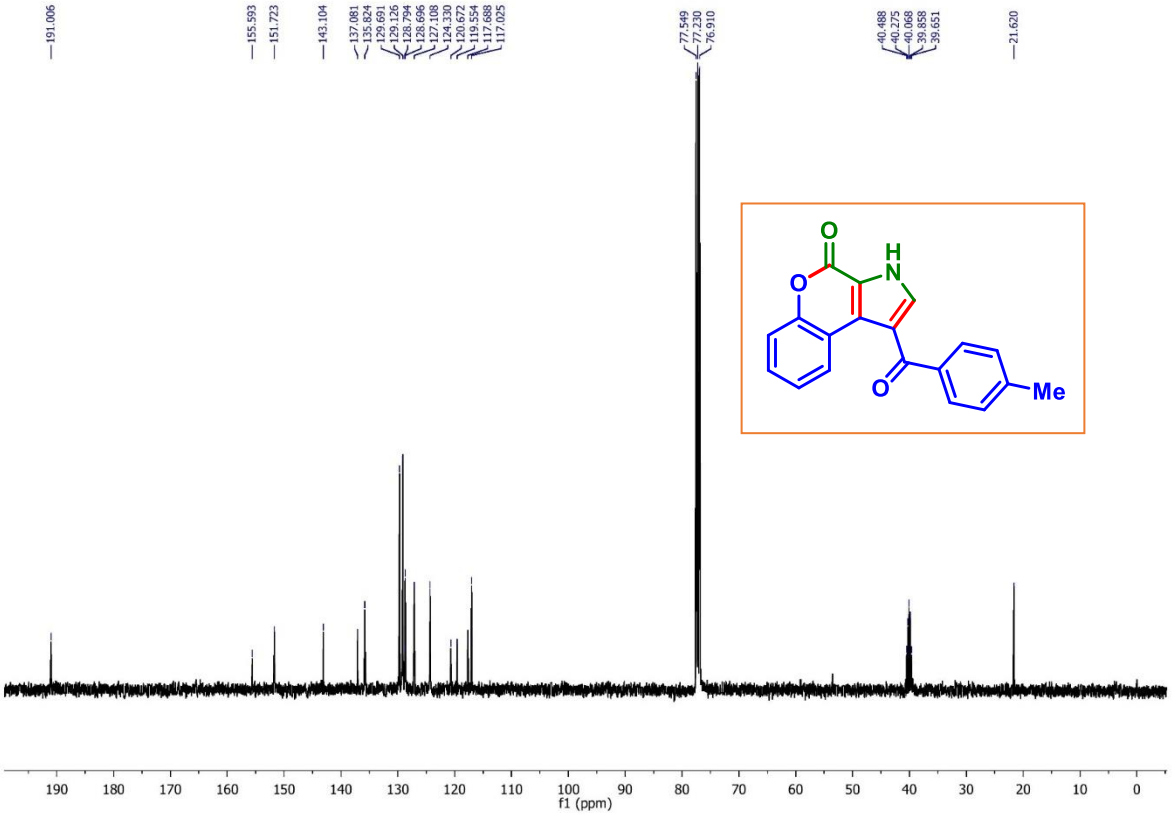

1-(3-Methylbenzoyl)chromeno[3,4-b]pyrrol-4(3H)-one (3a): **^{1}H NMR (DMSO-d$_6$, 500 MHz)**

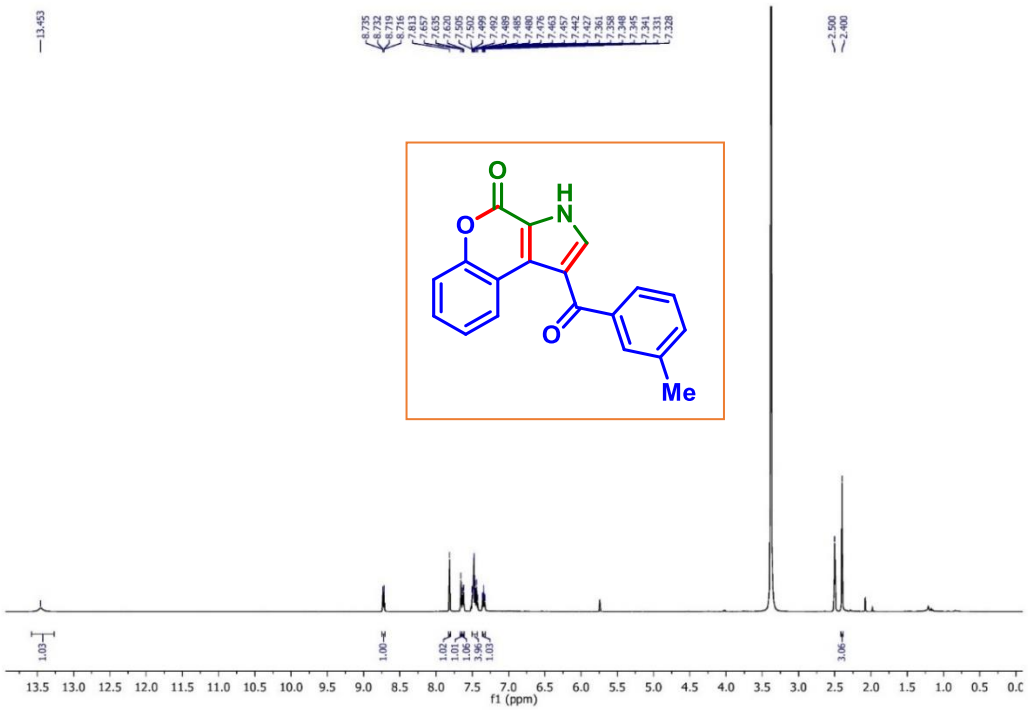

1-(3-Methylbenzoyl)chromeno[3,4-b]pyrrol-4(3H)-one (3a): **$^{13}C\{^{1}H\}$ NMR (DMSO-d_6, 125 MHz)**

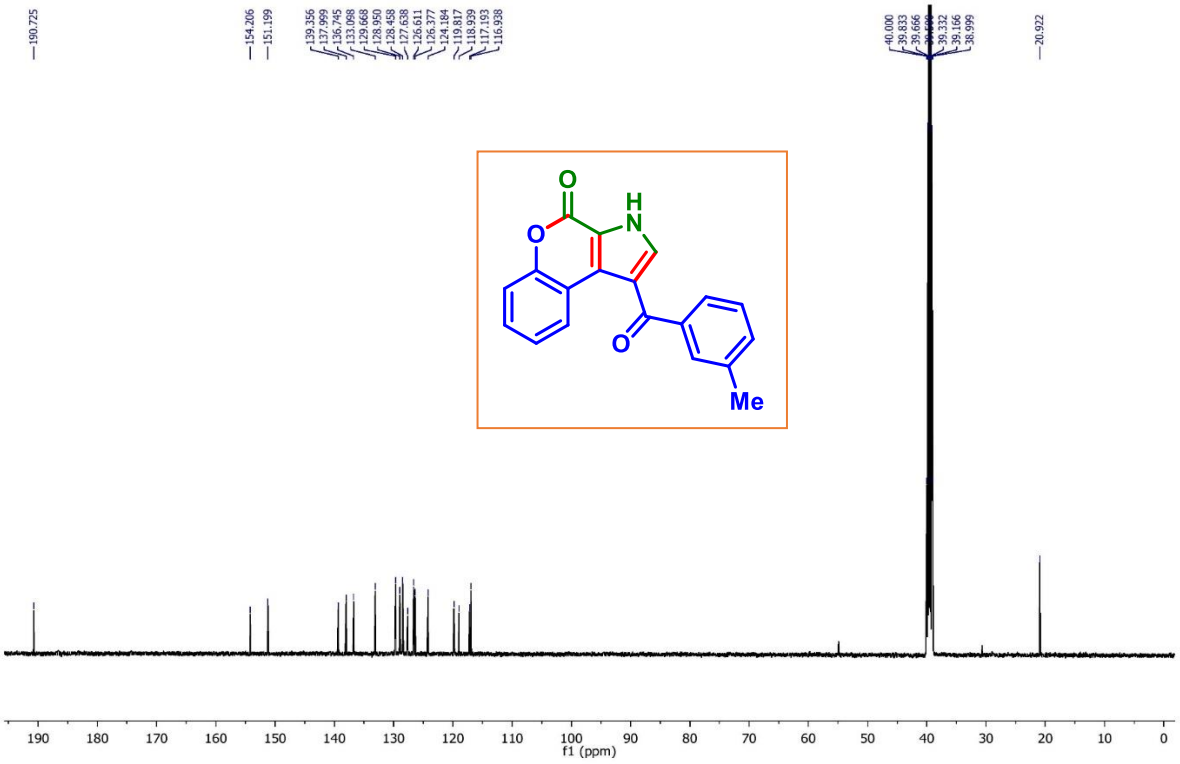

1-(4-Isopropoxybenzoyl)chromeno[3,4-b]pyrrol-4(3H)-one (6a): **^{1}H NMR (DMSO-d_6, 500 MHz)**

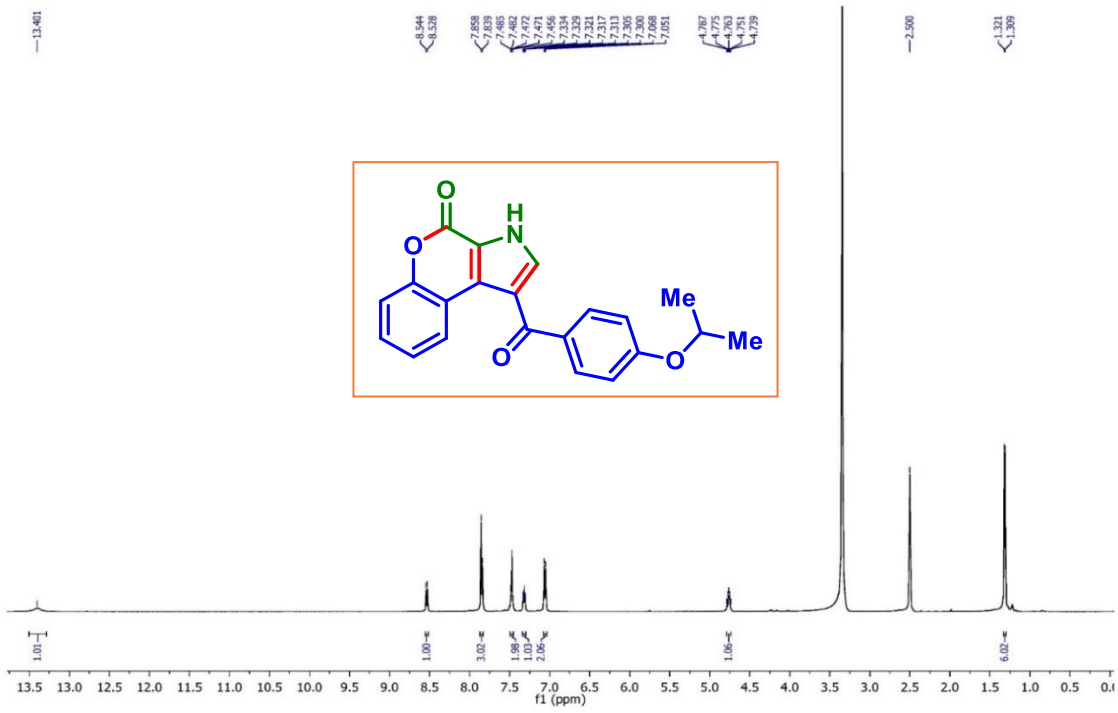

1-(4-Isopropoxybenzoyl)chromeno[3,4-b]pyrrol-4(3H)-one (6a): **$^{13}C\{^{1}H\}$ NMR (DMSO-d_6, 500 MHz)**

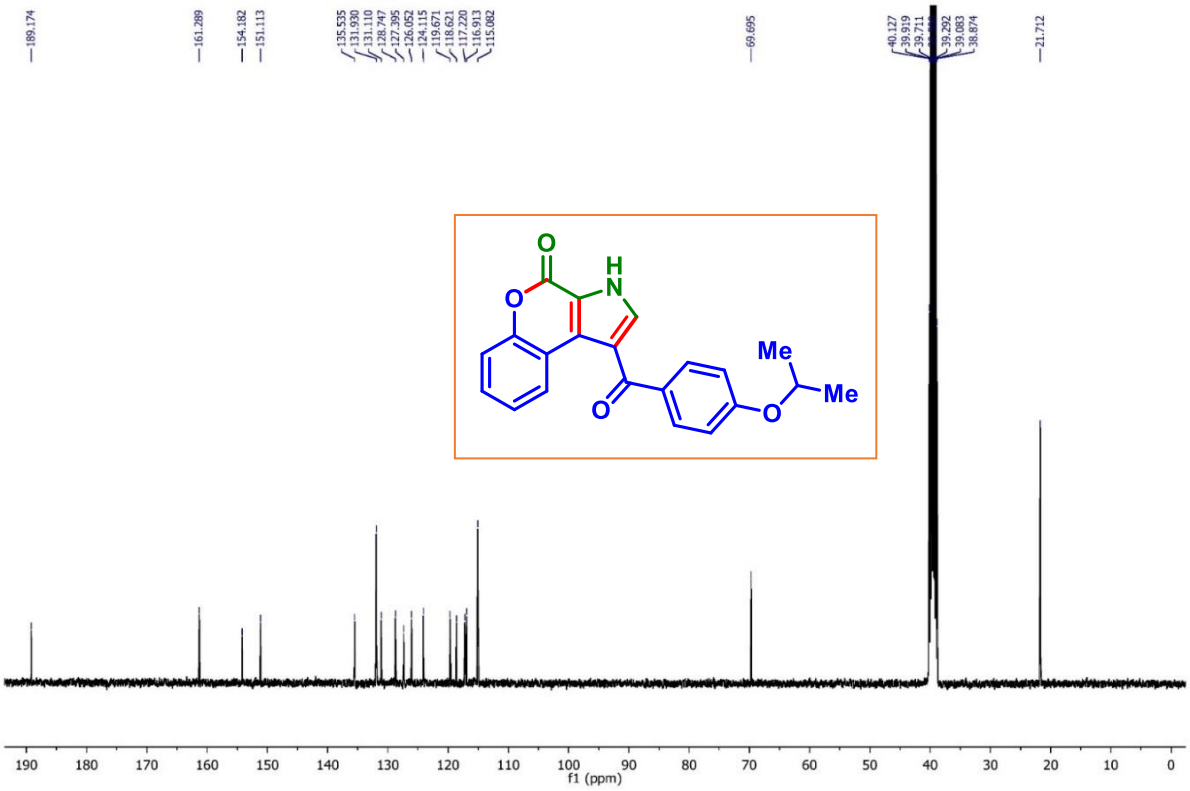

1-(4-Nitrobenzoyl)chromeno[3,4-b]pyrrol-4(3H)-one (13a): **^{1}H NMR (DMSO-d_6, 400 MHz)**

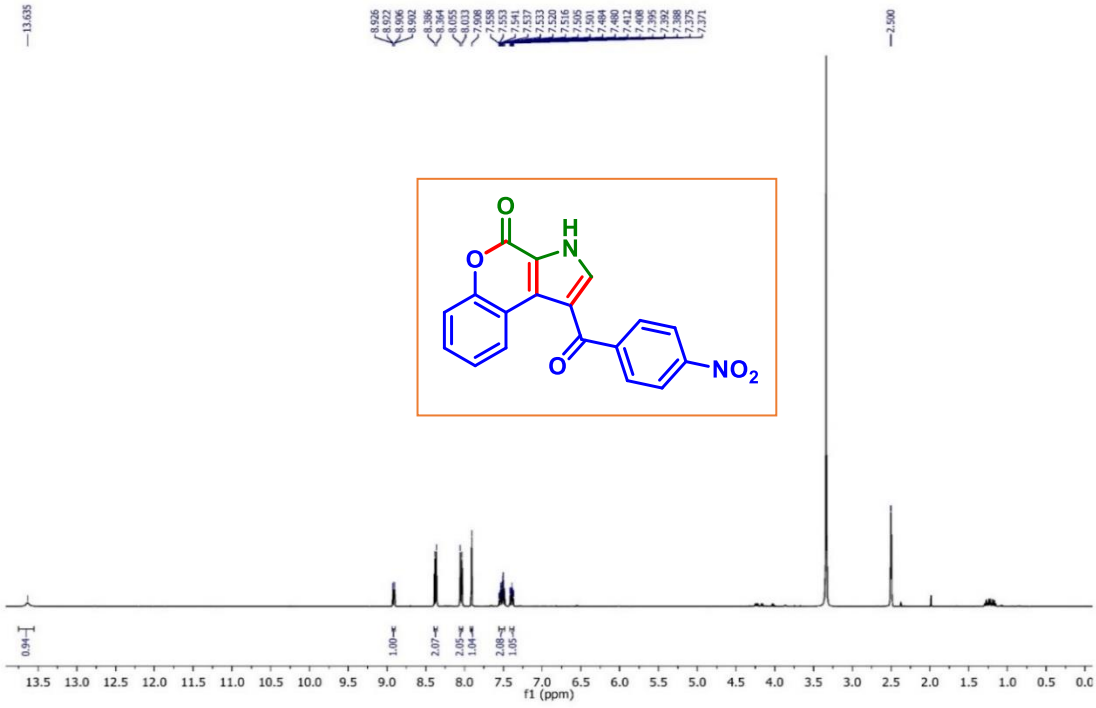

1-(4-Nitrobenzoyl)chromeno[3,4-b]pyrrol-4(3H)-one (13a): **$^{13}C\{^{1}H\}$ NMR (DMSO-d_6, 100 MHz)**

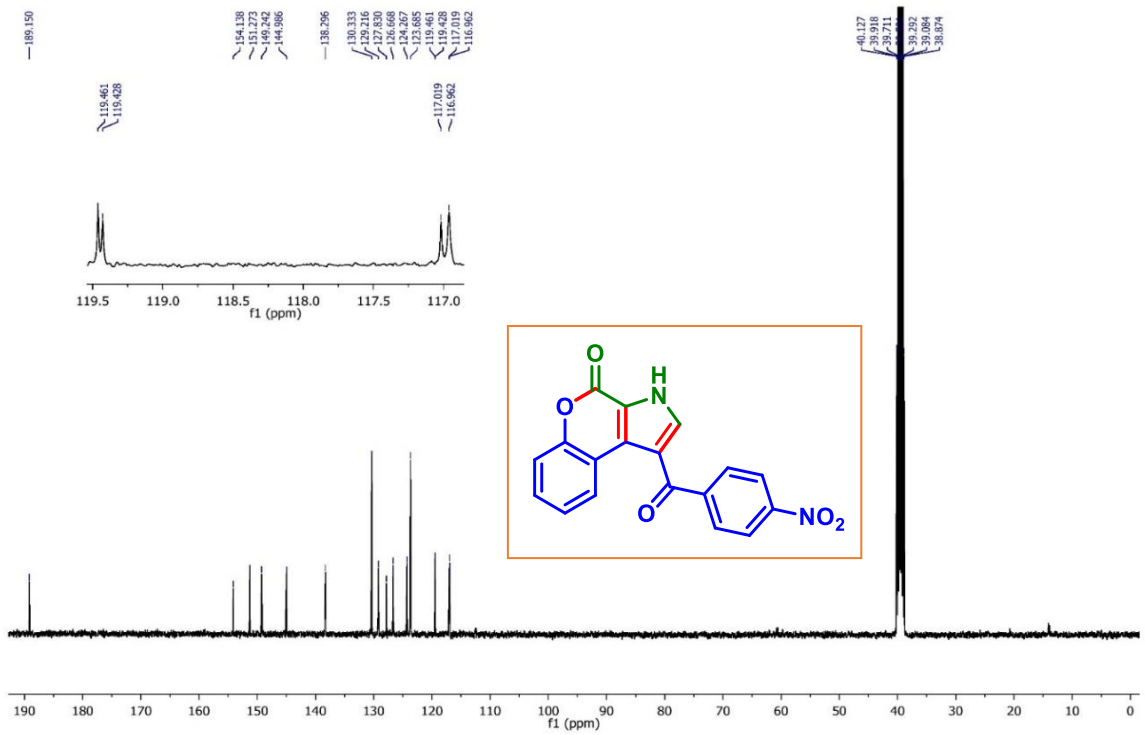

1-(2-ethoxy-4-fluorobenzoyl)chromeno[3,4-b]pyrrol-4(3H)-one (15a): **^{1}H NMR (DMSO-d_6, 400 MHz)**

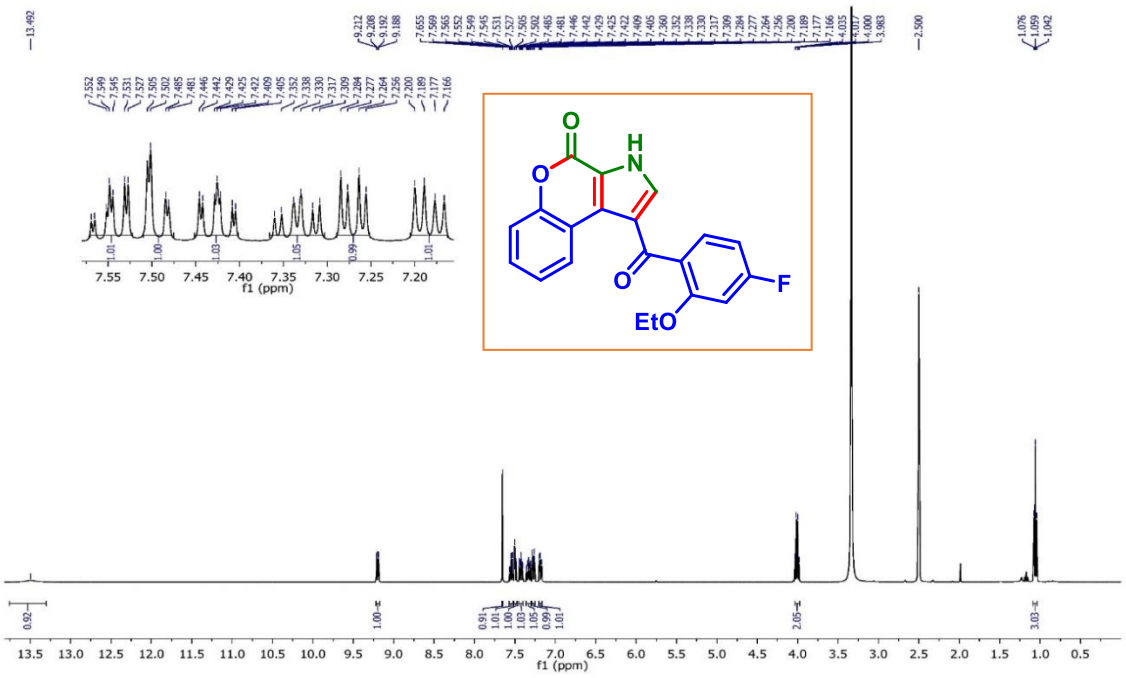

1-(2-Ethoxy-4-fluorobenzoyl)chromeno[3,4-b]pyrrol-4(3H)-one (15a): **$^{13}C\{^{1}H\}$ NMR (DMSO-d_6, 100 MHz)**

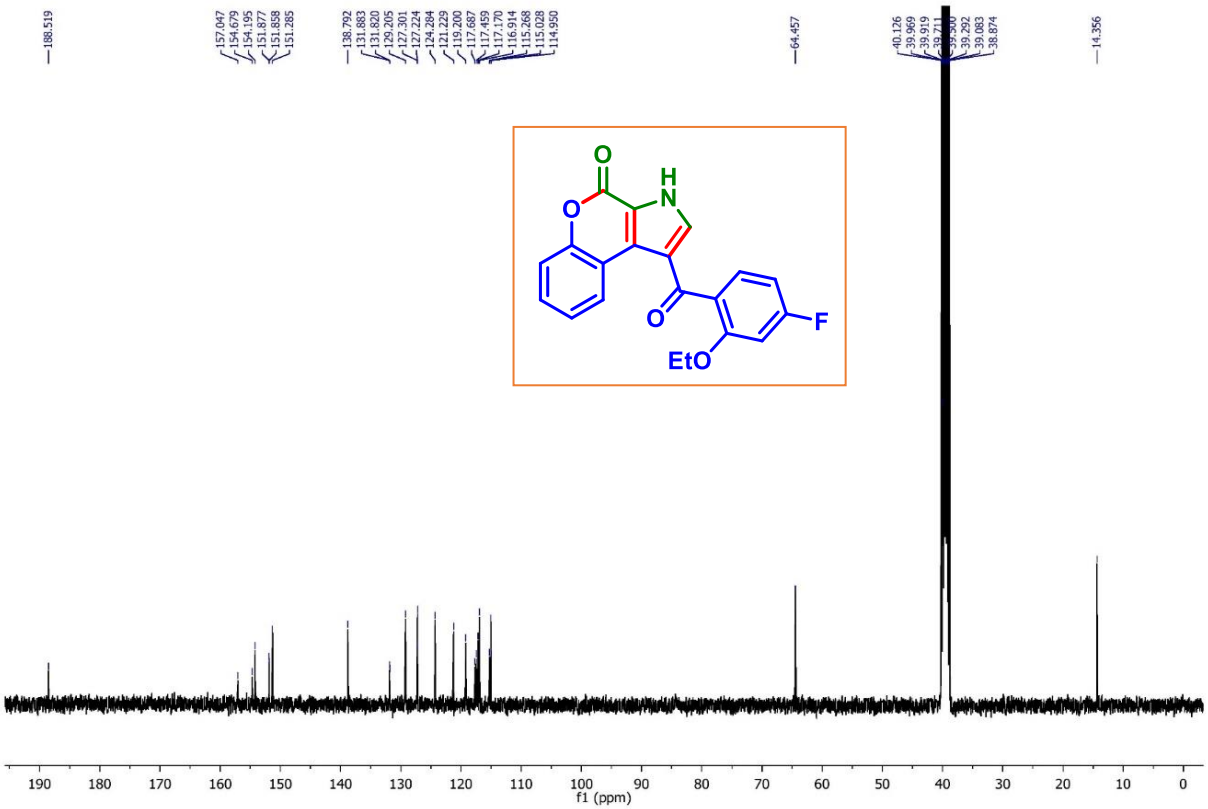

1-(2-Ethoxy-4-fluorobenzoyl)chromeno[3,4-b]pyrrol-4(3H)-one (15a): **^{19}F NMR (DMSO-d_6, 376 MHz)**

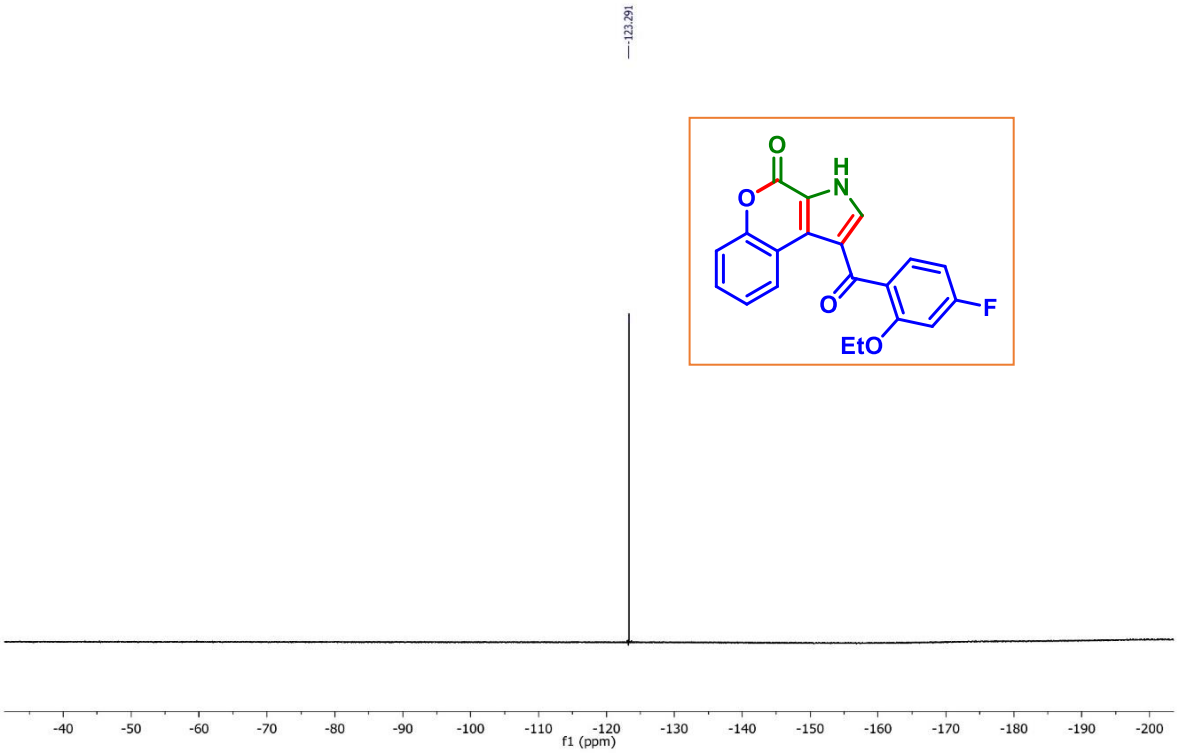

1-(Thiophene-2-carbonyl)chromeno[3,4-b]pyrrol-4(3H)-one (19a): **^{1}H NMR (DMSO-d$_6$, 500 MHz)**

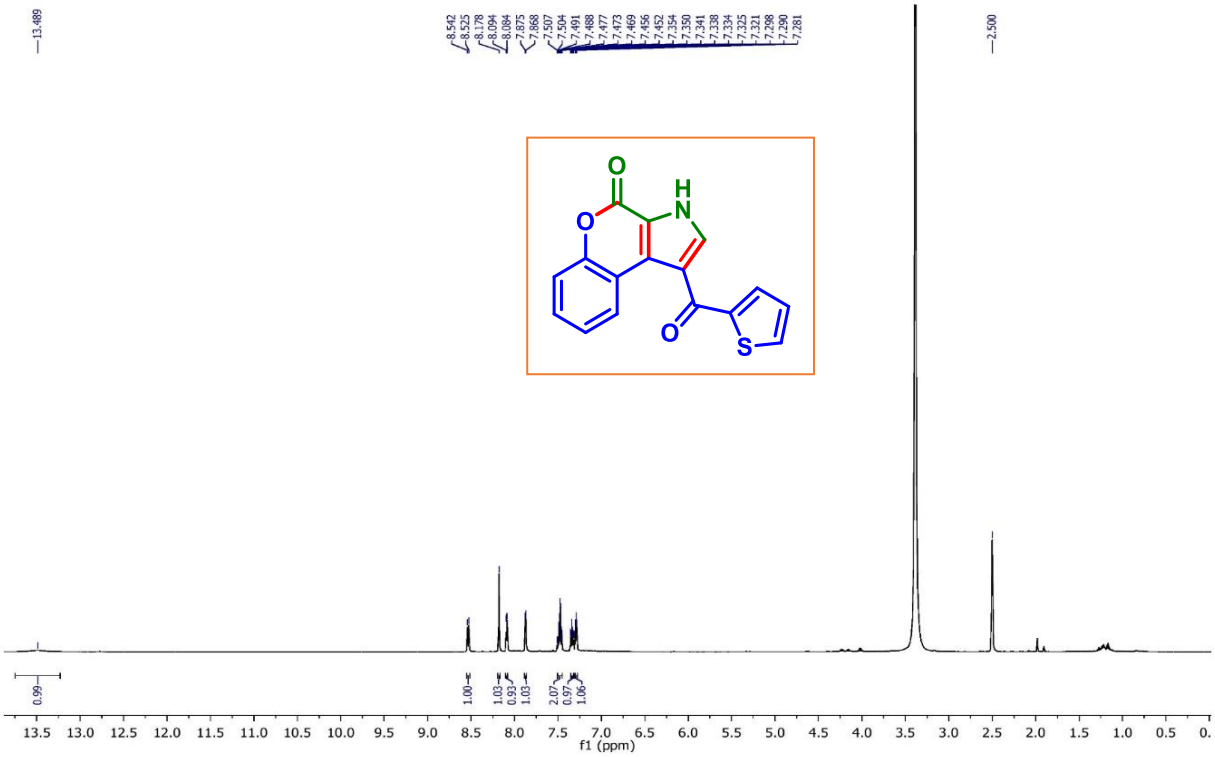

1-(Thiophene-2-carbonyl)chromeno[3,4-b]pyrrol-4(3H)-one (19a): **^{13}C{^{1}H} NMR (DMSO-d$_6$, 125 MHz)**

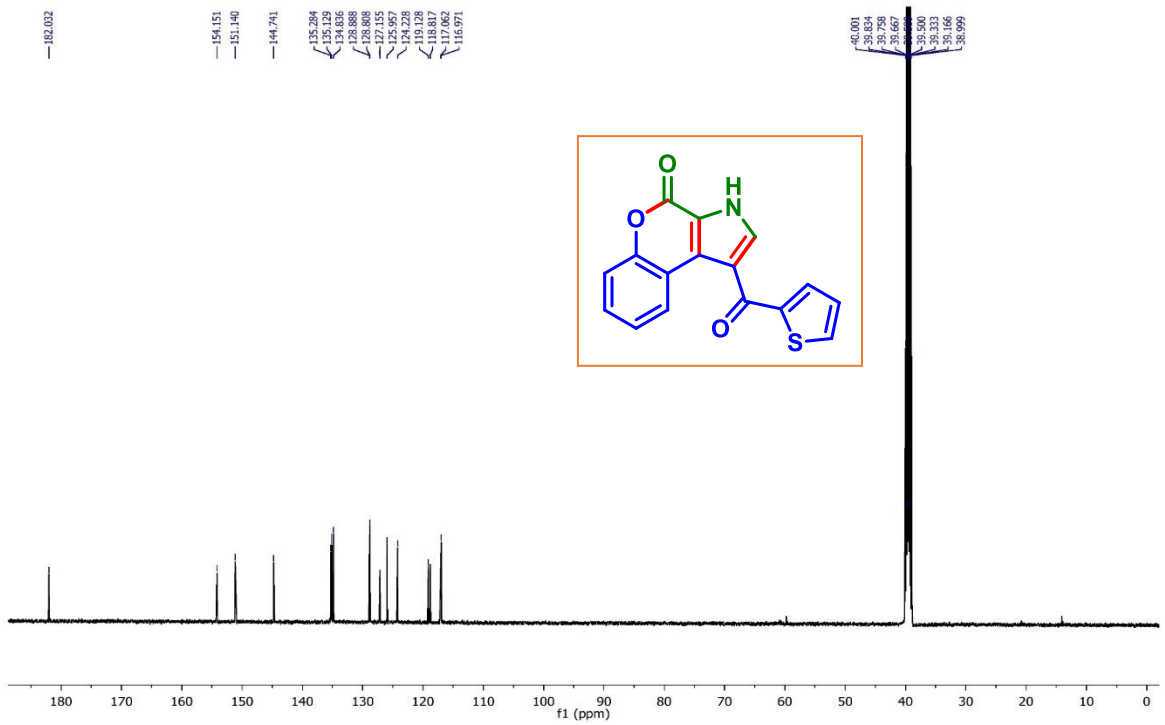

1-(Cyclopropanecarbonyl)chromeno[3,4-b]pyrrol-4(3H)-one (22a): **^{1}H NMR ($CDCl_3$, 400 MHz)**

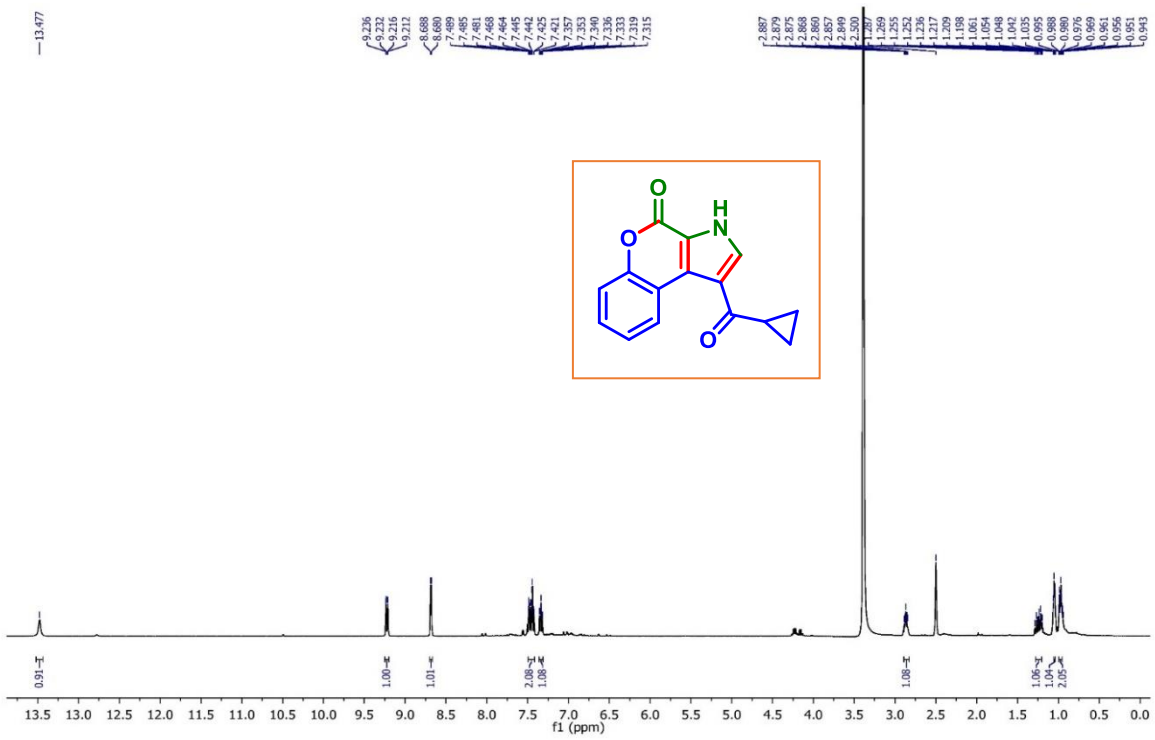

1-(Cyclopropanecarbonyl)chromeno[3,4-b]pyrrol-4(3H)-one (22a): **^{13}C{^{1}H} NMR ($CDCl_3$, 125 MHz)**

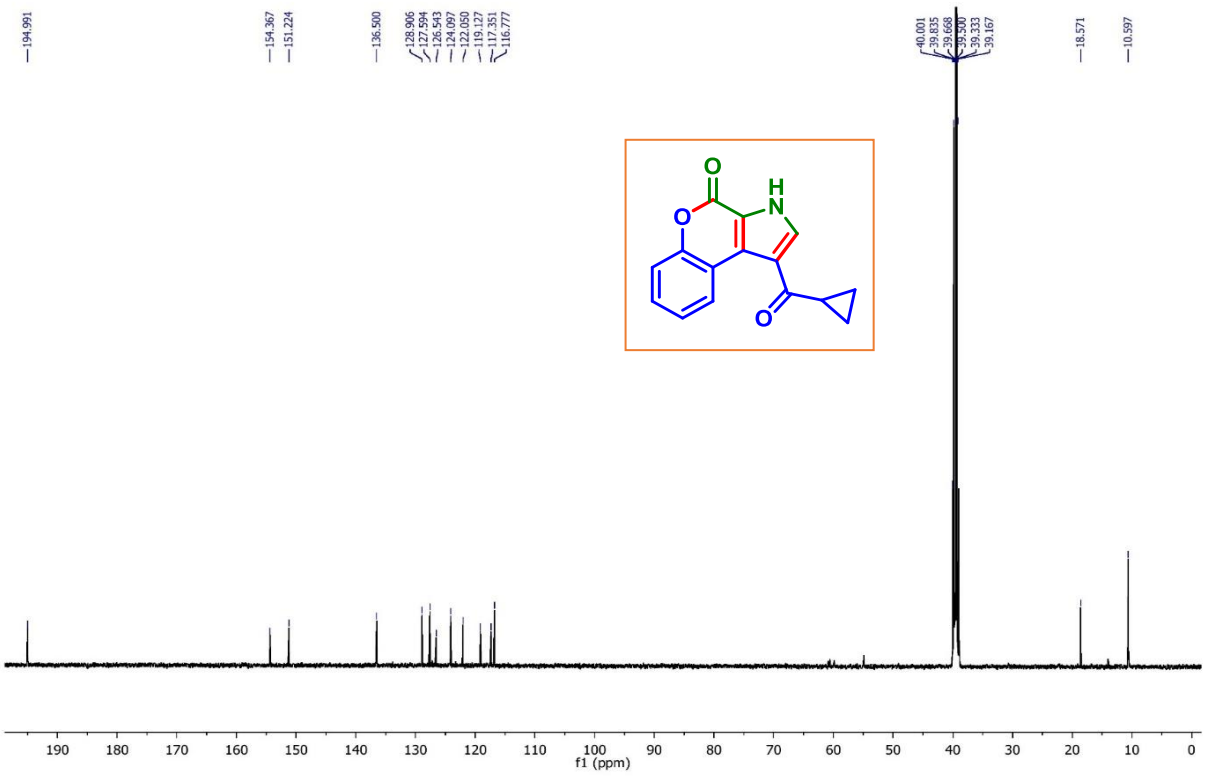

1-Benzoyl-8-iodochromeno[3,4-b]pyrrol-4(3H)-one (26a): **^{1}H NMR (DMSO-d$_6$, 400 MHz)**

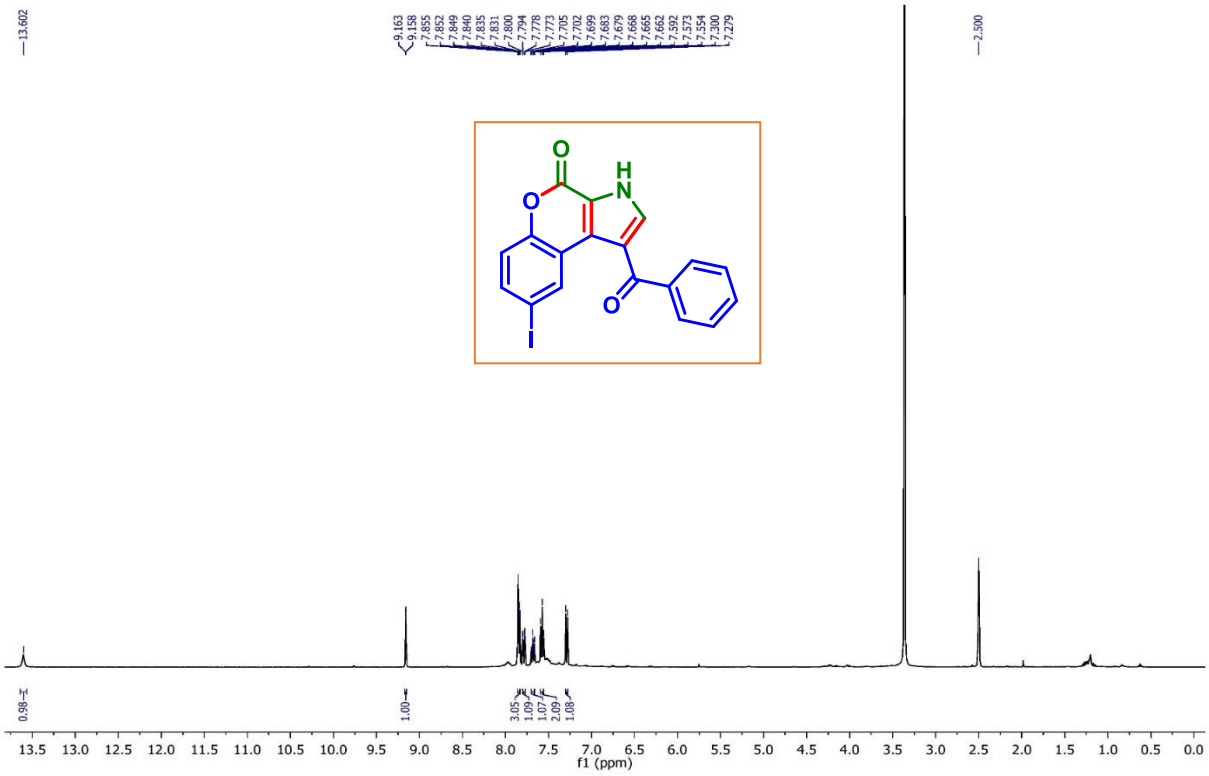

1-Benzoyl-8-iodochromeno[3,4-b]pyrrol-4(3H)-one (26a): **^{13}C{^{1}H} NMR (DMSO-d$_6$, 100 MHz)**

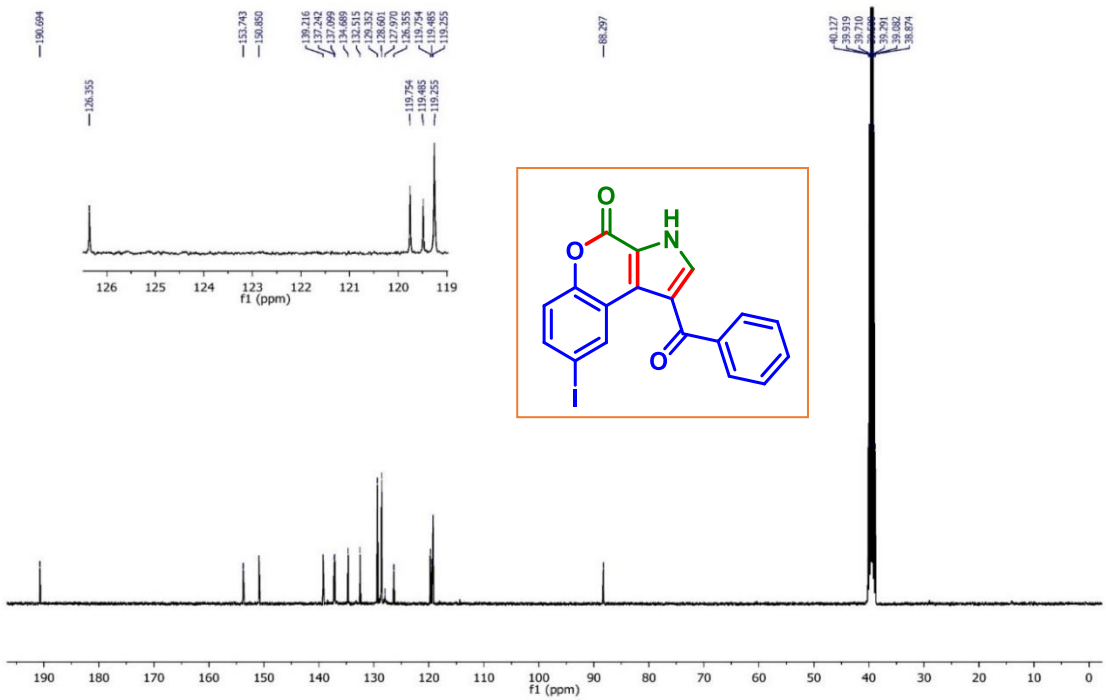

Ethyl 4-oxo-2,4-dihydrochromeno[3,4-c]pyrrole-1-carboxylate (1a'): **^{1}H NMR ($CDCl_3$, 400 MHz)**

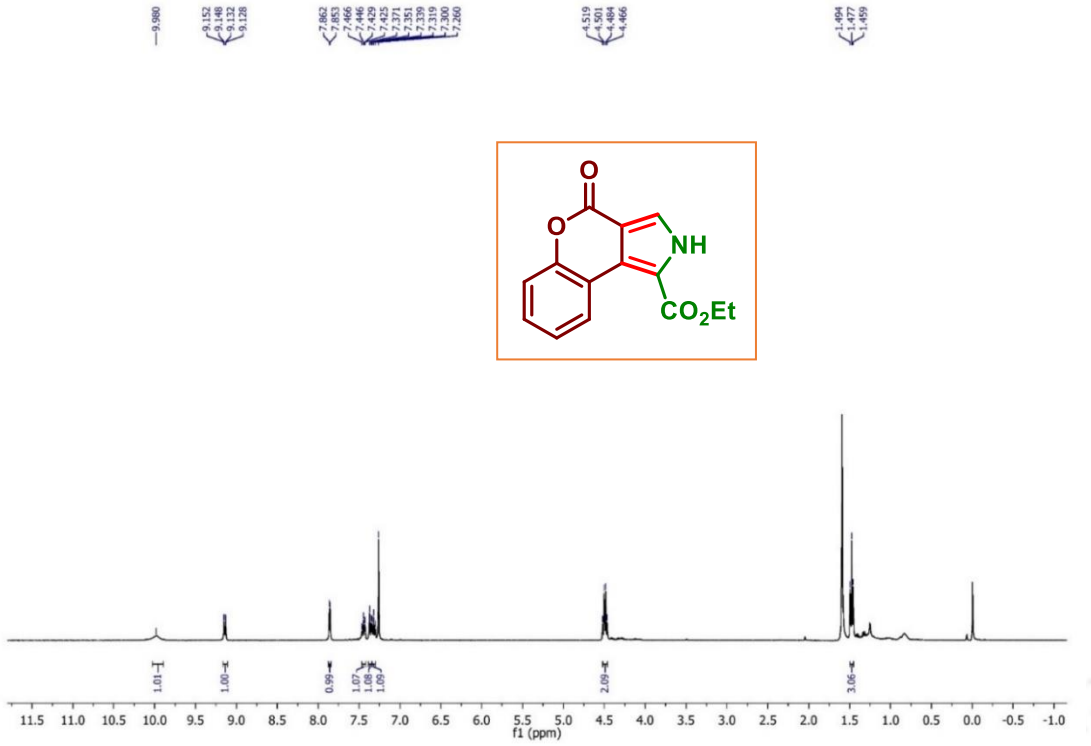

Ethyl 4-oxo-2,4-dihydrochromeno[3,4-c]pyrrole-1-carboxylate (1a'): **^{13}C{^{1}H} NMR ($CDCl_3$, 100 MHz)**

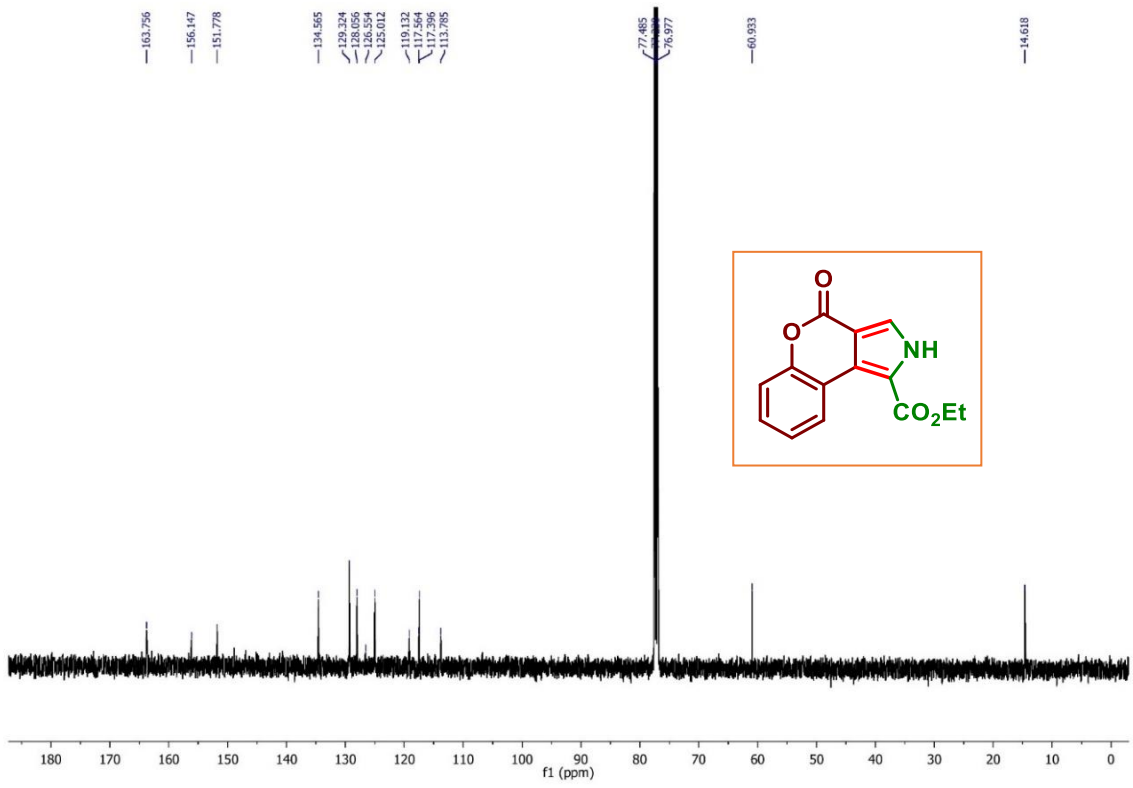

6H-Chromeno[3,4-b]indeno[2,1-d]pyrrole-6,12(7H)-dione (12aa): **^{1}H NMR (DMSO-d$_6$, 400 MHz)**

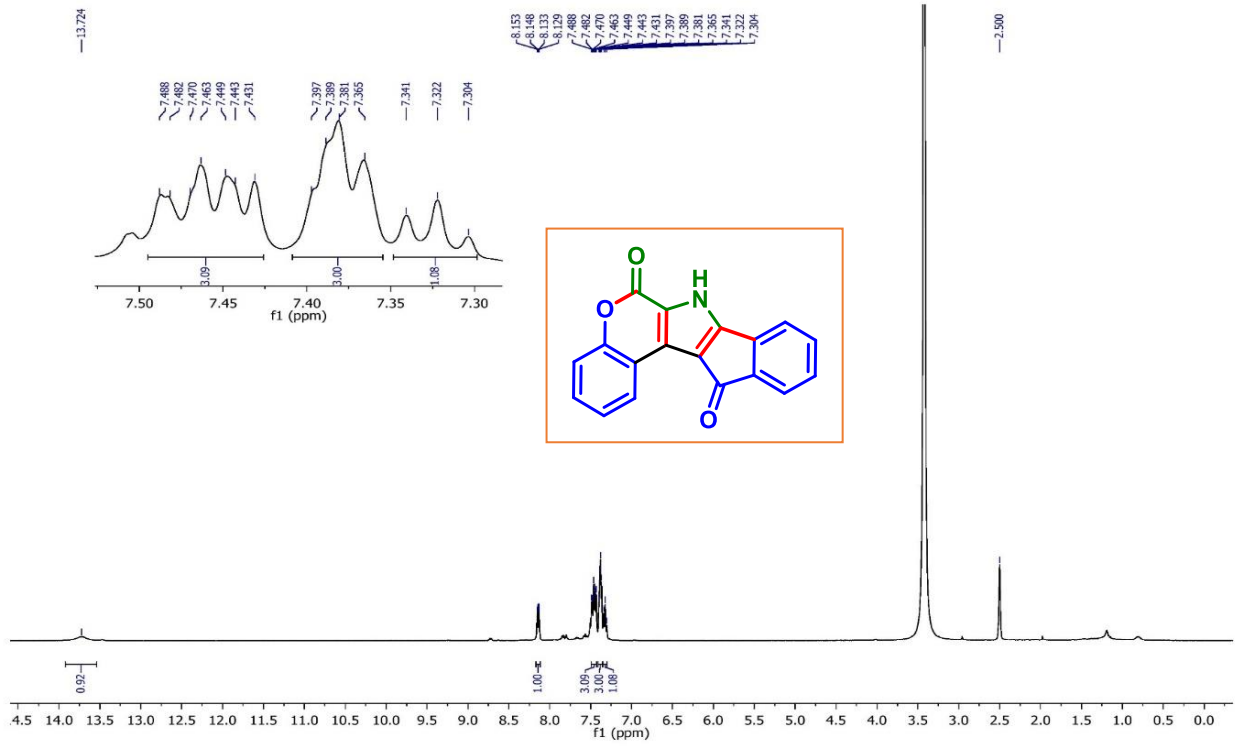

6H-Chromeno[3,4-b]indeno[2,1-d]pyrrole-6,12(7H)-dione (12aa): **^{13}C{^{1}H} NMR (DMSO-d$_6$, 125 MHz)**

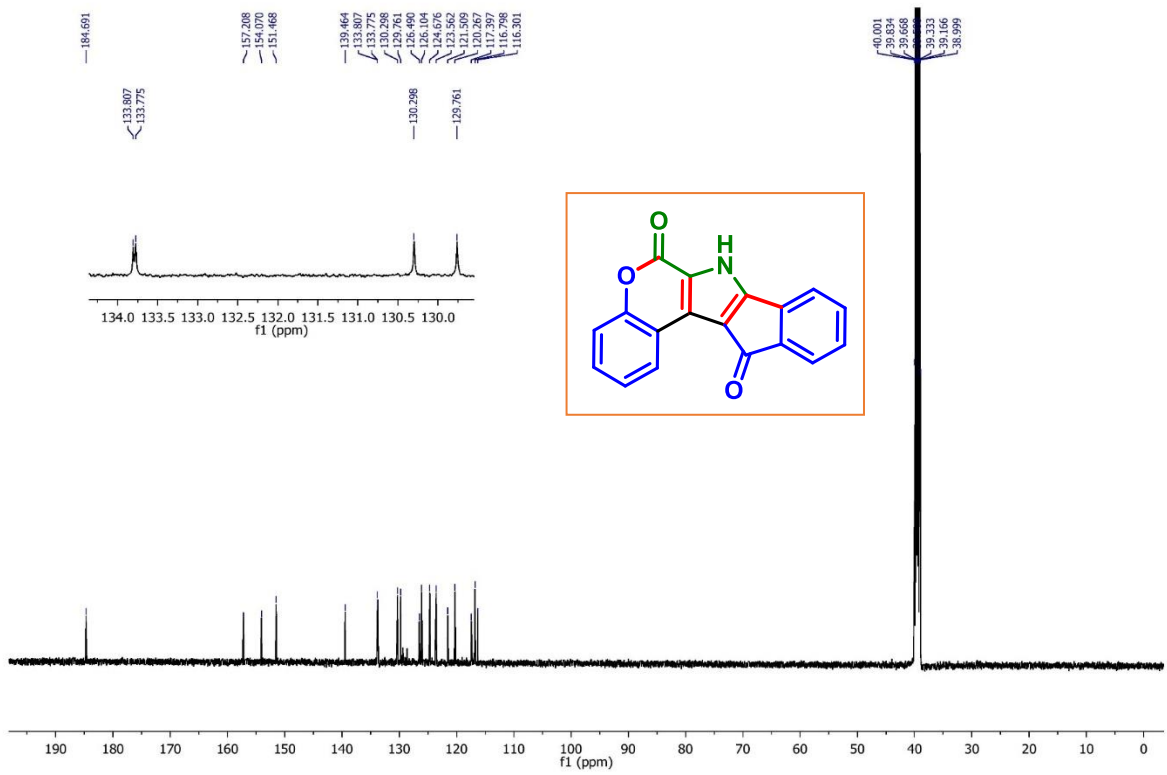

8-(Phenylethynyl)-1-(2-(phenylethynyl)benzoyl)chromeno[3,4-b]pyrrol-4(3H)-one (34ac):
^{1}H NMR (DMSO-d$_6$, 500 MHz)

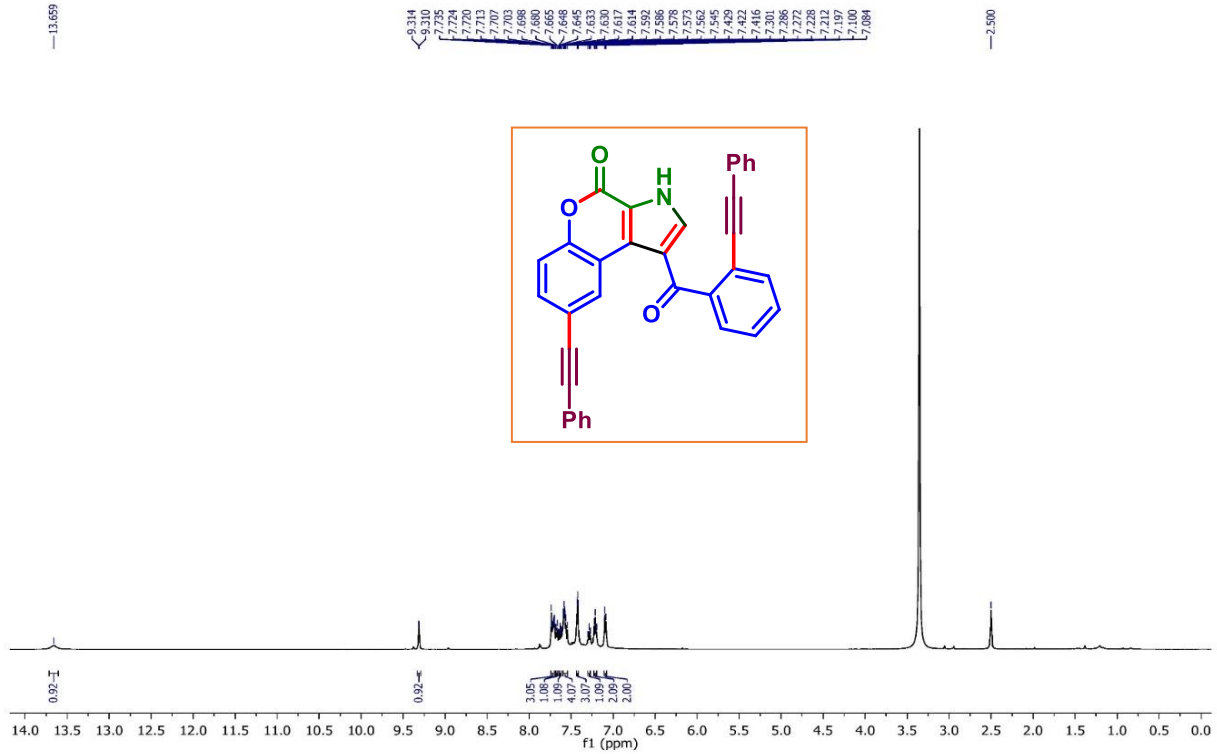

8-(Phenylethynyl)-1-(2-(phenylethynyl)benzoyl)chromeno[3,4-b]pyrrol-4(3H)-one (34ac):
^{1}H NMR (DMSO-d$_6$, 125 MHz)

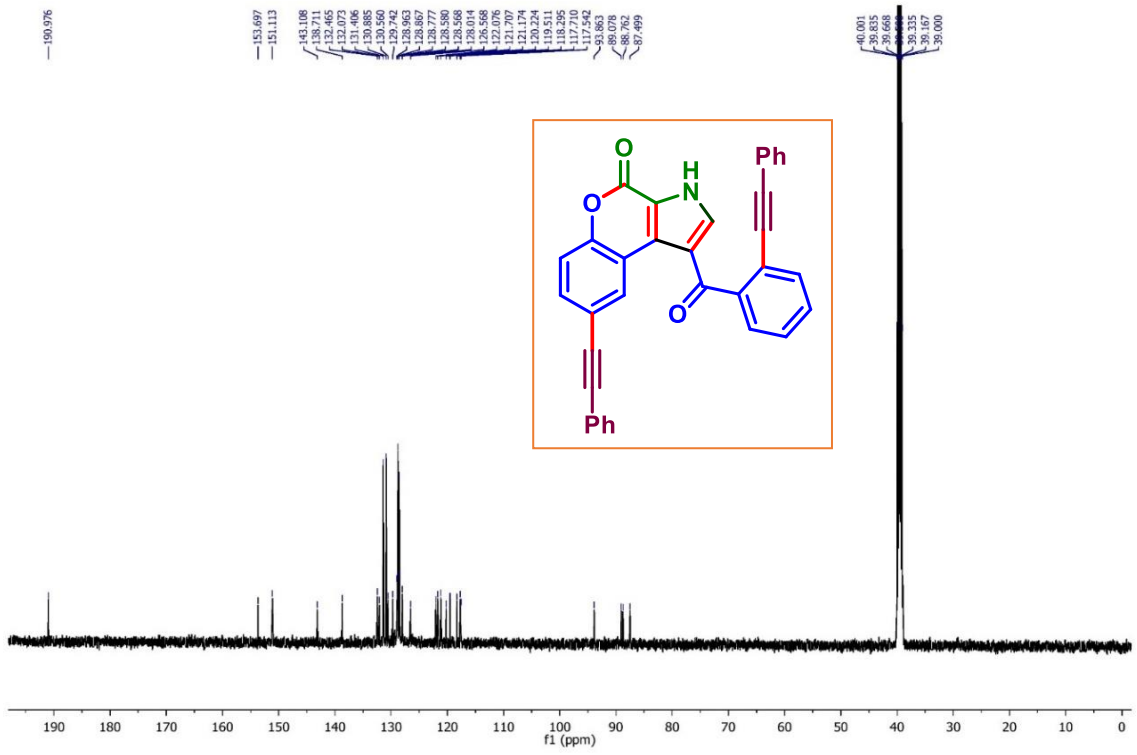

CHAPTER III

Access to Chromenopyrrole *via* Tandem (3 + 2) Cycloaddition and Intramolecular C–O Coupling

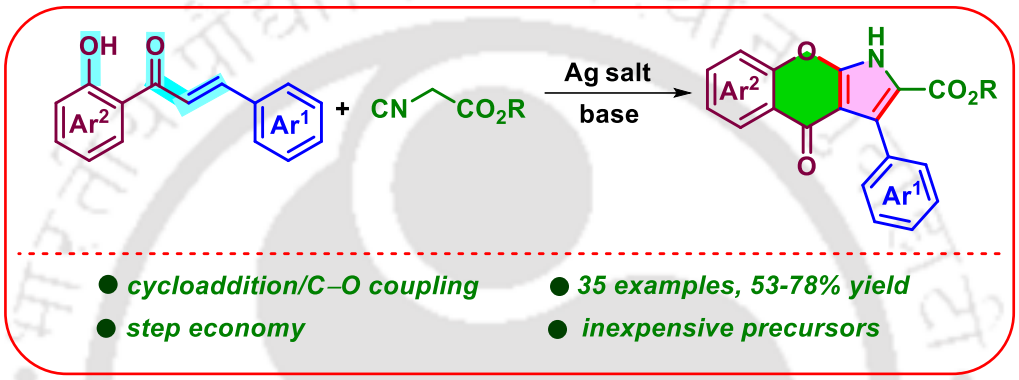

JOC The Journal of Organic Chemistry

J. Org. Chem. **2024**, *89*, 1331–1335.

pubs.acs.org/joc Note

ABSTRACT: ***A mild and concise method for the synthesis of chromenopyrrole from 2'-hydroxychalcone is devised. The reaction proceeds via an initial (3 + 2) cycloaddition on the C=C bond of 2'-hydroxychalcone and 1,3-dipole, generated in situ by the reaction of ethyl isocyanoacetate and AgOAc. This is then followed by an intramolecular C–O bond formation with the –OH group and C5-H of the in situ generated pyrrole leading to chromenopyrroles.***

CHAPTER III

Access to Chromenopyrrole *via* Tandem (3 + 2) Cycloaddition and Intramolecular C–O Coupling

III.1. Introduction

Pyrrole is a well-known *N*-containing structural motif, often found in some of the natural products and pharmacologically active molecules.[1a-b] Pyrrole ring is widespread in many natural products such as lamellarin, ningalin, purpurone as well as in synthetic drugs such as sunitinib, atorvastatin, URB447 among others.[1c-e] Polysubstituted pyrroles are valuable synthetic building blocks and chemistry has progressed far in the direction of pyrrole synthesis.[1f-j] Chromene too is a privileged core that occurs in many natural and synthetic biological molecules and potential starting precursor for the construction of bio-active heterocycles.[1d,2a-c] Chromene core is also found in many anticancer (PIK-108), antifungal, etc. drugs.[2] Both of these rings in the form of fused chromenopyrrole interest chemists and pharmacists as an exciting and versatile building block because of their excellent biological activities.[1e,3] Chromenopyrrole or benzopyranopyrrole structure was first reported as a heterocyclic core structure of TAN-876A isolated from a *Streptomyces sp*. by a group from Takeda company. Subsequently, this unique core was found in pyralomicins. Pyralomicins, a group of antibiotics isolated from the soil bacterium *Nonomuraea spiralis* IMC A-0156, contain a chromenopyrrole core. This core is linked to a C7-cyclitol (pyralomicins I-IV) or glycosylated by glucose (pyralomicins V-VII) (Figure.III.1). The pyralomicins are active against Gram-positive bacteria and their antibacterial activity depends on the position and number of chlorine atoms attached within the molecule and nature and methylation of glycone.[4a,b] The aglycon region of the molecule resembles pyoluteorin, the marinopyrroles, TAN-876A, and TAN-876B.[4a,c] Moreover, marine alkaloids such as lamellarins with a chromenopyrrole core display diverse biological activities including potential treatments for CNS orders.[1] Considering the remarkable utility of chromenopyrroles with unique structural characteristics, it is essential to plan newer sustainable methodologies for their synthesis through mild reaction conditions and readily available precursors.

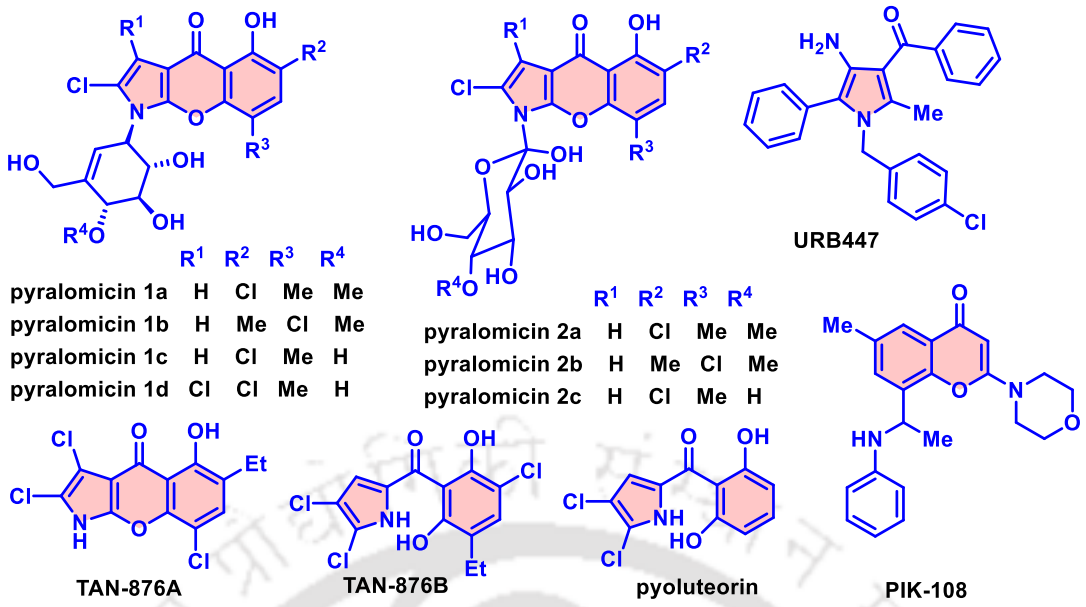

Figure III.1. *Bioactive pyrrole and chromenopyrrole core.*

III.2. Strategies for Synthesis of Chromenopyrrole

Most of the existing methods for the synthesis of chromenopyrrole involve constructing pyrrole moiety from a functionalized chromenone *via* transition metal-catalyzed coupling reactions.[5] A few significant synthetic methodologies include 1,3-dipolar cycloaddition, multi-component synthesis, transition metal-catalyzed annulation, etc. The existing methods mostly start with 3-substituted chromones and subsequent annulation or cyclization with some *N*-containing coupling partners.

Yan *et al*. demonstrated a Cu-catalyzed decarboxylative annulation of *N*-substituted glycines with 3-formylchromones for the synthesis of functionalized chromenopyrroles. This cascade protocol proceeded *via* initial decarboxylation of glycine which then underwent annulation with an acyl group of 3-formylchromones (Scheme III.2.1).[6a] The requirement of pre-synthesized 3-formylchromone demands additional steps for its synthesis.

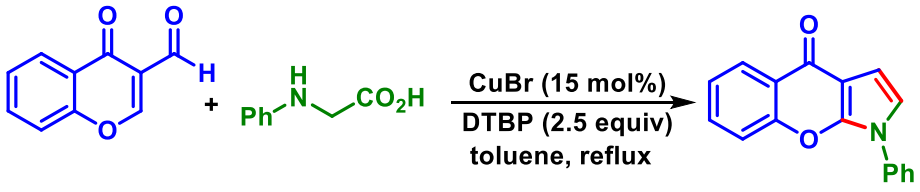

Scheme III.2.1. *Synthesis of chromenopyrroles via decarboxylative annulation.*

The same group in the following year developed a multi-component cascade strategy for the synthesis of functionalized chromenopyrrole by simply heating a mixture of 3-formylchromone and proline derivative under Cu catalysis. This decarboxylative annulation strategy provides an alternative route for the synthesis of these pyrrolidine derivatives (Scheme.III. 2.2).[6b]

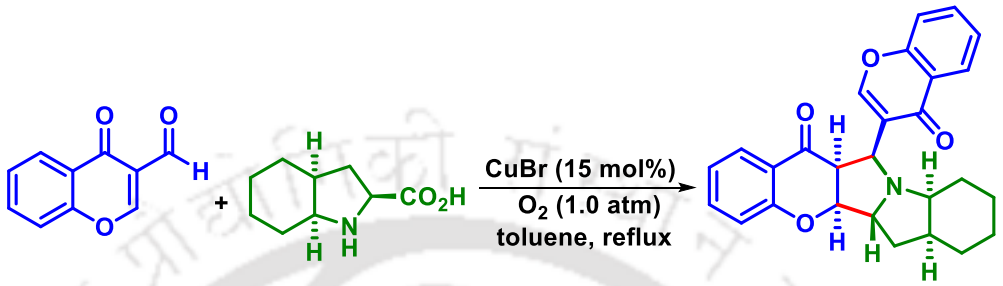

Scheme III.2.2. *Synthesis of chromenopyrrole via Cu-catalyzed decarboxylative annulation.*

Hu and his co-workers demonstrated a Cu-catalyzed methodology for the synthesis of imidazochromones by reacting 3-iodochromone and acetamidine hydrochloride in the presence of a base. The Cu-catalyzed aerobic C–H cyclo-etherification is found to be the key step for this cyclization protocol. Substrate scope analysis reveals that acyl phenols with electron-rich heterocycles efficiently participate in this C–H activation/C–O formation process (Scheme III.2.3).[6c]

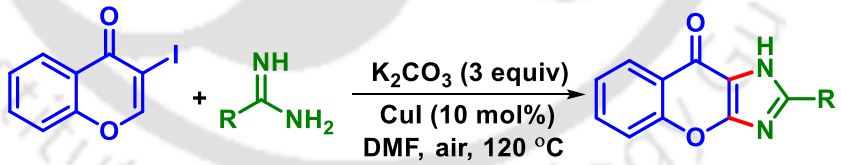

Scheme III.2.3. *Cu-catalyzed cascade synthesis of imidazochromone.*

Gao and Wu group disclosed a dual *α,β*-C(sp^2)–H functionalization of *o*-hydroxyphenyl enaminones to construct C2, C3-disubstituted chromenes which eventually undergoes intramolecular cascade cyclization to deliver diverse chromenopyrroles. Mechanistically, acetophenone oxidized to phenylglyoxal *via* iodination intermediate in the presence of I_2-DMSO (Kornblum oxidation) which subsequently undergoes nucleophilic attack by *o*-hydroxyphenyl enaminone. The resulting intermediate undergoes 1,4-addition with aniline which eventually delivers the product. This one-pot strategy constructs four new

bonds and two rings to form target compounds from readily accessible substrates (Scheme III.2.4).[6d]

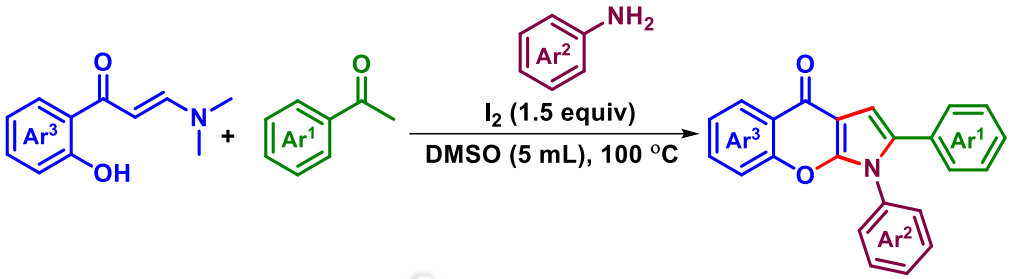

Scheme III.2.4. *I_2/DMSO-mediated synthesis of chromenopyrroles.*

Zhang and Yang group developed a facile and efficient methodology for the synthesis of tricyclic fused pyrazoles *via* a one-pot sequential path. The condensation of aldehyde and tosylhydrazine forms hydrazone which chemoselectively undergoes fusion with 3-chlorochromones in a sequential way through ring-opening and ring-closing to deliver chromeno[3,2-*c*]pyrazoles in moderate to excellent yields (Scheme III.2.5).[6e]

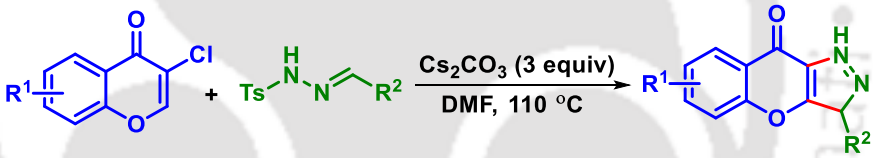

Scheme III.2.5. *Sequential synthesis of chromenopyrazoles.*

Another efficient approach for the synthesis of chromenopyrrole was developed by Yang group utilizing activated isocyanide. In the presence of an Ag catalyst, ethyl isocyanoacetate undergoes nucleophilic addition to the double bond of the chromanone. Subsequent ring-opening and intramolecular C–O bond formation lead to the construction of functionalized chromeno[2,3-*b*]pyrrol-4(1*H*)-ones (Scheme III.2.6).[6f]

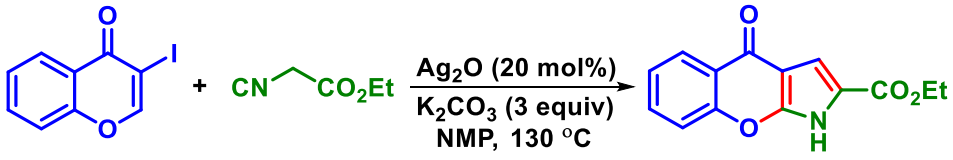

Scheme III.2.6. *Ag-catalyzed cascade synthesis of chromenopyrrole.*

Shao *et al*. described a transition metal-free synthesis of 2,3,4-substituted pyrrole from aurone analogues and methyl isocyanoacetate. This NaOH-catalyzed cyclization proceeds under mild reaction conditions and at room temperature and delivers diverse pyrrole in excellent yields (up to 99%). However, such pyrrole can be smoothly transformed into corresponding chromenopyrrole under alkaline conditions at high temperature in the presence of a catalytic amount of CuI. Gratifyingly, the reaction was also successful in a one-pot fashion when treated with CuI at high temperatures resulting in the chromenopyrrole in good yield (Scheme III.2.7).[6g]

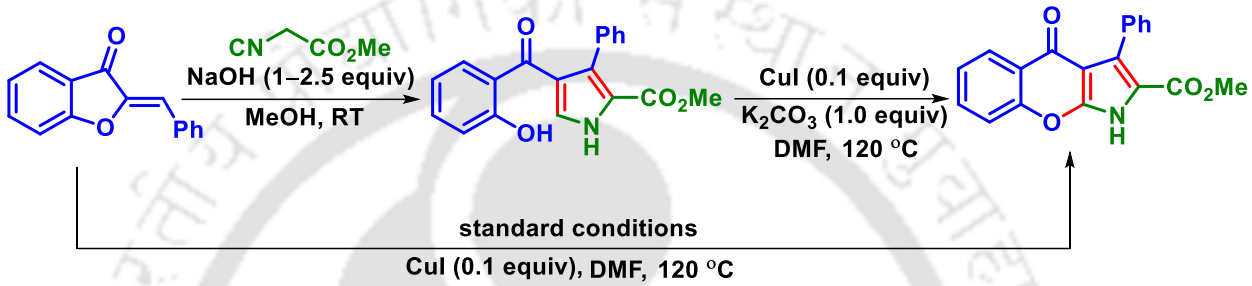

Scheme III.2.7. *Synthesis of chromenopyrrole from aurone and isocyanoacetate.*

Considering the importance of chromenopyrrole core in various biological activities, its synthesis has gained considerable attention in the recent past. However, simple reaction conditions and easily accessible precursors always find their usefulness in constructing heterocycles. Recently, we developed a one-pot tandem (3 + 2) cycloaddition-lactonization strategy utilizing 2-hydroxychalcone and ethyl isocyanoacetate for the synthesis of fused 2-chromenopyrroles (Scheme III.2.8).[7]

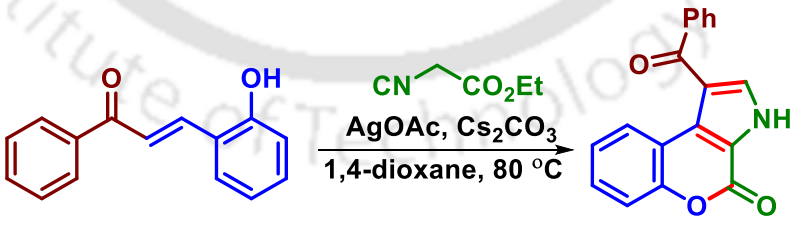

Scheme III.2.8. *Synthesis of 2-chromenopyrrole via (3 + 2) cycloaddition.*

III.3. Present Work

III.3.1. Our approach

Inspired by these approaches, we envisioned applying such a strategy to an appropriately designed substituted chalcone, where the hydroxy group is kept at a distal phenyl ring, thereby avoiding the chances of lactonization. Hence to execute our approach, 2′-hydroxychalcone (**1**) derived from 2′-hydroxyacetophenone and benzaldehyde was treated with ethyl isocyanoacetate (**a**) in the presence of AgOAc and K_2CO_3 in CH_3CN at 60 ^oC (Scheme III.3.1).

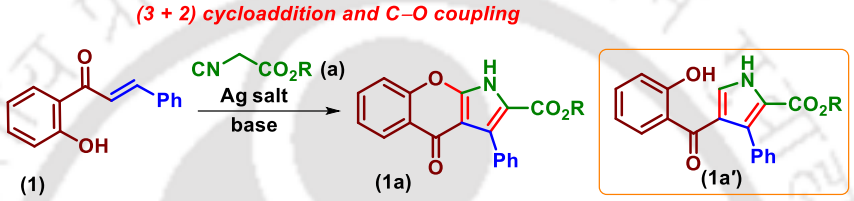

Scheme III.3.1. *Cascade cycloaddition and C–O coupling.*

Delightfully, after 12 h of reaction, two new products were obtained which were isolated and characterized by spectroscopic techniques (^1H, $^{13}C\{^1H\}$, and IR). The one having higher R_f was obtained in 37% yield and was found to be a formal (3 + 2) cycloadduct pyrrole (**1a'**). The other compound having lower R_f was isolated in 45% yield, and was characterized to be ethyl 4-oxo-3-phenyl-1,4-dihydrochromeno[2,3-*b*]pyrrole-2-carboxylate (**1a**). Here, unlike the previous approach,[7] the furthest located hydroxy group prefers C–O coupling with 2-*H* of the *in situ* generated pyrrole over lactonization. The exact structure of the chromenopyrrole was re-confirmed by single crystal XRD analysis of one of the derivatives (**28a**) (CCDC 2284347) (Figure III.3.1).

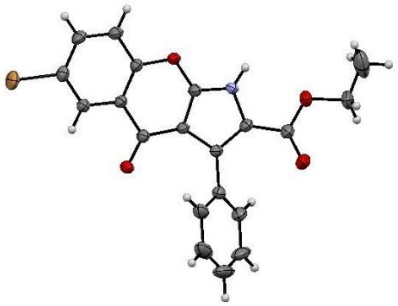

Figure. III.3.1. *ORTEP view of ethyl 6-bromo-4-oxo-3-phenyl-1,4-dihydrochromeno[2,3-b]pyrrole-2-carboxylate (**28a**) with 30% ellipsoid probability (CCDC 2284347).*

III.3.2. Optimization of the reaction conditions

To get a better yield of **1a** and to reduce the amount of uncyclized pyrrole (**1a′**), we started our optimization by taking hydroxy chalcone (**1**) and ethyl isocyanoacetate (**a**) as two model reacting partners (Table III.1). At first, different solvents such as 1,2-DCE, toluene, DMF, DMSO, THF, acetone, 1,4-dioxane, MeOH, and EtOH were screened. Solvents like 1,2-DCE and toluene delivered the anticipated product (**1a**) along with a substantial amount of uncyclized pyrrole (**1a′**) (Table III.1, entries 1–3). However, the reaction was completely unsuccessful in polar aprotic solvents such as DMF, DMSO, THF, acetone, and 1,4-dioxane (Table III.1, entries 4–6). In the polar protic solvent MeOH, the reaction led to almost equal amounts of **1a** and **1a′** (Table III.1, entry 7). Interestingly, in EtOH, the yield of **1a** improved to 70% and reduced the yield of **1a′** to a mere 10% (Table III. 1, entry 8). Thus, EtOH turned out to be the best among all the solvents screened, and hence, further optimizations were carried out using EtOH. The salts of Ag and Cu are known to activate alkyl isocyanoacetates by coordinating with the isocyanide group forming a 1,3-dipole. Therefore, different Ag and Cu salts such as Ag_2CO_3, Ag_2O, CuI, $Cu(OAc)_2{\cdot}H_2O$, and $CuBr_2$ were screened. While Ag_2CO_3, Ag_2O, and CuI were found to be inferior to AgOAc, but $Cu(OAc)_2{\cdot}H_2O$ and $CuBr_2$ were completely ineffective (Table III.1, entries 9–13). Then, we turned our attention to examining the effect of various bases, such as Cs_2CO_3, Na_2CO_3, KOAc, and DABCO in place of K_2CO_3. However, none of the examined bases could improve the yield or selectivity of **1a** over **1a′** as compared to K_2CO_3 (Table III.1, entries 14–17). Lowering the amount of AgOAc to 2 equiv reduces the yield of **1a** to 55% (Table III.1, entry 18). Similarly, lowering of the amount of base to 1 equiv decreases the yield of **1a** to 40% (Table III.1, entry 19). Further, reducing the reaction time to 4 h leads to the formation of uncyclized pyrrole **1a′** as the major product (**1a**/**1a′** = 35/40, Table III.1, entry 20). This suggested the intermediacy of pyrrole **1a′** in this overall strategy. Increasing the reaction temperature to 80 ^oC improves the product yield to 78% and reduces the formation of **1a′** to 5% (Table III.1, entry 21). However, an increase in temperature to 100 ^oC had no significant impact on the product yield (Table III.1, entry 22). Thus, after an extensive optimization, the best conditions for this chromenopyrrole synthesis is the use of **1** (1 equiv) and **a** (1.2 equiv) in the presence of AgOAc (3 equiv), K_2CO_3 (2 equiv) in EtOH at 80 ^oC (Table III.1, entry 21).

Table III.1. *Optimization of reaction conditions*[abc]

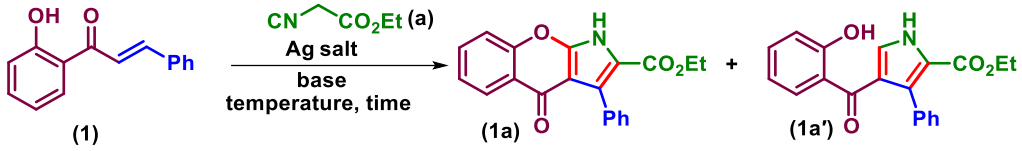

Entry	Solvent	Additive (equiv)	Base (equiv)	Temp. (°C)	Yield (%)[b] (1a/1a′)
1	CH_3CN	AgOAc (3)	K_2CO_3 (2)	60	45/37
2	1,2-DCE	AgOAc (3)	K_2CO_3 (2)	60	40/30
3	Toluene	AgOAc (3)	K_2CO_3 (2)	60	35/30
4	DMF, DMSO	AgOAc (3)	K_2CO_3 (2)	60	nd
5	THF, Acetone	AgOAc (3)	K_2CO_3 (2)	60	nd
6	1,4-Dioxane	AgOAc (3)	K_2CO_3 (2)	60	nd
7	MeOH	AgOAc (3)	K_2CO_3 (2)	60	43/40
8	EtOH	AgOAc (3)	K_2CO_3 (2)	60	70/10
9	EtOH	Ag_2CO_3 (3)	K_2CO_3 (2)	60	65/10
10	EtOH	Ag_2O (3)	K_2CO_3 (2)	60	50/15
11	EtOH	CuI (3)	K_2CO_3 (2)	60	65/10
12	EtOH	$Cu(OAc)_2{\cdot}H_2O$ (3)	K_2CO_3 (2)	60	nd
13	EtOH	$CuBr_2$ (3)	K_2CO_3 (2)	60	nd
14	EtOH	AgOAc (3)	Cs_2CO_3 (2)	60	55/15
15	EtOH	AgOAc (3)	Na_2CO_3	60	50/20
16	EtOH	AgOAc (3)	KOAc (2)	60	30/40
17	EtOH	AgOAc (3)	DABCO	60	50/15
18	EtOH	AgOAc (2)	K_2CO_3 (2)	60	55/15
19	EtOH	AgOAc (3)	K_2CO_3 (1)	60	40/25
20	EtOH	AgOAc (3)	K_2CO_3 (1)	60	35/40[c]
21	**EtOH**	**AgOAc (3)**	**K_2CO_3 (2)**	**80**	**78/05**
22	EtOH	AgOAc (3)	K_2CO_3 (2)	100	80/04

[a]Reaction conditions: **1** (0.25 mmol), **a** (0.30 mmol, 1.2 equiv), additive (equiv), base (equiv), solvent (4 mL), 10 h. [b]Isolated yield. [c]in 4 h. nd = not detected[d]

III.3.3. Substrate scope of chromenopyrrole

After successfully identifying the optimal conditions, a range of 2′-hydroxychalcones (**1**–**25**) were subjected to the present protocol to synthesize a library of chromenopyrroles (**1a**–**25a**) (Scheme III.3.2).

Scheme III.3.2. *Substrate scope for the synthesis of 4-chromenopyrrole*[a,b]

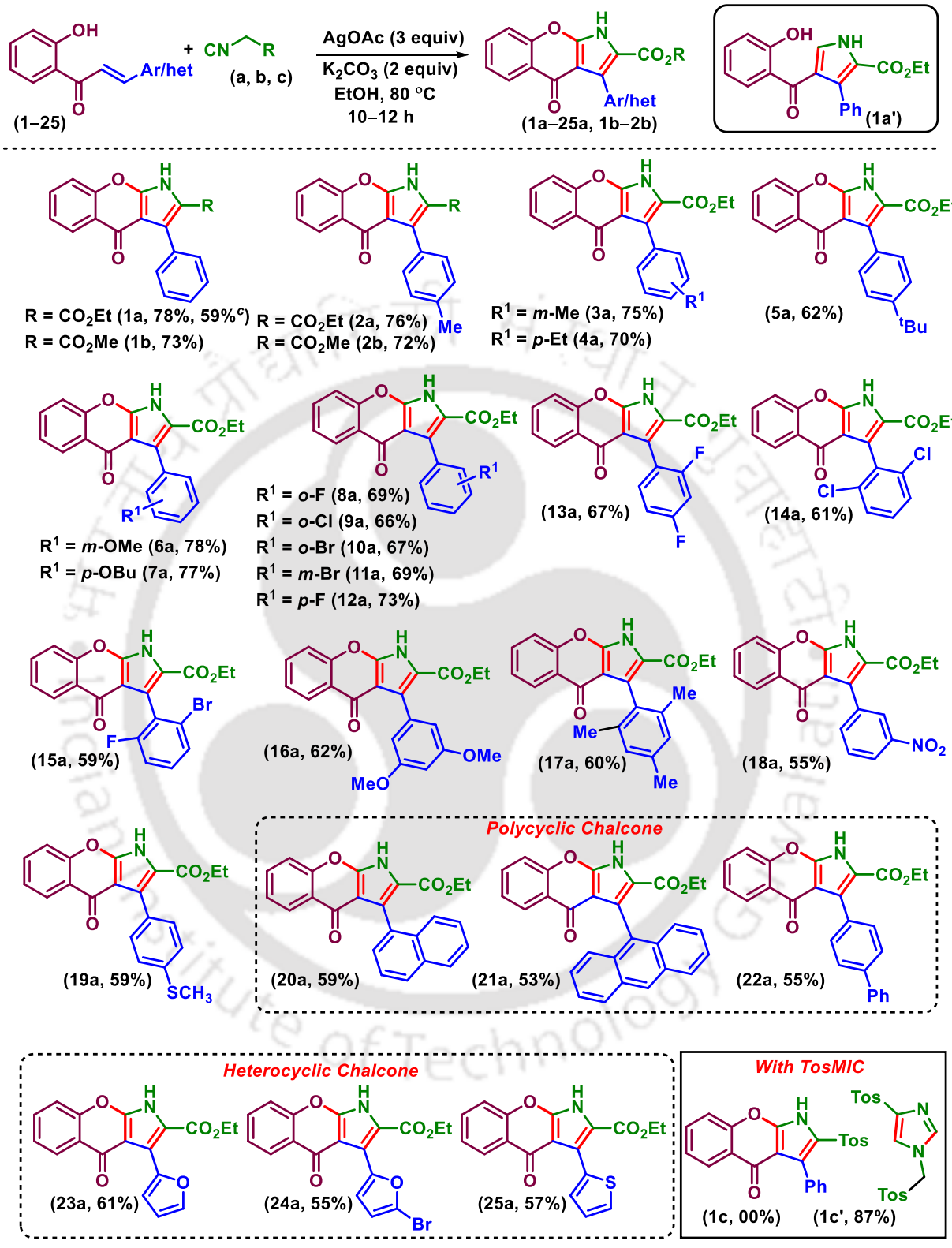

[a]Reaction conditions: **1**–**25** (0.5 mmol), **a**–**c** (1.2 equiv, 0.6 mmol), AgOAc (3 equiv, 1.5 mmol), K_2CO_3 (2 equiv, 1 mmol), EtOH (4 mL), 80 °C, 12 h. [b]Isolated yield of the product. [c]Gram-scale synthesis

Initially, electron-rich substituents (R^1) on the phenyl ring towards the alkene side (derived from benzaldehyde) of 2′-hydroxychalcones such as *p*-Me (**2**), *m*-Me (**3**), *p*-Et (**4**), *p*-^{t}Bu (**5**), *m*-OMe (**6**), *p*-OBu (**7**) were examined and all delivered their desired 4-chromenopyrroles (**2a**–**7a**) in yields ranging from 62–78%. Further, the protocol resulted in the production of chromenopyrrole from halogen-substituted precursors (**8**–**12**). Irrespective of the position of halo substituents such as *o*-F (**8**), *o*-Cl (**9**), *o*-Br (**10**), *m*-Br (**11**), and *p*-F (**12**), all were well compatible and resulted in the chromenopyrrole scaffold **8a**–**12a** in good yields of 66–73%. Further, di-substituted chalcones such as **13**, **14**, and **15** smoothly participated in this transformation and delivered the predicted chromenopyrrole **13a** (67%), **14a** (61%), and **15a** (59%), respectively. A slightly lower yield in the case of 2,6-disubstituted substrates **14a** and **15a** may be attributed to steric congestion. Di-methoxy substituted chalcone (**16**) and mesityl-derived chalcone (**17**) delivered their respective fused pyrrole **16a** and **17a** in 62% and 60% yield, respectively. A strongly electron-withdrawing $-NO_2$ substituted chalcone (**18**) furnished the product **18a** in a slightly lower yield of 55%. A *p*-methylthio group in 2′-hydroxychalcone (**19**) is also well tolerated under the reaction conditions and provided **19a** in 59% yield. 2′-Hydroxychalcones derived from polyaromatic aldehydes such as 1-naphthyl (**20**), 9-anthracenyl (**21**), and biphenyl (**22**) were smoothly converted to respective chromenopyrrole **20a** (59%), **21a** (53%) and **22a** (55%). Under the standard conditions, heteroaryl such as furyl (**23a**–**24a**) and thiophenyl (**25a**) containing fused chromenopyrroles were synthesized from their corresponding chalcones **23**, **24**, and **25** in moderate yields (55–61%). Analogues to ethyl isocyanoacetate (**a**), methyl isocyanoacetate (**b**) also underwent identical cycloaddition/C–O bond formation with 2′-hydroxychalcones (**1** and **2**), delivering corresponding 4-chromenopyrrole methyl esters, **1b** and **2b** in 73% and 72% yield. When an analogous *p*-tolylsulfonymethyl isocyanide (TosMIC) (**c**) was reacted with 2'-hydroxychalcone (**1**) in place of alkyl isocyanoacetate, the anticipated chromenopyrrole (**1c**) was not observed, rather, a dimer of TosMIC (**1c'**) was obtained in 87% yield. The scalability of the protocol was tested by reacting **1** (5 mmol, 1.12 g) with **a**, which yielded corresponding **1a** in 59% yield (Scheme III.3.2).

We subsequently sought to survey the effect of substituents on the hydroxy-bearing ring of chalcone for this transformation. Initially, 4-methyl hydroxychalcone (**26**) was treated independently with ethyl (**a)** and methyl isocyanoacetate (**b**) and both led to their corresponding product **26a** (75%) and **26b** (71%) in good yields. Mild electron-withdrawing

halo substituted 2′-hydroxychalcones *p*-Cl (**27**), *p*-Br (**28**), 5-Cl (**29**) also reacted with ethyl isocyanoacetate (**a**) and resulted in chromenopyrroles **27a**, **28a** and **29a** in 68%, 64% and 55% yields. 2,4-Dimethyl substituted 2′-hydroxychalcone (**30**) successfully delivered the corresponding chromenopyrrole (**30a**) in 59% yield. 2,4-Dihalo substituted chalcones (**31** and **32**) reacted well in this protocol, delivering **31a** and **32a** in modest yields of 58% and 55% (Scheme III.3.3).

Scheme III.3.3. *Substrate scope for the synthesis of 4-chromenopyrrole*[a,b]

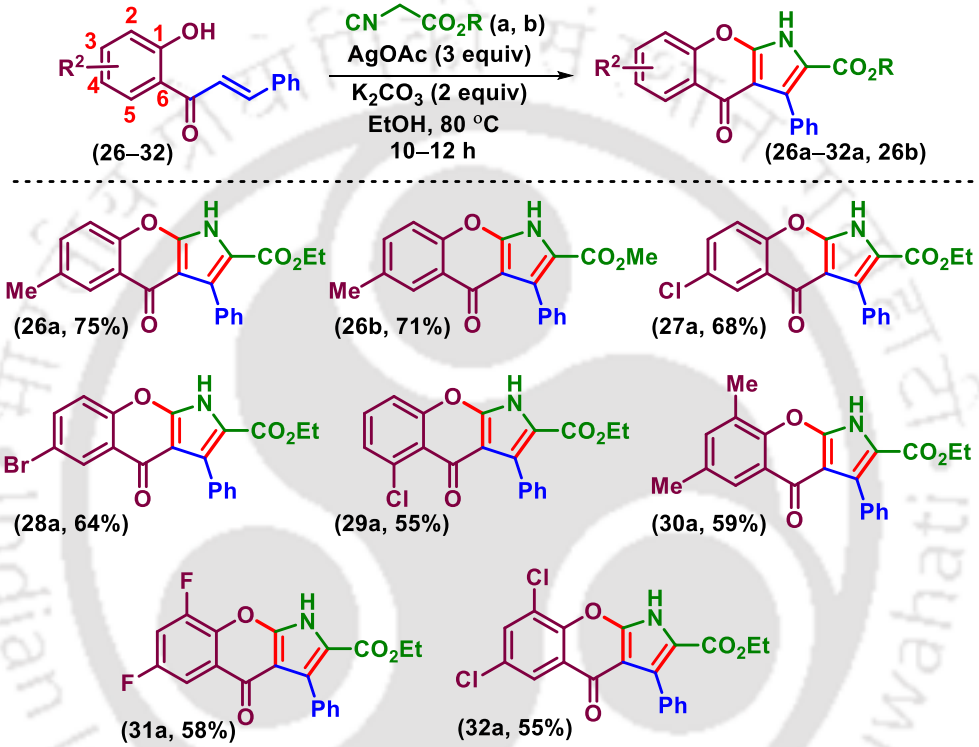

[a]Reaction conditions: **26**–**32** (0.5 mmol), **a**–**b** (1.2 equiv, 0.6 mmol), AgOAc (3 equiv, 1.5 mmol), K_2CO_3 (2 equiv, 1 mmol), EtOH (4 mL), 80 °C, 12 h. [b]Isolated yield of the product.

III.3.4. Mechanistic investigations:

Control experiments:

A few control experiments were performed to gain mechanistic insight into this cycloaddition/C–O coupling strategy. Two independent reactions were carried out between (**1**) and (**a**) to understand the role of silver salt and base. The one performed with only silver salt (without the base) resulted in the (3 + 2) cycloadduct **1a'** having a free –OH group as the sole product (Scheme III.3.4.1) while the other with only base (without Ag salt) gave no

product (Scheme III.3.4.2) This suggests the essential role of AgOAc in the initial cycloaddition yielding pyrrole **1a'** as the intermediate.

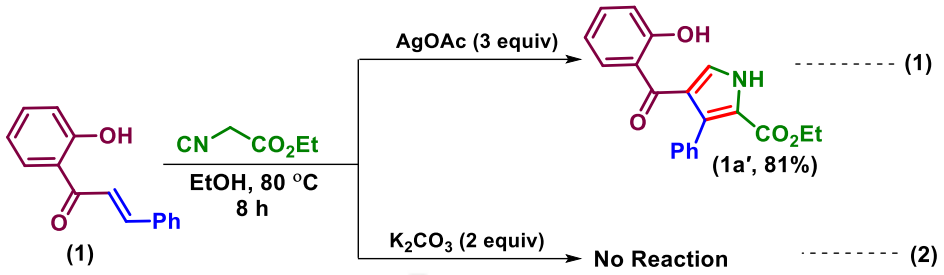

Scheme III.3.4. *Independent treatment of (**1**) with (**a**) in base and base-free condition.*

Treatment of **1a'** separately with either AgOAc or K_2CO_3 failed to provide the C–O coupled product **1a** (Scheme III.3.5).

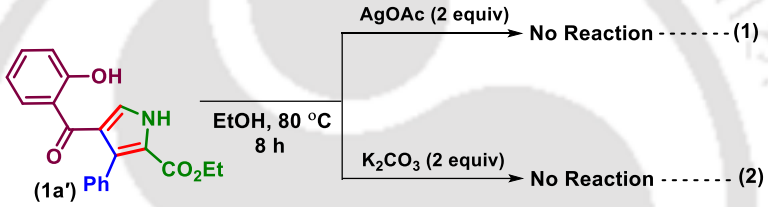

Scheme III.3.5. *Independent treatment of (**1a'**) with base nad base-free conditions.*

However, treatment of **1a'** in the presence of both AgOAc and K_2CO_3 under the standard condition, resulted in the chromenopyrrole (**1a**) (Scheme III.3.6), suggesting the cooperative role of silver salt and base in the final C–O coupling step.

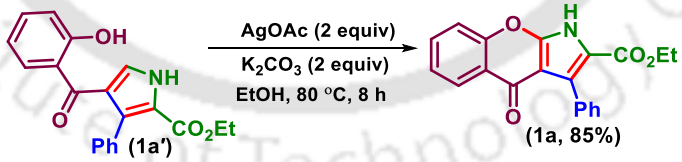

Scheme III.3.6. *Co-operative role of Ag salt and base in final C–O coupling.*

III.3.5. Plausible reaction mechanism:

Guided by these observations and from the literature reports, a possible silver-promoted mechanism for this transformation has been proposed as shown in Scheme III.3.7.[6c,7,8] Initially, ethyl isocyanoacetate (**a**) generates a 1,3-dipolar intermediate (**a'**) in the presence of AgOAc with the elimination of AcOH. Next, this 1,3-dipole (**a'**) undergoes a (3

+ 2) cycloaddition at the C=C double bond of chalcone (**1**) which results in the generation of pyrrole intermediate **1a'**.[7,8a,b] Following this, a six-membered cyclic transition state (**A**) arises because of the interaction between AgOAc and C5–*H* of the pyrrole ring of **1a'** which also involves the participation of the deprotonated phenolic group.[6c] Elimination of AcOH followed by activation of the pyrrole ring *via* insertion of Ag at C5 resulted in the formation of another intermediate **B**.[8c,d] Finally, C–O coupling at the electrophilic C5 site with release of Ag(0) gives the desired chromenopyrrole (**1a**) (Scheme III.3.7). The formation of Ag mirror at the surface of the reaction flask confirms the reduction of Ag(I) salt supporting the proposed mechanism (path a).

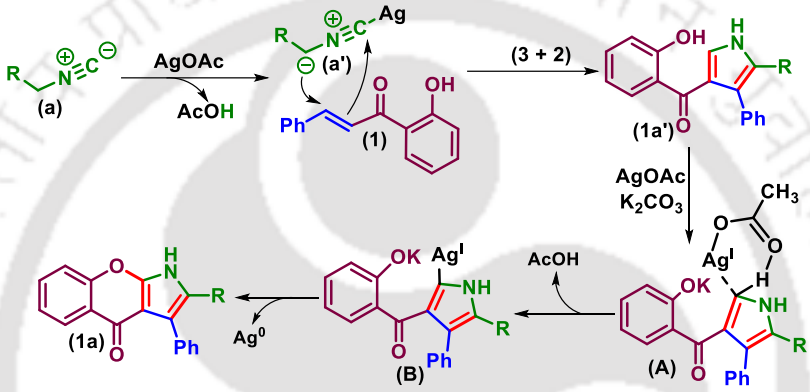

Scheme III.3.7.1. *Plausible mechanism (path a).*

The reaction may also proceed *via* a path as shown in the Scheme III.3.7.2. Here, the dipole generated from the initial attack of silver acetate on ethyl isocyanoacetate (**a**) will form a cyclic imine (**A'**) which will release Ag(0) in subsequent steps to give intermediate (**B'**). Through tautomerization, intermediate **B'** will form another intermediate **1a'** which *via* C–H oxidative etherification delivers the desired product (**1a'**) (path b).

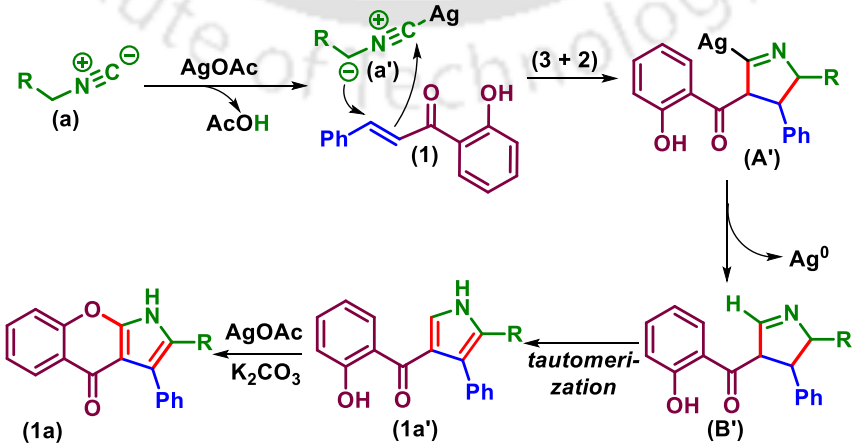

Scheme III.3.7.2. *Plausible mechanism (path b).*

III.3.6. Conclusion

In summary, this tandem cycloaddition and C–O coupling is an elegant approach for the synthesis of substituted 4-chromenopyrrole. The appropriately positioned hydroxy group and alkene double bond of the chalcone offer two reactive sites for this reaction. Mechanistic investigation infers that Ag salt has a crucial role in the activation of isocyanoacetate and in the final cyclization step. This methodology leads to the construction of C=C and C–O bonds in a step-economical manner under operationally simple reaction conditions. The developed method is scalable and has wide functional group tolerance, providing good to moderate yields of the product.

III.4. Experimental Section:

III.4.1. General information:

All the reagents were commercial grade and used without further purification unless otherwise stated. All the reactions were carried out in a 10 mL oven-dried round-bottom flask under aerobic conditions. Reactions were monitored by thin layer chromatography (TLC) on a 0.25 mm silica gel plates ($60F_{254}$) and visualized under UV illumination at 254 nm. Organic extracts were dried over anhydrous sodium sulfate (Na_2SO_4). Column chromatography was performed to purify the crude product on silica gel 60–120 mesh using a mixture of hexane and ethyl acetate as eluent. The isolated compounds were characterized by spectroscopic [^1H, $^{13}C\{^1H\}$ NMR, and IR] techniques and HRMS analysis. NMR spectra were recorded in deuterochloroform ($CDCl_3$) and in some cases deuterated dimethyl sulfoxide (CD_3SOCD_3). ^1H, $^{13}C\{^1H\}$ NMR was recorded in 500 (125) or 400 (100) MHz spectrometer and were calibrated using tetramethylsilane or residual undeuterated solvent for ^1H NMR, deuterochloroform for $^{13}C\{^1H\}$ NMR as an internal reference {$Si(CH_3)_4$: 0.00 ppm or $CHCl_3$: 7.260 ppm for ^1H NMR, 77.230 ppm for $^{13}C\{^1H\}$ NMR. ^{19}F NMR was calibrated without any internal standard in $CDCl_3$. The chemical shifts are quoted in δ units, parts per million (ppm). ^1H NMR data is represented as follows: Chemical shift, multiplicity (s = singlet, d = doublet, t = triplet, q = quartet, m = multiplet, dd = doublet of doublet, dt = doublet of triplet), integration and coupling constant(s) *J* in hertz (Hz). High-resolution mass spectra (HRMS) were recorded on a mass spectrometer using electrospray ionization-time of flight (ESI-TOF) reflection experiments. FT-IR spectra were recorded in neat and reported in the frequency of absorption (cm^{-1}).

III.4.2. Crystallographic information:

Sample preparation: The single crystal of compound **28a** was prepared by the slow evaporation method for which 10 mg of the compound (**28a**) was dissolved in 1 mL of DCM in a clean and dry 10 mL glass vial. MeOH (0.5 mL) was added to this solution slowly with a dropper. The mouth of the glass vial was covered with a cap having a small hole and kept for slow evaporation at room temperature. Crystals of **28a** were obtained after approximately 3–4 days as a transparent block-shaped crystal.

Data collection: Diffraction data were collected at 292 K with MoKα radiation (λ = 0.71073 Å) using a Bruker Nonius SMART APEX CCD diffractometer equipped with graphite monochromator and Apex CD camera. The SMART software was used for data collection and indexing the reflections and determining the unit cell parameters. Data reduction and cell refinement were performed using SAINT[9a-b] software and the space groups of these crystals were determined from systematic absences by XPREP and further justified by the refinement results. The structures were solved by direct methods and refined by full-matrix least-squares calculations using SHELXTL-973 software. All the non-H atoms were refined in the anisotropic approximation against F2 of all reflections.[9c]

Crystallographic description of *ethyl 6-bromo-4-oxo-3-phenyl-1,4-dihydrochromeno[2,3-b]pyrrole-2-carboxylate (28a)*:

$C_{20}H_{14}BrNO_4$, colourless block shaped crystal; crystal dimensions 0.25 x 0.23 x 0.17 mm, M_r = 412.24, monoclinic, space group P 1 21/c 1, Hall group –P 2ybc, a = 13.6571(10), b = 10.8213(8), c = 11.9303(9)Å, α = 90°, β = 93.856 (2)°, γ = 90°, V = 1759.2(2) Å^3, Z = 4, ρ = 1.557 g/cm^3, μ = 2.362 mm^{-1} , F(000)= 831.731, reflection collected / unique = 3085 / 2217, refinement method = full-matrix least-squares on F^2, final R indices [I > 2\s(I)]: R_1 = 0.0426, wR_2 = 0.1133, R indices (all data): R_1 = 0.0741, wR_2 = 0.1601, goodness of fit = 1.1807; CCDC = 2284347 for ***ethyl 6-bromo-4-oxo-3-phenyl-1,4-dihydrochromeno[2,3-b]pyrrole-2-carboxylate (28a)*** contains the supplementary crystallographic data for this paper. These data can be obtained free of charge from The Cambridge Crystallographic Data Centre via www.ccdc.cam.ac.uk/data_request/cif.

III.4.3. General procedures:

III.4.3.1. General procedure for the synthesis of (*E*)-1-(2-hydroxyphenyl)-3-phenylprop-2-en-1-one (1):

2'-Hydroxychalones are known and are synthesized according to the available literature procedure.[10a-c]

III.4.3.2. General procedure for the synthesis of ethyl 4-oxo-3-phenyl-1,4-dihydrochromeno[2,3-*b*]pyrrole-2-carboxylate (1a):

To a 10 mL oven-dried round bottom flask equipped with a magnetic bar was added (*E*)-1-(2-hydroxyphenyl)-3-phenylprop-2-en-1-one (**1**) (0.5 mmol, 112 mg), ethyl isocyanoacetate (**a**) (1.2 equiv, 68 mg), AgOAc (3 equiv, 250 mg), K_2CO_3 (2 equiv, 138 mg) and ethanol (4 mL). The reaction mixture was allowed to stir at 80 ^oC for 12 h in a pre-heated oil bath. After completion of the reaction as confirmed by TLC monitoring, the mixture was filtered through a thin bed of celite. After removing ethanol by rotary evaporator, the crude mixture was diluted by adding 20 mL ethyl acetate and washed with water (1 x 10 mL) followed by brine solution (1 x 5 mL). The organic layer was dried over anhydrous Na_2SO_4 and concentrated under reduced pressure. The crude product thus obtained was purified over a column of silica gel using hexane and ethyl acetate (3:1) to give pure product **1a** in 78% yield (130 mg).

III.4.3.3. General procedure for the synthesis of methyl 4-oxo-3-phenyl-1,4-dihydrochromeno[2,3-*b*]pyrrole-2-carboxylate (1b):

To a 10 mL oven-dried round bottom flask equipped with a magnetic bar was added (*E*)-1-(2-hydroxyphenyl)-3-phenylprop-2-en-1-one (**1**) (0.5 mmol, 112 mg), methyl isocyanoacetate (**b**) (1.2 equiv, 60 mg), AgOAc (3 equiv, 250 mg), K_2CO_3 (2 equiv, 138 mg) and ethanol (4 mL). The reaction mixture was allowed to stir at 80 ^oC for 12 h in a pre-heated oil bath. After completion of the reaction as confirmed by TLC monitoring, the mixture was filtered through a thin bed of celite. After removing the ethanol by a rotary evaporator, the crude mixture was diluted by adding 20 mL ethyl acetate and washed with water (1 x 10 mL) followed by brine solution (1 x 5 mL). The organic layer was dried over anhydrous Na_2SO_4 and concentrated under reduced pressure. The crude product thus obtained was purified over a column of silica gel using hexane and ethyl acetate (3:1) to give the pure product **1b** in 73% yield (116 mg).

III.4.3.4. Reaction between 2'-hydroxychalcone (1) and *p*-toluenesulfonylmethyl isocyanide (TosMIC) (c):

To a 10 mL oven-dried round bottom flask equipped with a magnetic bar was added (*E*)-1-(2-hydroxyphenyl)-3-phenylprop-2-en-1-one (**1**) (0.5 mmol, 112 mg), TosMIC (**c**) (1.2 equiv, 117 mg), AgOAc (3 equiv, 250 mg), K_2CO_3 (2 equiv, 138 mg) and ethanol (4 mL). The reaction mixture was allowed to stir at 80 ^oC for 12 h in a pre-heated oil bath. After completion of the reaction as confirmed by TLC monitoring, the mixture was filtered through a thin bed of celite. After removing the ethanol by a rotary evaporator, the crude mixture was diluted by adding 20 mL ethyl acetate and washed with water (1 x 10 mL) followed by brine solution (1 x 5 mL). The organic layer was dried over anhydrous Na_2SO_4 and concentrated under reduced pressure. The crude product thus obtained was purified over a column of silica gel using hexane and ethyl acetate (1:1) to pure product **1c'** in 87% yield (85 mg).

III.4.4. Mechanistic investigations:

III.4.4.1. Base (K_2CO_3)-free reactions of 2'-hydroxychalcone (1) and ethyl isocyanoacetate (a):

To a 10 mL oven-dried round bottom flask equipped with a magnetic bar was added (*E*)-1-(2-hydroxyphenyl)-3-phenylprop-2-en-1-one (**1**) (0.25 mmol, 56 mg), ethyl isocyanoacetate (**a**) (1.2 equiv, 34 mg), AgOAc (3 equiv, 125 mg), and ethanol (4 mL). The reaction mixture was allowed to stir at 80 ^oC for 12 h in a pre-heated oil bath. After completion of the reaction as confirmed by TLC monitoring, the mixture was filtered through a thin bed of celite. After evaporating ethanol, the crude mixture was diluted by adding 20 mL ethyl acetate and washed with water (1 x 10 mL) followed by brine solution (1 x 5 mL). The organic layer was dried over anhydrous Na_2SO_4 and concentrated under reduced pressure. The crude product thus obtained was purified over a column of silica gel using hexane and ethyl acetate (3:1) to give pure product **1a′** in 81% yield (68 mg).

Ethyl 4-(2-hydroxybenzoyl)-3-phenyl-1H-pyrrole-2-carboxylate (1a′)

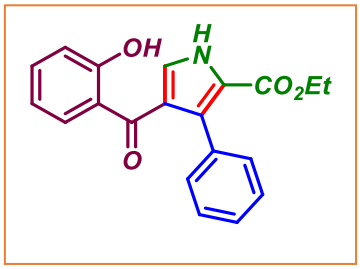

1a′ was obtained as gummy solid; purified over a column of silica gel (25% EtOAc in hexane); ^{1}H NMR ($CDCl_3$, 400 MHz): δ 11.83 (s, 1H), 9.89 (s, 1H), 7.57 (dd, 1H, J_1 = 8.0 Hz, J_2 = 1.6 Hz), 7.37–7.29 (m, 1H), 7.27–7.17 (m, 6H), 6.86 (dd, 1H, J_1 = 8.0 Hz, J_2 = 1.2 Hz), 6.70–6.66 (m, 1H), 4.13 (q, 2H, J = 6.8 Hz), 1.07 (t, 3H, J = 7.2 Hz); ^{13}C{^{1}H} NMR ($CDCl_3$, 125 MHz): δ 195.7, 162.7, 161.3, 135.9, 133.2, 132.9, 132.2, 130.1, 127.6, 127.5, 126.6, 124.5, 121.0, 120.7, 118.7, 118.1, 61.1, 14.1; IR (neat, cm^{-1}): 3321, 3219, 2919, 1730, 1665, 1645, 1611, 1569, 1523, 1442, 1419, 1282; HRMS (ESI/Q-TOF) (m/z): calcd. for $C_{20}H_{21}N_2O_4$, [M + NH_4]$^{+}$: 353.1496, found: 353.1496 (Figure III.4.4.1. and Figure III.4.4.2).

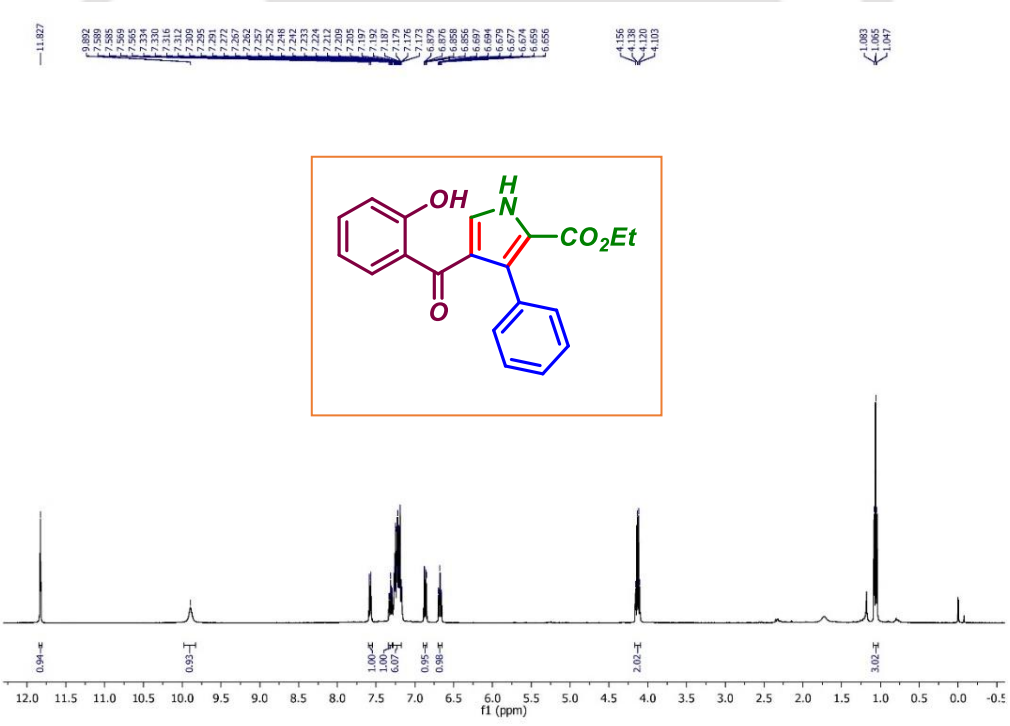

Figure III.4.4.1. *^{1}H spectra of intermediate* ***1a′*** *($CDCl_3$, 125 MHz).*

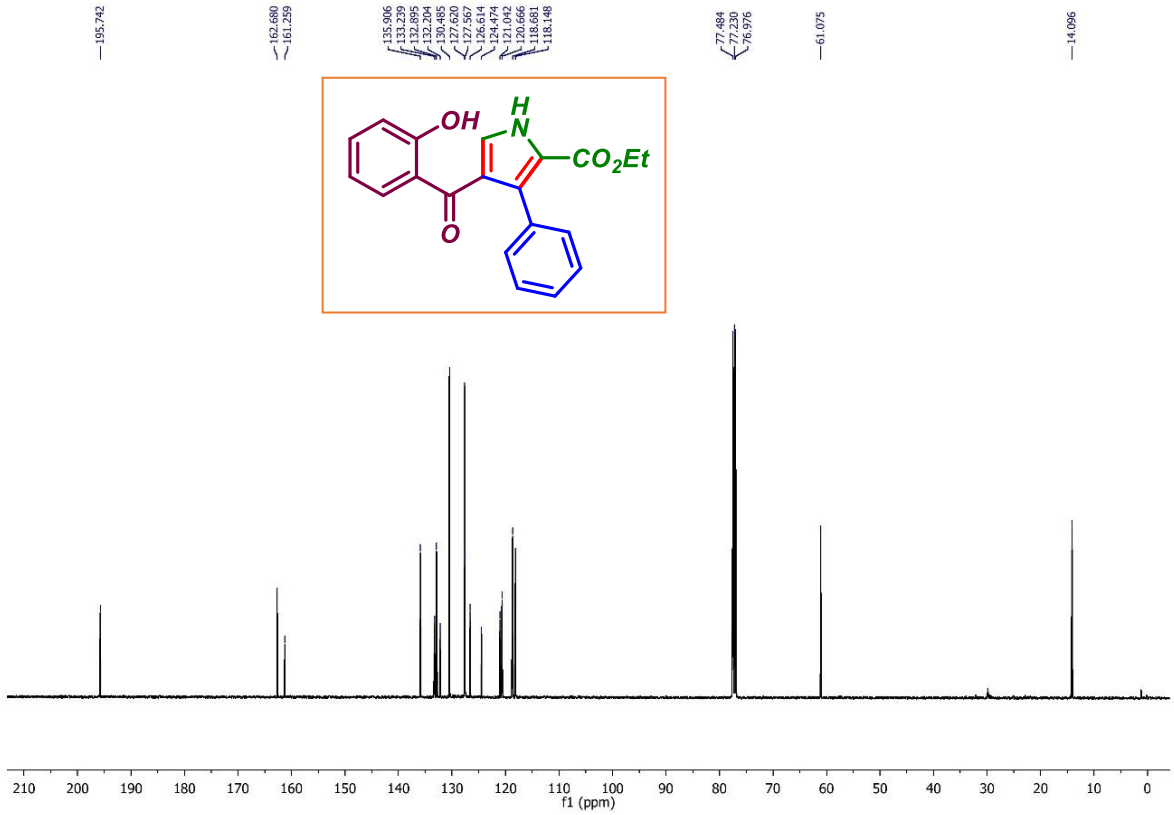

Figure III.4.4.2. *$^{13}C\{^{1}H\}$ spectra of intermediate **1a'** ($CDCl_3$, 400 MHz).*

III.4.4.2. AgOAc-free reactions of 2'-hydroxychalcone (1) and ethyl isocyanoacetate (a):

To a 10 mL oven-dried round bottom flask equipped with a magnetic bar was added (*E*)-1-(2-hydroxyphenyl)-3-phenylprop-2-en-1-one (**1**) (0.25 mmol, 56 mg), ethyl isocyanoacetate (**a**) (1.2 equiv, 34 mg), K_2CO_3 (2 equiv, 69 mg), and ethanol (3 mL). The reaction mixture was allowed to stir at 80 ^{o}C for 12 h in a pre-heated oil bath. However, careful observation of the reaction mixture found that the starting materials remain as it is even after 12 h.

III.4.4.3. Reaction of ethyl 4-(2-hydroxybenzoyl)-3-phenyl-1*H*-pyrrole-2-carboxylate (1a') with AgOAc:

To a 10 mL oven-dried round bottom flask equipped with a magnetic bar was added ethyl 4-(2-hydroxybenzoyl)-3-phenyl-1*H*-pyrrole-2-carboxylate (**1a'**) (0.15 mmol, 50 mg), AgOAc (2 equiv, 50 mg), and ethanol (4 mL). The reaction mixture was allowed to stir at

80 ^{o}C for 12 h in a pre-heated oil bath. However, careful observation of the reaction mixture up to 12 h found that the starting materials remain as it is.

III.4.4.4. Reaction of ethyl 4-(2-hydroxybenzoyl)-3-phenyl-1*H*-pyrrole-2-carboxylate (1a') with base K_2CO_3:

To a 10 mL oven-dried round bottom flask equipped with a magnetic bar was added ethyl 4-(2-hydroxybenzoyl)-3-phenyl-1*H*-pyrrole-2-carboxylate (**1a'**) (0.15 mmol, 50 mg), K_2CO_3 (2 equiv, 42 mg), and ethanol (2 mL). The reaction mixture was allowed to stir at 80 ^{o}C for 12 h in a pre-heated oil bath. However, careful observation of the reaction mixture up to 12 h found that the starting materials remain as it is.

III.4.4.5. Reaction of ethyl 4-(2-hydroxybenzoyl)-3-phenyl-*1*H-pyrrole-2-carboxylate (1a') in the standard condition:

To a 10 mL oven-dried round bottom flask equipped with a magnetic bar was added ethyl 4-(2-hydroxybenzoyl)-3-phenyl-1*H*-pyrrole-2-carboxylate (**1a'**) (0.15 mmol, 50 mg), K_2CO_3 (2 equiv, 42 mg), AgOAc (2 equiv, 50 mg), and ethanol (2 mL). The reaction mixture was allowed to stir at 80 ^{o}C for 8 h in a pre-heated oil bath. TLC analysis confirms the formation of the cyclized product **1a**. Subsequently, the mixture was filtered through a thin bed of celite. After evaporating the ethanol by a rotary evaporator, the crude mixture was diluted by adding 10 mL ethyl acetate and washed with water (1 x 5 mL) followed by brine solution (1 x 5 mL). The organic layer was dried over anhydrous Na_2SO_4 and concentrated under reduced pressure. The crude product thus obtained was purified over a column of silica gel using hexane and ethyl acetate (3:1) to give pure product **1a** in 85% yield (42 mg).

III.4.5. General procedure for the scale-up procedure:

To a 50 mL oven-dried round bottom flask equipped with a magnetic bar was added (*E*)-1-(2-hydroxyphenyl)-3-phenylprop-2-en-1-one (**1**) (5 mmol, 1.12 g), ethyl isocyanoacetate (**a**) (1.2 equiv, 6 mmol, 678 mg), AgOAc (3 equiv, 15 mmol, 2.5 g), K_2CO_3 (2 equiv, 10 mmol, 1.38 g) and ethanol (20 mL). The reaction mixture was allowed to stir at 80 ^{o}C for 12 h in a pre-heated oil bath. After completion of the reaction as confirmed by TLC monitoring, the mixture was filtered through a thin bed of celite. Evaporating ethanol by rotary evaporator, the crude mixture was diluted by adding 3 x 20 mL ethyl acetate and washed with water (3 x 15 mL) followed by brine solution (3 x 10 mL). The organic layer

was dried over anhydrous Na_2SO_4 and concentrated under reduced pressure. The crude product thus obtained was purified over a column of silica gel using hexane and ethyl acetate (3:1) to give pure product **1a** in 59% yield (982 mg).

III.5. Spectral Data

Spectral data of all compounds:

Ethyl 4-oxo-3-phenyl-1,4-dihydrochromeno[2,3-b]pyrrole-2-carboxylate (1a):

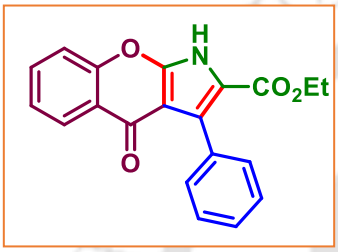

As off-white solid (130 mg, 78% yield), mp 260–262 °C; purified over a column of silica gel (25% EtOAc in hexane); ^{1}H NMR ($CDCl_3$, 400 MHz): δ 9.70 (s, 1H), 8.30 (d, 1H, J_1 = 8.0 Hz, J_2 = 2.0 Hz), 7.68–7.63 (m, 1H), 7.58–7.56 (m, 2H), 7.44 (dd, 1H, J_1 = 8.4 Hz, J_2 = 0.8 Hz), 7.42–7.36 (m, 4H), 4.23 (q, 2H, J = 7.2 Hz), 1.17 (t, 3H, J = 7.2 Hz); ^{13}C{^{1}H} NMR ($CDCl_3$, 100 MHz): δ 173.8, 161.4, 154.2, 150.4, 133.4, 131.9, 130.9, 128.8, 128.1, 127.3, 127.2, 125.1, 123.8, 117.3, 114.6, 106.4, 61.3, 14.1; IR (neat, cm^{-1}): 3075, 2982, 1721, 1609, 1567, 1533, 1508, 1471, 1432, 1274, 1204; HRMS (ESI/Q-TOF) (m/z): calcd. for $C_{20}H_{16}NO_4$, [M + H]$^+$: 334.1074, found: 334.1075.

Methyl 4-oxo-3-phenyl-1,4-dihydrochromeno[2,3-b]pyrrole-2-carboxylate (1b):

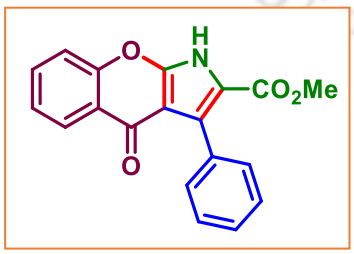

As off-white solid (116 mg, 73% yield), mp 264–266 °C; purified over a column of silica gel (25% EtOAc in hexane); ^{1}H NMR ($CDCl_3$, 400 MHz): δ 9.31 (s, 1H), 8.29 (d, 1H, J = 7.2 Hz), 7.67 (t, 1H, J = 7.6 Hz), 7.58 (d, 2H, J = 6.8 Hz), 7.47 (d, 1H, J = 8.4 Hz), 7.43–7.39 (m, 4H), 3.76 (s, 3H); ^{13}C{^{1}H} NMR ($CDCl_3$, 125 MHz): δ 173.7, 161.6, 154.2, 150.4, 133.5, 133.6, 130.9, 129.0, 128.3, 127.4, 127.3, 125.1, 123.8, 117.3, 114.1, 106.5, 52.1; IR (neat, cm^{-1}): 3051, 2924, 1716, 1635, 1611, 1567, 1537, 1520, 1463, 1431, 1271, 1205; HRMS (ESI/Q-TOF) (m/z): calcd. for $C_{19}H_{14}NO_4$, [M + H]$^+$: 320.0917, found: 320.0917.

Ethyl 4-oxo-3-(p-tolyl)-1,4-dihydrochromeno[2,3-b]pyrrole-2-carboxylate (2a):

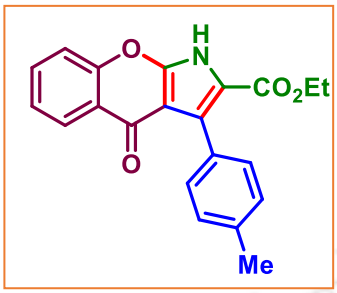

As off-white solid (132 mg, 76% yield), mp 259–261 °C; purified over a column of silica gel (25% EtOAc in hexane); ^{1}H NMR ($CDCl_3$, 400 MHz): δ 9.51 (s. 1H), 8.30 (dd, 1H, J_1 = 8 Hz, J_2 = 2.0 Hz), 7.67–7.63 (m, 1H), 7.48 (d, 2H, J = 8.0 Hz), 7.44 (d, 1H, J = 8.4 Hz), 7.39 (t, 1H, J = 7.2 Hz), 7.21 (d, 2H, J = 8.0 Hz), 4.25 (q, 2H, J = 6.8 Hz), 2.39 (s, 3H), 1.21 (t, 3H, J = 7.2 Hz); ^{13}C{^{1}H} NMR ($CDCl_3$, 125 MHz): δ 173.7, 161.3, 154.2, 150.5, 137.9, 133.4, 130.9, 129.1, 128.7, 128.1, 127.3, 125.0, 123.9, 117.3, 114.4, 106.5, 61.2, 21.6, 14.3; IR (neat, cm^{-1}): 3050, 2914, 1728, 1634, 1611, 1561, 1536, 1520, 1472, 1431, 1271; HRMS (ESI/Q-TOF) (m/z): calcd. for $C_{21}H_{18}NO_4$, $[M + H]^+$: 348.1230, found: 348.1232.

Methyl 4-oxo-3-(p-tolyl)-1,4-dihydrochromeno[2,3-b]pyrrole-2-carboxylate (2b):

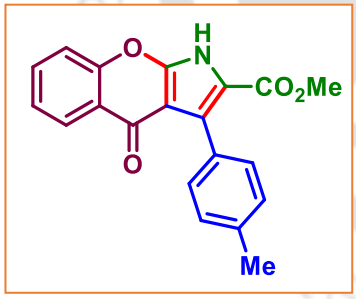

As off-white solid (120 mg, 72% yield), mp 248–250 °C; purified over a column of silica gel (25% EtOAc in hexane); ^{1}H NMR ($CDCl_3$, 500 MHz): δ 9.62 (s, 1H), 8.30 (dd, 1H, J_1 = 8.0 Hz, J_2 = 2.0 Hz), 7.67–7.63 (m, 1H), 7.47 (d, 2H, J = 8.0 Hz), 7.44 (d, 1H, J = 8.5 Hz), 7.41–7.38 (m, 1H), 7.21 (d, 2H, J = 7.5 Hz), 3.76 (s, 3H), 2.38 (s, 3H); ^{13}C{^{1}H} NMR ($CDCl_3$, 125 MHz): δ 173.8, 161.7, 154.1, 150.5, 138.0, 133.4, 130.8, 129.2, 128.6, 128.2, 127.2, 125.1, 123.8, 117.3, 114.0, 106.4, 52.0, 21.6; IR (neat, cm^{-1}): 3229, 2919, 1730, 1665, 1645, 1569, 1523, 1442, 1419, 1282; HRMS (ESI/Q-TOF) (m/z): calcd. for $C_{20}H_{15}NO_4Na$, $[M + Na]^+$: 356.0893, found: 356.0895.

Ethyl 4-oxo-3-(m-tolyl)-1,4-dihydrochromeno[2,3-b]pyrrole-2-carboxylate (3a):

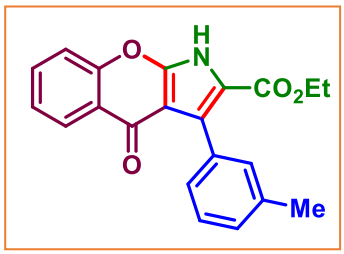

As off-white solid (130 mg, 75% yield), mp 218–220 °C; purified over a column of silica gel (25% EtOAc in hexane); ^{1}H NMR ($CDCl_3$, 500 MHz): δ 10.37 (s, 1H), 8.32 (dd, 1H, J_1 = 6.5 Hz, J_2 = 2.0 Hz), 7.65–7.61 (m, 1H), 7.39 (s, 1H), 7.38–7.35 (m, 3H), 7.24 (d, 1H, J = 7.5 Hz), 7.11 (d, 1H, J = 7.5 Hz), 4.20 (q, 2H, J = 7.5 Hz), 2.35 (s, 3H), 1.14 (t, 3H, J = 5.6 Hz); ^{13}C{^{1}H} NMR ($CDCl_3$, 125 MHz): δ 173.9, 161.6, 154.1, 150.7, 136.5, 133.3, 131.9, 131.5, 128.8, 128.7, 128.0, 127.2, 127.1, 124.9, 123.7, 117.3, 114.8, 106.4, 61.1, 21.6, 14.1; IR (neat, cm^{-1}): 3061, 2980, 1718, 1636, 1609, 1568, 1538, 1470, 1431, 1270, 1201; HRMS (ESI/Q-TOF) (m/z): calcd. for $C_{21}H_{18}NO_4$, $[M + H]^+$: 348.1230, found: 348.1232.

Ethyl 3-(4-ethylphenyl)-4-oxo-1,4-dihydrochromeno[2,3-b]pyrrole-2-carboxylate (4a):

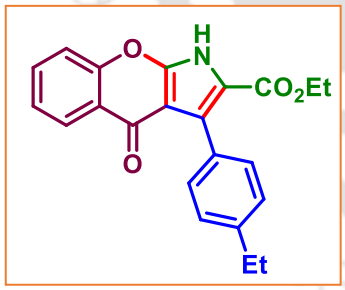

As off-white solid (126 mg, 70% yield), mp 225–227 °C; purified over a column of silica gel (25% EtOAc in hexane); ^{1}H NMR ($CDCl_3$, 500 MHz): δ 9.99 (s, 1H), 8.31 (dd, 1H, J_1 = 8.0 Hz, J_2 = 1.5 Hz), 7.66–7.62 (m, 1H), 7.51 (d, 2H, J = 7.5 Hz), 7.41 (d, 1H, J = 8.5 Hz), 7.38 (d, 1H, J = 7.5 Hz), 7.21 (d, 2H, J = 8.0 Hz), 4.23 (q, 2H, J = 7.0 Hz), 2.26 (q, 2H, J = 7.5 Hz), 1.25 (t, 3H, J = 7.5 Hz), 1.18 (t, 3H, J = 7.5 Hz); ^{13}C{^{1}H} NMR ($CDCl_3$, 125 MHz): δ 173.8, 161.4, 154.1, 150.6, 144.1, 133.3, 130.9, 129.1, 129.0, 127.2, 126.8, 125.0, 123.8, 117.3, 114.5, 106.4, 61.2, 28.9, 15.6, 14.2; IR (neat, cm^{-1}): 3048, 2924, 1715, 1631, 1610, 1564, 1537, 1519, 1470, 1433, 1271, 1202; HRMS (ESI/Q-TOF) (m/z): calcd. for $C_{22}H_{20}NO_4$, $[M + H]^+$: 362.1387, found: 362.1388.

Ethyl 3-(4-(tert-butyl)phenyl)-4-oxo-1,4-dihydrochromeno[2,3-b]pyrrole-2-carboxylate (5a):

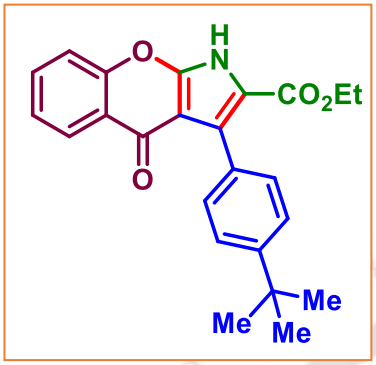

As off-white solid (121 mg, 62% yield), mp 243–245 °C; purified over a column of silica gel (25% EtOAc in hexane); ^{1}H NMR ($CDCl_3$, 400 MHz): δ 9.86 (s, 1H), 8.30 (dd, 1H, J_1 = 7.6 Hz, J_2 = 2.0 Hz), 7.66–7.62 (m, 1H), 7.54 (d, 2H, J = 8.4 Hz), 7.42 (d, 3H, J = 8.4 Hz), 7.39–7.37 (m, 1H), 4.24 (q, 2H, J = 7.2 Hz), 1.35 (s, 9H), 1.18 (t, 3H, J = 7.2 Hz); ^{13}C{^{1}H} NMR ($CDCl_3$, 125 MHz): δ 173.8, 161.5, 154.1, 150.9, 150.5, 133.3, 130.7, 129.1, 128.7, 127.2, 125.0, 124.2, 123.8, 117.3, 114.5, 106.4, 61.3, 34.8, 31.6, 14.1; IR (neat, cm^{-1}): 3207, 2959, 2866, 1651, 1609, 1562, 1530, 1458, 1429, 1280, 1200; HRMS (ESI/Q-TOF) (m/z): calcd. for $C_{24}H_{23}NO_4K$, $[M + K]^+$: 428.1259, found: 428.1278.

Ethyl 3-(3-methoxyphenyl)-4-oxo-1,4-dihydrochromeno[2,3-b]pyrrole-2-carboxylate (6a):

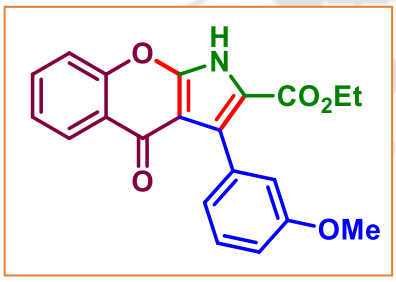

As off-white solid (142 mg, 78% yield), mp 237–239 °C; purified over a column of silica gel (25% EtOAc in hexane); ^{1}H NMR ($CDCl_3$, 500 MHz): δ 9.94 (s, 1H), 8.31 (dd, 1H, J_1 = 8.0 Hz, J_2 = 2.0 Hz), 7.66–7.63 (m, 1H), 7.42 (d, 1H, J = 8.0 Hz), 7.41–7.37 (m, 1H), 7.29 (t, 1H, J = 8.0 Hz), 7.14 (d, 1H, J = 7.5 Hz), 7.12 (t, 1H, J = 1.5 Hz), 6.90–6.88 (m, 1H), 4.22 (q, 2H, J = 7.5 Hz), 3.81 (s, 3H), 1.16 (t, 3H, J = 7.0 Hz); ^{13}C{^{1}H} NMR ($CDCl_3$, 125 MHz): δ 173.7, 161.4, 158.7, 154.2, 150.5, 133.4, 133.2, 128.4, 128.2, 127.2, 125.0, 123.8, 123.5, 117.3, 116.8, 114.8, 113.6, 106.5, 61.3, 55.4, 14.1; IR (neat, cm^{-1}): 3202, 2926, 1709, 1659, 1589, 1539, 1445, 1432, 1261, 1172; HRMS (ESI/Q-TOF) (m/z): calcd. for $C_{21}H_{18}NO_5$, $[M + H]^+$: 364.1179, found: 364.1186.

Ethyl 3-(4-butoxyphenyl)-4-oxo-1,4-dihydrochromeno[2,3-b]pyrrole-2-carboxylate (7a):

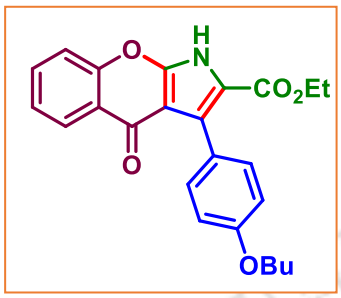

As off-white solid (157 mg, 77% yield), mp 243–245 °C; purified over a column of silica gel (25% EtOAc in hexane); ^{1}H NMR ($CDCl_3$, 400 MHz): δ 9.75 (s, 1H), 8.30 (dd, 1H, J_1 = 8.0 Hz, J_2 = 1.6 Hz), 7.66–7.62 (m, 1H), 7.52 (d, 2H, J = 8.8 Hz), 7.43–7.37 (m, 2H), 6.92 (d, 2H, J = 8.8 Hz), 4.25 (q, 2H, J = 7.2 Hz), 3.99 (t, 2H, J = 6.8 Hz), 1.81–1.74 (m, 2H), 1.56–1.45 (m, 2H), 1.21(t, 3H, J = 7.2 Hz), 0.98 (t, 3H, J = 7.2 Hz); ^{13}C{^{1}H} NMR ($CDCl_3$, 125 MHz): δ 173.9, 161.5, 159.3, 154.1, 150.5, 133.3, 132.4, 129.0, 127.2, 125.0, 123.8, 123.6, 117.3, 114.3, 113.3, 106.3, 67.8, 61.2, 31.6, 19.5, 14.3, 14.1; IR (neat, cm^{-1}): 3068, 2957, 2870, 1711, 1630, 1607, 1569, 1542, 1523, 1458, 1434, 1275, 1240; HRMS (ESI/Q-TOF) (m/z): calcd. for $C_{24}H_{23}NO_5K$, $[M + K]^+$: 444.1208, found: 444.1226.

Ethyl 3-(2-fluorophenyl)-4-oxo-1,4-dihydrochromeno[2,3-b]pyrrole-2-carboxylate (8a):

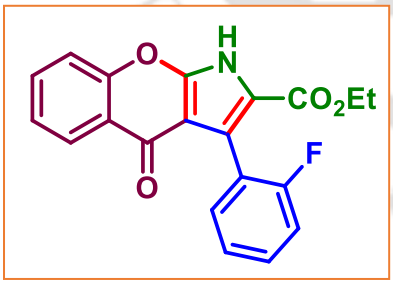

As off-white solid (121 mg, 69% yield), mp 249–251 °C; purified over a column of silica gel (25% EtOAc in hexane); ^{1}H NMR ($CDCl_3$, 400 MHz): δ 9.92 (s, 1H), 8.30 (d, 1H, J = 8.0 Hz), 7.66 (t, 1H, J = 8.0 Hz), 7.52–7.49 (m, 1H), 7.45 (d, 1H, J = 8.4 Hz), 7.40 (t, 1H, J = 7.2 Hz), 7.34 (d, 1H, J = 6.0 Hz), 7.18 (t, 1H, J = 7.6 Hz), 7.11 (t, 1H, J = 8.8 Hz), 4.22 (s, 2H), 1.14 (t, 3H, J = 7.2 Hz); ^{13}C{^{1}H} NMR ($CDCl_3$, 125 MHz): δ 173.8, 161.2, 154.3, 150.5, 133.5, 132.8, 130.1 (d, J_{C-F} = 8.5 Hz), 127.2, 125.1, 123.7, 123.2 (d, J = 2.9 Hz), 120.7, 120.5 (d, J = 15.6 Hz), 117.4, 115.9, 115.2, 115.1, 106.8, 61.4, 14.0; ^{19}F NMR ($CDCl_3$, 470 MHz): δ –113.6; IR (neat, cm^{-1}): 3190, 2957, 1712, 1630, 1607, 1568, 1541, 1458, 1433, 1276, 1240; HRMS (ESI/Q-TOF) (m/z): calcd. for $C_{20}H_{15}FNO_4$, $[M + H]^+$: 352.0980, found: 352.0995.

Ethyl 3-(2-chlorophenyl)-4-oxo-1,4-dihydrochromeno[2,3-b]pyrrole-2-carboxylate (9a):

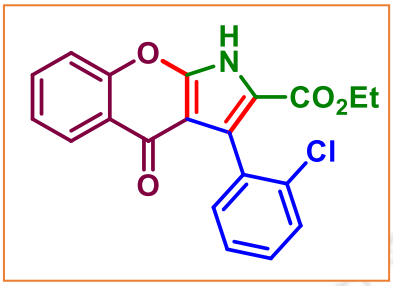

As off-white solid (121 mg, 66% yield), mp 212–214 °C; purified over a column of silica gel (25% EtOAc in hexane); ^{1}H NMR ($CDCl_3$, 400 MHz): δ 10.08 (s, 1H), 8.29 (dd, 1H, J_1 = 8.0 Hz, J_2 = 1.6 Hz), 7.68–7.64 (m, 1H), 7.47–7.38 (m, 4H), 7.28–7.26 (m, 2H), 4.20–4.14 (m, 2H), 1.07 (t, 3H, J = 7.2 Hz); ^{13}C{^{1}H} NMR ($CDCl_3$, 100 MHz): δ 173.7, 161.3, 154.4, 150.4, 134.2, 133.5, 132.3, 131.9, 129.3, 129.1, 127.2, 126.1, 125.1, 124.4, 123.7, 117.5, 115.9, 107.1, 61.3, 13.9; IR (neat, cm^{-1}): 3063, 2981, 1708, 1632, 1567, 1519, 1457, 1432, 1278; HRMS (ESI/Q-TOF) (m/z): calcd. for $C_{20}H_{15}ClNO_4$, $[M + H]^+$: 368.0684, found: 368.0684.

Ethyl 3-(2-bromophenyl)-4-oxo-1,4-dihydrochromeno[2,3-b]pyrrole-2-carboxylate (10a):

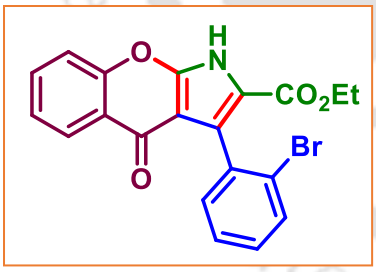

As off-white solid (138 mg, 67% yield), mp 235–237 °C; purified over a column of silica gel (25% EtOAc in hexane); ^{1}H NMR ($CDCl_3$, 400 MHz): δ 10.18 (s, 1H), 8.29 (dd, 1H, J_1 = 7.6 Hz, J_2 = 1.6 Hz), 7.68–7.64 (m, 1H), 7.61 (dd, 1H, J_1 = 8.0 Hz, J_2 = 1.2 Hz), 7.46–7.44 (m, 1H), 7.42–7.38 (m, 2H), 7.34–7.30 (m, 1H), 7.21–7.16 (m, 1H), 4.22–4.13 (m, 2H), 1.05 (t, 3H, J = 7.2 Hz); ^{13}C{^{1}H} NMR ($CDCl_3$, 100 MHz): δ 173.7, 161.3, 154.4, 150.4, 134.5, 133.5, 132.3, 131.7, 129.4, 127.2, 126.7, 126.2, 125.0, 124.4, 123.7, 117.5, 115.9, 106.9, 61.3, 13.9; IR (neat, cm^{-1}): 3063, 2981, 1708, 1632, 1567, 1519, 1457, 1432, 1278, 1198; HRMS (ESI/Q-TOF) (m/z): calcd. for $C_{20}H_{14}BrNO_4K$, $[M + K]^+$: 449.9738, found: 449.9743.

Ethyl 3-(3-bromophenyl)-4-oxo-1,4-dihydrochromeno[2,3-b]pyrrole-2-carboxylate (11a):

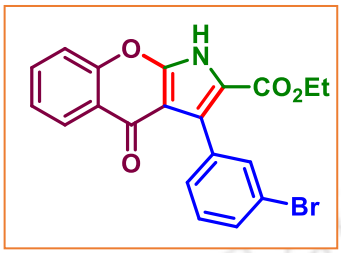

As off-white solid (142 mg, 69% yield), mp 228–230 °C; purified over a column of silica gel (25% EtOAc in hexane); ^{1}H NMR ($CDCl_3$, 400 MHz): δ 10.19 (s, 1H), 8.34 (dd, 1H, J_1 = 8.0 Hz, J_2 = 2.0 Hz), 7.75 (t, 1H, J = 1.6 Hz), 7.71–7.67 (m, 1H), 7.57–7.55 (m, 1H), 7.50–7.41 (m, 3H), 7.30–7.28 (m, 1H), 4.26 (q, 2H, J = 7.2 Hz), 1.22 (t, 3H, J = 7.2 Hz); ^{13}C{^{1}H} NMR ($CDCl_3$, 100 MHz): δ 173.9, 161.3, 154.2, 150.6, 134.0, 133.9, 133.5, 130.9, 129.8, 128.8, 127.2, 126.5, 125.1, 123.6, 121.1, 117.4, 115.1, 106.2, 61.5, 14.1; IR (neat, cm^{-1}): 3060, 2982, 1709, 1631, 1610, 1569, 1520, 1458, 1430, 1276, 1199; HRMS (ESI/Q-TOF) (m/z): calcd. for $C_{20}H_{15}BrNO_4$, $[M + H]^+$: 412.0179, found: 412.0180.

Ethyl 3-(4-fluorophenyl)-4-oxo-1,4-dihydrochromeno[2,3-b]pyrrole-2-carboxylate (12a):

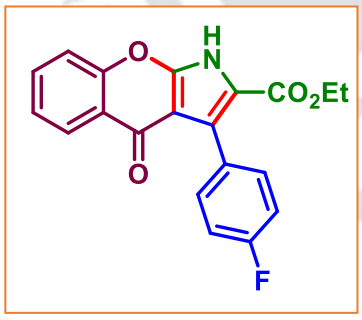

As off-white solid (128 mg, 73% yield), mp 191–193 °C; purified over a column of silica gel (25% EtOAc in hexane); ^{1}H NMR ($CDCl_3$, 400 MHz): δ 9.69 (s, 1H), 8.29 (dd, 1H, J_1 = 8.0 Hz, J_2 = 2.0 Hz), 7.68–7.64 (m, 1H), 7.57–7.54 (m, 2H), 7.44 (dd, 1H, J_1 = 8.8 Hz, J_2 = 1.2 Hz), 7.43–7.39 (m, 1H), 7.09 (t, 2H, J = 8.8 Hz), 4.25 (q, 2H, J = 7.2 Hz), 1.20 (t, 3H, J = 6.8 Hz); ^{13}C{^{1}H} NMR ($CDCl_3$, 125 MHz): δ 173.9, 162.9 (d, $J_{C–F}$ = 245.25 Hz), 161.2, 154.2, 150.4, 133.5, 132.8 (d, $J_{C–F}$ = 8.1 Hz), 127.7 (d, $J_{C–F}$ = 4.5 Hz), 127.2, 125.2, 123.7, 117.3, 114.6, 114.4, 114.2, 106.4, 61.4, 14.2; ^{19}F NMR ($CDCl_3$, 470 MHz): δ –114.2; IR (neat, cm^{-1}): 3291, 2985, 1722, 1698, 1609, 1590, 1567, 1372, 1273; HRMS (ESI/Q-TOF) (m/z): calcd. for $C_{20}H_{15}FNO_4$, $[M + H]^+$: 352.0980, found: 352.0999.

Ethyl-3-(2,4-difluorophenyl)-4-oxo-1,4-dihydrochromeno[2,3-b]pyrrole-2-carboxylate (13a):

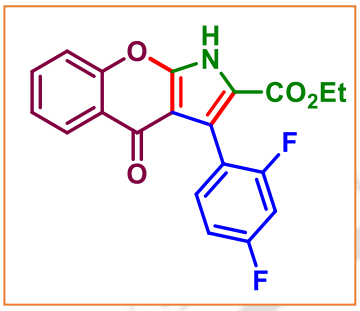

As off-white solid (124 mg, 67% yield), mp 255–257 °C; purified over a column of silica gel (25% EtOAc in hexane); ^{1}H NMR ($CDCl_3$, 400 MHz): δ 10.08 (s, 1H), 8.29 (dd, 1H, J_1 = 8.0 Hz, J_2 = 1.6 Hz), 7.68–7.64 (m, 1H), 7.53–7.48 (m, 1H), 7.45–7.39 (m, 2H), 6.95–6.85 (m, 2H), 4.28–4.21 (m, 2H), 1.17 (t, 3H, J = 7.2 Hz); ^{13}C{^{1}H} NMR ($CDCl_3$, 125 MHz): δ 173.8, 163.2 (dd, J_1 = 247.87 Hz, J_2 = 11.87 Hz), 161.1, 160.7 (dd, J_1 = 236.63 Hz, J_2 = 12.25 Hz), 154.3, 150.5, 133.7–133.6 (m), 133.6, 127.1, 125.2, 123.6, 119.8, 117.4, 116.0, 110.6 (d, J = 3.63 Hz), 110.5 (d, J = 3.37 Hz), 106.8, 103.7 (d, J = 25.5 Hz), 61.5, 14.1; ^{19}F NMR ($CDCl_3$, 376 MHz): δ –108.8 (d, $J_{F–F}$ = 8.1 Hz), –110.2 (d, $J_{F–F}$ = 7.8 Hz); IR (neat, cm^{-1}): 3227, 2921, 1721, 1650, 1607, 1567, 1531, 1460, 1425, 1263; HRMS (ESI/Q-TOF) (m/z): calcd. for $C_{20}H_{13}F_2NO_4K$, $[M + K]^+$: 408.0444, found: 408.0445.

Ethyl-3-(2,6-dichlorophenyl)-4-oxo-1,4-dihydrochromeno[2,3-b]pyrrole-2-carboxylate (14a):

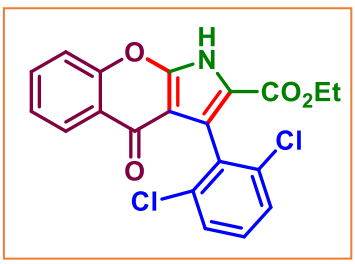

As off-white solid (123 mg, 61% yield), mp 260–262 °C; purified over a column of silica gel (25% EtOAc in hexane); ^{1}H NMR ($CDCl_3$, 400 MHz): δ 9.78 (s, 1H), 8.28 (dd, 1H, J_1 = 8.0 Hz, J_2 = 1.6 Hz), 7.69–7.65 (m, 1H), 7.49 (dd, 1H, J_1 = 8.8 Hz, J_2 = 1.2 Hz), 7.43–7.41 (m, 1H), 7.40–7.38 (m, 2H), 7.25–7.23 (m, 1H), 4.18 (q, 2H, J = 7.2 Hz), 1.06 (t, 3H, J = 7.2 Hz); ^{13}C{^{1}H} NMR ($CDCl_3$, 100 MHz): δ 173.5, 160.9, 154.5, 150.4, 135.6, 133.5, 129.6, 127.6, 127.1, 125.2, 123.6, 121.3, 117.6, 116.1, 111.9, 106.9, 61.4, 13.9; IR (neat, cm^{-1}): 3196, 2921, 1656, 1612, 1559, 1531, 1446, 1432, 1418, 1283; HRMS (ESI/Q-TOF) (m/z):

calcd. for $C_{20}H_{14}Cl_2NO_4$, $[M + H]^+$: 402.0294, found: 402.0295.

Ethyl 3-(2-bromo-6-fluorophenyl)-4-oxo-1,4-dihydrochromeno[2,3-b]pyrrole-2-carboxylate (15a):

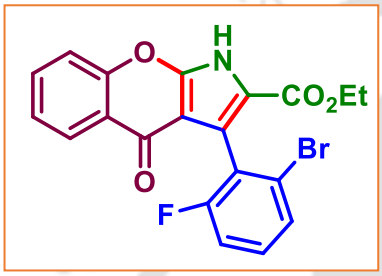

As off-white solid (127 mg, 59% yield), mp 258–260 °C, mp 271–273 °C; purified over a column of silica gel (25% EtOAc in hexane); ^{1}H NMR ($CDCl_3$, 400 MHz): δ 9.93 (s, 1H), 8.29 (dd, 1H, J_1 = 8.0 Hz, J_2 = 1.6 Hz), 7.70–7.65 (m, 1H), 7.57 (dd, 1H, J_1 = 8.8 Hz, J_2 = 5.2 Hz), 7.47 (dd, 1H, J_1 = 8.8 Hz, J_2 = 1.2 Hz), 7.43–7.39 (m, 1H), 7.15 (dd, 1H, J_1 = 8.8 Hz, J_2 = 3.2 Hz), 6.98–6.93 (m, 1H), 4.22–4.16 (m, 2H), 1.09 (t, 3H, J = 6.8 Hz); ^{13}C{^{1}H} NMR ($CDCl_3$, 125 MHz): δ 173.5, 161.5 (d, J_{C-F} = 244.9 Hz), 161.0, 154.5, 150.2, 136.4 (d, J_{C-F} = 8.7 Hz), 133.6, 133.2 (d, J_{C-F} = 8.2 Hz), 127.2, 125.2, 123.6, 119.0 (d, J_{C-F} = 23.2 Hz), 118.9 (d, J_{C-F} = 3.5 Hz), 117.5, 116.7, 116.5, 115.9, 106.8, 61.5, 14.0; ^{19}F NMR ($CDCl_3$, 470 MHz): δ –116.2; IR (neat, cm^{-1}): 3293, 3192, 2984, 1722, 1698, 1649, 1590, 1516, 1456, 1379, 1276; HRMS (ESI/Q-TOF) (m/z): calcd. for $C_{20}H_{13}BrFNO_4Na$, $[M + Na]^+$: 451.9904, found: 451.9916.

Ethyl 3-(3,5-dimethoxyphenyl)-4-oxo-1,4-dihydrochromeno[2,3-b]pyrrole-2-carboxylate (16a):

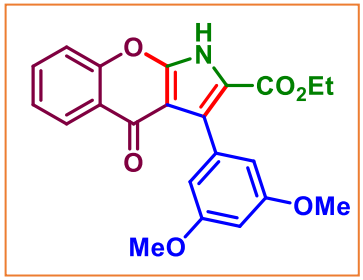

As off-white solid (122 mg, 62% yield), mp 230–232 °C; purified over a column of silica gel (25% EtOAc in hexane); ^{1}H NMR ($CDCl_3$, 500 MHz): δ 10.11 (s, 1H), 8.26 (dd, 1H, J_1 = 8.0 Hz, J_2 = 2.0 Hz), 7.61–7.57 (m, 1H), 7.37–7.33 (m, 2H), 6.96 (d, 1H, J = 2.5 Hz), 6.88–6.84 (m, 2H), 4.19–4.12 (m, 2H), 3.75 (s, 3H), 3.73 (s, 3H), 1.09 (t, 3H, J = 7.0 Hz); ^{13}C{^{1}H} NMR ($CDCl_3$, 125 MHz): δ 173.5, 161.5, 154.2, 153.0, 152.0, 150.5, 133.1, 127.1, 124.8, 123.8, 123.7, 122.9, 118.0, 117.3, 115.7, 114.2, 111.7, 107.1, 61.0, 56.5,

55.9, 14.1; IR (neat, cm^{-1}): 3076, 2984, 1714, 1697, 1610, 1547, 1491, 1456, 1270; HRMS (ESI/Q-TOF) (m/z): calcd. for $C_{22}H_{20}NO_6$, $[M + H]^+$: 394.1285, found: 394.1287.

Ethyl 3-mesityl-4-oxo-1,4-dihydrochromeno[2,3-b]pyrrole-2-carboxylate (17a):

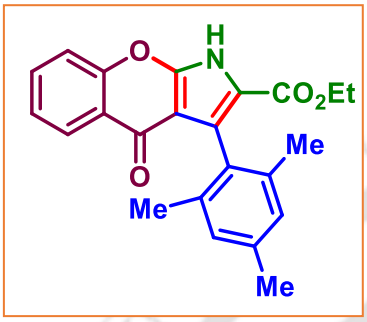

As off-white solid (112 mg, 60% yield), mp 238–240 °C; purified over a column of silica gel (25% EtOAc in hexane); ^1H NMR ($CDCl_3$, 400 MHz): δ 10.00 (s, 1H), 8.27 (dd, 1H, J_1 = 8.0 Hz, J_2 = 1.6 Hz), 7.68–7.63 (m, 1H), 7.45 (dd, 1H, J_1 = 8.4 Hz, J_2 = 1.2 Hz), 7.41–7.37 (m, 1H), 6.87 (s, 2H), 4.15 (q, 2H, J = 7.2 Hz), 2.24 (s, 3H), 2.05 (s, 6H), 1.04 (t, 3H, J = 7.2 Hz); $^{13}C\{^1H\}$ NMR ($CDCl_3$, 100 MHz): δ 173.7, 161.5, 154.4, 150.9, 136.9, 136.1, 133.3, 129.6, 127.9, 127.2, 127.0, 125.0, 123.7, 117.4, 115.0, 106.9, 61.0, 21.4, 20.7, 14.0; IR (neat, cm^{-1}): 3228, 2916, 1720, 1650, 1556, 1531, 1461, 1426, 1262, 1205; HRMS (ESI/Q-TOF) (m/z): calcd. for $C_{23}H_{22}NO_4$, $[M + H]^+$: 376.1543, found: 376.1549.

Ethyl 3-(3-nitrophenyl)-4-oxo-1,4-dihydrochromeno[2,3-b]pyrrole-2-carboxylate (18a):

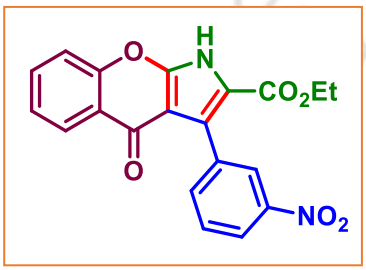

As off-white solid (104 mg, 55% yield), mp 265–267 °C; purified over a column of silica gel (25% EtOAc in hexane); ^1H NMR ($CDCl_3$, 400 MHz): δ 9.79 (s, 1H), 8.48 (s, 1H), 8.29 (dd, 1H, J_1 = 8.0 Hz, J_2 = 1.6 Hz), 8.25 (dd, 1H, J_1 = 8.4 Hz, J_2 = 2.4 Hz), 7.96 (d, 1H, J = 7.6 Hz), 7.72–7.67 (m, 1H), 7.58 (t, 1H, J = 8.0 Hz), 7.48 (d, 1H, J = 8.4 Hz), 7.43 (t, 1H, J = 7.6 Hz), 4.25 (q, 2H, J = 7.2 Hz), 1.16 (t, 3H, J = 6.8 Hz); $^{13}C\{^1H\}$ NMR ($CDCl_3$, 125 MHz): δ 173.8, 160.8, 154.2, 150.4, 147.5, 137.5, 133.8, 133.5, 128.2, 127.2, 126.5, 125.6, 125.4, 123.5, 123.1, 117.5, 115.2, 106.2, 61.8, 14.1; IR (neat, cm^{-1}): 3228, 2920, 1730, 1666, 1610, 1569, 1524, 1443, 1420, 1283, 1210; HRMS (ESI/Q-

TOF) (m/z): calcd. for $C_{20}H_{15}N_2O_6$, $[M + H]^+$: 379.0925, found: 379.0927.

Ethyl 3-(4-(methylthio)phenyl)-4-oxo-1,4-dihydrochromeno[2,3-b]pyrrole-2-carboxylate (19a):

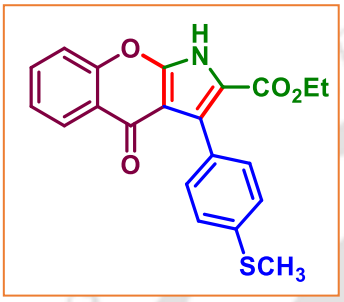

As off-white solid (112 mg, 59% yield), mp 255–257 °C; purified over a column of silica gel (25% EtOAc in hexane); ^{1}H NMR ($CDCl_3$, 400 MHz): δ 10.08 (s, 1H), 8.31 (dd, 1H, J_1 = 8.0 Hz, J_2 = 1.6 Hz), 7.66–7.62 (m, 1H), 7.52 (d, 2H, J = 8.4 Hz), 7.42–7.39 (m, 2H), 7.25 (d, 2H, J = 8.4 Hz), 4.23 (q, 2H, J = 7.2 Hz), 2.46 (s, 3H), 1.19 (t, 3H, J = 7.2 Hz); ^{13}C{^{1}H} NMR ($CDCl_3$, 125 MHz): δ 173.9, 161.3, 154.1, 150.6, 138.5, 133.4, 131.5, 128.5, 128.3, 127.2, 125.2, 125.0, 123.7, 117.3, 114.6, 106.3, 61.3, 15.8, 14.2; IR (neat, cm^{-1}): 3204, 2984, 1649, 1611, 1556, 1528, 1459, 1424, 1280, 1209; HRMS (ESI/Q-TOF) (m/z): calcd. for $C_{21}H_{18}NO_4S$, $[M + H]^+$: 380.0951, found: 380.0959.

Ethyl 3-(naphthalen-1-yl)-4-oxo-1,4-dihydrochromeno[2,3-b]pyrrole-2-carboxylate (20a):

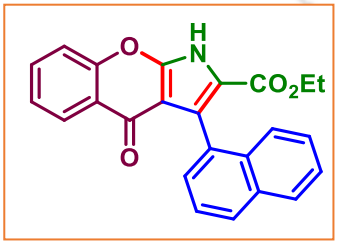

As off-white solid (113 mg, 59% yield), mp 266–268 °C; purified over a column of silica gel (25% EtOAc in hexane); ^{1}H NMR ($CDCl_3$, 400 MHz): δ 9.98 (s, 1H), 8.23 (dd, 1H, J_1 = 8.0 Hz, J_2 = 1.6 Hz), 7.85 (t, 2H, J = 7.6 Hz), 7.68–7.63 (m, 2H), 7.56 (dd, 1H, J_1 = 6.8 Hz, J_2 = 1.6 Hz), 7.53–7.49 (m, 1H), 7.44 (d, 1H, J = 8.4 Hz), 7.42–7.36 (m, 2H), 7.34–7.30 (m, 1H), 3.95 (q, 2H, J = 7.2 Hz), 0.69 (t, 3H, J = 7.2 Hz); ^{13}C{^{1}H} NMR ($CDCl_3$, 125 MHz): δ 173.6, 161.4, 154.3, 150.6, 133.5, 133.4, 132.8, 130.8, 128.4, 128.3, 128.1, 127.3, 126.0, 125.9, 125.8, 125.6, 125.0, 123.8, 117.4, 116.4, 107.8, 61.0, 13.5; IR (neat, cm^{-1}): 3043, 2917, 1716, 1634, 1607, 1566, 1532, 1457, 1431, 1274;

HRMS (ESI/Q-TOF) (m/z): calcd. for $C_{24}H_{18}NO_4$, $[M + H]^+$: 384.1230, found: 384.1214.

Ethyl 3-(anthracen-9-yl)-4-oxo-1,4-dihydrochromeno[2,3-b]pyrrole-2-carboxylate (21a):

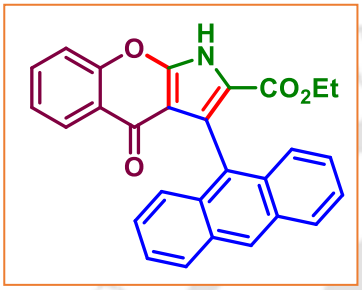

As off-white solid (115 mg, 53% yield), mp 266–268 °C; purified over a column of silica gel (25% EtOAc in hexane); ^{1}H NMR (DMSO-d_6, 400 MHz): δ 13.70 (s, 1H), 8.64 (s, 1H), 8.13 (d, 2H, J = 8.8 Hz), 7.89 (dd, 1H, J_1 = 8.0 Hz, J_2 = 2.0 Hz), 7.82–7.78 (m, 1H), 7.73 (d, 1H, J = 8.4 Hz), 7.66 (d, 2H, J = 8.8 Hz), 7.49–7.46 (m, 2H), 7.45–7.41 (m, 1H), 7.35–7.31 (m, 2H), 3.69 (q, 2H, J = 7.2 Hz), 0.37 (t, 3H, J = 7.2 Hz); ^{13}C{^{1}H} NMR (DMSO-d_6, 125 MHz): δ 172.1, 160.0, 154.0, 151.3, 133.7, 130.9, 130.3, 129.1, 128.2, 126.3, 126.1, 125.7, 125.3, 125.0, 124.8, 122.8, 122.1, 117.8, 117.3, 107.6, 59.6, 13.0; IR (neat, cm^{-1}): 3377, 2918, 1693, 1650, 1612, 1531, 1441, 1285, 1188; HRMS (ESI/Q-TOF) (m/z): calcd. for $C_{28}H_{20}NO_4$, $[M + H]^+$: 434.1387, found: 434.1387.

Ethyl 3-([1,1'-biphenyl]-4-yl)-4-oxo-1,4-dihydrochromeno[2,3-b]pyrrole-2-carboxylate (22a):

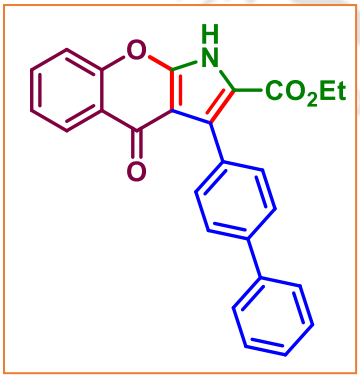

As off-white solid (112 mg, 55% yield), mp 220–222 °C; purified over a column of silica gel (25% EtOAc in hexane); ^{1}H NMR ($CDCl_3$, 500 MHz): δ 12.09 (s, 1H), 8.33–8.27 (m, 1H), 7.68–7.63 (m, 7H), 7.51–7.42 (m, 3H), 7.40–7.34 (m, 2H), 4.26–4.21 (m, 2H), 1.21–1.15 (m, 3H); ^{13}C{^{1}H} NMR ($CDCl_3$, 125 MHz): δ 173.7, 161.3, 154.0, 151.0, 141.1, 140.1, 133.0, 131.4, 131.7, 128.7, 127.5, 127.1, 127.0, 126.7, 125.6, 124.5, 123.5, 117.2, 115.2, 105.9, 60.7, 14.0; IR (neat, cm^{-1}): 3026, 2986, 1695, 1626, 1604, 1556, 1538, 1514, 1454, 1430, 1279; HRMS (ESI/Q-TOF) (m/z): calcd. for $C_{26}H_{20}NO_4$, $[M + H]^+$: 410.1387, found: 410.1392.

Ethyl 3-(furan-2-yl)-4-oxo-1,4-dihydrochromeno[2,3-b]pyrrole-2-carboxylate (23a):

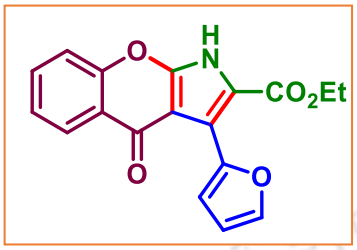

As off-white solid (98 mg, 61% yield), mp 247–249 °C; purified over a column of silica gel (25% EtOAc in hexane); ^{1}H NMR ($CDCl_3$, 400 MHz): δ 9.57 (s, 1H), 8.34 (dd, 1H, J_1 = 8.0 Hz, J_2 = 1.6 Hz), 7.68–7.64 (m, 1H), 7.58 (d, 1H, J = 2.0 Hz), 7.45–7.40 (m, 2H), 7.10 (d, 1H, J = 3.6 Hz), 6.56–6.55 (m, 1H), 4.35 (q, 2H, J = 7.2 Hz), 1.33 (t, 3H, J = 7.2 Hz); ^{13}C{^{1}H} NMR ($CDCl_3$, 125 MHz): δ 173.3, 160.9, 154.0, 150.3, 145.1, 142.7, 135.5, 127.3, 125.2, 123.8, 117.3, 116.9, 115.0, 113.5, 111.4, 106.5, 61.6, 14.4; IR (neat, cm^{-1}): 3179, 2976, 1681, 1651, 1607, 1560, 1529, 1454, 1416, 1278; HRMS (ESI/Q-TOF) (m/z): calcd. for $C_{18}H_{14}NO_5$, $[M + H]^+$: 324.0866, found: 324.0867.

Ethyl 3-(5-bromofuran-2-yl)-4-oxo-1,4-dihydrochromeno[2,3-b]pyrrole-2-carboxylate (24a):

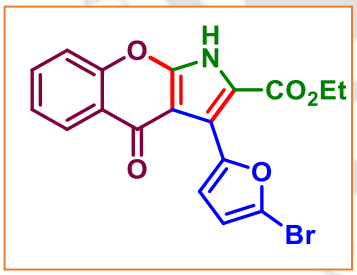

As off-white solid (115 mg, 55% yield), mp 214–216 °C; purified over a column of silica gel (25% EtOAc in hexane); ^{1}H NMR ($CDCl_3$, 400 MHz): δ 9.95 (s, 1H), 8.33 (dd, 1H, J_1 = 8.0 Hz, J_2 = 1.6 Hz), 7.68–7.64 (m, 1H), 7.43 (d, 2H, J = 8.0 Hz), 7.15 (d, 1H, J = 3.6 Hz), 6.46 (d, 1H, J = 3.6 Hz), 4.38 (q, 2H, J = 7.2 Hz), 1.38 (t, 3H, J = 7.2 Hz); ^{13}C{^{1}H} NMR ($CDCl_3$, 125 MHz): δ 173.4, 161.2, 154.0, 150.4, 147.2, 135.6, 127.3, 125.2, 123.7, 121.9, 117.3, 116.1, 115.5, 115.3, 113.2, 105.5, 62.0, 14.4; IR (neat, cm^{-1}): 3187, 2973, 1649, 1610, 1563, 1525, 1454, 1415, 1279, 1206; HRMS (ESI/Q-TOF) (m/z): calcd. for $C_{18}H_{13}BrNO_5$, $[M + H]^+$: 401.9972, found: 401.9972.

Ethyl 4-oxo-3-(thiophen-2-yl)-1,4-dihydrochromeno[2,3-b]pyrrole-2-carboxylate (25a):

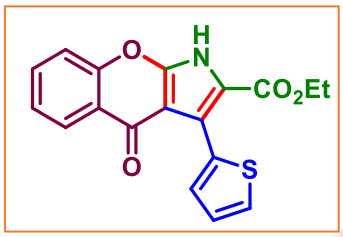

As off-white solid (97mg, 57% yield), mp 254–256 °C; purified over a column of silica gel (25% EtOAc in hexane); ^{1}H NMR ($CDCl_3$, 400 MHz): δ 9.61 (s, 1H), 8.31 (d, 1H, J = 8.0 Hz), 7.66 (t, 1H, J = 7.6 Hz), 7.45–7.39 (m, 4H), 7.10 (t, 1H, J = 4.4 Hz), 4.30 (q, 2H, J = 7.2 Hz), 1.27 (t, 3H, J = 7.2 Hz); ^{13}C{^{1}H} NMR ($CDCl_3$, 125 MHz): δ 173.5, 160.9, 154.0, 150.3, 133.5, 130.7, 127.3, 127.0, 126.3, 125.2, 123.8, 120.9, 117.3, 115.4, 106.7, 61.5, 14.3; IR (neat, cm^{-1}): 3182, 2978, 1679, 1649, 1607, 1550, 1520, 1436, 1408, 1272; HRMS (ESI/Q-TOF) (m/z): calcd. for $C_{18}H_{14}NO_4S$, $[M + H]^+$: 340.0638, found: 340.0641.

Ethyl 6-methyl-4-oxo-3-phenyl-1,4-dihydrochromeno[2,3-b]pyrrole-2-carboxylate (26a):

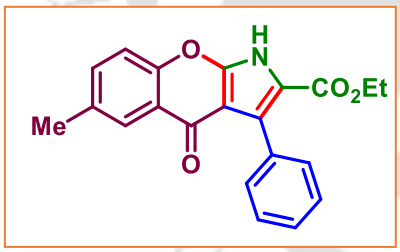

As off-white solid (130 mg, 75% yield), mp 247–249 °C; purified over a column of silica gel (25% EtOAc in hexane); ^{1}H NMR ($CDCl_3$, 400 MHz): δ 9.75 (s, 1H), 8.07 (d, 1H, J = 2.4 Hz), 7.58–7.56 (m, 2H), 7.45 (dd, 1H, J_1 = 8.4 Hz, J_2 = 2.4 Hz), 7.41–7.36 (m, 3H), 7.32 (d, 1H, J = 8.4 Hz), 4.22 (q, 2H, J = 7.2 Hz), 2.44 (s, 3H), 1.16 (t, 3H, J = 7.2 Hz); ^{13}C{^{1}H} NMR ($CDCl_3$, 125 MHz): δ 174.0, 161.4, 152.3, 150.6, 134.8, 134.4, 131.9, 131.0, 128.8, 128.1, 127.3, 126.7, 123.4, 117.0, 114.5, 106.4, 61.3, 21.1, 14.1; IR (neat, cm^{-1}): 2980, 2926, 1719, 1637, 1612, 1570, 1519, 1474, 1434, 1273; HRMS (ESI/Q-TOF) (m/z): calcd. for $C_{21}H_{18}NO_4$, $[M + H]^+$: 348.1230, found: 348.1230.

Methyl 6-methyl-4-oxo-3-phenyl-1,4-dihydrochromeno[2,3-b]pyrrole-2-carboxylate (26b):

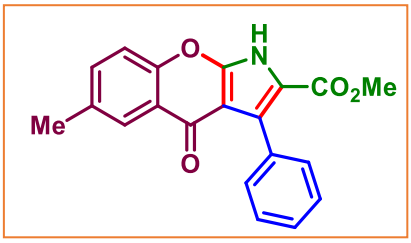

As off-white solid (118 mg, 71% yield), mp 263–265 °C; purified over a column of silica gel (25% EtOAc in hexane); ^{1}H NMR ($CDCl_3$, 400 MHz): δ 9.51 (s, 1H), 8.06 (d, 1H, J = 2.0 Hz), 7.57 (d, 2H, J = 6.4 Hz), 7.45 (dd, 1H, J_1 = 8.4 Hz, J_2 = 2.0 Hz), 7.43–7.37 (m, 3H), 7.34 (d, 1H, J = 8.4 Hz), 3.75 (s, 3H), 2.44 (s, 3H); ^{13}C{^{1}H} NMR ($CDCl_3$, 125 MHz): δ 173.9, 161.7, 152.4, 150.6, 134.9, 134.5, 131.7, 130.9, 129.0, 128.2, 127.4, 126.8, 123.4, 117.0, 114.1, 106.4, 52.1, 21.1; IR (neat, cm^{-1}): 3198, 2926, 1711, 1656, 1601, 1584, 1560, 1432, 1236; HRMS (ESI/Q-TOF) (m/z): calcd. for $C_{20}H_{16}NO_4$, $[M + H]^+$: 334.1074, found: 334.1081.

Ethyl 6-chloro-4-oxo-3-phenyl-1,4-dihydrochromeno[2,3-b]pyrrole-2-carboxylate (27a):

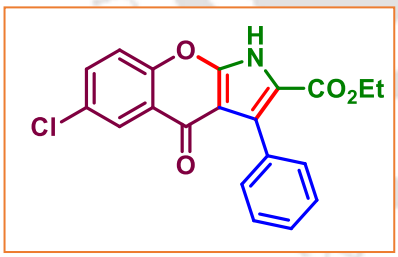

As off-white solid (125 mg, 68% yield), mp 265–267 °C; purified over a column of silica gel (25% EtOAc in hexane); ^{1}H NMR (DMSO-d_6, 400 MHz): δ 13.44 (s, 1H), 7.98 (d, 1H, J = 2.8 Hz), 7.80 (dd, 1H, J_1 = 8.8 Hz, J_2 = 2.8 Hz), 7.71 (d, 1H, J = 8.8 Hz), 7.47–7.45 (m, 2H), 7.36–7.34 (t, 3H), 4.12 (q, 2H, J = 7.2 Hz), 1.09 (t, 3H, J = 7.2 Hz); ^{13}C{^{1}H} NMR (DMSO-d_6, 125 MHz): δ 171.1, 160.2, 152.1, 150.7, 133.3, 132.0, 130.8, 129.0, 127.3, 126.7, 124.9, 124.4, 124.2, 120.0, 115.1, 104.9, 60.2, 13.8; IR (neat, cm^{-1}): 3062, 2980, 1709, 1632, 1609, 1567, 1520, 1457, 1432, 1279, 1198; HRMS (ESI/Q-TOF) (m/z): calcd. for $C_{20}H_{15}ClNO_4$, $[M + H]^+$: 368.0684, found: 368.0682.

Ethyl 6-bromo-4-oxo-3-phenyl-1,4-dihydrochromeno[2,3-b]pyrrole-2-carboxylate (28a):

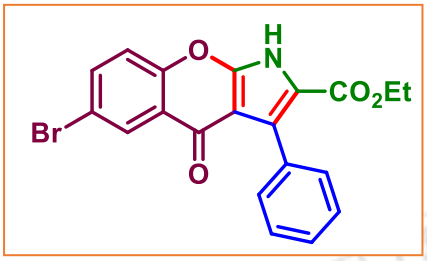

As off-white solid (132 mg, 64% yield), mp 290–292 °C; purified over a column of silica gel (25% EtOAc in hexane); ^{1}H NMR ($CDCl_3$, 500 MHz): δ 9.73 (s, 1H), 8.39 (d, 1H, J = 2.5 Hz), 7.73 (dd, 1H, J_1 = 8.5 Hz, J_2 = 2.5 Hz), 7.56–7.54 (m, 2H), 7.41–7.33 (m, 4H), 4.23 (q, 2H, J = 7.0 Hz), 1.16 (t, 3H, J = 7.0 Hz); ^{13}C{^{1}H} NMR ($CDCl_3$, 125 MHz): δ 172.3, 161.2, 152.9, 150.3, 136.3, 131.5, 130.9, 129.9, 128.7, 128.3, 127.3, 125.2, 119.2, 118.3, 115.0, 106.3, 61.4, 14.1; IR (neat, cm^{-1}): 3064, 2983, 1710, 1630, 1569, 1517, 1459, 1434, 1280, 1199; HRMS (ESI/Q-TOF) (m/z): calcd. for $C_{20}H_{15}BrNO_4$, [M + H]$^{+}$: 412.0179, found: 412.0182.

Ethyl 5-chloro-4-oxo-3-phenyl-1,4-dihydrochromeno[2,3-b]pyrrole-2-carboxylate (29a):

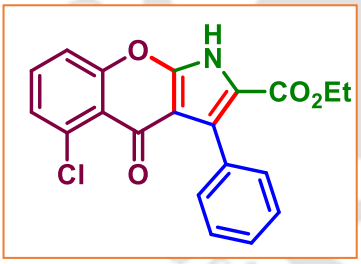

As off-white solid (101 mg, 55% yield), mp 263–265 °C; purified over a column of silica gel (25% EtOAc in hexane); ^{1}H NMR ($CDCl_3$, 500 MHz): δ 9.52 (s, 1H), 7.54–7.51 (m, 2H), 7.49 (dd, 1H, J_1 = 8.5 Hz, J_2 = 2.0 Hz), 7.39–7.37 (m, 4H), 7.26 (s, 1H), 4.22–4.18 (m, 2H), 1.15–1.12 (m, 3H); ^{13}C{^{1}H} NMR ($CDCl_3$, 125 MHz): δ 172.7, 161.3, 156.0, 149.0, 135.2, 132.3, 131.8, 130.8, 129.1, 128.8, 128.1, 127.4, 120.7, 116.8, 114.8, 106.9, 61.3, 14.1; IR (neat, cm^{-1}): 3198, 2926, 1711, 1656, 1601, 1588, 1538, 1432, 1264, 1236; HRMS (ESI/Q-TOF) (m/z): calcd. for $C_{20}H_{15}ClNO_4$, [M + H]$^{+}$: 368.0684, found: 368.0685.

Ethyl 6,8-dimethyl-4-oxo-3-phenyl-1,4-dihydrochromeno[2,3-b]pyrrole-2-carboxylate (30a):

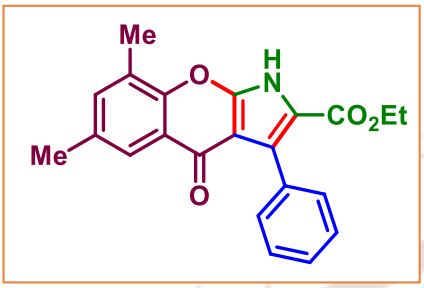

As off-white solid (106 mg, 59% yield), mp 225–227 °C; purified over a column of silica gel (25% EtOAc in hexane); ^{1}H NMR ($CDCl_3$, 400 MHz): δ 9.51 (s, 1H), 7.91 (d, 1H, J = 2.5 Hz), 7.59–7.57 (m, 2H), 7.42–7.37 (m, 3H), 7.31 (d, 1H, J = 2.0 Hz), 4.24 (q, 2H, J = 7.0 Hz), 2.48 (s, 3H), 2.39 (s, 3H), 1.18 (t, 3H, J = 7.0 Hz); ^{13}C{^{1}H} NMR ($CDCl_3$, 125 MHz): δ 174.2, 161.3, 150.9, 150.5, 135.8, 134.2, 131.9, 131.0, 128.8, 128.1, 127.3, 126.2, 124.4, 123.3, 114.4, 106.2, 61.2, 21.0, 15.8, 14.2; IR (neat, cm^{-1}): 3232, 2918, 1650, 1609, 1567, 1535, 1425, 1384, 1261; HRMS (ESI/Q-TOF) (m/z): calcd. for $C_{22}H_{20}NO_4$, $[M + H]^+$: 362.1387, found: 362.1391.

Ethyl 6,8-difluoro-4-oxo-3-phenyl-1,4-dihydrochromeno[2,3-b]pyrrole-2-carboxylate (31a):

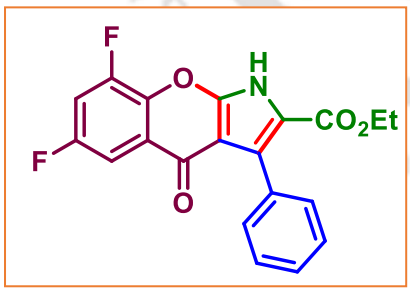

As off-white solid (107 mg, 58% yield), mp 238–240 °C; purified over a column of silica gel (25% EtOAc in hexane); ^{1}H NMR ($CDCl_3$, 400 MHz): δ 10.01 (s, 1H), 7.74–7.71 (m, 1H), 7.56–7.53 (m, 2H), 7.43–7.38 (m, 3H), 7.25–7.21 (m, 1H), 4.27 (q, 2H, J = 7.2 Hz), 1.19 (t, 3H, J = 7.2 Hz); ^{13}C{^{1}H} NMR ($CDCl_3$, 125 MHz): δ 171.6, 161.2, 157.3, 149.8, 131.4, 130.9, 128.6, 128.4, 127.4, 126.4 (d, J_{C-F} = 7.8 Hz), 115.3, 108.9 (d, J_{C-F} = 20.4 Hz), 108.7 (d, J_{C-F} = 20.5 Hz), 107.7 (d, J_{C-F} = 3.5 Hz), 107.5 (d, J_{C-F} = 3.7 Hz), 106.2, 61.6, 14.1; ^{19}F NMR ($CDCl_3$, 376 MHz): δ –(113.5–113.6) (m), –(129.3–129.4) (m); IR (neat, cm^{-1}): 3392, 3047, 1708, 1655, 1627, 1571, 1538, 1470, 1424, 1230; HRMS (ESI/Q-TOF) (m/z): calcd. for $C_{20}H_{14}F_2NO_4$, $[M + H]^+$: 370.0885, found: 370.0889.

Ethyl 6,8-dichloro-4-oxo-3-phenyl-1,4-dihydrochromeno[2,3-b]pyrrole-2-carboxylate (32a):

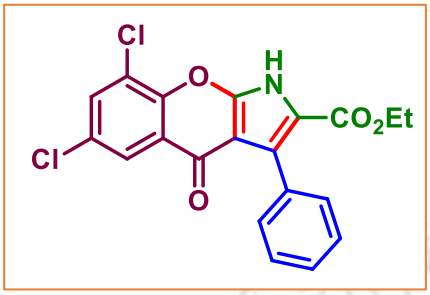

As off-white solid (110 mg, 55% yield), mp 233–235 °C; purified over a column of silica gel (25% EtOAc in hexane); ^{1}H NMR (DMSO-d_6, 400 MHz): δ 13.64 (s, 1H), 8.12 (d, 1H, J = 2.8 Hz), 7.94 (d, 1H, J = 2.8 Hz), 7.47–7.44 (m, 2H), 7.37–7.35 (m, 3H), 4.13 (q, 2H, J = 6.8 Hz), 1.11 (t, 3H, J = 7.2 Hz); ^{13}C{^{1}H} NMR (DMSO-d_6, 125 MHz): δ 170.4, 160.0, 150.3, 148.2, 132.9, 131.8, 130.9, 128.8, 127.4, 126.8, 125.3, 124.2, 122.8, 115.4, 104.8, 60.3, 13.8; IR (neat, cm^{-1}): 3060, 2981, 1709, 1631, 1610, 1569, 1520, 1457, 1433, 1277, 1197; HRMS (ESI/Q-TOF) (m/z): calcd. for $C_{20}H_{13}Cl_2NO_4Na$, [M + Na]$^{+}$: 424.0114, found: 424.0114.

4-Tosyl-1-(tosylmethyl)-1H-imidazole (1c'):

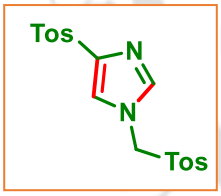

As a yellow solid (85 mg, 87% yield); mp 177–179 °C purified over a column of silica gel (80% EtOAc in hexane); ^{1}H NMR ($CDCl_3$, 500 MHz): δ 7.86 (d, 2H, J = 8.0 Hz), 7.45 (d, 2H, J = 8.0 Hz), 7.39 (s, 1H), 7.33 (d, 2H, J = 8.0 Hz), 7.29 (s, 1H), 7.23 (d, 2H, J = 8.0 Hz), 5.11 (s, 2H), 2.44 (s, 3H), 2.43 (s, 3H); ^{13}C{^{1}H} NMR (125 MHz): δ 147.0, 144.7, 143.3, 139.7, 137.6, 131.5, 130.7, 129.9, 128.8, 128.1, 124.0, 65.5, 21.9, 21.8; IR (neat, cm^{-1}): 3377, 2924, 1705, 1622, 1438, 1264, 1172; HRMS (ESI/Q-TOF) (m/z): calcd. for $C_{18}H_{18}N_2O_4S_2Na$, [M + H]$^{+}$: 413.0600, found: 413.0601.

III.6. References

[1] (a) Gupton, J. Pyrrole Natural Products with Antitumor Properties. In Lee, M. (eds) *Heterocyclic Antitumor Antibiotics*; Topics in Heterocyclic Chemistry; Springer Berlin Heidelberg: Berlin, Heidelberg, **2006**; Vol. 2, pp 53–92. (b) Hu, D. X.; Withall, D. M.; Challis, G. L.; Thomson, R. J. *Chem. Rev.* **2016**, *116*, 7818–7853. (c) Fan, H.; Peng,

J.; Hamann, M. T.; Hu, J.-F. *Chem. Rev*. **2008**, *108*, 264–287. (d) Carloni, S.; Crinelli, R.; Palma, L.; Álvarez, F. J.; Piomelli, D.; Duranti, A.; Balduini, W.; Alonso-Alconada, D. *ACS Chem. Neurosci*. **2020**, *11*, 1291–1299. (e) Paludetto, M.-N.; Bijani, C.; Puisset, F.; Bernardes-Génisson, V.; Arellano, C.; Robert, A. *J. Med. Chem*. **2018**, *61*, 7849–7860. (f) Blunt, J. W.; Copp, B. R.; Keyzers, R. A.; Munro, M. H. G.; Prinsep, M. R. *Nat. Prod. Rep*. **2012**, *29*, 144–222. (g) Snieckus, V.; Demchuk, O. M. *Synfacts* **2005**, *0*, 0020–0020. (h) Gulevich, A. V.; Zhdanko, A. G.; Orru, R. V. A.; Nenajdenko, V. G. *Chem. Rev*. **2010**, *110*, 5235–5331. (i) Liao, J.-Y.; Shao, P.-L.; Zhao, Y. *J. Am. Chem. Soc*. **2015**, *137*, 628–631. (j) Qi, X.; Xiang, H.; Yang, Y.; Yang, C. *RSC Adv*. **2015**, *5*, 98549–98552.

[2] (a) Zhang, X.; He, Q.; Xiang, H.; Song, S.; Miao, Z.; Yang, C. *Org. Biomol. Chem*. **2014**, *12*, 355–361. (b) Yan, J.; Cheng, M.; Hu, F.; Hu, Y. *Org. Lett.* **2012**, *14*, 3206–3209. (c) Zhao, L.; Xie, F.; Cheng, G.; Hu, Y. A. *Angew. Chem. Int. Ed.* **2009**, *48*, 6520–6523. (d) Chen, J. S.; Zhou, L. J.; Entin-Meer, M.; Yang, X.; Donker, M.; Knight, Z. A.; Weiss, W.; Shokat, K. M.; Haas-Kogan, D.; Stokoe, D. *Mol. Cancer Ther.* **2008**, *7*, 841–850. (e) Bharate, S. B.; Kumar, V.; Jain, S. K.; Mintoo, M. J.; Guru, S. K.; Nuthakki, V. K.; Sharma, M.; Bharate, S. S.; Gandhi, S. G.; Mondhe, D. M.; Bhushan, S.; Vishwakarma, R. A. *J. Med. Chem*. **2018**, *61*, 1664–1687. (f) Morales, G. A.; Garlich, J. R.; Su, J.; Peng, X.; Newblom, J.; Weber, K.; Durden, D. L. *J. Med. Chem*. **2013**, *56*, 1922–1939. (g) Lucas, M.; Freitas, M.; Silva, A. M. S.; Fernandes, E.; Ribeiro, D. *Oxid. Med. Cell. Longev* **2021**, *2021*, 1–47. (h) Eshghi, H.; Pirani, F.; Khoshnevis, M. *Frontiers in Natural Product Chemistry*; Atta-ur-Rahman, Ed.; BENTHAM SCIENCE PUBLISHERS, **2021**; Vol. 8, pp 239–304.

[3] (a) Schilf, P.; Srinivasulu, V.; Bolognesi, M. L.; Ibrahim, S.; Majdalawieh, A. F.; Abu-Yousef, I. A.; Omar, H. A.; ElAwady, R.; Al-Tel, T. H. *Med. Chem. Res.* **2021**, *30*, 635–646. (b) Fukuda, T.; Ishibashi, F.; Iwao, M. *The Alkaloids: Chemistry and Biology*; Elsevier, **2020**; Vol. 83, pp 1–112. (c) Chittchang, M.; Batsomboon, P.; Ruchirawat, S.; Ploypradith, P. *ChemMedChem* **2009**, *4*, 457–465.

[4] (a) Kawamura, N.; Kinoshita, N.; Sawa, R.; Takahashi, Y.; Sawa, T.; Naganawa, H.; Hamada, M.; Takeuchi, T. *J. Antibiot*. **1996**, *49*, 706–709. (b) Kawamura, N.; Sawa, R.; Takahashi, Y.; Isshiki, K.; Sawa, T.; Naganawa, H.; Takeuchi, T. *J. Antibiot*. **1996**,

49, 651–656. (c) Flatt, P. M.; Wu, X.; Perry, S.; Mahmud, T. *J. Nat. Prod*. **2013**, *76*, 939–946.

[5] (a) Balakrishna, A.; Aguiar, A.; Sobral, P. J. M.; Wani, M. Y.; Almeida E Silva, J.; Sobral, A. J. F. N. *Catal. Rev.* **2019**, *61*, 84–110. (b) Leonardi, M.; Estévez, V.; Villacampa, M.; Menéndez, J. *Synthesis* **2019**, *51*, 816–828. (c) Qi, X.; Xiang, H.; Yang, C. *Org. Lett*. **2015**, *17*, 5590–5593. (d) Sun, J.; Zhang-Negrerie, D.; Du, Y.; Zhao, K. *J. Org. Chem*. **2015**, *80*, 1200–1206. (e) Li, X.; Huang, Y. *Chem. Commun*. **2021**, *57*, 9934–9937. (f) Tong, Q.; Xiu, R.-F.; Chen, J.-H.; Zhang, Y.; Cui, B.-D.; Wan, N.-W.; Chen, Y.-Z.; Han, W.-Y. *ACS Catal*. **2023**, *13*, 12692–12699. (g) Zhou, X.; Zhang, B.; Wu, P.; Xu, W.; Wang, R.; Li, J.; Zhai, H.; Cheng, B.; Wang, T. *Org. Lett*. **2023**, *25*, 7512–7517. (h) Li, D.; Wang, Z.; Zhang, H.; Lu, N.; Cui, L.; Wu, N.; Li, C.; Li, J. *Adv. Synth. Catal*. **2022**, *364*, 3168–3172.

[6] (a) Chen, L.; Li, Y.-D.; Lv, Y.; Lu, Z.-H.; Yan, S.-J. *Chem. Commun*. **2022**, *58*, 10194–10197. (b) Chen, L.; Qi, J.-M.; Yang, S.; Sun, S.-N.; Yan, S.-J. *Org. Chem. Front*. **2023**, *10*, 2994–2999. (c) Sheng, J.; Chao, B.; Chen, H.; Hu, Y. *Org. Lett*. **2013**, *15*, 4508–4511. (d) Lei, S.-G.; Zhou, Y.; Wang, L.-S.; Yu, Z.-C.; Chen, T.; Wu, Y.-D.; Gao, M.; Wu, A. -X. *Org. Chem. Front.* **2023**, *10*, 4843–4847. (e) Dai, T.; Li, Q.; Zhang, X.; Yang, C. *J. Org. Chem.* **2019**, *84*, 5913–5921. (f) Qi, X.; Xiang, H.; Yang, C. *Org. Lett.* **2015**, *17*, 5590–5593. (g) Wang, Z.-P.; He, Y.; Shao, P.-L. *Org. Biomol. Chem.* **2018**, *16*, 5422–5426.

[7] Das, B.; Dahiya, A.; Chakraborty, N.; Patel, B. K. *Org. Lett*. **2023**, *25*, 5209–5213.

[8] (a) Gulevich, A. V.; Zhdanko, A. G.; Orru, R. V. A.; Nenajdenko, V. G. *Chem. Rev*. **2010,** *110*, 5235–5331. (b) Gao, M.; He, C.; Chen, H.; Bai, R.; Cheng, B.; Lei, A. *Angew. Chem. Int. Ed*. **2013**, *52*, 6958–6961. (c) Wang, F.; Lu, S.; Chen, B.; Zhou, Y.; Yang, Y.; Deng. G. *Org. Lett.* **2016**, *18*, 6248−6251. (d) Hack, D.; Chauhan, P.; Deckers, K.; Hermann, G. N.; Mertens, L.; Raabe, G.; Enders, D. *Org. Lett.* **2014**, *16*, 5188−5191.

[9] (a) Sheldrick, G. M. SHELXL-2014, Program for the Refinement of Crystal Structures; University of Göttingen: Göttingen (Germany), **1997**. (b) Dolomanov, O.V.; Bourhis, L.J.; Gildea, R.J.; Howard, J. A. K.; Puschmann, H. *J. Appl.*

Crystallogr. **2009**, *42*, 339–341. (c) Sheldrick, G.M. *Acta. Crystallogr. A Found. Adv.* **2015**, *71*, 3–8.

[10] (a) Guo, G.; Wan, S.; Si, X.; Jiang, Q.; Jia, Y.; Yang, L.; Zhou, W. *Org. Lett.* **2017**, *19*, 5026–5029. (b) Mundhe, P.; Bhanwala, N.; Saini, S. M.; Sumanth, G.; Shivaprasad, K.; Shende, S. U.; Reddy, K.; Chandrashekharappa, S. *Tetrahedron* **2023**, *132*, 133265. (c) López, G.; Mellado, M.; Werner, E.; Said, B.; Godoy, P.; Caro, N.; Besoain, X.; Montenegro, I.; Madrid, A. *Antibiotics* **2020**, *9*, 576.

III.7. Representative Spectra

Ethyl 4-oxo-3-phenyl-1,4-dihydrochromeno[2,3-b]pyrrole-2-carboxylate (1a): **^{1}H NMR (CDCl$_3$, 400 MHz)**

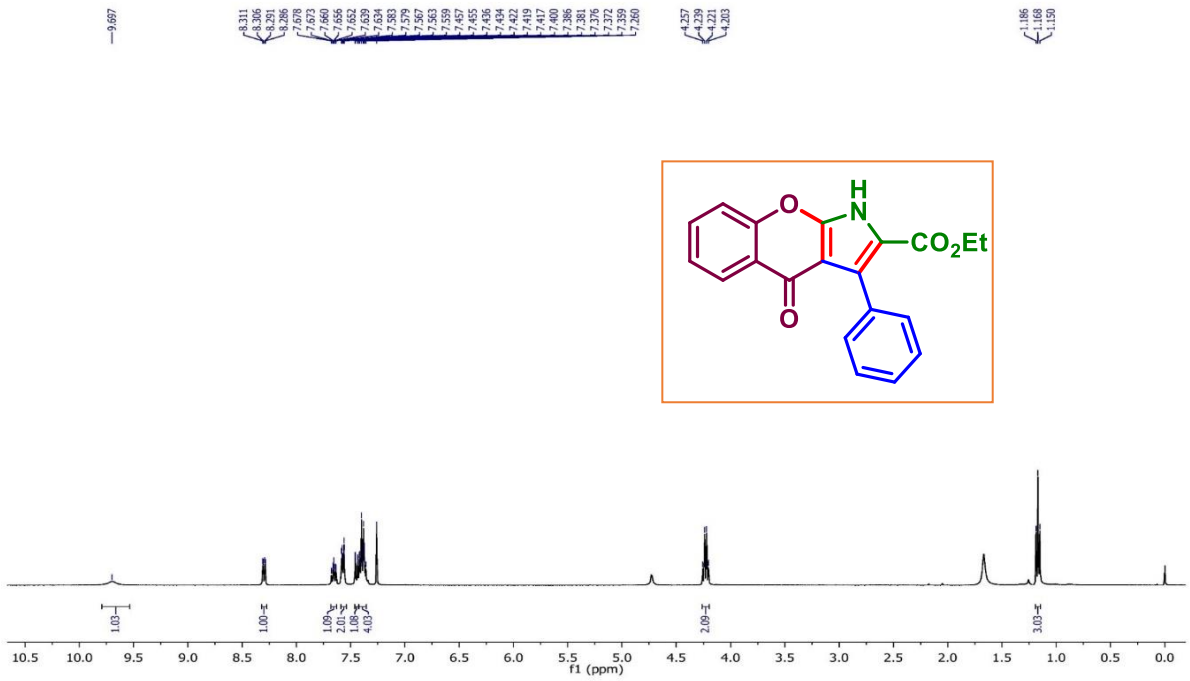

Ethyl 4-oxo-3-phenyl-1,4-dihydrochromeno[2,3-b]pyrrole-2-carboxylate (1a): **$^{13}C\{^1H\}$ NMR ($CDCl_3$, 400 MHz)**

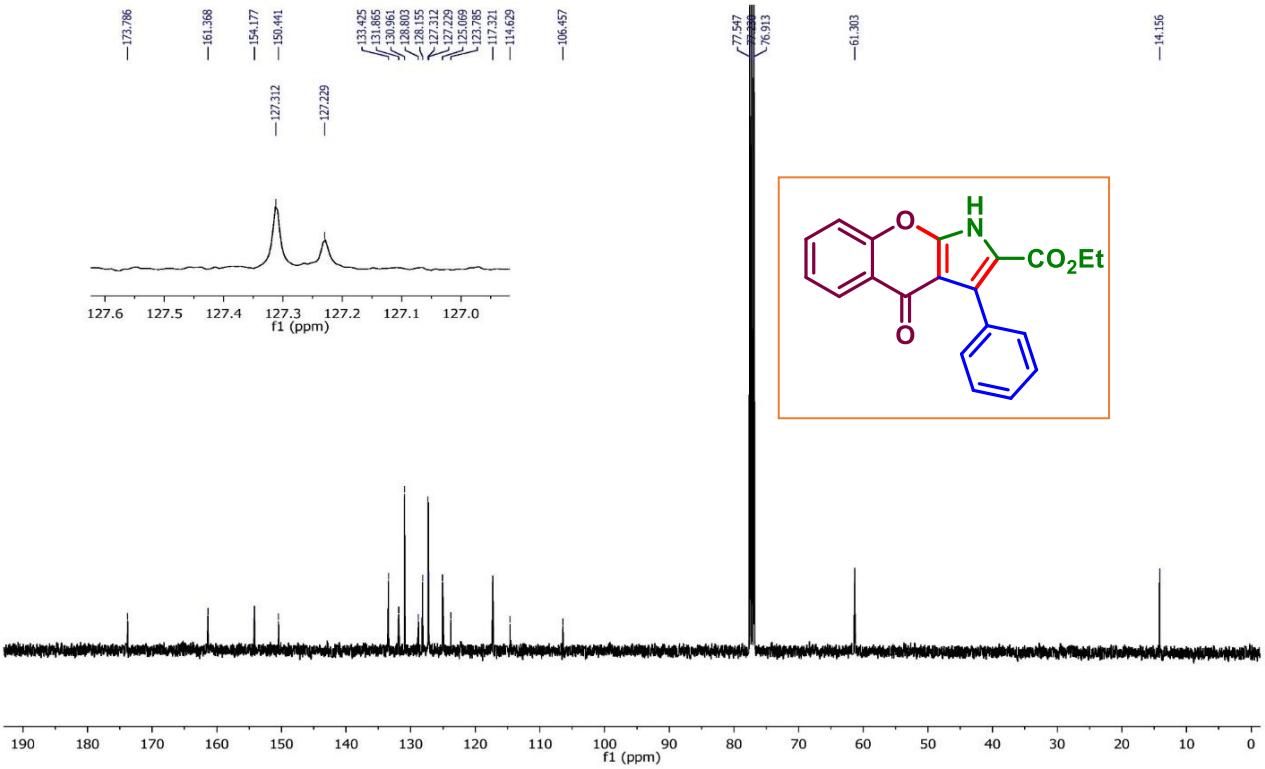

Methyl 4-oxo-3-phenyl-1,4-dihydrochromeno[2,3-b]pyrrole-2-carboxylate (1b): **^1H NMR ($CDCl_3$, 400 MHz)**

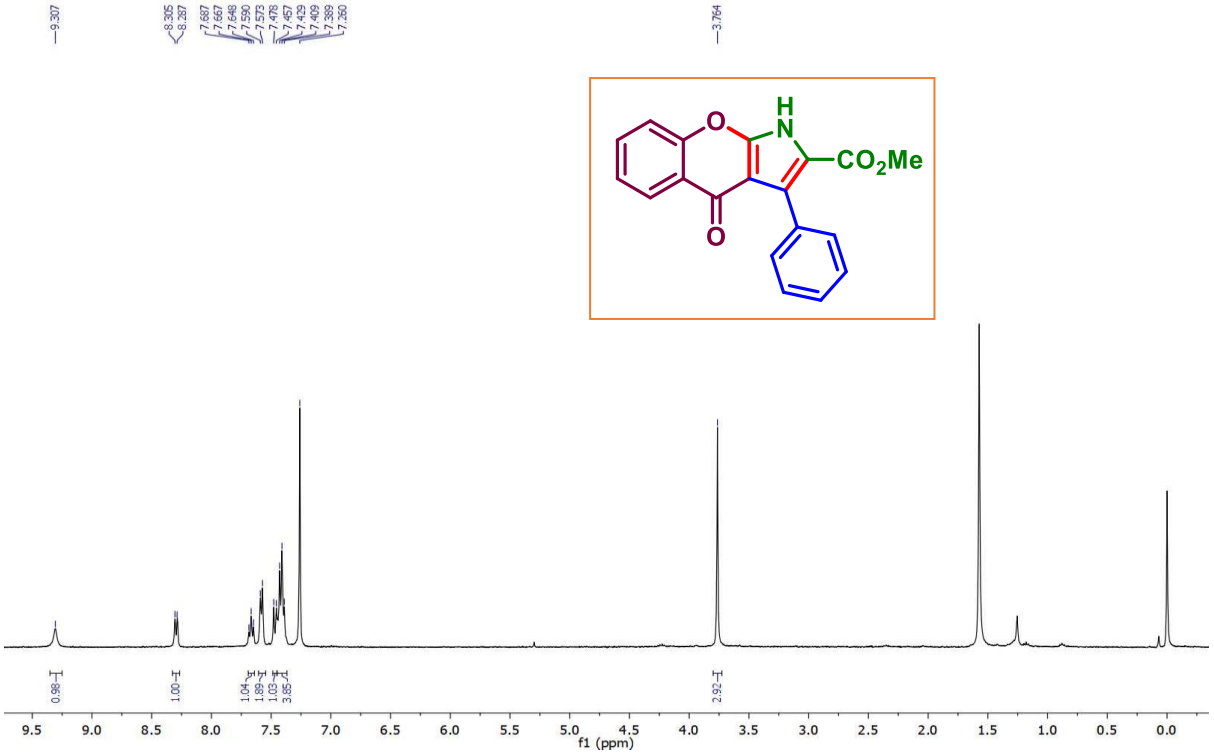

Methyl 4-oxo-3-phenyl-1,4-dihydrochromeno[2,3-b]pyrrole-2-carboxylate (1b): **$^{13}C\{^1H\}$ NMR (CDCl, 125 MHz)**

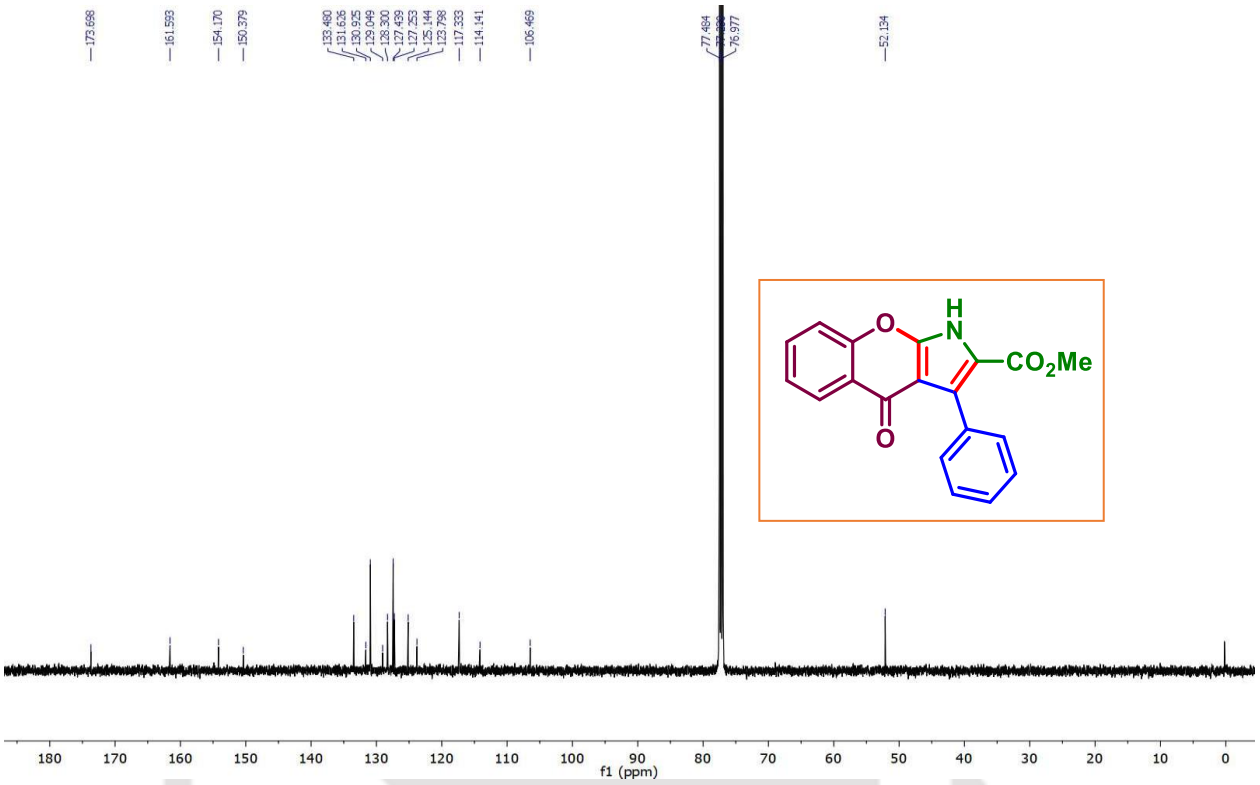

Ethyl 4-oxo-3-(p-tolyl)-1,4-dihydrochromeno[2,3-b]pyrrole-2-carboxylate (2a): **^1H NMR ($CDCl_3$, 400 MHz)**

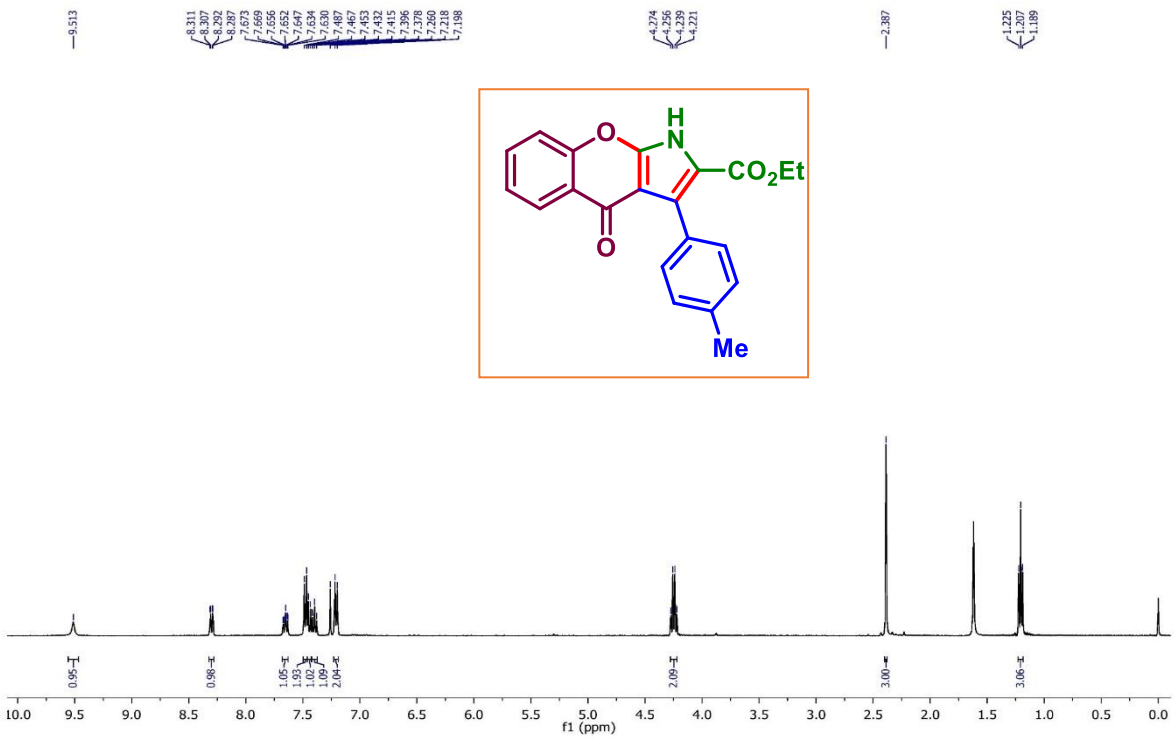

Ethyl 4-oxo-3-(p-tolyl)-1,4-dihydrochromeno[2,3-b]pyrrole-2-carboxylate (2a): **$^{13}C\{^1H\}$ NMR ($CDCl_3$, 125 MHz)**

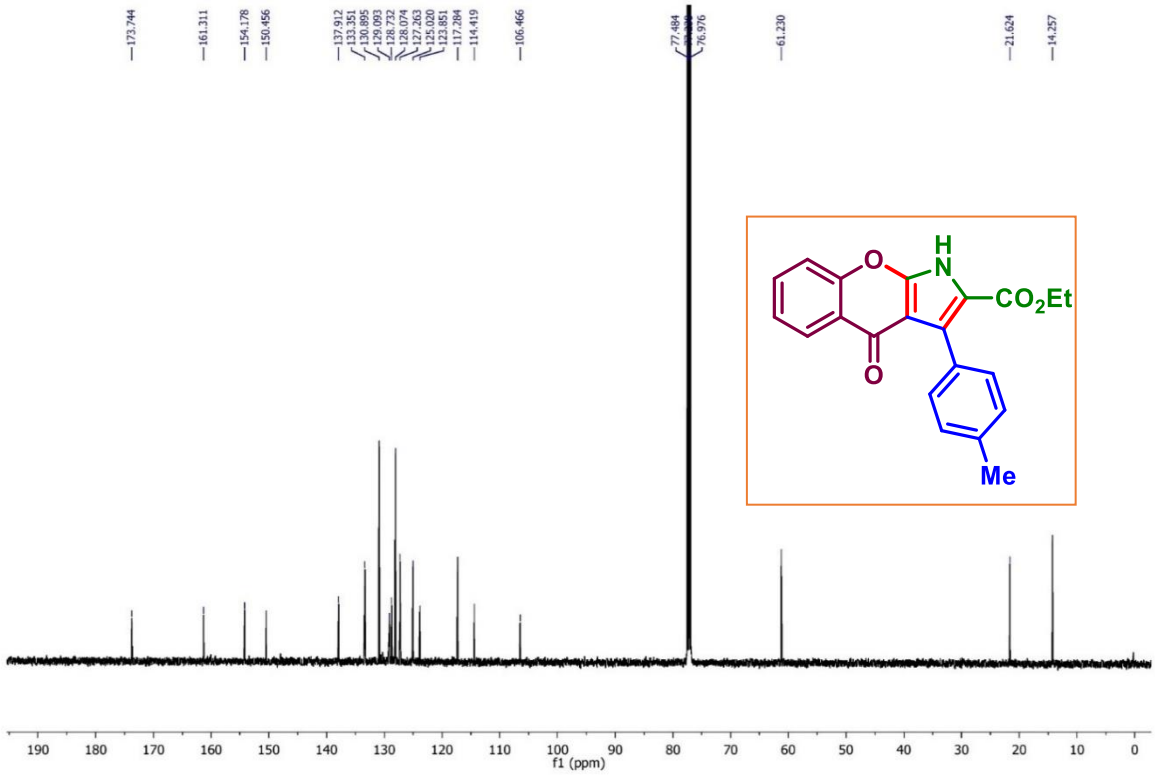

Methyl 4-oxo-3-(p-tolyl)-1,4-dihydrochromeno[2,3-b]pyrrole-2-carboxylate (2b): **^1H NMR ($CDCl_3$, 500 MHz)**

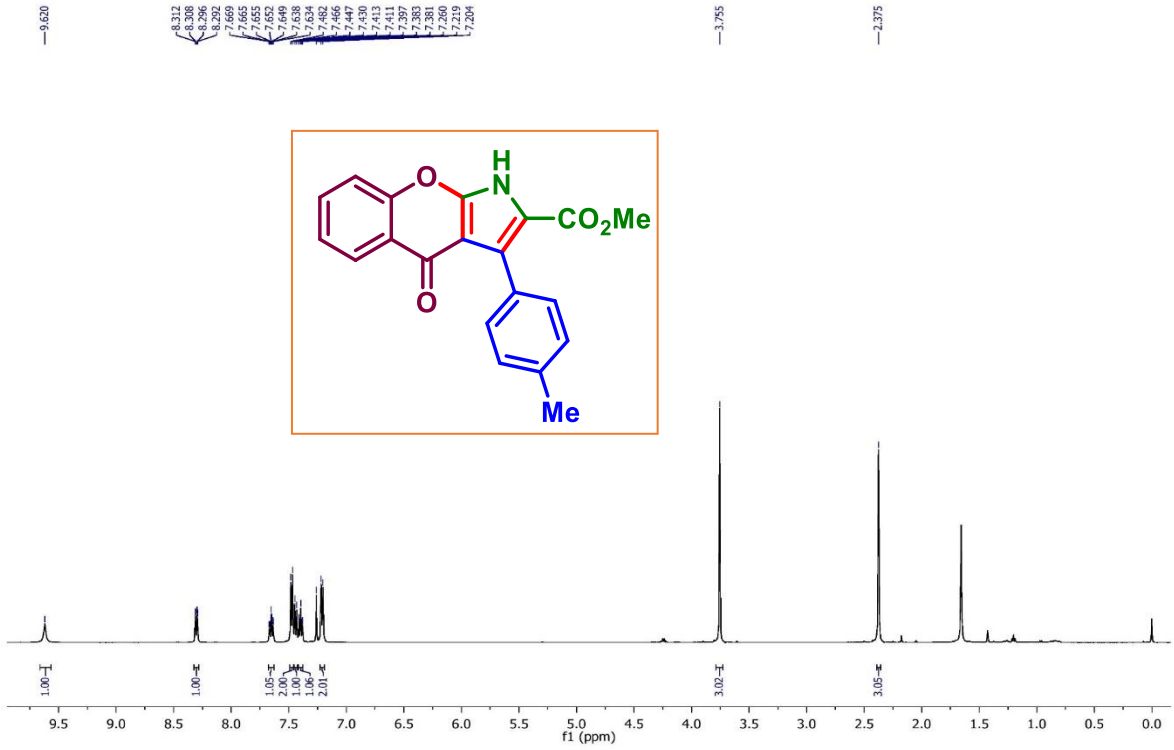

Methyl 4-oxo-3-(p-tolyl)-1,4-dihydrochromeno[2,3-b]pyrrole-2-carboxylate (2b): **$^{13}C\{^1H\}$ NMR ($CDCl_3$, 125 MHz)**

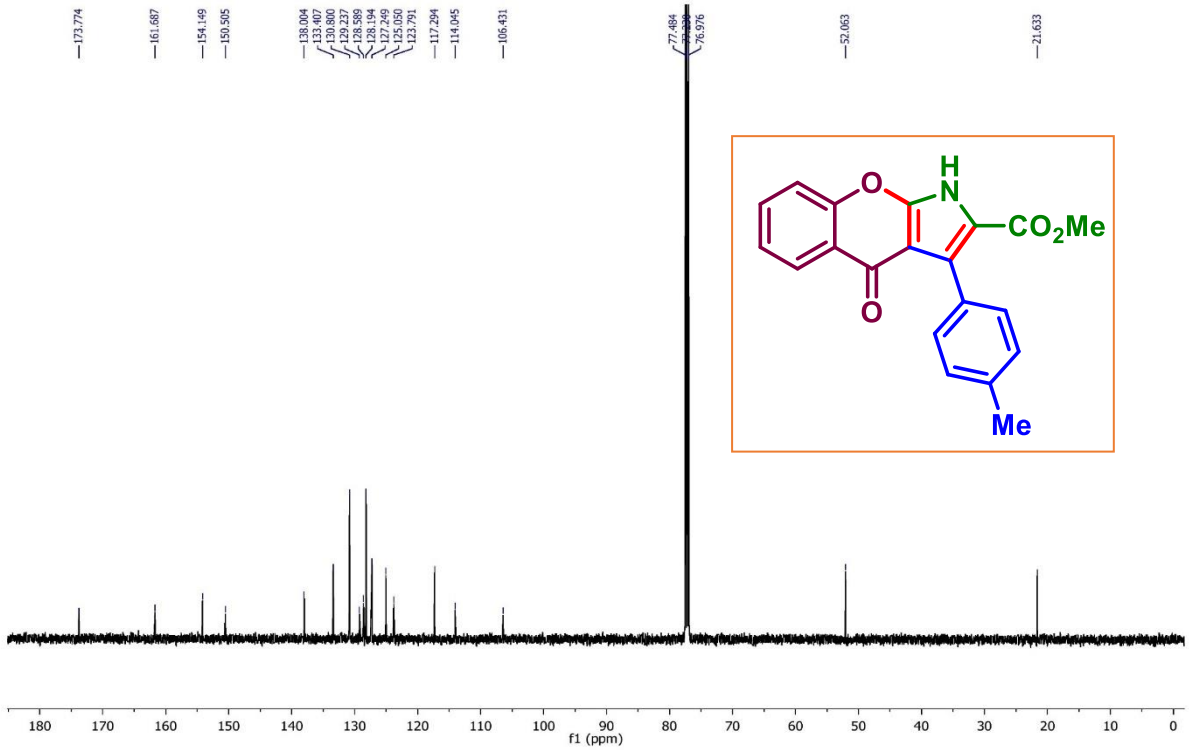

Ethyl 3-(4-(tert-butyl)phenyl)-4-oxo-1,4-dihydrochromeno[2,3-b]pyrrole-2-carboxylate (5a) : **^1H NMR ($CDCl_3$, 400 MHz)**

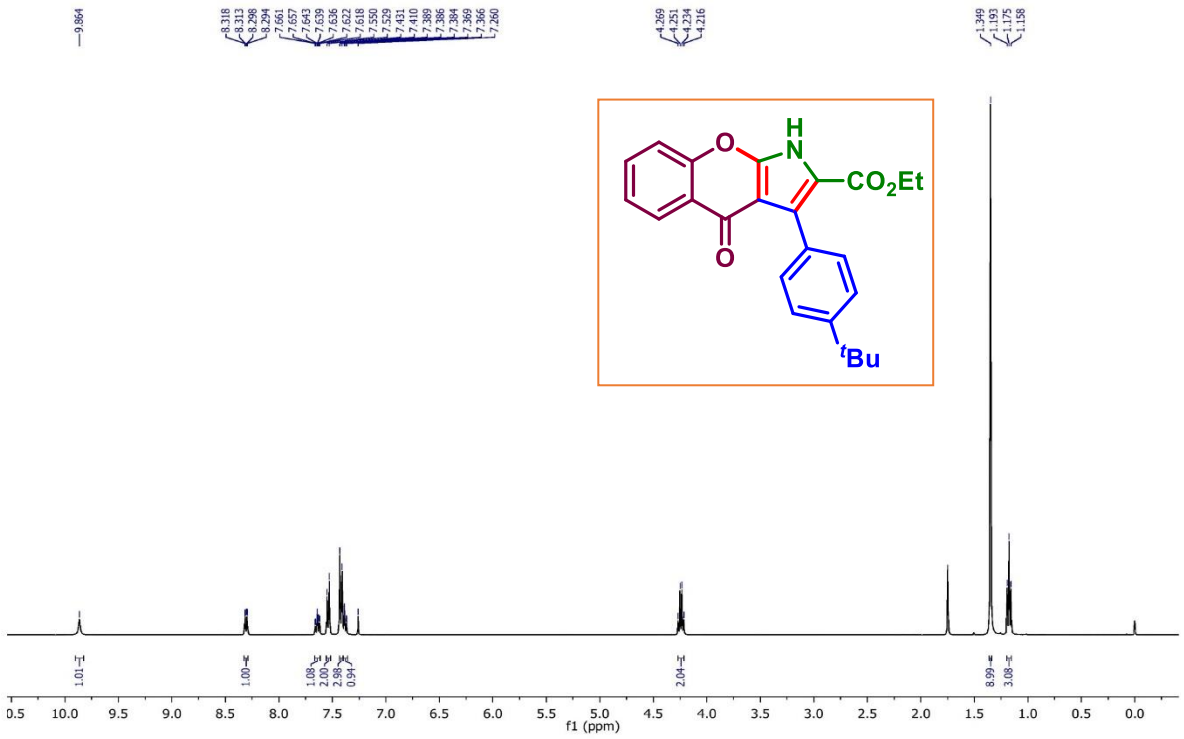

***Ethyl 3-(4-(tert-butyl)phenyl)-4-oxo-1,4-dihydrochromeno[2,3-b]pyrrole-2-carboxylate (5a):* $^{13}C\{^1H\}$ NMR ($CDCl_3$, 125 MHz)**

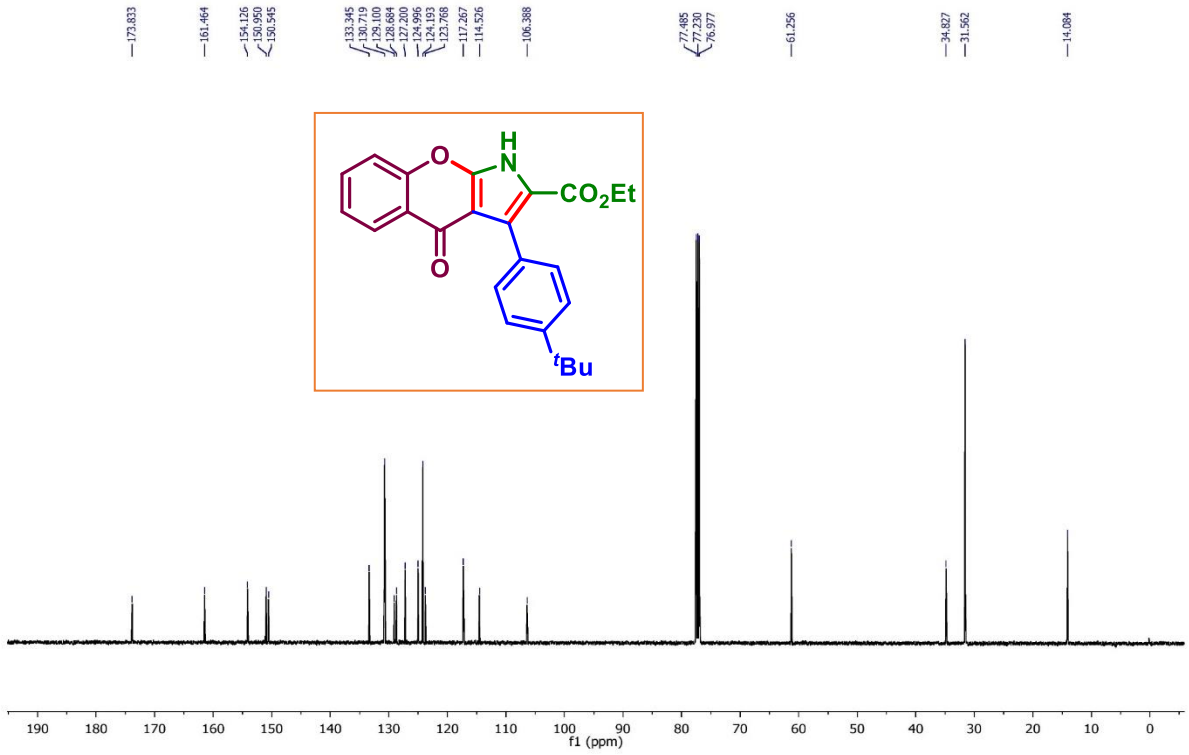

***Ethyl 3-(4-butoxyphenyl)-4-oxo-1,4-dihydrochromeno[2,3-b]pyrrole-2-carboxylate (7a):* ^1H NMR ($CDCl_3$, 400 MHz)**

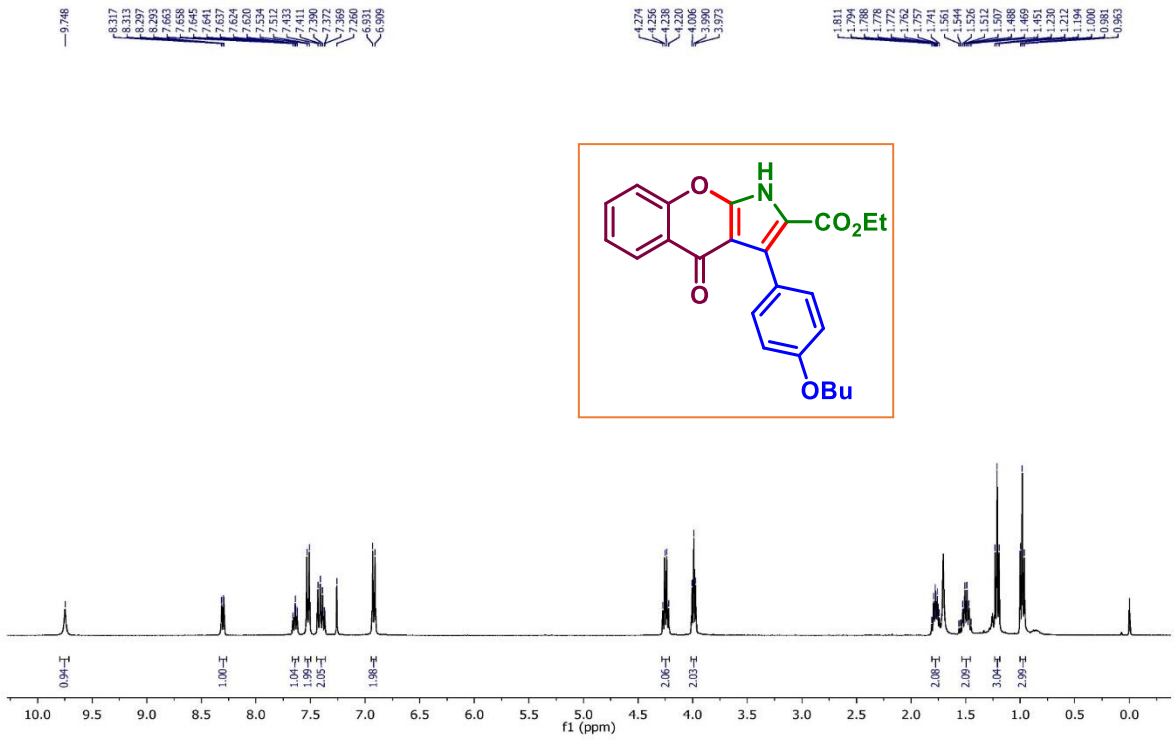

Ethyl 3-(4-butoxyphenyl)-4-oxo-1,4-dihydrochromeno[2,3-b]pyrrole-2-carboxylate (7a):
$^{13}C\{^1H\}$ NMR ($CDCl_3$, 125 MHz)

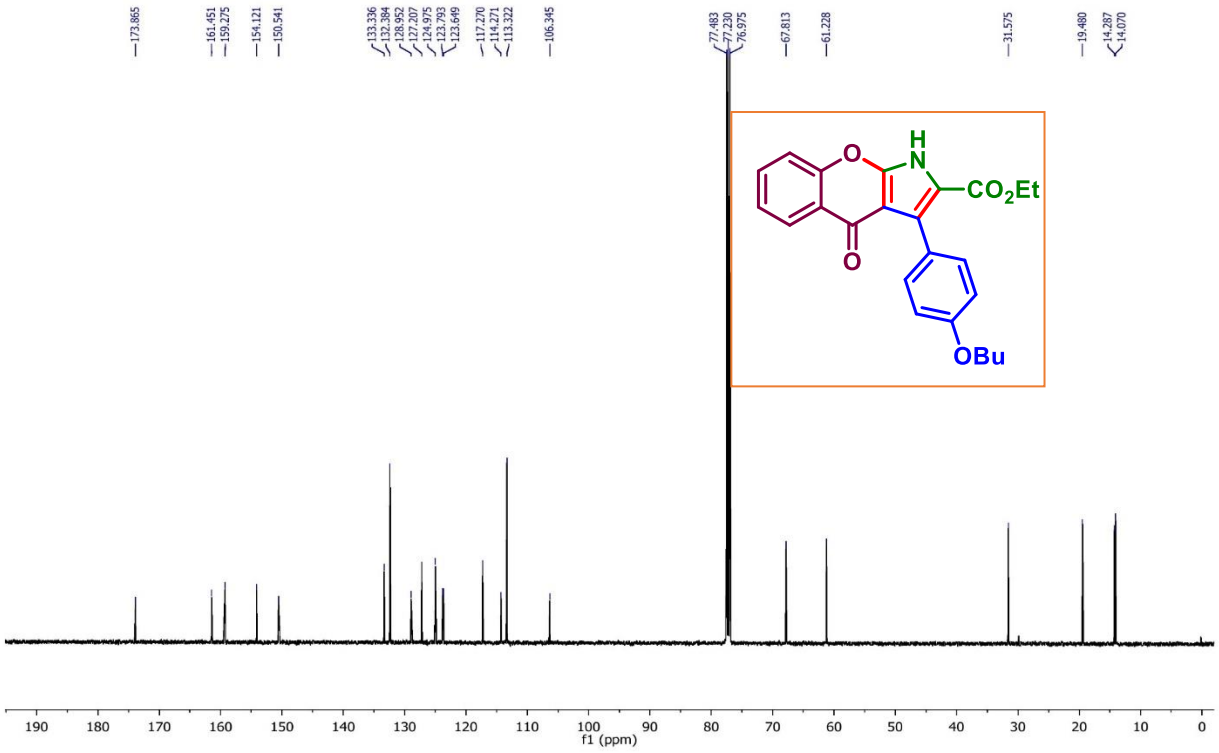

Ethyl 3-(4-fluorophenyl)-4-oxo-1,4-dihydrochromeno[2,3-b]pyrrole-2-carboxylate (12a):
^1H NMR ($CDCl_3$, 400 MHz)

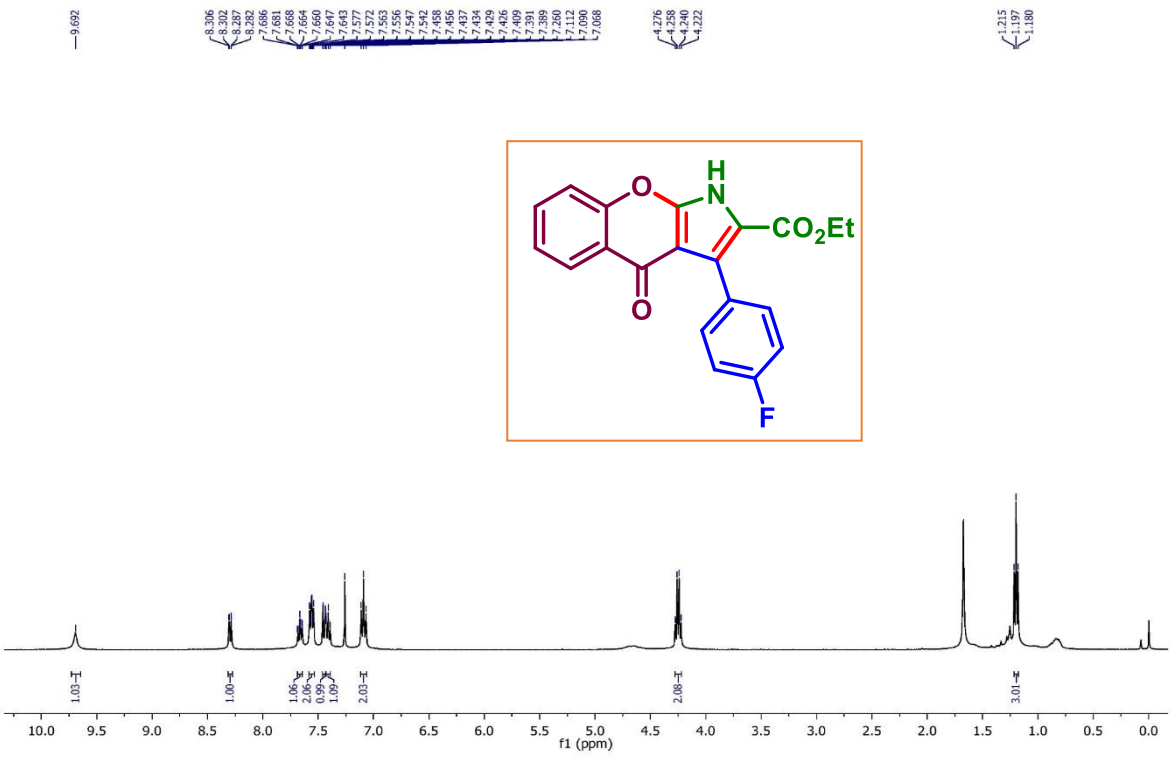

Ethyl 3-(4-fluorophenyl)-4-oxo-1,4-dihydrochromeno[2,3-b]pyrrole-2-carboxylate (12a): **$^{13}C\{^{1}H\}$ NMR ($CDCl_3$, 400 MHz)**

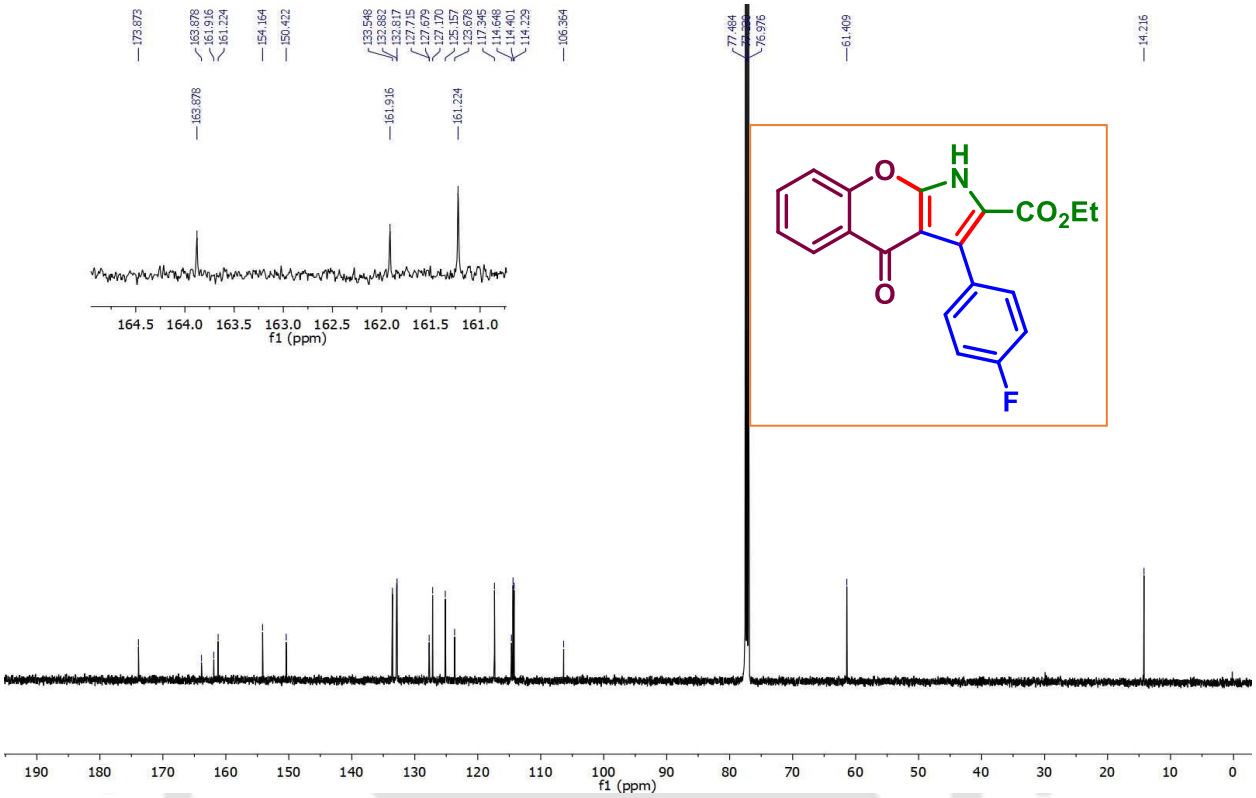

Ethyl 3-(4-fluorophenyl)-4-oxo-1,4-dihydrochromeno[2,3-b]pyrrole-2-carboxylate (12a): **^{19}F NMR ($CDCl_3$, 470 MHz)**

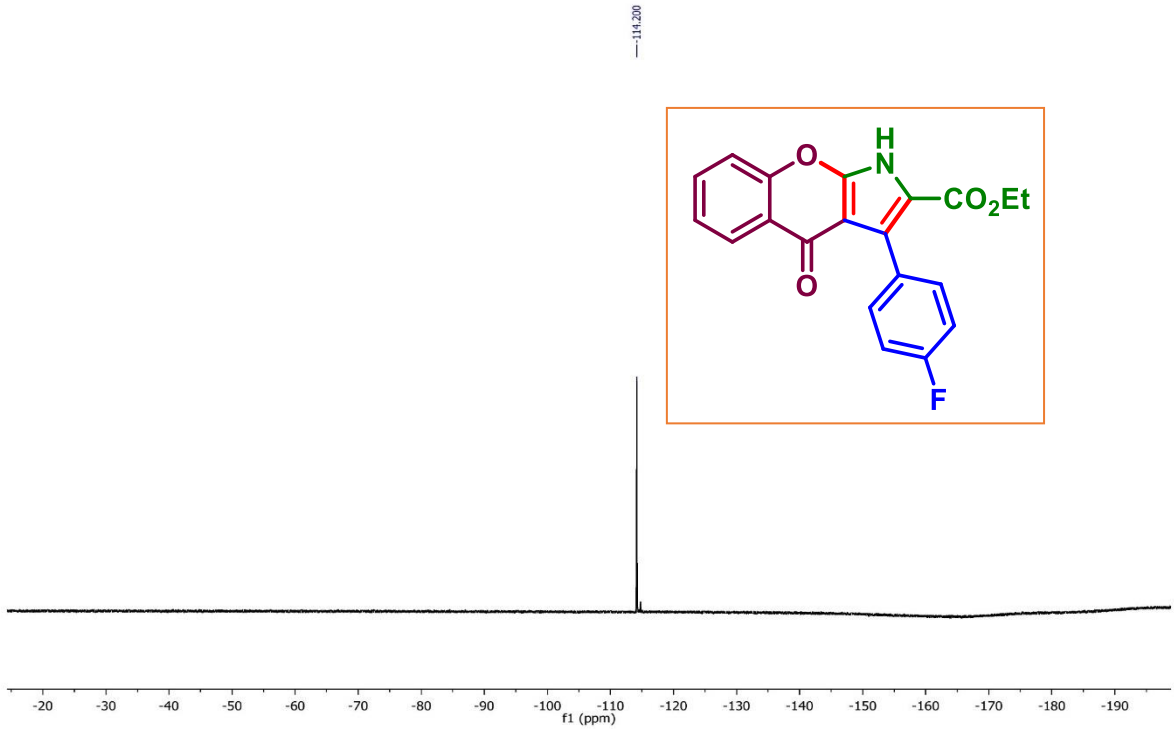

Ethyl 3-(anthracen-9-yl)-4-oxo-1,4-dihydrochromeno[2,3-b]pyrrole-2-carboxylate (21a):
^{1}H NMR (DMSO-d$_6$, 400 MHz)

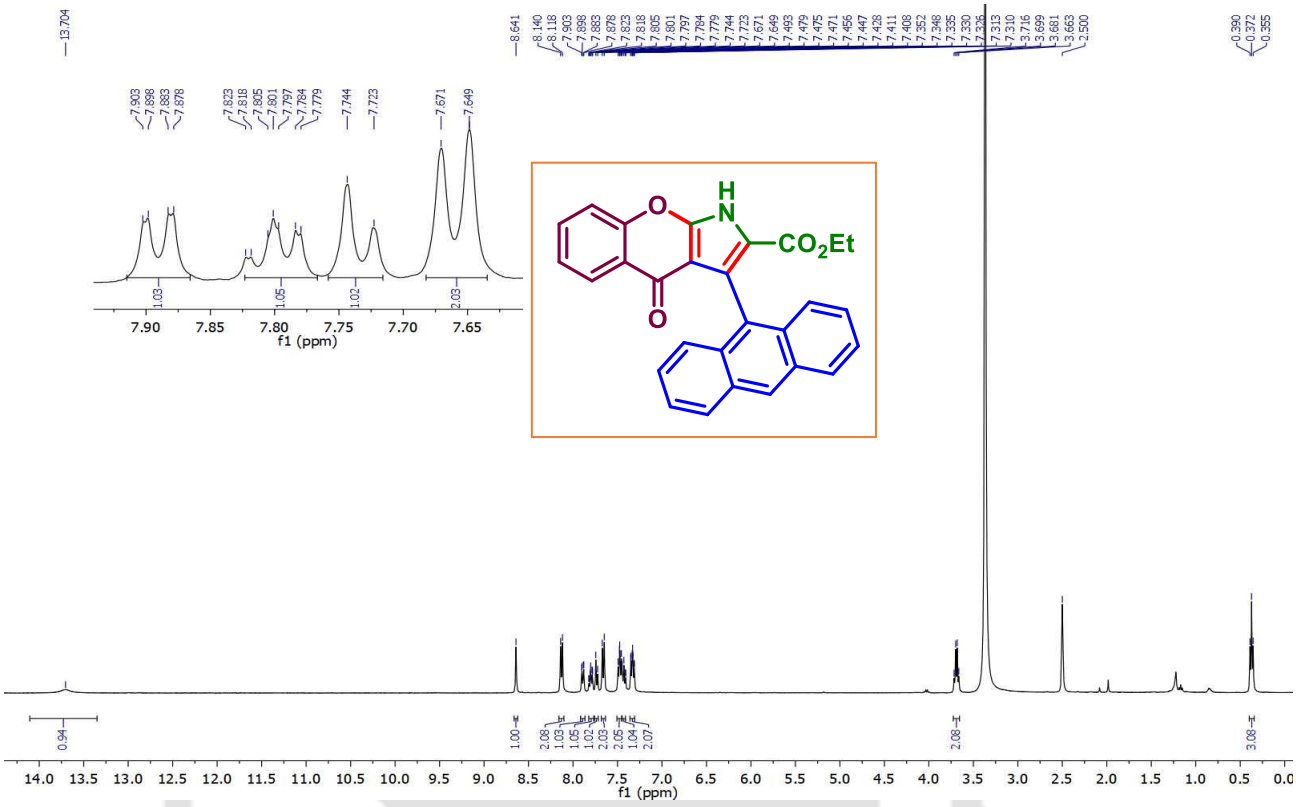

Ethyl 3-(anthracen-9-yl)-4-oxo-1,4-dihydrochromeno[2,3-b]pyrrole-2-carboxylate (21a):
^{13}C{^{1}H} NMR (DMSO-d$_6$, 125 MHz)

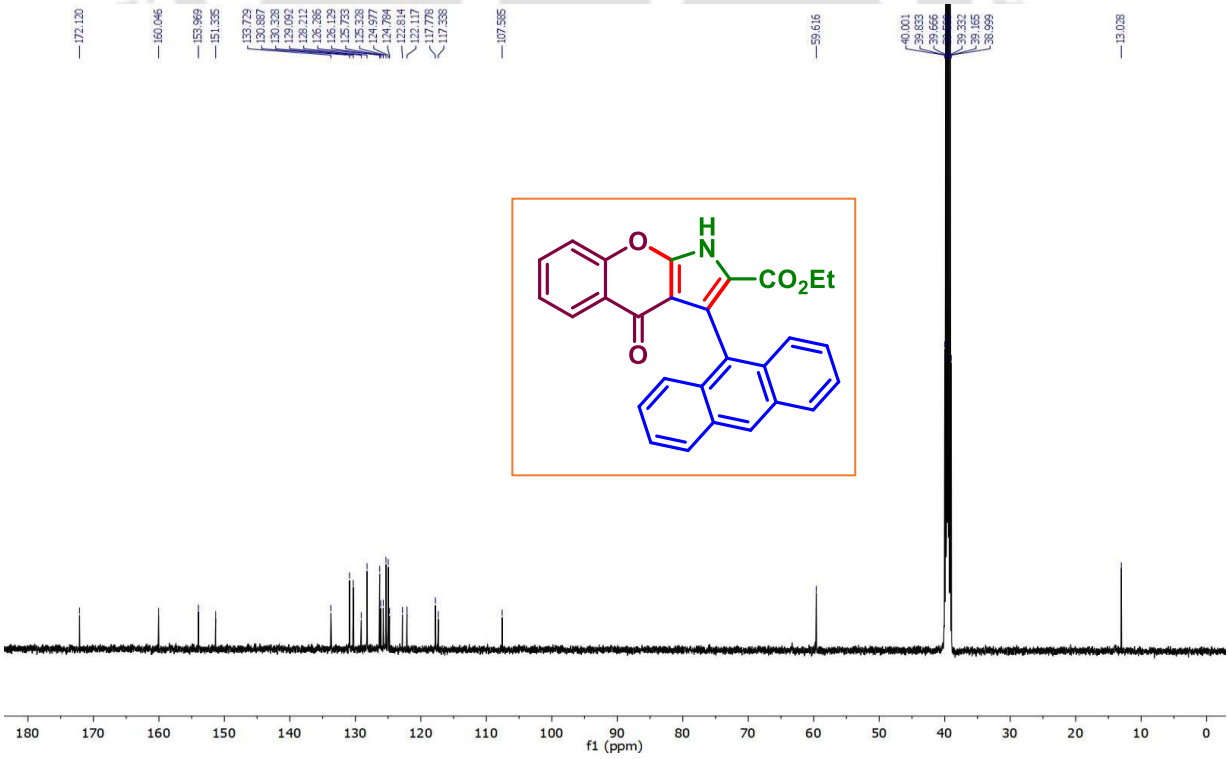

***Ethyl 3-(5-bromofuran-2-yl)-4-oxo-1,4-dihydrochromeno[2,3-b]pyrrole-2-carboxylate (24a):* ^{1}H NMR ($CDCl_3$, 400 MHz)**

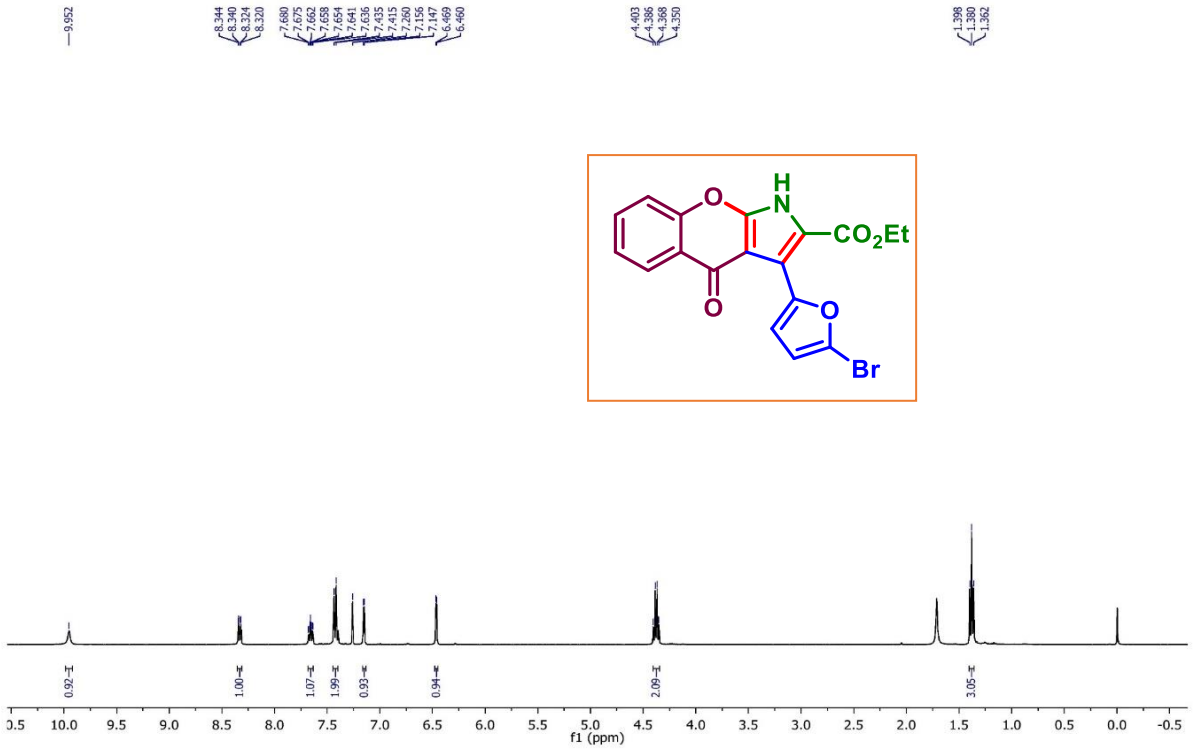

***Ethyl 3-(5-bromofuran-2-yl)-4-oxo-1,4-dihydrochromeno[2,3-b]pyrrole-2-carboxylate (24a):* ^{13}C{^{1}H} NMR ($CDCl_3$, 125 MHz)**

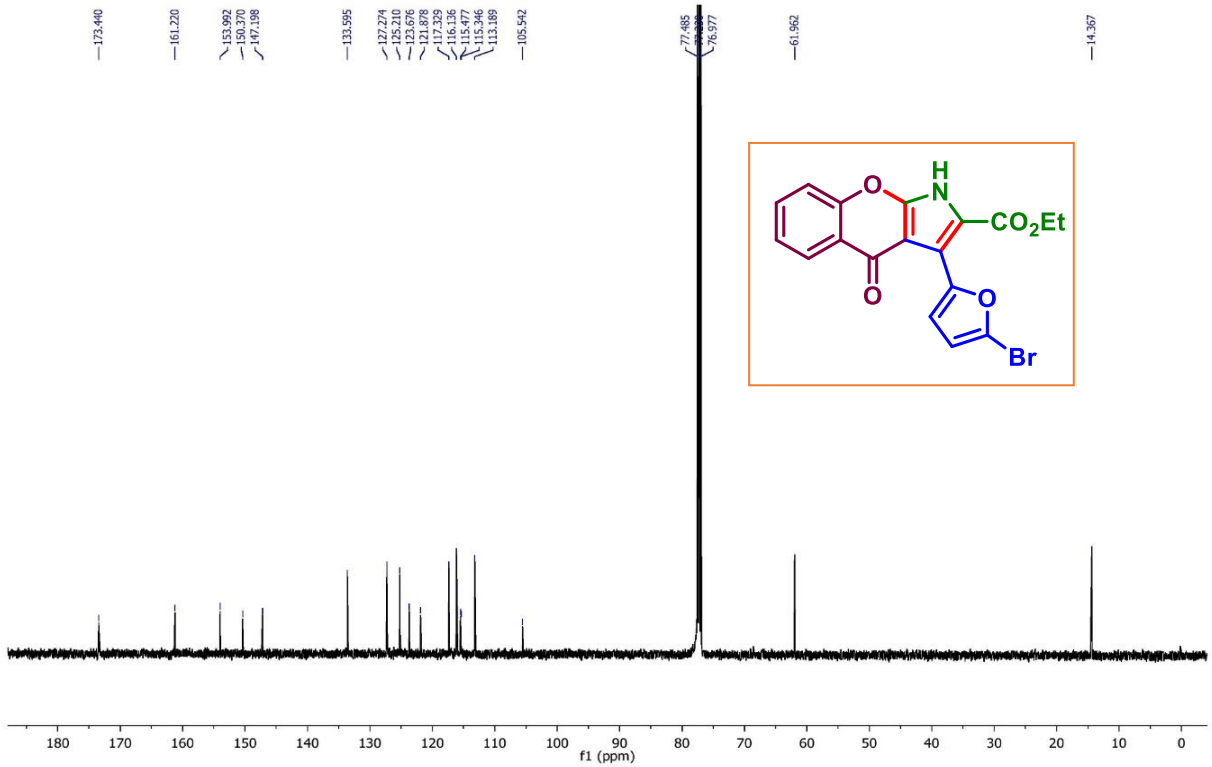

Ethyl 6-chloro-4-oxo-3-phenyl-1,4-dihydrochromeno[2,3-b]pyrrole-2-carboxylate (27a):
^{1}H NMR (DMSO-d$_6$, 400 MHz)

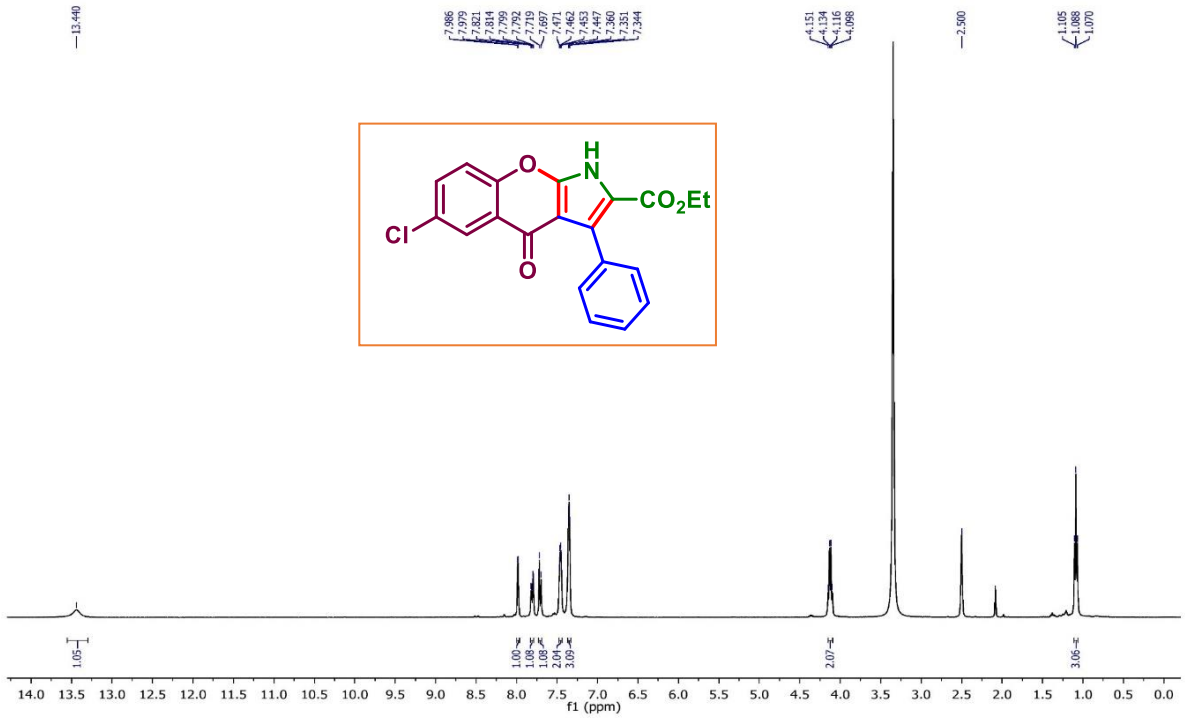

Ethyl 6-chloro-4-oxo-3-phenyl-1,4-dihydrochromeno[2,3-b]pyrrole-2-carboxylate (27a):
^{13}C{^{1}H} NMR (DMSO-d$_6$, 125 MHz)

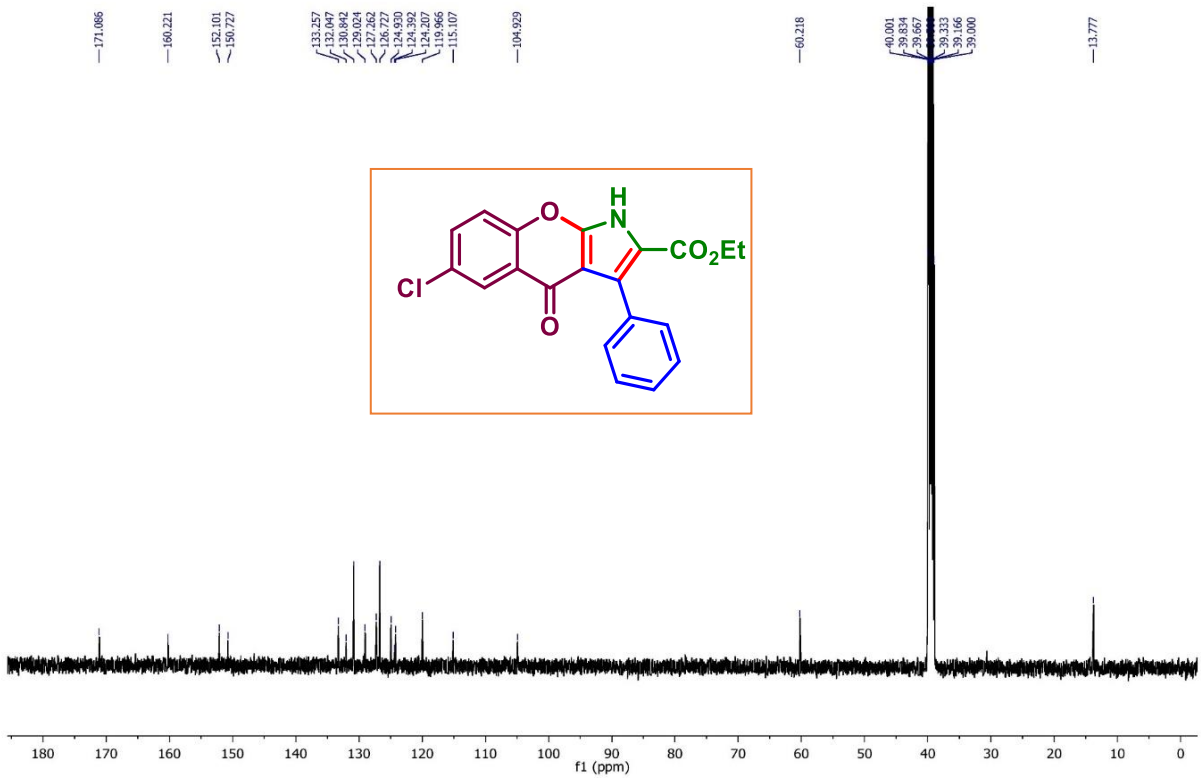

***Ethyl 6,8-dimethyl-4-oxo-3-phenyl-1,4-dihydrochromeno[2,3-b]pyrrole-2-carboxylate (30a):* ^{1}H NMR ($CDCl_3$, 400 MHz)**

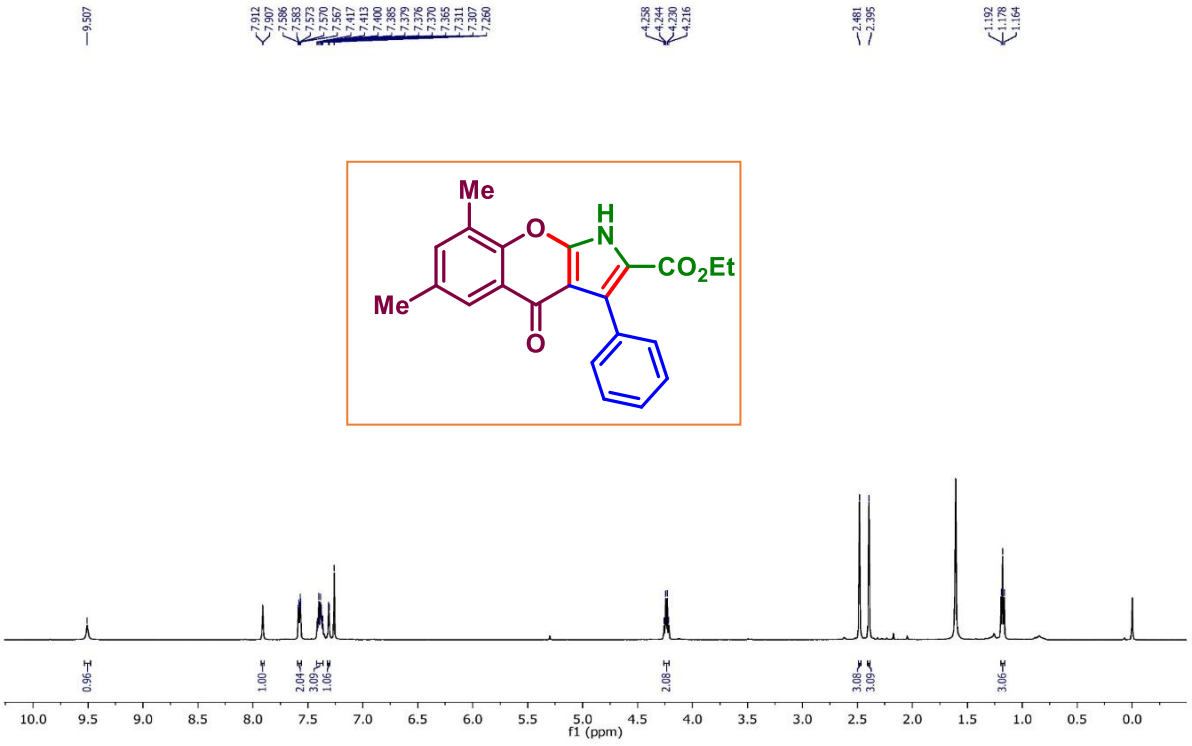

***Ethyl 6,8-dimethyl-4-oxo-3-phenyl-1,4-dihydrochromeno[2,3-b]pyrrole-2-carboxylate (30a):* ^{13}C{^{1}H} NMR ($CDCl_3$, 125 MHz)**

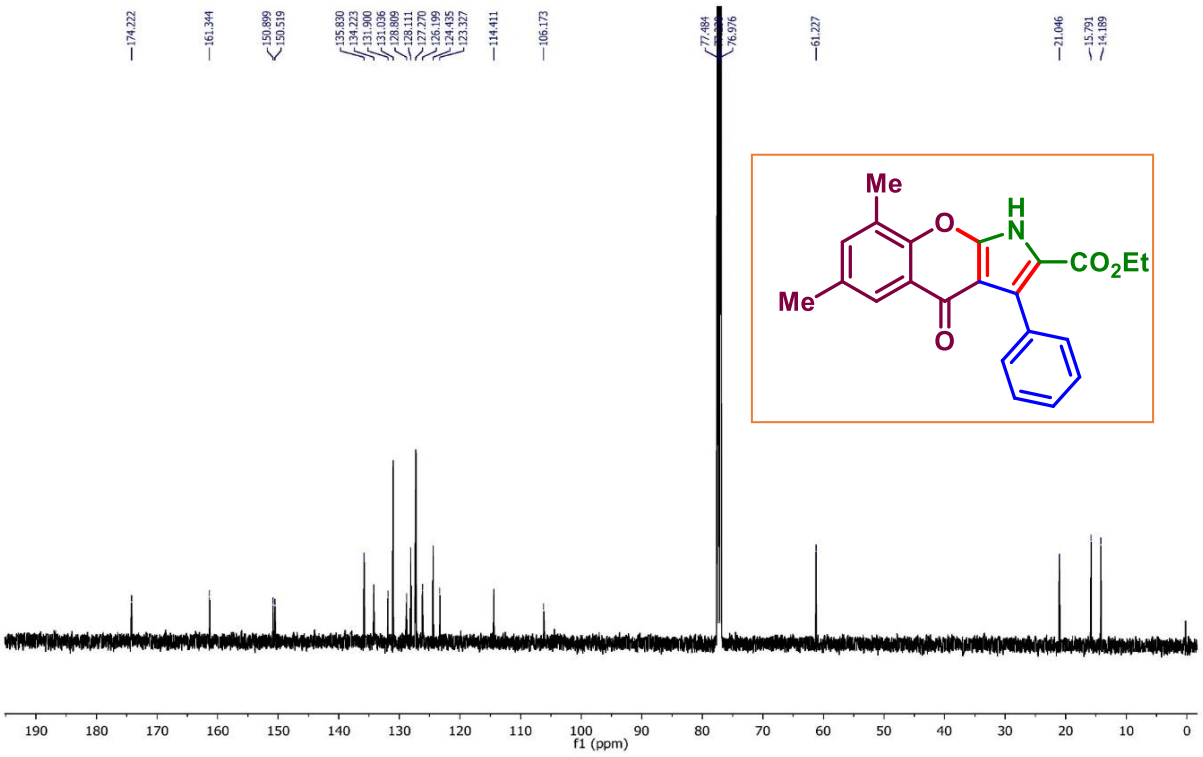

CHAPTER IV

Transformable Transient Directing Group Assisted C(sp^2)–H Activation: Synthesis and Late-Stage Functionalizations of *o*-Alkenylanilines

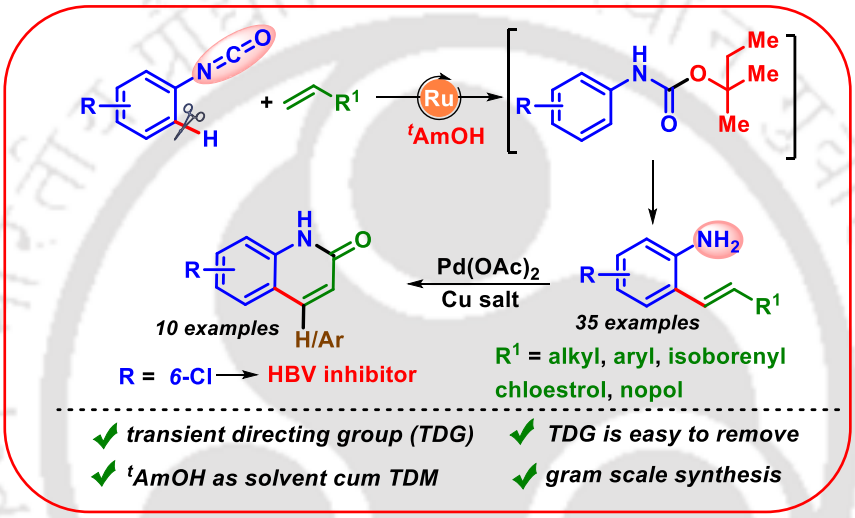

JOC The Journal of Organic Chemistry

J. Org. Chem. **2022**, *87*, 13383–13387.

pubs.acs.org/joc Note

ABSTRACT: ***The isocyanate group in aryl isocyanates serves as a transformable transient directing group in a Ru(II)-catalyzed o-olefination leading to o-alkenylanilines. In alcoholic solvents, aryl isocyanates are transformed into carbamates which initiate the insertion of acrylates via o-C–H activation. In particular, ^{t}AmOH serves the dual role of solvent-cum transient directing mediator. The o-alkenylanilines are converted to azacoumarins and subsequently into C-4 aryl-substituted azacoumarins using aryl iodides as coupling partners via Pd(II) catalyzed C–H functionalizations.***

CHAPTER IV

Transformable Transient Directing Group Assisted C(sp^2)–H Activation: Synthesis and Late-Stage Functionalizations of *o*-Alkenylanilines

II.1. Introduction

The formation of C–C, and C–X bonds *via* direct C–H bond activation continues to be an important and stimulating thrust in academic and industrial research. The high abundance of C–H bonds in organic compounds makes their functionalization an extensively investigated topic of research. The C–H activation strategy has attained prominent space in the field of organic chemistry and has emerged as an alternative pathway to overcome the necessary pre-activation of substrates as required in traditional cross-coupling reactions. Thus, this strategy could shorten the synthetic sequence and allow the utilization of cheap and environmentally benign reactants (eg., hydrocarbons instead of organic halides).[1a-d] For example, an alternative to Mizoroki-Heck coupling is the oxidative coupling of arenes with an alkene to form vinylarenes which proceeds in step economical way by avoiding functionalized coupling partners. Similar strategies for the construction of C–C bonds by C–X activation such as Stille, Negishi, Suzuki, and Kumada face limited functional group tolerance, the toxicity of starting materials, and harsh reaction conditions. Although several efficient catalytic systems have emerged with modifications in original reaction conditions, the requirement of good leaving groups (eg., halide, triflate) and subsequent formation of halide salts as by-product limits the usefulness of such cross-coupling reactions. The direct C–H activation is an invaluable alternative to answer all the concerns raised on coupling reactions about their site-selectivity and step-economy (Scheme IV.1.1).[1e] However, the wide abundance of C–H bonds in organic compounds, makes their selective functionalization difficult. The high bond dissociation energy and low polarity of the C–H bond, make it fairly unreactive. Thus, easy and straightforward installation of diverse functional groups to fabricate complex molecular entities through the C–H bond activation strategy is highly intriguing. Over the years, techniques have developed which focus on the use of specially designed ligands, modified reactors, and catalytic conditions which enable to overcome concerns regarding regio-, stereoselectivity and efficiency of C–H activation.[1]

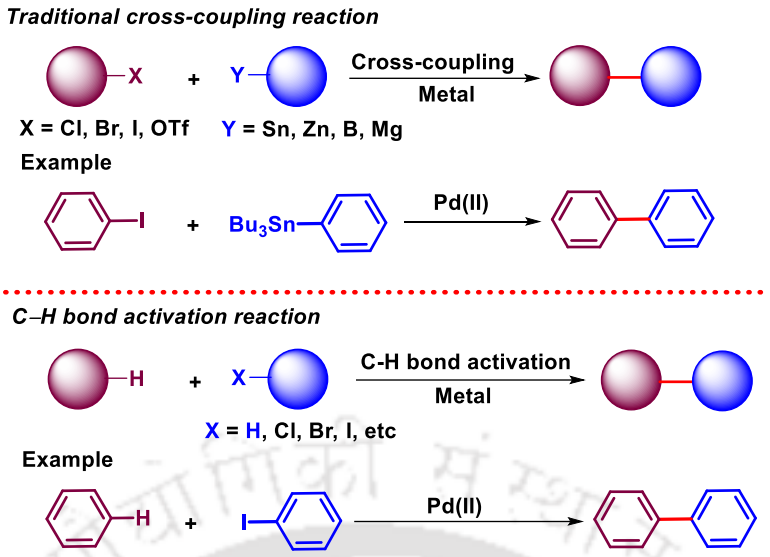

Scheme IV.1.1. *Traditional cross-coupling and C–H activation process.*

The conversion of desired C–H bonds into C–C bonds can be selectively achieved with the help of directing groups (DGs). The usage of DGs can help in the preferential functionalization of a particular C–H bond in the presence of several equivalent C–H bonds. The introduction of DGs results in the rapid expansion of this field and employs C–H bonds as versatile functional groups in synthetic molecule assembly. DGs are usually *σ*-coordinating functional groups that in combination with a transition metal control the site selectivity and activate the relatively strong C–H bonds by coordinating through the heteroatoms of DGs to the reactive metal catalysts. Directing groups are required to direct the positioning of the metal catalyst so that the desired C–H bond can be activated. DGs basically refers to coordinating functional groups that either may be already present in the molecule or can be *in situ* installed *via* functional group transformations. DGs help in achieving maximum coordination with a metal for specific C–H bond functionalization. In principle, an ideal directing group should be an intrinsic part of the substrate, which avoids installation and detachment after desired transformations. The coordination of the DG with the metal determines the efficiency of the protocol otherwise leads to unprecedented side reactions. Therefore, to achieve optimum coordination, a proper combination of the metal as well as directing group is very much essential.[2] Based on the coordination ability of the DGs with metal, they may be classified as strong and weakly coordinating DGs. Although, the borderline of this classification is not so hard, yet it presents significant information on the nature of the coordination ability of the heteroatom of the DGs. A strongly coordinating DG forms a stable metallacycle with the transition metal mostly through the *N*-atom of the DGs. *N*-containing DGs such as pyridin-2-

yl, oxazolin-2-yl or pyrazol-1-yl groups act strong σ-donors. This thermodynamically stable metallacycle demands additional steps or harsh reaction conditions for their installation and removal after desired transformations. On the contrary, ketones, carboxylic acids, ethers, and esters weakly coordinate with the metal and are more versatile for subsequent transformations. The resulting metallacycles are thermodynamically less stable and subsequent modification or removal is easier (Scheme IV.1.2).[3]

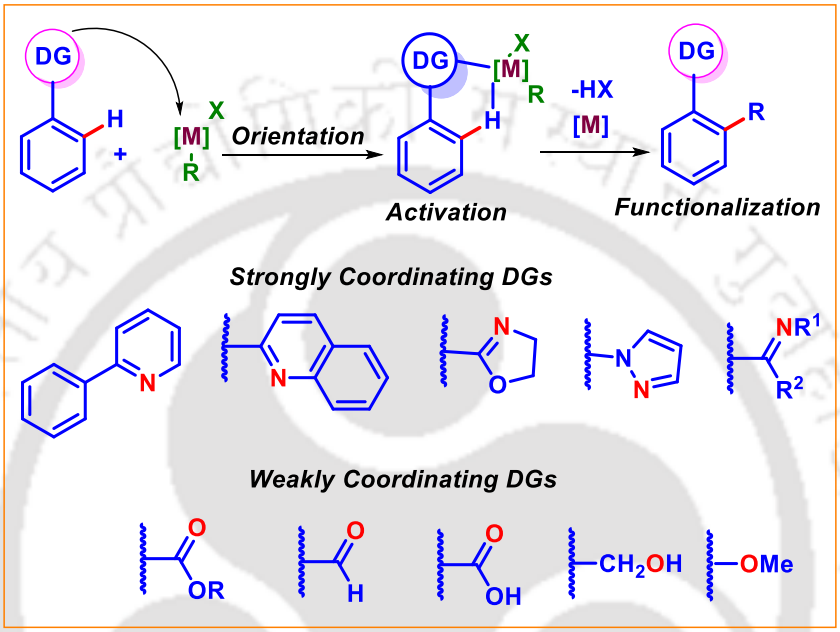

Scheme. IV.1.2. *Types of directing groups.*

Transition metals-catalyzed C–H bond functionalization arguably constitutes the most valuable synthetic tool for activation of the desired C–H bond. The most widely studied transition metals for the activation of inert C–H bonds are Pd,[3] Rh,[4] Ru,[5] Ir,[7] Mn,[8] Co,[9] Ni,[10a-c] Cu[10d-f], etc. The directing group brings transition metal to proximity and is positioned at an appropriate place for versatile C–H bond functionalization upon trapping with electrophiles or nucleophiles under basic or oxidative conditions respectively. Directing groups accelerate C–H bond activation through the formation of carbon-metal bonds *via* a chelation-controlled cyclometallation process. The field of directed C–H bond activations has grown tremendously and many chelating groups have been explored that can serve as auxiliaries.[11] Though the directing group-assisted C–H activation is a well-established methodology for inert C–H bond activation, the detachment of these groups after completion of the desired transformations is a cumbersome process. Thus, the step economical issue is an added disadvantage of DG-assisted C–H activation.

Compared to traditional DG-assisted C–H bond activation, transient DGs (TDG) assisted C–H bond activation has become a new strategy for the challenges of prior installation and removal of auxiliaries.[12a-d] TDGs are modified *in situ* with an external transient directing mediator (TDM), used either in catalytic or stoichiometric amounts. TDMs are functional moieties that transform a weakly coordinating functional group into a better σ-donor motif by tethering to the TDGs. Moreover, this TDM must be cleaved *in situ* after the functionalization (Figure IV.1.1). For instance, derivatives of phenols, aldehydes, and ketones, etc. are some examples of transient DGs that have been utilized in the C–H bond functionalizations.[12e-i]

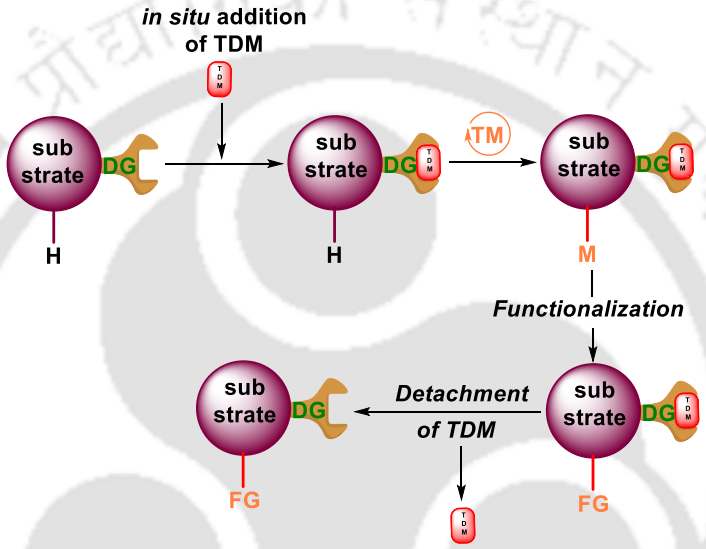

Figure IV.1.1. *Activation C–H of bond through transient directing groups.*

Being closer to the DGs, the *ortho* C–H bonds of arenes can be activated easily compared to furthest located *meta* or *para* C–H bonds. Thus, most of the traditional DGs usually activate proximate *ortho* C–H bonds. These activated C–H bonds then can be coupled with a variety of coupling partners for desired transformations. In recent years, outstanding progress has been achieved in *o*-C–H alkenylation using activated alkenes.[14a-c,] Alkenes are essential feedstock in industrial processes, and their utilization for the synthesis of a variety of important biological and materially relevant molecules has become immensely important in organic synthesis.[14d] However, the direct introduction of olefinic C(sp^2)–H bonds into aryl rings is challenging and thus becomes a potential area of research for organic chemists. DGs-assisted C–H activation has overcome many such limitations and has significantly improved the arsenal of synthetic chemistry for synthesizing such exotic molecules.[14a]

IV.2. Metal-Catalyzed *o*-C–H Functionalization Strategy

IV.2.1. Transient directing group assisted C–H functionalization:

Lewis and Smith are two pioneers of the transient-directing catalytic C–H bond activation field. Lewis independently studied the *ortho* deuteration of phenols using Ru complex (TDM-1) by transesterification of the phenoxy group to phosphites under D_2 atmosphere. The catalytic KOPh was found to be very crucial for rapid transesterification. The *ortho* selectivity of the protocol was believed to be due to the formation *o*-metallated complex as the key intermediate (Scheme IV.2.1).[13a]

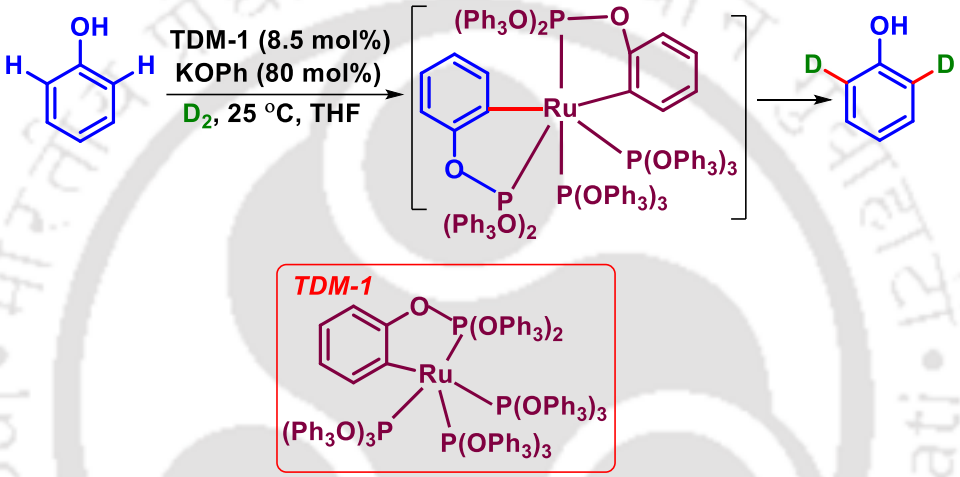

Scheme IV.2.1. *Pioneering work by Lewis for o-C–H deuteration using TDG*

Although most of the transient directing mediator results in the generation of oxime and imine TDGs, but oximes are mostly synthesized separately before the functionalization. The oxygen atom of the carbonyl has low basicity for proximal C–H bond activation. However, transformation to an imine functionality enhances the basicity of carbonyl carbon. Shi *et al*. reported such a strategy where the *ortho* C–H bond is silylated using imine as the transient auxillary. The condensation of biaryl aldehyde and 3-aminophenylpropionic acid generates imine which serves as the actual directing group for this Pd-catalyzed *ortho* silylation. As suggested by control experiments, the presence of amino acid as an additive is essential to facilitate C–H activation, which imparts its role as TDM (Scheme IV.2.2).[13b]

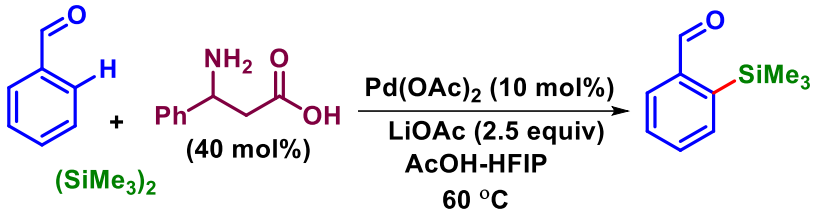

Scheme IV.2.2. *ortho-C–H silylation of biaryl aldehydes using transient DG.*

IV.2.2. Directing group-assisted C–H olefination

A new transient directing group for the selective C–H functionalizations is highly desirable as well as appreciable in organic synthesis. Directing group-assisted C–H activation can be used for the synthesis of olefinated compounds using olefin as the coupling partner. *o*-Alkenylanilines are important building blocks in many organic transformations and are prevalent in many bioactive compounds.[15]. Activated olefins are widely introduced in the *ortho* position of anilines with the assistance of directing groups such as –NHCOMe,[16a-e] urea[16f,g] (Scheme IV.2.3).

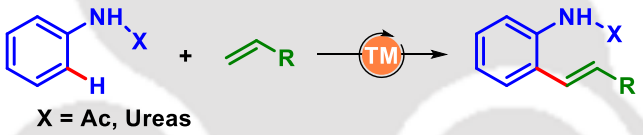

Scheme IV.2.3. *Transition-metal-catalyzed o-olefination.*

In 2017, Satoh, and Miura reported a carbamate (Boc) directed olefination protocol using Rh catalyst.[16i] The weakly coordinating carbonyl oxygen of carbamate coordinates to the Rh metal in an environmentally benign alcoholic solvent (^{t}BuOH). However, an additional step is required for the cleavage of the Boc directing group after the desired olefination (Scheme IV.2.4).

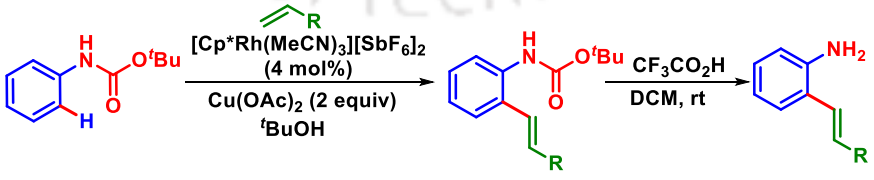

Scheme IV.2.4. *Carbamate-directed C–H activation.*

Recently, Li and co-workers developed a method that enables the Rh(III)-catalyzed C−H alkenylation of aryldiazenecarboxylates using acrylate esters as the alkenylating partner with concomitant hydrogenation of the N=N bond in the resulting product (Scheme IV.2.5).[16j]

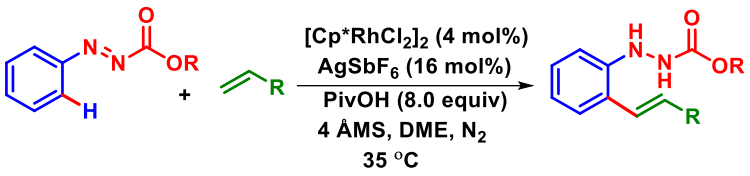

Scheme IV.2.5. *Olefination of aryldiazenecarboxylate.*

Yi *et al*. in 2017, disclosed a regioselective mono-alkenylation of arenes with polar acrylates using urea moiety as a transformable directing group.[16k] This Rh(III)-catalyzed and MeOH-involved *ortho* alkenylation utilizes transformable $NHCONMe_2$ directing group for the synthesis of *ortho* acrylated *N*-phenyl carbamates with good functional group tolerance delivering products in good to excellent yields. After the desired C–H functionalization, the solvent molecule *in situ* hydrolyzed urea substrate to a new functional moiety (Scheme IV.2.6).

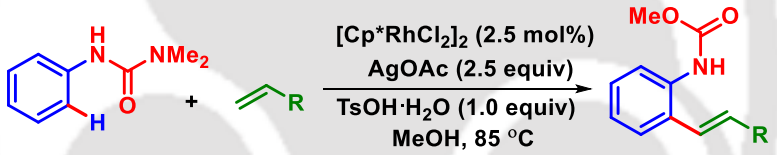

Scheme IV.2.6. *N-aryl urea as directing group for ortho-alkenylation.*

IV.3. Present Work

IV.3.1. Our approach

Searching for new and innovative TDG, we came across a relatively unexplored phenyl isocyanate moiety. To the best of our knowledge, in DG-assisted C–H activation reactions, alkyl and phenyl isocyanates have been widely employed only as reacting partner due to their strong electrophilic nature.[17] The inertness of phenyl isocyanate towards proximal C–H activation is attributed to the strategic structure of the functional group. Despite having both *N* and *O* atoms, its σ-donor ability is very less as both are unable to form metallacycles by coordinating with neighbouring C–H bonds. Hence, the use of phenyl isocyanate as a directing group in the proximal C–H bond activation is completely unexplored. To exploit this inertness, herein we report an efficient synthesis of *o*-alkenylanilines *via* a regioselective *o*-C–H

olefination using phenyl isocyanate as the transient directing group under Ru catalysis (Scheme IV.3.1).

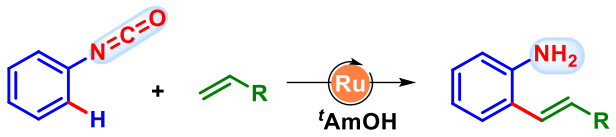

Scheme IV.3.1. *Phenyl isocyanate as transformable directing group.*

We commenced our investigation using *p*-tolyl isocyanate (**2**) and methyl acrylate (**a**) as the coupling partner in the presence of $[Ru(p\text{-cymene})Cl_2]_2$ (5 mol %), $AgSbF_6$ (15 mol %), $Cu(OAc)_2{\cdot}H_2O$ (0.5 equiv), and *tert*-amyl alcohol (^{t}AmOH) (2 mL) in a sealed tube at 120 ^{o}C. To our delight, a yellow fluorescent spot was observed which was isolated and identified by spectroscopic analysis (^{1}H NMR, ^{13}C{^{1}H} NMR, and IR) as an *ortho*-olefinated product of *p*-tolylaniline (**2a**). The new product was obtained in a satisfactory yield of 78%. XRD analysis of one of the substrates reconfirmed its structure to be *p*-tolyl (*E*)-3-(2-amino-5-methylphenyl)acrylate (**1l**) (Figure IV.3.1).

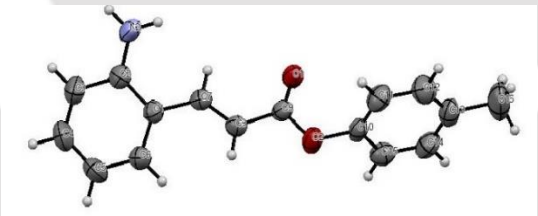

Figure IV.3.1. *ORTEP view of (**1l**) with 50% ellipsoid probability (CCDC 2165893).*

IV.3.2. Optimization of the reaction conditions

To further improve the yield, extensive screening of reaction parameters was conducted. In solvent screening, it was revealed that only alcoholic solvents gave a positive outcome while other solvents such as DMSO, DMF, and DCE were completely ineffective (Table IV.1, entries 2–8). Among the alcoholic solvents, ^{t}AmOH (78%) was found to be superior as compared to ^{t}BuOH (54%) and ^{i}PrOH (47%) (Table IV.1, entries 2 and 3). In case of EtOH and MeOH, *ortho*-olefinated ethyl *N*-phenylcarbamate (**I**) and methyl *N*-phenylcarbamate (**II**) were obtained in 37% and 41% yields respectively (Table IV.1, entries 4 and 5) (Figure IV.3.2 and Figure IV.3.3). Further, it was found that silver salts other than $AgSbF_6$, such as AgOAc, AgOTf, $AgNO_3$ and $AgOCOCF_3$ failed to improve the yield beyond 78% (Table IV.1, entries 9–12). Keeping $AgSbF_6$ as the additive, further screening was done to get the suitable oxidant for this protocol.

***Table IV.1**. Optimization of the reaction conditions*[a,b]

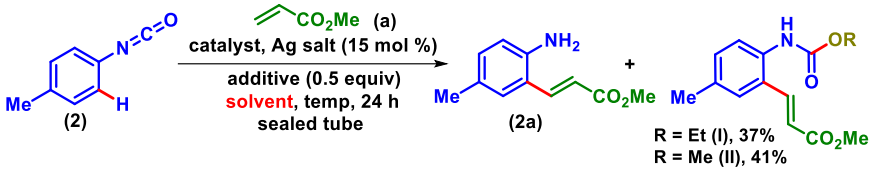

Entry	Catalyst (mol %)	Additive/Oxidant	Solvent	Temp (°C)	Yield[b]
1.	**[Ru(*p*-cymene)Cl_2]$_2$ (5)**	**$AgSbF_6$/ $Cu(OAc)_2.H_2O$**	**^{t}AmOH**	**120**	**78**
2.	[Ru(*p*-cymene)Cl_2]$_2$ (5)	$AgSbF_6$/ $Cu(OAc)_2.H_2O$	^{t}BuOH	120	54
3.	[Ru(*p*-cymene)Cl_2]$_2$ (5)	$AgSbF_6$/ $Cu(OAc)_2.H_2O$	^{i}PrOH	120	47
4.	[Ru(*p*-cymene)Cl_2]$_2$ (5)	$AgSbF_6$/ $Cu(OAc)_2.H_2O$	EtOH	120	37[c]
5.	[Ru(*p*-cymene)Cl_2]$_2$ (5)	$AgSbF_6$/ $Cu(OAc)_2.H_2O$	MeOH	120	41[c]
6.	[Ru(*p*-cymene)Cl_2]$_2$ (5)	$AgSbF_6$/ $Cu(OAc)_2.H_2O$	DMSO	120	N.D
7.	[Ru(*p*-cymene)Cl_2]$_2$ (5)	$AgSbF_6$/ $Cu(OAc)_2.H_2O$	DMF	120	N.D
8.	[Ru(*p*-cymene)Cl_2]$_2$ (5)	$AgSbF_6$/ $Cu(OAc)_2.H_2O$	DCE	120	N.D
9.	[Ru(*p*-cymene)Cl_2]$_2$ (5)	AgOAc/$Cu(OAc)_2.H_2O$	^{t}AmOH	120	N.D
10.	[Ru(*p*-cymene)Cl_2]$_2$ (5)	AgOTf/$Cu(OAc)_2.H_2O$	^{t}AmOH	120	10
11.	[Ru(*p*-cymene)Cl_2]$_2$ (5)	$AgNO_3$/$Cu(OAc)_2.H_2O$	^{t}AmOH	120	<5
12.	[Ru(*p*-cymene)Cl_2]$_2$ (5)	$AgOCOCF_3$/$Cu(OAc)_2.H_2O$	^{t}AmOH	120	15
13.	[Ru(*p*-cymene)Cl_2]$_2$ (5)	$AgSbF_6$/$CuCl_2.2H_2O$	^{t}AmOH	120	N.D
14.	[Ru(*p*-cymene)Cl_2]$_2$ (5)	$AgSbF_6$/$Cu(CH_3CN)_4PF_6$	^{t}AmOH	120	N.D
15.	[Ru(*p*-cymene)Cl_2]$_2$ (5)	$AgSbF_6$/Cu_2O	^{t}AmOH	120	N.D
16.	[Ru(*p*-cymene)Cl_2]$_2$ (5)	$AgSbF_6$/CuI	^{t}AmOH	120	N.D
17.	[Ru(*p*-cymene)Cl_2]$_2$ (5)	$AgSbF_6$/$CuBr_2$	^{t}AmOH	120	N.D
18.	[Ru(*p*-cymene)Cl_2]$_2$ (7)	$AgSbF_6$/$Cu(OAc)_2.H_2O$	^{t}AmOH	120	73
19.	[Ru(*p*-cymene)Cl_2]$_2$ (3)	$AgSbF_6$/$Cu(OAc)_2.H_2O$	^{t}AmOH	120	50
20.	[Ru(*p*-cymene)Cl_2]$_2$ (5)	$AgSbF_6$/$Cu(OAc)_2.H_2O$	^{t}AmOH	110	68
21.	[Ru(*p*-cymene)Cl_2]$_2$ (5)	$AgSbF_6$/$Cu(OAc)_2.H_2O$	^{t}AmOH	130	75

[a]Reaction conditions: **1** (0.5 mmol), **a** (1 mmol, 2 equiv), [Ru(*p*-cymene)Cl_2]$_2$ (5 mol %), additive (15 mol %), oxidant (0.5 equiv), solvent (2 mL) in a sealed tube, 120 °C, 24 h. [b]Isolated yield of the product. [c]Non-anticipated product formation.

It was found that the use of various copper salts such as $CuCl_2 \cdot 2H_2O$, $Cu(CH_3CN)_4PF_6$, Cu_2O, CuI, $CuBr_2$ were all unable to improve the yield as compared to the use of $Cu(OAc)_2 \cdot H_2O$. (Table IV.1, entries 13–17). Thus, $Cu(OAc)_2 \cdot H_2O$ served as the best oxidant for our protocol. An increase (7 mol %) or a decrease (3 mol %) in the catalyst loading had a detrimental effect on the product yield (Table IV.1, entries 18 and 19). Similarly, the yield of the reaction at lower (100 °C) and higher (130 °C) temperatures was found to be inferior to that of at 120 °C (Table IV.1, entries 20 and 21). Based on our extensive screening of different solvents, additives, and catalysts; the best condition for the present alkenylation strategy was determined to include phenyl isocyanate (**1**) (1 equiv), methyl acrylate (**a**) (2 equiv), [Ru(*p*-cymene)Cl_2]$_2$ (5 mol %), $AgSbF_6$ (15 mol %), $Cu(OAc)_2 \cdot H_2O$ (0.5 equiv), and ^{t}AmOH (2 mL) in a 21 mL sealed tube at 120 °C for 24 h (Table IV.1, entry 1).

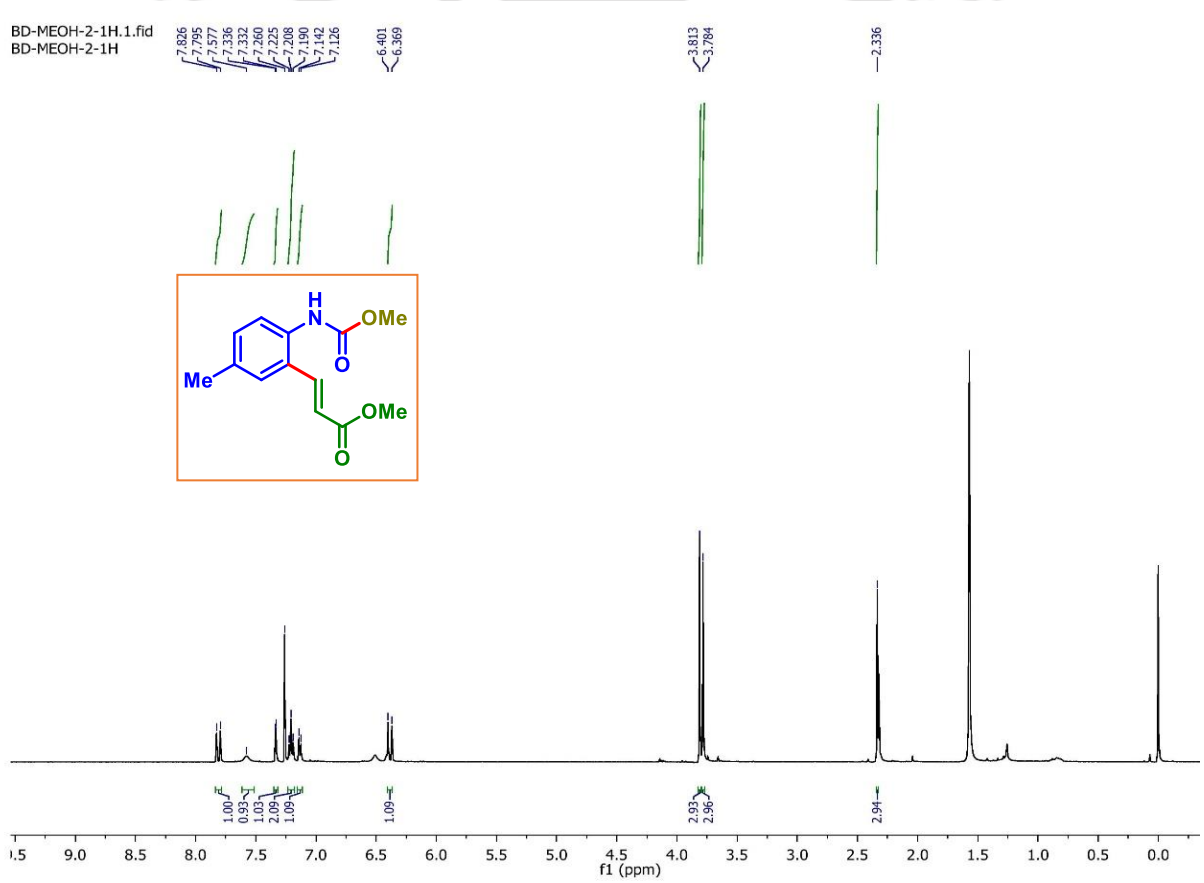

Figure IV.3.2. *^{1}H NMR spectra of **II** ($CDCl_3$, 500 MHz).*

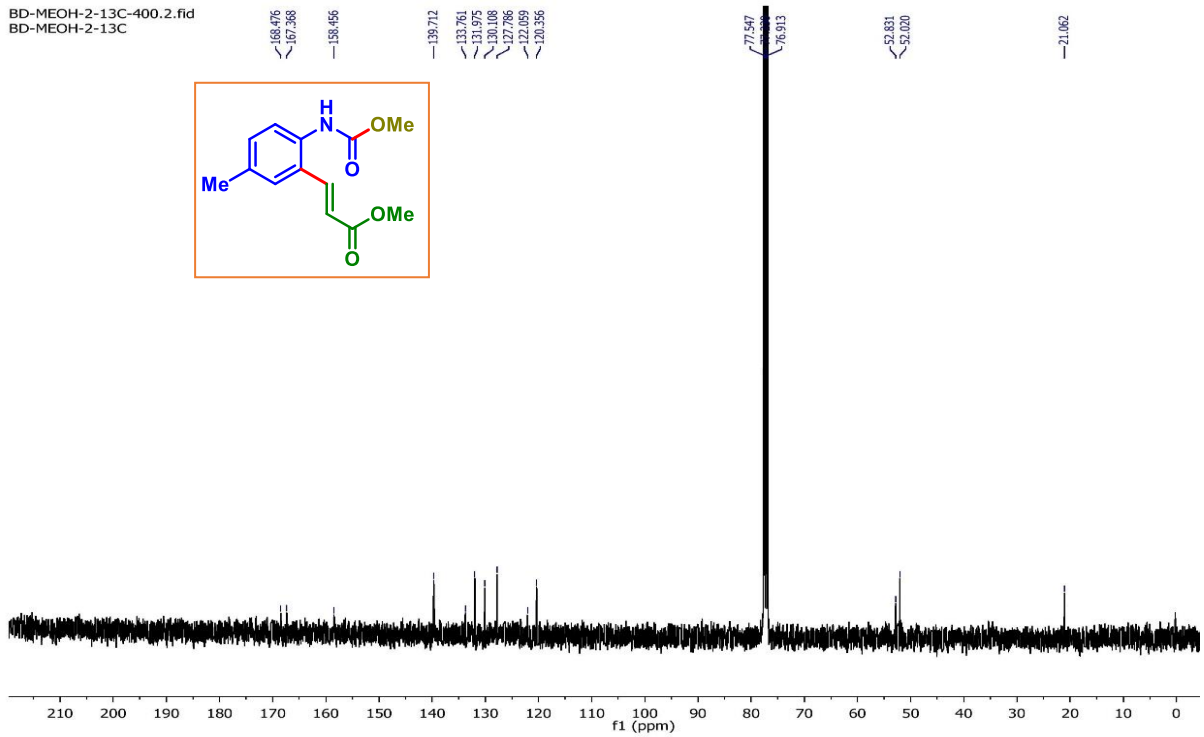

Figure IV.3.3. *$^{13}C\{^{1}H\}$ NMR spectra of* ***II*** *($CDCl_3$, 100 MHz).*

IV.3.3. Substrate scope of phenyl isocyanate and acrylates

With the established conditions in our hand, a series of acrylates (**a–q**) were treated with phenyl isocyanate (**1**) to produce *ortho*-alkenylated anilines (**1a–1q**) in good to moderate yields (47–77%) (Scheme IV.3.2). It was observed that the yields of the anticipated *o*-alkenylanilines decreased for long-chain and branched acrylates compared to those of their short-chain and linear analogues. Acrylates such as methyl (**a**), ethyl (**b**), *n*-butyl (**c**), *n*-hexyl (**d**), lauryl (**e**), stearyl (**f**), isobutyl (**g**), and *tert*-amyl acrylate (**h**) were successfully converted into their *ortho*-alkenylated products **1a** (77%), **1b** (73%), **1c** (69%), **1d** (61%), **1e** (59%), **1f** (53%), **1g** (70%), and **1h** (66%), respectively. In addition, 2-methoxyethyl (**i**), 2-methyl tetrahydrofuran (**j**), benzyl (**k**), aromatic acrylates (**l** and **m**), hexafluoroisopropyl (**n**), and isoborenyl acrylates (**o**) were all well-tolerated irrespective of their electronic and steric effects and delivered corresponding *o*-alkenylated aniline **1i** (62%), **1j** (55%), **1k** (63%), **1l** (67%), **1m** (66%) and **1n** (71%) in moderate to good yields. To show the diversification of the protocol presented here, homomyrtenol (**p**) and cholesterol-derived acrylate (**q**) yielded their anticipated *o*-alkenylanilines (**1p**) and (**1q**) in 55% and 47% yields respectively. Further, on the gram scale, the reaction delivered 56% of the product **1a** when treated phenyl isocyanate (**1**) with acrylate (**a**) (Scheme IV.3.2).

Scheme IV.3.2. *Substrate scope of different acrylates*[a,b,c]

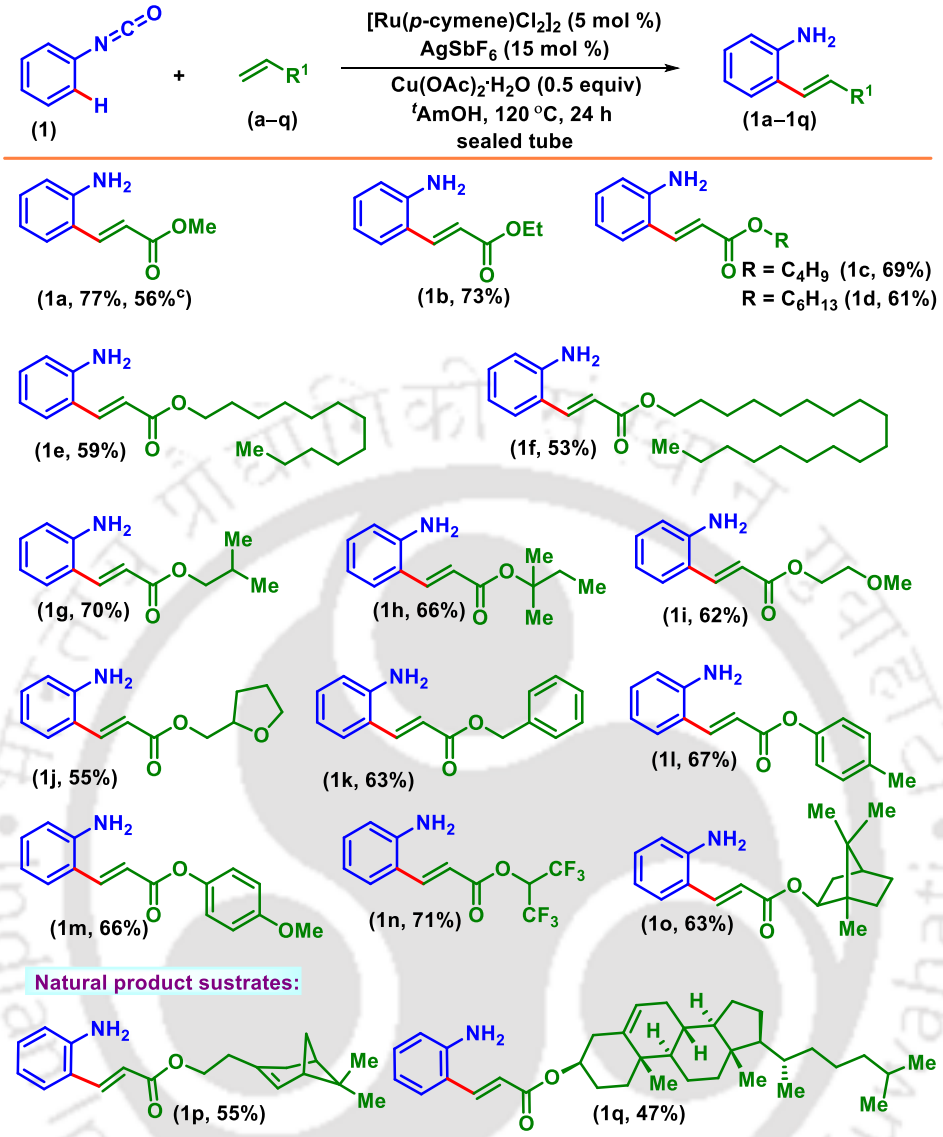

[a]Reaction conditions: **1** (0.5 mmol), **a**–**q** (1 mmol), [Ru(*p*-cymene)Cl_2]$_2$ (5 mol %), $AgSbF_6$ (15 mol %), $Cu(OAc)_2{\cdot}H_2O$ (0.5 equiv), and ^{t}AmOH (2 mL) in a sealed tube, 120 °C, 24 h. [b]Isolated yield of the product. [c]On a 7 mmol scale.

Next, the viability of this methodology was tested with various phenyl isocyanates (**2–13**) and acrylates (**a**–**c**, **g**, and **r**) (Scheme IV.3.3). Thus, *p*-tolyl isocyanate (**2**) upon reaction with methyl (**a**), ethyl (**b**), butyl (**c**), isobutyl (**g**) and dodecafluoroheptyl acrylate (**r**) afforded their corresponding products **2a** (78%), **2b** (76%), **2c** (74%), **2g** (73%), and **2r** (58%), respectively, in moderate yields. Likewise, *p*-*tert*-butylphenyl isocyanate (**3**) provided the anticipated product (**3a**, 65%) in good yields. The reaction showed a satisfactory outcome with *p*-fluorophenyl isocyanate (**4**) and different acrylates, *viz*., methyl (**a**), ethyl (**b**), and isobutyl (**g**).

Scheme IV.3.3. *Scopes of different phenyl isocyanates with acrylates*[a,b]

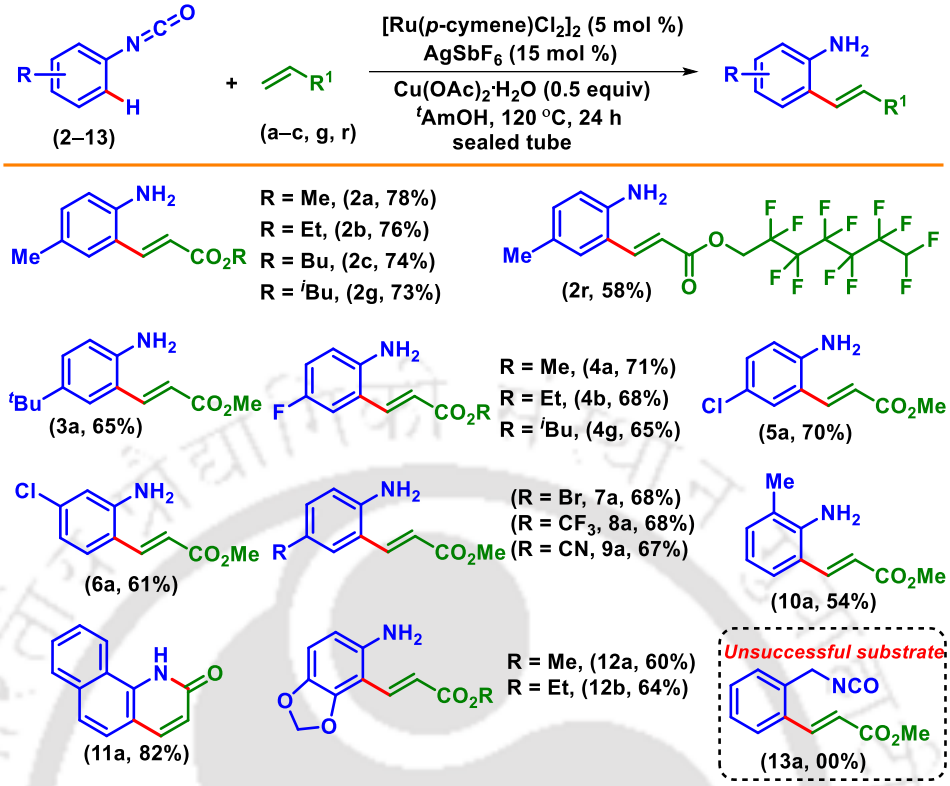

[a]Reaction conditions: **2**–**13** (0.5 mmol), **a**–**c**, **g**, or **r** (1 mmol), [Ru(*p*-cymene)Cl_2]$_2$ (5 mol %), $AgSbF_6$ (15 mol %), $Cu(OAc)_2{\cdot}H_2O$ (0.5 equiv), and ^{t}AmOH (2 mL) in a sealed tube, 120 °C, 24 h. [b]Isolated yield of the product.

Phenyl isocyanates having different electron-withdrawing groups such as *p*-Cl (**5**), *m*-Cl (**6**), *p*-Br (**7**), *p*-CF_3 (**8**), and *p*-CN (**9**) reacted smoothly with methyl acrylate (**a**), producing **5a** (70%), **6a** (61%), **7a** (68%), **8a** (68%), and **9a** (67%), respectively, in good yields. An *ortho*-substituted isocyanate (**10**) was successfully employed under standard conditions, yielding the corresponding product (**10a**) in 54% yield. Surprisingly, 1-naphthyl isocyanate (**11**) afforded the corresponding azacoumarin **11a** in 82% yield under the standard conditions (Scheme IV.3.3) instead of methyl (*E*)-3-(1-aminonaphthalen-2-yl)acrylate. This might be due to the ease in accessibility of the ester group to undergo aminolysis. The reaction of heterocycle-fused isocyanate 5-isocyanatobenzo[*d*][1,3]dioxole (**12**) proceeded smoothly with methyl (**a**) and ethyl acrylate (**b**), affording the corresponding *o*-alkenylanilines [**12a** (60%), and **12b** (64%) respectively] in moderate yields. On the contrary, benzyl isocyanate (**13**) failed to give the anticipated olefinated product; instead, benzylamine was obtained as the major product (Scheme IV.3.3). This might be due to the inability to form a six-membered ruthenocycle

intermediate. The corresponding carbamate of benzyl isocyanate reacts with another molecule of ^{t}AmOH to give benzylamine and di-*tert*-amyl carbonate.[12f]

IV.3.4. Mechanistic studies

IV.3.4.1. Intramolecular competitive experiment

After synthesizing a library of *o*-alkenylanilines, we performed a few control experiments to improve our understanding of the mechanism (Scheme IV.3.4). To assess the electronic effect of substituents on phenyl isocyanates, an equimolar mixture of *p*-tolyl isocyanate (**2**) and *p*-fluorophenyl isocyanate (**4**) was reacted with methyl acrylate (**a**). The corresponding *o*-alkenylanilines **2a** and **4a** were obtained in nearly identical yields (1:0.93) suggesting the negligible electronic effect (Scheme IV.3.4).

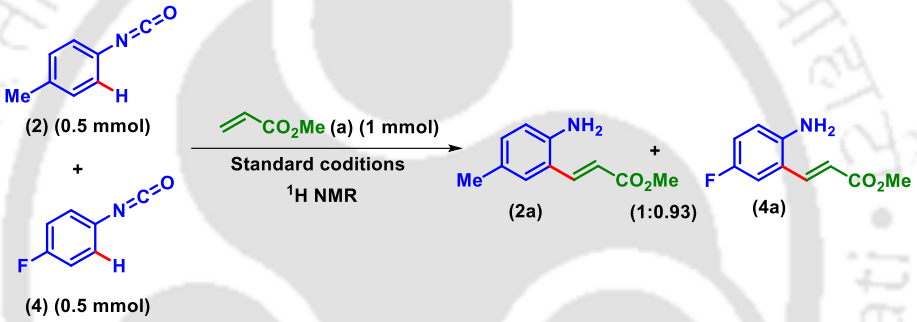

Scheme IV.3.4. *Intermolecular competitive experiment.*

IV.3.4.2. Kinetic Isotope Effect (KIE)

To understand the C–H activation process, the kinetic isotope effect (KIE) was measured based on parallel reactions between phenyl isocyanate (**1**) and its deuterated analogue (**1*d*$_5$**) with methyl acrylate (**a**). The measured KIE value (k_H/k_D = 4) indicates that C–H bond cleavage is the rate-determining step (RDS) (Scheme IV.3.5).

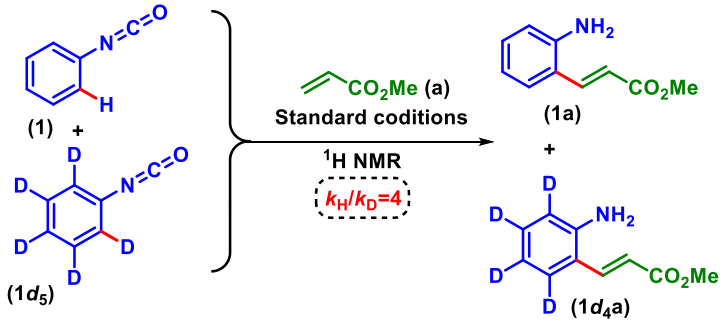

Scheme IV.3.5. *Determination of KIE value.*

IV.3.4.3. Synthesis of carbamate intermediate

To ascertain the exact role of the solvent, phenyl isocyanate was treated with ^{t}AmOH at 120 °C. The nucleophilic attack by the solvent results in the synthesis of *tert*-pentyl phenylcarbamate (**P**) in 93% yield (Scheme IV.3.6).

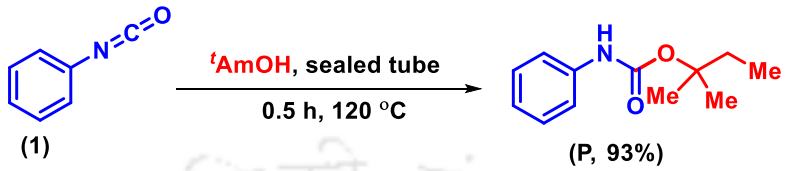

Scheme IV.3.6. *Ex-situ isolation of carbamte intermediate (P).*

Then, the carbamate (**P**) was then subjected to standard reaction conditions, and the anticipated product **1a** was obtained in 75% yield (Scheme IV.3.7). This indicates that ^{t}AmOH acts as a transient directing mediator, and this protocol proceeds *via* carbamate-assisted C−H ruthenation.

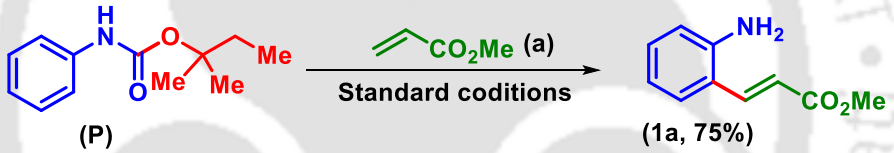

Scheme IV.3.7. *Treatment of isolated carbamate in the standard reaction conditions.*

IV.3.4.4. Dual role of solvent ^{t}AmOH

Next, a standard reaction was performed taking only 5 equiv of ^{t}AmOH in DCE solvent. The anticipated product was obtained in a lower yield (35%) compared to that when ^{t}AmOH (77%) was used as the solvent. This confirms the dual role of ^{t}AmOH as a solvent-cum transient directing mediator (TDM) (Scheme IV.3.8).

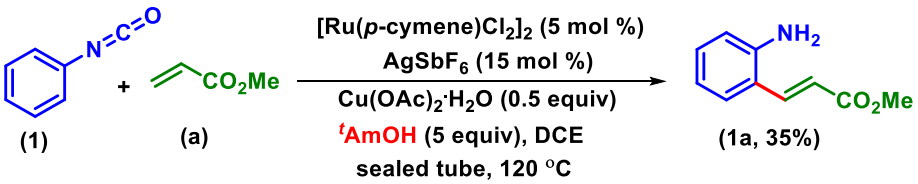

Scheme IV.3.8. *Examination of role of other solvent.*

IV.3.5. Plausible reaction mechanism

On the basis of the control experiments and literature precedent,[6f,12a,16h,18] a plausible mechanism for the *ortho* alkenylation (**1** with **a**) is illustrated in Scheme IV.3.9. Initially, the nucleophilic attack of the solvent ^{t}AmOH on the phenyl isocyanate (**1**) forms a carbamate intermediate (**P**). The *in situ*-generated carbamate coordinates to the ruthenium center *via* the carbonyl oxygen. This coordination triggers the activation of the proximal C(sp^2)–H bond forming a six-membered ruthenocycle intermediate (**A**). Intermediate **A** undergoes an olefin insertion to give intermediate **B** with subsequent elimination of acetic acid. Later, a β-hydride elimination gives the *ortho*-alkenylated carbamate (**C**). Finally, the acetic acid cleaves the *ortho*-alkenylated carbamate (**C**) to afford the final product (**1a**) with the release of 2-methylbut-2-ene (**E**) and carbon dioxide. The removal of carbamate depends on the stability of the carbocation formed after its cleavage to produce a substituted alkene. In the case of primary alcohol such as methanol and ethanol, the reaction stops prior to the removal of carbamate, which is due to the lower stability of the primary carbocation (Scheme IV.3.9).

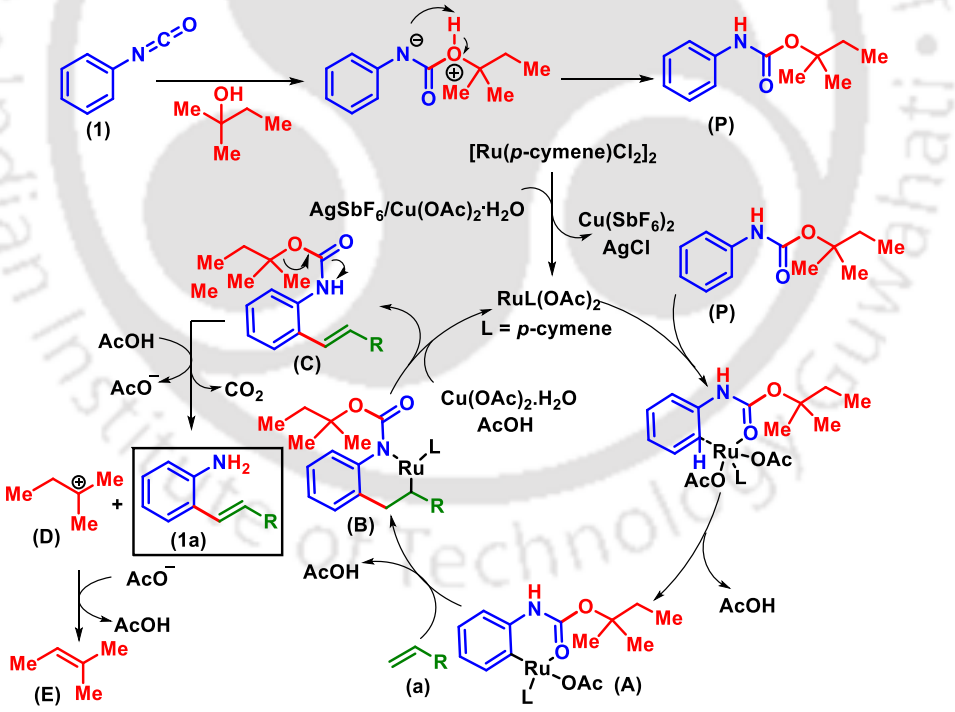

Scheme IV.3.9. *Proposed mechanism.*

IV.3.6. Post-synthetic modifications

The *ortho*-alkenylated anilines are widely used in the synthesis of useful bioactive compounds. To explore the synthetic utility of the protocol presented here, the synthesized

ortho-alkenylated anilines were subjected to various late-stage functionalizations. Treatment of *o*-alkenylanilines (**1a**, **2a**, **5a**, **6a**, and **8a**) with $Pd(OAc)_2$ resulted in the formation of azacoumarins **1a′**, **2a′**, **5a′**, **6a′**, and **8a′**, respectively *via* the nucleophilic attack of the amine on ester (Scheme IV.3.10). During the control experiments, we found that both Pd and Cu are indispensable for this transformation. Both Pd(II) and Cu(II) help in the *cis-trans* isomerization of the alkene bond that brings the ester group proximal to the amine group, which helps in the nucleophilic attack resulting in azacoumarins.[19a] Such azacoumarins are reported to have various biological activities, viz., anti-inflammatory, antimicrobial, anticancer, etc.[19b,c]

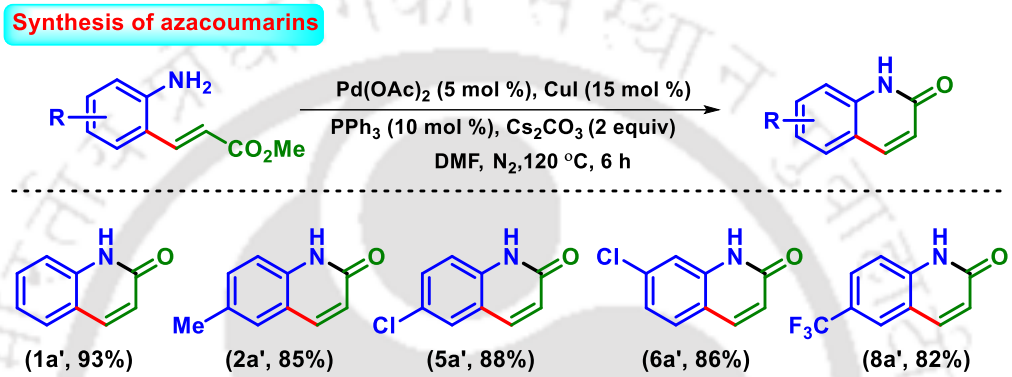

Scheme IV.3.10. *Synthesis of azacoumarin.*

On the contrary, a similar one-pot reaction in the presence of aryl iodides provided C-4 aryl-substituted azacoumarins **1ab** (86%), **2ab** (72%), **5ab** (76%), and **6ab** (75%) *via* Heck coupling followed by cyclization. Following this protocol, HBV inhibitor **5aa** was synthesized in 74% yield (Scheme IV.3.11).[19d]

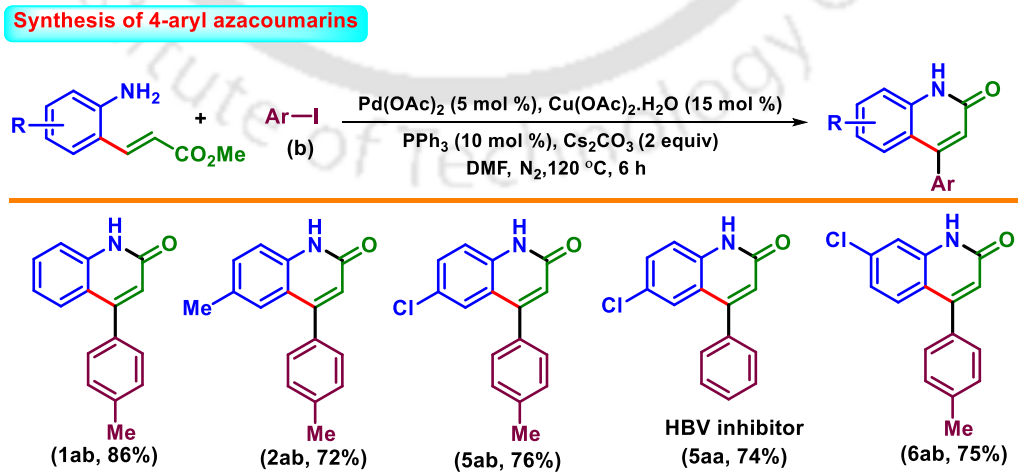

Scheme IV.3.11. *Synthesis of 4-aryl-azacoumarin.*

In addition, a Sonogashira coupling of a bromo-substituted product (**7a**) with 4-ethynyltoluene at 120 °C provided an alkynylated azacoumarin (**7ac′**) (Scheme IV.3.12.1),[22b] whereas the same reaction at 60 °C gave only alkynylation of **7a** (Scheme IV.3.12.2).

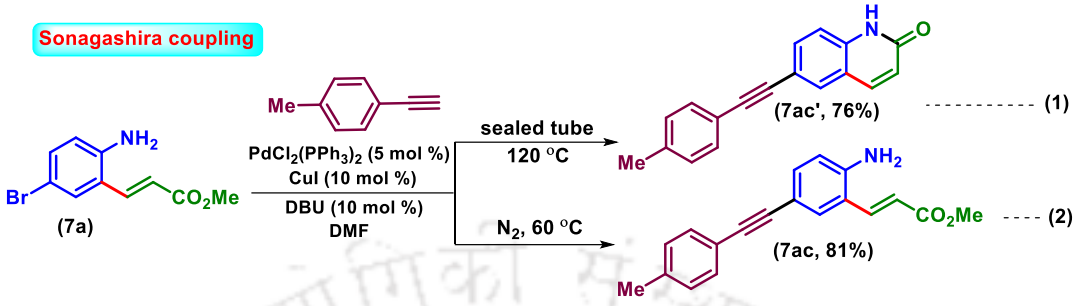

Scheme IV.3.12. *Sonogashira coupling.*

Further, if desired, the amino group can be easily removed *via* photochemical diazotization. Following this, deamination of **1a** gave methyl cinnamate in 65% yield (Scheme IV.3.13).[22c]

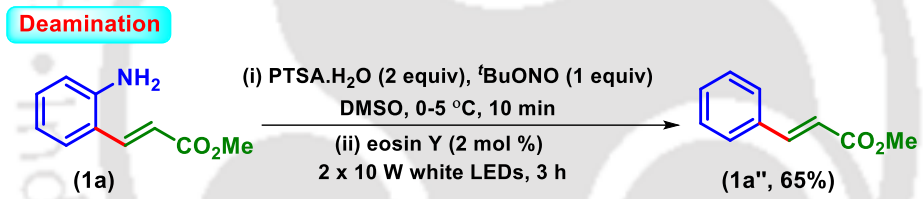

Scheme IV.3.13. *Deamination of o-alkylaniline.*

IV.3.7. Conclusion:

In summary, we have developed a Ru-catalyzed *ortho*-olefination strategy using phenyl isocyanate as a transformable transient directing group. *tert*-Amyl alcohol not only serves as a transient directing mediator (TDM) by forming its carbamate *in situ* but also as an effective solvent. An isotope labeling experiment (k_H/k_D = 4) established that irreversible C–H bond cleavage is the rate-limiting step. The salient features of this protocol are the broad substrate scope in terms of phenyl isocyanate and acrylates, no requirement for external TDM, and *in situ* transformation of the transient directing group (NCO to NH_2). The olefinated anilines were successfully transformed into azacoumarins and C-4 aryl-substituted azacoumarins. The scalability of the reaction demonstrates the practical acceptability of the phenyl isocyanates as a transient directing group.

IV.4. Experimental Section:

IV.4.1. General information:

All the reagents were commercial grade and used without further purification unless otherwise stated. Phenyl isocyanates (**1**–**13**) and acrylates (**a**–**q**) are obtained from commercial sources unless mentioned specifically and used without further purification. All the reactions were carried out in an oven-dried pressure tube (20.3 cm x 19 mm, 21 mL) (Figure IV.4.1) under aerobic conditions. Reactions were monitored by thin layer chromatography (TLC) on a 0.25 mm silica gel plates ($60F_{254}$) and visualized under UV illumination at 254 nm. Organic extracts were dried over anhydrous sodium sulfate (Na_2SO_4). Column chromatography was performed to purify the crude product on silica gel 60–120 mesh using a mixture of hexane and ethyl acetate as eluent. The isolated compounds were characterized by spectroscopic [^{1}H, ^{13}C{^{1}H} NMR, and IR] techniques and HRMS analysis. NMR spectra were recorded in deuterochloroform ($CDCl_3$) and in some cases deuterated dimethyl sulfoxide. ^{1}H, ^{13}C{^{1}H} were recorded in 500 (125) or 400 (100) MHz spectrometer and were calibrated using tetramethylsilane or residual undeuterated solvent for ^{1}H NMR, deuterochloroform for ^{13}C NMR as an internal reference {$Si(CH_3)_4$: 0.00 ppm or $CHCl_3$: 7.260 ppm for ^{1}H NMR, 77.230 ppm for ^{13}C NMR}. ^{19}F NMR was calibrated without any internal standard in $CDCl_3$. The chemical shifts are quoted in δ units, parts per million (ppm). ^{1}H NMR data is represented as follows: Chemical shift, multiplicity (s = singlet, d = doublet, t = triplet, q = quartet, m = multiplet, dd = doublet of doublet, dt = doublet of triplet), integration and coupling constant(s) *J* in hertz (Hz). High-resolution mass spectra (HRMS) were recorded on a mass spectrometer using electrospray ionization-time of flight (ESI-TOF) reflection experiments. FT-IR spectra were recorded in neat and reported in the frequency of absorption (cm^{-1}).

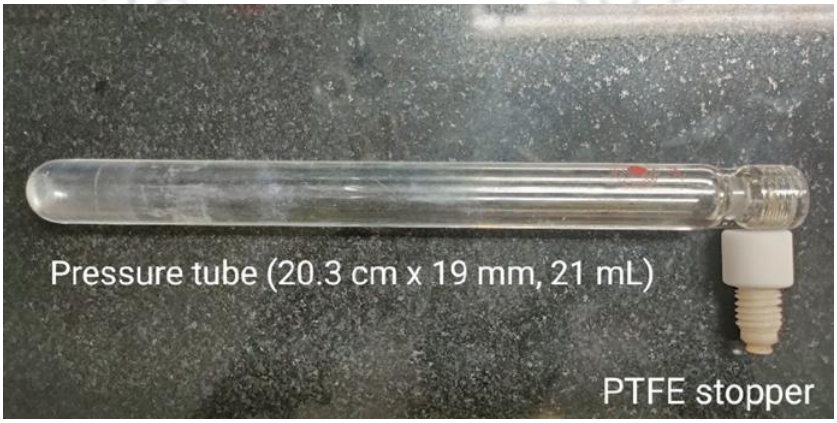

Figure IV.4.1. Pressure tube.

IV.4.2. Crystallographic information:

Sample preparation: The single crystal of compound **1l** was prepared by the slow evaporation method for which 10 mg of the compound (**1l**) was dissolved in 1 mL of DCM in a clean and dry 10 mL glass vial. MeOH (0.5 mL) was added to this solution slowly with a dropper. The mouth of the glass vial was covered with a cap having a small hole and kept for slow evaporation at room temperature. Crystals of **1l** were obtained after approximately 3–4 days as a transparent block-shaped crystal.

Data collection: Crystal data were collected with Bruker Smart Apex-II CCD diffractometer using graphite monochromated MoKα radiation (λ = 0.71073Å) at 273 K. Cell parameters were retrieved using SMART[20a] software and refined with SAINT[20a] on all observed reflections. Data reduction was performed with the SAINT software and corrected for Lorentz and polarization effects. Absorption corrections were applied with the program SADABS[20b]. The structure was solved by direct methods implemented in SHELXT 2014/5 (Sheldrick, 2014)[20c] program and refined by full-matrix least-squares methods on F2. All non-hydrogen atomic positions were located in different Fourier maps and refined anisotropically. The hydrogen atoms were placed in their geometrically generated positions. Yellowish crystals were isolated in rod-shaped from DCM at room temperature.

Crystallographic description of *p-tolyl (E)-3-(2-aminophenyl)acrylate* (1l):

$C_{16}H_{15}NO_2$, crystal dimensions 0.28 x 0.22 x 0.16 mm, M_r = 253.29, Monoclinic, space group P/21 c, a = 6.0711(5), b = 29.030(2), c =7.8308(6) Å, α = 90°, β = 98.105(2)°, γ = 90°, V = 1366.35(18) Å^3, Z = 4, ρ = 1.231 g/cm^3, μ = 0.081 mm^{-1} , F(000)= 536.0, reflection collected / unique = 1953 / 2389, refinement method = full-matrix least-squares on F^2, final R indices [I > 2\s(I)]: R_1 = 0.0782, wR_2 = 0.2424, R indices (all data): R_1 = 0.079, wR_2 = 0.2195, goodness of fit = 1.220; CCDC = 2165893 for ***p-tolyl (E)-3-(2-aminophenyl)acrylate*** **(1l)** contains the supplementary crystallographic data for this paper. These data can be obtained free of charge from The Cambridge Crystallographic Data Centre via www.ccdc.cam.ac.uk/data_request/cif.

IV.4.3. General procedures:

IV.4.3.1. General procedure for the synthesis of acrylates (h, l, m, p, q)

The acrylates (**h**, **l**, **m**, **p**, **q)** were synthesized according to the modified literature procedure.[21a]

IV.4.3.2. General procedure for the synthesis of alkyl/aryl (*E*)-3-(2-aminophenyl)acrylate (**1a**)

An oven-dried pressure tube (20.3 cm x 19 mm, 21 mL) equipped with a magnetic bar was charged with phenyl isocyanate (**1**, 0.5 mmol, 60 mg), $Cu(OAc)_2$. H_2O (0.25 mmol, 50 mg), $AgSbF_6$ (0.075 mmol, 26 mg), $[Ru(p\text{-cymene})Cl_2]_2$ (0.025 mmol, 15.3 mg), acrylate (**a**, 0.5 mmol) and *tert*-amyl alcohol (2 mL). The reaction mixture was allowed to stir for 24 h at 120 ^oC. After 24 h, the reaction mixture was filtered through a thin bed of celite. The filtrate was evaporated and admixed with EtOAc (20 mL). The organic layer was washed with water (2 x 10 mL), followed by brine solution (1 x 5 mL). The organic layer was dried over anhydrous Na_2SO_4 and solvent and concentrated under reduced pressure. The crude product thus obtained was purified over a column of silica gel using hexane and ethyl acetate in (9:1) to give pure methyl (*E*)-3-(2-aminophenyl)acrylate (**1a**) in 77% yield. The identity and purity of the product were confirmed by spectroscopic analysis.

IV.4.4. Mechanistic investigations

IV.4.4.1. Intermolecular competitive experiment

An oven-dried pressure tube (20.3 cm x 19 mm, 21 mL) equipped with a magnetic bar was charged with *p*-tolyl phenyl isocyanate (**2)** (0.5 mmol, 67 mg), 4-fluorophenyl isocyanate (**4**) (0.5 mmol, 69 mg), $Cu(OAc)_2$. H_2O (0.25 mmol, 50 mg), $AgSbF_6$ (0.075 mmol, 26 mg), $[Ru(p\text{-cymene})Cl_2]_2$ (0.025 mmol, 15.3 mg), methyl acrylate (**a**) (1 mmol) and *tert*-amyl alcohol (2 mL). The reaction mixture was allowed to be stirred for 24 h at 120 ^oC. After completion, the reaction mixture was filtered through a thin bed of celite. The filtrate was evaporated and diluted with EtOAc (20 mL). The organic layer was washed with water (2 x 10 mL) followed by a saturated brine solution (1 x 5 mL). The organic layer was dried over anhydrous Na_2SO_4 and solvent and concentrated under reduced pressure. The crude product so obtained was purified over a column of silica gel using hexane and ethyl acetate (17:3) to give a mixture of methyl (*E*)-3-(2-amino-5-methylphenyl)acrylate (**2a**) and methyl (*E*)-3-(2-amino-

5-fluorophenyl)acrylate (**4a**) (Scheme IV.4.4.1). The ratio of the product obtained for **2a**:**4a** was (1:0.93) (as determined from ^{1}H spectra) (Figure IV.4.2).

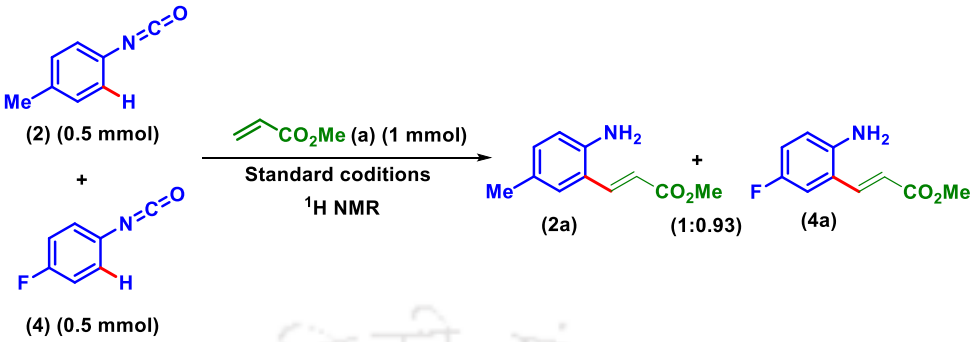

Scheme IV.4.4.1. *Intermolecular competitive experiment.*

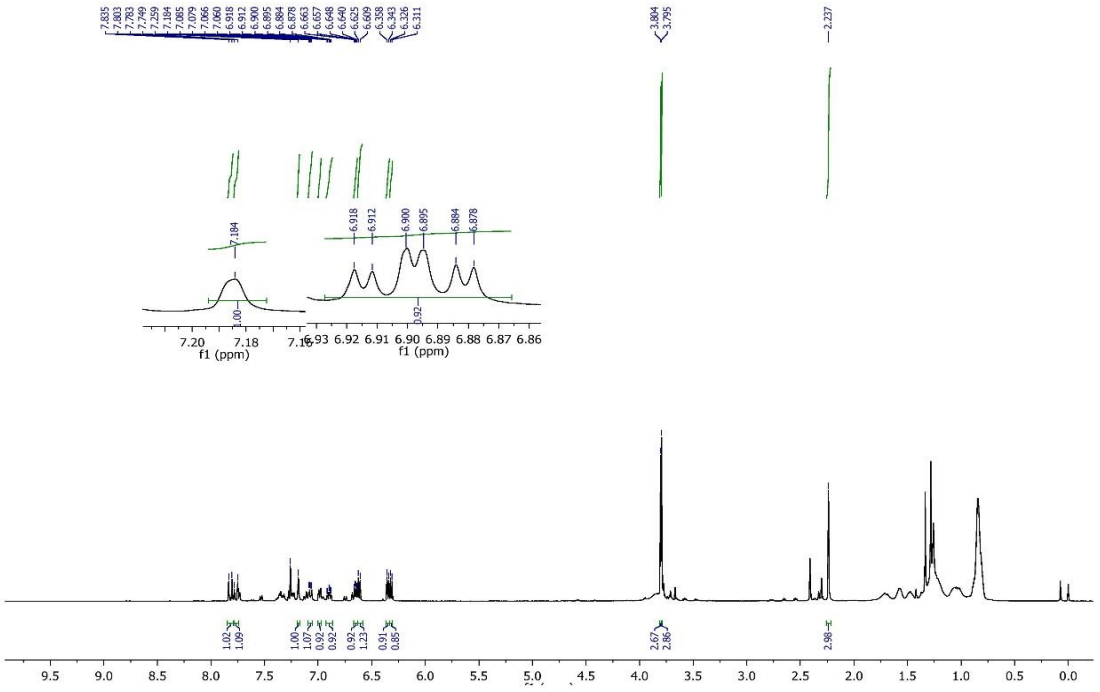

Figure IV.4.2. *^{1}H NMR spectra of intermolecular competitive experiment ($CDCl_3$, 500 MHz).*

IV.4.4.2. Synthesis of phenyl isocyanate-d_5 (**1d_5**):

The deuterated phenyl isocyanate (**1d_5**) was synthesized according to the modified literature procedure.[22a] ^{13}C {^{1}H} spectra of the product confirm the deuteration of phenyl isocyanate (**1d_5**).

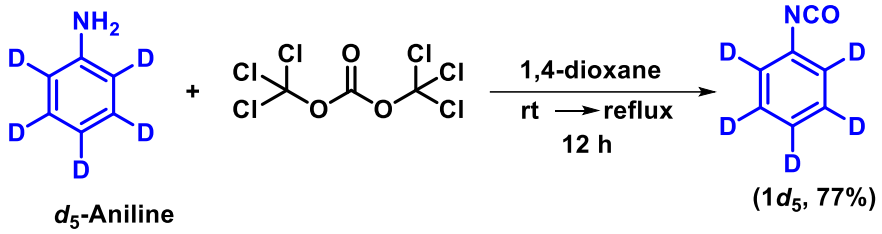

Scheme IV.4.4.2. *Synthesis of deuterated phenyl isocyanate.*

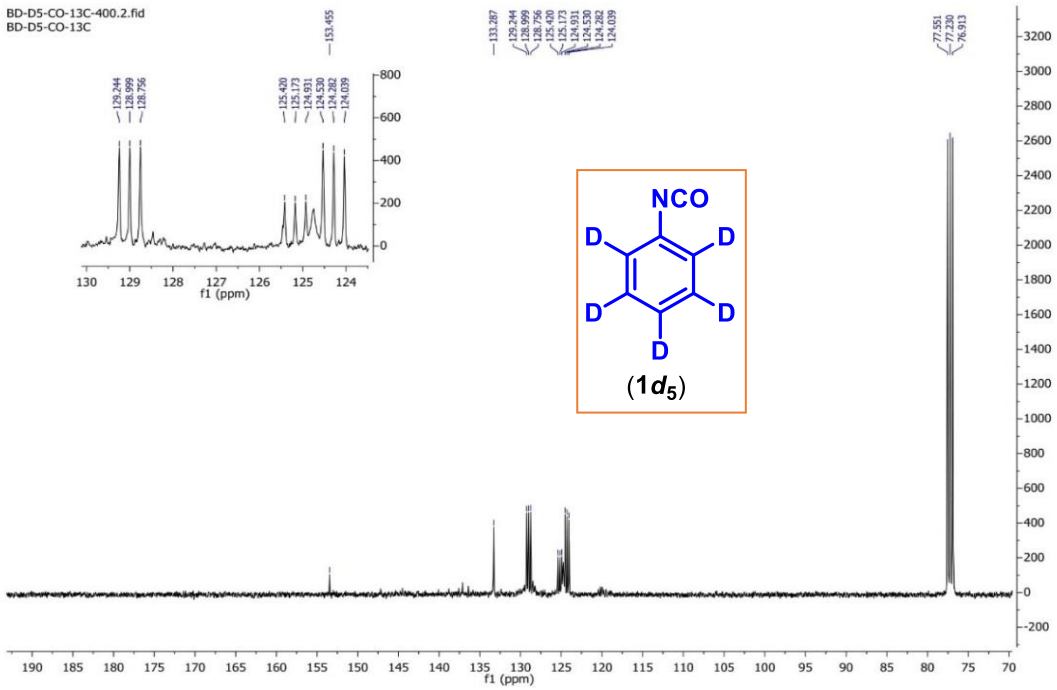

Figure IV.4.3. *$^{13}C\{^1H\}$ NMR spectra of* ***1d*$_5$** *($CDCl_3$, 100 MHz).*

IV.4.4.3. Kinetic isotope experiment

An oven-dried pressure tube (20.3 cm x 19 mm, 21 mL) equipped with a magnetic bar was charged with phenyl isocyanate (**1**) (0.5 mmol, 67 mg), phenyl isocyanate-d_5 (**1*d*$_5$**) (0.5 mmol, 62 mg), $Cu(OAc)_2.H_2O$ (0.25 mmol, 50 mg), $AgSbF_6$ (0.075 mmol, 26 mg), [Ru(*p*-cymene)Cl_2]$_2$ (0.025 mmol, 15.3 mg), methyl acrylate (**a**, 1 mmol) and *tert*-amyl alcohol (2 mL). The reaction mixture was heated in an oil bath for 24 h at 120 ^oC. After 24 h, the reaction mixture was filtered through a thin bed of celite. The filtrate was evaporated and diluted with EtOAc (20 mL). The organic layer was washed with water (2 x 10 mL), followed by brine solution (2 x 5 mL). The organic layer was dried over anhydrous Na_2SO_4 and solvent and concentrated under reduced pressure. The crude product so obtained was purified over a column of silica gel using hexane and ethyl acetate (10:1) to give a mixture of expected

products methyl (*E*)-3-(2-aminophenyl)acrylate (**1a**) and methyl (*E*)-3-(2-aminophenyl-3,4,5,6-d$_4$)acrylate (**1*d*$_4$a**) respectively (Scheme IV.4.4.3) (Figure IV.4.4).

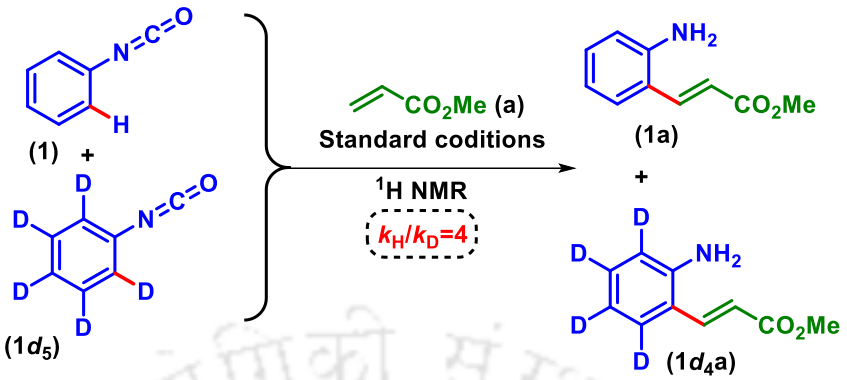

Scheme IV.4.4.3. *Determination of KIE value.*

The ratio of the deuterated (**1*d*$_4$a**) and non-deuterated (**1a**) product was calculated on the basis of the integration ratio of the aromatic proton peak at 7.38–7.37 (obtained as doublets) and an alkene doublet proton peak at 7.85–7.82 (Figure IV.4.4).

Calculation:

For one proton at 7.83, the integration value is 1.00.

Thus, for a single proton, the integration corresponds to 1.00/1 = 1.00.

Now the integration value of the protons originating from doublet at 7.38 is 0.8.

Thus, the number of protons corresponding to this integration value is 0.8/1.00 = 0.8.

Upon correlation with the original spectra of (**1a**) the number of protons at 7.38 should be 1.

Hence the proton difference in this region is 1 – 0.8 = 0.2

Thus, the k_H / k_D = 0.8 / 0.2 = 4.

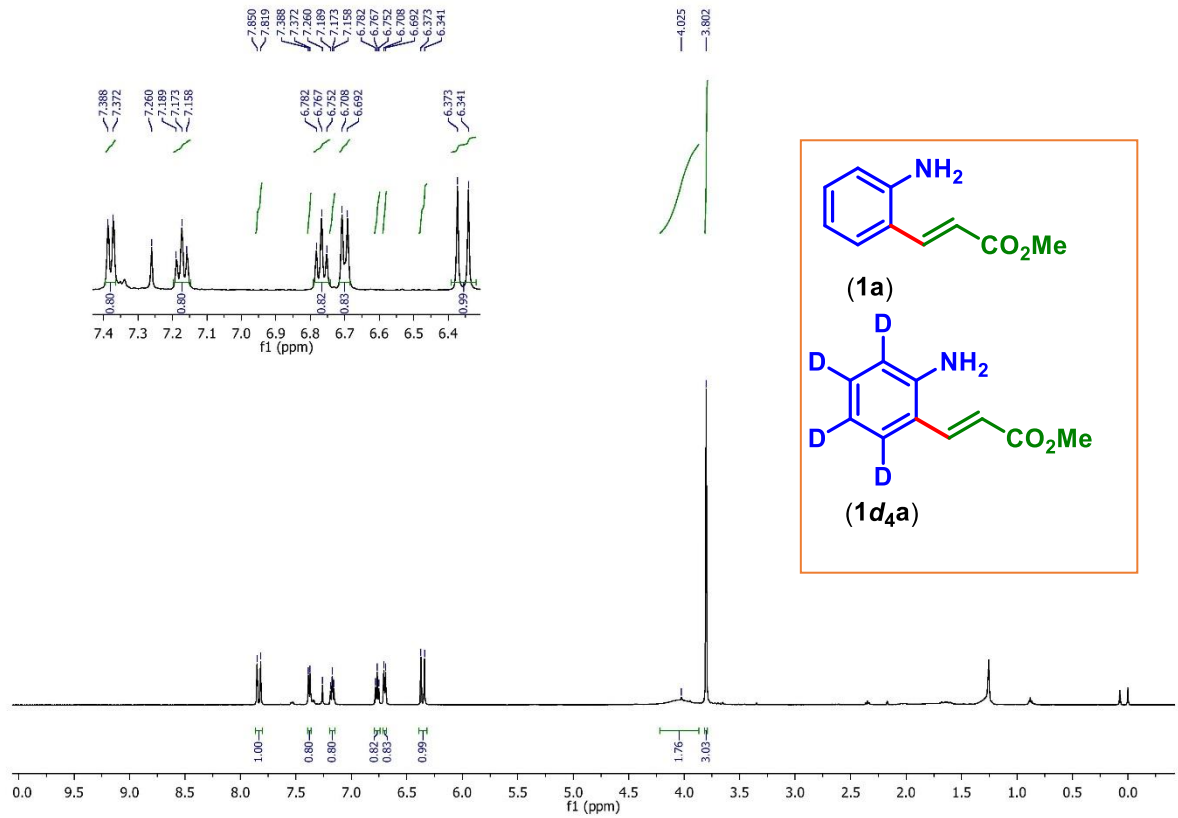

Figure IV.4.4. *^{1}H NMR spectra of kinetic isotope effect study.*

IV.4.4.4. Synthesis of *tert*-pentyl phenyl carbamate (**P**)

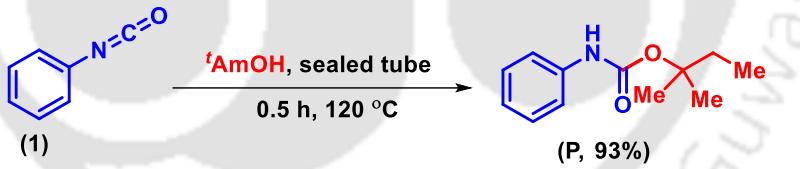

Scheme IV.4.4.4. *Ex-situ isolation of carbamte intermediate (P).*

An oven-dried pressure tube (20.3 cm x 19 mm, 21 mL) equipped with a magnetic bar was charged with phenyl isocyanate (**1**) (0.5 mmol, 60 mg) and solvent *tert*-amyl alcohol (2 mL). The reaction mixture was allowed to stir at 120 °C for 30 minutes. After completion of the reaction, the solvent was evaporated and the crude mixture was admixed with EtOAc (20 mL). The organic layer was washed with water (2 x 10 mL), and brine solution (1 x 5 mL). The organic layer was dried over anhydrous Na_2SO_4 solvent and concentrated under reduced pressure. The crude product so obtained was purified over a column of silica gel using an increasing percentage of ethyl acetate in hexane (3:10) to give pure *tert*-pentyl phenylcarbamate (**P**) in 93% yield (96 mg) (Scheme IV.4.4.4).

tert-Pentyl phenylcarbamate (P):

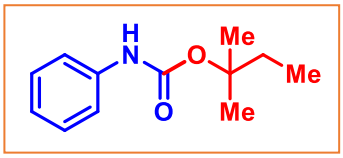

As a colourless liquid (96 mg, 93% yield); ^{1}H NMR ($CDCl_3$, 500 MHz): δ 7.27 (d, 2H, J = 8.0 Hz), 7.17 (t, 2H, J = 8.0 Hz), 6.91 (t, 1H, J = 7.5 Hz), 6.58 (s, 1H), 1.74 (q, 2H, J = 7.5 Hz), 1.39 (s, 6H), 0.83 (t, 3H, J = 7.5 Hz); ^{13}C{^{1}H} NMR ($CDCl_3$, 125 MHz): δ 152.6, 138.5, 129.0, 123.0, 118.7, 82.9, 33.7, 25.9, 8.4; IR (neat, cm^{-1}): 3435, 3338, 2932, 1723, 1599, 1520, 1439, 1371, 1263, 1154; HRMS (ESI/Q-TOF) (m/z): calcd. for $C_{12}H_{18}NO_2$, [M + H]$^{+}$: 208.1332, found: 208.1336 (Figure IV.4.5 and Figure IV.4.6).

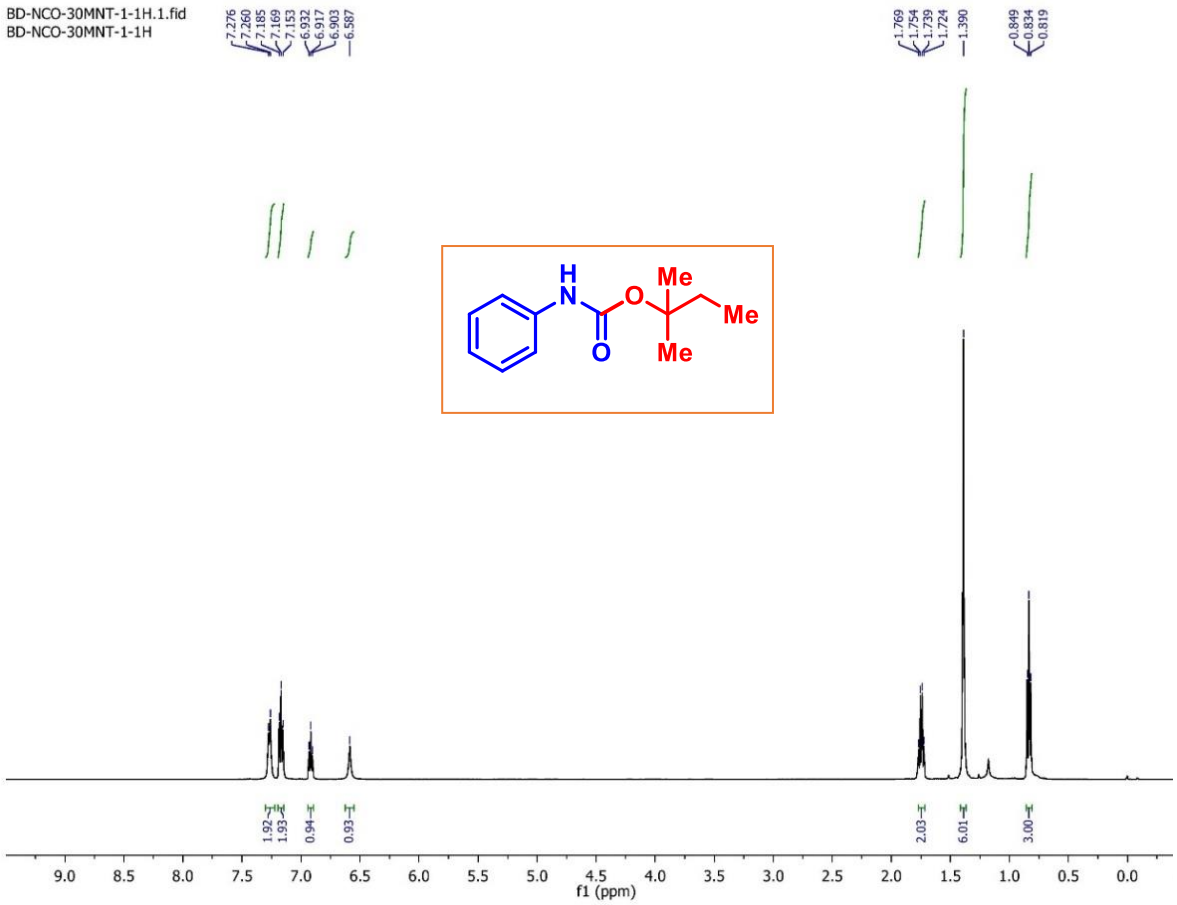

Figure IV.4.5. *^{1}H NMR spectra of **P** ($CDCl_3$, 500 MHz).*

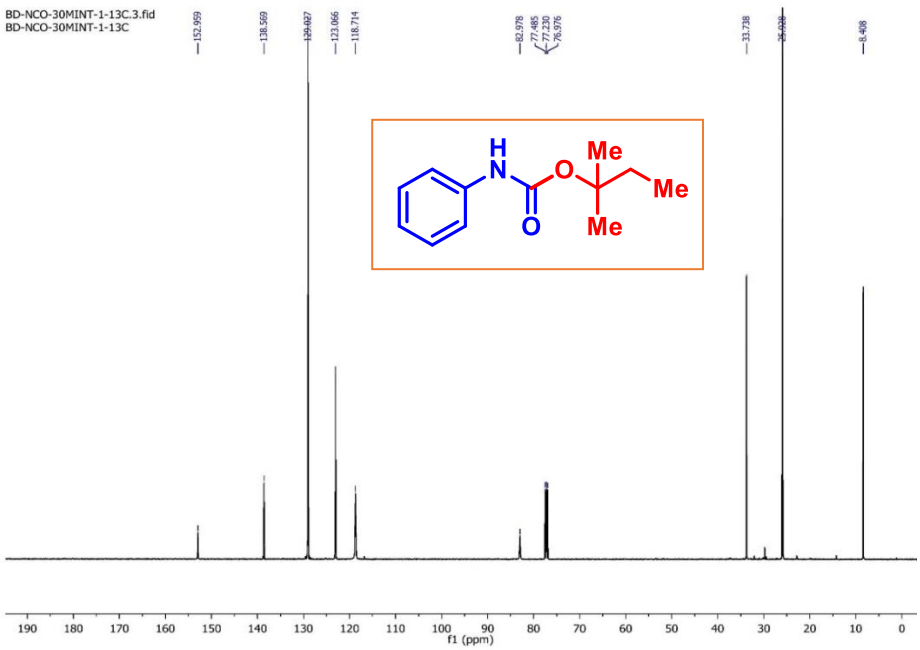

Figure IV.4.6. *$^{13}C\{^{1}H\}$ NMR spectra of* ***P*** *($CDCl_3$, 125 MHz).*

IV.4.4.5. Treatment of carbamate P in the standard conditions:

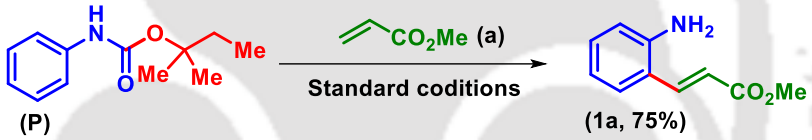

Scheme IV.4.4.5. *Treatment of isolated carbamate in the standard reaction conditions.*

An oven-dried pressure tube (20.3 cm x 19 mm, 21 mL) equipped with a magnetic bar was charged with *tert*-pentyl phenyl carbamate (**P**) (0.25 mmol, 52 mg), $Cu(OAc)_2$. H_2O (0.25 mmol, 25 mg), $AgSbF_6$ (0.0375 mmol, 13 mg), $[Ru(p\text{-cymene})Cl_2]_2$ (0.0125 mmol, 8 mg), acrylate (**a**, 0.5 mmol) and *tert*-amyl alcohol (2 mL). The reaction mixture was allowed to stir at 120 ^{o}C for 24 h. After completion of the reaction, the solvent was evaporated and the crude mixture was admixed with EtOAc (20 mL). The organic layer was washed with water (2 x 10 mL), and brine solution (1 x 5 mL). The organic layer was dried over anhydrous Na_2SO_4 solvent and concentrated under reduced pressure. The crude product so obtained was purified over a column of silica gel using an increasing percentage of ethyl acetate in hexane (1:9) to give pure methyl (*E*)-3-(2-aminophenyl)acrylate (**1a**) in 75% yield (33 mg) (Scheme IV.4.4.5).

IV.4.4.6. Dual role of solvent ^{t}AmOH:

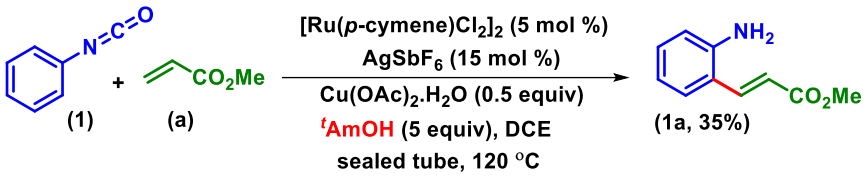

Scheme IV.4.4.6. *Examination of role of other solvent.*

An oven-dried pressure tube (20.3 cm x 19 mm, 21 mL) equipped with a magnetic bar was charged with phenyl isocyanate (**1**, 0.5 mmol, 60 mg), $Cu(OAc)_2$. H_2O (0.25 mmol, 50 mg), $AgSbF_6$ (0.075 mmol, 26 mg), $[Ru(p\text{-cymene})Cl_2]_2$ (0.025 mmol, 15.3 mg), acrylate (**a**, 0.5 mmol), *tert*-amyl alcohol (5 equiv, 220 mg) and solvent DCE (2 mL). The reaction mixture was allowed to stir for 24 h at 120 °C. After 24 h, the reaction mixture was filtered through a thin bed of celite. The filtrate was evaporated and admixed with EtOAc (20 mL). The organic layer was washed with water (2 x 10 mL), followed by brine solution (1 x 5 mL). The organic layer was dried over anhydrous Na_2SO_4 and solvent and concentrated under reduced pressure. The crude product thus obtained was purified over a column of silica gel using hexane and ethyl acetate in (9:1) to give pure methyl (*E*)-3-(2-aminophenyl)acrylate (**1a**) in 35% yield (31 mg). The identity and purity of the product were confirmed by spectroscopic analysis (Scheme IV.4.4.6).

IV.4.5. Post-synthetic modifications

IV.4.5.1. General procedure for synthesis of quinolin-2(1*H*)-one (1a') from methyl (*E*)-3-(2-aminophenyl)acrylate (1a)

To an oven-dried round bottom flask containing a magnetic bar was added methyl (*E*)-3-(2-aminophenyl)acrylate (**1a**) (0.25 mmol, 44 mg), $Pd(OAc)_2$ (0.0125 mmol, 3 mg), CuI (0.0375 mmol, 7.1 mg), PPh_3 (0.025 mmol, 6.5 mg), Cs_2CO_3 (0.5 mmol, 162 mg), 2 mL dry DMF in nitrogen atmosphere. The reaction mixture was allowed to stir for 6 h at 120 °C. The completion of the reaction was monitored by TLC. After completion, the mixture was filtered through a thin bed of celite. The filtrate was evaporated and diluted with EtOAc (20 mL). The organic layer was thoroughly washed with water (2 x 10 mL), and brine solution (1 x 5 mL) and dried over anhydrous Na_2SO_4. The organic layer was concentrated under reduced pressure. The crude product so obtained was purified over a column of silica gel using ethyl acetate in hexane (1:2) to give the desired azacoumarin in 93% yield (34 mg).

IV.4.5.2. General procedure for synthesis of 4-(*p*-tolyl)quinolin-2(1*H*)-one (1ab) from methyl (*E*)-3-(2-aminophenyl)acrylate (1a)

An oven dried 10 mL round bottom flask equipped with a magnetic bar was charged with methyl (*E*)-3-(2-aminophenyl)acrylate (**1a**) (0.25 mmol, 44 mg), 4-iodotoluene (0.25 mmol, 55 mg), $Pd(OAc)_2$ (0.0125 mmol, 2.8 mg), CuI (0.0375 mmol, 7.1 mg), PPh_3 (0.025 mmol, 6.6 mg), Cs_2CO_3 (0.5 mmol, 162 mg), dry DMF (2 mL) under nitrogen atmosphere. The reaction mixture was allowed to stir for 12 h at 120 ^oC. After completion, the mixture was filtered through a thin bed of celite. The filtrate was evaporated and diluted with EtOAc (20 mL). The organic layer was washed with water (2 x 10 mL) followed by brine solution (1 x 5 mL). The organic layer was dried over anhydrous Na_2SO_4 and solvent and concentrated under reduced pressure. The crude product so obtained was purified over a column of silica gel using ethyl acetate in hexane (1:2) to give the product in 86% yield (50 mg).

IV.4.5.3. General procedure for the synthesis of 6-(*p*-tolylethynyl)quinolin-2(1H)-one (7ac') from methyl (*E*)-3-(2-amino-5-bromophenyl)acrylate (7a):

The alkynylated azacoumarin (**7ac′**) was synthesized according to the modified literature procedure.[22b]

IV.4.5.4. General procedure for the synthesis of Methyl (E)-3-(2-amino-5-(*p*-tolylethynyl)phenyl)acrylate (7ac) from methyl (*E*)-3-(2-amino-5-bromophenyl)acrylate (7a):

The alkynylation of *o*-alkenylanilines was performed according to the modified literature procedure.[22b]

IV.4.5.5. General procedure for the removal of amino group:

The removal of the amine group was carried out according to the modified literature procedure.[22c]

IV.4.5.6. General procedure for gram-scale synthesis:

An oven-dried pressure tube (20.3 cm x 19 mm, 21 mL) containing a magnetic bar was added phenyl isocyanate (**1**, 10 mmol, 1.19 g), $Cu(OAc)_2$. H_2O (2.5 mmol, 500 mg), $AgSbF_6$ (0.75 mmol, 260 mg), $[Ru(p\text{-cymene})Cl_2]_2$ (0.25 mmol, 153 mg), methyl acrylate (**a**, 20 mmol) and *tert*-amyl alcohol (10 mL). The reaction mixture was allowed to stir for 24 h at 120 ^oC. After 24 h, the reaction mixture was filtered through a thin bed of celite and the filtrate was

evaporated. The crude mixture was admixed with EtOAc (25 mL). The organic layer was washed with water (2 x 10 mL) followed by brine solution (1 x 5 mL). The organic layer was dried over anhydrous Na_2SO_4 and solvent and concentrated under reduced pressure. The crude product so obtained was purified over a column of silica gel using an increasing percentage of ethyl acetate in hexane to give pure methyl (*E*)-3-(2-aminophenyl)acrylate (**1a**) in 56% yield (991 mg).

IV.5. Spectral Data

Spectral data of all compounds:

Methyl (E)-3-(2-aminophenyl)acrylate (1a)[22d]:

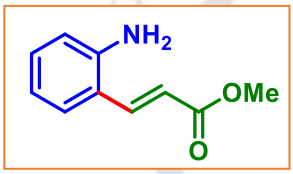

As yellow solid (68 mg, 77% yield); mp 70–72 °C; ^{1}H NMR ($CDCl_3$, 400 MHz): δ 7.83 (d, 1H, J = 15.6 Hz), 7.38 (d, 1H, J = 7.6 Hz), 7.17 (t, 1H, J = 8.4 Hz), 6.77 (t, 1H, J = 7.2 Hz), 6.70 (d, 1H, J = 8.0 Hz), 6.36 (d, 1H, J = 15.6 Hz), 3.96 (s, 2H), 3.80 (s, 3H); ^{13}C{^{1}H} NMR ($CDCl_3$, 100 MHz): δ 167.9, 145.7, 140.5, 131.5, 128.3, 120.0, 119.2, 117.9, 116.9, 51.8; IR (neat, cm^{-1}): 3377, 2924, 1705, 1622, 1438, 1264, 1172; HRMS (ESI/Q-TOF) (m/z): calcd. for $C_{10}H_{12}NO_2$, $[M + H]^+$: 178.0863, found: 178.0873.

Ethyl (E)-3-(2-aminophenyl)acrylate (1b)[22e]:

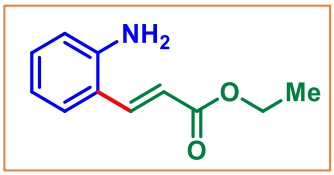

As yellow solid (70 mg, 73% yield); mp 67–69 °C; ^{1}H NMR ($CDCl_3$, 400 MHz): δ 7.82 (d, 1H, J = 16.0 Hz), 7.38 (d, 1H, J = 8.0 Hz), 7.16 (t, 1H, J = 8.0 Hz), 6.76 (t, 1H, J = 7.2 Hz), 6.70 (d, 1H, J = 8.0 Hz), 6.35 (d, 1H, J = 15.6 Hz), 4.26 (q, 2H, J = 7.2 Hz), 3.98 (s, 2H), 1.33 (t, 3H, J = 7.2 Hz); ^{13}C{^{1}H} NMR ($CDCl_3$, 100 MHz): δ 167.5, 145.7, 140.2, 131.4, 128.3, 120.1, 119.1, 118.3, 116.9, 60.6, 14.5; IR (neat, cm^{-1}): 3374, 2981, 1699, 1622, 1490, 1264, 1176; HRMS (ESI/Q-TOF) (m/z): calcd. for $C_{11}H_{14}NO_2$, $[M + H]^+$: 192.1019, found: 192.1026.

Butyl (E)-3-(2-aminophenyl)acrylate (1c):

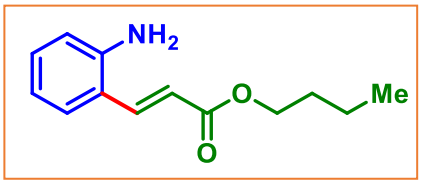

As brown gummy (76 mg, 69% yield); ^{1}H NMR ($CDCl_3$, 500 MHz): δ 7.81 (d, 1H, J = 15.5 Hz), 7.38 (dd, 1H, J_1 = 7.5 Hz, J_2 = 1.5 Hz), 7.18–7.15 (m, 1H), 6.76 (t, 1H, J =7.5 Hz), 6.70 (dd, 1H, J_1 = 8.0 Hz, J_2 = 1.5 Hz), 6.35 (d, 1H, J = 16.0 Hz), 4.21 (t, 2H, J = 6.5 Hz), 3.95 (s, 2H), 1.71–1.66 (m, 2H), 1.46–1.42 (m, 2H), 0.96 (t, 3H, J = 7.5 Hz); ^{13}C{^{1}H} NMR ($CDCl_3$, 125 MHz): δ 167.6, 145.7, 140.2, 131.4, 128.3, 120.2, 119.1, 118.5, 116.9, 64.6, 31.0, 19.4, 13.9; IR (neat, cm^{-1}): 3056, 2959, 1732, 1630, 1410, 1264, 1046; HRMS (ESI/Q-TOF) (m/z): calcd. for $C_{13}H_{18}NO_2$, [M + H]$^{+}$: 220.1332, found: 220.1327.

Hexyl (E)-3-(2-aminophenyl)acrylate (1d):

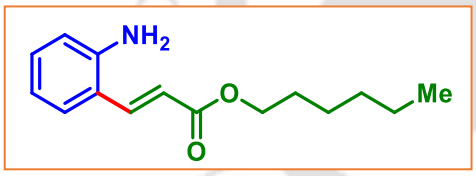

As yellow solid (75 mg, 61% yield); mp 58–60 ^{o}C; ^{1}H NMR ($CDCl_3$, 400 MHz): δ 7.82 (d, 1H, J = 16.0 Hz), 7.38 (dd, 1H, J_1 = 6.4 Hz, J_2 = 1.2 Hz), 7.16 (t, 1H, J = 8.0 Hz), 6.76 (t, 1H, J = 7.6 Hz), 6.70 (d, 1H, J = 8.0 Hz), 6.36 (d, 1H, J = 16.0 Hz), 4.19 (t, 2H, J = 6.8 Hz), 3.96 (s, 2H), 1.73–1.66 (m, 3H), 1.34–1.32 (m, 5H), 0.90 (t, 3H, J = 6.8 Hz); ^{13}C{^{1}H} NMR ($CDCl_3$, 125 MHz): δ 167.6, 145.7, 140.2, 131.4, 128.3, 120.2, 119.1, 118.4, 116.9, 64.9, 31.6, 28.9, 25.8, 22.7, 14.1; IR (neat, cm^{-1}): 3379, 3056, 2957, 1732, 1626, 1377, 1264, 1046; HRMS (ESI/Q-TOF) (m/z): calcd. for $C_{15}H_{22}NO_2$, [M + H]$^{+}$: 248.1645, found: 248.1648.

Dodecyl (E)-3-(2-aminophenyl)acrylate (1e):

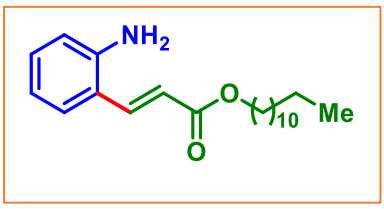

As yellowish solid (100 mg, 59% yield), 76–78 ^{o}C; ^{1}H NMR ($CDCl_3$, 500 MHz): δ 7.81 (d, 1H, J = 16.0 Hz), 7.38 (dd, 1H, J_1 = 8.0 Hz, J_2 = 1.5 Hz), 7.18–7.15 (m, 1H), 6.76 (t, 1H, J = 7.5 Hz), 6.70 (d, 1H, J = 8.0 Hz), 6.36 (d, 1H, J = 16.0 Hz), 4.19 (t, 2H, J = 7.0 Hz), 1.71–1.69 (m, 4H), 1.26 (s, 18 H),

0.88 (t, 3H, J = 7.0 Hz); $^{13}C\{^1H\}$ NMR ($CDCl_3$, 125 MHz): δ 167.6, 145.7, 140.2, 131.4, 128.4, 120.2, 119.1, 118.5, 116.9, 64.9, 32.1, 29.87, 29.85, 29.80, 29.75, 29.6, 29.5, 29.0, 26.2, 22.9, 14.3; IR (neat, cm^{-1}): 3055, 2983, 1733, 1626, 1425, 1374, 1264, 1046; HRMS (ESI/Q-TOF) (m/z): calcd. for $C_{21}H_{34}NO_2$, $[M + H]^+$: 332.2584, found: 332.2578.

Octadecyl (E)-3-(2-aminophenyl)acrylate (1f):

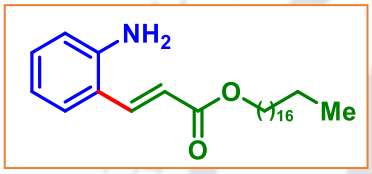

As yellowish solid (110 mg, 53% yield), 81–83 °C; ^1H NMR ($CDCl_3$, 500 MHz): δ 7.82 (d, 1H, J = 16.0 Hz), 7.38 (dd, 1H, J_1 = 8.0 Hz, J_2 = 1.5 Hz), 7.16 (t, 1H, J = 7.0 Hz), 6.75 (t, 1H, J = 7.5 Hz), 6.69 (d, 1H, J = 8.0 Hz), 6.36 (t, 1H, J = 16.0 Hz), 4.19 (t, 2H, J = 7.0 Hz), 3.98 (s, 2H), 1.72–1.67 (m, 2H), 1.26 (s, 3H), 0.88 (t, 3H, J = 7.0 Hz); $^{13}C\{^1H\}$ NMR ($CDCl_3$, 125 MHz): δ 167.6, 145.7, 140.2, 131.4, 128.3, 120.1, 119.1, 118.4, 116.9, 64.9, 32.1, 29.89, 29.88, 29.85, 29.8, 29.7, 29.6, 29.5, 29.0, 26.2, 22.9, 14.3; IR (neat, cm^{-1}): 3368, 2954. 2919, 2851, 1734, 1698, 1622, 1460, 1375, 1264, 1046; HRMS (ESI/Q-TOF) (m/z): calcd. for $C_{27}H_{46}NO_2$, $[M + H]^+$: 416.3523, found: 416.3529.

Isobutyl (E)-3-(2-aminophenyl)acrylate (1g):

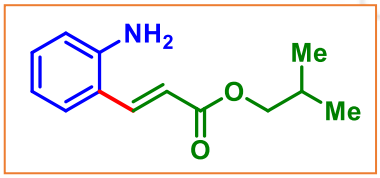

As light yellow solid (77 mg, 70% yield); mp 79–81 °C; ^1H NMR ($CDCl_3$, 400 MHz): δ 7.82 (d, 1H, J = 15.6 Hz), 7.41–7.37 (m, 1H), 7.18–7.14 (m, 1H), 6.78–6.74 (m, 1H), 6.70 (d, 1H, J = 8.0 Hz), 6.37 (d, 1H, J = 16.0 Hz), 4.29 (s, 2H), 3.99 (d, 2H, J = 6.8 Hz), 2.05–1.98 (m, 1H), 0.98 (d, 6H, J = 6.8 Hz); $^{13}C\{^1H\}$ NMR ($CDCl_3$, 125 MHz): δ 167.5, 145.7, 140.3, 131.4, 128.4, 120.2, 119.2, 118.5, 116.9, 70.8, 28.1, 19.3; IR (neat, cm^{-1}): 3377, 2962, 1701, 1623, 1491, 1263, 1171; HRMS (ESI/Q-TOF) (m/z): calcd. for $C_{13}H_{18}NO_2$, $[M + H]^+$: 220.1332, found: 220.1332.

tert-Pentyl (E)-3-(2-aminophenyl)acrylate (1h):

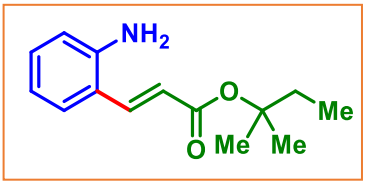

Gummy (77 mg, 66% yield); ^{1}H NMR ($CDCl_3$, 500 MHz): δ 7.72 (d, 1H, J = 16.0 Hz), 7.37 (d, 1H, J = 8.0 Hz), 7.15 (t, 1H, J = 7.5 Hz), 6.75 (t, 1H, J = 7.5 Hz), 6.69 (d, 1H, J = 8.0 Hz), 6.29 (d, 1H, J = 16.0 Hz), 3.93 (s, 2H), 1.86 (q, 2H, J = 7.5 Hz), 1.50 (s, 6H), 0.93 (t, 3H, J = 7.5 Hz); ^{13}C{^{1}H} NMR ($CDCl_3$, 125 MHz): δ 166.7, 145.5, 139.2, 131.1, 128.3, 120.5, 120.4, 119.1, 116.8, 83.1, 33.8, 25.9, 8.4; IR (neat, cm^{-1}): 3054, 2983, 1733, 1626, 1425, 1374, 1264, 1045; HRMS (ESI/Q-TOF) (m/z): calcd. for $C_{14}H_{20}NO_2$, $[M + H]^+$: 234.1489, found: 234.1488.

2-Methoxyethyl(E)-3-(2-aminophenyl)acrylate (1i):

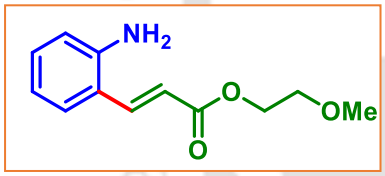

As brown solid (68 mg, 62% yield), mp 124–126 ^{o}C; ^{1}H NMR ($CDCl_3$, 500 MHz): δ 7.85 (d, 1H, J = 15.5 Hz), 7.37 (d, 1H, J = 8.0 Hz), 7.16 (t, 1H, J = 7.0 Hz), 6.75 (t, 1H, J = 7.5 Hz), 6.69 (d, 1H, J = 8.0 Hz), 6.40 (d, 1H, J = 16.0 Hz), 4.36 (s, 2H), 3.99 (s, 2H), 3.66 (s, 2H), 3.42 (s, 3H); ^{13}C{^{1}H} NMR ($CDCl_3$, 100 MHz): δ 167.4, 145.8, 140.8, 131.5, 128.3, 119.9, 119.1, 117.7, 116.9, 70.7, 63.7, 59.2; IR (neat, cm^{-1}): 3371, 2927, 1704, 1622, 1494, 1263, 1173; HRMS (ESI/Q-TOF) (m/z): calcd. for $C_{12}H_{16}NO_3$, $[M + H]^+$: 222.1125, found: 222.1115.

(Tetrahydrofuran-2-yl)methyl (E)-3-(2-aminophenyl)acrylate (1j):

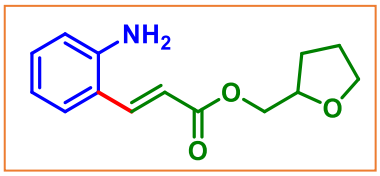

As a brown solid (68 mg, 55% yield), mp 114–116 ^{o}C; ^{1}H NMR ($CDCl_3$, 400 MHz): δ 7.85 (d, 1H, J = 16.0 Hz), 7.37 (dd, 1H, J_1 = 8.0 Hz, J_2 = 1.6 Hz), 7.18–7.14 (m, H), 6.75 (t, 1H, J = 7.6 Hz), 6.69 (d, 1H, J = 8.4 Hz), 6.40 (d, 1H, J = 15.6 Hz), 4.29 (dd, 1H, J_1 = 11.2 Hz, J_2 = 3.2 Hz), 4.21–4.17 (m, 1H), 4.15–4.11 (m, 1H), 3.99 (s, 2H), 3.95–3.89 (m, 1H), 3.85–3.79 (m, 1H), 2.08–2.00 (m, 1H), 1.98–1.89 (m, 2H),

1.71–1.63 (m, 1H); $^{13}C\{^{1}H\}$ NMR ($CDCl_3$, 100 MHz): δ 167.4, 145.8, 140.8, 131.5, 128.4, 120.0, 119.1, 117.8, 116.9, 76.8, 68.6, 66.7, 28.2, 25.8; IR (neat, cm^{-1}): 3367, 2973, 1702, 1620, 1490, 1263, 1167; HRMS (ESI/Q-TOF) (m/z): calcd. for $C_{14}H_{21}N_2O_3$, $[M + NH_4]^+$: 265.1547, found: 265.1560.

Benzyl (E)-3-(2-aminophenyl)acrylate (1k):

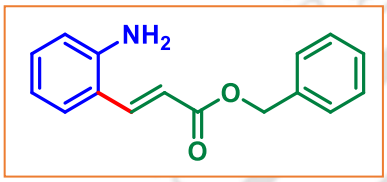

As yellow solid (80 mg, 63% yield), mp 127–129 °C; ^{1}H NMR ($CDCl_3$, 400 MHz): δ 7.88 (d, 1H, J = 15.6 Hz), 7.44–7.34 (m, 6H), 7.19–7.15 (m, 1H), 6.76 (t, 1H, J = 7.6 Hz), 6.69 (d, 1H, J = 8.0 Hz), 6.41 (d, 1H, J = 16.0 Hz), 5.26 (s, 2H), 3.98 (s, 2H); $^{13}C\{^{1}H\}$ NMR ($CDCl_3$, 100 MHz): δ 167.3, 145.8, 140.9, 136.3, 131.5, 128.7, 128.5, 128.4, 128.3, 119.9, 119.1, 117.9, 116.5, 66.5; IR (neat, cm^{-1}): 3377, 3057, 1704, 1621, 1491, 1263, 1161; HRMS (ESI/Q-TOF) (m/z): calcd. for $C_{16}H_{16}NO_2$, $[M + H]^+$: 254.1176, found: 254.1172.

p-Tolyl (E)-3-(2-aminophenyl)acrylate (1l):

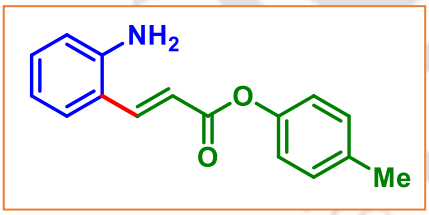

As yellow solid (85 mg, 67% yield), mp 146–148 °C; ^{1}H NMR ($CDCl_3$, 500 MHz): δ 8.00 (d, 1H, J = 16.0 Hz), 7.45 (d, 1H, J = 7.5 Hz), 7.20 (d, 3H, J = 7.0 Hz), 7.05 (d, 2H, J = 7.5 Hz), 6.80 (t, 1H, J = 6.5 Hz), 6.71 (d, 1H, J = 7.5 Hz), 6.54 (d, 1H, J = 15.5 Hz), 4.02 (s, 2H), 2.36 (s, 3H); $^{13}C\{^{1}H\}$ NMR ($CDCl_3$, 125 MHz): δ 166.1, 148.8, 146.1, 142.0, 135.5, 131.9, 130.1, 128.4, 121.5, 119.8, 119.2, 117.2, 117.1, 21.0; IR (neat, cm^{-1}): 3463, 3380, 3239, 2920, 1707, 1638, 1621, 1489, 1460, 1345, 1211, 1159; HRMS (ESI/Q-TOF) (m/z): calcd. for $C_{16}H_{16}NO_2$, $[M + H]^+$: 254.1176, found: 254.1178.

4-Methoxyphenyl (E)-3-(2-aminophenyl)acrylate (1m):

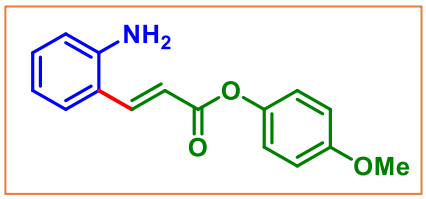

As yellowish solid (89 mg, 66% yield), mp: 157–160 °C; ^{1}H NMR ($CDCl_3$, 400 MHz): δ 7.99 (d, 1H, J = 15.6 Hz), 7.45 (d, 1H, J = 8.0 Hz), 7.20 (t, 1H, J = 7.6 Hz), 7.08 (d, 2H, J = 8.4 Hz), 6.92 (d, 2H, J = 8.4 Hz), 6.80 (t, 1H, J = 7.6 Hz), 6.72 (d, 1H, J = 8.0 Hz), 6.54 (d, 1H, J = 15.6 Hz), 4.01 (s, 2H), 3.81 (s, 3H); ^{13}C{^{1}H} NMR ($CDCl_3$, 100 MHz): δ 166.3, 157.4, 146.0, 144.5, 142.0, 131.9, 128.5, 122.6, 119.8, 119.2, 117.2, 117.0, 114.7, 55.8; IR (neat, cm^{-1}): 3388, 3054, 2983, 1733, 1640, 1402, 1374, 1267, 1046; HRMS (ESI/Q-TOF) (m/z): calcd. for $C_{16}H_{16}NO_3$, $[M + H]^+$: 270.1125, found: 270.1126.

1,1,1,3,3,3-Hexafluoropropan-2-yl (E)-3-(2-aminophenyl)acrylate (1n):

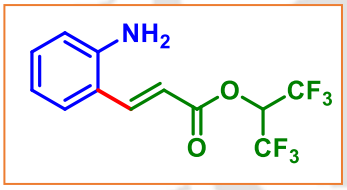

As yellowish solid (111 mg, 71% yield); mp: 89–91 °C ^{1}H NMR ($CDCl_3$, 400 MHz): δ 8.02 (d, 1H, J = 15.6 Hz), 7.42 (d, 1H, J = 7.6 Hz), 7.23 (t, 1H, J = 7.6 Hz), 6.79 (t, 1H, J = 7.2 Hz), 6.72 (d, 1H, J = 8.0 Hz), 6.44 (d, 1H, J = 16.0 Hz), 5.91 (hept, 1H, $J_{H\text{-}F}$ = 6.4 Hz), 4.04 (s, 2H); ^{13}C{^{1}H} NMR ($CDCl_3$, 125 MHz): δ 164.1, 146.5, 145.0, 132.8, 128.8, 121.6 (q, $J_{C\text{-}F}$ = 1.6 Hz), 119.4, 119.1, 117.3, 113.5, 67.27–66.17 (m); ^{19}F NMR ($CDCl_3$, 471 MHz): δ –73.2 (s); IR (neat, cm^{-1}): 3371, 3238, 2957, 2924, 2861, 1741, 1657, 1615, 1564, 1461, 1355, 1284, 1112; HRMS (ESI/Q-TOF) (m/z): calcd. for $C_{12}H_{10}F_6NO_2$, $[M + H]^+$: 314.0610, found: 314.0613.

1,7,7-Trimethylbicyclo[2.2.1]heptan-2-yl €-3-(2-aminophenyl)acrylate (1o):

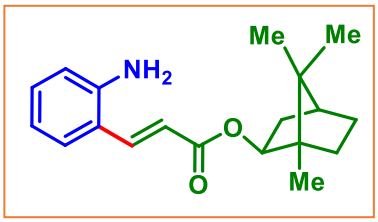

As yellow solid (94 mg, 63% yield); 108–112 °C; ^{1}H NMR ($CDCl_3$, 400 MHz): δ 7.78 (d, 1H, J = 16.0 Hz), 7.38 (dd, 1H, J_1 = 8.4 Hz, J_1 = 1.6 Hz), 7.18–7.14 (m, 1H), 6.76 (t, 1H, J = 8.4 Hz), 6.70 (d, 1H, J = 8.0 Hz), 6.32 (d, 1H, J = 15.6 Hz), 4.80 (dd, 1H, J_1 = 7.2 Hz, J_1 = 4.0 Hz), 3.94 (s, 2H),

1.87–1.83 (m, 2H), 1.76 (t, 2H, J = 4.4 Hz), 1.61–1.57 (m, 1H), 1.26–1.20 (m, 2H), 1.05 (s, 3H), 0.89 (s, 3H), 0.86 (s, 3H); $^{13}C\{^{1}H\}$ NMR ($CDCl_3$, 100 MHz): δ 167.0, 145.6, 139.9, 131.3, 128.3, 120.2, 119.1, 119.0, 116.9, 81.2, 49.1, 47.2, 45.3, 39.1, 33.9, 27.3, 20.3, 20.2, 11.7; IR (neat, cm^{-1}): 3351, 2959, 1699, 1623, 1424, 1264; HRMS (ESI/Q-TOF) (m/z): calcd. for $C_{19}H_{26}NO_2$, $[M + H]^+$: 300.1958, found: 300.1956.

2-(6,6-Dimethylbicyclo[3.1.1]hept-2-en-2-yl)ethyl (E)-3-(2-aminophenyl)acrylate (1p):

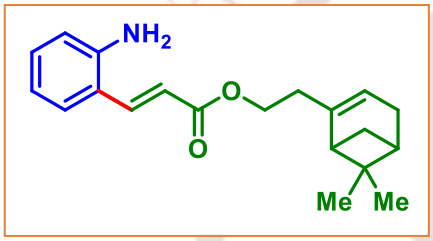

As gummy (85 mg, 55% yield); ^{1}H NMR ($CDCl_3$, 500 MHz): δ 7.81 (d, 1H, J = 15.5 Hz), 7.37 (d, 1H, J = 8.0 Hz), 7.16 (t, 1H, J = 8.0 Hz), 6.76 (t, 1H, J = 7.5 Hz), 6.69 (d, 1H, J = 8.0 Hz), 6.33 (d, 1H, J = 16.5 Hz), 5.33 (s, 1H), 4.21 (q, 2H, J = 6.5 Hz), 3.96 (s, 2H), 2.39–2.35 (m, 3H), 2.24 (q, 2H, J = 17.5 Hz), 2.09 (d, 2H, J = 6.0 Hz), 1.28 (s, 3H), 1.17 (d, 1H, J = 8.5 Hz), 0.85 (s, 3H); $^{13}C\{^{1}H\}$ NMR ($CDCl_3$, 125 MHz): δ 167.4, 145.7, 144.4, 140.2, 131.4, 128.3, 120.1, 119.1, 119.0, 118.4, 116.9, 63.0, 45.9, 40.9, 38.2, 36.2, 31.8, 31.5, 26.5, 21.3; IR (neat, cm^{-1}): 3374, 2983, 2912, 1728, 1700, 1623, 1404, 1263; HRMS (ESI/Q-TOF) (m/z): calcd. for $C_{20}H_{26}NO_2$, $[M + H]^+$: 312.1958, found: 312.1956.

(3S,8S,9S,10R,13R,14S,17R)-10,13-dimethyl-17-((R)-6-methylheptan-2-yl)-2,3,4,7,8,9,10,11,12,13,14,15,16,17-tetradecahydro-1H-cyclopenta[a]phenanthren-3-yl (E)-3-(2-aminophenyl)acrylate (1q):

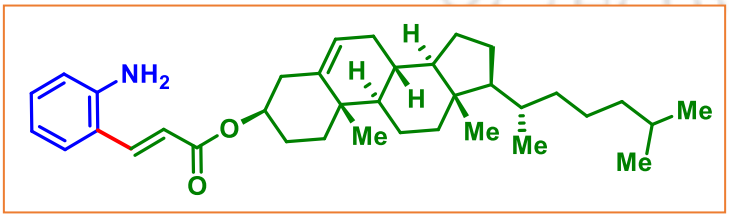

As yellow solid (125 mg, 47% yield), mp 148–150 °C; ^{1}H NMR ($CDCl_3$, 500 MHz): δ 7.80 (d, 1H, J = 15.5 Hz), 7.37 (dd, 1H, J_1 = 8.0 Hz, J_2 = 1.5 Hz), 7.17–7.14 (m, 1H), 6.76 (t, 1H, J = 8.0 Hz), 6.69 (d, 1H, J = 8.0 Hz), 6.33 (d, 1H, J = 16.0 Hz), 5.40 (d, 1H, J = 5.0 Hz), 4.78–4.71 (m, 1H), 3.96 (s, 2H), 2.41–2.38 (m, 2H), 2.03–1.82 (m, 6H),

1.61–1.45 (m, 9H), 1.37–1.33 (m, 3H), 1.19–1.08 (m, 7H), 1.05 (s, 4H), 1.01–0.97 (m, 3H), 0.92 (d, 3H, J = 7.0 Hz), 0.87 (d, 3H, J = 2.5 Hz), 0.86 (d, 3H, J = 2.0 Hz); $^{13}C\{^{1}H\}$ NMR ($CDCl_3$, 125 MHz): δ 166.9, 145.7, 140.1, 140.0, 131.4, 128.4, 122.9, 120.3, 119.2, 118.9, 116.9, 74.3, 57.0, 56.4, 50.3, 42.6, 40.0, 39.8, 38.5, 37.3, 36.9, 36.4, 36.0, 32.1, 28.5, 28.2, 28.1, 24.5, 24.1, 23.0, 22.8, 21.3, 19.6, 19.0, 12.1; IR (neat, cm^{-1}): 3378, 2980, 2914, 1725, 1709, 1628, 1400, 1253;HRMS (ESI/Q-TOF) (m/z): calcd. for $C_{36}H_{54}NO_2$, $[M + H]^+$: 532.4149, found: 532.4149.

Methyl (E)-3-(2-amino-5-methylphenyl)acrylate (2a)[22d]:

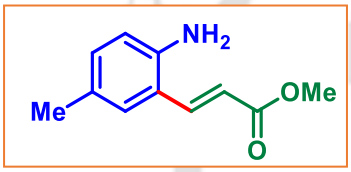

As yellow solid (74 mg, 78% yield); mp 80–90 °C; ^{1}H NMR ($CDCl_3$, 400 MHz): δ 7.82 (d, 1H, J = 15.6 Hz), 7.19 (s, 1H), 6.99 (d, 1H, J = 8.0 Hz), 6.62 (d, 1H, J = 8.0 Hz), 6.34 (d, 1H, J = 16.0 Hz), 3.79 (s, 3H), 2.24 (s, 3H); $^{13}C\{^{1}H\}$ NMR ($CDCl_3$, 125 MHz): δ 167.9, 143.4, 140.6, 132.4, 130.0, 128.4, 120.0, 117.6, 117.1, 51.8, 20.5; IR (neat, cm^{-1}): 3374, 2960, 1728, 1658, 1431, 1262; HRMS (ESI/Q-TOF) (m/z): calcd. for $C_{11}H_{14}NO_2$, $[M + H]^+$: 192.1019, found: 192.1023.

Ethyl (E)-3-(2-amino-5-methylphenyl)acrylate (2b)[22g]:

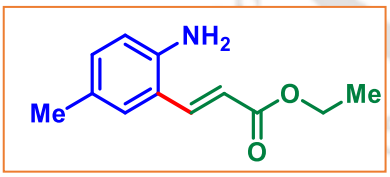

As yellow solid (78 mg, 76% yield); mp 72–74 °C; ^{1}H NMR ($CDCl_3$, 400 MHz): δ 7.81 (d, 1H, J = 15.6 Hz), 7.19 (s, 1H), 6.99 (d, 1H, J = 7.2 Hz), 6.62 (d, 1H, J = 8.0 Hz), 6.34 (d, 1H, J = 16.0 Hz), 4.25 (q, 2H, J = 7.2 Hz), 3.86 (s, 2H), 2.23 (s, 3H), 1.33 (t, 3H, J = 6.8 Hz); $^{13}C\{^{1}H\}$ NMR ($CDCl_3$, 100 MHz): δ 167.5, 143.4, 140.3, 132.3, 128.4, 128.3, 120.1, 118.0, 117.1, 60.6, 20.5, 14.5; IR (neat, cm^{-1}): 3371, 2922, 1707, 1620, 1500, 1427, 1264; HRMS (ESI/Q-TOF) (m/z): calcd. for $C_{12}H_{16}NO_2$, $[M + H]^+$: 206.1176, found: 206.1188.

Butyl (E)-3-(2-amino-5-methylphenyl)acrylate (2c):

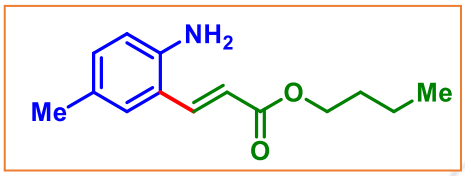

As gummy (86 mg, 74% yield); ^{1}H NMR ($CDCl_3$, 500 MHz): δ 7.80 (d, 1H, J = 16.0 Hz), 7.19 (s, 1H), 6.98 (d, 1H, J = 8.0 Hz), 6.62 (d, 1H, J = 8.5 Hz), 6.34 (d, 1H, J = 15.5 Hz), 4.20 (t, 2H, J = 7.0 Hz), 3.84 (s, 2H), 2.24 (s, 3H), 1.70–1.67 (m, 2H), 1.46–1.41 (m, 2H), 0.96 (t, 3H, J = 7.5 Hz); ^{13}C{^{1}H} NMR ($CDCl_3$, 125 MHz): δ 167.6, 143.4, 140.3, 132.3, 128.4, 128.3, 120.2, 118.1, 117.1, 64.5, 31.0, 20.5, 19.4, 13.9; IR (neat, cm^{-1}): 3374, 2958, 2926, 1703, 1621, 1501, 1462, 1377, 1263, 1162, 1044; HRMS (ESI/Q-TOF) (m/z): calcd. for $C_{14}H_{20}NO_2$, $[M + H]^+$: 234.1489, found: 234.1492.

Isobutyl (E)-3-(2-amino-5-methylphenyl)acrylate (2g):

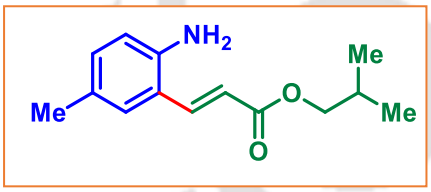

As yellow solid (85 mg, 73% yield); mp: 77–79 ^{o}C; ^{1}H NMR ($CDCl_3$, 400 MHz): δ 7.81 (d, 1H, J = 15.6 Hz), 7.21 (s, 1H), 6.99 (d, 1H, J = 8.0 Hz), 6.62 (d, 1H, J = 8.0 Hz), 6.36 (d, 1H, J = 16.0 Hz), 3.98 (d, 2H, J = 6.4 Hz), 3.85 (s, 2H), 2.24 (s, 3H), 2.04–1.97 (m, 1H), 0.98 (d, 6H, J = 6.8 Hz); ^{13}C{^{1}H} NMR ($CDCl_3$, 100 MHz): δ 167.7, 143.4, 140.3, 132.3, 128.4, 128.3, 120.2, 118.1, 117.1, 70.8, 28.1, 20.6, 19.4; IR (neat, cm^{-1}): 3373, 2926, 1702, 1622, 1501, 1263, 1162; HRMS (ESI/Q-TOF) (m/z): calcd. for $C_{14}H_{20}NO_2$, $[M + H]^+$: 234.1489, found: 234.1476.

2,2,3,3,4,4,5,5,6,6,7,7-Dodecafluoroheptyl (E)-3-(2-amino-5-methylphenyl)acrylate (2r):

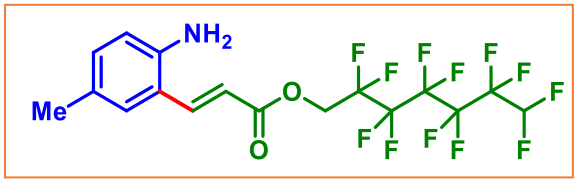

As yellowish solid (142 mg, 58% yield), mp: 110–112 ^{o}C; ^{1}H NMR ($CDCl_3$, 500 MHz): δ 7.91 (d, 1H, J = 16.0 Hz), 7.22 (d, 1H, J = 2.0 Hz), 7.02 (dd, 1H, J_1 = 8.0 Hz, J_2 = 2.0 Hz), 6.63 (d, 1H, J = 8.0 Hz), 6.39 (d, 1H, J = 16.0 Hz), 6.05 (tt, 1H, J_1 = 5.2 Hz, J_2 = 5.0 Hz), 4.71 (t, 2H, J = 14.0 Hz), 3.87 (s, 2H), 2.24 (s, 3H); ^{13}C{^{1}H} NMR ($CDCl_3$, 125 MHz): δ 165.8,

143.9, 143.0, 133.2, 128.5 (d, J_{C-F} = 3.4 Hz), 121.6, 119.6, 117.4, 115.2, 113.1 (t, J_{C-F} = 30.8 Hz), 111.3 (t, J_{C-F} = 8.3 Hz), 110.9 (t, J_{C-F} = 1.25 Hz), 109.8 (t, J_{C-F} = 31.4 Hz), 107.8 (t, J_{C-F} = 31.8 Hz), 105.8 (t, J_{C-F} = 22.4 Hz), 59.8 (t, J_{C-F} = 26.5 Hz), 20.5; ^{19}F NMR ($CDCl_3$, 471 MHz): δ –119.3, –122.0, –123.3, –129.3, –137.0; IR (neat, cm^{-1}): 3056, 2986, 1732, 1615, 1422, 1374, 1254, 1244, 1045; HRMS (ESI/Q-TOF) (m/z): calcd. for $C_{17}H_{14}F_{12}NO_2$, $[M + H]^+$: 492.0827, found: 492.0808.

Methyl (E)-3-(2-amino-5-(tert-butyl)phenyl)acrylate (3a):

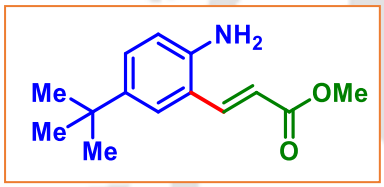

As gummy (76 mg, 65% yield); ^{1}H NMR ($CDCl_3$, 500 MHz): δ 7.85 (d, 1H, J = 16.0 Hz), 7.37 (s, 1H,), 7.23 (dd, 1H, J_1 = 8.5 Hz, J_2 = 2.5 Hz), 6.66 (d, 1H, J = 8.5 Hz), 6.37 (d, 1H, J = 15.5 Hz), 3.89 (s, 2H), 3.81 (s, 3H), 1.29 (s, 9H); ^{13}C{^{1}H} NMR ($CDCl_3$, 125 MHz): δ 167.7, 143.5, 142.0, 141.2, 128.9, 124.8, 119.6, 117.5, 116.9, 51.8, 34.1, 31.5; IR (neat, cm^{-1}): 3378, 2954, 2927, 2857, 1703, 1615, 1517, 1502, 1435, 1262, 1162; HRMS (ESI/Q-TOF) (m/z): calcd. for $C_{14}H_{19}NO_2Na$, $[M + Na]^+$: 256.1308, found: 256.1301.

Methyl (E)-3-(2-amino-5-fluorophenyl)acrylate (4a)[22d]:

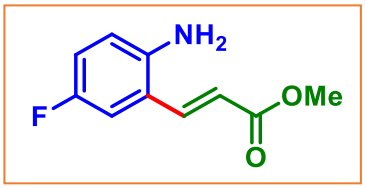

As yellow (69 mg, 71% yield), mp: 93–95; ^{o}C ^{1}H NMR ($CDCl_3$, 400 MHz): δ 7.76 (d, 1H, J = 16.0 Hz), 7.07 (dd, 1H, J_1 = 9.6 Hz, J_2 = 2.8 Hz), 6.90 (dt, 1H, J_1 = 8.4 Hz, J_2 = 2.8 Hz), 6.65 (dd, 1H, J_1 = 8.6 Hz, J_2 = 5.2 Hz), 6.33 (d, 1H, J = 16.0 Hz), 3.80 (s 3H); ^{13}C{^{1}H} NMR ($CDCl_3$, 125 MHz): δ 167.5, 156.5 (d, J_{C-F} = 235.6 Hz), 141.9 (d, J_{C-F} = 2.12 Hz), 139.3 (d, J_{C-F} = 2.5 Hz), 121.0 (d, J_{C-F} = 7.1 Hz), 119.1, 118.5 (d, J_{C-F} = 7.75 Hz), 113.6 (d, J_{C-F} = 22.5 Hz), 51.9; ^{19}F NMR ($CDCl_3$, 376 MHz): δ –125.7; IR (neat, cm^{-1}): 3375, 3057, 1706, 1626, 1495, 1435, 1263, 1176; HRMS (ESI/Q-TOF)

(m/z): calcd. for $C_{10}H_{11}FNO_2$, $[M + H]^+$: 196.0768, found: 196.0786.

Ethyl (E)-3-(2-amino-5-fluorophenyl)acrylate (4b)[22h]:

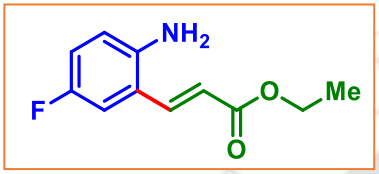

As yellowish solid (71 mg, 68% yield), mp: 79–81 °C; ^{1}H NMR ($CDCl_3$, 500 MHz): δ 7.75 (d, 1H, J = 16.0 Hz), 7.07 (dd, 1H, J_1 = 6.5 Hz, J_2 = 2.5 Hz), 6.91–6.87 (m, 1H), 6.64 (dd, 1H, J_1 = 4.0 Hz, J_2 = 5.0 Hz), 6.32 (d, 1H, J = 16.0 Hz), 4.26 (q, 2H), 3.84 (s, 2H), 1.33 (s, 3H, J = 7.0 Hz); ^{13}C{^{1}H} NMR ($CDCl_3$, 125 MHz): δ 167.1, 156.5 (d, $J_{C\text{-}F}$ = 235.7 Hz), 141.9 (d, $J_{C\text{-}F}$ = 1.9 Hz), 139.1 (d, $J_{C\text{-}F}$ = 2.4 Hz), 121.2 (d, $J_{C\text{-}F}$ = 7.0 Hz), 119.7, 118.4 (d, $J_{C\text{-}F}$ = 22.87 Hz), 118.2 (d, $J_{C\text{-}F}$ = 7.8 Hz), 113.6 (d, $J_{C\text{-}F}$ = 22.5 Hz), 60.8, 14.5; ^{19}F NMR ($CDCl_3$, 471 MHz): δ –112.8; IR (neat, cm^{-1}): 3372, 3241, 2982, 2927, 1698, 1622, 1493, 1434, 1368, 1256, 1152, 1032; HRMS (ESI/Q-TOF) (m/z): calcd. for $C_{11}H_{13}FNO_2$, $[M + H]^+$: 210.0925, found: 210.0927.

Isobutyl (E)-3-(2-amino-5-fluorophenyl)acrylate (4g):

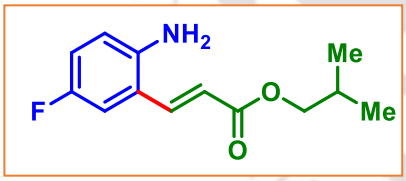

As yellowish solid (77 mg, 65% yield), mp: 81–83 °C; ^{1}H NMR ($CDCl_3$, 500 MHz): δ 7.75 (d, 1H, J = 16.5 Hz), 7.07 (d, 1H, J = 10.0 Hz), 6.92–6.88 (m, 1H), 6.66–6.63 (m, 1H), 6.35 (d, 1H, J = 16.0 Hz), 3.99 (d, 2H, J = 6.0 Hz), 3.83 (s, 2H), 2.04–1.98 (m, 1H), 0.98 (d, 6H, J = 6.5 Hz); ^{13}C{^{1}H} NMR ($CDCl_3$, 125 MHz): δ 167.2, 156.5 (d, $J_{C\text{-}F}$ = 235.7 Hz), 141.9 (d, $J_{C\text{-}F}$ = 1.87 Hz), 139.1 (d, $J_{C\text{-}F}$ = 2.37 Hz), 121.2 (d, $J_{C\text{-}F}$ = 7.25 Hz), 119.6, 118.4 (d, $J_{C\text{-}F}$ = 22.87 Hz), 118.1 (d, $J_{C\text{-}F}$ = 7.62 Hz), 113.7 (d, $J_{C\text{-}F}$ = 22.6 Hz), 71.0, 28.0, 19.3; ^{19}F NMR ($CDCl_3$, 471 MHz): δ –125.8; IR (neat, cm^{-1}): 3373, 3053, 2960, 2925, 1705, 1627, 1496, 1375, 1263, 1157; HRMS (ESI/Q-TOF) (m/z): calcd. for $C_{13}H_{17}FNO_2$, $[M + H]^+$: 238.1238, found: 238.1246.

Methyl (E)-3-(2-amino-5-chlorophenyl)acrylate (5a)[22g]:

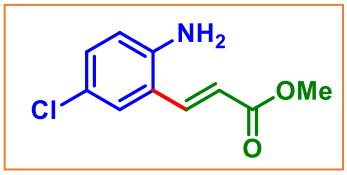

As yellow solid (74 mg, 70% yield), mp: 89–91 °C; ^{1}H NMR ($CDCl_3$, 500 MHz): δ 7.72 (d, 1H, J = 16.0 Hz), 7.33 (d, 1H, J = 2.5 Hz), 7.11 (dd, 1H, J_1 = 8.5 Hz, J_2 = 2.0 Hz), 6.63 (d, 1H, J = 8.5 Hz), 6.34 (d, 1H, J = 15.5 Hz), 3.96 (s, 2H), 3.80 (s, 3H); ^{13}C{^{1}H} NMR ($CDCl_3$, 125 MHz): δ 167.5, 144.2, 139.0, 131.1, 127.5, 123.9, 121.2, 119.1, 118.1, 52.0; IR (neat, cm^{-1}): 3055, 29881732, 1631, 1421, 1374, 1264, 1046; HRMS (ESI/Q-TOF) (m/z): calcd. for $C_{10}H_{11}ClNO_2$, $[M + H]^+$: 212.0473, found: 212.0476.

Methyl (E)-3-(2-amino-4-chlorophenyl)acrylate (6a):

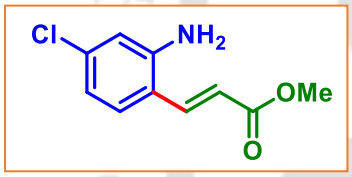

As yellow solid (64 mg, 61% yield), mp: 119–121 °C; ^{1}H NMR ($CDCl_3$, 500 MHz): δ 7.73 (d, 1H, J = 15.5 Hz), 7.28 (d, 1H, J = 8.0 Hz), 6.73 (d, 1H, J = 9.0 Hz), 6.70 (d, 1H, J = 2.0 Hz), 6.32 (d, 1H, J = 16.0 Hz), 4.03 (s, 3H), 3.80 (s, 3H); ^{13}C{^{1}H} NMR ($CDCl_3$, 125 MHz): δ 167.7, 146.6, 139.3, 137.1, 129.4, 119.3, 118.4, 118.3, 116.4, 51.9; IR (neat, cm^{-1}): 3453, 3055, 2988, 1733, 1620, 1422, 1374, 1264; HRMS (ESI/Q-TOF) (m/z): calcd. for $C_{10}H_{11}ClNO_2$, $[M + H]^+$: 212.0473, found: 212.0474.

Methyl (E)-3-(2-amino-5-bromophenyl)acrylate (7a):

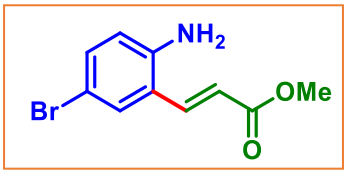

As a yellowish solid (87 mg, 68% yield), mp: 122–124 °C; ^{1}H NMR ($CDCl_3$, 500 MHz): δ 7.71 (d, 1H, J = 16.0 Hz), 7.47 (d, 1H, J = 2.5 Hz), 7.24 (dd, 1H, J_1 = 8.0 Hz, J_2 = 2.5 Hz), 6.58 (d, 1H, J = 8.5 Hz), 6.34 (d, 1H, J = 16.0 Hz), 3.97 (s, 2H), 3.80 (s, 3H); ^{13}C{^{1}H} NMR ($CDCl_3$, 125 MHz): δ 167.5. 144.6, 138.9, 133.9, 130.5, 121.8, 119.2, 118.4, 110.8, 51.9; IR (neat, cm^{-1}): 3055, 2988, 1732, 1629, 1422, 1374, 1264, 1046; HRMS (ESI/Q-TOF) (m/z): calcd. for $C_{10}H_{11}BrNO_2$, $[M + H]^+$: 255.9968, found: 255.9964.

Methyl (E)-3-(2-amino-5-(trifluoromethyl)phenyl)acrylate (8a):

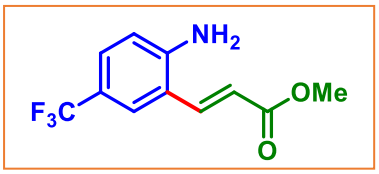

As a yellow solid (83 mg, 68% yield), mp: 86–89 °C; ^{1}H NMR ($CDCl_3$, 400 MHz): δ 7.76 (d, 1H, J = 15.6 Hz), 7.60 (t, 1H, J = 1.6 Hz), 7.40–7.37 (m, 1H), 6.73 (d, 1H, J = 9.2 Hz), 6.40 (d, 1H, J = 16.0 Hz), 4.27 (s, 2H), 3.81 (s, 3H); ^{13}C{^{1}H} NMR ($CDCl_3$, 125 MHz): δ 167.4, 148.1, 139.0, 128.0 (q, J_{C-F} = 3.62 Hz), 125.6 (q, J_{C-F} = 3.62 Hz), 123.5, 121.0 (q, J_{C-F} = 32.75 Hz), 119.8, 119.3, 116.4, 52.0; ^{19}F NMR ($CDCl_3$, 471 MHz): δ –61.6; IR (neat, cm^{-1}): 3381, 3253, 3053, 2956, 1707, 1630, 1511, 1438, 1264, 1077; HRMS (ESI/Q-TOF) (m/z): calcd. for $C_{11}H_{11}F_3NO_2$, $[M + H]^+$: 246.0736, found: 246.0737.

Methyl (E)-3-(2-amino-5-cyanophenyl)acrylate (9a):

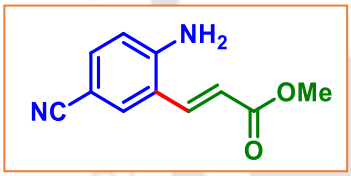

As yellow solid (68 mg, 67% yield), mp: 69–71 °C; ^{1}H NMR ($CDCl_3$, 500 MHz): δ 7.68 (d, 1H, J = 16.0 Hz), 7.63 (d, 1H, J = 1.5 Hz), 7.40 (dd, 1H, J_1 = 8.5 Hz, J_2 = 2.0 Hz), 6.70 (d, 1H, J = 9.0 Hz), 6.37 (d, 1H, J = 15.5 Hz), 4.47 (s, 2H), 3.82 (s, 3H); ^{13}C{^{1}H} NMR ($CDCl_3$, 125 MHz): δ 167.1, 148.9, 138.0, 134.4, 132.7, 120.6, 119.9, 119.4, 116.5, 101.5, 52.1; IR (neat, cm^{-1}): 3450, 3373, 3261, 2956, 2918, 2217, 1709, 1663, 1629, 1608, 1505, 1480, 1225, 1017; HRMS (ESI/Q-TOF) (m/z): calcd. for $C_{11}H_{11}N_2O_2$, $[M + H]^+$: 203.0815, found: 203.0813.

Methyl (E)-3-(2-amino-3-methylphenyl)acrylate (10a):

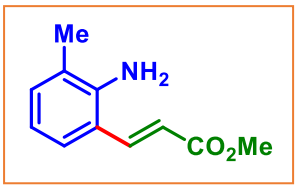

As yellow solid (52 mg, 54% yield), mp: 70–72 °C; ^{1}H NMR ($CDCl_3$, 400 MHz): δ 7.88 (d, 1H, J = 16.0 Hz), 7.27 (d, 1H, J = 5.6 Hz), 7.09 (d, 1H, J = 7.6 Hz), 6.70 (t, 1H, J = 7.6 Hz), 6.35 (d, 1H, J = 15.6 Hz), 3, 98 (s, 2H), 3.81 (s, 3H), 2.12 (s, 3H); ^{13}C{^{1}H} NMR ($CDCl_3$, 100 MHz): δ 167.9, 144.0, 140.9, 132.5, 126.1, 123.3, 119.6, 118.5, 118.0, 51.8, 17.7; IR (neat, cm^{-1}): 3388, 3055, 1714, 1656, 1438, 1264; HRMS (ESI/Q-

TOF) (m/z): calcd. for $C_{11}H_{14}NO_2$, $[M + H]^+$: 192.1019, found: 192.1023.

Benzo[h]quinolin-2(1H)-one (11a):

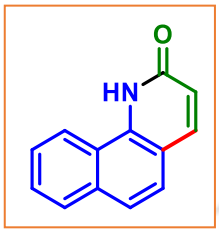

As yellow solid (80 mg, 82% yield), mp: 190–192 °C; ^{1}H NMR ($CDCl_3$, 400 MHz): δ 8.24 (s, 1H), 7.64 (d, 1H, J = 8.0 Hz), 7.36 (d, 1H, J = 8.0 Hz), 7.29–7.25 (m, 2H), 7.15 (d, 1H, J = 7.2 Hz), 6.83 (d, 1H, J = 12.4 Hz), 6.77 (d, 1H, J = 8.0 Hz), 5.84 (dd, 1H, J_1 = 12.8, J_2 = 2.0 Hz); ^{13}C{^{1}H} NMR ($CDCl_3$, 125 MHz): δ 166.2, 144.6, 136.8, 136.7, 133.2, 132.0, 131.9, 127.4, 126.2, 125.4, 123.8, 122.2, 115.5; IR (neat, cm^{-1}): 3208, 3060, 2958, 1674, 1621, 1529, 1446, 1266, 1047; HRMS (ESI/Q-TOF) (m/z): calcd. for $C_{13}H_{10}NO$, [M + H]+: 196.0757, found: 196.0758.

Methyl (E)-3-(5-aminobenzo[d][1,3]dioxol-4-yl)acrylate (12a):

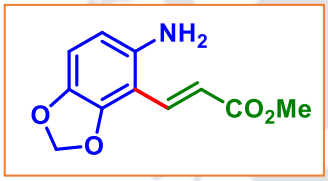

As yellow solid (66 mg, 60% yield), mp: 111–113 °C; ^{1}H NMR ($CDCl_3$, 400 MHz): δ 7.80 (d, 1H, J = 16.0 Hz), 6.71 (d, 1H, J = 16.0 Hz), 6.65 (d, 1H, J = 8.4 Hz), 6.17 (d, 1H, J = 8.4), 5.96 (s, 2H), 3.80 (s, 3H), 3.72 (s, 2H); ^{13}C{^{1}H} NMR ($CDCl_3$, 100 MHz): δ 168.2, 147.5, 140.7, 140.6, 134.7, 121.0, 110.7, 108.2, 106.7, 101.5, 51.8; IR (neat, cm^{-1}): 3395, 2968, 1710, 1629, 1460, 1359, 1319, 1262, 1180; HRMS (ESI/Q-TOF) (m/z): calcd. for $C_{11}H_{12}NO_4$, $[M + H]^+$: 222.0761, found: 222.0770.

Ethyl (E)-3-(5-aminobenzo[d][1,3]dioxol-4-yl)acrylate (12b):

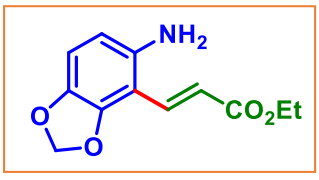

As yellow solid (75 mg, 64% yield), mp: 117–119 °C; ^{1}H NMR ($CDCl_3$, 400 MHz): δ 7.69 (d, 1H, J = 16.0 Hz), 6.70 (d, 1H, J = 16.0 Hz), 6.65 (d, 1H, J = 8.4 Hz), 6.17 (d, 1H, J = 8.4 Hz), 5.96 (s, 2H), 4.25 (q, 2H, J = 7.2 Hz), 3.71 (s, 2H), 1.33 (t, 3H, J = 7.2 Hz); ^{13}C{^{1}H} NMR ($CDCl_3$, 100 MHz): δ 167.8, 147.4, 140.7, 140.6, 134.4, 121.5, 110.6, 108.2, 106.8,

101.4, 60.6, 14.5; IR (neat, cm^{-1}): 3398, 2906, 1704, 1625, 1461, 1368, 1318, 1260, 1186; HRMS (ESI/Q-TOF) (m/z): calcd. for $C_{12}H_{14}NO_4$, $[M + H]^+$: 236.0917, found: 236.0920.

Quinolin-2(1H)-one (1a')[22f]:

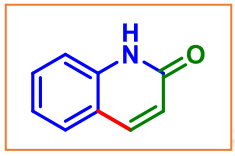

As white solid (34 mg, 93% yield), mp: 160–162 °C; ^1H NMR ($CDCl_3$, 500 MHz): δ 12.69 (s, 1H), 7.82 (d, 1H, J = 9.5 Hz), 7.56 (d, 1H, J = 8.0 Hz), 7.51 (d, 1H, J = 8.0 Hz), 7.46 (d, 1H, J = 8.0 Hz), 7.21 (t, 1H, J = 9.5 Hz), 6.73 (d, 1H, J = 9.5 Hz); $^{13}C\{^1H\}$ NMR ($CDCl_3$, 125 MHz): δ 164.9, 141.2, 138.7, 130.8, 127.9, 122.8, 121.5, 120.1, 116.4; IR (neat, cm^{-1}): 3396, 3057, 2989, 1733, 1657, 1429, 1374, 1264, 1045; HRMS (ESI/Q-TOF) (m/z): calcd. for C_9H_8NO, $[M + H]^+$: 146.0600, found: 146.0613.

6-Methylquinolin-2(1H)-one (2a'):

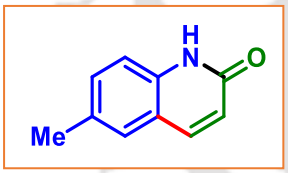

As yellowish solid (34 mg, 85% yield), mp: 165–167 °C; ^1H NMR ($CDCl_3$, 400 MHz): δ 11.73 (s, 1H), 7.75 (d, 1H, J = 10.0 Hz), 7.34 (d, 2H, J = 9.6 Hz), 7.29 (d, 1H, J = 8.0 Hz), 6.68 (d, 1H, J = 9.2 Hz), 2.41 (s, 3H); $^{13}C\{^1H\}$ NMR ($CDCl_3$, 125 MHz): δ 164.3, 140.9, 136.6, 132.4, 132.2, 127.6, 121.6, 120.1, 116.0, 21.0; IR (neat, cm^{-1}): 3422, 3054, 2988, 1733, 1661, 1425, 1374, 1264, 1046; HRMS (ESI/Q-TOF) (m/z): calcd. for $C_{10}H_{10}NO$, $[M + H]^+$: 160.0757, found: 160.0759.

6-Chloroquinolin-2(1H)-one (5a'):

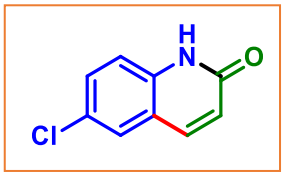

As yellowish solid (39 mg, 88% yield), mp: 179–181 °C; ^1H NMR ($CDCl_3$, 400 MHz): δ 12.03 (s, 1H), 7.74 (d, 1H, J = 9.6 Hz), 7.56 (d, 1H, J = 2.4 Hz), 7.47 (dd, 1H, J_1 = 6.8 Hz, J_2 = 2.0 Hz), 7.34 (d, 1H, J = 8.8 Hz), 6.74 (d, 1H, J = 9.6 Hz); $^{13}C\{^1H\}$ NMR ($CDCl_3$ + DMSO-d_6, 125 MHz): δ 161.4, 138.0, 136.5, 129.1, 125.6, 125.5, 122.0, 119.4, 116.2; IR (neat, cm^{-1}): 3055, 2957, 1733, 1669, 1424, 1374, 1264, 1046;

HRMS (ESI/Q-TOF) (m/z): calcd. for C_9H_7ClNO, $[M + H]^+$: 180.0211, found: 180.0211.

7-Chloroquinolin-2(1H)-one (6a'):

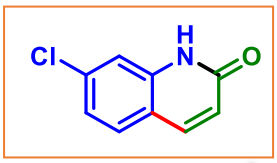

As white solid (38 mg, 86% yield), mp: 169–171 °C; ^{1}H NMR ($CDCl_3$ + DMSO-d_6 400 MHz): δ 11.71 (s, 1H), 7.69 (dd, 1H, J_1 = 10.4 Hz, J_2 = 2.8 Hz), 7.46 (dd, 1H, J_1 = 8.4 Hz, J_2 = 2.8 Hz), 7.29 (s, 1H), 7.04 (d, 1H, J = 8.4 Hz), 6.44 (dd, 1H, J_1 = 9.6 Hz, J_2 = 4.0 Hz); ^{13}C{^{1}H} NMR NMR ($CDCl_3$ + DMSO-d_6, 100 MHz): δ 161.3, 138.6, 138.3, 134.3, 127.9, 120.9, 120.8, 116.8, 113.8; IR (neat, cm^{-1}): 3054, 2957, 1733, 1674, 1425, 1374, 1254, 1046; HRMS (ESI/Q-TOF) (m/z): calcd. for C_9H_7ClNO, $[M + H]^+$: 180.0211, found: 180.0213.

6-Trifluoromethylquinolin-2(1H)-one (8a'):

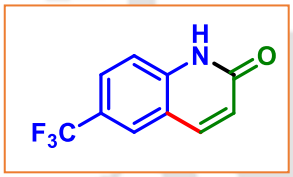

As yellowish solid (44 mg, 82% yield), mp: 178–180 °C; ^{1}H NMR ($CDCl_3$, 500 MHz): δ 12.52 (s, 1H), 7.87 (d, 2H, J = 7.2 Hz), 7.73 (d, 1H, J = 7.2 Hz), 7.52 (d, 1H, J = 6.8 Hz), 6.81 (d, 1H, J = 7.6 Hz); ^{13}C{^{1}H} NMR ($CDCl_3$, 125 MHz): δ 160.3, 139.6, 138.2, 124.8–124.7 (m), 123.7–123.6 (m), 121.6, 121.5, 120.5 (q, $J_{C\text{-}F}$ = 32.3 Hz), 117.0, 114.4; ^{19}F NMR ($CDCl_3$, 471 MHz): δ –61.8; IR (neat, cm^{-1}): 3055, 2983, 1733, 1674, 1373, 1324, 1264, 1046; HRMS (ESI/Q-TOF) (m/z): calcd. for $C_{10}H_7F_3NO$, $[M + H]^+$: 214.0474, found: 214.0476.

4-(p-Tolyl)quinolin-2(1H)-one (1ab)[19a]:

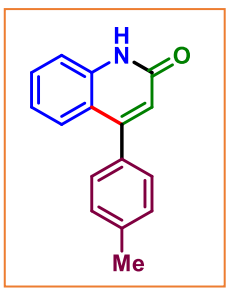

As white solid (50 mg, 86% yield), mp: 237–239 °C; ^{1}H NMR ($CDCl_3$, 500 MHz): δ 12.80 (s, 1H), 7.59 (dd, 1H, J_1 = 8.0 Hz, J_2 = 1.5 Hz), 7.58–7.50 (m, 2H), 7.37 (d, 2H, J = 8.0 Hz), 7.32 (d, 2H, J = 8.0 Hz), 7.17–7.14 (m, 1H), 6.69 (s, 1H), 2.46 (s, 3H); ^{13}C{^{1}H} NMR ($CDCl_3$, 125 MHz): δ 164.5, 153.7, 139.1, 139.0, 134.4, 130.8, 129.5, 129.0, 126.9, 122.6, 120.7, 119.9,

116.9, 21.5; IR (neat, cm^{-1}): 3419, 3049, 2992, 1735, 1659, 1431, 1369, 1266, 1047;HRMS (ESI/Q-TOF) (m/z): calcd. for $C_{16}H_{14}NO$, $[M + H]^+$: 236.1070, found: 236.1071.

6-Methyl-4-(p-tolyl)quinolin-2(1H)-one (2ab):

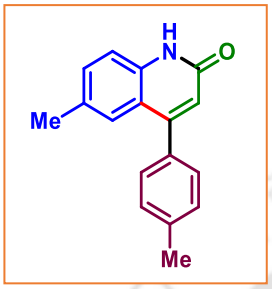

As white solid (46 mg, 75% yield), mp 170–172 °C; ^1H NMR ($CDCl_3$, 400 MHz): δ 11.57 (s, 1H), 7.34–7.33 (m, 6H), 7.26 (s, 1H), 6.63 (s, 1H), 2.46 (s, 3H), 2.33 (s, 3H); $^{13}C\{^1H\}$ NMR ($CDCl_3$, 100 MHz): δ 163.8, 153.4, 138.9, 136.9, 134.5, 132.3, 132.2, 129.5, 128.9, 126.5, 120.8, 119.8, 116.4, 21.5, 21.3; IR (neat, cm^{-1}): 3419, 3044, 2982, 1731, 1661, 1423, 1372, 1269, 1041; HRMS (ESI/Q-TOF) (m/z): calcd. for $C_{17}H_{16}NO$, $[M + H]^+$: 250.1226, found: 250.1228.

6-Chloro-4-(p-tolyl)quinolin-2(1H)-one (5ab):

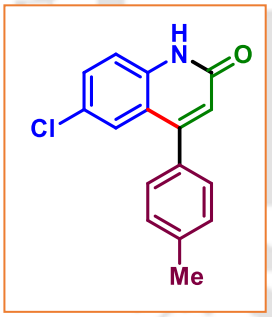

As white solid (51 mg, 76% yield), 230–232 °C; ^1H NMR ($CDCl_3$, 400 MHz): δ 11.34 (s, 1H), 7.56–7.52 (m, 2H), 7.49–7.45 (m, 2H), 7.34 (s, 3H), 6.69 (s, 1H), 2.47 (s, 3H); $^{13}C\{^1H\}$ NMR ($CDCl_3$ + DMSO-d_6, 100 MHz): δ 161.1, 150.2, 137.8, 137.0, 129.3, 128.5, 127.5, 125.8, 124.5, 121.2, 119.3, 116.8, 20.3; IR (neat, cm^{-1}): 3432, 3044, 2982, 1733, 1663, 1421, 1377, 1265, 1049; HRMS (ESI/Q-TOF) (m/z): calcd. for $C_{16}H_{13}ClNO$, $[M + H]^+$: 270.0680, found: 270.0686.

6-Chloro-4-phenylquinolin-2(1H)-one (5aa):

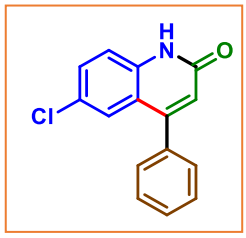

As white solid (47 mg, 74% yield), mp 258–260 °C; ^1H NMR ($CDCl_3$, 500 MHz): δ 6.71 (s, 1H), 7.44 (d. 3H, J = 8 Hz), 7.49–7.47 (m, 1H), 7.54–7.51 (m, 4H), 12.53 (s, 1H); ^{13}C NMR ($CDCl_3$, 125 MHz): δ 163.9, 152.8, 137.5, 136.6, 131.2, 129.4, 129.1, 128.9, 128.3, 126.3, 122.0, 120.9, 118.1; IR (neat, cm^{-1}): 3351, 2954, 2920, 1730, 1663, 1519, 1439, 1371, 1258, 1177; HRMS (ESI/Q-TOF) (m/z): calcd. for $C_{15}H_{11}ClNO$, $[M + H]^+$: 256.0524, found: 256.0522.

7-Chloro-4-(p-tolyl)quinolin-2(1H)-one (6ab):

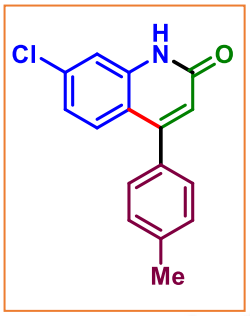

As white solid (50 mg, 75% yield), 223–225 °C; ^{1}H NMR ($CDCl_3$ + DMSO-d_6, 400 MHz): δ 11.72 (s, 1H), 7.62 (s, 1H), 7.42 (d, 1H, J = 6.8 Hz), 7.36 (d, 2H, J = 1.6 Hz), 7.34–7.31 (m, 2H), 6.96 (dd, 1H, J_1 = 8.8 Hz, J_2 = 2.0 Hz), 2.36 (s, 3H); ^{13}C{^{1}H} NMR ($CDCl_3$ + DMSO-d_6, 100 MHz): δ 161.6, 150.9, 139.3, 137.8, 135.0, 132.9, 128.4, 127.6, 127.1, 121.2, 120.3, 116.9, 114.7, 20.3; IR (neat, cm^{-1}): 3341, 2954, 2921, 1724, 1669, 1512, 1437, 1374, 1258, 1170; HRMS (ESI/Q-TOF) (m/z): calcd. for $C_{16}H_{13}ClNO$, $[M + H]^+$: 270.0680, found: 270.0686.

6-(p-tolylethynyl)quinolin-2(1H)-one (7ac'):

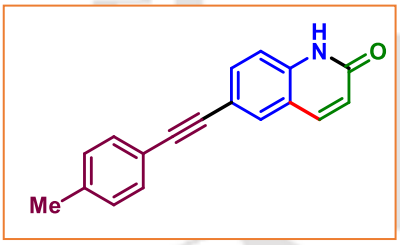

As white solid (49 mg, 76% yield), 159–161 °C; ^{1}H NMR ($CDCl_3$, 400 MHz): δ 10.9 (s, 1H), 7.78–7.75 (m, 2H,), 7.64 (d, 1H, J = 8.4 Hz), 7.43 (d, 2H, J = 8.0 Hz), 7.28 (d, 1H, J = 8.4 Hz), 717 (d, 2H, J = 8.0 Hz), 6.71 (d, 1H, J = 9.2 Hz), 2.37 (s, 3H); ^{13}C{^{1}H} NMR ($CDCl_3$, 100 MHz): δ 164.4, 140.7, 138.7, 138.0, 133.9, 131.6, 131.0, 129.3, 128.6, 122.2, 120.0, 118.2, 116.4, 89.8, 87.9, 21.7; IR (neat, cm^{-1}): 3351, 2954, 2920, 2210, 1694, 1660, 1510, 1438, 1374, 1258, 1173; HRMS (ESI/Q-TOF) (m/z): calcd. for $C_{18}H_{14}NO$, $[M + H]^+$: 260.1070, found: 260.1077.

Methyl (E)-3-(2-amino-5-(p-tolylethynyl)phenyl)acrylate (7ac):

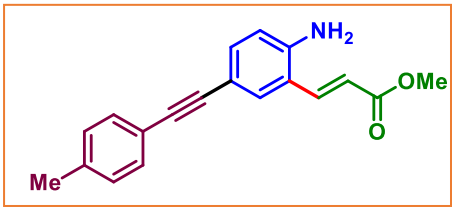

As yellow solid (59 mg, 81% yield), mp 158–160 °C; ^{1}H NMR ($CDCl_3$, 400 MHz): δ 7.77 (d, 1H, J = 16.0 Hz), 7.57 (d, 1H, J = 2.5 Hz), 7.39 (d, 2H, J = 16.0 Hz), 7.32 (d, 1H, J_1 = 6.4 Hz, J_2 = 2.0 Hz), 7.14 (d, 2H, J = 8.0 Hz), 6.65 (d, 1H, J = 8.4 Hz), 6.39 (d, 1H, J = 15.6 Hz), 4.14 (s, 2H), 3.80 (s, 3H), 2.36 (s, 3H); ^{13}C{^{1}H} NMR ($CDCl_3$, 100 MHz): δ 167.7, 145.9, 139.4, 138.1, 134.5, 131.5, 131.4, 129.2,

120.6, 119.7, 118.7, 116.7, 113.6, 88.6, 88.1, 51.9, 21.6; IR (neat, cm^{-1}): 3484, 3385, 3241, 2949, 2202, 1696, 1620, 1512, 1496, 1342, 1268, 1172, 1115, 1040; HRMS (ESI/Q-TOF) (m/z): calcd. for $C_{19}H_{18}NO_2$, $[M + H]^+$: 292.1332, found: 292.1335.

Methyl cinnamate (1a''):

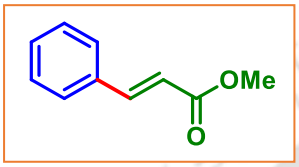

As gummy (53 mg, 65% yield); ^1H NMR ($CDCl_3$, 400 MHz): δ 7.70 (d, 1H, J = 16.0 Hz), 7.54–7.51 (m, 2H), 7.38 (t, 3H, J = 3.6 Hz), 6.44 (d, 1H, J = 16.0 Hz), 3.81 (s, 3H); $^{13}C\{^1H\}$ NMR ($CDCl_3$, 100 MHz): δ 167.6, 145.1, 134.5, 130.5, 129.1, 128.2, 118.0, 51.9; IR (neat, cm^{-1}): 3056, 2959, 1733, 1635, 1422, 1374, 1264, 1046; HRMS (ESI/Q-TOF) (m/z): calcd. for $C_{10}H_{11}O_2$, $[M + H]^+$: 163.0754, found: 163.0756.

tert-Pentyl acrylate (h)[21a]:

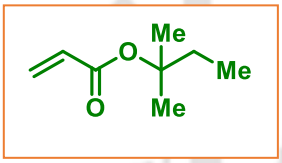

As colorless liquid: ^1H NMR ($CDCl_3$, 500 MHz): δ 7.15 (dd, 1H, J_1 = 17.5 Hz, J_2 = 11.0 Hz), 6.06 (d, 1H, J = 17.0 Hz), 5.40 (d, 1H, J = 11.0 Hz), 1.60 (q, 2H, J = 7.5 Hz), 1.24 (s, 6H), 0.64 (t, 3H, J = 7.5 Hz). The obtained ^1H NMR spectra matched with the reported procedure in ref. 21a.

p-Tolyl acrylate (l)[21b]:

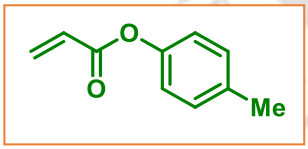

As colorless liquid: ^1H NMR ($CDCl_3$, 400 MHz): δ 7.16 (d, 2H, J = 8.4 Hz), 6.99 (d, 2H, J = 8.4 Hz), 6.57 (d, 1H, J = 18.0 Hz), 6.29 (dd, 1H, J_1 = 17.2 Hz, J_2 = 9.2 Hz), 5.97 (d, 1H, J = 9.2 Hz), 2.33 (s, 3H). The obtained ^1H NMR spectra matched with the reported procedure in ref. 21b.

4-Methoxyphenyl acrylate (m)[21c]:

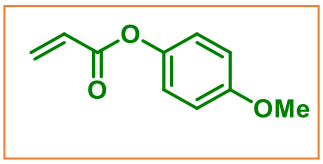

As colorless liquid: ^1H NMR ($CDCl_3$, 500 MHz): δ 7.05 (d, 2H, J = 9.0 Hz), 6.89 (d, 2H, J = 9.0 Hz), 6.57 (d, 1H, J = 17.5 Hz), 6.30 (dd, 1H, J_1 = 17.5 Hz, J_2 = 10.5 Hz), 5.96 (d, 1H, J = 10.5 Hz), 3.76 (s, 3H); $^{13}C\{^1H\}$ NMR ($CDCl_3$, 125 MHz): δ 164.8, 157.3, 144.1, 132.2, 127.9, 122.2, 114.4, 56.4; IR (neat, cm^{-1}): 2979,1720, 1639, 1545, 1340, 1282, 1152. The

obtained ^{1}H and $^{13}C\{^{1}H\}$ NMR spectra matched with the reported procedure in ref. 21c.

2-(6,6-Dimethylbicyclo[3.1.1]hept-3-en-2-yl)ethyl acrylate (p):

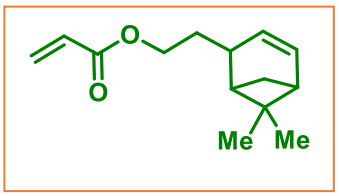

As colorless liquid: ^{1}H NMR ($CDCl_3$, 400 MHz): δ 6.29 (dd, 1H, J_1 = 5.6 Hz, J_2 = 2.0 Hz), 6.06–5.99 (m, 1H), 5.72 (dd, 1H, J_1 = 10.4 Hz, J_2 = 1.6 Hz), 5.24 (s, 1H), 4.11–4.09 (m, 2H), 2.29–2.25 (m, 3H), 2.17–2.14 (m, 2H), 2.01 (s, 2H), 1.20 (s, 3H), 1.09 (d, 1H, J = 8.4 Hz), 0.76 (s, 3H); $^{13}C\{^{1}H\}$ NMR ($CDCl_3$, 100 MHz): δ 166.1, 144.2, 130.3, 128.7, 118.9, 62.8, 45.8, 40.8, 38.0, 35.6, 31.7, 31.4, 26.3, 21.1; IR (neat, cm^{-1}): 2915, 1721, 1635, 1407, 1267, 1189,1058.

(3S,8S,9S,10R,13R,14S,17R)-10,13-Dimethyl-17-((R)-6-methylheptan-2-yl)-2,3,4,7,8,9,10,11,12,13,14,15,16,17-tetradecahydro-1H-cyclopenta[a]phenanthren-3-yl acrylate (q)[21d]***:***

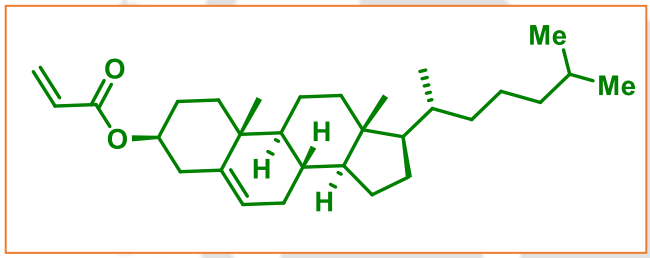

Yellow solid: ^{1}H NMR ($CDCl_3$, 500 MHz): δ 6.38 (dd, 1H, J_1 = 17.5 Hz, J_2 = 1.5 Hz), 6.10 (dd, 1H, J_1 = 17.0 Hz, J_2 = 10.5 Hz), 5.79 (dd, 1H, J_1 = 10.5 Hz, J_2 = 1.5 Hz), 5.38 (d, 1H, J = 5.0 Hz), 4.72–4.67 (m, 1H), 2.36 (d, 2H, J = 8.5 Hz), 2.03–1.95 (m, 2H), 1.92– 1.81 (m, 3H), 1.65–1.44 (m, 9H), 1.35–1.33(m, 3H), 1.28–1.22(m, 1H), 1.19–1.01 (m, 6H), 1.03–0.96 (m, 5H), 0.90 (d, 3H, J = 6.5 Hz), 0.87 (d, 3H, J = 2.5 Hz), 0.86 (d, 3H, J = 2.0 Hz), 0.68 (s, 3H). The obtained ^{1}H NMR spectra matched with the reported procedure in ref. 21d.

IV.6. References

[1] (a) Lyons, T. W.; Sanford, M. S. *Chem. Rev.* **2010**, *110*, 1147–1169. (b) Rogge, T.; Kaplaneris, N.; Chatani, N.; Kim, J.; Chang, S.; Punji, B.; Schafer, L. L.; Musaev, D. G.; Wencel-Delord, J.; Roberts, C. A.; Sarpong, R.; Wilson, Z. E.; Brimble, M. A.; Johansson, M. J.; Ackermann, L. *Nat. Rev. Methods Primers* **2021**, *1*, 43. (c) Li, Z.;

Shi, Z. *Acc. Chem. Res*. **2024**, *57*, 1057–1072. (d) Kuhl, N.; Hopkinson, M. N.; Wencel-Delord, J.; Glorius, F. *Angew. Chem. Int. Ed.* **2012**, *51*, 10236–10254. (e) Ryu, J.; Kwak, J.; Shin, K.; Lee, D.; Chang, S. *J. Am. Chem. Soc*. **2013**, *135*, 12861–12868.

[2] (a) Sambiagio, C.; Schönbauer, D.; Blieck, R.; Dao-Huy, T.; Pototschnig, G.; Schaaf, P.; Wiesinger, T.; Zia, M. F.; Wencel-Delord, J.; Besset, T.; Maes, B. U. W.; Schnürch, M. *Chem. Soc. Rev*. **2018**, *47*, 6603–6743. (b) Chen, Z.; Wang, B.; Zhang, J.; Yu, W.; Liu, Z.; Zhang, Y. *Org. Chem. Front*. **2015**, *2*, 1107–1295.

[3] (a) Ackermann, L. *Chem. Rev*. **2011**, *111*, 1315–1345. (b) Kumar, G. S.; Kumar, P.; Kapur, M. *Org. Lett*. **2017**, *19*, 2494–2497. (c) De Sarkar, S.; Liu, W.; Kozhushkov, S. I.; Ackermann, L. *Adv. Synth. Catal*. **2014**, *356*, 1461–1479. (d) Hummel, J. R.; Boerth, J. A.; Ellman, J. A. *Chem. Rev*. **2017**, *117*, 9163–9227. (e) Ogiwara, Y.; Tamura, M.; Kochi, T.; Matsuura, Y.; Chatani, N.; Kakiuchi, F. *Organometallics* **2014**, *33*, 402–420.

[4] (a) Boele, M. D. K.; van Strijdonck, G. P. F.; de Vries, A. H. M.; Kamer, P. C. J.; de Vries, J. G.; van Leeuwen, P. W. N. M. *J. Am. Chem. Soc.* **2002**, *124*, 1586–1587. (b) Sun, C.-L.; Li, B.-J.; Shi, Z.-J. *Chem. Commun*. **2010**, *46*, 677–685. (c) Schreib, B. S.; Fadel, M.; Carreira, E. M. *Angew. Chem. Int. Ed*. **2020**, *59*, 7818–7822. (d) Carral-Menoyo, A.; Sotomayor, N.; Lete, E. *Catal. Sci. Technol*. **2020**, *10*, 5345–5361. (e) Zhan, B.-B.; Li, Y.; Xu, J.-W.; Nie, X.-L.; Fan, J.; Jin, L.; Shi, B.-F. *Angew. Chem. Int. Ed*. **2018**, *57*, 5858–5862. (f) Hao, D.; Yang, Z.; Liu, Y.; Li, Y.; Li, C.; Gu, Y.; Vaccaro, L.; Liu, J.; Liu, P. *Org. Biomol. Chem*. **2022**, *20*, 847–851.

[5] (a) Liu, L.; Li, J.; Dai, W.; Gao, F.; Chen, K.; Zhou, Y.; Liu, H. *Molecules* **2020**, *25*, 268. (b) Zhao, F.; Zhou, Z.; Lu, Y.; Qiao, J.; Zhang, X.; Gong, X.; Liu, S.; Lin, S.; Wu, X.; Yi, W. *ACS Catal*. **2021**, *11*, 13921–13934. (c) Kumaran, S.; Parthasarathy, K. *J. Org. Chem*. **2021**, *86*, 7987–7999. (d) Wang, C.; Chen, F.; Qian, P.; Cheng, J. *Org. Biomol. Chem*. **2021**, *19*, 1705–1721. (e) Sasmal, S.; Prakash, G.; Dutta, U.; Laskar, R.; La-hiri, G. K.; Maiti, D. *Chem. Sci*. **2022**, *13*, 5616–5621. (f) Rej, S.; Chatani, N. *Angew. Chem. Int. Ed*. **2019**, *58*, 8304–8329.

[6] (a) Dethe, D. H.; Beeralingappa, N. C.; Kumar, V. *Org. Lett*. **2021**, *23*, 6267–6271. (b) Yu, C.; Li, F.; Zhang, J.; Zhong, G. *Chem. Commun*. **2017**, *53*, 533–536. (c) Duarah, G.; Kaishap, P. P.; Begum, T.; Gogoi, S. *Adv. Synth. Catal*. **2019**, *361*, 654–672. (d) Shan, C.; Zhu, L.; Qu, L.-B.; Bai, R.; Lan, Y. *Chem. Soc. Rev*. **2018**, *47*, 7552–7576.

(e) Gramage-Doria, R.; Bruneau, C. *Coord. Chem. Rev*. **2021**, *428*, 213602–213618. (f) Mohanty, S. R.; Prusty, N.; Nanda, T.; Banjare, S. K.; Ravikumar, P. C. *J. Org. Chem*. **2022**, *87*, 6189–6201.

[7] (a) Li, X.; Ouyang, W.; Nie, J.; Ji, S.; Chen, Q.; Huo, Y. *ChemCatChem* **2020**, *12*, 2358–2384. (b) Woźniak, Ł.; Tan, J.-F.; Nguyen, Q.-H.; Madron Du Vigné, A.; Smal, V.; Cao, Y.-X.; Cramer, N. *Chem. Rev*. **2020**, *120*, 10516–10543. (c) Haldar, C.; Hoque, M. E.; Chaturvedi, J.; Hassan, M. M. M.; Chattopadhyay, B. *Chem. Commun*. **2021**, *57*, 13059–13074.

[8] (a) Mohanty, S. R.; Prusty, N.; Banjare, S. K.; Nanda, T.; Ravikumar, P. C. *Org. Lett*. **2022**, *24*, 848–852. (b) Cano, R.; Mackey, K.; McGlacken, G. P. *Catal. Sci. Technol*. **2018**, *8*, 1251–1266. (c) Ghosh, S.; Khandelia, T.; Patel, B. K. *Org. Lett*. **2021**, *23*, 7370–7375.

[9] (a) Lukasevics, L.; Grigorjeva, L. *Org. Biomol. Chem*. **2020**, *18*, 7460–7466. (b) Dey, A.; Volla, C. M. R. *Org. Lett*. **2020**, *22*, 7480–7485. (c) Ujwaldev, S. M.; Harry, N. A.; Divakar, M. A.; Anilkumar, G. *Catal. Sci. Technol*. **2018**, *8*, 5983–6018. (d) Yang, J.; Hu, X.; Liu, Z.; Li, X.; Dong, Y.; Liu, G. *Chem. Commun*. **2019**, *55*, 13840–13843.

[10] (a) Chatani, N. *Acc. Chem. Res.* **2023**, *56*, 3053–3064. (b) Harry, N. A.; Saranya, S.; Ujwaldev, S. M.; Anilkumar, G. *Catal. Sci. Technol*. **2019**, *9*, 1726–1743. (c) Khake, S. M.; Chatani, N. *Trends Chem.* **2019**, *1*, 524–539. (d) Rao, W.-H.; Shi, B.-F. *Org. Chem. Front*. **2016**, *3*, 1028–1047. (e) Guo, X.-X.; Gu, D.-W.; Wu, Z.; Zhang, W. *Chem. Rev.* **2015**, *115*, 1622–1651. (f) Gandeepan, P.; Müller, T.; Zell, D.; Cera, G.; Warratz, S.; Ackermann, L. *Chem. Rev*. **2019**, *119*, 2192–2452.

[11] (a) Lukasevics, L.; Grigorjeva, L. *Org. Biomol. Chem*. **2020**, *18*, 7460–7466. (b) Dey, A.; Volla, C. M. R. *Org. Lett*. **2020**, *22*, 7480–7485. (c) Ujwaldev, S. M.; Harry, N. A.; Divakar, M. A.; Anilkumar, G. *Catal. Sci. Technol*. **2018**, *8*, 5983–6018. (d) Yang, J.; Hu, X.; Liu, Z.; Li, X.; Dong, Y.; Liu, G. *Chem. Commun*. **2019**, *55*, 13840–13843.

[12] (a) Gandeepan, P.; Ackermann, L. *Chem*. **2018**, *4*, 199–222. (b) Liu, Z.; Oxtoby, L. J.; Liu, M.; Li, Z.-Q.; Tran, V. T.; Gao, Y.; Engle, K. M. *J. Am. Chem. Soc*. **2021**, *143*, 8962–8969. (c) Jacob, C.; Maes, B. U. W.; Evano, G. *Chem. Eur. J*. **2021**, *27*, 13899–13952. (d) Liao, G.; Zhang, T.; Lin, Z.-K.; Shi, B.-F. *Angew. Chem. Int. Ed.* **2020**, *59*,

19773–19786. (e) Bag, S.; Jana, S.; Pradhan, S.; Bhowmick, S.; Goswami, N.; Sinha, S. K.; Maiti, D. *Nat. Commun*. **2021**, *12*, 1393–1400. (f) Xu, J.; Liu, Y.; Wang, Y.; Li, Y.; Xu, X.; Jin, Z. *Org. Lett*. **2017**, *19*, 1562–1565. (g) Zhang, M.; Zhong, Z.; Liao, L.; Zhang, A. Q. *Org. Chem. Front*. **2022**, *9*, 3882–3896. (h) Liao, G.; Chen, H.-M.; Xia, Y.-N.; Li, B.; Yao, Q.-J.; Shi, B.-F. *Angew. Chem. Int. Ed.* **2019**, *58*, 11464–11468. (i) Liao, G.; Li, B.; Chen, H.-M.; Yao, Q.-J.; Xia, Y.-N.; Luo, J.; Shi, B.-F. *Angew. Chem. Int. Ed.* **2018**, *57*, 17151–17155.

[13] (a) Lewis, L. N. *Inorg. Chem*. **1985**, *24*, 4433–4435. (b) Wu, Y.-J.; Yao, Q.-J.; Chen, H.-M.; Liao, G.; Shi, B.-F. *Sci. China Chem*. **2020**, *63*, 875–880.

[14] (a) Ali, W.; Prakash, G.; Maiti, D. *Chem. Sci*. **2021**, *12*, 2735–2759. (b) Shang, X.; Liu, Z.-Q. *Chem. Soc. Rev*. **2013**, *42*, 3253–3260. (c) Cheel, J.; Theoduloz, C.; Rodríguez, J.; Saud, G.; Caligari, P. D. S.; Schmeda-Hirschmann, G. *J. Agric. Food Chem*. **2005**, *53*, 8512–8518. (d) Jana, R.; Begam, H. M.; Dinda, E. *Chem. Commun*. **2021**, *57*, 10842–10866.

[15] (a) Grimsdale, A. C.; Leok Chan, K.; Martin, R. E.; Jokisz, P. G.; Holmes, A. B. *Chem. Rev*. **2009**, *109*, 897–1091. (b) Nguyen, P.-H.; Yang, J.-L.; Uddin, M. N.; Park, S.-L.; Lim, S.-I.; Jung, D.-W.; Williams, D. R.; Oh, W.-K. *J. Nat. Prod*. **2013**, *76*, 2080–2087. (c) Singh, R. S.; Michel, D.; Das, U.; Dimmock, J. R.; Alcorn, J. *Bioorg. Med. Chem. Lett*. **2014**, *24*, 5199–5202.

[16] (a) Patureau, F. W.; Glorius, F. *J. Am. Chem. Soc*. **2010**, *132*, 9982–9983. (b) Ferlin, F.; Santoro, S.; Ackermann, L.; Vaccaro, L. *Green Chem*. **2017**, *19*, 2510–2514. (c) Bai, P.; Li, Y.-Q.; Huang, Z.-Z. *Org. Lett*. **2017**, *19*, 1374–1377. (d) Zhang, H.-J.; Lin, W.; Su, F.; Wen, T.-B. *Org. Lett*. **2016**, *18*, 6356–6359. (e) Sharma, S.; Han, S.; Kim, M.; Mishra, N. K.; Park, J.; Shin, Y.; Ha, J.; Kwak, J. H.; Jung, Y. H.; Kim, I. S. *Org. Biomol. Chem*. **2014**, *12*, 1703–1706. (f) Leitch, J. A.; Cook, H. P.; Bhonoah, Y.; Frost, C. G. *J. Org. Chem*. **2016**, *81*, 10081–10087. (g) Guo, L.; Chen, Y.; Zhang, R.; Peng, Q.; Xu, L.; Pan, X. *Chem. - Asian J*. **2017**, *12*, 289–292. (h) Kumar, A.; Tadigoppula, N. *Org. Lett.* **2021**, *23*, 8–12. (i) Morita, T.; Satoh, T.; Miura, M. *Org. Lett*. **2017**, *19*, 1800–1803. (j) Zhang, X.; Zhang, B.; Li, X. *Org. Lett*. **2021**, *23*, 1687–1691. (k) Lv, H.; Shi, J.; Huang, J.; Zhang, C.; Yi, W. *Org. Biomol. Chem*. **2017**, *15*, 7088–7092.

[17] (a) Liang, H.; Li, G.; Zhang, L.; Wang, G.; Song, M.; Li, H.; Yuan, B. *Org. Lett*. **2021**, *23*, 5821–5825. (b) McKay, A. I.; Altalhi, W. A. O.; McInnes, L. E.; Czyz, M. L.; Canty, A. J.; Donnelly, P. S.; O'Hair, R. A. J. *J. Org. Chem*. **2020**, *85*, 2680–2687. (c) Pan, Z.; Shi, S.; Yang, X.; Xiao, X.; Zhang, W.; Wang, S.; Ma, Y. *Green Chem*. **2021**, *23*, 2944–2949. (d) Govindan, K.; Jayaram, A.; Duraisamy, T.; Chen, N.-Q.; Lin, W.-Y. *J. Org. Chem*. **2022**, *87*, 8719–8729.

[18] (a) Zhang, X.; Si, W.; Bao, M.; Asao, N.; Yamamoto, Y.; Jin, T. *Org. Lett*. **2014**, *16*, 4830–4833. (b) Bera, S. S.; Maji, M. S. *Org. Lett*. **2020**, *22*, 2615–2620. (c) Han, X.; Shan, L.-X.; Zhu, J.-X.; Zhang, C.-S.; Zhang, X.-M.; Zhang, F.-M.; Wang, H.; Tu, Y.-Q.; Yang, M.; Zhang, W.-S. *Angew. Chem. Int. Ed*. **2021**, *60*, 22688–22692. (d) Yang, L.; Fu, L.; Li, G. *Adv. Synth. Catal*. **2017**, *359*, 2235–2240. (e) Manikandan, R.; Madasamy, P.; Jeganmohan M. *ACS Catal*. **2016**, *6*, 230−234. (f) Li, J.; Kornhaaß, C.; Ackermann, L. *Chem. Commun*. **2012**, *48*, 11343–11345. (g) Song, L.; Zhang, X.; Tang, X.; Van Meervelt, L.; Van der Eycken, J.; Harvey, J. N.; Van der Eycken, E. V. *Chem. Sci*. **2020**, *11*, 11562–11569.

[19] (a) Gupta, S.; Ganguly, B.; Das, S. *RSC Adv*. **2014**, *4*, 41148–41151. (b) Patra, P. *ChemistrySelect* **2019**, *4*, 2024–2043. (c) Medina, F. G.; Marrero, J. G.; Macías-Alonso, M.; González, M. C.; Córdova-Guerrero, I.; Teissier García, A. G.; Osegueda-Robles, S. *Nat. Prod. Rep*. **2015**, *32*, 1472–1507. (d) Inamoto, K.; Saito, T.; Hiroya, K.; Doi, T. *J. Org. Chem*. **2010**, *75*, 3900–3903.

[20] (a) SMART V 4.043 Software for the CCD Detector System; Siemens Analytical Instruments Division: Madison, WI, **2008**. (b) SAINT Plus (v 6.14) Bruker AXS Inc., Madison, WI, **2008**. (c) Sheldrick, G. M. SHELXL-2014, Program for the Refinement of Crystal Structures; University of Göttingen: Göttingen (Germany), **1997**. (d) Dolomanov, O. V.; Bourhis, L. J.; Gildea, R. J.; Howard, J. A. K.; Puschmann, H.*J. Appl. Crystallogr*. **2009**, *42*, 339–341. (e) Sheldrick, G. M. *Acta. Crystallogr. A Found. Adv*. **2015**, *71, 3–8*. (f) Sheldrick, G. M. *Acta. Crystallogr. C Struct. Chem.* **2015**, *71, 3–8*..

[21] (a) Kumar, M.; Verma, S.; Verma, A. K. *Org. Lett.* **2020**, *22*, 4620–4626. (b) Maddocks, C. J.; Ermanis, K; Clarke, P. A. *Org. Lett*. **2020**, *22*, 8116–8121. (c) Fernandes, R. A.; Yadav, S. S; Kumar, P. *Org. Biomol. Chem*. **2022**, *20*, 427–443. (d)

Chen, H.; Farizyan, M.; Ghiringhelli, F.; Gemmeren M. van. *Angew. Chem. Int. Ed*. **2020**, *59*, 12213–12220.

[22] (a) Jiang, N.; Bu, Y.; Wang, Y.; Nie, M.; Zhang, D.; Zhai, X. *Molecules* **2016**, *21*, 1572. (b) Rakshit, A.; Dhara, H. N.; Alam, T.; Dahiya, A.; Patel, B. K. *J. Org. Chem*. **2021**, *86*, 17504–17510. (c) Dahiya, A.; Das, B.; Sahoo, A. K.; Patel, B. K. *Adv. Synth. Catal*. **2022**, *364*, 966–973. (d) Sharif, S. A. I.; Calder, E. D. D.; Delolo, F. G.; Sutherland, A. *J. Org. Chem*. **2016**, *81*, 6697–6706. (e) Lee, S. J.; Seo, H.-A.; Cheon, C.-H. *Adv. Syn. Catal*. **2016**, *358*, 1566–1570. (f) Xie, D.; Zhang, S. *J. Org. Chem*. **2022**, *87*, 8757–8763. (g) Adepu, R.; Rajitha, A.; Ahuja, D.; Sharma, A. K.; Ramudu, B.; Kapavarapu, R.; Parsaa, K. V. L.; Pal, M. *Org. Biomol. Chem*. **2014**, *12*, 2514–2518. (h) Palanimuthu, A.; Chen, C.; Lee, G.-H. *RSC Adv*. **2020**, *10*, 13591–13600.

IV.7. Representative Spectra

***Methyl (E)-3-(2-aminophenyl)acrylate (1a)*: ^{1}H NMR (CDCl$_3$, 400 MHz)**

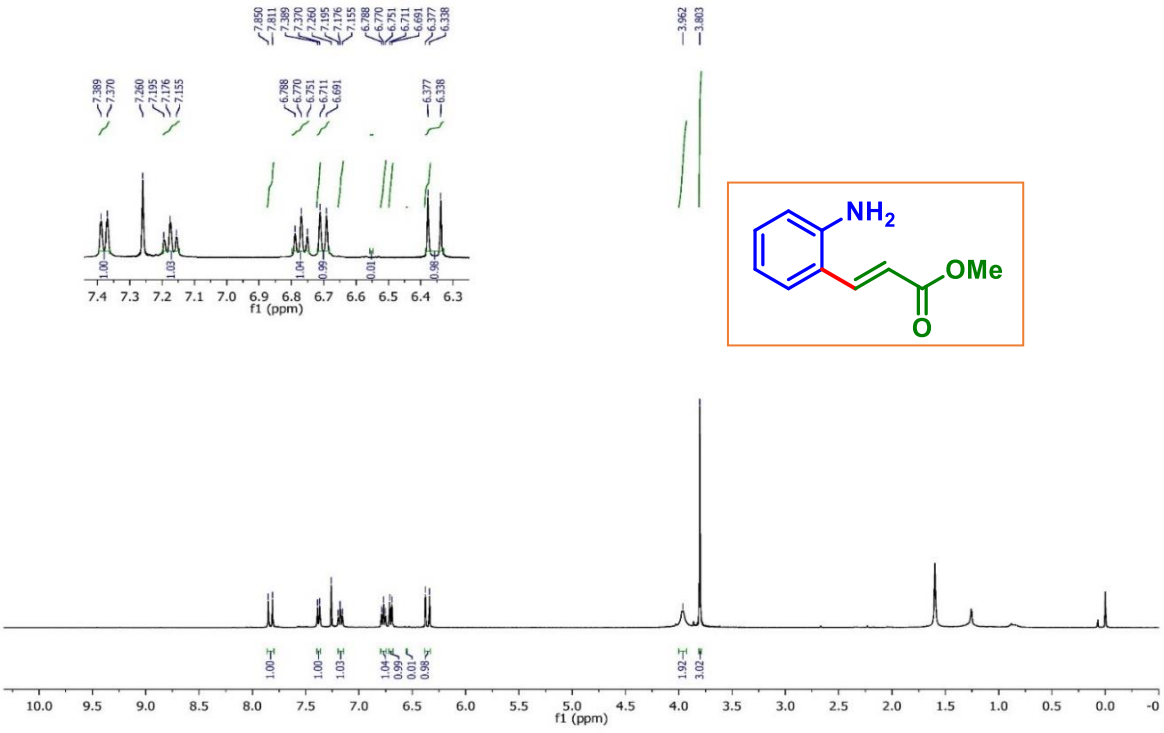

***Methyl (E)-3-(2-aminophenyl)acrylate (1a)*: $^{13}C\{^{1}H\}$ NMR ($CDCl_3$, 100 MHz)**

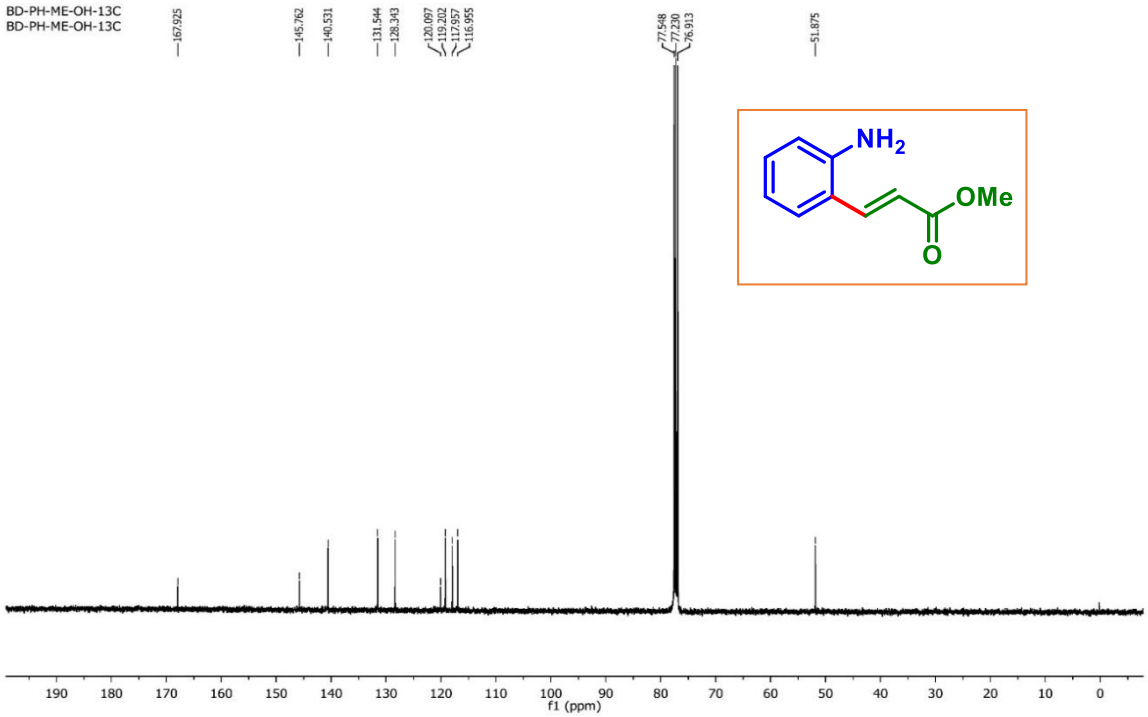

***Ethyl (E)-3-(2-aminophenyl)acrylate (1b)*: ^{1}H NMR ($CDCl_3$, 400 MHz)**

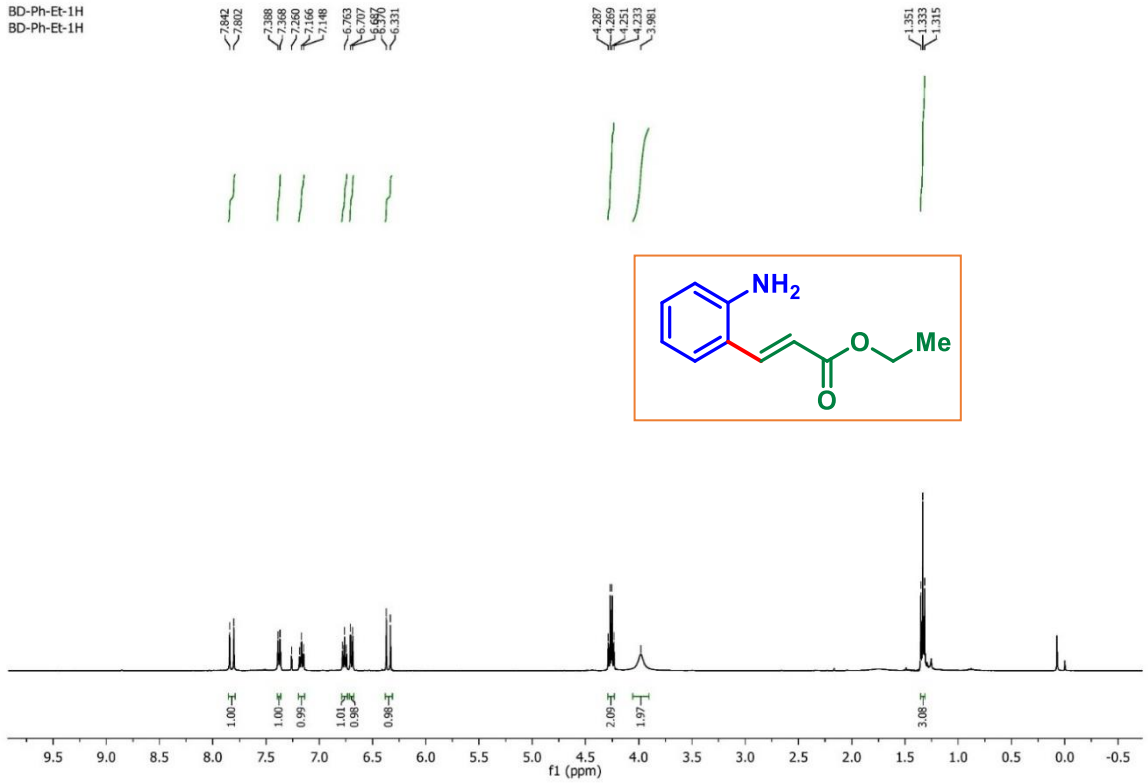

Ethyl (E)-3-(2-aminophenyl)acrylate (1b): **$^{13}C\{^{1}H\}$ NMR ($CDCl_3$, 100 MHz)**

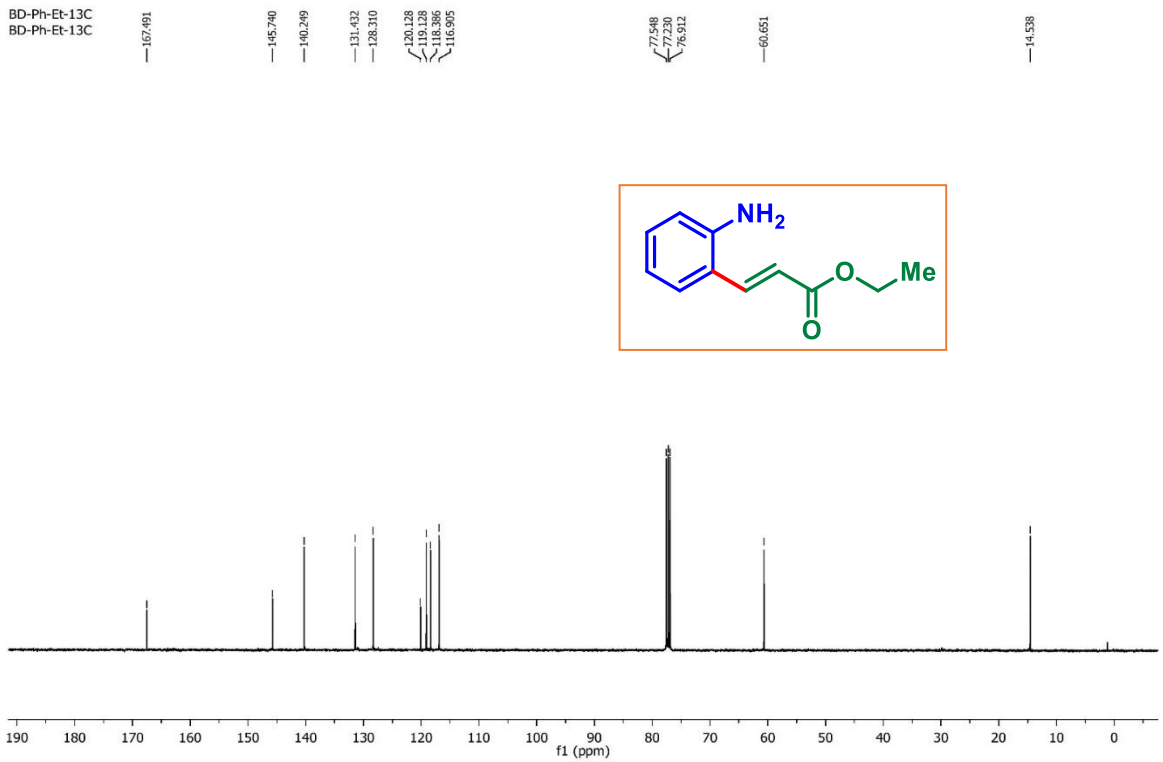

Dodecyl (E)-3-(2-aminophenyl)acrylate (1e): **^{1}H NMR ($CDCl_3$, 500 MHz)**

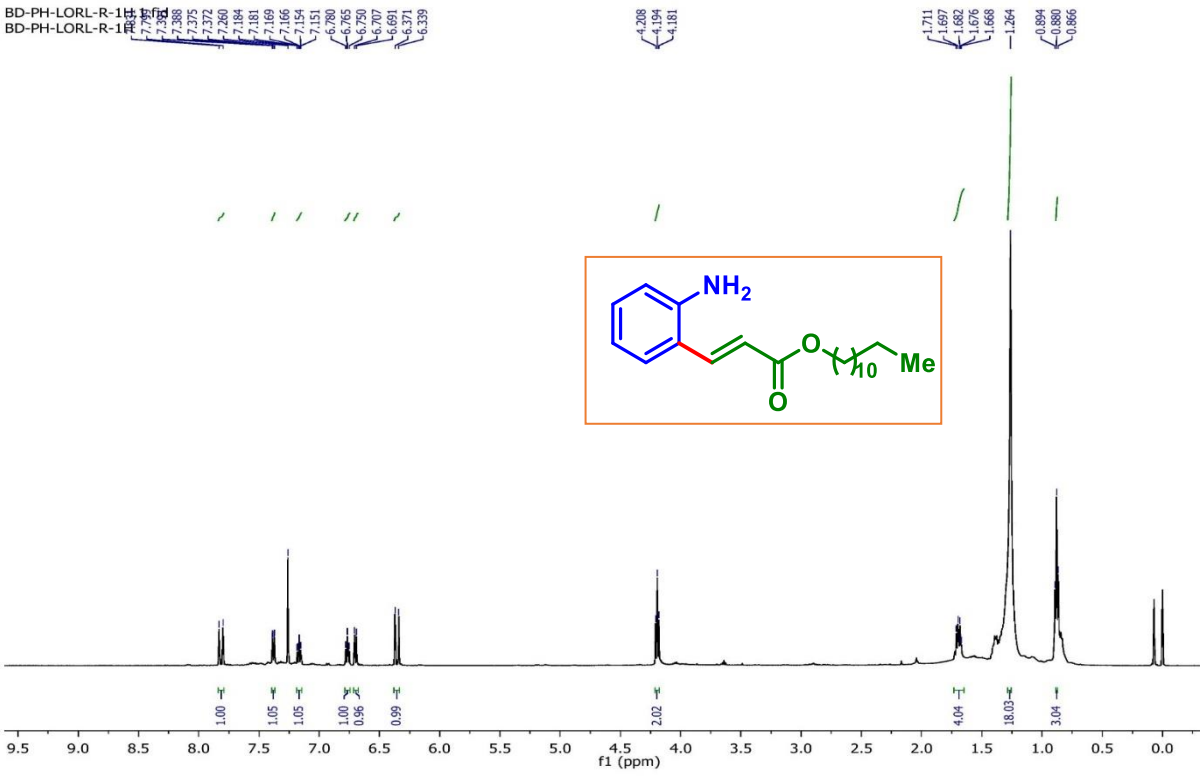

Dodecyl (E)-3-(2-aminophenyl)acrylate (1e): **$^{13}C\{^1H\}$ NMR (CDCl$_3$, 125 MHz)**

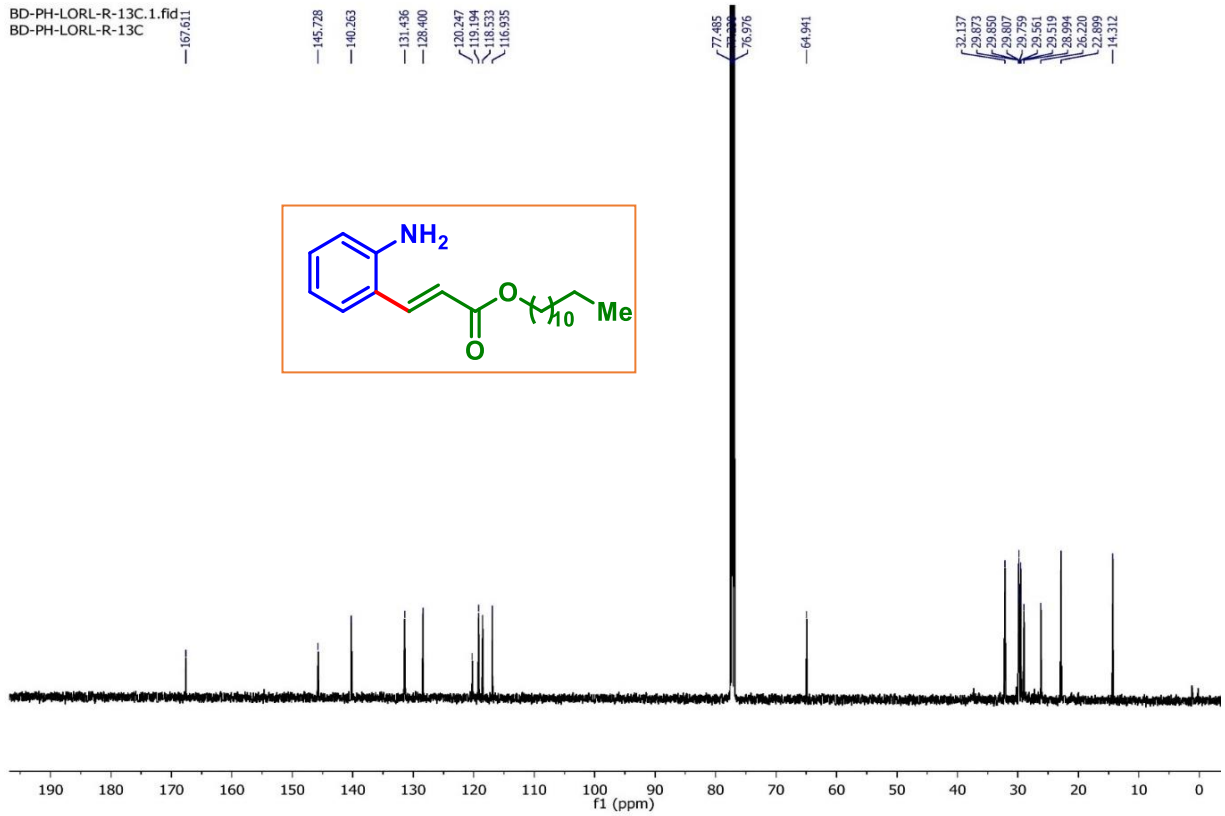

(Tetrahydrofuran-2-yl)methyl (E)-3-(2-aminophenyl)acrylate (1j)**: ^1H NMR (CDCl$_3$, 400 MHz)**

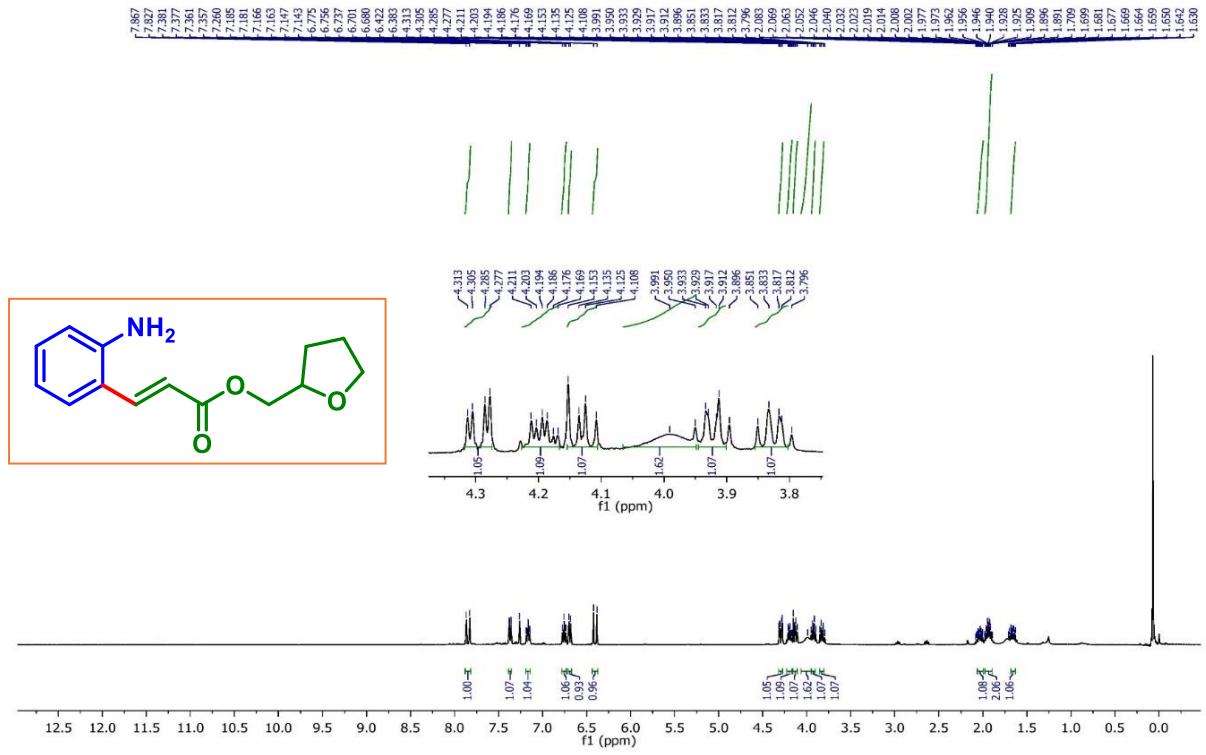

***(Tetrahydrofuran-2-yl)methyl (E)-3-(2-aminophenyl)acrylate (1j)*: $^{13}C\{^1H\}$ NMR ($CDCl_3$, 100 MHz)**

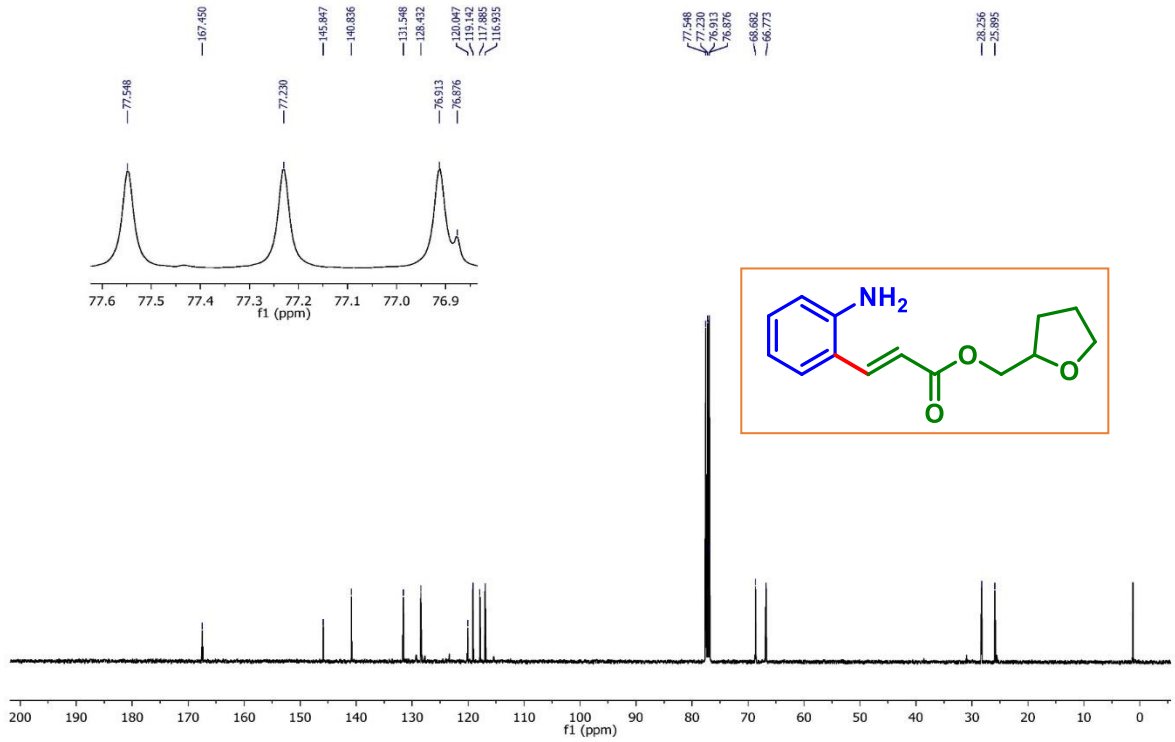

***p-Tolyl (E)-3-(2-aminophenyl)acrylate (1l)*: ^1H NMR ($CDCl_3$, 500 MHz)**

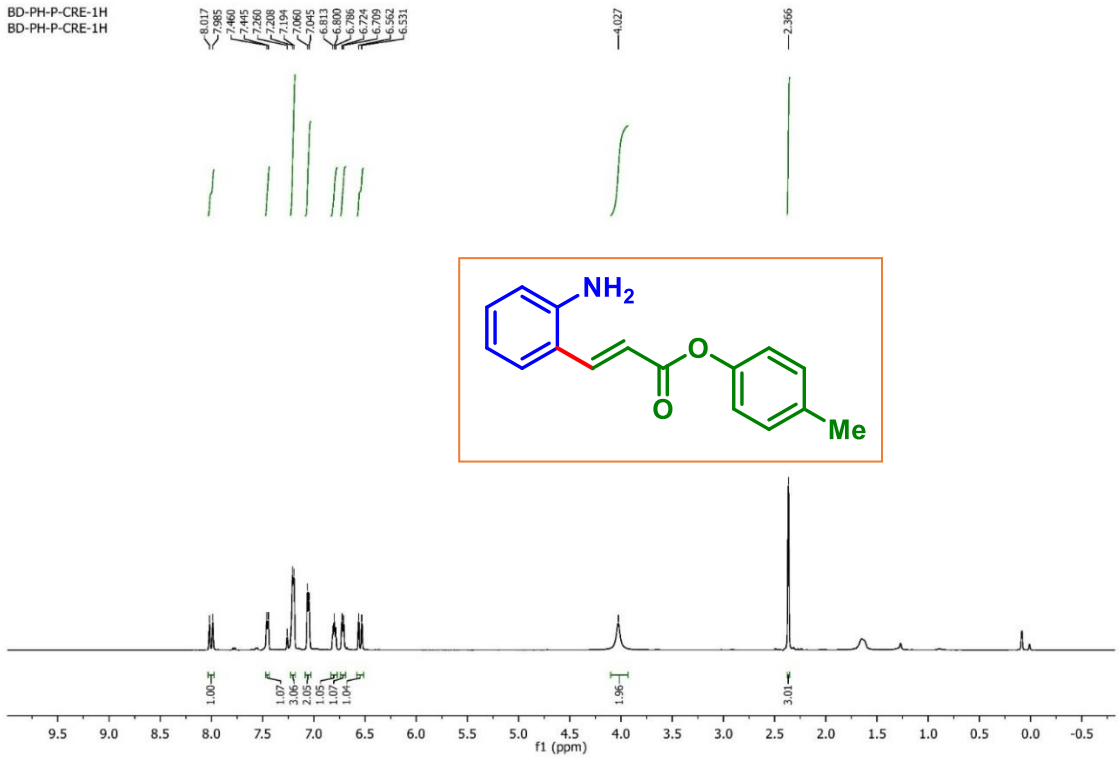

***p-Tolyl (E)-3-(2-aminophenyl)acrylate (1l)*: $^{13}C\{^{1}H\}$ NMR (CDCl$_3$, 125 MHz)**

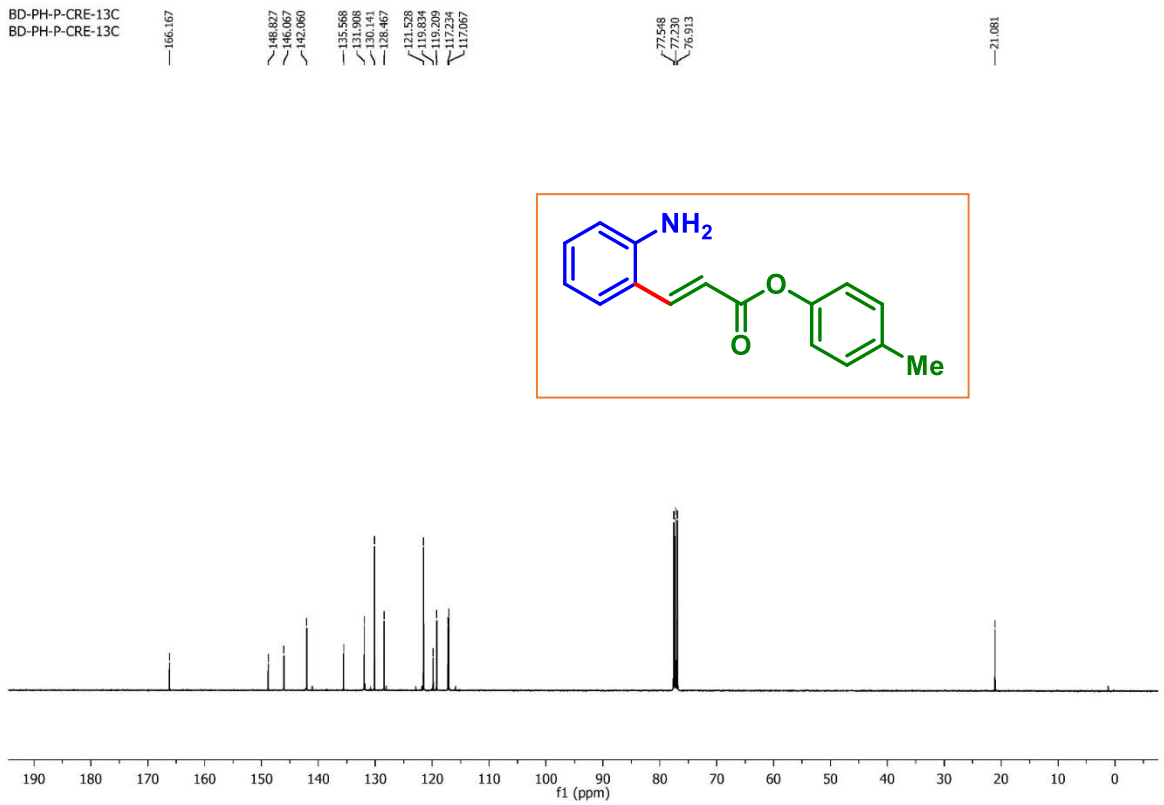

***1,7,7-Trimethylbicyclo[2.2.1]heptan-2-yl €-3-(2-aminophenyl)acrylate (1o)*: ^{1}H NMR (CDCl$_3$, 400 MHz)**

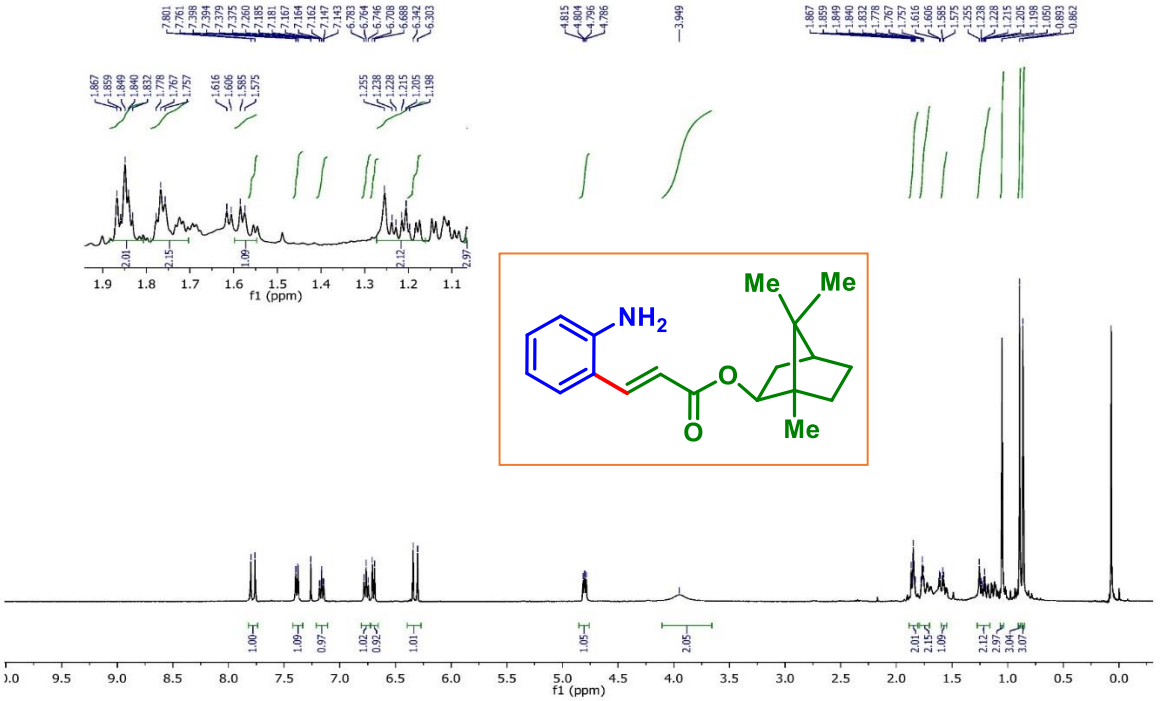

***1,7,7-Trimethylbicyclo[2.2.1]heptan-2-yl €-3-(2-aminophenyl)acrylate (1o)*: $^{13}C\{^1H\}$ NMR (CDCl$_3$, 100 MHz)**

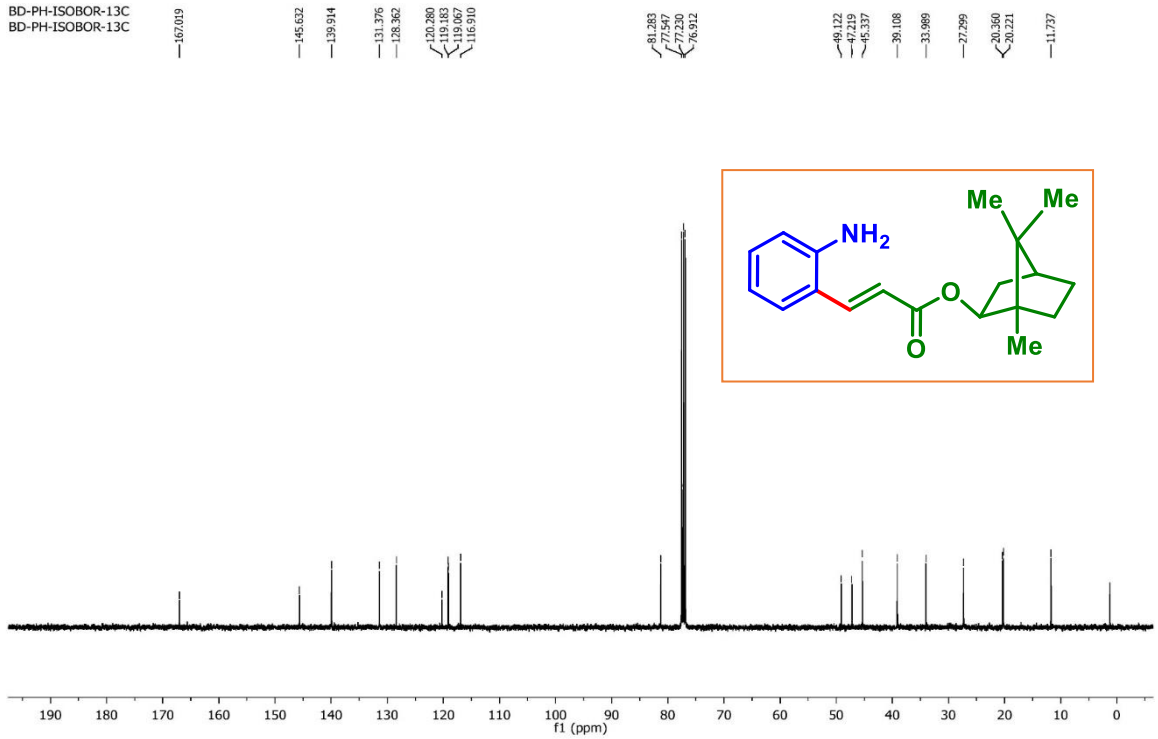

***2-(6,6-Dimethylbicyclo[3.1.1]hept-2-en-2-yl)ethyl (E)-3-(2-aminophenyl)acrylate (1p)*: ^1H NMR (CDCl$_3$, 500 MHz)**

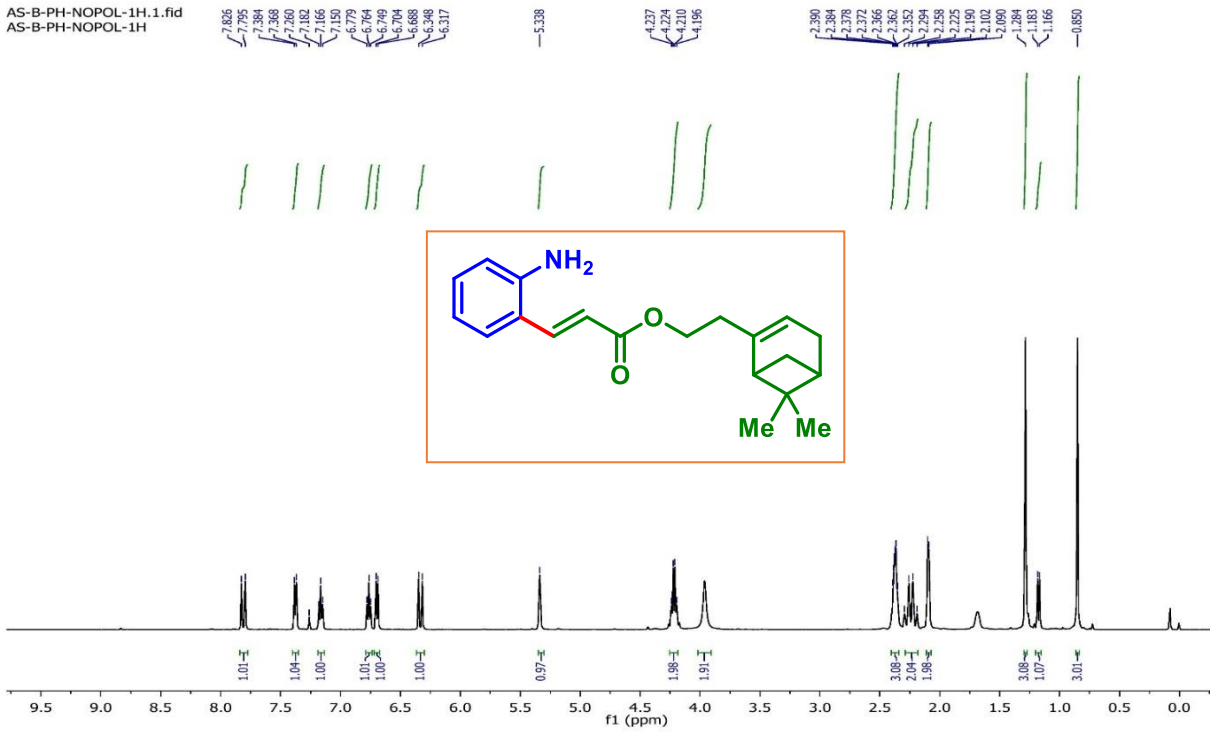

***2-(6,6-Dimethylbicyclo[3.1.1]hept-2-en-2-yl)ethyl (E)-3-(2-aminophenyl)acrylate (1p)*: $^{13}C\{^1H\}$ NMR ($CDCl_3$, 125 MHz)**

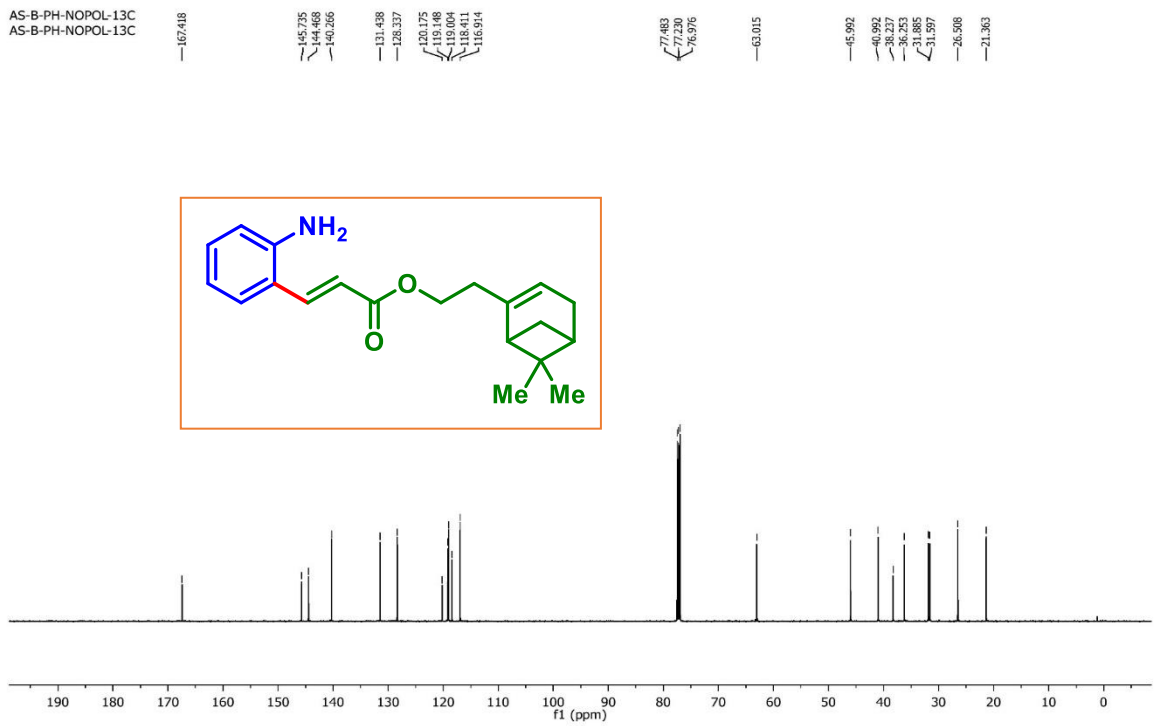

***(3S,8S,9S,10R,13R,14S,17R)-10,13-dimethyl-17-((R)-6-methylheptan-2-yl)-2,3,4,7,8,9,10,11,12,13,14,15,16,17-tetradecahydro-1H-cyclopenta[a]phenanthren-3-yl (E)-3-(2-aminophenyl)acrylate (1q)*: ^1H NMR ($CDCl_3$, 500 MHz)**

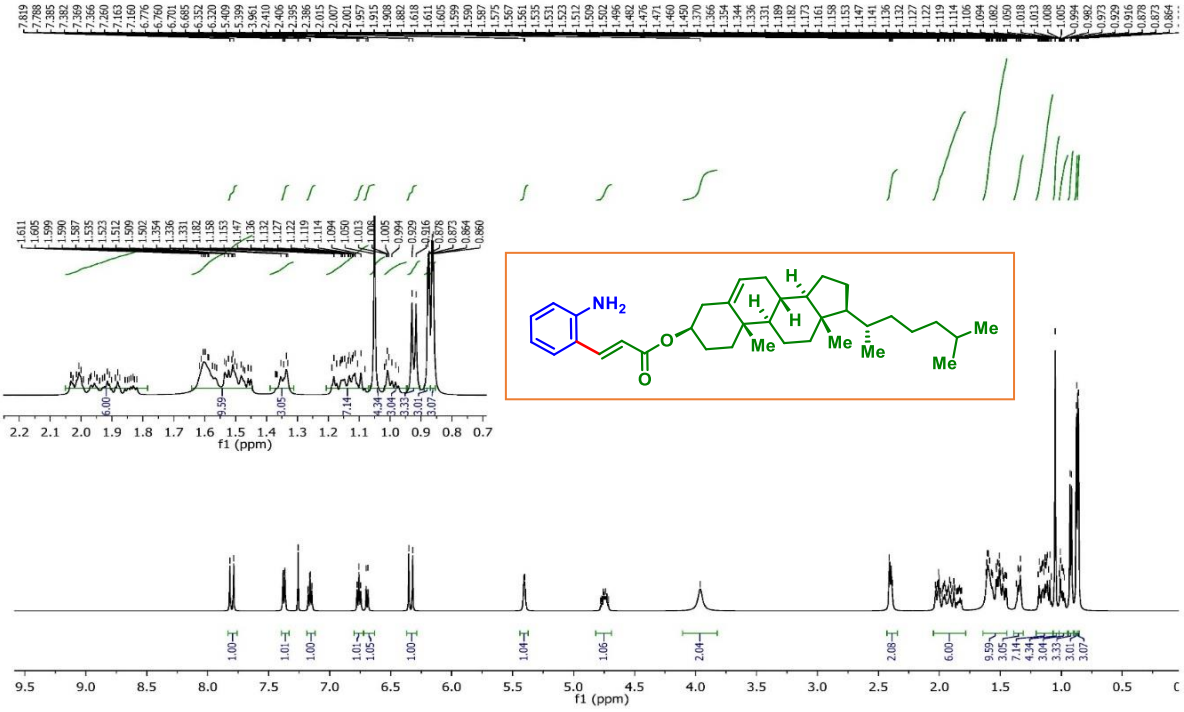

***(3S,8S,9S,10R,13R,14S,17R)-10,13-dimethyl-17-((R)-6-methylheptan-2-yl)-2,3,4,7,8,9,10,11,12,13,14,15,16,17-tetradecahydro-1H-cyclopenta[a]phenanthren-3-yl (E)-3-(2-aminophenyl)acrylate (1q)*: $^{13}C\{^{1}H\}$ NMR (CDCl$_3$, 125 MHz)**

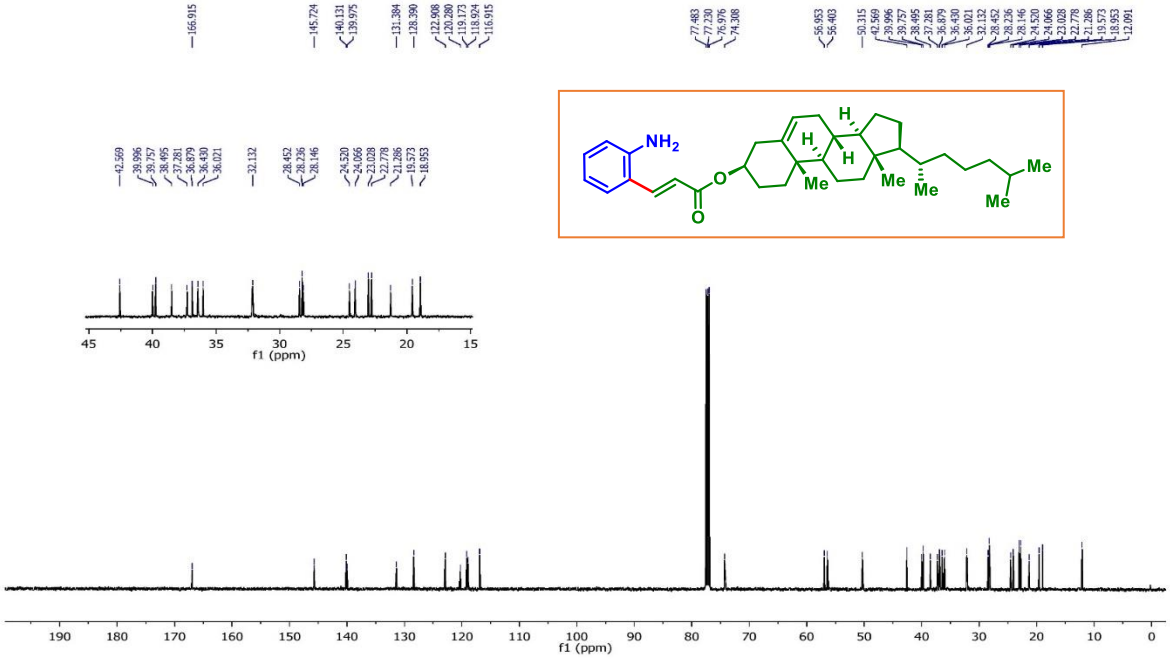

***Methyl (E)-3-(2-amino-5-fluorophenyl)acrylate (4a)*: ^{1}H NMR (CDCl$_3$, 400 MHz)**

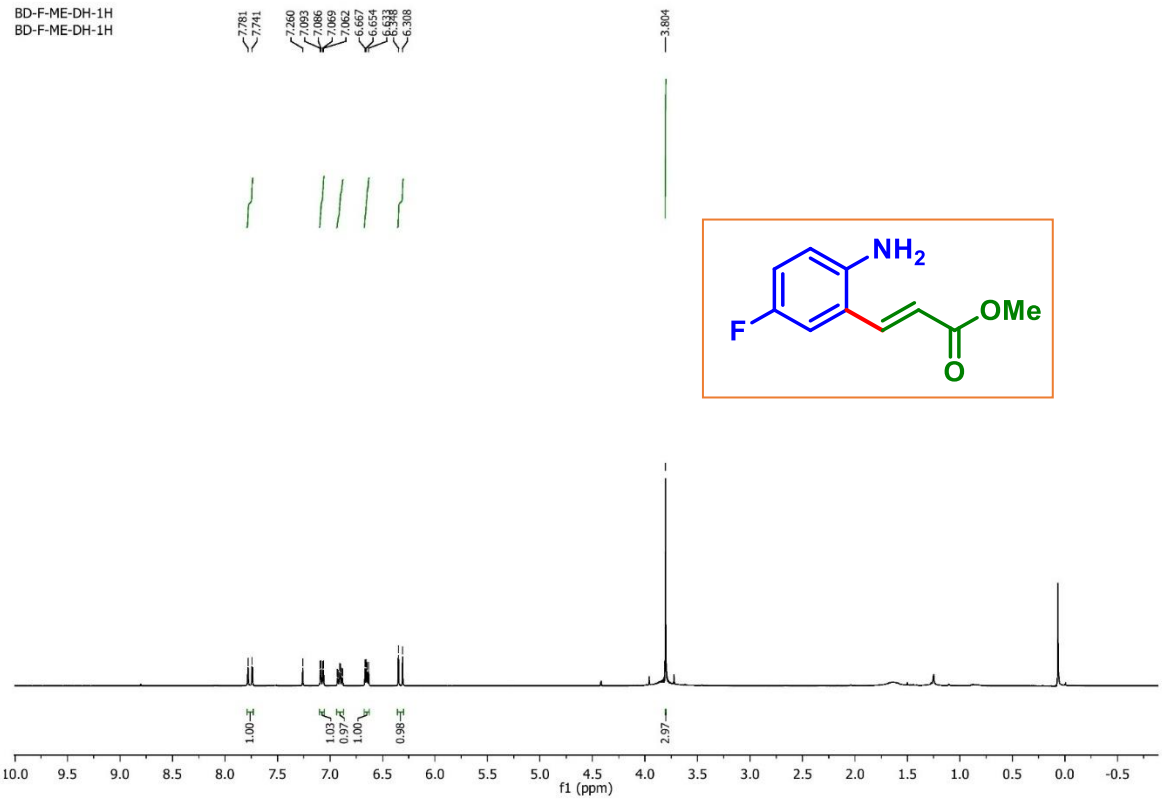

***Methyl (E)-3-(2-amino-5-fluorophenyl)acrylate (4a)*: $^{13}C\{^{1}H\}$ NMR ($CDCl_3$, 125 MHz)**

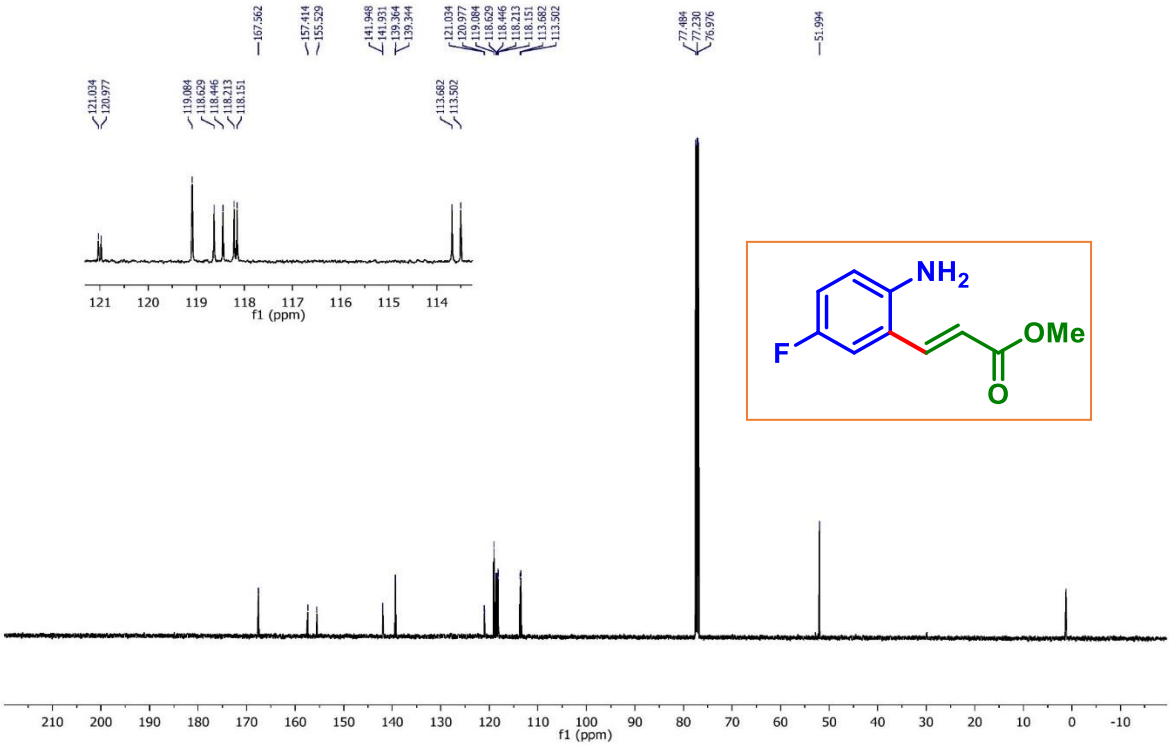

***Methyl (E)-3-(2-amino-5-fluorophenyl)acrylate (4a)*: ^{19}F NMR ($CDCl_3$, 376 MHz)**

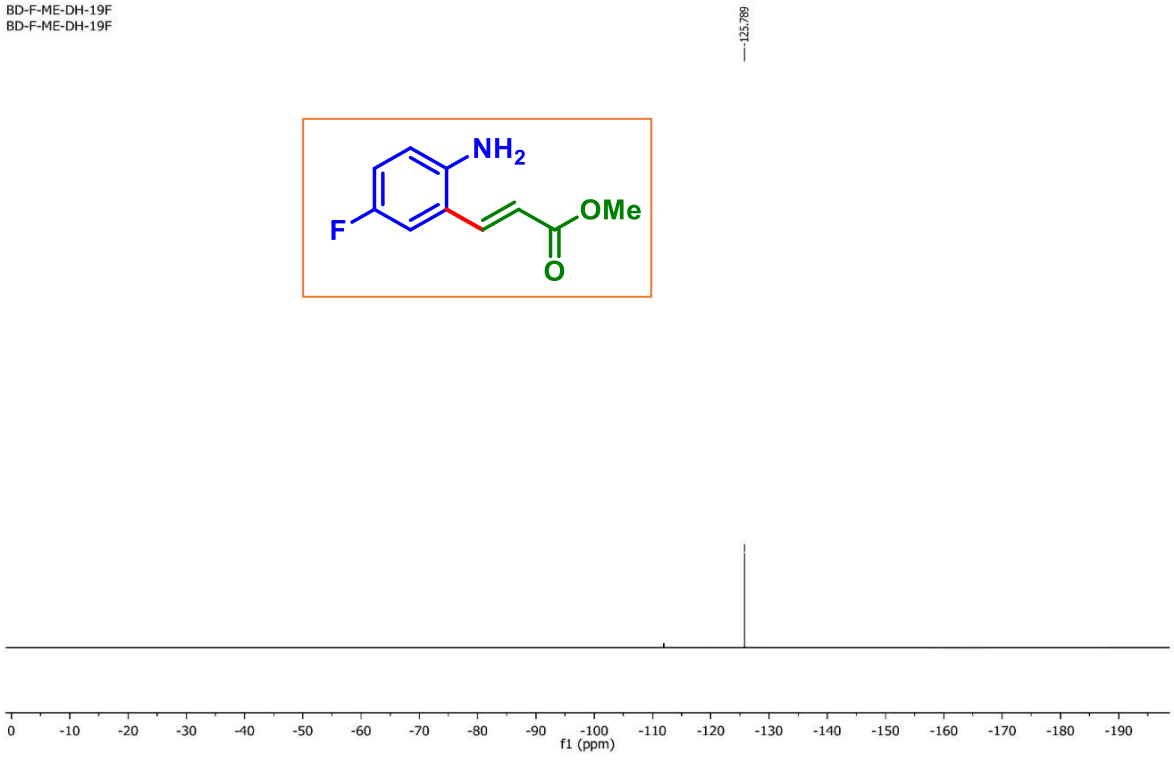

***Methyl (E)-3-(2-amino-5-bromophenyl)acrylate (7a)*: ^{1}H NMR (CDCl$_3$, 500 MHz)**

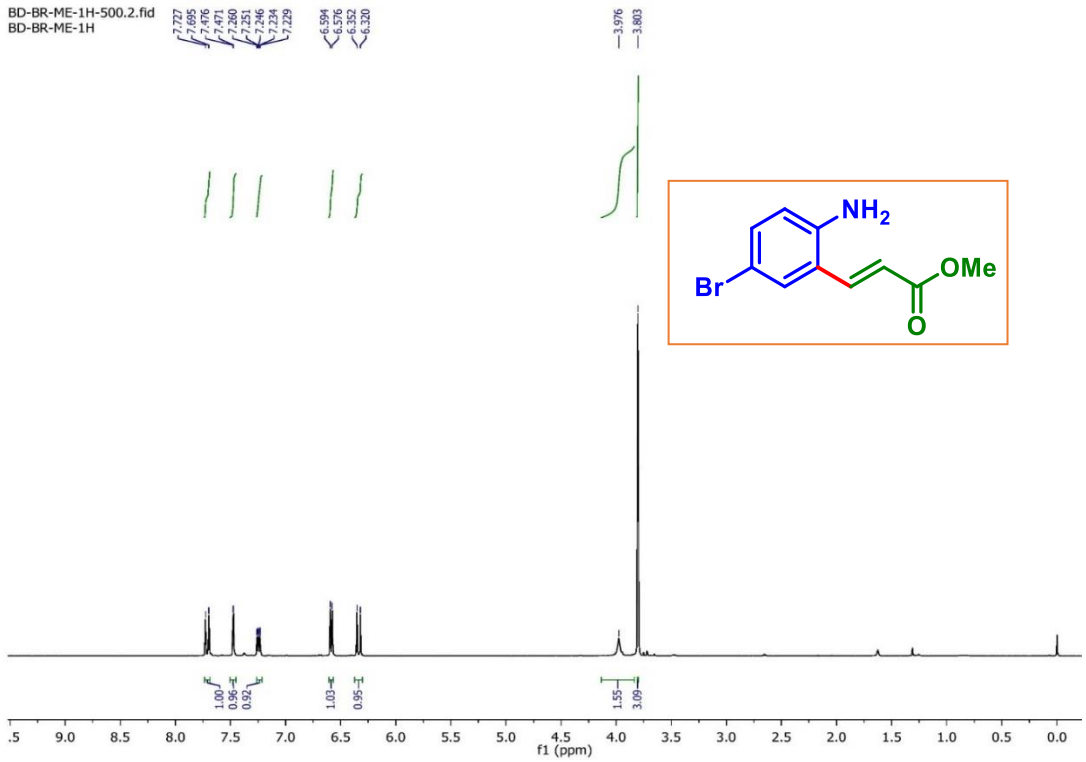

***Methyl (E)-3-(2-amino-5-bromophenyl)acrylate (7a)*: ^{13}C{^{1}H} NMR (CDCl$_3$, 125 MHz)**

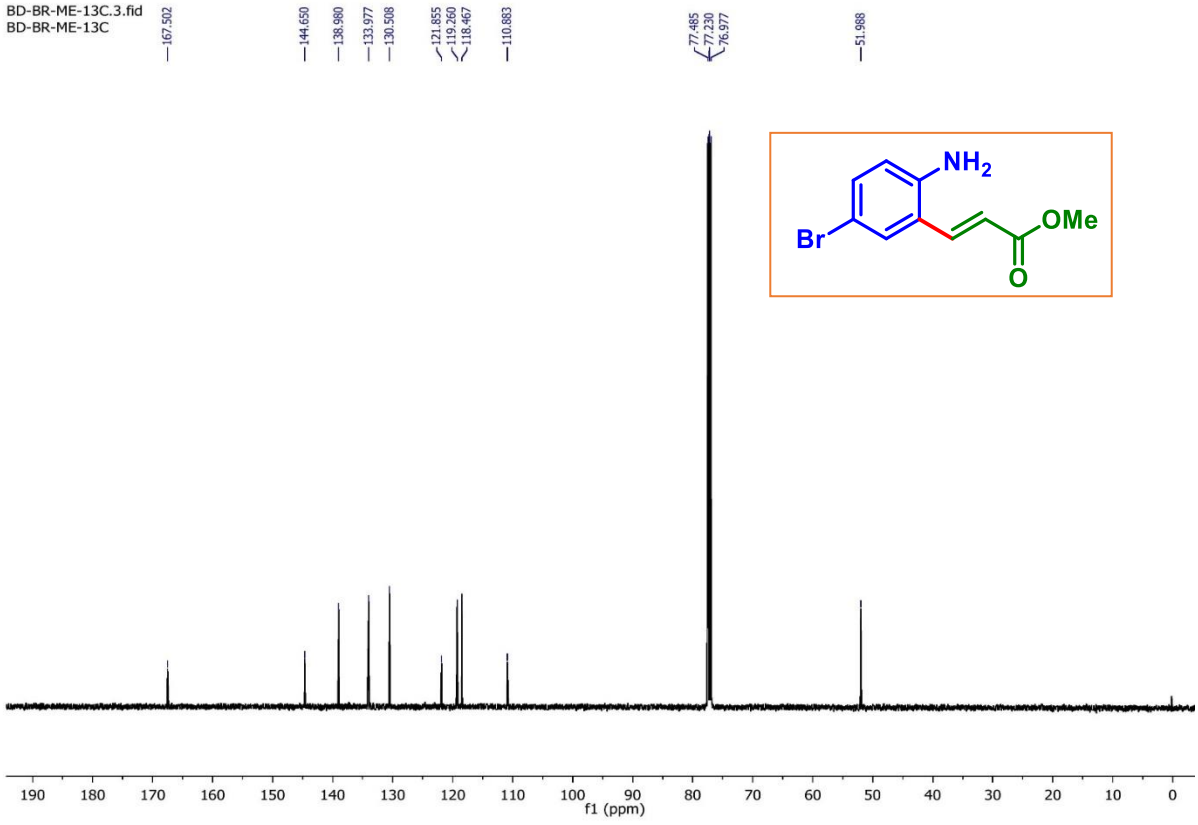

***Quinolin-2(1H)-one (1a')*: ^{1}H NMR (CDCl$_3$, 500 MHz)**

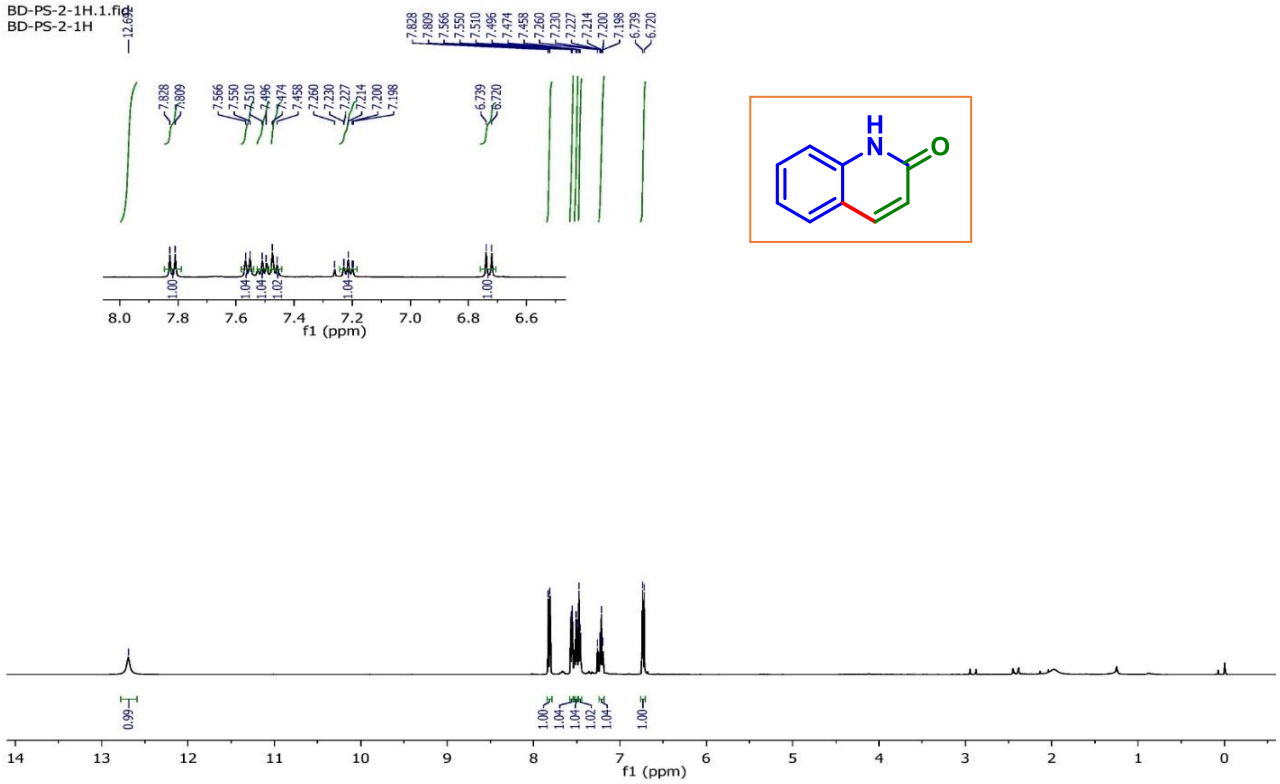

***Quinolin-2(1H)-one (1a')*: ^{13}C{^{1}H} NMR (CDCl$_3$, 125 MHz)**

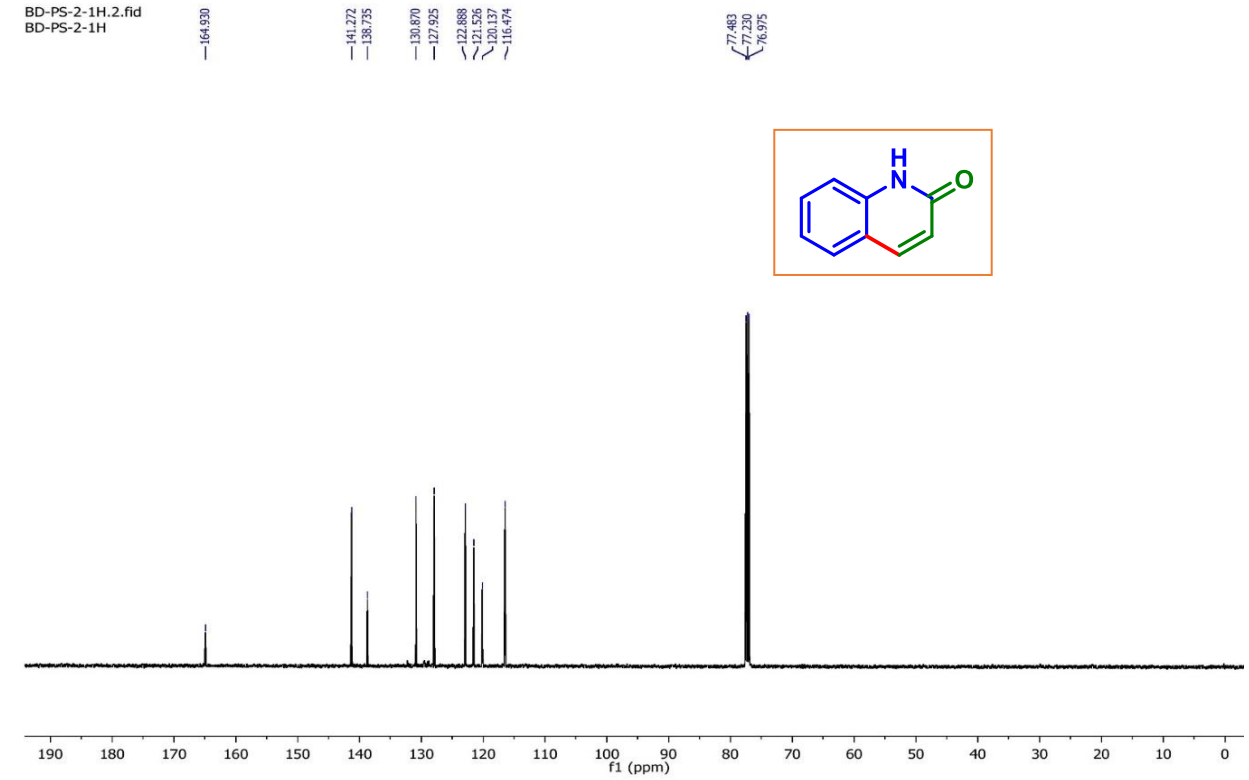

***6-Methyl-4-(p-tolyl)quinolin-2(1H)-one (2ab)*: ^{1}H NMR (CDCl$_3$, 400 MHz)**

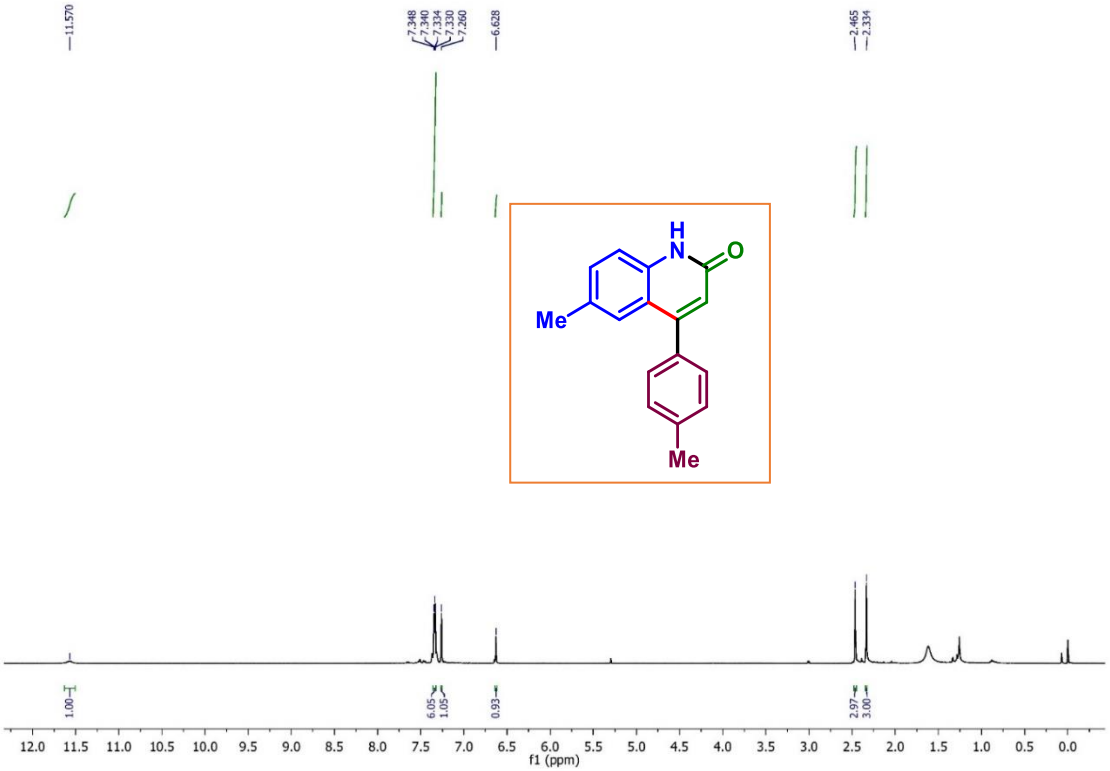

***6-Methyl-4-(p-tolyl)quinolin-2(1H)-one (2ab)*: ^{13}C{^{1}H} NMR (CDCl$_3$, 100 MHz)**

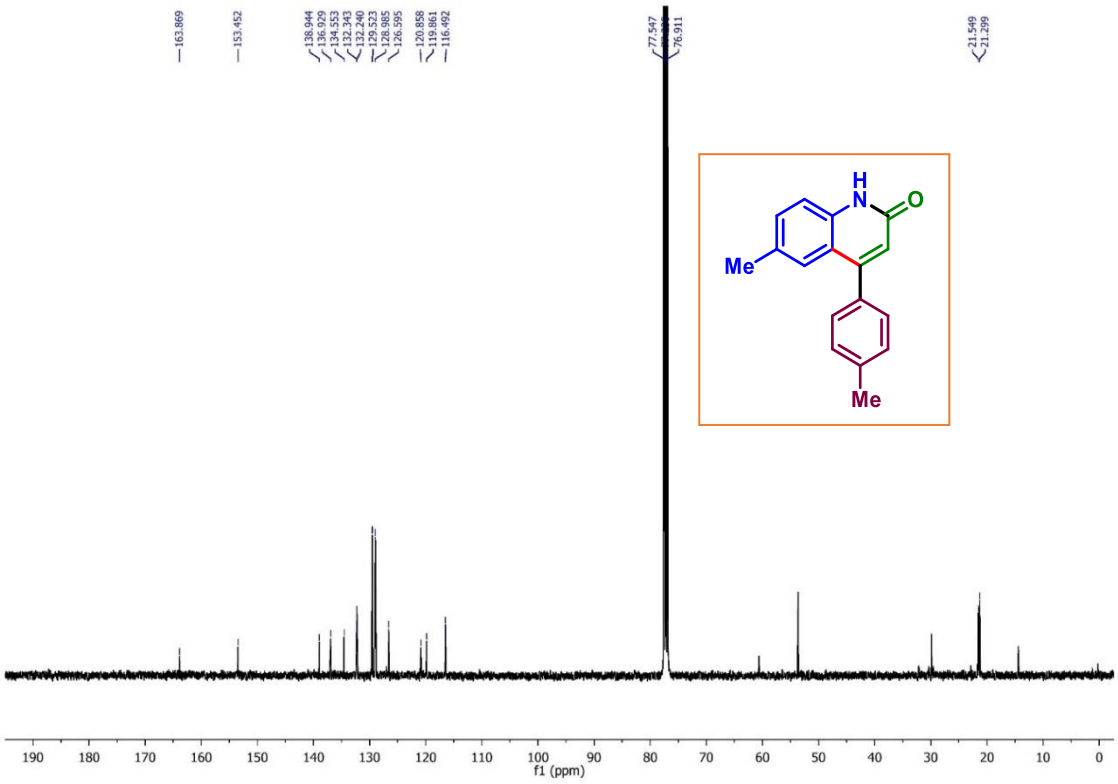

***Methyl (E)-3-(2-amino-5-(p-tolylethynyl)phenyl)acrylate (7ac)*: ^{1}H NMR ($CDCl_3$, 400 MHz)**

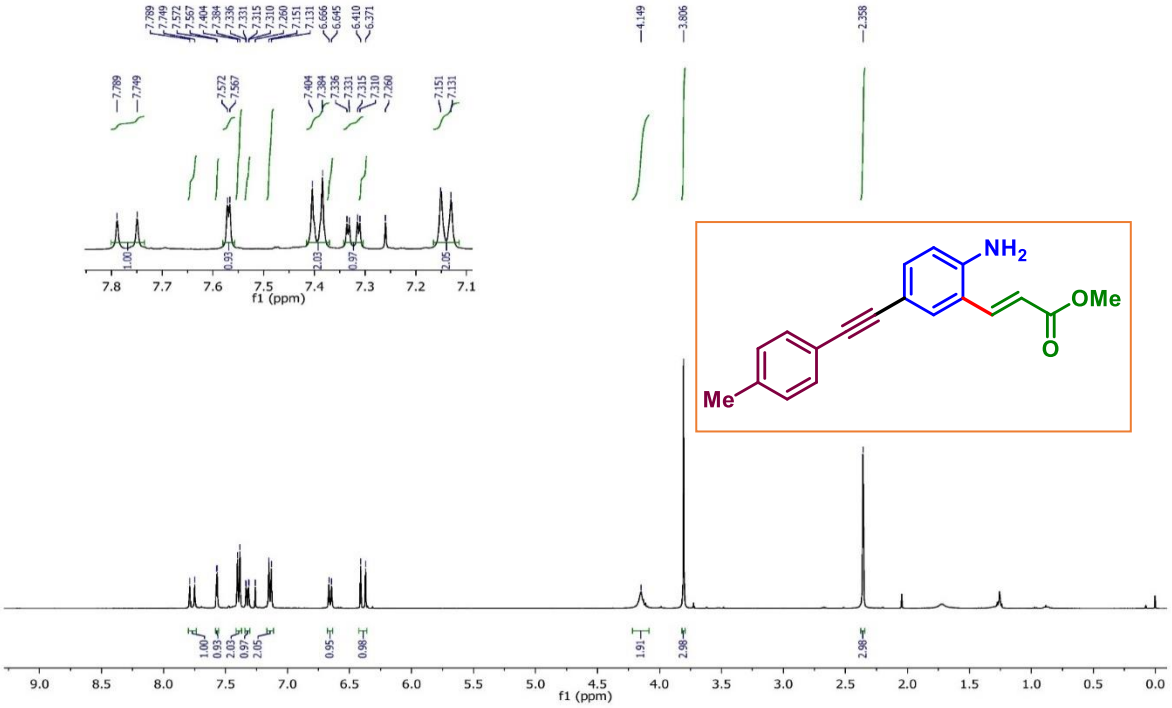

***Methyl (E)-3-(2-amino-5-(p-tolylethynyl)phenyl)acrylate (7ac)*: ^{13}C{^{1}H} NMR ($CDCl_3$, 100 MHz)**

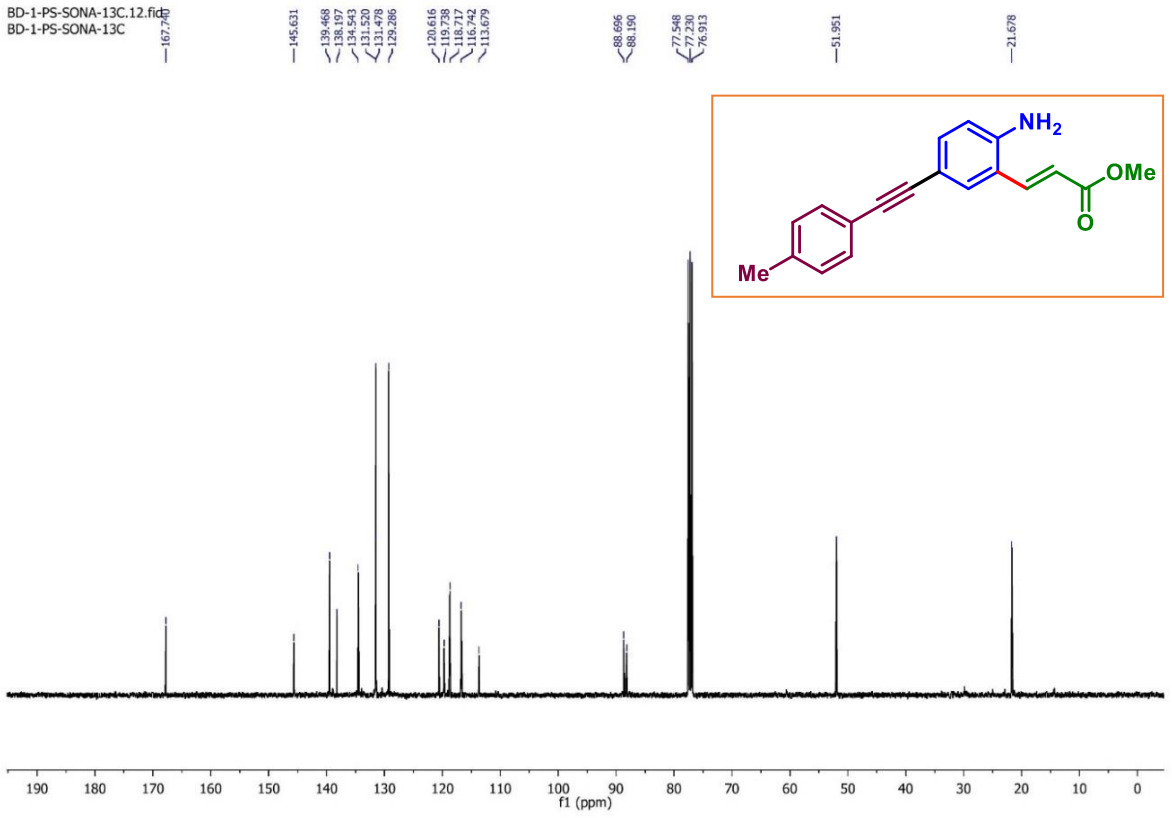

***Methyl cinnamate (1a'')*: ^{1}H NMR ($CDCl_3$, 400 MHz)**

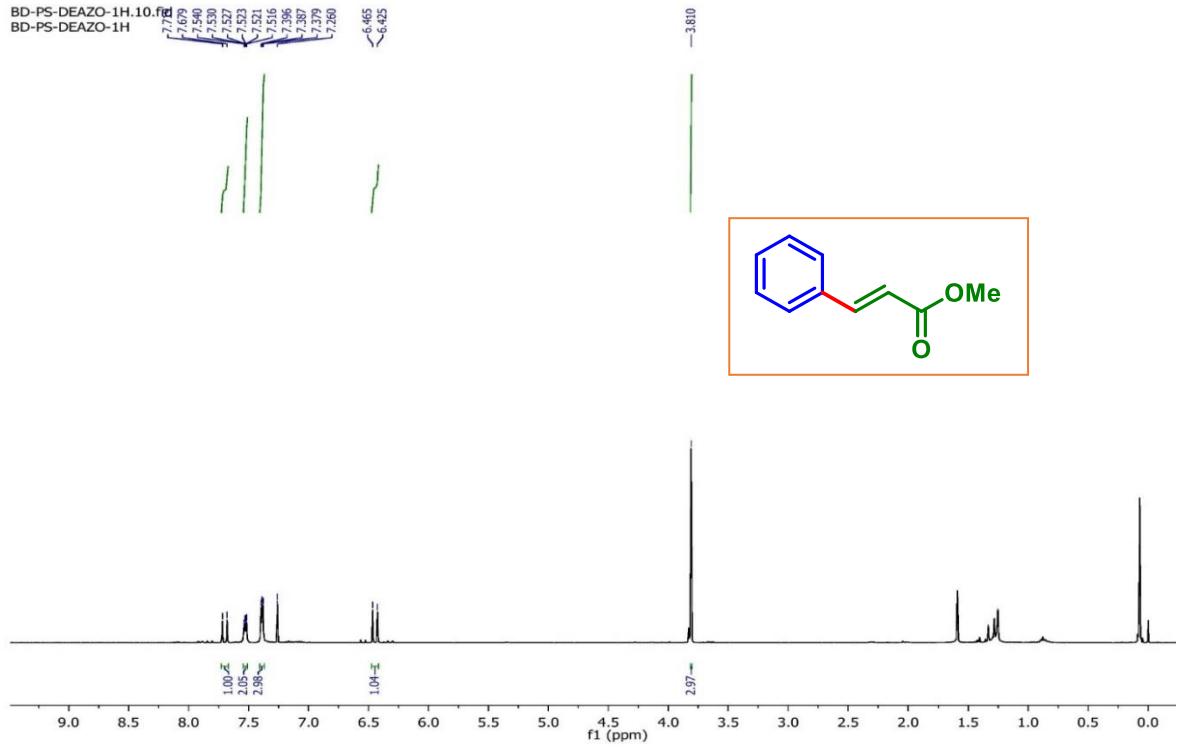

***Methyl cinnamate (1a'')*: ^{13}C{^{1}H} NMR ($CDCl_3$, 100 MHz)**

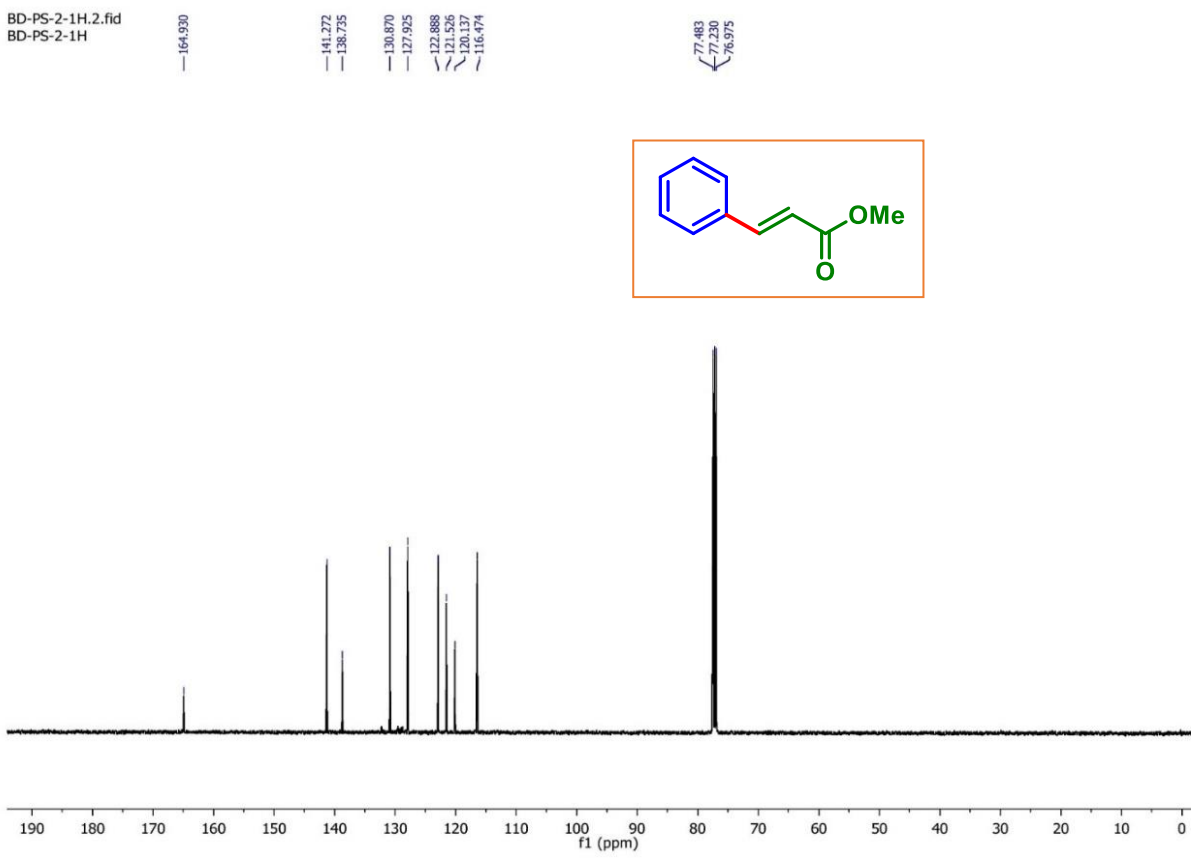

List of Publications

Research Articles

1. Synthesis of chromenopyrroles (azacoumestans) from functionalized enones and alkyl isocyanoacetates: **Bubul Das**, Anjali Dahiya, Nikita Chakraborty, and Bhisma K. Patel,* *Org. Lett.* **2023**, *25*, 5209. (***IF: 4.9***)

2. Access to chromenopyrrole *via* tandem [3 + 2] cycloaddition and intramolecular C–O coupling: **Bubul Das**, Nikita Chakraborty, Hirendra Nath Dhara and Bhisma K. Patel,* *J. Org. Chem*. **2024**, *89*, 1331. (***IF: 3.3***)

3. Transformable transient directing group-assisted C(sp^2)–H activation: synthesis and late-stage functionalizations of *o*-alkenylanilines: **Bubul Das**, Anjali Dahiya, Ashish K. Sahoo, and Bhisma K Patel *J. Org. Chem*. **2022**, *87*, 13383. (***IF: 3.3***)

4. Pd(II)-catalyzed three-component synthesis of furo[2,3-*d*]pyrimidines from *β*-ketodinitriles, boronic acids, and aldehydes: Hirendra Nath Dhara, **Bubul Das**, Dinabandhu Barik, Supriya Manna, and Bhisma K. Patel,* *Org. Lett*. **2023**, *25*, 9070. (***IF: 4.9***)

5. Visible-light-driven isocyanide insertion to *o*-alkenylanilines: A route to isoindolinone synthesis: Anjali Dahiya, **Bubul Das**, Ashish Kumar Sahoo, and Bhisma K. Patel* *Adv. Synth. Catal*. **2022**, *364*, 5, 966. (***IF: 4.4***)

6. Base-promoted synthesis of *S*-arylisothiazolones *via* intramolecular dehydrative cyclization of *α*-keto-*N*-acylsulfoximines: Nikita Chakraborty, **Bubul Das**, Dinabandhu Barik, Kamal Krishna Rajbongshi and Bhisma K. Patel,* *J. Org. Chem*. **2024**, 89, 778. (***IF: 3.3***)

7. Visible-light-mediated difunctionalization of alkynes: synthesis of *β*-substituted vinylsulfones using *O*- and *S*-centered nucleophiles: Ashish Kumar Sahoo, Anjali Dahiya, **Bubul Das**, Ahalya Behera, and Bhisma K. Patel,* *J. Org. Chem*. **2021**, *86*, 11968. (***IF: 3.3***)

8. NIS-initiated Photo-induced oxidative decarboxylative sulfoximidation of cinnamic acids: Nikita Chakraborty, Kamal Krishna Rajbongshi, Anjali Dahiya, **Bubul Das**, Akshar Vaishnani and Bhisma K. Patel,* *Chem. Commun*. **2023**, *59*, 2779. (***IF: 4.3***)

Review Articles

1. Synthetic utility of styrenes in the construction of diverse heterocycles *via* annulation/cycloaddition. **Bubul Das**, Nikita Chakraborty, Kamal K. Rajbongshi and Bhisma K. Patel,* *Tetrahedron*, **2023**, *134*, 133270. ***(IF: 2.1)***

2. Isothiocyanates: happy-go-lucky reagents in organic synthesis: **Bubul Das**, Anjali Dahiya, and Bhisma K. Patel,* *Org. Bimol. Chem*. **2024**, *22*, 3772. ***(IF: 2.9)***

3. Combined power of organo- and transition metal catalysis in organic synthesis: Nikita Chakraborty, **Bubul Das**, Kamal K. Rajbongshi and Bhisma K. Patel*, *Eur. J. Org. Chem*. **2022**, e202200273. ***(IF: 2.5)***

4. Graphitic carbon nitride materials in dual metallo-photocatalysis: a promising concept in organic synthesis: Binoyargha Dam, **Bubul Das**, and Bhisma K. Patel,* *Green Chem*., **2023**, *25*, 3374. ***(IF: 9.3)***

5. Updates on hypervalent-iodine reagents: metal free functionalisation of alkenes, alkynes and heterocycles: Anjali Dahiya, Ashish Kumar Sahoo, Nikita Chakraborty, **Bubul Das**, and Bhisma K. Patel,* *Org. Biomol. Chem*. **2022**, *20*, 2005. ***(IF: 2.9)***

Book Chapters

1. **Bubul Das**, Anjali Dahiya, Ashish K. Sahoo, and Bhisma K. Patel,* A book chapter entitled "Conventional Liquid Biofuels" for the book "Bio-Clean Energy Technologies Volume 2" published by Springer Nature Singapore, eBook ISBN: 978-981-16-8094-6, Print: ISBN 978-981-16-8093-9.

2. **Bubul Das**, Hirendra Nath Dhara, Anjali Dahiya, and Bhisma K. Patel,* A book chapter entitled "Recent Advances in Photocatalytic Degradation of Dyes Using Heterogeneous Catalysts" for the book "Trends and Contemporary Technologies for Photocatalytic Degradation of Dyes" published by Springer International Publishing, eBook: ISBN 978-3-031-08991-6, Print ISBN: 978-3-031-08990-9.

****